

NASA
Reference
Publication
1313

November 1993

The Atmospheric Effects of Stratospheric Aircraft: A Third Program Report

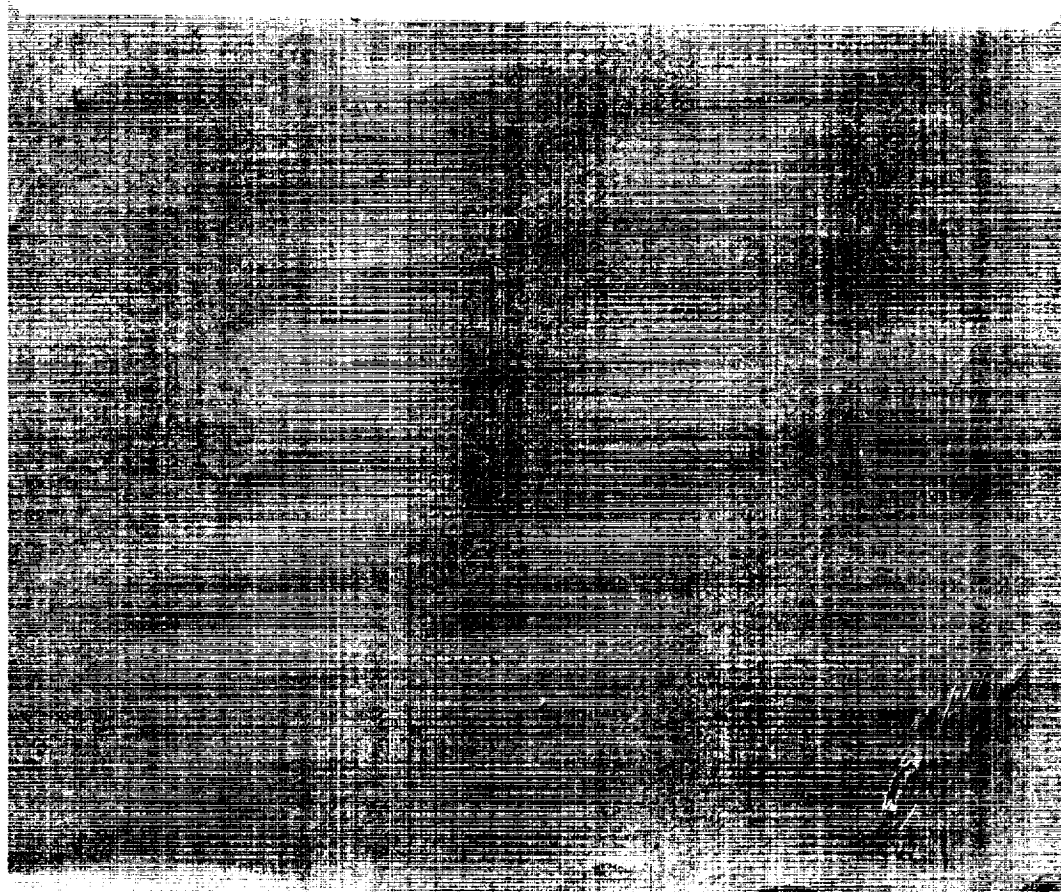
(NASA-RP-1313) THE ATMOSPHERIC
EFFECTS OF STRATOSPHERIC AIRCRAFT:
A THIRD PROGRAM REPORT (NASA)
405 p

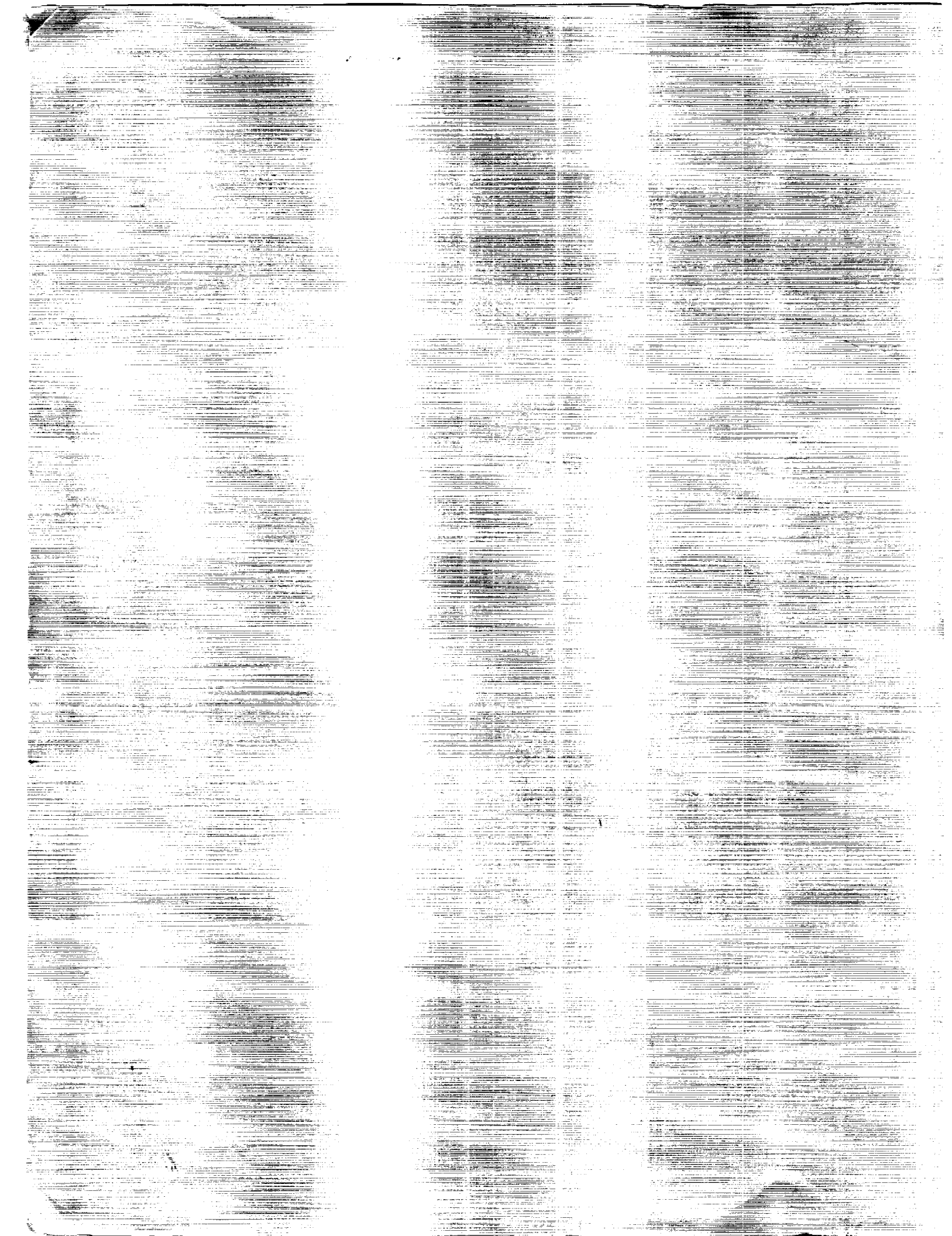
N94-24104

Unclass

H1/45 0199888

NASA





**NASA
Reference
Publication
1313**

1993

The Atmospheric Effects of Stratospheric Aircraft: A Third Program Report

Edited by
Richard S. Stolarski
Goddard Space Flight Center
Greenbelt, Maryland

Howard L. Wesoky
NASA Office of Aeronautics
Washington, D.C.



National Aeronautics and
Space Administration
Office of Management
Scientific and Technical
Information Program

Contents

1	Program Summary <i>Richard Stolarski and Howard Wesoky</i>	1
2	Plans for Atmospheric Observations <i>William Brune</i>	25
3	Emissions Scenarios Development: Emissions Scenarios Committee Report <i>Donald Wuebbles et al.</i>	63
4	Update of Model Simulations for the Effects of Stratospheric Aircraft <i>Malcolm Ko and Anne Douglass</i>	209
5	Engine Exhaust Trace Chemistry Committee Report <i>Frederick Dryer et al.</i>	245
6	Exhaust Plume/Aircraft Wake Vortex Interaction Committee Report <i>Charles Kolb et al.</i>	317
7	High-Speed Research Program/Atmospheric Effects of Stratospheric Aircraft Research Summaries	339
A	Appendix: List of Reviewers	A-1

Chapter 1

Program Summary

Richard S. Stolarski
Program Scientist
Goddard Space Flight Center
National Aeronautics and Space Administration
Greenbelt, MD

Howard L. Wesoky
Program Manager
Office of Aeronautics
Headquarters
National Aeronautics and Space Administration
Washington, DC

INTRODUCTION

This report effectively marks the midpoint of the Atmospheric Effects of Stratospheric Aircraft (AESA) investigation (Prather et al., 1992, Stolarski and Wesoky, 1993) of the NASA High-Speed Research Program (HSRP). The AESA element of the HSRP began in FY 1990 and has an approved budget plan through FY 1995. Although it has been proposed to augment and continue the HSRP, at this time only the original plan has been authorized, and only AESA activities that will be completed by the end of FY 1995 are sponsored by NASA.

Progress has been made in all areas of the HSRP (Rosen and Williams, 1993, Shaw, 1991), including community noise and sonic boom research. However, most important to the AESA studies is that related combustion research has achieved the goal emissions level of 5 grams of equivalent NO_2 per kilogram of fuel in laboratory level facilities (i.e., flame tubes) for two basic concepts at simulated high-speed civil transport (HSCT) aircraft cruise conditions. Plans are progressing to next test these concepts in facilities that better simulate aircraft engines, and research and technology development has also begun with the composite materials that will be required for practical application of the low NO_x ($= \text{NO} + \text{NO}_2$) concepts.

AESA is a directed research program which relies heavily on the underlying base investigations of the NASA Upper Atmosphere Research Program (UARP) and the NASA Atmospheric Chemistry Modeling and Analysis Program (ACMAP). A primary question at the beginning of the program was the impact of aircraft-generated NO_x on stratospheric ozone. The other possible effects of importance to the program spanned the broad range of known fundamental problems of stratospheric science. AESA support is used to emphasize those elements of UARP and ACMAP that are most relevant to the evaluation of the effects of stratospheric aircraft and to focus efforts of many of the researchers in those programs in directions most beneficial to AESA. As indicated by the organizational association of the investigators listed in Table 1, AESA has similarly benefited from base investigations that are sponsored by other agencies of the U.S. government as well as programs sponsored by other governments. In particular, recognition should be given to the National Oceanic and Atmospheric Administration, the U.S. Department of Energy, and the National Science Foundation. Likewise, it should be recognized that the investigators from other nations are being financially supported by their governments for participation in AESA.

The general direction for the HSRP-sponsored atmospheric research has continued to be guided by a panel of experts (Table 2) representing important constituencies of the scientific and related communities. Investigators have been selected for sponsorship through a series of NASA Research Announcements, which solicited worldwide participation in a wide range of topics (Prather et al., 1992). In the past year a significant number of newly sponsored investigations were begun, and these will probably be the last additions to the phase I program. Therefore, the studies now under way will likely serve as the basis for the atmospheric assessment to be conducted for the program in 1995. To ensure that the scientific plan for that assessment is appropriate, the program status and plan reported here will be evaluated by the National Research Council. The panel's evaluation of the interim assessment will, in turn, be later utilized in the United Nations atmospheric assessment process which has resulted in a series of major reports (e.g., World Meteorological Organization, 1992) to the Montreal Protocol Parties (Benedick, 1991).

The overall plan for accomplishing the assessment activities and supporting the definition of standards for acceptable levels of HSCT aircraft engine emissions is shown in Figure 1, where the shaded areas represent completed milestones. The plan consists of three basic elements: technology, science, and policy. The thrust of the AESA Program is towards the evaluation of the scientific basis for technology directions and for any subsequent policy decisions. In order to

provide a basis for evaluation of the scientific program, brief discussions of the technology and policy issues are included in the chapter.

TECHNOLOGY

Low Emission Combustors

The Low Emission Combustor Technology element of the HSRP focuses on reducing oxides of nitrogen (NO_x) from proposed HSCT engines (Rosen and Williams, 1993). Related research encompasses conceptual design of low NO_x combustors, evaluation of their technical feasibility, analytical prediction of cruise emissions levels for the selected configurations, and combustor concept experiments. During the past 3 years, NASA, university investigators, and the aircraft engine industry have established the foundation for the required technology under the HSRP.

Successful development of this technology poses significant challenges. The need for substantial increases in fuel efficiency dictates considerable increases in combustor pressure and temperature operating conditions in order to achieve viable aircraft performance and economics. These conditions associated with fuel efficient engines cause NO_x levels to increase exponentially. Thus, significant departures from conventional combustor designs are required to achieve program goals.

Advanced combustors, based on the Lean-Premixed-Prevaporized (LPP) and the Rich Burn/Quick-Quench/Low-Burn (RQL) concepts, shown schematically in Figure 2, offer the potential for achieving the low NO_x goals. In both concepts, combustion is designed to occur where NO_x formation is at a minimum: fuel lean for the LPP and fuel rich for the RQL (i.e., away from stoichiometric, or an equivalence ratio of 1). In the LPP concept, air and fuel are mixed upstream of the burning zone to produce a homogeneous mixture. The liquid fuel is also fully vaporized in this zone. This mixture burns downstream of the flameholder at a relatively low temperature (below 3000°F) producing very low NO_x emissions. The RQL combustor is a staged combustion system in which the rich zone burns fuel in an air-deficient environment which is conducive to very low NO_x formation. This partially burned mixture has large quantities of air injected into it as it passes through the quick-quench zone of the combustor. The air must be added quickly to avoid burning at stoichiometric conditions. Final combustion then occurs in the lean stage.

The HSRP goal is shown in Figure 3 relative to operational engines and an earlier NASA research program, the Experimental Clean Combustor Program (ECCP). This program demonstrated the technology required to design and develop advanced commercial, subsonic aircraft engines with significantly lower pollutant levels. In that program the research combustor attained NO_x -emissions indices considerably lower than those of the operational General Electric CF6-50 or Pratt & Whitney JT9D engine combustors. These results are highlighted in Figure 3, showing a plot of total NO_x emissions, expressed as grams of equivalent NO_2 per kilogram of fuel, as a function of a NO_x severity parameter (i.e., proportional to increased severity of operating conditions). The top curve shows NO_x levels from the conventional combustors, while the bottom curve shows NO_x levels obtained under the ECCP. For comparison, the ambitious HSR Program goal is shown as a band around an emissions index (EI) of 5 grams of equivalent NO_2 per kilogram fuel.

Many NASA and industry tests in flame tube facilities now show a laboratory-level capability to achieve the low emissions goal (Shaw, 1991), and it is planned to verify the capability for both concepts in sector rig (i.e., a piece of a full annular combustor) tests before the end of FY 1995. Full annular rig and testbed engine experiments have been proposed for the next phase of the HSRP which has not yet been authorized. Simultaneously with the combustion research, an Enabling Propulsion Materials project (Aviation Week, 1992) was initiated in FY

1992 to develop the Ceramic Matrix Composite (CMC) materials that will be necessary to fully implement the low NO_x concepts in aircraft engines. The goal of the project is a material that can operate at 2500° to 3000° F for 75% to 80% of the 18,000 hours of proposed engine combustor liner lifetime. As shown in Figure 1, validation of the materials technology in an engine combustor test has been proposed for around the year 2000.

Fleet Emission Scenarios

Although designs for HSCT aircraft and engines are only in the conceptual stage, it is important to assess their potential atmospheric impact on the basis of predicted flight patterns and technology specifications that are as realistic as possible. To this end the HSRP has supported the development of a database of present and future fleet operational mission scenarios by the Boeing Commercial Airplane Group and the McDonnell Douglas Corporation.

As indicated in Figure 1, this effort has been managed as an element of the AESA scientific assessment process, but the task has been implemented within the HSRP aircraft technology system studies (see Chapter 3). In earlier AESA sensitivity studies (Prather et al., 1992, Stolarski and Wesoky, 1993), the scenarios did not fully consider all aspects of normal flight patterns (e.g., takeoff, climb, etc), and it was assumed that all fuel would be consumed within narrow ranges of cruise altitude. No longitudinal variation in fuel burn or emissions was considered, and only scheduled commercial passenger traffic in the earlier non-Communist world was included.

For this report, the aircraft fleet emissions scenarios utilized with the assessment models have been further developed (see Chapter 3). They now provide a detailed geographic distribution for fuel burn and exhaust emissions (i.e., 1 degree latitude by 1 degree longitude by 1 km altitude). The simulated fleets include military as well as civil aircraft and also consider operations in the former Soviet bloc. Besides including the present scheduled airline subsonic jet fleet, projected future subsonic fleets, and various assumptions for future HSCT fleets, the new scenarios also include estimates for cargo, turboprop, military, charter, and nonscheduled flights.

For all scenarios, fuel burned was estimated along with emissions of nitrogen oxides, hydrocarbons, and carbon monoxide. Estimates were made for relevant subsonic fleets in 1990 and 2015 and for HSCTs in 2015 flying at Mach 1.6, 2.0, or 2.4. Emissions of water vapor and carbon dioxide are estimated directly from the fuel burned. Two versions of the 2015 subsonic emission levels were developed: one of these assumed no HSCTs would fly, while the other assumed that HSCTs would be used to satisfy part of the projected market thereby lowering the projected subsonic growth. For the HSCT emissions of nitrogen oxides, estimates were made for several values of the emission index (EI) for each of the Mach numbers. Nominal emission indices at cruise altitudes of 5 (the HSRP goal) and 15 g NO_x as NO₂ per kg of fuel were calculated. Scenarios for EI of 45 were constructed by linear scaling.

Exhaust Characterization and Wake-Vortex Interaction

The programmatic interface between HSRP technology and atmospheric science figuratively occurs at the exhaust plane of the aircraft engines. Assessment of the potential impact of an HSCT on the stratosphere is dependent upon accurate knowledge of what is emitted from the aircraft, and studies (Prather et al., 1992) show that the products of combustion in the engine exhaust are the primary source of significant reactive chemical species. These studies have determined that perturbations to atmospheric chemistry may occur from NO_x, SO_x, H₂O, and soot constituents of engine exhaust. Traditional consideration of NO_x-driven homogeneous (i.e., gas phase) catalysis of ozone has been supplemented with a recent general concern about the impact of particulate soot and condensable gases (e.g., HNO₃, H₂SO₄, H₂O) on the aerosol content of the stratosphere, and the possible resulting effect on heterogeneous chemistry which also influences ozone chemistry. Although no HSCT engines will have been developed during

the lifetime of this study, plans (see Chapter 5) are being formulated for measurements of the exhaust products from flame-tube and other combustor test rigs. Accurate determination of exhaust NO_x , based on redundant instrumentation, is the highest priority. Efforts to measure soot properties, SO_x speciation, and OH concentrations have also been instituted.

The global atmospheric models that assess the impact of engine emissions simulate the exhaust products with a grid box in which simple dilution occurs with the required amount of air. This assumes that there are no nonlinear, irreversible processes which change the character of the exhaust products, and the exhaust products chemical balance is assumed to be controlled by the conditions in the ambient atmosphere. To test this idea, the program has supported development of a plume and wake-vortex interaction model that couples fluid dynamics, chemical kinetics, and condensation physics. Initial calculations (Zhao and Turco, 1992, Miake-Lye et al., 1993) suggest that binary homogeneous nucleation of small particles could occur rapidly in the plume because of high concentrations of nitric and sulfuric acid. If small particles are rapidly formed, and if the particles do not coagulate with the background aerosol, then the sulfur in the exhaust will produce a larger perturbation to the background sulfate surface area than would be the case for coagulation. The potential importance of this effect is dependent on the amount of the surface area increase and on the role of the sulfate in determining stratospheric chemical balances. Calculations of the range of possible increases in the surface area are being done, and these must be evaluated in the context of the sensitivity of the stratospheric chemical balance to sulfate additions. Evaluation of the sulfate effect on the lower stratosphere is ongoing, as understanding of the chemistry develops (see Chapter 5).

SCIENCE

Background and Issues

Early assessments of the potential impact of stratospheric aircraft were done during the Climatic Impact Assessment Program (CIAP) (Grobecker, et al., 1974) and the following High Altitude Pollution Program (HAPP). CIAP and HAPP concluded that the two primary potential impacts of aviation were on stratospheric ozone and on climate. Exhaust constituents considered included, NO_x , H_2O , sulfur compounds, soot, hydrocarbons, metals, CO, and CO_2 . Based on these results and research since the end of CIAP and HAPP, the AESA investigation has placed its primary focus on the problem of the effects of NO_x and H_2O on ozone. CO, CO_2 , and hydrocarbons have been considered in assessments, but their calculated effects are small, and, therefore, minimal research has been done on them. The problem of sulfur and soot on particle formation has also been considered in the program, but with less emphasis. The effects of changes in particle concentrations and ozone on climate have been deferred until a better understanding of those changes. An initial study to evaluate the potential changes in radiative forcing from aircraft effluents is now under way.

The scientific studies of AESA have been conducted simultaneously with the technology effort. Previous AESA reports (Prather et al., 1992, Stolarski and Wesoky, 1993) have discussed the general program plan and early results. At this midpoint of the program, a number of the major milestones (Figure 1) have been accomplished.

For an HSCT fleet with low NO_x combustors, the predictions of ozone depletion are now small (see Interim Assessment Report, chapter 7). This is mostly because of the realization gained from the observational and laboratory programs that lower stratospheric chemistry is significantly modified by heterogeneous chemical reactions. The AESA program was designed to focus on the impacts of stratospheric aircraft flight identified to be of primary concern. At the same time, the program supports a broad base of research to ensure that all aspects of the problem are evaluated. This broad base provides flexibility, so that the program can respond to changes in the understanding of stratospheric science. Thus, the program started with a focus on

the homogeneous gas-phase chemistry of the lower stratosphere, but has now been refocused to emphasize the heterogeneous aspects of the chemistry.

The importance of heterogeneous chemistry in the lower stratosphere has led to the realization that the effect of aircraft exhaust on the stratospheric particulate surface area may be a more important problem than previously believed. The researchers funded by AESA and by UARP and ACMAP are leading the way in defining these important new foci. This process is strongly supported by the Advisory Panel which has helped select the research proposals to be funded and the directions in which to encourage further investigation by those researchers already funded by the program. As the assessment process has matured, the foci of the program and the related investigations have shifted with the emerging understanding, but the overall scientific issues have remained unchanged. These are:

1. What emissions could occur from high-speed civil transport (HSCT) aircraft?
2. What ozone-related chemical processes are important in today's atmosphere and in a future atmosphere perturbed by HSCT emissions?
3. How consistent are atmospheric observations with the current understanding of the HSCT-related chemistry?
4. What are the predicted atmospheric changes associated with HSCTs?
5. What are the uncertainties in these perturbation predictions?

As explained in a previous section of this chapter, the first issue is being addressed with a detailed evaluation and prediction of worldwide aircraft operations, related fuel consumption, and relevant emissions. Investigations of the other four issues draw from scientific research sponsored by AESA and other programs in three basic areas: laboratory studies, atmospheric observations, and theoretical modeling.

A baseline assessment was reported at the beginning of 1992 (Prather et al., 1992), with two-dimensional global atmospheric models and homogeneous chemistry assumptions serving as the basis for sensitivity studies. The models were relatively unchanged from those being applied at the time to calculate the effects of CFCs (i.e., chlorine) on the atmosphere, and did not yet incorporate heterogeneous reactions on particle surfaces in the stratosphere. Laboratory studies and atmospheric observations, supported by AESA and other programs, later demonstrated the important role of heterogeneous reactions in determining the chemical speciation of NO_x and chlorine compounds, which has profoundly affected the calculated sensitivity of ozone to these pollutants.

Laboratory Studies

Interpretation and understanding of the results of atmospheric observations in terms of numerical models rests on fundamental experiments carried out in the laboratory. Since a majority of the needed information is fundamental to various other areas of atmospheric chemistry, laboratory studies have been an ongoing effort in various programs. A number of basic research programs, including the UARP, have funded researchers doing such chemistry studies, with augmentation from AESA to focus on the questions specific to the evaluation of the effects of stratospheric aircraft; particularly the major impact of heterogeneous reactions on the prediction of HSCT effects.

Results from several laboratories now agree that the reaction of N_2O_5 with H_2O proceeds rapidly on liquid sulfate aerosols and its rate is apparently independent of the composition of the

sulfate particles. The dependence of the ClONO_2 plus H_2O reaction on sulfate particles as a function of the water content of the particles has been determined, and ongoing studies will quantify the effects of water vapor and temperature on sulfate aerosol composition for inclusion in assessment models.

Characterizing the reactions occurring on nitric acid trihydrate (NAT) and water ice surfaces continues. A recently important aspect of this research is the question of the exact conditions required for the formation of frozen NAT particles in the stratosphere. Aircraft exhaust contains NO_x , which will be converted to HNO_3 , and water vapor. Together these can increase the probability of the formation of NAT clouds both inside and outside the polar vortex. Calculation of their impact depends on questions like the degree of supersaturation required for NAT formation and also whether pure NAT will form. Aircraft exhaust also contains compounds that will add to the sulfur loading of the stratosphere. The possible increase in surface area will depend on whether the emitted sulfur is in the form of new or separate small particles or deposited on existing particles to make them larger. AESA laboratory work will be continued (and coordinated with exhaust characterization efforts) to improve knowledge of the properties of aerosols associated with HSCT atmospheric impact (issue 2) and to reduce uncertainties in the related predictions of ozone perturbations (issue 5).

Atmospheric Observations

Because atmospheric observation programs are expensive to run, and because it was perceived that such programs held the key to new discoveries which would modify our understanding of the stratosphere, the AESA program has devoted a large part of its available budget to this aspect of the program. Initial involvement in atmospheric observations was through the second Airborne Arctic Stratospheric Expedition (AASE-II) where AESA augmented the primary support of the UARP. That mission included six 2- to 3-week segments of flights of an instrumented ER-2 aircraft from Bangor, Maine, and Fairbanks, Alaska, which were carried out from October 1991 through March 1992. Measurements from these flights were augmented with others obtained from an instrumented DC-8 aircraft on flights from Moffett Field, California to Stavanger, Norway via Fairbanks, and back to Moffett Field. A result of direct importance to AESA was the finding of chemically perturbed air (e.g., high ClO , low NO) at middle and low latitudes of the northern hemisphere lower stratosphere. These findings were consistent with the idea that the air had been subjected to heterogeneous reactions on the surfaces of stratospheric particles.

Investigators associated with AASE-II have further reported (Fahey et al., 1993) on their observations, combining laboratory and modeling efforts to show how "the reaction of N_2O_5 on sulfate aerosols likely alters the partitioning of the reactive nitrogen reservoir in the lower stratosphere." Measured estimates of the NO_x/NO_y ratio are far lower than predicted by photochemical models that include only gas phase reactions. Inclusion of the sulfate aerosol reaction in the models results in better agreement with observations and indicates a greater sensitivity of ozone to growth in anthropogenic chlorine, but a lessened impact of NO_x . The apparent cause of the lessened NO_x effect has been suggested by laboratory studies which show a large reaction rate for $\text{N}_2\text{O}_5 + \text{H}_2\text{O} \rightarrow 2\text{HNO}_3$, where the HNO_3 reservoir is not directly involved in ozone chemistry, as indicated in Figure 4.

Although it is clear that the presence of heterogeneous chemistry reduces the calculated potential impact of NO_x from stratospheric aircraft on ozone, questions still remain about the relative contributions of reactions on background sulfate aerosols, volcanic sulfate aerosols, and polar stratospheric clouds to midlatitude chemistry. It is now necessary to investigate how widespread the impact of heterogeneous chemistry is as a function of geography and season.

To better understand these effects, more atmospheric observations are being conducted in the Stratospheric Photochemistry, Aerosols and Dynamics Expedition (SPADE). The SPADE measurements will emphasize free radical chemistry over a full diurnal cycle at the northern midlatitudes most important to aviation. Flights of the ER-2 aircraft from Moffett Field, California, will extend the results from AASE-II by addressing the primary question: What are the key chemical processes that potentially affect ozone levels in the part of the stratosphere most strongly influenced by stratospheric aviation? A secondary question is: What will be the distribution of exhaust effluents in the stratosphere?

The SPADE mission uses the same basic payload flown on AASE-II augmented by three new instruments, two of which were developed under the AESA program: 1) an OH/HO₂ instrument developed at Harvard University to measure the key missing radicals, 2) a CO₂ instrument also developed at Harvard, which will provide a measure of the length of time that air has been in the stratosphere, and 3) an ultraviolet/visible spectrometer developed by the Canadian Atmospheric Environment Service, which will provide a measurement of the solar flux available at the aircraft for the dissociation of key molecules. A more detailed description of the plans for SPADE is provided in Chapter 2.

A 1994 field campaign is planned to be conducted in conjunction with the NASA UARP Airborne Southern Hemisphere Ozone Experiment (ASHOE). ASHOE is expected to provide further understanding of basic atmospheric chemistry and dynamics through studies in the Antarctic region. Measurements for Assessing the Effects of Stratospheric Aircraft (MAESA) is an AESA/HSRP-sponsored effort which will support enhanced ER-2 flights between Christchurch, New Zealand, and Moffett Field, with stopovers in Hawaii and Fiji. The combined ASHOE/MAESA mission will provide observations of important chemistry and dynamics in the equatorial regions, as well as in the middle latitudes. The measurements will greatly increase knowledge of seasonal and geographic distribution of the chemical partitioning of stratospheric radicals to allow an improved assessment of the global importance of heterogeneous chemistry and its importance for the evaluation of HSCT perturbations.

An augmented altitude capability for observations will be provided in MAESA by the new Perseus autonomous aircraft (Russell et al., 1991). Along with the UARP, AESA has provided a significant portion of the funding for the development of Perseus. AESA has also funded the development of four new lightweight instruments for Perseus (see Chapter 2 for more details). The current plan is for the first Perseus test flights to be from the NASA Ames-Dryden Flight Research Facility at Edwards Air Force Base, California, and then for deployment at an equatorial base to specifically study tropical dynamics and chemistry. Those measurements are to be coordinated with observations from the ER-2 and the Upper Atmosphere Research Satellite (UARS) and will help to fill the gap between their altitude capabilities.

Modeling

The major advances in understanding from the atmospheric observations and laboratory measurements must be incorporated into a comprehensive model to quantitatively assess the effects of stratospheric aircraft. Together with ACMAP, the AESA program has supported development of a number of research and assessment models.

Research models extend understanding of the best ways to model the stratospheric system. These include simulations that are used to search for better ways to incorporate the essential features of the three-dimensional world into two dimensions (i.e., altitude and latitude). Three-dimensional models are primarily aimed at understanding the detailed nature of the transport of stratospheric pollutants to the troposphere, providing the fundamental advances that are incorporated into the two-dimensional assessment models, often implemented by the same groups.

Models and Measurements Intercomparison

During the CIAP program in the early 1970s and the early evaluations of the fluorocarbon-ozone problem, the basic assessment tool used was a one-dimensional (i.e., altitude) eddy-diffusion model. Limited observations of long-lived tracer species were used to define the transport coefficients, and equally limited observations of important stratospheric radicals were used to test the model. Discrepancies were usually explained as indications of meteorological variability that the simple model could not be expected to represent. Progress in the understanding of the stratosphere has led to a more critical view of models. Now two-dimensional models (i.e., latitude and altitude) are relied on to predict the seasonal and geographic distribution of the zonal mean concentrations of stratospheric species. The database of observations has expanded significantly, allowing comparisons which place a larger degree of constraint on the models.

A major milestone in advancing the understanding and credibility of assessment models was the Models & Measurements (M&M) Workshop (Prather and Remsberg, 1993) conducted in early 1992. This forum provided a foundation for establishing the credibility of stratospheric assessment models and represents a significant extension of previous model intercomparisons. A set of predetermined experiments tested different aspects of the models. In addition, a group of experimenters and data analysts assessed the existing observational database and provided an evaluated set which could be used to further critically test the models.

The M&M Workshop was directed towards two goals: the intercomparison of models on highly constrained problems of prediction and comparison to carefully selected data on the concentrations of stratospheric gases. The modelers were given specified inputs for the key tracers and absorbing species and asked to calculate several fundamental parameters such as chemical partitioning and rates of photodissociation. The model-to-model agreement obtained was far better than in previous model intercomparisons. Although some disagreements still exist, there is now a core set of models that appear to be calculating nearly the same impacts under the same set of assumptions. These models are used to make the basic assessment of the impact of aircraft, augmented by offline calculations of effects not incorporated into the 2-D models as well as by 3-D model evaluations of the accuracy of the transport calculations.

The models being used for assessments in the AESA program began as gas-phase 2-D photochemical models of the troposphere-stratosphere system. They have been improved through the incorporation of updated gas-phase reaction rate coefficients, improvements in their dynamical representation, and the inclusion of parameterized rates for heterogeneous processes on the surfaces of aerosols. The M&M Workshop and the research efforts of the modelers have identified several areas of possible improvements for future assessment models. These include:

- 1) *Parameterization of heterogeneous chemistry* - Present models include reactions on assumed surface areas, which are consistent with the laboratory measurements of sticking or reaction coefficients. Questions concerning the possibility of increased aerosol surface area or NAT formation due to exhaust products (e.g., SO₂, H₂O, NO_x converted to HNO₃) will require a more detailed examination of the conditions under which particles are formed. This will require continued laboratory studies and the incorporation of aerosol formation processes in assessment models.
- 2) *Vortex and subtropical jet barriers* - Aircraft data have shown sharp gradients of tracers such as N₂O at the boundary of the winter polar vortex in both hemispheres. These gradients are indicative of the existence of barriers to transport which limit the exchange of air between the vortex and the surrounding midlatitudes. These barriers, and the degree of containment or leakiness of polar-processed air, may be crucial to the accurate evaluation of the effects of stratospheric aircraft. Present assessment models show no

significant barrier and thus mix air rapidly between the two regions. Promising results were shown by Garcia at the M&M Workshop (Prather and Remsberg, 1993) indicating that a simple parameterization of the waves in the longitudinal direction effectively isolated the vortex and led to predictions of sharp gradients. Some practical method must be found to incorporate this vortex isolation into the assessment models. A further problem is the apparent (i.e., weaker) barrier to transport between the tropics and midlatitudes. This shows up in the analysis of data from ER-2 measurements and, dramatically, in the SAGE observations of the aerosol cloud from Mount Pinatubo.

- 3) *Synoptic-scale processes and stratosphere-troposphere exchange* - Although some overall constraints can be put on stratosphere-troposphere exchange from the slopes of tracer isolines (see Chapter 4 by Plumb in Stolarski and Wesoky, 1993), aircraft exhaust will be injected in narrow areas near the tropopause. Its lifetime in the stratosphere will often be determined by the details of the synoptic-scale processes occurring in the region near the injection. This requires 3-D studies that are closely keyed to observations. It is not now clear how the 2-D assessment models can be changed to accurately include these processes, but 3-D simulation results will probably be used in some way to improve the existing dynamics in the 2-D models.

Current Assessment

The present assessment uses 2-D models as described in the M&M Workshop Report. In many cases, these models include improvements based on results from that workshop. Detailed predictions from the current assessment models are presented and discussed in Chapter 4 and summarized in Table 3. A range of aircraft operational scenarios has been examined, and the predictions indicate the possibility of relatively small effects of HSCT emissions on atmospheric ozone. However, the results are also clearly dependent on the heterogeneous chemistry assumptions, which require further study. There is also an expected effect of background chlorine and its interaction with emitted NO_x .

As previously noted (Stolarski and Wesoky, 1993), much more effort will be required to confirm and interpret the AASE-II observations regarding sulfate aerosol chemistry over the full operating range of possible future HSCT aircraft. Similarly, the heterogeneous reactions which form the polar stratospheric clouds associated with the Antarctic ozone hole (WMO, 1992) require further study because additional NO_x from aircraft emissions may cause an increase in the geographic extent of that phenomenon. The formation of NAT in aircraft corridors, particularly at near polar latitudes, may trigger ozone depletion through enhanced chlorine chemistry.

Final Assessment Plans

The AESA program plans to use what might be called the next generation of models for the final program assessment in 1995. Between now and that assessment in 1995, it is expected that models will incorporate better representations of some of the processes described above. The assessment models should benefit from the knowledge gained from both laboratory and observational data.

Observations from SPADE and MAESA will address many of the remaining important questions. Additional information from exhaust characterization and wake-vortex studies, continuing laboratory investigations, and improved global models should all contribute to an improved assessment capability by 1995. Other capabilities which have been added to the overall AESA effort, and should even further enhance the quality of the final AESA assessment planned for 1995, include climate modeling and uncertainty analysis of the global simulations.

POLICY

Policy (Figure 1) is the third element of the plan to define acceptable levels of HSCT emissions. Although the establishment of standards for regulatory policy is not a specific NASA responsibility, it is assumed that the scientific and technical data derived from the HSRP will provide significant assistance to regulatory authorities. Therefore, the program plan has attempted to coordinate research with ongoing United Nations activities, which recommend standards for global environmental acceptability of certain atmospheric pollutants, as well as with the national and international organizations that establish aircraft certification standards.

The International Civil Aviation Organization (ICAO) is the U.N. body that recommends standards for the worldwide aviation industry. ICAO, in turn, has established the Committee on Aviation Environmental Protection (CAEP) "to undertake specific studies, as approved by the Council, related to the control of aircraft noise and gaseous emissions from aircraft engines." CAEP is to take into account:

- Reasonableness and environmental benefit of certification schemes.
- Developments in other fields (e.g., emissions control through operational procedures).
- International and national programs of relevant research.

In its first work program, CAEP proposed to recommend "appropriate provisions for the control of emissions from aircraft in the vicinity of airports" and to monitor "research into pollution of the atmosphere above 900 metres and propose appropriate action if it appears that aircraft are significant contributors to this pollution." Currently, aircraft emissions standards only exist for the landing-takeoff cycle (i.e., the airport vicinity below 900 meters altitude) (ICAO, 1981), but the following recommendation was included in the report of the second meeting of CAEP in December 1991:

"It was generally agreed that the main aim of this part of the future work programme was to minimize or, if necessary, decrease the adverse impacts of aircraft emissions on the environment around airports, on the ozone layer, and on global climate change. In particular, this work should address the possibility of increasing the stringency of the gaseous emissions requirements for subsonic aircraft and establishing standards for supersonic aircraft, when the environmental need has been accepted by an international scientific consensus (e.g. by UNEP/WMO), and is technologically feasible and economically reasonable."

A working group was established by CAEP to pursue this recommendation, with the following instruction in its governing Terms of Reference:

"The working group should review the environmental needs for reducing aircraft emissions. The working group should assess the results of the further development of modelling of the atmosphere, in order to improve the prediction of the environmental effects of aircraft emissions. The assessment should include, but not be limited to, the results of the research sponsored by ECAC, EC, the NASA High-Speed Research Program, and UNEP/WMO."

It was recommended at the second meeting of CAEP that the third meeting occur as early as late-1994 where standards for aircraft cruise emissions might first be considered.

Results of the AESA studies have already been included in a previous assessment by UNEP/WMO (WMO, 1992) where it was recommended that future research should include:

- Stratosphere-troposphere exchange.
- Ozone budget in the lower stratosphere.
- Plume dispersion and plume chemistry.
- Effects of sulfur and particulates.
- Effects of polar stratospheric clouds and coupling to ozone chemistry.

Ongoing results of the AESA studies are to be included in future UNEP/WMO scientific assessment reports, and specifically are to serve as a primary source for the planned "Scientific Assessment of Ozone Depletion: 1994," which is to be submitted to the Montreal Protocol Parties in 1995 (D. L. Albritton, personal communication, 1992). These results are to be coordinated with other similar research efforts being conducted throughout the world. In particular, the European Community is now sponsoring a number of aircraft-focused investigations with possibly the most relevant being the 1992 initiated AERONOX (U. Schumann, personal communication, 1992) program for "studies concerning the impact of subsonic air traffic at cruising altitude on the atmosphere." Therefore the policy processes implied in Figure 1 for achieving international emissions standards, and possible national regulations are well under way.

CONCLUSION

The NASA High-Speed Research Program is sponsoring a comprehensive study of the scientific issues associated with the Atmospheric Effects of Stratospheric Aircraft. Included are significant projects to characterize engine exhaust and interactions with the aircraft vortex-wake, investigations of relevant chemistry in the laboratory, observations of related processes in the atmosphere, and development of accurate computer models of the global processes. The scientific studies are coordinated with low NO_x combustor research and technology and the projection of growth in airline markets. Results of the scientific studies are also being used by international organizations that assess environmental effects of atmospheric pollutants and establish standards for aircraft certification.

A range of aircraft operational scenarios has been examined with 2-D global models, and the predictions indicate the possibility of relatively small effects of proposed low NO_x combustor emissions on atmospheric ozone. These models have relied on limited in situ observations of heterogeneous chemical processes in the upper atmosphere which have been shown to be robust in laboratory studies. However, the history of ozone and climate change science and policy has been complex and contentious (Benedick, 1991, Roan, 1990). Therefore, to ensure that appropriate simulations serve as the basis for future assessments, much work remains to confirm whether the observed chemistry is representative of all seasons and geographic locations and that the assessment models are accurately simulating all relevant aspects of atmospheric chemistry and dynamics as well as the proposed aircraft emissions and operations.

ACKNOWLEDGMENTS

We gratefully acknowledge the contributions from the Lewis Research Center Combustion Technology Branch and the work of the scientists and engineers who authored and reviewed this report. The principal authors and contributors are listed with each chapter, and the reviewers are given in the Appendix. The tireless efforts of Ms. Cindy Alami, Ms. Nancy Brown, Ms. Rose Kendall, Ms. Kathy Wolfe, and other staff members of the ARC Professional Services Group were essential in the preparation and editing of this document.

Table 1. AESA Principal Investigators

Theoretical Studies*2-D Global Chemical Models and Stratospheric Ozone Assessment*

Name	Affiliation
G. P. Brasseur	NCAR
D. B. Considine	NASA/Goddard Space Flight Center
V. Dosov	Central Aerological Obs., Russia
A. R. Douglass	NASA/Goddard Space Flight Center
R. S. Harwood	University of Edinburgh, United Kingdom
I. S. A. Isaksen	University of Oslo, Norway
M. K. W. Ko	AER, Inc.
M. J. Prather	University of California, Irvine
J. A. Pyle	University of Cambridge, United Kingdom
D. H. Rind	Goddard Institute for Space Studies
J. M. Rodriguez	AER, Inc.
M. R. Schoeberl	NASA/Goddard Space Flight Center
R. K. Seals	NASA/Langley Research Center
R. L. Shia	AER, Inc.
O. B. Toon	NASA/Ames Research Center
R. P. Turco	University of California, Los Angeles
G. Visconti	Universita' degli Studi L'Aquila, Italy
D. J. Wuebbles	Lawrence Livermore National Laboratory

3-D Chemical Transport Models and Longitudinal Asymmetry

Name	Affiliation
G. P. Brasseur	NCAR
A. R. Douglass	NASA/Goddard Space Flight Center
R. A. Plumb	Massachusetts Institute of Technology
R. B. Rood	NASA/Goddard Space Flight Center
H. R. Schneider	AER, Inc.

Emissions, Plume Chemistry, and Other Modeling

Name	Affiliation
A. J. Bilanin	Continuum Dynamics, Inc.
T. J. Dunkerton	NorthWest Research Associates, Inc.
D. E. Hagen	University of Missouri-Rolla
V. U. Khattatov	Central Aerological Obs., Russia
C. E. Kolb	Aerodyne Research, Inc.
R. C. Miake-Lye	Aerodyne Research, Inc.
O. B. Toon	NASA/Ames Research Center
K. K. Tung	University of Washington
R. P. Turco	University of California, Los Angeles
G. K. Yue	NASA/Langley Research Center

Laboratory and Theoretical Studies of Chemical Mechanisms

Name	Affiliation
W. H. Brune	Pennsylvania State University
K. L. Carleton	Physical Sciences, Inc.
D. R. Crosley	SRI International
R. R. Friedl	NASA/Jet Propulsion Laboratory
C. E. Kolb	Aerodyne Research, Inc.
M.-T. Leu	NASA/Jet Propulsion Laboratory
M. J. Molina	Massachusetts Institute of Technology
K. R. Ryan	CSIRO, Australia
M. A. Tolbert	University of Colorado
D. R. Worsnop	Aerodyne Research, Inc.

Table 1. AESA Principal Investigators

Atmospheric Observations and Field Experiments

Name	Affiliation
J. G. Anderson	Harvard University
D. Baumgardner	NCAR
D. R. Blake	University of California, Irvine
K. A. Boering	Harvard University
W. H. Brune	Pennsylvania State University
K. R. Chan	NASA/Ames Research Center
J. E. Dye	NCAR
J. W. Elkins	NOAA Environmental Research Lab
D. W. Fahey	NOAA Aeronomy Lab
G. V. Ferry	NASA/Ames Research Center
P. Hamill	San Jose State University
S. Hipskind	NASA/Ames Research Center
M. H. Hitchman	University of Wisconsin, Madison
K. Kelly	NOAA Aeronomy Lab
J. S. Langford	Aurora Flight Sciences Corp.
M. Loewenstein	NASA/Ames Research Center
D. M. Murphy	NOAA Aeronomy Lab
P. A. Newman	NASA/Goddard Space Flight Center
S. J. Oltmans	NOAA Environmental Research Lab
L. Pfister	NASA/Ames Research Center
M. J. Prather	University of California, Irvine
M. H. Proffitt	NOAA Aeronomy Lab
R. F. Pueschel	NASA/Ames Research Center
B. A. Ridley	NCAR
J. M. Rodriguez	AER, Inc.
F. S. Rowland	University of California, Irvine
G. W. Sachse	NASA/Langley Research Center
P. J. Sheridan	NOAA Environmental Research Lab
A. F. Tuck	NOAA Aeronomy Lab
G. Visconti	Universita' degli Studi L'Aquila, Italy
C. R. Webster	NASA/Jet Propulsion Laboratory
S. Wegener	NASA/Ames Research Center
P. D. Whitefield	University of Missouri, Rolla
J. C. Wilson	University of Denver
S. C. Wofsy	Harvard University

Table 2. AESA Scientific Advisory Panel**Scientific Panel Members**

Name	Affiliation
William H. Brune	Pennsylvania State University
Frederick L. Dryer	Princeton University
Dieter H. Ehhalt	Institute for Atmospheric Chemistry, FRG
Neil Harris	Cambridge University, UK
James R. Holton	University of Washington
Harold S. Johnston	University of California, Berkeley
Nicole Louisnard	Office National d'Etudes et Recherches Aerospatiales, France
Jerry D. Mahlman	NOAA/Geophysical Fluid Dynamics Laboratory
Mario J. Molina	Massachusetts Institute of Technology
Michael Oppenheimer	Environmental Defense Fund
Alan Plumb	Massachusetts Institute of Technology
Michael J. Prather	University of California, Irvine
A. R. Ravishankara	NOAA/Environmental Research Laboratory
Arthur L. Schmeltekopf	NOAA, Retired
Adrian Tuck	NOAA/Aeronomy Laboratory
Steven C. Wofsy	Harvard University
Donald J. Wuebbles	Lawrence Livermore National Laboratory
Robert T. Watson	NASA Headquarters, Chairman
Richard S. Stolarski	NASA Goddard Space Flight Center, Program Scientist
Howard L. Wesoky	NASA Headquarters, Program Manager

Ex-Officio Members

Name	Affiliation
Stephen Seidel	Environmental Protection Agency
Nicholas P. Krull	Federal Aviation Administration
Estelle P. Condon	NASA/Ames Research Center
James J. Margitan	NASA/Jet Propulsion Laboratory
William L. Grose	NASA/Langley Research Center
Richard W. Niedzwiecki	NASA/Lewis Research Center
Jack A. Kaye	NASA Headquarters
Michael J. Kurylo	NIST/NASA Headquarters
Robert E. Anderson	NASA Headquarters
Joel M. Levy	NOAA Headquarters
Jarvis Moyers	National Science Foundation

Observers

Name	Affiliation
Willard J. Dodds	General Electric Aircraft Engines
Richard W. Hines	Pratt & Whitney
Michael L. Henderson	Boeing Commercial Airplanes
Alan K. Mortlock	McDonnell Douglas
Richard L. Kurkowski	NASA/Ames Research Center
Allen H. Whitehead	NASA/Langley Research Center
Edwin J. Graber	NASA/Lewis Research Center
Thomas A. Jackson	Wright-Patterson Air Force Base

Table 3. Summary of Current Assessment Model Predictions

SCENARIOS		
HSCT FLEET MACH NO.	HSCT EMISSIONS INDEX gm equiv NO ₂ /kg fuel	BACKGROUND CI (ppbv)
1.6	5	3.7
1.6	15	3.7
2.4	5	3.7
2.4	15	3.7
2.4	15	2.0
2.4	45	3.7

HSCT FLEET MACH NO.	ASSESSMENT MODEL*					
	COLUMN OZONE CHANGE (%), 40 TO 50 DEG N LATITUDE					
	AER	CAMED	GSFC	LLNL	NCAR	OSLO
1.6	-0.04	0.69	-0.11	-0.22	-0.01	0.04
1.6	-0.02	0.48	-0.07	-0.57	-0.60	0.15
2.4	-0.47	0.38	-0.29	-0.58	-0.26	-0.47
2.4	-1.2	-0.45	-0.86	-2.1	-1.8	-1.3
2.4	-2.0	-1.1	-1.3	-2.7	-2.3	-0.42
2.4	-5.5	-2.8	-4.1	-8.3	-6.9	-3.5

*See Chapter 4 for definition of models and other details.

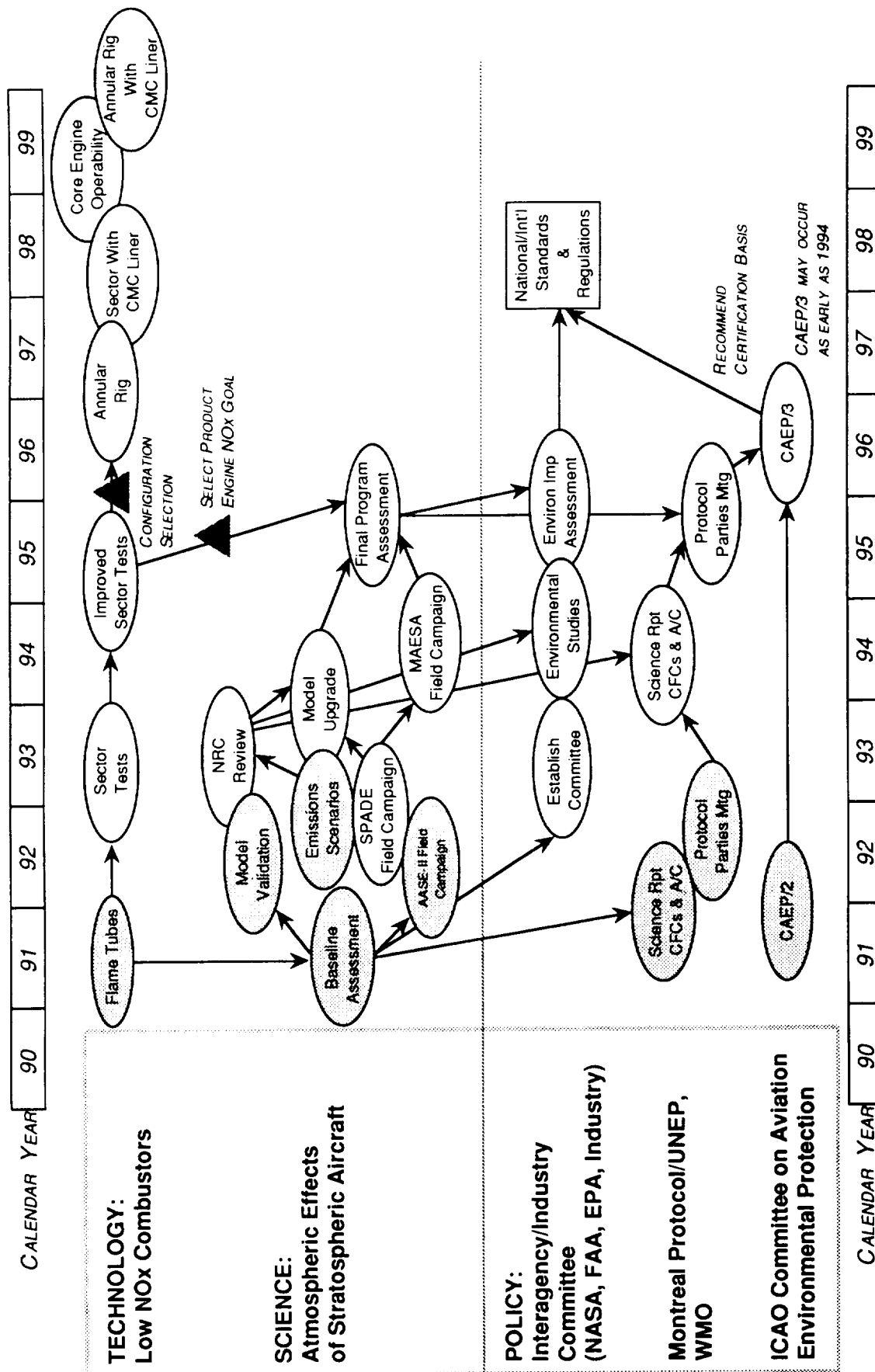
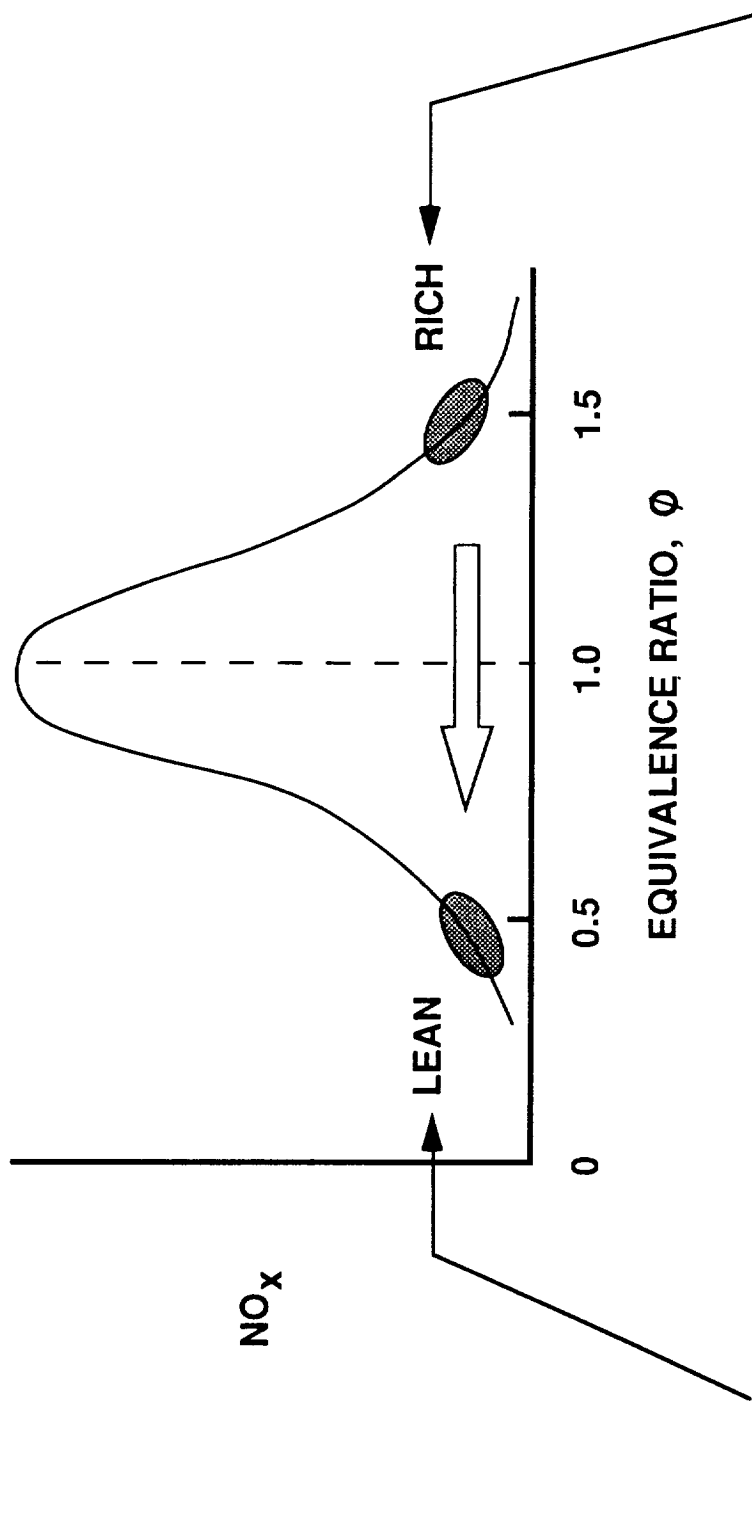


Figure 1. High-Speed Research Program plan for establishing environmental standards for HSCT aircraft certification.



LEAN PREMIXED PREVAPORIZED

RICH BURN/QUICK QUENCH/LEAN BURN

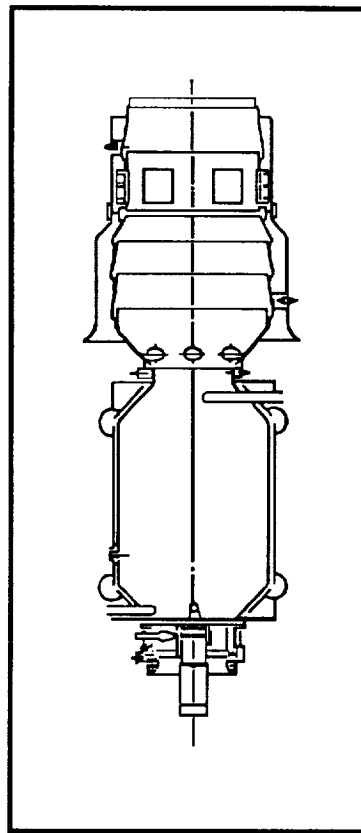
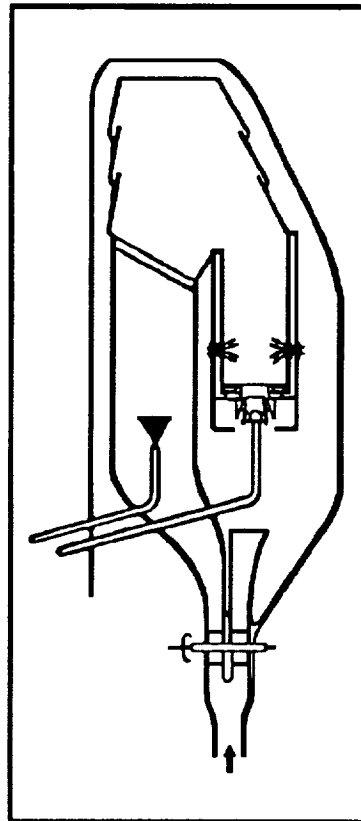


Figure 2. Low NO_x combustor concepts where equivalence ratio of 1.0 corresponds to stoichiometric conditions.

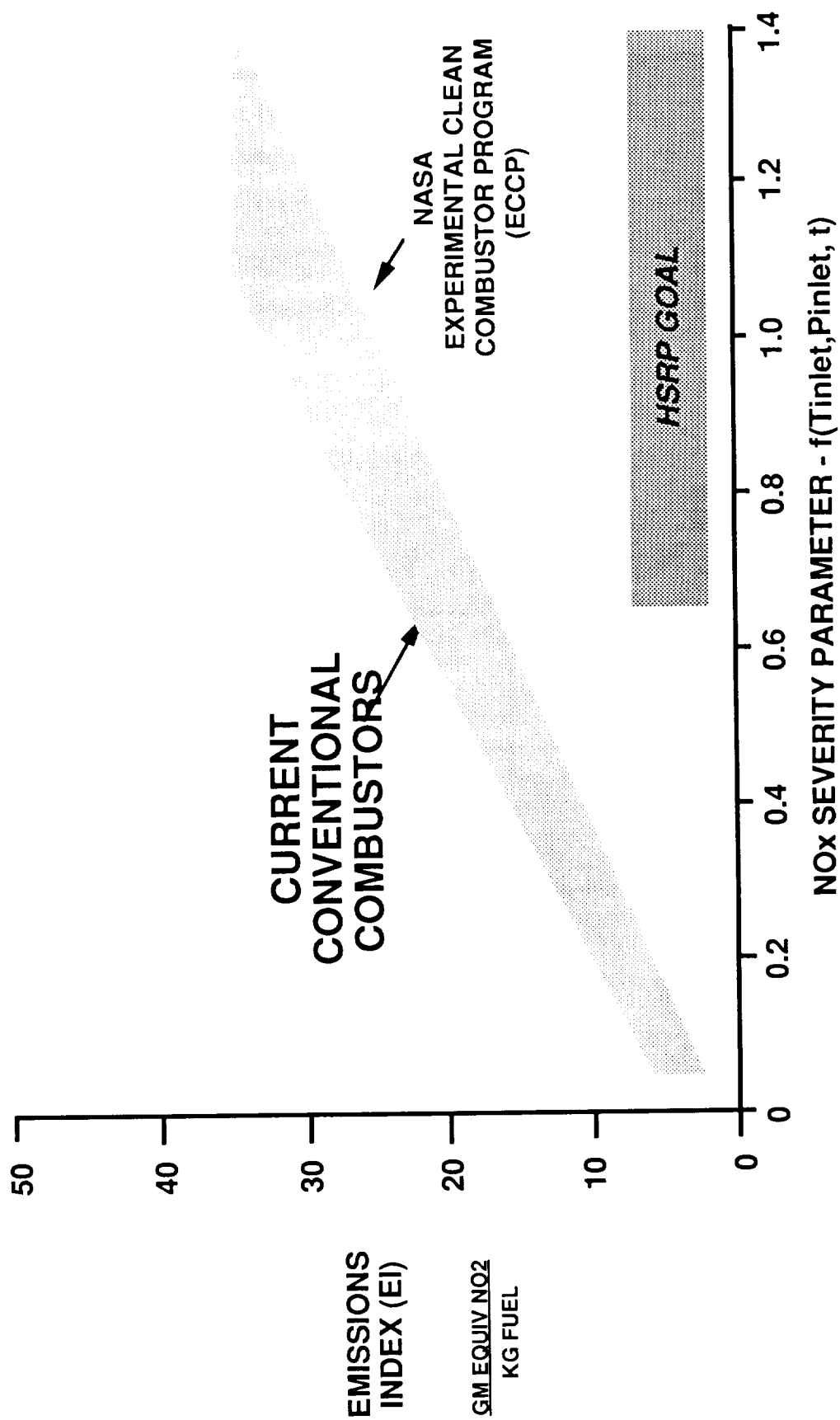


Figure 3. High-Speed Research Program low NO_x emissions goal, where T_{inlet} and P_{inlet} are combustor inlet temperature and pressure and t is the fuel residence time.

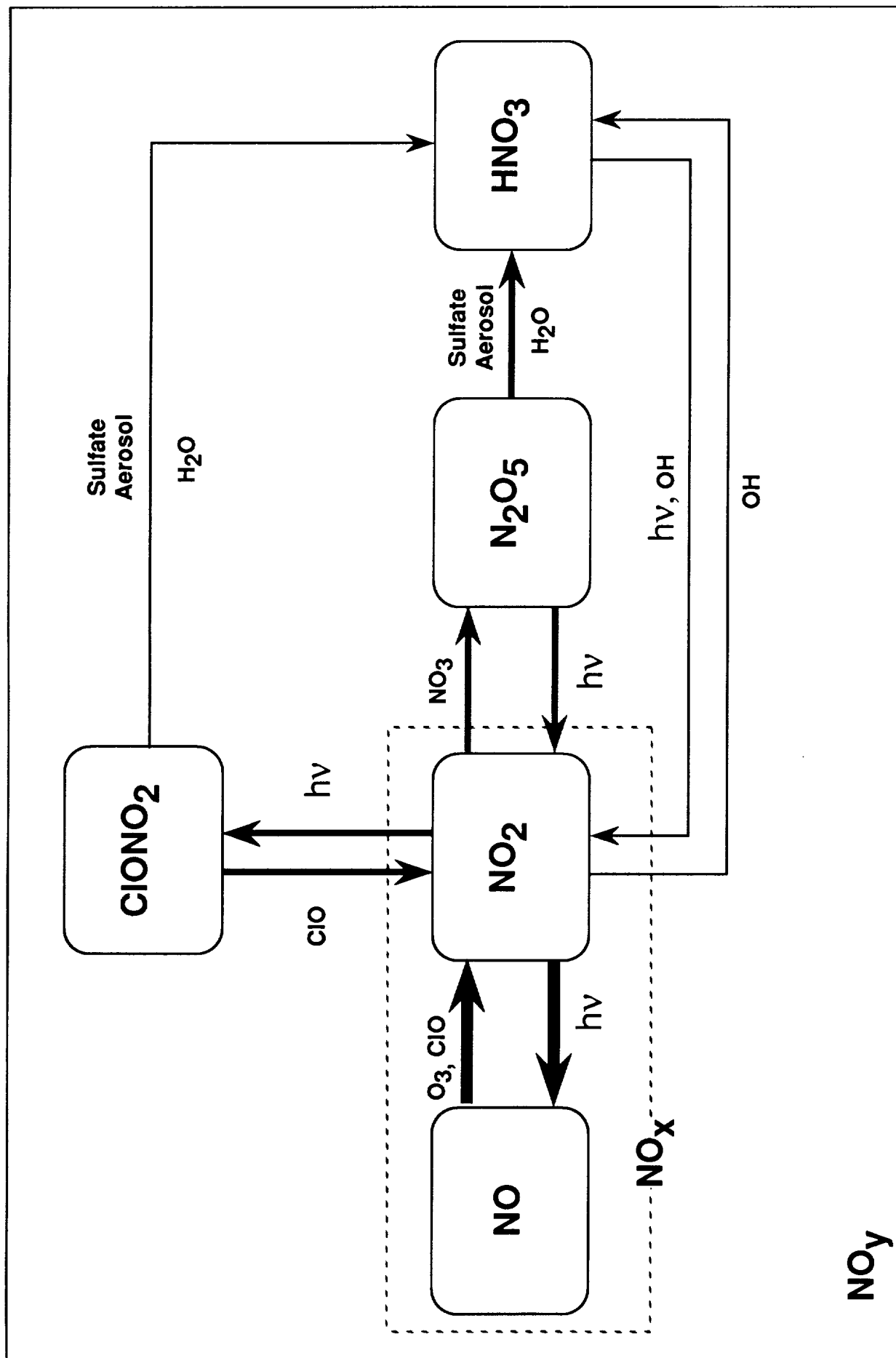


Figure 4. Diagram denoting the processes that determine the NO_x/NO_y ratio, where the thickness of the arrows is nominally proportional to the conversion rate (Fahey et al., 1993; reprinted with permission from *Nature*, 363, 509-514, 1993, Macmillan Magazine Limited).

REFERENCES

- Aviation Week & Space Technology*, "GE, Pratt Studying Combustor, Nozzle Materials for HSCT," p. 66, August 31, 1992.
- Benedick, R. E., *Ozone Diplomacy*, Harvard University Press, Cambridge, MA, 1991.
- Fahey, D. W. et al., In situ measurements constraining the role of reactive nitrogen and sulphate aerosols in mid-latitude ozone depletion, *Nature*, in press, 1993.
- Grobecker, A. J. et al., Climatic Impact Assessment Program (CIAP), Report of Findings: The Effects of Stratospheric Pollution by Aircraft, DOT-TST-75-50, U.S. Department of Transportation, Washington, D.C., 1974.
- International Civil Aviation Organization (ICAO), *International Standards and Recommended Practices, Environmental Protection*, Annex 16, Volume II, Aircraft Engine Emissions, First Edition, ICAO, 1981.
- Miake-Lye, R. C., R. C. Brown, M. Martinez-Sanchez, C. E. Kolb, Plume and Wake Dynamics, Mixing, and Chemistry, *Proceedings of the 1993 JANNAF Exhaust Plume Technology Subcommittee Meeting*, Kirtland AFB, NM, Chemical Propulsion Information Agency, in press, 1993.
- Prather, M. J., et al., *The Atmospheric Effects of Stratospheric Aircraft: A First Program Report*, NASA Reference Publication 1272, NASA, Washington, D.C., 1992.
- Prather, M. J., and E. E. Remsberg, Eds., *The Atmospheric Effects of Stratospheric Aircraft: Report of the 1992 Models and Measurements Workshop*, NASA Reference Publication 1292, NASA, Washington, D.C., 1993.
- Roan, S. L., *Ozone Crisis*, John Wiley & Sons, New York, 1990.
- Rosen, R., and L. J. Williams, The Rebirth of Supersonic Transport, *Technology Review*, Edited at the Massachusetts Institute of Technology, February/March 1993.
- Russell, P. et al., *Advanced Aircraft for Atmospheric Research*, AIAA 91, 3162, 1991.
- Shaw, R. J., Propulsion Challenges for a 21st Century Economically Viable, Environmentally Compatible High-Speed Civil Transport, Tenth International Symposium on Air Breathing Engines, ISABE 91, 7008, 1991.
- Stolarski, R. S., and H. L. Wesoky, Eds., *The Atmospheric Effects of Stratospheric Aircraft: A Second Program Report*, NASA Reference Publication 1293, NASA, Washington, D.C., 1993.
- Wesoky, H. L., and Prather, M. J., Atmospheric Effects of Stratospheric Aircraft: A Status Report From NASA's High-Speed Research Program, Tenth International Symposium on Air Breathing Engines, ISABE 91, 7020, 1991.
- WMO, (World Meteorological Organization), *Scientific Assessment of Ozone Depletion: 1991*, Global Ozone Research and Monitoring Project, Report No. 25, WMO, Geneva, 1992.
- Zhao, J., and R. P. Turco, Particle Nucleation in the Wake of a Jet Aircraft in Stratospheric Flight, *J. Aerosol Sci.*, submitted for publication, 1992.

Chapter 2

Plans for Atmospheric Observations

William H. Brune
Department of Meteorology
Pennsylvania State University
University Park, PA

Contributors

James G. Anderson
Steven C. Wofsy
Harvard University

James L. Barrilleaux
Max Loewenstein
Leonhard Pfister
Owen B. Toon
Ames Research Center
National Aeronautics and Space
Administration

Anne R. Douglass
Paul A. Newman
Richard B. Rood
Richard S. Stolarski
Goddard Space Flight Center
National Aeronautics and Space
Administration

David W. Fahey
Daniel M. Murphy
Alex Weaver
Aeronomy Laboratory
National Oceanic and Atmospheric
Administration

James R. Holton
University of Washington

Harold S. Johnston
University of California, Berkeley

Malcolm K. W. Ko
Jose M. Rodriguez
Nien D. Sze
Atmospheric and Environmental Research,
Inc.

James J. Margitan
Jet Propulsion Laboratory

R. Alan Plumb
Massachusetts Institute of Technology

Michael J. Prather
Darrell W. Toohey
University of California, Irvine

Ellis E. Remsberg
Langley Research Center
National Aeronautics and Space
Administration

Arthur L. Schmeltkopf
Retired, NOAA Aeronomy Laboratory

Douglas R. Worsnop
Aerodyne Research, Inc.

INTRODUCTION

To understand how high-speed civil transports might affect the stratosphere, particularly stratospheric ozone, we must first build an understanding of stratospheric photochemistry and dynamics that can be used to predict what will happen. Simply put, we need to know where aircraft exhaust will go and what photochemical transformations will occur. Such an understanding requires a combination of assessment and process models, laboratory experiments, and atmospheric measurements.

The Stratospheric Photochemistry, Aerosols and Dynamics Experiment (SPADE) and Measurements for Assessing the Effects of Stratospheric Aircraft (MAESA) will yield observations of reactive and long-lived trace gases and their relationships. These observations can contribute to the assessment of the effects of stratospheric aircraft in two ways:

- They improve our understanding and computer simulations of stratospheric processes.
- They help establish the credibility of the atmospheric models that will be used to assess the effects of stratospheric aircraft on stratospheric ozone and climate.

The quality of our assessment—the level of the uncertainties that must be part of any quantitative assessment of future aircraft effects that we report to regulators, legislators, and decision-makers—depends critically on how well we are able to measure and understand the current atmosphere.

We already have a number of existing aircraft measurements, particularly information from Stratosphere-Troposphere Exchange Program (STEP), the Airborne Arctic Stratospheric Expedition II (AASE II), and various test flights. To these, we will add observations from SPADE in 1992 and 1993, and from the Airborne Southern Hemisphere Experiment (ASHOE) and MAESA programs in 1994. In addition to aircraft observations are the existing and future observations from instruments on the UARS satellite, which provide global coverage but with poorer spatial resolution and a higher minimum altitude than aircraft, from instruments on large helium-filled balloons, and from ground-based instruments. Our goal and our challenge is to combine these measurements with those to be taken from aircraft in 1994 to provide the essential, basic knowledge of stratospheric processes for the assessment of the atmospheric effects of stratospheric aircraft (Figure 1).

SPADE is being conducted with the ER-2 aircraft from NASA Ames Research Center at Moffett Field, California. The experiment has two segments: one already completed in October and November of 1992; another in April-May of 1993. Significant advances in instrumentation since the AASE II in 1991-1992 will produce significant advances in the scientific observations in the lower stratosphere at middle latitudes.

The MAESA experiment will use flights of opportunity of the ER-2 that occur for ASHOE, both the test flights and the transit flights, combined with flights of the remotely-piloted Perseus A aircraft, and perhaps helium-filled balloons. The number and position of the flights are constrained by the requirements of ASHOE, the capabilities of the instrument platforms, and the duration of the HSRP.

SPADE and MAESA will contribute significant new information to our understanding of the stratosphere for at least five reasons.

- Studies will be made of the diurnal variation of reactive trace gases in nitrogen, hydrogen, chlorine, and bromine chemical families.

- Needed measurements will be made where few have been made before—in the lower stratosphere, especially at latitudes between 40°N and 40°S.
- Measurements will be made over a range of seasons, from February to October, and in months when few measurements have been made—in the summer months of the northern hemisphere.
- New and improved measurement capabilities for reactive and reservoir trace gases, tracers, and aerosols have been developed—each flight will provide unique observations that can be obtained no other way.
- A new remotely piloted platform, Perseus A, once operational, should allow controlled flights to higher altitudes extending upward a subset of these unique observations above ER-2 altitudes.

ASHOE and MAESA are tightly linked, complementary experiments. The goals of ASHOE are to understand the stratospheric processes of the polar and middle latitudes; their effects on the partitioning of the nitrogen, hydrogen, chlorine, and bromine reservoir and reactive species; and the evolution of the Antarctic polar vortex (Tuck, 1992). The goals of SPADE and MAESA are to understand stratospheric processes that will be the most influenced by HSCT effluents and to observe regions and seasons of the stratosphere that are currently severely undersampled. Thus, SPADE and MAESA are focused on the middle to low latitudes. We recognize, however, that no one region of the stratosphere operates in isolation from the others, and that we need to consider all of these observations for the Assessment of the Effects of Stratospheric Aircraft (AESA).

These proposed science objectives and plans for MAESA are the product of many comments by the contributors to this chapter. However, neither the objectives nor the plans are immutable. We expect that some of the issues outlined below will become better understood and that new issues will arise by 1994. This document is intended to continue these discussions.

SCIENTIFIC ISSUES THAT ARE IMPORTANT FOR AESA

The observations during SPADE and MAESA can contribute to the understanding of several issues important for the AESA. Particularly important is the effect of heterogeneous chemistry on the roles of reactive nitrogen, hydrogen, chlorine, and bromine in the control of ozone, and way that HSCTs might alter that effect. Also important is the transport of trace gases both among the polar, middle latitude, and tropical regions of the stratosphere, and between the stratosphere and troposphere. These two issues hold the most uncertainty for AESA.

An important tool that has been technologically practical only in the last decade is the simultaneous observations of several reactive and long-lived species. Recent observations have shown that long-lived chemical species observed in the lower stratosphere at middle latitudes have simple relationships with each other (Kelly et al., 1989; Fahey et al., 1990). Thus, these relationships provide a powerful method to extend measurements from one region to a much larger scale, to test some chemical transformations, and to assimilate observations from different platforms into an integrated picture of stratospheric chemical and dynamical processes. Also, these simple relationships have confirmed the view that rapid, quasi-horizontal transport occurs in the middle latitudes.

In this section, we consider some questions important for AESA that the observations of SPADE and MAESA can help to answer. Questions will continue to be raised and resolved during the next year as more information becomes available from UARS, SPADE, and the analyses of older observations. The instrumentation for MAESA/ASHOE is best for resolving photochemical issues, and we give photochemical issues our highest priority. Studies of the most important

issues in stratospheric transport are difficult with these measurements and they have lower priority than the photochemical studies. Nonetheless, the aircraft observations most relevant to transport may be an important part of the overall assessment of this critical issue.

Photochemistry and Aerosols

- How do the abundances of chemical species, particularly NO, NO₂, HNO₃, NO_y, ClO, HCl, BrO, OH, HO₂, and their ratios vary from 40°N to 70°S latitude in the lower stratosphere? How do they vary over a range of altitudes and solar zenith angles? How do they vary from late spring to mid-summer to late fall? Does the budget of reactive nitrogen balance? Do the observed ratios of reactive species agree with those calculated for photochemical steady state?
- How do the abundances of these same chemical species vary as a function of aerosol loading of the lower stratosphere? In particular, we know that the partitioning of chemical species in the nitrogen, chlorine, and hydrogen families changed with aerosol loading from the Mt. Pinatubo eruption. How will they change as the aerosol loading slowly decreases over the next few years?
- At what rates do the reactive species in the nitrogen, hydrogen, chlorine, and bromine chemical families catalytically destroy ozone at latitudes from 40°N to 70°S in the lower stratosphere during late spring, mid-summer, and late fall?
- Do the characteristics of sulfate aerosols vary with temperature in a way that is consistent with ideas of liquid aerosol growth? Can this observed relationship be used to determine if the aerosols are liquid or solid?

Transport of Trace Species

- How do the abundances and correlations of tracer species, such as N₂O, CH₄, O₃, H₂O, CO₂, condensation nuclei, aerosols, and NO_y, vary between the middle latitudes of both hemispheres and the tropics? How do they vary in different seasons with different temperature characteristics?
- Can relatively undiluted air be found within a few kilometers above the tropopause in the tropics? In other words, is tropical transport dominated by upwelling, or does significant mixing occur along surfaces, as in the middle latitudes?
- Do these measurements indicate restricted exchange between the tropics and the middle latitudes? How do such restrictions affect the photochemistry of the tropics and the middle latitudes?
- What is the character of the exchange of trace gases between the stratosphere and troposphere? Can we improve our understanding by measuring the abundances and relationships among trace gases?

Other Scientific Issues to Which MAESA Might Contribute

A number of other issues are important for the assessment of the atmospheric effects of stratospheric aircraft. However, the platforms, instruments, locations, and timing of MAESA may limit its contribution to our understanding of these issues. We are aware of these issues and will take advantage of opportunities to combine measurements from MAESA with those from other sources to address them.

- Does heterogeneous chemistry occur on the tropical ice clouds that form in the western Pacific near the tropopause? Can it affect the photochemistry of either the tropics or the middle latitudes?
- Does air from middle latitudes, rich in NO_y and H_2O , pass through the cold regions on the margins of the tropics? Can subtropical stratospheric clouds (SSCs) with a composition similar to polar stratospheric clouds (PSCs) form. Does significant heterogeneous chemistry occur?
- In the tropics, will the tracer abundances and correlations differ during the easterly and westerly phases of the Quasi-Biennial Oscillation (QBO)? Can this information be reconciled with satellite observations of volcanic aerosol transport out of the tropics?

INSTRUMENTATION AND PLATFORMS FOR SPADE AND MAESA

ER-2 Platform and Instruments

The instrument payload for the ER-2 has evolved steadily since STEP in 1987. The list of measurements (Table 1), taken from the experiment plan for ASHOE (Tuck, 1992) shows a wide array of measurements of long-lived tracers, reservoir and reactive trace gases, aerosols and their properties, and the atmospheric environment near the aircraft. Those in bold lettering are new since 1991.

In fact, we now have, for the first time, direct measurements of those reactive chemicals in the four major chemical families—nitrogen, hydrogen, chlorine, and bromine—that control the abundance of ozone. We now can measure many of the important reservoir species in those chemical families. We also have for the first time a reasonable measure of the radiation field that will be useful in constraining the uncertain radiation environment near the aircraft. And we have new stratospheric tracers, including CO_2 , that will be necessary to understand transport issues. This ER-2 payload is a significant advance over payloads of just a few years ago.

Perseus Platform and Instruments

Another instrument platform, the Perseus A remotely piloted aircraft, is currently being designed, constructed, and tested for a September 1993 delivery date from Aurora Flight Sciences Corporation. Our most immediate need for this aircraft is high-altitude flights in the tropics and middle latitudes, as will be discussed. In this mode, Perseus A can carry a payload of at least 50 kg for a short duration to an altitude of 25 km, but with only small horizontal coverage of a few degrees of latitude, limited by the line-of-sight of the radio control. The list of measurements is in Table 2.

The group of instruments for Perseus presently cannot be flown simultaneously because their requirements exceed the payload capabilities of the aircraft. In addition, ALIAS II will be developed for experiments after 1994 and will not be deployed during MAESA. If we assume that Perseus A, once flown and proven, will be able to carry about 120 kg to 25 km and provide 900 watts of instrument power (which is within the computer-calculated abilities of Perseus), then two useful payloads can be flown.

- Payload 1 consists of instruments to measure NO_y , N_2O , and CH_4 (by Argus), O_3 , pressure, and temperature. This configuration is designed for studies of relationships among long-lived chemical species.
- Payload 2 consists of instruments to measure ClO , BrO , NO , NO_y , O_3 , pressure, and temperature. This configuration is designed for studies of reactive trace gases and rapid

photochemistry. NO_y and O_3 can be used as tracers once their relationships with N_2O have been established with Payload 1.

These two payloads are being designed so that they can be readily interchanged during deployment. Eventually, a third payload configuration consisting of the full instrument complement will be possible, and Payloads 1 and 2 are being designed to simplify this eventual coalescence.

Critical observations of aerosol characteristics, particularly surface area, are missing from the Perseus payloads. These measurements are crucial if we are to understand the results from Payload 2, the reactive gas payload. To solve this problem, we will deploy a ground-based lidar with Perseus to measure the aerosol backscattering, which can be correlated with aerosol surface area. When Perseus is deployed in the United States at NASA Dryden Flight Research Facility, the JPL lidar at Table Mountain will be used. In Darwin, the GSFC mobile lidar will be used. These lidars can measure aerosol backscattering, temperature, and ozone up and through the altitude range of Perseus. The GSFC lidar will be operated in New Zealand during the early part of ASHOE/MAESA. These lidar measurements will be made as part of the Network for Detection of Stratospheric Change (NDSC).

Scientific Balloon Platform and Instruments

In the event that Perseus is not ready for the 1994 mission, we will consider the use of helium-filled scientific balloons in the 1 to 10 million cubic feet class. The payload would consist of the Perseus instruments, and instruments that have recently flown on balloons:

- ClO and BrO (existing balloon instrument);
- NO and NO_y (existing balloon instrument);
- O_3 (existing balloon instrument);
- N_2O and CH_4 (Argus, under construction);
- N_2O , CH_4 , and H_2O (ALIAS; under construction);
- CFC-11, CFC-113, CFC-12 (needs to be built—could be whole air sampling);
- Pressure and temperature (existing balloon instrument).

Scientific flights of the balloon payload would be conducted primarily in the tropics, with earlier test flights conducted in middle latitudes.

DISCUSSION OF SCIENTIFIC ISSUES AND MEASUREMENT STRATEGIES

In this section, we consider the scientific issues in more detail. We will discuss the importance of the issue for AESA, and the flight plans that will provide the observations to answer the question.

Photochemistry and Aerosols

How do the abundances of chemical species, particularly NO, NO_2 , HNO_3 , NO_y , ClO, HCl, BrO, OH, HO_2 , and their ratios vary from 40°N to 70°S latitude in the lower stratosphere? How do they vary over a range of altitudes and solar zenith angles? How do they vary from late spring to mid-summer to late fall? Does the budget of reactive nitrogen balance? Do the observed ratios of reactive species agree with those calculated for photochemical steady state?

Much of what we learn about stratospheric processes we learn best from observing changes or differences in trace gas abundances (or ratios of abundances) for differing environmental conditions.

SPADE is designed to measure changes in reactive trace gas amounts in the middle latitudes in two seasons — early fall and late spring. Several flights during sunrise and sunset transitions will provide information about fast photochemical processes. Changes in reactive trace gas amounts will also be observed over latitudes that span the northern middle latitudes and altitudes from 15 to 20 km.

MAESA is also designed to observe altitude and latitude changes in the middle latitudes, but at different seasons. A primary component of MAESA, however, is the observations in the lower, tropical stratosphere, where high quality, simultaneous observations are scarce. The photochemical environment is radically different from that of the middle to high latitudes. The sunlight is more intense and constant from season to season, the abundances of reservoir species are small in the chlorine and nitrogen chemical families, and photochemical production activity is great. The tropical stratosphere starts with tropospheric air containing little ozone, and thus production of ozone greatly exceeds loss. This condition is opposite to that in the middle to high latitudes where descending air brings in large amounts of ozone, and ozone loss exceeds production. Most of the recent ER-2 observations have been made only at the extra-tropical latitudes during winter, when the production of ozone is negligible. Thus, tropical measurements from MAESA can be contrasted with those from middle latitudes. The latitudinal dependencies, particularly when taken during different seasons, are as powerful a tool for diagnosing stratospheric processes as the sunrise and sunset transits that are part of SPADE.

Importance to AESA

We must know the climatology of as many members of the nitrogen, hydrogen, chlorine, and bromine chemical families as possible (Prather and Remsberg, 1992, see page 161). These measurements over a large range of latitudes, three seasons, and limited range of altitudes will add significantly to our knowledge of this climatology. Satellite and balloon observations, although they contribute significantly to the climatologies in their own ways, cannot substitute for the observations we will get from aircraft.

By making these simultaneous observations over such a large range of conditions, we can reduce the uncertainty in our understanding of photochemical processes. We can develop a better understanding of the interaction of the chemical families and of the competition between gas-phase and heterogeneous processes in partitioning these chemical families. These tests are particularly important for any processes that increased amounts of reactive nitrogen and water might affect.

An important example is the competition between the hydrolysis of N_2O_5 to remove NO_x and produce HNO_3 and the photolysis and reaction with OH to remove HNO_3 and produce NO_x . The hydrolysis of N_2O_5 on sulfate aerosols is the reaction $\text{N}_2\text{O}_5 + \text{H}_2\text{O} \rightarrow 2 \text{HNO}_3$. This heterogeneous reaction affects not only the nitrogen family but also those of chlorine and hydrogen. It indirectly affects the abundances of ClO primarily through the reduction of NO_x in two ways: by shifting the daytime balance of ClONO_2 and ClO toward ClO, and by enhancing the abundance of OH through the reduced destruction of OH by NO_2 and increased production by photolysis of HON_3 , which then produces more Cl by reaction with HCl. This competition should be highly dependent on latitude and season. The hydrolysis of N_2O_5 is one of the most important processes dictating the effect that stratospheric aircraft will have on ozone.

Current Observations and Calculations

The variation of reactive trace gases during sunrise and sunset transitions has now been observed on several occasions from both balloon (Webster et al., 1990) and aircraft instruments (Brune et al., 1990; Kawa et al., 1990). The balloon measurements contained a fairly complete set of measurements in the reactive nitrogen family above 30 km, and observations and model calculations using gas-phase chemistry are in excellent agreement. The aircraft measurements, on the other hand, did not have enough simultaneous measurements to demonstrate with small uncertainty that the partitioning among ClO, NO, and ClONO₂ is completely understood. For instance, no measurement was made of NO₂. Until SPADE, no measurement has been made of the sunset and sunrise transitions of OH.

The SPADE measurements in November had the potential to observe effects of the hydrolysis of N₂O₅ on NO_x. The darkness of night was long enough that considerable NO_x could be heterogeneously lost to HNO₃ and yet PSCs had not yet occurred. However, the results from the sunrise flight have not yet been fully analyzed.

Aircraft observations in the tropics consist of transit flights for the STEP and AAOE programs in 1987 and a few earlier observations from Panama. However, the instrument complements for these two experiments were insufficient to answer the questions that we now pose for MAESA. As a result, we have an extremely limited data set of reactive trace gas abundances for the tropical region, and even less seasonal information. These tropical measurements are important for establishing and testing the current ideas about gas-phase chemistry.

The situation for the northern middle latitudes and the high latitudes in winter and spring is much better than that for the tropics. We have many measurements that span the middle latitudes for many of the chemical species, and observations from instruments placed on balloons, the space shuttle, and satellites contribute to our understanding of the abundances at these latitudes. The number of aircraft observations in the summer is small however.

Observations of reactive nitrogen and chlorine are inconsistent with models that contain only gas-phase chemistry. They support an important role for the hydrolysis of N₂O₅ in middle latitudes. Particularly relevant are observations of NO and NO_y by Fahey et al. (1993) during AASE II, from which the inferred ratio of NO_x to NO_y is in much better agreement with models containing the hydrolysis of N₂O₅ than with those containing only gas-phase chemistry. No measurements of species in the nitrogen family are in conflict with the concept of hydrolysis of N₂O₅.

However, some observations, particularly in the background levels of sulfate aerosol that existed prior to the Mt. Pinatubo eruption, indicate that the reaction efficiencies measured in the laboratory may not be the same for the stratospheric sulfate aerosols under all circumstances (Considine et al., 1992). The LIMS measurements of HNO₃ and the seasonal variation of NO₂ both agree best with models that contain the hydrolysis of N₂O₅, but the absolute abundance of NO₂ agrees better with models that contain only gas-phase chemistry.

No observations of ClO are in conflict with the concept of hydrolysis of N₂O₅ either. The persistently enhanced abundance of ClO observed from the ER-2 during AASE II is strong indirect evidence, as are the variations of ClO with latitude, (as shown in Figure 2), season, and aerosol surface area (King et al., 1991; Avallone et al., 1993; Toohey et al., 1993; Wilson et al., 1993), and the ClO/HCl ratio (C. Webster, private communication, 1993).

Aircraft in situ measurements of HCl, which were made for the first time during AASE II, are not explained by current model calculations (C. Webster, private communication, 1993). The HCl abundances observed for ER-2 altitudes at middle to high latitudes in winter were substantially

lower than predicted by photochemical models, whether they included heterogeneous chemistry or not. This observation implies that HCl was not the major inorganic chlorine reservoir in the lower stratosphere.

Three possible causes, if no problem with the ER-2 instrument is uncovered during ongoing tests, have been suggested for the discrepancies in HCl abundances. First, the representation of the heterogeneous chemistry in the models is either incomplete or incorrect. Effects due to temperature, aerosol impurities, aerosol phase, or photochemistry on the reaction rates may not be properly characterized. A second possibility is that the abundances of OH are substantially different from model predictions. If the OH abundances are much larger than predicted in these environments, then the reaction of OH with HCl would reduce the HCl abundances. A third possibility is that key photolysis rates are in error. New instrumentation for SPADE and MAESA and comparisons with observations from UARS and ATMOS should tell us if either of the last two possibilities is the cause.

If we cannot simulate the observations of reactive and reservoir species in the chlorine and nitrogen families, then we can have no confidence that the photochemistry included in the HSRP assessment models is complete and accurate. Only more data with tighter constraints on the possible mechanisms (with more and better simultaneous measurements over a wider range of conditions), combined with additional laboratory studies of the heterogeneous chemistry and all of its nuances, can resolve these issues.

Measurement Collection Strategy

The goal is to gather as much data as possible on the abundances of reservoir and reactive species in the nitrogen, chlorine, and hydrogen chemical families. These measurements must be made along with tracer, aerosol, and meteorological measurements to put them in an understandable reference frame. To collect these data, we will need both ER-2 and Perseus flights. The ER-2 can give us good spatial and seasonal coverage, but over a limited altitude range. The Perseus can give us fewer simultaneous measurements, but over a greater altitude range at a few latitudes and seasons.

The ER-2 test flights from ASHOE in February 1994 can be used to resolve questions left over from SPADE, including possible flights in the morning or evening. These flights will also provide the opportunity to examine the photochemical state of the middle latitudes in 1994 through the measurement of trace gases and aerosol abundances. Flights north would reestablish the measurements from AASE I and AASE II.

The transit flights will provide data about the seasonal and latitudinal variations of these trace gases, and hence the photochemistry, because the four transit flights occur in March, June, July, and October. Each transit will consist of four flights: Ames to Hawaii; a stop-over flight at Hawaii; Hawaii to Fiji; and Fiji to Christchurch. During these transit flights, the aircraft will be fully loaded with instruments and fuel, and probably will not be able to exceed a pressure altitude of 64,000 ft (J. Barrilleaux, private communication, 1993), which is roughly equivalent to a potential temperature of 430-450 K. At these altitudes in the tropics the abundances of reactive trace gases will be quite low and the range of useful measurements will be highly restricted. A greater altitude range, up to roughly 68,000 ft, can be obtained if the aircraft takes off and lands at Hawaii because it can be loaded with less fuel and still reach alternate landing sites. Thus, to extend the altitude range of the measurements in the tropics, flights could be made from Hawaii. The tropical region should be accessible from Hawaii, and if not, the possibility of stop-over flights from Fiji will need to be examined.

The Perseus A aircraft will also be used to address our concerns about the photochemistry. Because it can attain an altitude of 25 km, but has limited horizontal range, we will stage it for

flights from only a few locations. One will be at middle latitudes, probably at Dryden Flight Research Facility and in conjunction with the ER-2. We have chosen Darwin, Australia as the tropical deployment site for Perseus and the ground-based lidar. The observations generated from the limited number of instruments on the Perseus does not supplant the need to cover a greater altitude range with the ER-2 and its more complete instrument package. It does extend the altitude range considerably, however, giving us a view of ClO and NO and a tracer to higher altitudes, and allowing us a better view of the photochemistry in a different environment.

We need the greater altitude capability of Perseus, even with the limited payload, for several reasons. First, in the tropics, the ER-2 will be able to sample N₂O only to about 260 ppbv and NO_y to a few ppbv. Perseus, on the other hand, will be able to sample N₂O to about 200 ppbv and NO_y to about 6 ppbv. This additional range could be very important for measurements of NO, NO_y, ClO, and BrO.

Second, NO_y/N₂O is a valuable diagnostic of reactive nitrogen. It measures exactly the quantity that HSCTs will perturb the most. It has been used to indicate denitrification in the polar vortices, and displays some interesting differences between hemispheres. Model calculations (Plumb and Ko, 1992) suggest that NO_y/N₂O may be about 10% greater in the tropical lower stratosphere than at middle latitudes. This observable difference may indicate the photodestruction of NO (and thus NO_y) above about 30 km. In addition, NO_y/N₂O may be affected by the injection of tropical NO_y that is produced by lightning. However, we need a measure of this relationship over a sufficient range in N₂O in order to ensure the use of this diagnostic. Perseus provides us with this range.

Third, the amounts of trace gases change rapidly in the lower stratosphere. From ER-2 altitudes to 25 km, ClO and NO_y are calculated to change by a factor of 10, NO by a factor of 2, and O₃ by a factor of 30. These steep gradients result from changes in both trace gases and photochemical environment.

Specific Measurements

The enhanced instrument capabilities give us the tools to make many measurements that have never been made before (Figure 3). However, each measurement has an instrumental absolute uncertainty and a limit to the precision. For most measurements of reactive species, the uncertainty is 20 to 35%. For most measurements of reservoir species, the uncertainty is 5 to 30%. The precision of these measurements is generally a few percent for a few minutes (or less) of integration time. These uncertainties, coupled with the uncertainties in laboratory measurements, permit test of simple photochemical balances to an uncertainty of 50 to 80% in many cases. The variation of relationships during sunrise or sunset, or over a range of latitudes or seasons, can be measured much more accurately. With this uncertainty in mind, we can consider combining measurements from instruments in a way that tests photochemical and heterogeneous mechanisms that involve the nitrogen, chlorine, and hydrogen chemical families and the interactions among them.

Many tests are possible with the ER-2 payload. Four that have a high priority for AESA are:

- balancing the reactive nitrogen budget with measurements of NO, NO₂, HNO₃, and NO_y, and inferred values for ClONO₂, NO₃, and N₂O₅. (uncertainty: less than a factor of 2);
- the photochemical balance of OH, NO₂, and HNO₃, and measurements of the photolysis rate (uncertainty: about 70% in the photolysis rate);
- the photochemical balance of ClO, NO₂, and inferred ClONO₂ during sunrise and sunset (uncertainty: about 70% in the photolysis rate);

- the photochemical balance of OH, HO₂, O₃, NO, and CO (uncertainty: 10% in the ratio of OH to HO₂, about 50% for the entire balance).

The uncertainties in these tests are estimates. Tests over a range of altitudes and latitudes in differing photochemical environments will expose inconsistencies in measurements and will reduce the uncertainties. Other specific studies are listed under other questions.

How do the abundances of these same chemical species vary as a function of aerosol loading of the lower stratosphere? In particular, we know that the partitioning of chemical species in the nitrogen, chlorine, and hydrogen families changed with aerosol loading from the Mt. Pinatubo eruption. How will these amounts change as the aerosol loading slowly decreases over the next few years?

Observations of the aerosols injected by volcanoes into the stratosphere suggest that aerosols have a stratospheric lifetime of 1 to 2 years (WMO, 1991). Thus, SPADE and MAESA are opportunities to study stratospheric processes in 1994, when the aerosol loading will probably be several times lower than in 1992. When these measurements are combined with those taken prior to the Mt. Pinatubo eruption, we will have observed the effects that different aerosol surface areas have on the trace gas distributions.

Importance to AESA

The revelation that heterogeneous chemistry on sulfate aerosols was changing the NO_x abundances in the stratosphere has significantly altered the assessment of the impact of high-speed aircraft on the stratosphere. From the comparison between observations and model results, we know that heterogeneous chemistry on sulfate aerosols needs to be included in our assessment models. But questions remain. First, have we accounted correctly for the heterogeneous processes and do we understand their effects on trace gas abundances? Second, how much of the detailed heterogeneous mechanism do we need to consider for making the assessment? Measurements of trace gas abundances that are affected by heterogeneous chemistry and the variations of those abundances as a result of different aerosol loadings should give us some indication of the complexity of the problem.

Current Observations and Calculations

As discussed for the first question, we have large uncertainties in the detailed processes that are occurring on sulfate aerosols in the lower stratosphere. Measurements of NO and NO_y during AASE II show that the observed increase in the sulfate aerosol surface area due to Mt. Pinatubo resulted in a less-than-proportional reduction in NO_x due to the hydrolysis of N₂O₅ (Fahey et al., 1993). This saturation effect, which occurs because the formation and gas-phase destruction of N₂O₅ is slower than the hydrolysis of N₂O₅ even with background aerosols, apparently reduces the sensitivity of stratospheric chemistry to the observed variability of stratospheric aerosol loading. Observations from SPADE in 1993 and from MAESA in 1994 will allow us to plot the ratios of NO_x/NO_y and ClO/Cl_y for several values of sulfate aerosol surface area and to compare this plot with model results.

The NO_x/NO_y ratio that was derived from AASE II observations appears to agree with models that include hydrolysis of N₂O₅ for the volcanic aerosol; the ratio measured in the background aerosol appears to be slightly larger than model results (Fahey et al., 1993). The model fits the observations better if the heterogeneous reaction efficiency is reduced a factor of two. SPADE and MAESA will provide more observations of NO_x/NO_y at different aerosol loadings so that this possible discrepancy can be resolved.

Measurement Collection Strategies

Relatively few measurements exist for those reactive species that are most affected by heterogeneous chemistry. As significant, no measurements have been made of NO₂, OH, and HO₂ in the lower stratosphere where the effects are the greatest. Because the hydrolysis of N₂O₅ has such a powerful effect on reactive nitrogen photochemistry and the injection of additional NO_x by HSCTs, we need to have many more measurements over a wider range on conditions than are currently available.

The measurement strategy is to collect observations of those species most affected by this reaction over a range of seasons, latitudes, and altitudes. Measurements toward the Arctic during the test flights in February 1994 and from New Zealand during ASHOE will augment the existing measurement set for middle to high latitudes, but at a smaller sulfate aerosol surface area. Measurements in the tropics will test the assumption that gas-phase chemistry dominates in the tropics. Measurements to higher altitudes with Perseus will do the same.

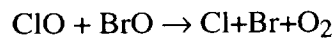
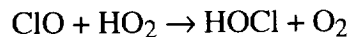
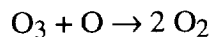
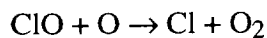
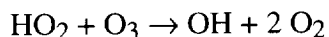
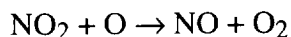
Specific Measurements

A test with high priority is the measurement of ratios of species that are most susceptible to heterogeneous chemistry. For the sulfate aerosol surface area that is likely to exist in 1994, the ratios of HO₂/NO₂, ClO/HCl, NO_x/NO_y are all calculated to be several times different from gas-phase in the middle latitudes (McElroy et al., 1992). Because these ratios can all be measured with an uncertainty of less than 50%, they will be powerful tests of N₂O₅ hydrolysis.

The decrease in the sulfate aerosol surface area with time permits a good test of the saturation effect. We already have several measurements of NO_x/NO_y from 1991 through May 1993 from AASE II and SPADE, and the surface area has gone from background levels, to 30 times larger after the Mt. Pinatubo eruption, and is now about 2 to 3 times smaller. In 1994, the surface area will have decreased even more. The combination of these measurements in middle latitudes for a number of reactive species over these 3 years will permit us study the trace gas ratios given above as a function of sulfate aerosol surface area and HNO₃ photolysis rate.

At what rates do the reactive species in the nitrogen, hydrogen, chlorine, and bromine chemical families catalytically destroy ozone at latitudes from 40°N to 70°S in the lower stratosphere during late spring, mid-summer, and late fall?

The primary catalytic destruction mechanisms for ozone in the lower stratosphere include the reactions:



Except for O atoms, we will be able to measure all the reactants in these rate-limiting reactions for these ozone-destroying photochemical cycles. We can establish the relative importance of these cycles and compare relative destruction rates with expectations for computer models.

The inclusion of the hydrolysis of N_2O_5 into photochemical models results in a larger role for the hydrogen-catalysis in the destruction of ozone (McElroy et al., 1992). In fact, these model calculations suggest that HO_x catalysis dominates over NO_x catalysis of ozone up to as high as 23 km altitude. Thus, observations of OH and HO_2 in the lower stratosphere appear to be essential for determining the rates of ozone catalysis in the lower stratosphere.

We do not have any simultaneous measurements of all the reactive species in these equations, but the ER-2 instruments for SPADE and MAESA will significantly improve this situation. Previously, attempts have been made to infer abundances of reactive species that were not directly measured. These exercises have been valuable, but do not provide low enough uncertainty to test our understanding of the ozone destruction rates in middle or low latitudes.

Measurement Collection Strategies

Studies of the catalytic cycles is a high priority for AESA because it is through these cycles that the HSCT effluents and their photochemical by-products will interact with ozone. The flights proposed for the other photochemical studies above and for the dynamical studies below will give us a good look at this issue because we will be measuring these species all the time.

An analysis of uncertainties for the measurements of the trace gases and the rate constants shows that the rates of each cycle can be determined with an uncertainty of about 50%. The overall catalytic destruction rate should be only slightly more uncertain. This level of uncertainty, while not sufficient to eliminate the possibility of any other unknown catalytic cycles, is nonetheless a significant advance over present conditions, where lack of measurements of one or more of the key radicals has prevented any reasonable attempts at determining the ozone destruction rate.

Do the characteristics of sulfate aerosols vary with temperature in a way that is consistent with ideas of liquid aerosol growth? Can this observed relationship be used to determine if the aerosols are liquid or solid?

The phase of the stratospheric sulfate aerosols—be it liquid or solid—is important to both the global heterogeneous chemistry and the nucleation of PSCs in the cold polar regions. If the sulfate aerosol is liquid, then hydrolysis of N_2O_5 is efficient but hydrolysis of ClONO_2 is relatively inefficient, except at temperatures below about 205 K. On the other hand, if the sulfate aerosols are frozen, then the heterogeneous reaction of $\text{HCl} + \text{ClONO}_2$ is more efficient, mimicking processes on PSCs. The nucleation of PSCs is thought to occur on frozen sulfate aerosols, so that in the wintertime polar regions, the phase of the sulfate aerosol may be important to PSC formation.

Importance to AESA

How the introduction of HSCT effluents will affect the stratospheric heterogeneous processes is currently unknown. However, these effluents are expected to double NO_y abundances, increase H_2O and sulfate aerosols by 20-30%. These species are all condensables that can affect the partitioning of the nitrogen, hydrogen, and chlorine chemical species that control ozone. The increase in water vapor in particular could increase the occurrence and duration of PSCs. The presence of accumulations of aircraft-generated sulfate aerosols in corridors that stretch through cold regions could increase the possibility of heterogeneous processing in the nitrogen and chlorine chemical families. These issues must be resolved before we can have any assurance that HSCTs will not cause substantial depletion of stratospheric ozone.

Particularly important is the phase of the sulfate particles. If they are liquid, then the hydrolysis of N_2O_5 is relatively fast and the conversion of reservoir chlorine to reactive chlorine is relatively slow. If they are frozen solid, then the conversion of N_2O_5 to HNO_3 is relatively slow but the reaction of HCl with ClONO_2 is relatively fast. In addition, the sulfate aerosols must be frozen to act as good condensation nuclei for the formation of PSCs. Some approaches for measuring aerosol phase will be attempted during ASHOE/MAESA.

Current Observations and Calculations

No direct stratospheric measurements of the phase of the sulfate aerosol exist. Some measurements of the change in sulfate aerosol size as a function of temperature suggest that sulfate aerosols can stay liquid to temperatures as low as 193 K (Dye et al., 1992). The lack of depolarization in the lidar backscattered light indicates that the most sulfate aerosol particles are spherical, but they do not necessarily have to be liquid. This issue of aerosol phase remains to be resolved.

Measurement Collection Strategies

The observations of the change in aerosol characteristics with changes in temperature is an indirect method to distinguish liquid from solid sulfate aerosol particles. This observation also provides a test of the laboratory measurements and theoretical calculations for how the liquid aerosols should change with temperature. Despite the low amounts of water vapor available in the tropics, the variation in temperature just above the tropical tropopause (see Figure 4) should provide a test of this relationship between aerosol size and temperature. Observations during SPADE in May should also provide an opportunity to examine this issue at middle latitudes after the break-up of the Arctic polar vortex, which in 1993 has experienced substantial low temperatures.

Transport of Trace Species

The ER-2 and Perseus are better suited for studies of photochemistry than they are for studies of dynamics. Nonetheless, very limited aircraft observations have had a role in shaping the discussions about transport within the stratosphere and between the stratosphere and troposphere. We expect flights during SPADE and MAESA/ASHOE to provide observations that are complementary to those taken by UARS and that are significant on their own.

How do the abundances and correlations of tracer species, such as N_2O , CH_4 , O_3 , H_2O , CO_2 , condensation nuclei, aerosols, and NO_y , vary between the middle latitudes of both hemispheres and the tropics? How do they vary in different seasons with different temperature characteristics?

Can relatively undiluted tropospheric air be found within a few kilometers above the tropopause in the tropics? In other words, is tropical transport dominated by upwelling, or does significant mixing occur along surfaces, as in the middle latitudes?

Do these measurements indicate restricted exchange between the tropics and the middle latitudes? How do such restrictions affect the photochemistry of the tropics and the middle latitudes?

What is the character of the exchange of trace gases between the stratosphere and troposphere? Can we improve our understanding by measuring the abundances and relationships among trace gases?

We can learn about dynamical processes, as well as photochemical processes, by observing changes or differences in trace gas abundances (or ratios of abundances) for different dynamical environments. For dynamical studies, however, we are most interested in those trace gases that have lifetimes that are longer than or comparable to the dynamical time constants N_2O , CH_4 , CFCs, H_2O , O_3 (which is roughly the same as O_x in the lower stratosphere), CO_2 , and NO_y . Analyses of the distributions of trace gas abundances measured during MAESA and other aircraft programs, along with the satellite observations of trace gases and volcanic debris, will help develop our understanding of how stratospheric transport occurs in the tropical regions.

Because all the issue about transport of trace species have the same importance to AESA and require the same measurement strategy, we consider them all at once.

Importance to AESA

Knowledge of tropical transport and the exchange between the tropics and the middle latitudes is important for AESA. We must know what the distribution of aircraft exhaust is likely to be. If any exhaust emissions that are released in middle latitudes are mixed into the tropics, they might be lofted to higher altitudes before they descend and enter the troposphere at middle latitudes. Similarly, emissions released directly in the tropics, currently estimated to be about 25% of the total emissions, may also be lofted. Once NO_x emissions rise to higher altitudes, they have a longer stratospheric residence time and they pass through a region of the stratosphere where increased NO_x catalytically destroys ozone. In addition, we need to know when and where transport and exchange might occur and whether it is fairly constant or sporadic. The character of the transport will affect the distribution of the aircraft exhaust. Thus, the seasonal and quasi-biennial dynamical effects must be understood.

Current Observations and Calculations

Few measurements of stratospheric tracers exist for the tropics, and simultaneous measurements of tracers are even rarer. Only a few tropical balloon and aircraft measurements of CFCs, CH_4 , and N_2O exist too few to derive meaningful correlations. An interesting compilation of NO_y , O_3 , and the NO_y/O_3 ratio from STEP and AAOE (Murphy et al., 1992) do exist and point to the importance of such ratios for testing photochemical and dynamical processes (Figure 5). Some satellite and shuttle measurements exist, with some simultaneous measurements of tracers, but the increasing uncertainty and poorer horizontal resolution of these measurements degrades the value of the correlations of the observations.

The concept of correlations among tracer abundances has been used as a test of the occurrence of PSCs in the polar stratosphere (Fahey et al., 1990) and as a means for initializing process-oriented computer simulations. An explanation for these observed compact correlation curves is that rapid mixing occurs on surfaces that slant poleward with respect to isentropic surfaces (Plumb and Ko, 1992). The question is, then, what do these correlations look like in the tropics, and can the assessment models, or the 3-D models for that matter, reproduce them? If we examine the modeled correlations of long-lived species with respect to N_2O (Prather and Remsberg, 1992), we see that the correlation curves for CH_4 , the CFCs, and NO_y are calculated to be relatively compact. However, they are not perfectly compact for most models. For species such as CFC-11 and CCl_4 , the abundances are predicted to be more than five times lower in the tropics than in middle latitudes for N_2O abundances of 180-250 ppbv (Figure 6). For other species, such as methane and CFC-12, the variation is predicted to be about 20%. At present, we have no measurements to test these predictions.

Two features of correlations of NO_y remain to be fully explained. First is the observation that the NO_y - N_2O correlation is measured to be slightly different in the two hemisphere at middle to high latitudes (Fahey et al., 1990). The second is the shape of the latitudinal variation of the ratio

NO_y/O_3 (Murphy et al., 1992). This first observation may give us a hint about either the different sources and sinks of NO_y in the two hemispheres and help provide another limit to the transport time between the two hemispheres across the tropics. The second observation indicates the presence of a barrier between the middle and tropical latitudes at about 10° - 20° in both hemispheres. These abrupt shifts cannot be simulated by the 2-D models.

The observations that show evidence of restricted exchange between the tropics and the middle latitudes are the satellite maps of the extinction by the aerosols released by Mt. Pinatubo in June, 1991 (McCormick and Veiga, 1992). However, the NO_y/O_3 ratio (Murphy et al., 1992), the abundances of ClO and O_3 from one flight (King et al., 1991), and the analyses of potential vorticity with the ECMWF model at high resolution (Tuck et al., 1992) also show evidence of restricted exchange.

More observations are required from aircraft, perhaps balloons, and UARS for us to better understand this issue.

The transport of trace gases between the tropics and middle latitudes appears to vary depending on the time of the year and the phase of the quasi-biennial oscillation (QBO). Eruptions from two different tropical volcanoes in 1984 and 1988 occurred during a different phase of the QBO, and the resultant spread of the volcanic aerosol was dramatically different during the easterly and westerly phases, as in Figure 7 (Trepte and Hitchman, 1992). When the QBO was easterly below 23 km and westerly above, the aerosol distribution suggested that the air was descending at 25 km, causing a lateral spread in the air near 23 km. When the QBO was easterly above 23 km and westerly below, less lateral spreading and more vertical lofting in the tropics occurred. These satellite observations also suggest that transport between the tropics and middle latitudes is rapid within a few kilometers of the tropopause. These observations may have implications for the spread of aircraft exhaust to higher altitudes.

Recent work (Rood et al., 1992; Douglass et al., 1992) using a 3-D assimilation model suggests that little aircraft exhaust released in the lower stratosphere, even in the tropics, will be lofted to higher altitudes and that essentially all of it will end up in the troposphere at middle latitudes. Even though these calculations indicate that the amount of exhaust being lofted to 30 km altitude is only a few hundredths of a ppbv, this question is so critically important to the assessment of aircraft effects that additional observations and calculations are required. No large gradients in trace species are evident in the tropics in the 2-D assessment models. Thus, these models do not represent correctly some of the important dynamical features of the lower stratosphere. We must understand the underlying physical processes that create these gradients in order to evaluate the importance of these failings in the models to the assessment of stratospheric aircraft effects.

Measurements of CO_2 on the ER-2 during SPADE in November 1992 and on the DC-8 during AASE II indicate that its variation may be significant for understanding stratospheric-tropospheric exchange. The November SPADE flights show a clear signature of the annual oscillation of the tropospheric CO_2 abundances extending up to 17 km. This result indicates that tropospheric air can enter the stratosphere from regions other than the energetic convection regions over Micronesia. Either tropospheric air can enter the stratosphere more globally, or the lower stratosphere above the tropopause is all connected by rapid quasi-horizontal transport. These two models predict significantly different behavior for the transport of HSCT effluents.

Measurement Collection Strategy

We need to make as many measurements of tracers from 40°N to 40°S for different seasons, and if possible, different phases of the QBO. We need the ER-2 to carry instruments to measure a wide variety of tracers including H_2O , N_2O , O_3 , NO_y , CH_4 , CO_2 , condensation nuclei, aerosols

and their properties, and a number of the CFCs (particularly CFC-11). We will be able to observe differences in the abundances of trace gases and their correlations over a range of seasons.

However, in the tropics, the ER-2 can fly less than 5 km above the tropopause on the transit flights. Any greater altitude that can be gained by stop-over flights from Hawaii into the tropics, projected to be 0.7 km, will allow us to make measurements closer to the altitudes where the restrictions to exchange seem to exist. They will also allow us to examine tropical correlations over more substantial ranges in N₂O.

Perseus, or balloons, have an important role in the study of tropical dynamics. Measurements from these platforms permit us to tie together measurements from the ER-2 aircraft and the UARS satellite because the altitude range of this aircraft bridges those of the other two platforms.

Other Scientific Issues to Which MAESA Might Contribute

Does heterogeneous chemistry occur on the tropical ice clouds that form in the western Pacific near the tropopause? Can it affect the photochemistry of either the tropics or the middle latitudes?

The mission plan for MAESA does not contain any attempt to look for or at ice clouds in the western Pacific. An entirely separate mission must be planned if such a study is thought to be important. However, it is doubtful that heterogeneous chemistry on these ice clouds can be very effective at repartitioning the trace gas constituents of the tropical stratosphere. It is also doubtful that chasing such clouds would yield much, or any, unambiguous information about the processes (Murphy et al., 1992). However, Perseus will be deployed in Darwin in October, and should encounter some very low temperatures near the tropopause. Any opportunity to sample this cold air will be taken.

Does air from middle latitudes, rich in NO_y and H₂O, pass through the cold regions on the margins of the tropics? Can subtropical stratospheric clouds (SSCs) with a composition similar to polar stratospheric clouds (PSCs) form. Does significant heterogeneous chemistry occur?

We now understand that if clouds form in the stratosphere, they exert a large nonlinear perturbation on the photochemistry of a region. Thus, the possibility of tropical stratospheric clouds, and if they are occurring, the possibility that they will be more frequent and intense with the addition of aircraft emissions, are good reasons to search for their existence under the aegis of AESA. The large nonlinear perturbations of increased occurrences of stratospheric clouds could easily offset any amelioration that heterogeneous chemistry might have on the NO_x catalytic cycles in the lower stratosphere. Observations of a thin layer of a high abundance of ClO at 22°N during AASE II in February 1992 may be an indication of subtropical stratospheric cloud formation.

In the tropics, will the tracer abundances and correlations differ during the easterly and westerly phases of the Quasi-Biennial Oscillation (QBO)? Can this information be reconciled with satellite observations of volcanic aerosol transport out of the tropics?

No provisions are being made to look at this interesting phenomenon. The ER-2 can fly only up to 20 km, which is at least 3 km below the region where restricted exchange between the tropics and middle latitudes occurs. Because of the uncertainty of the changes in the phase of the QBO, no plans can be made at this time to even use Perseus, which can sample into the restricted region of the tropics. The chosen deployment site for Perseus — Darwin, Australia — is at a latitude that does not experience oscillations from the QBO. This issue will have to wait for future studies.

COORDINATION WITH OTHER MEASUREMENTS

The measurements from this experiment need to be used in conjunction with measurements from other systems, primarily helium-filled balloons and satellites such as UARS. The combination of all the measurements from all the platforms is far more powerful than the individual measurements for testing the assessment models and providing an improved understanding of stratospheric processes. Thus, we are actively seeking out possible links with the other sources of observations.

Intercomparisons of Instruments on Different Platforms During MAESA

The ability to combine observations by different instruments on different platforms (and perhaps at different times) relies on the intercomparison of those different instruments. An important feature of MAESA is the intercomparison of these data sources. For tropospheric measurements, a good method for intercomparing instruments has been to make them sample the same standard gases on the ground, before they are flown. However, for the stratospheric measurements, the platforms are as important as the instruments in determining the measured values, and the platforms and measurement techniques are both remote and in situ. The best intercomparison for these is to measure the same trace gases in roughly the same volume of air at roughly the same time. We will endeavor to perform such intercomparisons whenever and where ever possible.

Some examples of intercomparisons are:

1. ER-2 and the balloon-borne Mark IV FTIR (G. Toon) measurements of O_3 , NO_y , CH_4 , N_2O , H_2O , some CFCs, HCl , HNO_3 , and NO_2 during May, 1993 (SPADE);
2. ER-2, Perseus, and UARS measurements of O_3 , NO , H_2O , CH_4 , HCl (but not Perseus), ClO , and NO_y (not UARS) during February and July 1994;
3. Perseus and UARS measurements of O_3 , NO , H_2O , CH_4 , and ClO in the tropics during October 1994.

A number of intercomparisons between UARS and balloon-borne instruments have already been made as part of the UARS Correlative Measurements program. Such intercomparisons can only reduce the uncertainty in our total observational data set.

The UARS Satellite Instruments

By early 1994, the UARS satellite will have been operational for about 2 years. Unfortunately, by that time, both the ISAMS and CLAES infrared instruments will have quit working and no observations will be available for N_2O , HNO_3 , CFC-11, and CFC-12. We will need to relate the observations of these species during 1992 to those made by instruments on the ER-2 and Perseus in 1994. Comparisons of the measurements by the UARS and ER-2 instruments during SPADE must be made whenever possible in order to bridge this gap in time.

The HALOE and MLS instruments on UARS may (presumably) still be operating in 1994. Measurements include those for: O_3 , NO , NO_2 , H_2O , CH_4 , ClO , and HCl . This observational data set includes radicals, reservoir species, and tracers.

The global observations over several seasons are more easily compared to assessment model results than in situ observations are. For this reason, such observations are preferred by assessment modelers, even though satellite observations tend to have lower accuracy and altitude

resolution in the lower stratosphere than in situ observations do. One of our goals is to learn to best use these two types of observations.

MAESA EXPERIMENT PLAN

MAESA will consist of two components: ER-2 flights associated with ASHOE and Perseus A (or helium-filled balloon) flights.

ER-2 Flights

Flights will be out of four locations:

1. Moffett Field, California (37°N, 122° W);
2. Barber's Point NAS, Hawaii (20°N, 155°W);
3. Nadi Airport, Fiji (17°S, 179°E);
4. Christchurch, New Zealand (44°S, 172°E).

Flights will consist of:

1. One to three test flights out of Moffett Field in mid-February; *The flights will be planned later, after SPADE.*
2. Four transits (3 legs) between Moffett Field and Christchurch; *The estimated flight path is shown in Figure 8.*
3. A stop-over flight from either Hawaii or Fiji during each transit; *The purpose of these flights, which may be only a few hours long, is to attain measurements at higher altitudes in the tropics than are possible on the transit legs.*
4. One flight north from Christchurch during each of the four phases of ASHOE, to be made as flights of opportunity. *These flights will define the trace gas distributions in the southern middle latitudes — just as the flights south from Bangor did during AASE II.*

The estimated flight times for the transit flight legs are (J. Barrilleaux, private communication, 1993):

1. Moffett Field to Barber's Point: 6 hrs
2. Barber's Point to Nadi: 7.5 hrs
3. Nadi to Christchurch: 4.5 hrs

Because of the stop-over flight on each transit, the total number of days for a transit will be 8. Thus, the total number of days devoted to HSRP that are not required by ASHOE is 8, two for each transit.

Facilities

Hangar facilities are available for all the sites. Laboratory space for the ER-2 instruments is being developed at Moffett Field and at Christchurch. Hangar space only will be provided for the Hawaii and Fiji transit stops, even though a stop-over flight will occur on each of the four transits between Moffett Field and Christchurch. The scientists' activities will thus be limited to maintenance and preparation of the instruments for either the stop-over or the transit flight. Go-no-go criteria for the transit flights will be developed with the PIs prior to 1994.

Perseus A

A tropical deployment of Perseus is planned for October and early November from Darwin, Australia. The change in the temperatures at the tropical tropopause and the southward movement of the ITCZ toward Darwin are the greatest during this period. Thus, observations over this 5-week period permits sampling of a wide cross section of the tropical lower stratosphere from one site.

Perseus will be deployed in middle latitudes at Dryden to coincide with flights of the ER-2 out of Moffett Field. These deployments will be in mid-February at the same time as the ER-2 test flights from ASHOE/MAESA and in July at the same time as the short test flight and departure of the ER-2 for Hawaii.

Flights will consist of:

1. Four flights (two of each payload) from Dryden in mid-February (these will be engineering/science flights);
2. Four flights (two of each payload) from Dryden in mid-July;
3. Ten to fifteen flights from Darwin, Australia.

Because Perseus A must remain in radio contact with the control station, it can cover only about 2 degrees of latitude from the launch site. Perseus operations will thus be conducted as if it were a balloon platform, and flights will consist of a scan up to 25 km and back. This simplified flight planning in the tropics results from the expected homogeneity of the trace gas distributions over the 2 degrees of latitude that can be covered by Perseus; by the lack of a good observational meteorological network to guide the meteorological forecasts accurately; and by the need to keep operations simple for the new Perseus platform and new instruments on a foreign deployment.

Some flight planning considerations for Perseus flights in the tropics are:

1. weather conditions, primarily lack of extensive convective activity;
2. low temperatures at the tropopause, as determined by radiosondes and lidar;
3. types of stratospheric airmasses that are forecast to move into the range of Perseus.

The flights at middle latitudes will also consist only of vertical scans to 25 km altitude. However, the flight planning considerations will include:

1. coincidences with ER-2 flight paths;
2. operational constraints such as wind and poor weather;
3. types of stratospheric airmasses that are forecast to move into the range of Perseus.

Sites and Facilities

These criteria for the tropical deployment of Perseus are met by the site at Darwin, Australia. It was the location of the STEP mission in 1987, and is known to have good facilities. Furthermore, convective storms that could endanger Perseus can be tracked by the excellent radar facility there. The facilities at Dryden should meet the needs of the aircraft and the investigators for the two deployments in middle latitudes.

The Helium-Filled Balloon Option

If for some reason the Perseus aircraft or its key instruments are not ready for deployment in 1994, then helium-filled balloons will have to be used for the platforms for the higher altitude measurements. We will not know if this option is necessary until after the Perseus test flights in

mid-to-late 1993. Thus, we will pursue any details of the planning until after these test flights. However, we have some preliminary ideas about deployment.

The flights will consist of:

1. two flights (one engineering, the second science) from Ft. Sumner, New Mexico in July;
2. two flights from Caico, Brazil in October.

Sites and Facilities

Complete balloon and laboratory facilities already exist in Ft. Sumner, New Mexico. The site in Brazil was to be used for UARS correlative measurements balloon flights in March 1993, but this activity was canceled. The personnel from the National Scientific Balloon Facility have examined this site, however, and could develop it if necessary.

MAESA PRELIMINARY FLIGHT SCHEDULE

The preliminary flight schedule for the ER-2 and Perseus components of MAESA are given in the MAESA Timetable. The timing of the ER-2 flights are fixed by the requirements of ASHOE. The timing of the Perseus component is dependent on the coincidences with the ER-2 flights and the stratospheric conditions in October in Darwin. An expanded calendar for ASHOE/MAESA is given in Appendix A.

Meteorological Support

ER-2

The timing of the transit flights is dictated by the requirements of ASHOE, and the flight plans, maximum altitude cruise climbs, are dictated by the requirements of flight operations. Meteorological support for these flights is in the form of satellite imagery, trajectories, and other dynamical and meteorological analyses. Flight planning capabilities, similar to those provided by Goddard Space Flight Center during the AASE II mission, will be required for the test flights from Ames and the flights out of Hawaii or Fiji.

Perseus

The required meteorological support for Perseus is similar to that for the ER-2, only perhaps not quite as extensive.

Additional Meteorological Support

The need for additional radiosonde launches must be assessed, particularly for the tropical flights of all the platforms where observational meteorological data will be otherwise scarce. Additional sondes may be necessary for flight planning for the ER-2 flying north out of Christchurch and out of Hawaii or Fiji. Otherwise, they may be necessary for the analyses of the meteorological conditions that will be required for all the flights. They may also be necessary for the flight planning and meteorological analyses for either Perseus or balloons in the tropics.

Data Reduction and Submission to the Archives

Traditionally, the data submission protocol has been relaxed for transit flights to the polar missions. On occasion, data from these flights have not been submitted to the archives until well after the mission was completed. However, for ASHOE and MAESA, the data taken on the transit

flights may be important for planning the flight north from Christchurch or for planning the stopover flight in Hawaii or Fiji.

Thus, a plan for submission of data to the archives needs to be developed by the principal investigators. The most reasonable possibility is the submission of transit flight data to the archives within a week of arrival at either Christchurch or Moffett Field. Although no immediate action is required on this subject, it needs some careful thought.

We see no need to have real-time data transmission capabilities from the Perseus or balloon sites of this program to either Moffett Field or Christchurch. Data from Perseus or from balloon flights would be submitted to the archives on the same schedule as is developed for the ER-2. Thus, Perseus PIs should be involved in the discussions on data submission protocol.

Science Team

For the most part, the science team for ASHOE should also be the science team for MAESA. However, the HSRP program has some special, pressing requirements that will require additional analytical capabilities on site. First, the AESA assessment is mandated for early 1995. Data from MAESA must be analyzed, understood, and incorporated into the assessment models, which then must be run in a very short time. It is therefore important that at least one member of the AESA assessment team be present during all of MAESA and ASHOE to act as the eyes and ears of this community. At the appropriate time after the flights (as determined by the science team), this person can then help speed the assimilation of these data sets by the other groups involved in the assessment process. Very likely, more process-oriented models will be required for analysis of the data and the improvement of the assessment models. These scientists who use such models may also be required to be present in the field. Second, the MAESA mission may also need modeling capability associated with the Perseus or balloon part of the mission. However, it is not clear that such capability must be present with Perseus or the balloons. Instead, Perseus or balloon data should be submitted within the agreed time limits to the main archives for dissemination to the MAESA and ASHOE participants.

Table 1. Measurements from the ER-2

	Measurement	Principal Investigator
<i>Reactive Species</i>	NO	Fahey (NOAA/AL)
	NO ₂	Webster (JPL); Fahey (NOAA/AL)
	ClO and BrO	Anderson and Stimpfle (Harvard)
	OH and HO ₂	Anderson and Wennberg (Harvard)
<i>Reservoir Species</i>	NO _y	Fahey (NOAA/AL)
	HNO ₃	Webster (JPL)
	HCl	Webster (JPL)
<i>Tracer Species</i>	O ₃	Proffitt (NOAA/AL-CIRES)
	H ₂ O	Kelly (NOAA/AL)
	N ₂ O	Loewenstein (NASA/Ames), Webster (JPL), Elkins (CMDL)
	CH ₄	Webster (JPL)
	CFC11, 113, 12, HCFC22	Elkins (NOAA/CMDL)
	CO ₂	Boering (Harvard)
	condensation nuclei	Wilson (U. Denver)
	aerosols (PCAS)	Wilson (U. Denver)
	aerosols (FSSP)	Dye, Baumgardner (NCAR)
	aerosols (impactor)	Pueschel (NASA Ames)
<i>Environment</i>	pressure	Chan (NASA Ames)
	temperature	Chan (NASA Ames)
	winds	Chan (NASA Ames)
	temperature profile	Gary (JPL)
	UV flux	McElroy (AES, Canada)

Table 2. Measurements from Perseus A

Measurement	Investigator	Weight (kg)	Power (watts)
ClO, BrO, O ₃ , P, & T	Anderson	48	600
NO and NO _y	Wofsy	35	350
N ₂ O and CH ₄	Loewenstein (Argus)	20	100
N ₂ O, CH ₄ , & H ₂ O	Webster (ALIAS II)	30	200
<i>Telemetry & data system</i>		6	50
<i>Parachute</i>		15	0

Table 3. A Proposed Timetable for MAESA/ASHOE

Deployment	Dates in 1994	Location/Path	Durations/# of Flights
ER-2			
Test flights	mid-February -- TBD	Moffett Field	14 days / 3 flights
MAESA 1	20 - 28 March	Moffett Field to Christchurch	9 days / 4 flights
ASHOE 1	29 March - 12 April	Christchurch	15 days / 3 - 5 flights
ASHOE 2	24 May - 6 June	Christchurch	14 days / 3 - 5 flights
MAESA 2	8 - 13 June	Christchurch to Moffett Field	7 days / 4 flights
MAESA 3	16 - 24 July	Moffett Field to Christchurch	9 days / 4 flights
ASHOE 3	25 July - 8 August	Christchurch	15 days / 3 - 5 flights
ASHOE 4	8 - 22 October	Christchurch	15 days / 3 - 5 flights
MAESA 4	24 - 29 October	Christchurch to Moffett Field	7 days / 4 flights
Totals			105 days / 35 flights
Perseus A			
Test flights	mid - February -- TBD	Dryden	14 days / 4 - 6 flights
Midlatitude	8 - 22 July	Dryden	14 days / 4 - 6 flights
Tropical	1 October - 5 November	Darwin, Australia	36 days / 12-15 flights
Totals			64 days / 24 flights

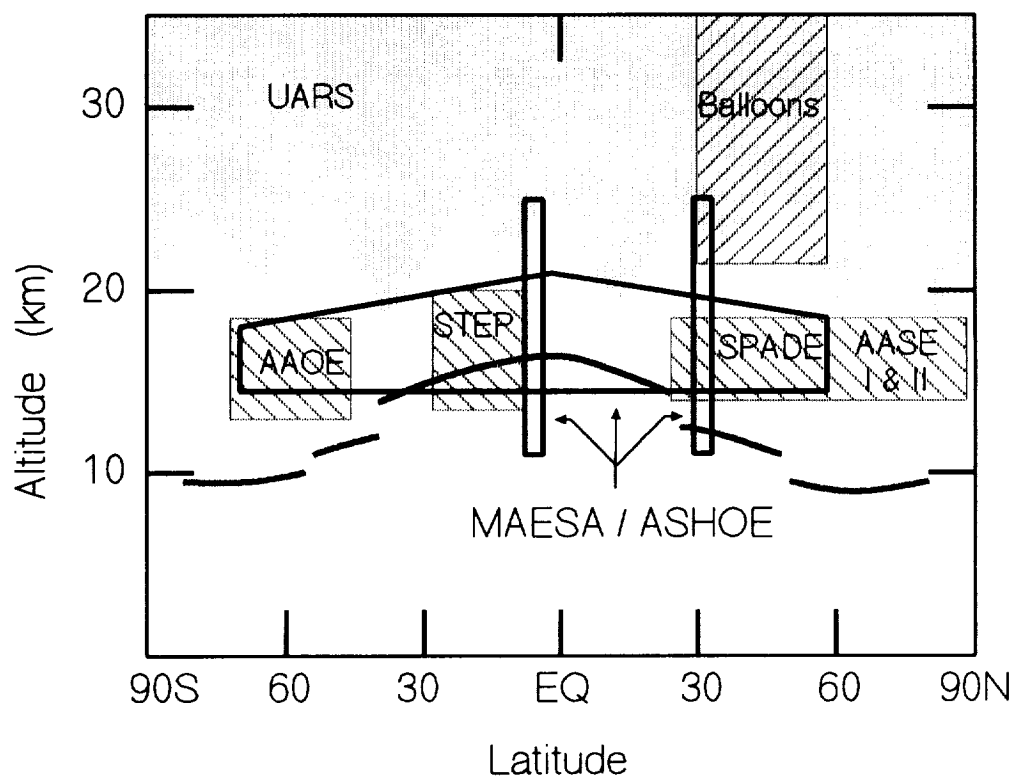


Figure 1. Schematic of the spatial coverage of the stratosphere provided by MAESA and ASHOE in 1994. The wedge-shaped box is covered by the ER-2; the two vertical boxes by Perseus or balloons. Striped boxes show the approximate locations of measurements from STEP, AAOE, AASE I & II, SPADE, and balloons. The shaded area indicates measurements from UARS -- the bottom is jagged to indicate the uncertainty in the lower altitude limits for the UARS instruments.

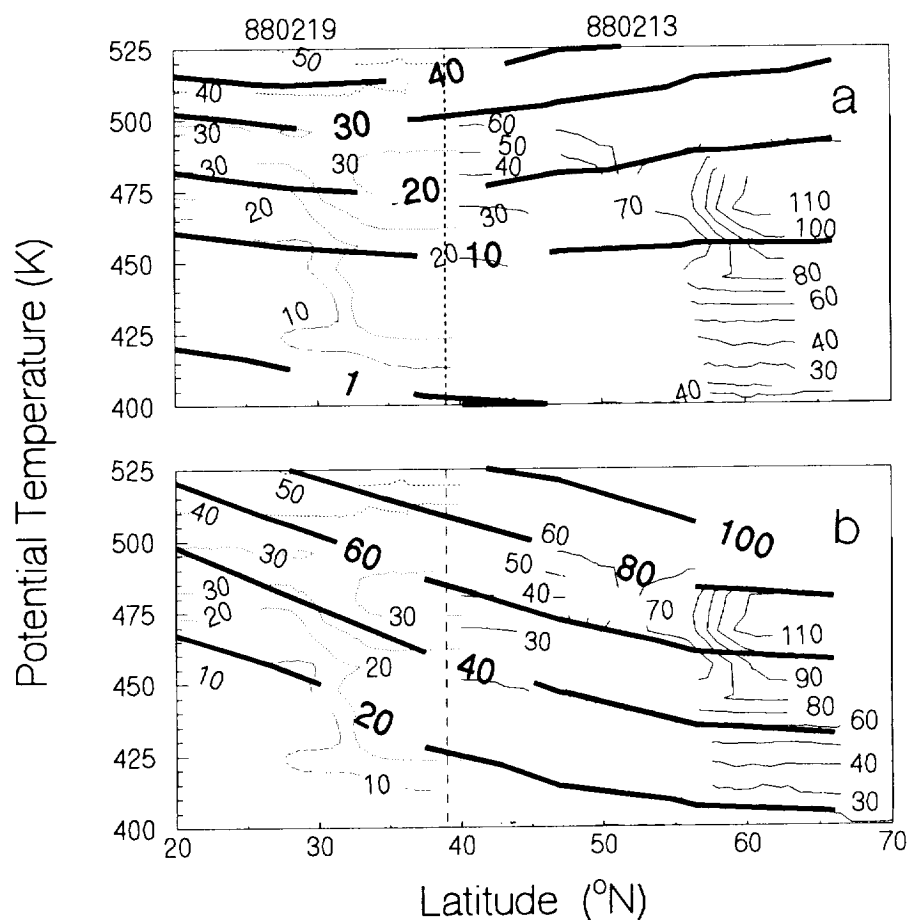


Figure 2. Comparisons between the observed ClO mixing ratios (pptv) in February 1988 with the results of model calculations (heavy lines) that contain gas-phase chemistry only (a) and those that contain currently known heterogeneous chemistry ($\text{N}_2\text{O}_5 + \text{H}_2\text{O}$) on sulfate aerosols (b). ClO data from Feb 19 (21°N to 38°N) and Feb 13 (39°N to 61°N) were separately converted to contours and then plotted together, separated by a vertical dotted line. These few ClO observations are better simulated at latitudes >30°N by the model with heterogeneous chemistry on sulfate aerosols and at latitudes <30°N by the model with only gas-phase chemistry (King et al., 1991).

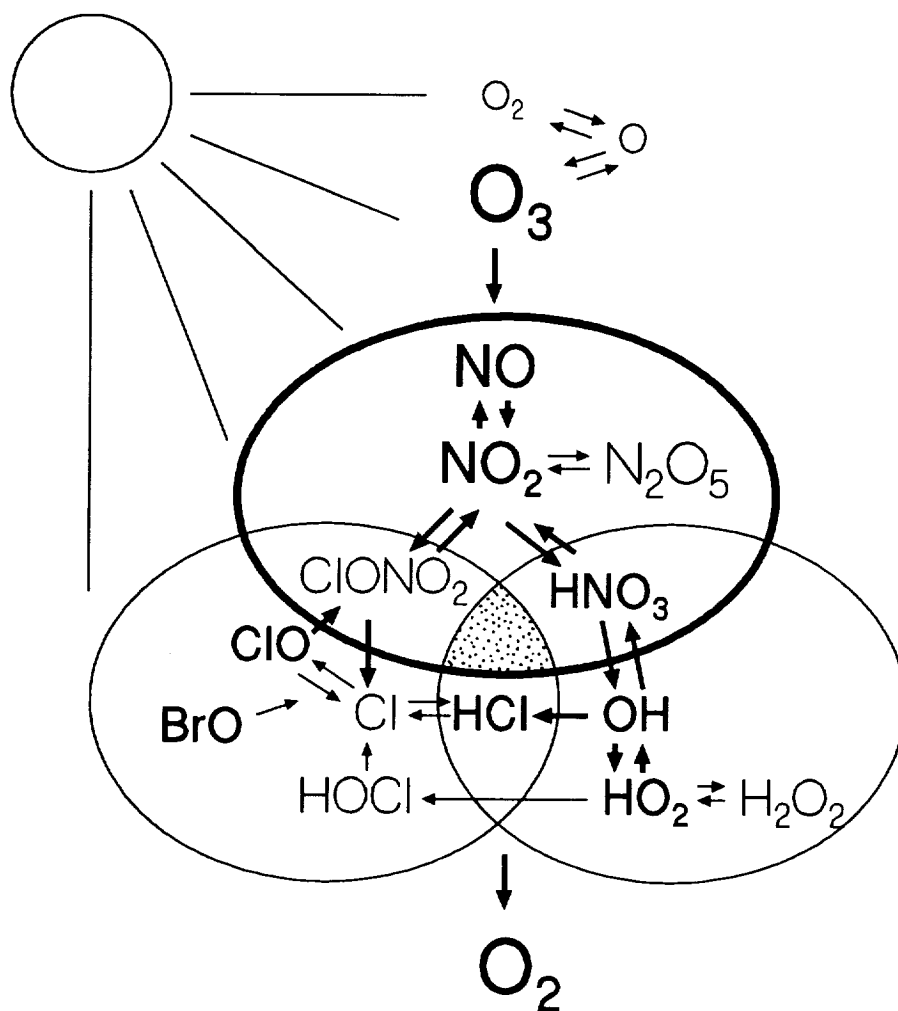


Figure 3. A schematic of stratospheric photochemistry, showing the links among the oxygen, nitrogen, halogen, and hydrogen chemical families. ER-2 instruments can measure the chemical species shown in bold print. These measurements enable the study of the photochemical processes that are shown with bold arrows. The central, dotted area indicates heterogeneous chemistry. The highlighted ellipse indicates the importance of the nitrogen family in assessing the effects of HSCTs.

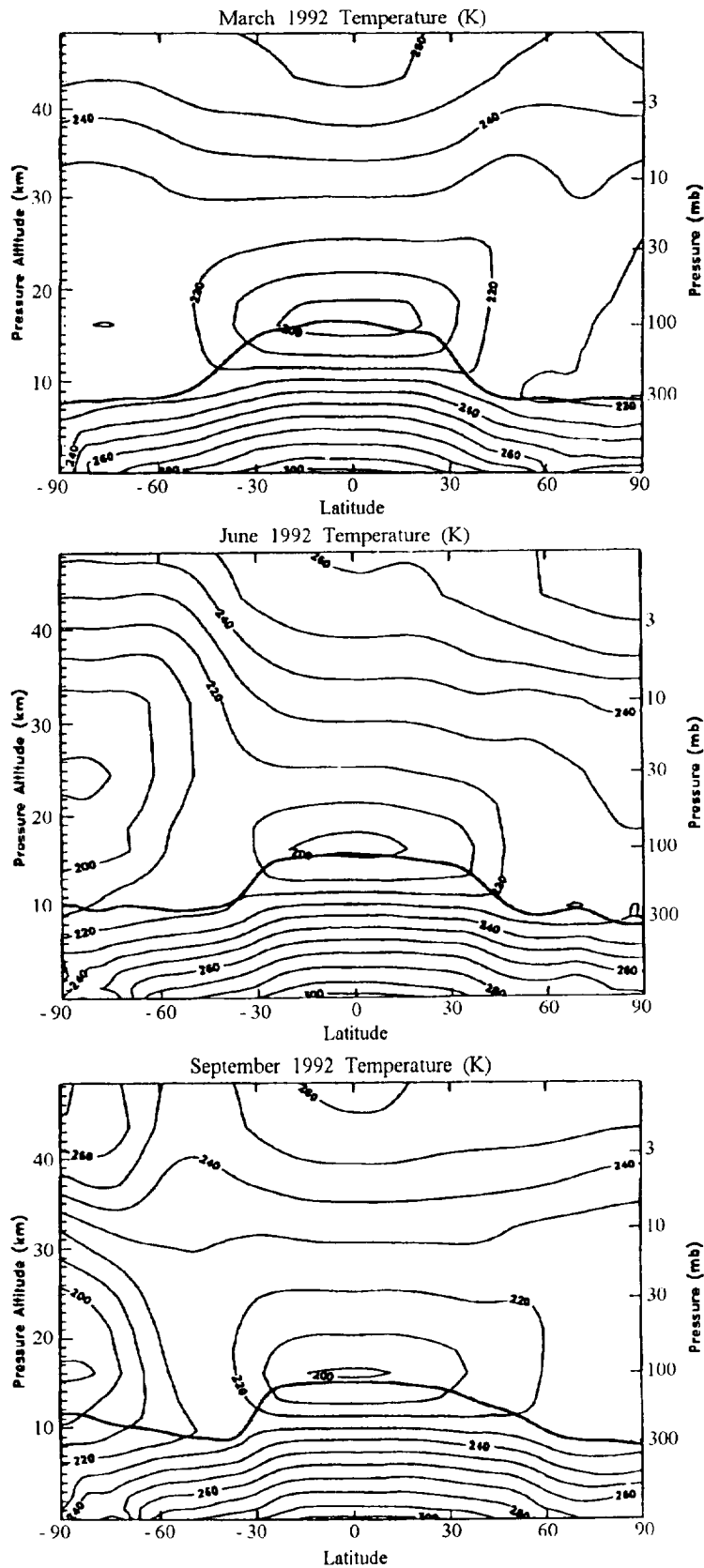


Figure 4. The monthly mean values of the tropopause height and potential temperature at a longitude of 185°E for (a.) March 1992, (b) June 1992, and (c) September, 1992. Vertical scales are pressure altitude (km) and pressure (mb). Transit flights between Moffett Field and Christchurch will occur in these months at longitudes near 185°E. Note that the ER-2 transit flight ceiling of 64,000 ft (19.5 km) is only a few kilometers above the tropopause. (P. Newman, private communication, 1992).

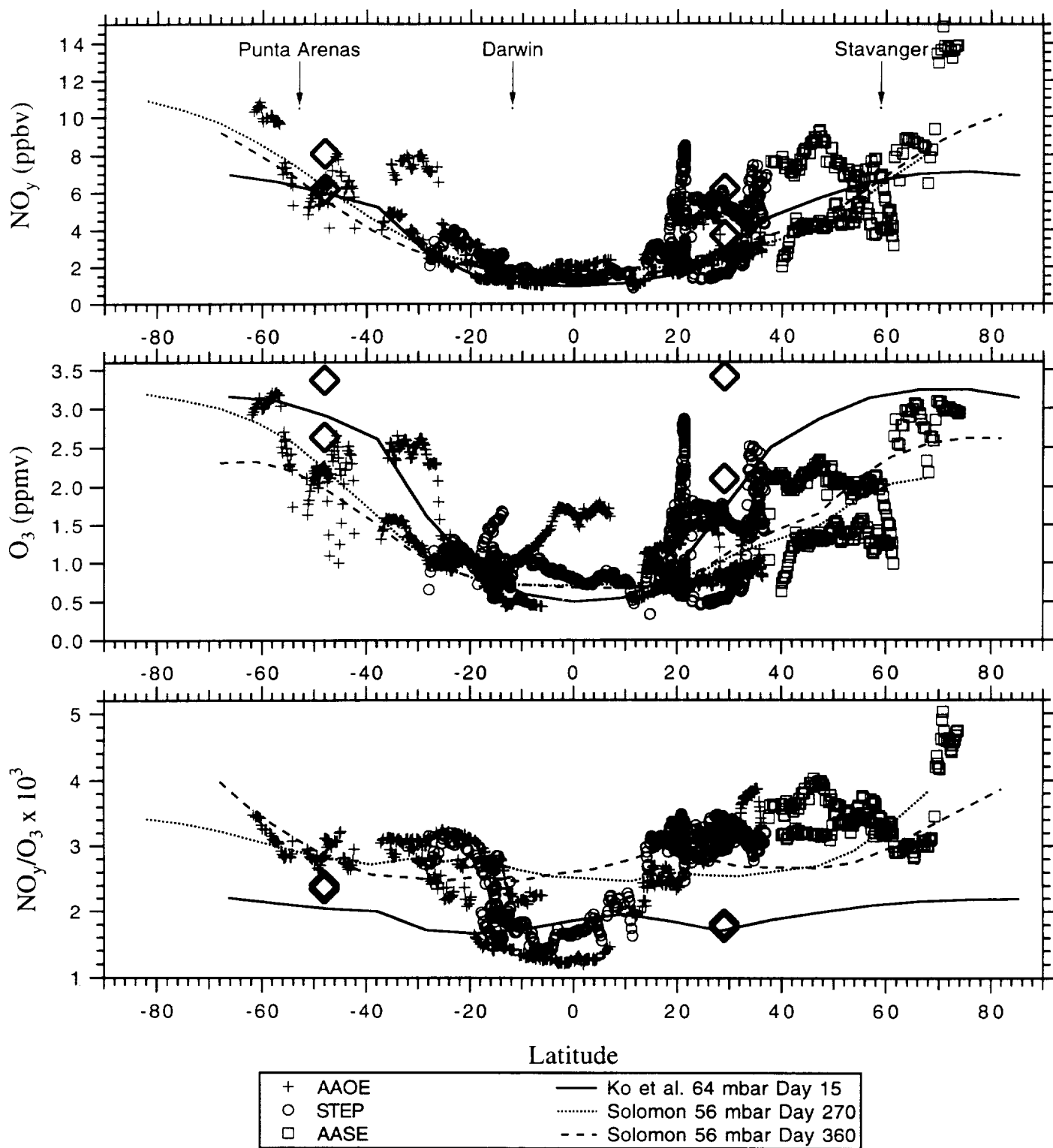


Figure 5. Comparisons of measurements and model results for NO_y , O_3 , and NO_y/O_3 plotted against latitude. The ER-2 observations come from all seasons and potential temperatures greater than 430 K. ATMOS observations (diamonds) are added for comparison. Model results come from Solomon and Garcia and Ko et al. (Murphy et al., 1993)

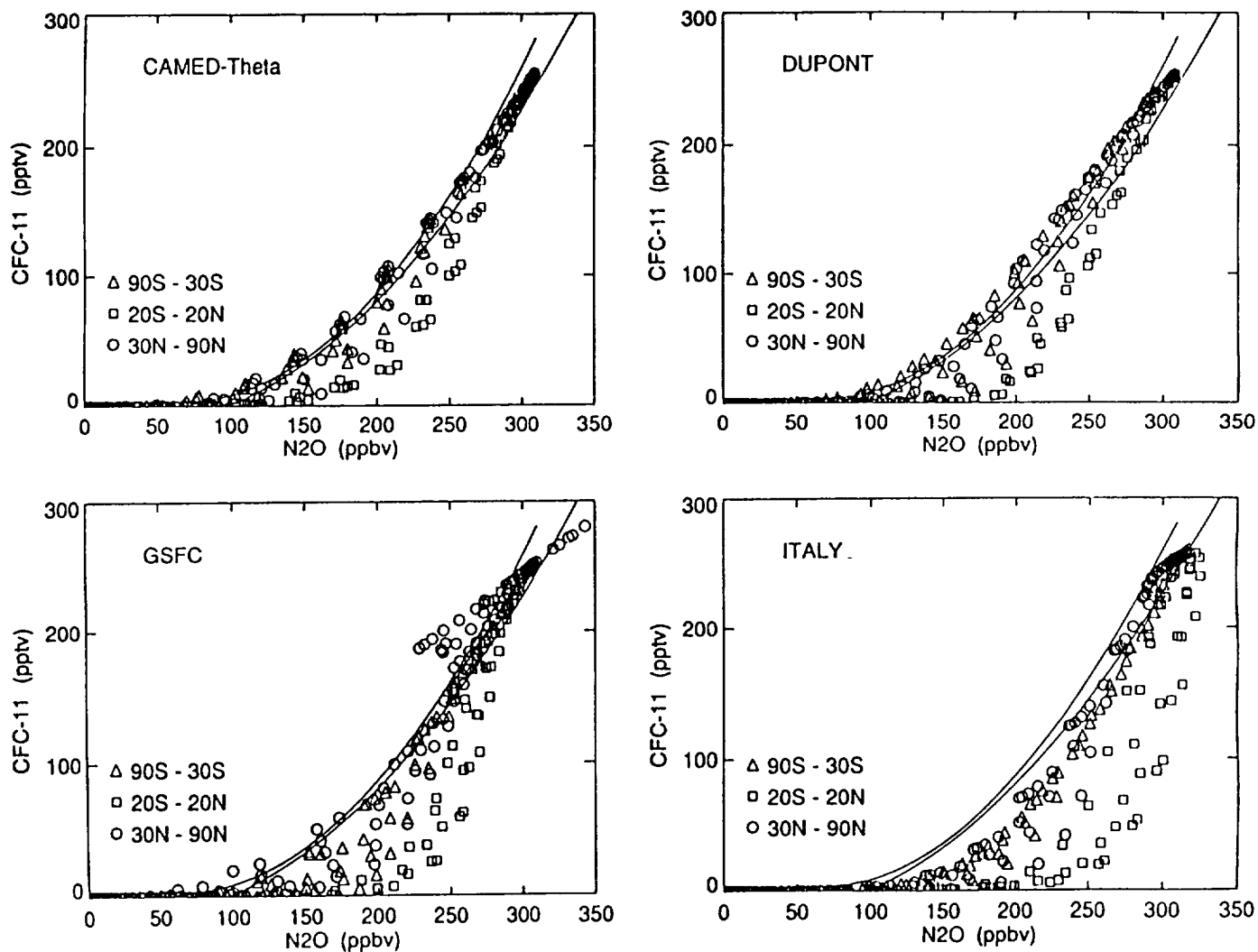


Figure 6. Comparison of observed correlation plot for N_2O and $CFCI_3$ (solid lines) with the results from four 2-D assessment models. The upper solid line is the fit to the ACATS measurements from AASE II and the lower solid line is the fit from all observations. Note the large modeled differences in the correlation at low latitudes and at the middle to high latitudes. (Remsberg and Prather, 1992).

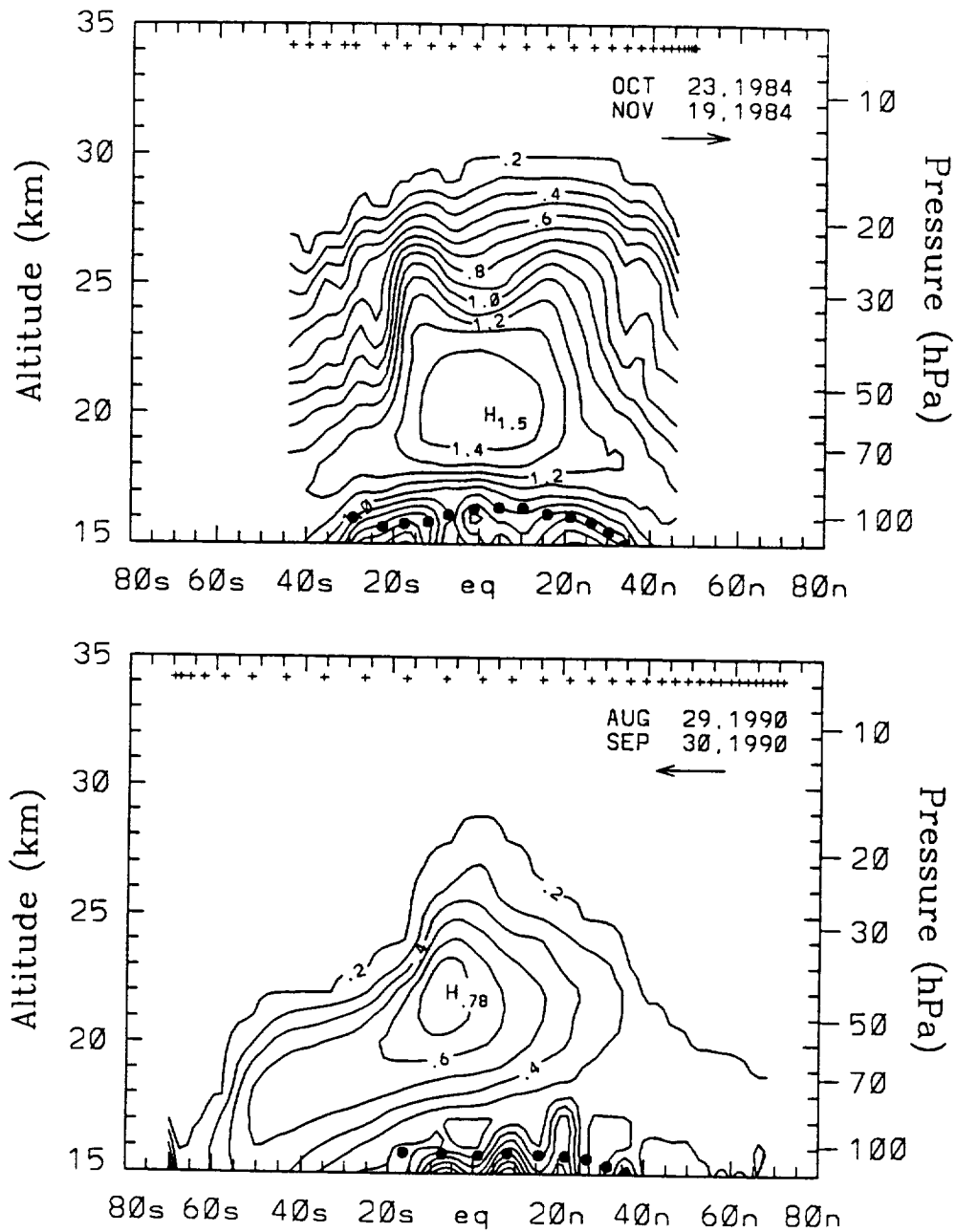


Figure 7. (a) The 1-mm aerosol extinction ratio (\log_{10}) from SAGE II for September 1990. The 50 mb winds at Singapore are westerly. (b) The same extinction for November 1984, when the 50-mb winds at Singapore were easterly. The tropopause is marked as a heavy dotted line. Note the large differences in the spreading of the aerosol between the two phases. (Trepte and Hitchman, 1992).

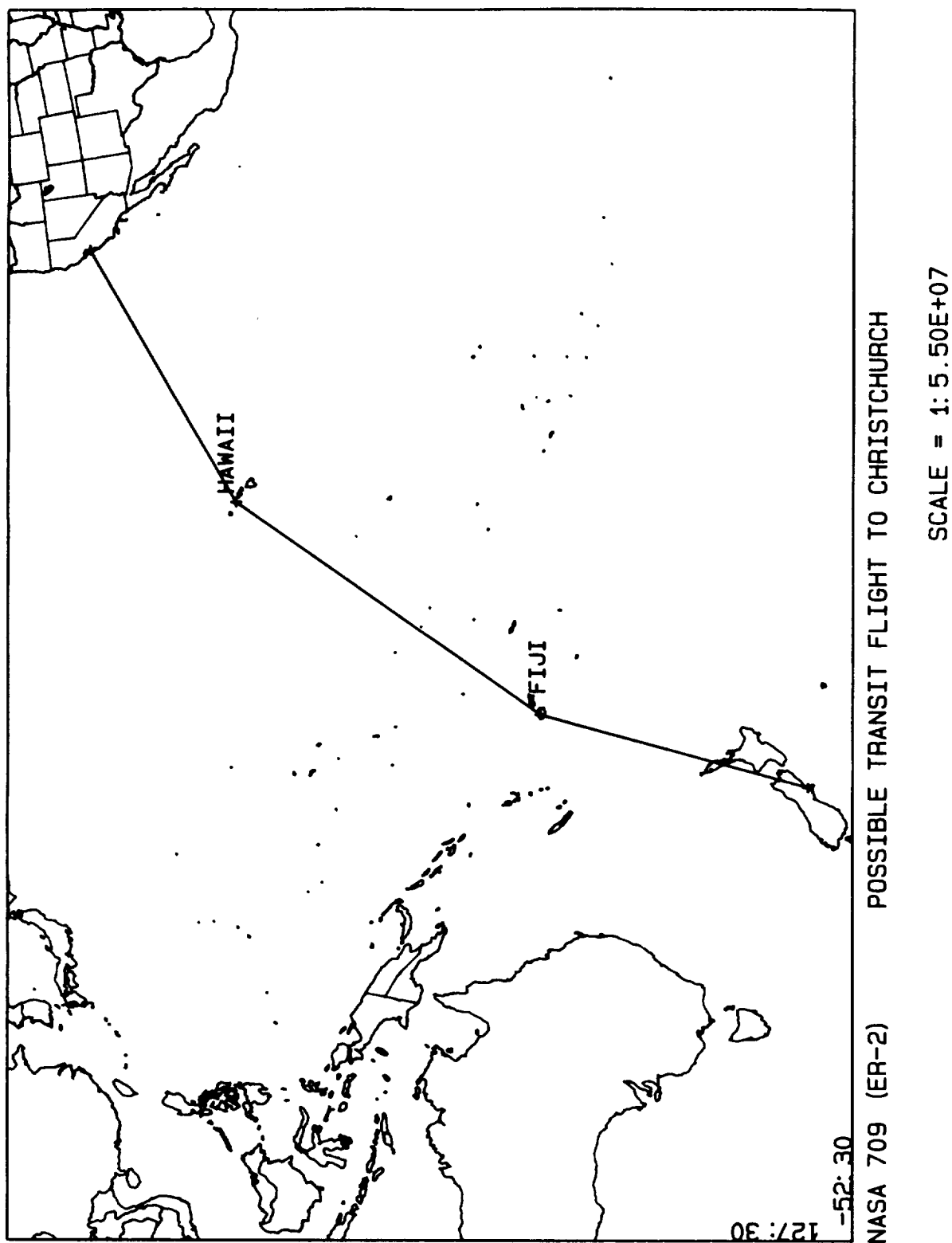








Figure 8. The proposed transit flight route between Moffett Field and Christchurch, through Hawaii and Fiji. (P. Hathaway, private communication, 1992).

Appendix A

PROPOSED CALENDAR for MAESA

 = ER-2
  = Perseus
  = tests
 = ASHOE
  = travel
  = meeting

	Sunday	Monday	Tuesday	Wed'day	Thursday	Friday	Saturday
January	2	3	4	5	6	7	8
	9	10	11	12	13	14	15
	16	17	18	19	20	21	22
	23	24	25	26	27	28	29
	30	31					
February			1	2	3	4	5
	6	7	8	9	10	11	12
	13	14	15	16	17	18	19
	20	21	22	23	24	25	26
	27	28					
March			1	2	3	4	5
	6	7	8	9	10	11	12
	13	14	15	16	17	18	19
	20	21	22	23	24	25	26
	27	28	29	30	31		
April						1	2
	3	4	5	6	7	8	9
	10	11	12	13	14	15	16
	17	18	19	20	21	22	23
	24	25	26	27	28	29	30
May	1	2	3	4	5	6	7
	8	9	10	11	12	13	14
	22	23	24	25	26	27	28

Appendix A

June	29	30	31				
				1	2	3	4
	5	6	7	8	9	10	11
	12	13	14	15	16	17	18
	19	20	21	22	23	24	25
	26	27	28	29	30		
						1	2
July	3	4	5	6	7	8	9
	10	11	12	13	14	15	16
	17	18	19	20	21	22	23
	24	25	26	27	28	29	30
	31						
		1	2	3	4	5	6
	7	8	9	10	11	12	13
August	14	15	16	17	18	19	20
	21	22	23	24	25	26	27
					1	2	3
	4	5	6	7	8	9	10
	11	12	13	14	15	16	17
	18	19	20	21	22	23	24
	25	26	27	28	29	30	
September							1
	2	3	4	5	6	7	8
	9	10	11	12	13	14	15
	16	17	18	19	20	21	22
	23	24	25	26	27	28	29
	30	31					
			1	2	3	4	5
October	13	14	15	16	17	18	19
November							

REFERENCES

- Avallone, L. M., D. W. Toohey, W. H. Brune, R. J. Salawitch, In situ measurements of ClO and ozone: implications for heterogeneous chemistry and midlatitude ozone loss, submitted to *Geophys. Res. Lett.*, 1993.
- Brune, W. H., D. W. Toohey, S. A. Lloyd, and J. G. Anderson, The sunrise and sunset variation of ClO in the lower stratosphere, *Geophys. Res. Lett.*, 17, 509, 1990.
- Considine, D. B., A. R. Douglass, and R. S. Stolarski, Heterogeneous conversion of N_2O_5 to HNO_3 on background stratospheric aerosols: Comparisons of model results with data, *Geophys. Res. Lett.*, 19, 397, 1992.
- Douglass, A. R., R. B. Rood, C. J. Weaver, M. C. Cerniglia, and K. F. Brueske, Implications of 3-D tracer studies for 2-D assessments of the impact of supersonic aircraft on stratospheric ozone, to appear in *J. Geophys. Res.*, 1993.
- Dye, J. E., D. Baumgardner, B. W. Gandrud, S. R. Kawa, K. K. Kelly, M. Loewenstein, G. V. Ferry, K. R. Chan, and B. L. Gary, Particle size distributions in Arctic polar stratospheric clouds, growth and freezing of sulfuric acid droplets, and implications for cloud formation, *J. Geophys. Res.*, 97, 8015, 1992.
- Fahey, D. W., S. Solomon, S. R. Kawa, M. Loewenstein, J. R. Podolske, S. E. Strahan, and K. R. Chan, A diagnostic for denitrification in the winter polar stratosphere, *Nature*, 345, 698-702, 1990.
- Fahey, D. W., S. R. Kawa, and K. R. Chan, Nitric oxide measurements in the Arctic winter stratosphere, *Geophys. Res. Lett.*, 17, 489, 1990.
- Fahey, D. W., S. R. Kawa, E. L. Woodbridge, P. Tin, J. C. Wilson, H. H. Jonsson, J. E. Dye, D. Baumgardner, S. Bormann, D. W. Toohey, L. M. Avallone, M. H. Proffitt, J. J. Margitan, R. J. Salawitch, S. C. Wofsy, M. K. W. Ko, D. E. Anderson, M. R. Schoeberl, and K. R. Chan, In situ measurements constraining the role of reactive nitrogen and sulphate aerosols in mid-latitude ozone depletion, to appear in *Nature*, 1993.
- Kawa, S. R., D. W. Fahey, S. Solomon, W. H. Brune, M. H. Proffitt, D. W. Toohey, D. E. Anderson, L. C. Anderson, and K. R. Chan, Interpretation of aircraft measurements of NO, ClO, and O₃ in the lower stratosphere, *J. Geophys. Res.*, 95, 18,597, 1990.
- Kawa, S. R., D. W. Fahey, L. E. Heidt, W. H. Pollock, S. Solomon, D. E. Anderson, M. Loewenstein, M. H. Proffitt, J. J. Margitan, K. R. Chan, Photochemical partitioning of the reactive nitrogen and chlorine reservoirs in the high-latitude stratosphere, *J. Geophys. Res.*, 97, 7905, 1992.
- Kawa, S. R., R. A. Plumb, and U. Schmidt, Correlation of long-lived species in simultaneous observations, *The Atmospheric Effects of Stratospheric Aircraft: Report of the 1992 Models and Measurements Workshop*, M. J. Prather and E. E. Remsberg, Eds., Reference Publication 1292, NASA, Washington, D.C., 1993.
- Kelly, K. K., A. F. Tuck, D. M. Murphy, M. H. Proffitt, D. W. Fahey, R. L. Jones, D. S. McKenna, M. Loewenstein, J. R. Podolske, S. E. Strahan, G. V. Ferry, K. R. Chan, J. F. Vedder, G. L. Gregory, W. D. Hynes, M. P. McCormick, E. V. Browell, and L. E. Heidt, Dehydration in the lower Antarctic stratosphere during late winter and early spring 1987, *J. Geophys. Res.*, 94, 11,317, 1989.

- King, J. C., W. H. Brune, D. W. Toohey, J. M. Rodriguez, W. L. Starr, and J. F. Vedder, Measurement of ClO and O₃ from 21°N to 61°N in the lower stratosphere during February 1988: Implications for heterogeneous chemistry, *Geophys. Res. Lett.*, 18, 2273, 1991.
- McCormick, M. P., and E. E. Veiga, SAGE II measurements of early Pinatubo aerosols, *Geophys. Res. Lett.*, 19, 155, 1992.
- McElroy, M. B., R. J. Salawitch, and K. Minschwaner, The changing stratosphere, *Planet. Space Sci.*, 40, 373, 1992.
- Murphy, D. M., D. W. Fahey, M. H. Proffitt, S. C. Liu, K. R. Chan, C. S. Eubank, S. R. Kawa, and K. K. Kelly, Reactive nitrogen and its correlation with ozone in the lower stratosphere and upper troposphere, *J. Geophys. Res.*, in press, 1992.
- Plumb, R. A., and M. K. W. Ko, Interrelationships between mixing ratios of long-lived stratospheric constituents, *J. Geophys. Res.*, 97, 10,195, 1992.
- Prather, M. J., and H. Wesoky, Eds., *The Atmospheric Effects of Stratospheric Aircraft: A First Program Report*, NASA Reference Publication 1272, NASA, Washington D. C., 1992.
- Remsberg, E. E., and M. J. Prather, Eds., *The Atmospheric Effects of Stratospheric Aircraft: Report of the 1992 Models and Measurements Workshop*, Reference Publication 1292, NASA, Washington, D.C., 1993.
- Rood, R. B., A. R. Douglass, and C. Weaver, Tracer exchange between tropics and middle latitudes, *Geophys. Res. Lett.*, 19, 805, 1992.
- Toohey, D. W., L. M. Avallone, M. R. Schoeberl, P. A. Newman, L. R. Lait, D. W. Fahey, E. L. Woodbridge, C. R. Webster, R. D. May, and J. G. Anderson, Observations of the temporal evolution of reactive chlorine in the northern hemisphere stratosphere, submitted to *Science*, 1993.
- Trepte, C. R., and M. H. Hitchman, Tropical stratospheric circulation deduced from satellite aerosol data, *Nature*, 355, 626, 1992.
- Tuck, A., Airborne Southern Hemisphere Ozone Mission, ER-2 Science and Support Document, March, 1992 Draft.
- Tuck, A. F., T. Davies, S. J. Hovde, M. Noguera-Alba, D. W. Fahey, S. R. Kawa, K. K. Kelly, D. M. Murphy, M. H. Proffitt, J. J. Margitan, M. Loewenstein, J. R. Podolske, S. E. Strahan, and K. R. Chan, Polar stratospheric cloud processed air and potential vorticity in the northern hemisphere lower stratosphere at mid-latitudes during winter, *J. Geophys. Res.*, 97, 7883, 1992.
- Webster, C. R., R. D. May, R. Toumi, and J. A. Pyle, Active nitrogen partitioning and the nighttime formation of N₂O₅ in the stratosphere: Simultaneous measurements of NO, NO₂, HNO₃, O₃, and N₂O using the BLISS diode laser spectrometer, *J. Geophys. Res.*, 95, 13,851, 1990.

Wilson, J. C., H. H. Jonsson, C. A. Brock, D. Baumgardner, J. E. Dye, S. Borrmann, L. R. Poole, D. C. Woods, R. J. DeCoursey, M. Osborn, M. C. Pitts, K. K. Kelly, K. R. Chan, G. V. Ferry, M. Loewenstein, J. R. Podolske, A. Weaver, D. W. Toohey, and L. M. Avallone, In situ observations of the stratospheric aerosol following the eruption of Mt. Pinatubo, submitted to *Science*, 1993.

WMO, *Stratospheric Assessment of Ozone Depletion: 1991*, Global Ozone Research and Monitoring Project, Report No. 25, WMO, Geneva, Switzerland, 1992.

Chapter 3

Emissions Scenarios Development: Report of the Emissions Scenarios Committee

Donald J. Wuebbles
Lawrence Livermore National Laboratory
Livermore, CA

Donald Maiden and Robert K. Seals, Jr.
Langley Research Center
National Aeronautics and Space Administration
Hampton, VA

Steven L. Baughcum
Boeing Commercial Airplane Group
Seattle, WA

Munir Metwally and Alan Mortlock
McDonnell Douglas Corporation
Long Beach, CA

The report of the Emissions Scenarios Committee is divided into four parts to reflect the significant accomplishments during the last year in developing the database for the 1990 and 2015 fleet emissions scenarios for the 1993 HSRP/AESA Interim Assessment. Subchapter 3–1 provides an overview of the scenarios developed and reviews the basic methodology and requirements for preparation of the database. Subchapter 3–2 describes the model and scenarios database development at Boeing Commercial Airplane Group. Subchapter 3–3 similarly describes the model and scenarios database development at McDonnell Douglas. Subchapter 3–4 describes the combined scenarios database, describes validation studies and consistency checks on the database, evaluates the strengths and weaknesses in the database developed, and describes future needs.

Subchapter 3-1

Emissions Scenarios Development: Overview and Methodology

Donald J. Wuebbles
Lawrence Livermore National Laboratory
Livermore, CA

Steven L. Baughcum
Boeing Commercial Airplane Group
Seattle, WA

Munir Metwally
McDonnell Douglas Corporation
Long Beach, CA

Robert K. Seals, Jr.
Langley Research Center
National Aeronautics and Space Administration
Hampton, VA

INTRODUCTION

Analyses of scenarios of past and possible future emissions are an important aspect of assessing the potential environmental effects from aircraft, including the proposed high-speed civil transports (HSCTs). The development of a detailed three-dimensional database that accurately represents the integration of all aircraft emissions along realistic flight paths for such scenarios requires complex computational modeling capabilities. Within the NASA High-Speed Research Program, the Emissions Scenarios Committee provides a forum for identifying the required scenarios and evaluating the resulting database being developed with the advanced emissions modeling capabilities at the Boeing Company and McDonnell Douglas Corporation. This chapter describes the scenarios and resulting database that have been developed for the 1993 NASA HSRP interim assessment.

1993 INTERIM ASSESSMENT SCENARIOS

It is premature to base scenarios on actual HSCT aircraft designs, as such designs are only in conceptual stages. However, the goal in the scenario development was to represent flight patterns and aircraft specifications as realistically as possible. Prior scenario databases for aircraft emissions have greatly simplified the emissions from aircraft. For example, the earlier scenarios evaluated by Boeing (1990) determined emissions at cruise altitudes only.

The scenarios developed for the 1993 interim assessment are described in Table 3-1.1. Fuel burned and emissions of nitrogen oxides (NO_x), hydrocarbons (HC), and carbon monoxide (CO) were to be developed for fleets of subsonic aircraft operating in 1990 and 2015, and for assumed fleets of HSCTs in 2015 flying at either Mach 1.6, 2.0, or 2.4. From the fuel burned, emissions of water vapor and carbon dioxide can also be determined. The subsonic scenarios evaluate the fuel burned and emissions for scheduled airliner (jet aircraft), scheduled cargo, scheduled turboprop, military, charter, and nonscheduled air traffic.

It was necessary to limit the scenarios evaluated to those shown in Table 3-1.1 because of the time required to develop the databases in a timely manner. All but the Mach 2.0 scenarios (H and I) have been completed and are described here. Although not directly relevant to evaluating HSCTs, the 1990 emissions database does provide a relative basis for evaluating the future environmental effects from fleets of these aircraft.

Individual components of the HSRP aircraft emissions database were developed by the Boeing Commercial Airplane Group and the McDonnell Douglas Corporation (MDC). Boeing was responsible for evaluating the scheduled (Official Airline Guide) airline, cargo, and turboprop emissions for the 1990 and 2015 subsonic fleets and for the Mach 2.4 and Mach 2.0 HSCT emissions. McDonnell Douglas was responsible for the military, charter, and nonscheduled (non-OAG flights within Russia and China) emissions for the 1990 and 2015 subsonic fleets and for the Mach 1.6 HSCT emissions.

Two versions of the 2015 subsonic emissions were developed. Scenario B is the 2015 subsonic case assuming there to be no HSCT fleet. A modified 2015 subsonic case was developed to reflect the reduced number of subsonic flights when HSCTs are included in the scenarios. The modified subsonic emissions were used in all of the scenarios that include HSCTs. At the request of the assessment modeling group, a special Mach 2.4, EI=45, scenario was developed in which the HSCT component was obtained from the Mach 2.4, EI=15, HSCT data set by multiplying NO_x emissions by a factor of three. This Scenario G was developed to examine the outer envelope of aircraft emissions effects on ozone.

REQUIREMENTS AND METHODOLOGY

The previous NASA HSRP Program reports (Wuebbles, et al., 1992, 1993) describe the guidelines and basic methodology used in the scenarios developed for the 1993 assessment. The guidelines developed for the emissions database recommend that it be properly documented, publicly available, continuous in space and time, open ended, flexible, and well scrutinized.

In order to generate the emissions for each scenario, it is necessary to account for the aircraft performance, engine characteristics, and marketing forecasts (traffic projections, flight frequencies, city-pairs, routing). For example, the flight altitude of an HSCT will vary with its cruise Mach number, increasing with higher speeds. The cruise altitude will also increase during the flight as fuel is burned and the aircraft becomes lighter.

Total Passenger Demand

Passenger demand, which forms the basis of the year 2015 route system emissions analysis, was projected by Boeing and McDonnell Douglas. Data regarding growth rate forecasts were exchanged, and a single growth scenario was devised which resulted in a common forecast for passenger demand. Both companies produce passenger demand projections as part of normal business activity. These projections were used as each company's submittal to create the common forecast.

After exchanging forecast growth rate data, Boeing and McDonnell Douglas agreed that a simple averaging of growth rates by regional market would suffice to create a common forecast. Table 3-1.2 shows the McDonnell Douglas forecast (McDonnell Douglas, 1992), the Boeing forecast (from Boeing, 1992), and the common forecast used in the analysis.

Projected passenger demand, which for 2015 is shown in Figure 3-1.1, with daily passengers and the percent of total passenger demand for each region shown separately. The North America-Asia and North America-Europe markets dominate.

The HSCT demand network was developed using the following ground rules:

- no more than 50% over land routing;
- flight distance greater than 2000 nautical miles;
- no supersonic flight over land;
- flight paths could be altered using waypoints to avoid flying over land but with no more than 20% diversion from great circle routing;
- great circle paths used between waypoints.

Based on these criteria, McDonnell Douglas and Boeing both produced a set of candidate city-pairs and route paths. After much negotiation and several iterations, a single set of city-pairs and flight frequencies was agreed upon which met the criteria described above and met the further requirement that the HSCT route system and market penetration as devised, would need about 500 Mach 2.4 HSCTs with 300 seat capacity to meet the passenger demand.

The passenger demand estimate for the year 2015 was partitioned between the different city-pairs to create a single universal airline network. Flights were scheduled to satisfy local airport curfews. The HSCT network was then developed as follows:

- Equal penetration assumed in all markets.
- City-pairs unable to support at least one HSCT flight per day with at least 70% of load capacity in 2015 were allocated to the subsonic fleet and dropped from the HSCT network.

- HSCT aircraft were then allocated to maximize the utilization of 500 Mach 2.4 HSCTs.
- One hour through times (flights with refueling stops) and 1.5 hour turnaround times were assumed.

The results are summarized for different HSCTs and for the subsonic aircraft they replace in Table 3-1.3. The higher speed aircraft would be able to fly more trips and thereby carry more people per day. A larger number of HSCT's would be required for slower aircraft to meet the same passenger demand. The HSCT fleet would carry 387,000 people/day, with an average load factor of 70%. The average stage length was 3400 nautical miles with an average diversion from great circle routing of 4.2%. Based on these assumptions of high utilization, the HSCT would achieve a market penetration of 48% on these routes. These high utilization rates are consistent with the scheduling guidelines; they probably represent an upper limit utilization for 500 Mach 2.4 HSCTs.

These calculations result in a Mach 2.4 HSCT flying 16.3 hours/day, while a Mach 1.6 HSCT would be used, on average, about 17.2 hours per day. While 500 Mach 2.4 aircraft are required to meet this utilization, the Mach 1.6 HSCT would require 594 aircraft to meet the same passenger demand. The average fleet utilization would likely be lower than this as additional aircraft would be needed for spares, replacement aircraft during periodic maintenance, etc.

The HSCT emissions study departure network is tabulated in Table 3-1.4 and graphically depicted in Figure 3-1.2. The table lists origin, destination, and "via" cities (refueling stops required when the origin-destination distance is greater than the 5000 nautical mile nominal range for the HSCT designs now contemplated). Also listed are flights per day and great circle paths and flight-path distances between cities. Since it was assumed for this study that supersonic flight over land will be prohibited, the flight path distances are greater than the great circle paths due to the routings that have been defined to minimize subsonic overland flight. This resulted in HSCT service between 199 city-pairs. Because some HSCT flights are routed through the same cities, 386 mission profiles were calculated to fly this network.

Flight Profiles

Actual flight profiles between city-pairs were used to distribute emissions during takeoff, subsonic and supersonic climb and cruise, and descent. Based on these mission profiles, the fuel burned and emissions were then calculated onto the database grid. Generic examples of HSCT flight profiles were given in the Second Program Report (Wuebbles et al., 1992b). Two missions which are representative of the way in which an actual HSCT would be flown are shown in Figures 3-1.3 and 3-1.4. The simplest mission (Figure 3-1.3) is a flight almost exclusively over water, such as Los Angeles to Tokyo. The HSCT would take off and climb subsonically and then supersonically to a supersonic cruise altitude. It would then fly at supersonic cruise at the optimum altitude determined by its gross weight. As it approached Tokyo, it would descend and land. The cumulative fraction of the total NO_x emissions is plotted on the right axis. The plot illustrates that about 40% of the NO_x emissions would occur during takeoff, climb, and supersonic climb.

A more complicated but still common mission is a flight in which one leg would be flown subsonically over land. This is illustrated in Figure 3-1.4 by the flight from Seattle to London. The HSCT would take off and climb to subsonic cruise altitudes. It would then cruise at subsonic speeds until reaching Hudson Bay where it would begin to climb supersonically. It would then cruise at supersonic speeds (altitude determined by the optimum performance) until descending near London. A substantial amount of the NO_x emissions would occur during the subsonic climb, subsonic cruise, and supersonic climb.

A still more complicated mission, which was included in the calculations but not shown graphically, is a flight in which the aircraft might descend and climb several times to avoid flying supersonically over land. An example would be Madrid, Spain, to Mexico City. In this case, the HSCT would fly subsonically over Spain, supersonically over the Atlantic, subsonically over Florida, supersonically over the Gulf of Mexico, and then subsonically inland over Mexico. Because of the extensive fuel required for supersonic climb, such flight profiles were kept to a minimum in the scenario development.

Other Considerations

An analysis of the potential importance of considering seasonal variations in emissions by MDC indicated that emissions from commercial jet flights from 1976–1991 show very strong variations in the subsonic traffic with season (see Wuebbles et al., 1993). However, the HSCT fleets may be more dependent on business traffic and therefore less seasonal. Although the effect of seasonality still needs to be evaluated, there was insufficient time to do further analysis for the Interim Assessment and the effects of seasonality are not included in the database developed for any of the scenarios.

OVERVIEW OF EMISSIONS CALCULATION

Once a schedule of city-pairs and departures has been determined, the next step in the development of the scenario data set is to use aircraft/engine performance and emissions data to calculate the fuel use and emissions as a function of altitude and location. For each mission, fuel consumption and emissions are calculated including all the flight segments (taxi out, takeoff, climb, cruise, descent, landing, taxi in), distributing the emissions as a function of space along the route between city-pairs. The emissions are then combined for all flights into the resulting three-dimensional database. The details of the calculations are described in Subchapters 3-2 and 3-3 which follow this section. Summary results are presented in Subchapter 3-4.

ACKNOWLEDGMENT

Work performed at LLNL was under the auspices of the U.S. Department of Energy by the Lawrence Livermore National Laboratory under contract No. W-7405-Eng-48 and was supported in part by the NASA High-speed Research Program. The emission scenario work by Boeing and by McDonnell Douglas were funded under the NASA High-speed Systems Research Studies Contracts NAS1-19360 and NAS1-19345, respectively.

Table 3-1.1. Emissions Scenarios Developed for the 1993 Assessment (Components of Each Scenario are Also Shown)

Scenario		Components of Scenario
A	1990 Fleet	Scheduled (OAG) airline, cargo, and turboprop; charter; military; and other (non-OAG, including internal former Soviet Union, China)
B	2015 Subsonic Fleet (without HSCTs)	Scheduled (OAG) airline, cargo, and turboprop; charter; military; and other (non-OAG, including internal former Soviet Union, China)
C	2015 Mach 1.6 HSCT (EI=5)*	2015 subsonic (scenario B with scheduled airlines revised to account for HSCTs; Mach 1.6 HSCT with EI=5
D	2015 Mach 1.6 HSCT (EI=15)*	2015 subsonic (scenario B with scheduled airlines revised to account for HSCTs; Mach 1.6 HSCT with EI=15
E	2015 Mach 2.4 HSCT (EI=5)*	2015 subsonic (scenario B with scheduled airlines revised to account for HSCTs; Mach 2.4 HSCT with EI=5
F	2015 Mach 2.4 HSCT (EI=15)*	2015 subsonic (scenario B with scheduled airlines revised to account for HSCTs; Mach 2.4 HSCT with EI=15
G	2015 Mach 2.4 HSCT (EI=45)*	2015 subsonic (scenario B with scheduled airlines revised to account for HSCTs; Mach 2.4 HSCT with EI=45
H	2015 Mach 2.0 HSCT (EI=5)*	2015 subsonic (scenario B with scheduled airlines revised to account for HSCTs; Mach 2.0 HSCT with EI=5
I	2015 Mach 2.0 HSCT (EI=15)*	2015 subsonic (scenario B with scheduled airlines revised to account for HSCTs; Mach 2.0 HSCT with EI=15

*Scheduled subsonic fleet emissions are revised to account for flights from HSCTs. Also, NO_x Emission Index (EI, in grams of NO_x as NO₂ emitted per kg of fuel) are approximate and refer to the nominal emission levels at cruise altitudes for the HSCT fleet in the scenarios; EI for subsonics will be different for each projected aircraft type.

Table 3-1.2. Growth Rates in Scheduled Passenger Demand Determined by Boeing and McDonnell Douglas

Emission Study Scheduled Passenger Demand Growth Rates

	Passenger Demand Growth Rate Percentage							
	McDonnell-Douglas	Boeing			"Common" Rates*			
From (Year)	1990	1990	2000	2005	1990	2000	2005	2010
To (Year)	2000	2000	2005	2010	2000	2005	2010	2015
Region:								
North America - Europe	5.00	5.10	4.30	4.20	5.00	4.20	4.10	4.00
North America - Asia	11.70	8.50	7.40	7.20	10.10	8.80	8.60	8.00
North America - Latin America	6.60	6.50	5.00	5.00	6.60	5.10	5.10	5.00
Europe - Asia	8.40	8.80	7.80	7.30	8.60	7.60	7.10	7.00
Intra Asia	10.70	8.10	7.20	7.00	9.40	8.40	8.10	8.00

*Common rates refer to the commonly agreed upon passenger demand developed jointly by Boeing and McDonnell Douglas.

Table 3-1.3. HSCT Network Analysis

	Mach Number			
	0.84	1.6	2.0	2.4
Passengers/Day	386,224	386,778	386,778	386,778
Seats	300	300	300	300
Load Factor (%)	69.6	70.0	70.0	70.0
Units Required	961	594	532	500
Daily Utilization (hours)	17.0	17.2	16.6	16.3
ASM/Year (Billions)	809.6	830.8	830.8	830.8

Table 3-1.4. Emission Network City-pairs and Daily Frequencies for Year 2015
Demand, Assuming 500 Unit Fleet of 300 Seat Mach=2.4 HSCTs

City-Pairs Served			Flights/ day	GC Dist	Path Dist	City-Pairs Served			Flights/ day	GC Dist	Path Dist
Org	Via	Des				Org	Via	Des			
AKL	MNL	HKG	2	4937	5022	AMS		NYC	5	3155	3248
HKG	MNL	AKL	2	4937	5022	NYC		AMS	5	3155	3248
AKL		HNL	12	3826	3827	AMS	BAH	SIN	2	5669	6573
HNL		AKL	12	3826	3827	SIN	BAH	AMS	2	5669	6573
AKL	HNL	LAX	9	5659	6044	AMS	HEL	TYO	1	5028	5579
LAX	HNL	AKL	9	5659	6044	TYO	HEL	AMS	1	5028	5579
AKL		PPT	1	2209	2210	AMS		YMQ	1	2972	3349
PPT		AKL	1	2209	2210	YMQ		AMS	1	2972	3349
AKL		SIN	3	4541	4838	AMS		YYZ	2	3232	3519
SIN		AKL	3	4541	4838	YYZ		AMS	2	3232	3519
AKL		TYO	5	4768	4769	ANC		HKG	1	4397	4947
TYO		AKL	5	4768	4769	HKG		ANC	1	4397	4947
AMS		ATL	2	3812	4002	ANC		LON	1	3885	4011
ATL		AMS	2	3812	4002	LON		ANC	1	3885	4011
AMS		BOS	1	2993	3133	ANC		PAR	1	4057	4155
BOS		AMS	1	2993	3133	PAR		ANC	1	4057	4155
AMS		CCS	1	4230	4232	ANC		TPE	2	4057	4234
CCS		AMS	1	4230	4232	TPE		ANC	2	4057	4234
AMS		CHI	1	3567	3876	ANC		TYO	8	2975	3045
CHI		AMS	1	3567	3876	TYO		ANC	8	2975	3045
AMS		DFW	1	4262	4630	ATH		NYC	1	4274	4318
DFW		AMS	1	4262	4630	NYC		ATH	1	4274	4318
AMS	YYC	LAX	2	4832	5158	ATH	BAH	SIN	1	4885	5654
LAX	YYC	AMS	2	4832	5158	SIN	BAH	ATH	1	4885	5654
AMS		MSP	1	3607	4106	ATL		FRA	5	3997	4215
MSP		AMS	1	3607	4106	FRA		ATL	5	3997	4215

Table 3-1.4. Continued

City-Pairs Served			Flights/ day	GC Dist	Path Dist	City-Pairs Served			Flights/ day	GC Dist	Path Dist
Org	Via	Des				Org	Via	Des			
ATL		GVA	1	4005	4147	PAR		BOM	1	3774	4232
GVA		ATL	1	4005	4147	BOS		FRA	2	3177	3286
ATL		LON	5	3648	3807	FRA		BOS	2	3177	3286
LON		ATL	5	3648	3807	BOS		GVA	1	3185	3278
ATL		PAR	1	3806	3967	GVA		BOS	1	3185	3278
PAR		ATL	1	3806	3967	BOS		LON	6	2827	2937
BAH		BOM	3	1302	1423	LON		BOS	6	2827	2937
BOM		BAH	3	1302	1423	BOS		PAR	1	2985	3101
BAH		FRA	3	2395	2721	PAR		BOS	1	2985	3101
FRA		BAH	3	2395	2721	BOS		SNN	2	2506	2608
BAH		GVA	1	2422	2673	SNN		BOS	2	2506	2608
GVA		BAH	1	2422	2673	BRU		CHI	1	3602	3868
BAH		JKT	9	3801	3861	CHI		BRU	1	3602	3868
JKT		BAH	9	3801	3861	BRU		NYC	4	3176	3240
BAH		MNL	1	3976	4672	NYC		BRU	4	3176	3240
MNL		BAH	1	3976	4672	BRU	HEL	TYO	1	5103	5646
BAH		SIN	14	3412	3659	TYO	HEL	BRU	1	5103	5646
SIN		BAH	14	3412	3659	BRU		YMQ	1	3000	3115
BKK		CAI	2	3915	4463	YMQ		BRU	1	3000	3115
CAI		BKK	2	3915	4463	BUD		NYC	1	3785	3895
BKK	BAH	CPH	3	4644	6456	NYC		BUD	1	3785	3895
CPH	BAH	BKK	3	4644	6456	BUE	DKR	MAD	2	5441	6098
BOM		GVA	1	3623	4045	MAD	DKR	BUE	2	5441	6098
GVA		BOM	1	3623	4045	CCS		LIS	1	3508	3509
BOM		NBO	1	2446	2505	LIS		CCS	1	3508	3509
NBO		BOM	1	2446	2505	CCS		MAD	2	3779	3780
BOM		PAR	1	3774	4232	MAD		CCS	2	3779	3780

Table 3-1.4. Continued

City-Pairs Served			Flights/ day	GC Dist	Path Dist	City-Pairs Served			Flights/ day	GC Dist	Path Dist
Org	Via	Des				Org	Via	Des			
CCS		ROM	1	4497	4498	PAR		DFW	2	4286	4595
ROM		CCS	1	4497	4498	DFW	SEA	TYO	3	5569	5572
CHI		FRA	6	3761	4030	TYO	SEA	DFW	3	5569	5572
FRA		CHI	6	3761	4030	DHA		BOM	2	1327	1441
CHI		GVA	2	3806	4014	BOM		DHA	2	1327	1441
GVA		CHI	2	3806	4014	DHA		LON	3	2731	3006
CHI		LON	6	3423	3681	LON		DHA	3	2731	3006
LON		CHI	6	3423	3681	DHA		MNL	7	4001	4690
CHI		PAR	2	3595	3845	MNL		DHA	7	4001	4690
PAR		CHI	2	3595	3845	DHA		PAR	1	2584	2836
CHI		ROM	2	4176	4363	PAR		DHA	1	2584	2836
ROM		CHI	2	4176	4363	DHA		SIN	5	3436	3677
CHI	SEA	TYO	13	5435	5622	SIN		DHA	5	3436	3677
TYO	SEA	CHI	13	5435	5622	DKR		PAR	6	2280	2494
CPH		LAX	1	4871	4909	PAR		DKR	6	2280	2494
LAX		CPH	1	4871	4909	DTW		FRA	2	3603	3827
CPH		NYC	1	3339	3481	FRA		DTW	2	3603	3827
NYC		CPH	1	3339	3481	DTW		LON	1	3261	3478
CPH		SEA	1	4214	4346	LON		DTW	1	3261	3478
SEA		CPH	1	4214	4346	DTW		PAR	2	3430	3616
CPH	HEL	TYO	1	4700	5239	PAR		DTW	2	3430	3616
TYO	HEL	CPH	1	4700	5239	DTW	SEA	SEL	5	5738	6347
DFW		FRA	2	4455	4784	SEL	SEA	DTW	5	5738	6347
FRA		DFW	2	4455	4784	DTW	SEA	TYO	5	5542	5801
DFW		LON	6	4115	4435	TYO	SEA	DTW	5	5542	5801
LON		DFW	6	4115	4435	FRA	YYC	LAX	3	5029	5137
DFW		PAR	2	4286	4595	LAX	YYC	FRA	3	5029	5137

Table 3-1.4. Continued

City-Pairs Served			Flights/ day	GC Dist	Path Dist	City-Pairs Served			Flights/ day	GC Dist	Path Dist
Org	Via	Des				Org	Via	Des			
						GVA		NYC	4	3346	3386
FRA		SFO	1	4936	4953	NYC		GVA	4	3346	3386
SFO		FRA	1	4936	4953	GVA		YMQ	1	3191	3258
FRA		MIA	4	4188	4238	YMQ		GVA	1	3191	3258
MIA		FRA	4	4188	4238	HEL		NYC	1	3565	3742
FRA		NYC	13	3340	3402	NYC		HEL	1	3565	3742
NYC		FRA	13	3340	3402	HKG	TYO	LAX	7	6282	6590
FRA	DKR	RIO	2	5163	5606	LAX	TYO	HKG	7	6282	6590
RIO	DKR	FRA	2	5163	5606	HKG	TYO	SEA	3	5625	5998
FRA	BAH	SIN	3	5543	6380	SEA	TYO	HKG	3	5625	5998
SIN	BAH	FRA	3	5543	6380	HKG	TYO	SFO	11	5994	6306
FRA	HEL	TYO	5	5054	5587	SFO	TYO	HKG	11	5994	6306
TYO	HEL	FRA	5	5054	5587	HKG		SYD	11	3981	4532
FRA		WAS	3	3534	3590	SYD		HKG	11	3981	4532
WAS		FRA	3	3534	3590	HKG	TYO	YVR	8	5533	5919
FRA		YMQ	1	3161	3502	YVR	TYO	HKG	8	5533	5919
YMQ		FRA	1	3161	3502	HNL		LAX	31	2216	2217
FRA		YYC	1	4062	4090	LAX		HNL	31	2216	2217
YYC		FRA	1	4062	4090	HNL		MNL	5	4597	4598
FRA		YYZ	3	3422	3672	MNL		HNL	5	4597	4598
YYZ		FRA	3	3422	3672	HNL		OSA	14	3557	3558
GUM		HNL	5	3296	3297	OSA		HNL	14	3557	3558
HNL		GUM	5	3296	3297	HNL		PHX	1	2528	2529
GUM		SIN	1	2533	2534	PHX		HNL	1	2528	2529
SIN		GUM	1	2533	2534	HNL		PPT	7	2383	2384
GUM		SYD	1	2869	3062	PPT		HNL	7	2383	2384
SYD		GUM	1	2869	3062	HNL		SEA	4	2324	2324

Table 3-1.4. Continued

City-Pairs Served			Flights/ day	GC Dist	Path Dist	City-Pairs Served			Flights/ day	GC Dist	Path Dist
Org	Via	Des				Org	Via	Des			
SEA		HNL	4	2324	2324	LAX		PPT	3	3567	3568
HNL		SEL	7	3950	4602	PPT		LAX	3	3567	3568
SEL		HNL	7	3950	4602	LAX	LIM	RIO	1	5470	5757
HNL		SFO	18	2080	2081	RIO	LIM	LAX	1	5470	5757
SFO		HNL	18	2080	2081	LAX	NYC	ROM	1	5504	5884
HNL		SYD	18	4409	4420	ROM	NYC	LAX	1	5504	5884
SYD		HNL	18	4409	4420	LAX	HNL	SYD	7	6508	6637
HNL		TPE	4	4394	4395	SYD	HNL	LAX	7	6508	6637
TPE		HNL	4	4394	4395	LAX	TYO	TPE	8	5893	5912
HNL		TYO	54	3311	3311	TPE	TYO	LAX	8	5893	5912
TYO		HNL	54	3311	3311	LAX		TYO	35	4723	4724
HNL		YVR	5	2347	2348	TYO		LAX	35	4723	4724
YVR		HNL	5	2347	2348	LIM		MIA	3	2276	2402
JKT		TYO	5	3145	3288	MIA		LIM	3	2276	2402
TYO		JKT	5	3145	3288	LIS		NYC	2	2916	2917
JNB		RIO	1	3859	3859	NYC		LIS	2	2916	2917
RIO		JNB	1	3859	3859	LIS		RIO	2	4163	4337
LAX		LON	7	4726	4870	RIO		LIS	2	4163	4337
LON		LAX	7	4726	4870	LON		MIA	7	3835	3842
LAX	HNL	MEL	4	6884	7017	MIA		LON	7	3835	3842
MEL	HNL	LAX	4	6884	7017	LON		MSP	1	3476	3910
LAX		OSA	3	4955	4956	MSP		LON	1	3476	3910
OSA		LAX	3	4955	4956	LON		NYC	27	2990	3053
LAX	YYC	PAR	2	4910	5189	NYC		LON	27	2990	3053
PAR	YYC	LAX	2	4910	5189	LON	DKR	RIO	2	4993	5347
LAX	TYO	PEK	1	5415	5876	RIO	DKR	LON	2	4993	5347
PEK	TYO	LAX	1	5415	5876	LON		SEA	1	4156	4307

Table 3-1.4. Continued

City-Pairs Served			Flights/ day	GC Dist	Path Dist	City-Pairs Served			Flights/ day	GC Dist	Path Dist
Org	Via	Des				Org	Via	Des			
SEA		LON	1	4156	4307	RIO		MAD	3	4395	4591
LON		SFO	3	4649	4778	MAD		SJU	2	3444	3443
SFO		LON	3	4649	4778	SJU		MAD	2	3444	3443
LON	BAH	SIN	8	5868	6689	MIA		PAR	2	3976	3989
SIN	BAH	LON	8	5868	6689	PAR		MIA	2	3976	3989
LON		SJU	4	3633	3634	MIA		SCL	2	3592	3690
SJU		LON	4	3633	3634	SCL		MIA	2	3592	3690
LON		STL	1	3638	3825	MNL		SYD	3	3380	3920
STL		LON	1	3638	3825	SYD		MNL	3	3380	3920
LON	HEL	TYO	11	5175	5754	MOW		NYC	2	4037	4208
TYO	HEL	LON	11	5175	5754	NYC		MOW	2	4037	4208
LON		WAS	6	3184	3241	MRU		SIN	1	3013	3014
WAS		LON	6	3184	3241	SIN		MRU	1	3013	3014
LON		YMQ	2	2817	3153	MRU		TPE	1	4602	4698
YMQ		LON	2	2817	3153	TPE		MRU	1	4602	4698
LON		YVR	1	4090	4286	MSP	SEA	TYO	2	5154	5343
YVR		LON	1	4090	4286	TYO	SEA	MSP	2	5154	5343
LON		YYC	1	3786	3916	NYC		OSL	1	3192	3341
YYC		LON	1	3786	3916	OSL		NYC	1	3192	3341
LON		YYZ	7	3079	3323	NYC		PAR	12	3148	3216
YYZ		LON	7	3079	3323	PAR		NYC	12	3148	3216
MAD		MEX	2	4892	4893	NYC		ROM	10	3704	3740
MEX		MAD	2	4892	4893	ROM		NYC	10	3704	3740
MIA		MAD	2	3834	3835	NYC	SEA	SEL	5	5974	6775
MAD		NYC	5	3109	3124	SEL	SEA	NYC	5	5974	6775
NYC		MAD	5	3109	3124	NYC		SNN	2	2669	2723
MAD		RIO	3	4395	4591	SNN		NYC	2	2669	2723

Table 3-1.4. Continued

City-Pairs Served			Flights/ day	GC Dist	Path Dist	City-Pairs Served			Flights/ day	GC Dist	Path Dist
Org	Via	Des				Org	Via	Des			
NYC		STO	1	3395	3549	TYO		PDX	3	4177	4178
STO		NYC	1	3395	3549	PER		TYO	3	4287	4288
NYC	ROM	TLV	2	4920	5200	TYO		PER	3	4287	4288
TLV	ROM	NYC	2	4920	5200	PPT		SFO	1	3649	3650
NYC	SEA	TYO	21	5844	6229	SFO		PPT	1	3649	3650
TYO	SEA	NYC	21	5844	6229	PPT		SYD	1	3301	3302
NYC		WAW	1	3695	3786	SYD		PPT	1	3301	3302
WAW		NYC	1	3695	3786	PPT	GUM	TYO	2	5096	5665
OSA		SIN	7	2668	2843	TYO	GUM	PPT	2	5096	5665
SIN		OSA	7	2668	2843	RIO	DKR	ROM	2	4949	5771
PAR	DKR	RIO	2	4956	5311	ROM	DKR	RIO	2	4949	5771
RIO	DKR	PAR	2	4956	5311	ROM	HEL	TYO	1	5343	5962
PAR		SJU	8	3734	3725	TYO	HEL	ROM	1	5343	5962
SJU		PAR	8	3734	3725	ROM		YYZ	1	3823	4031
PAR	BAH	SIN	1	5783	6519	YYZ		ROM	1	3823	4031
SIN	BAH	PAR	1	5783	6519	SEA		SEL	1	4503	4678
PAR	HEL	TYO	5	5239	5798	SEL		SEA	1	4503	4678
TYO	HEL	PAR	5	5239	5798	SEA	TYO	TPE	1	5264	5320
PAR		WAS	3	3343	3405	TPE	TYO	SEA	1	5264	5320
WAS		PAR	3	3343	3405	SEA		TYO	9	4131	4132
PAR		YMQ	6	2984	3317	TYO		SEA	9	4131	4132
YMQ		PAR	6	2984	3317	SEL		SIN	1	2511	2573
PAR		YYZ	1	3248	3461	SIN		SEL	1	2511	2573
YYZ		PAR	1	3248	3461	SEL		YVR	2	4411	4455
PDX		SEL	3	4566	4728	YVR		SEL	2	4411	4455
SEL		PDX	3	4566	4728	SFO	HNL	SYD	2	6448	6501
PDX		TYO	3	4177	4178	SYD	HNL	SFO	2	6448	6501

Table 3-1.4. Continued

City-Pairs Served			Flights/ day	GC Dist	Path Dist
Org	Via	Des			
SFO	TYO	TPE	5	5607	5628
TPE	TYO	SFO	5	5607	5628
SFO		TYO	29	4439	4440
TYO		SFO	29	4439	4440
SIN		TLV	1	4293	4641
TLV		SIN	1	4293	4641
SIN		TPE	2	1740	1742
TPE		SIN	2	1740	1742
SIN		TYO	32	2893	2947
TYO		SIN	32	2893	2947
SIN	BAH	VIE	1	5232	6302
VIE	BAH	SIN	1	5232	6302
SYD		TYO	20	4226	4385
TYO		SYD	20	4226	4385
TPE	TYO	YVR	1	5176	5241
YVR	TYO	TPE	1	5176	5241
TYO	SEA	WAS	6	5851	6129
WAS	SEA	TYO	6	5851	6129
TYO		YVR	9	4050	4053
YVR		TYO	9	4050	4053
TYO	YVR	YYZ	2	5557	5858
YYZ	YVR	TYO	2	5557	5858

Total HSCT Passenger Demand
 Passengers Carried per Day
 Year 2015

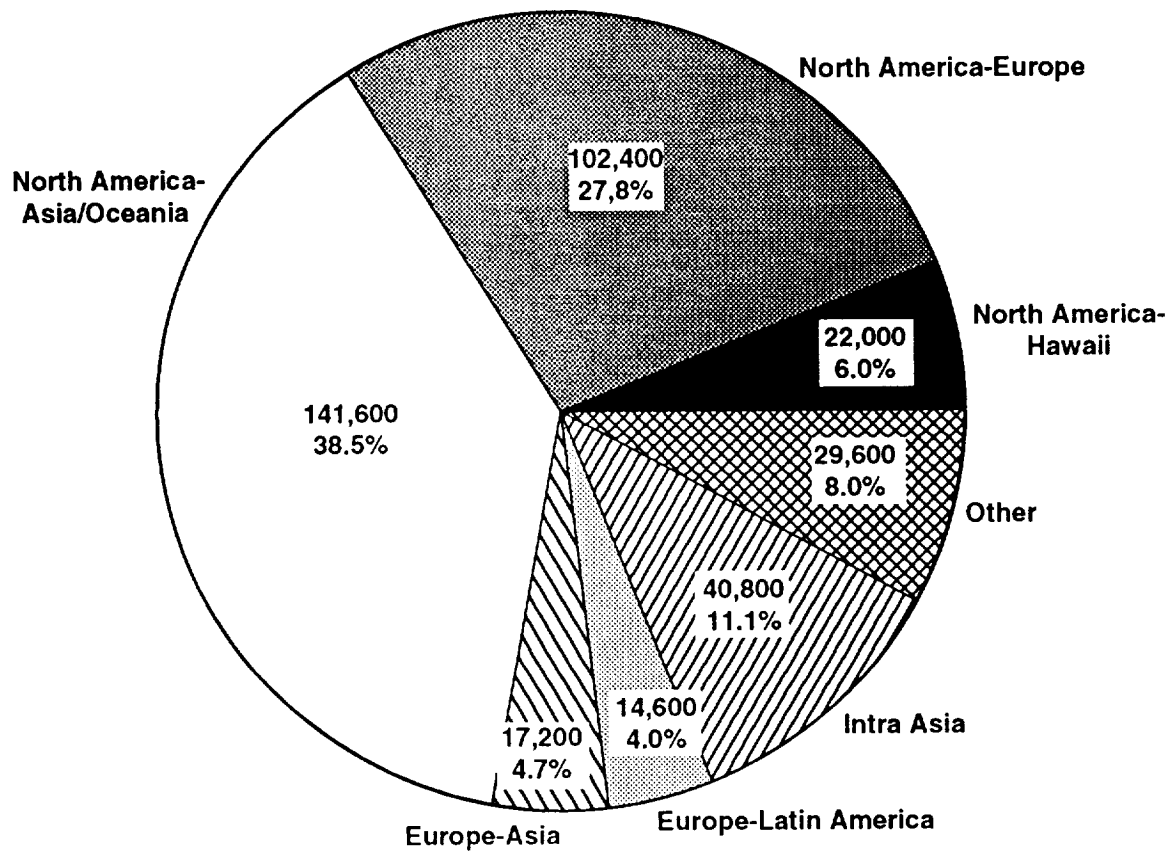


Figure 3-1.1. Total HSCT passenger demand for 2015 by region, including the projected number of daily passengers and percentage of total passenger demand for each region.

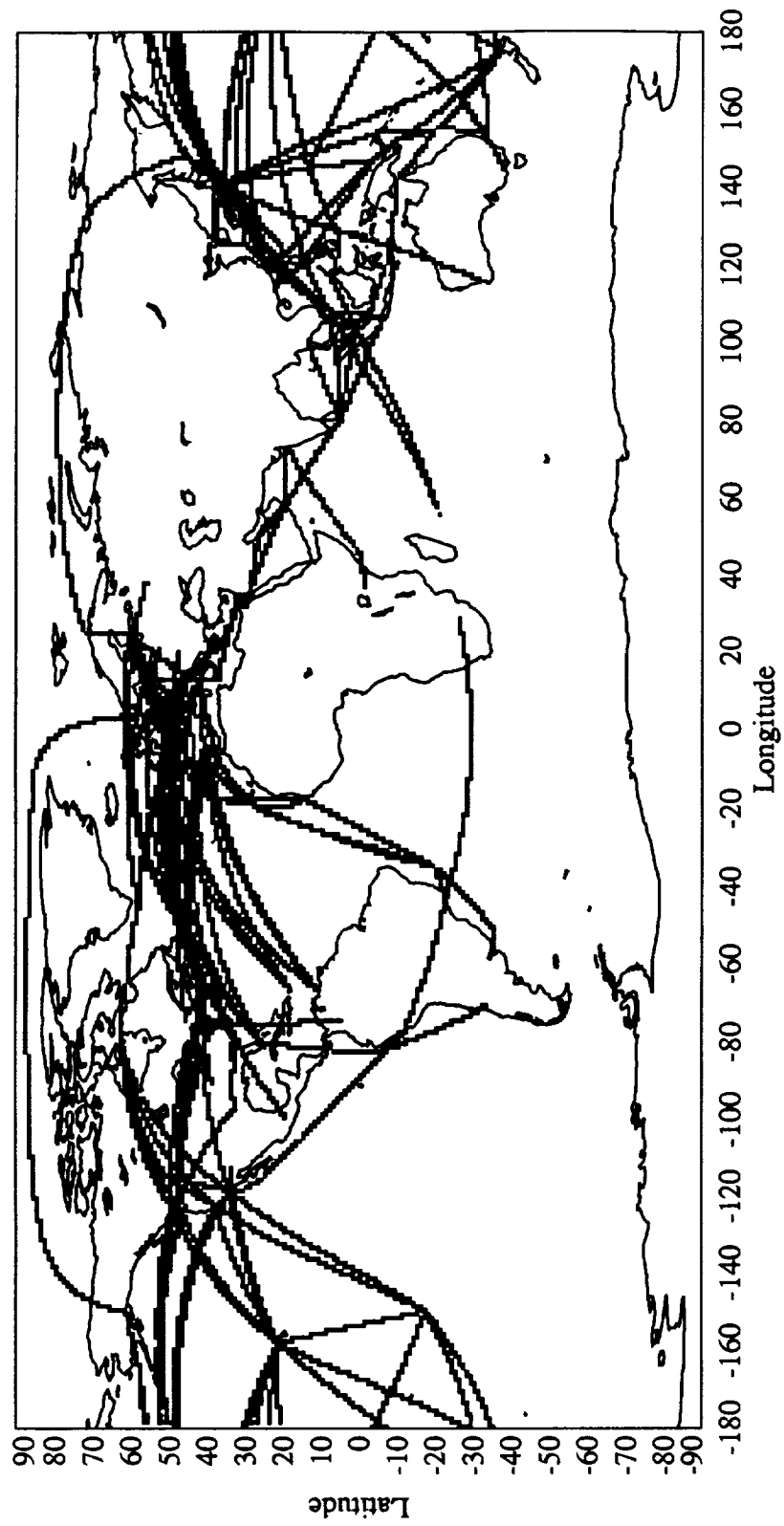


Figure 3-1.2. HSCT route system for the year 2015.

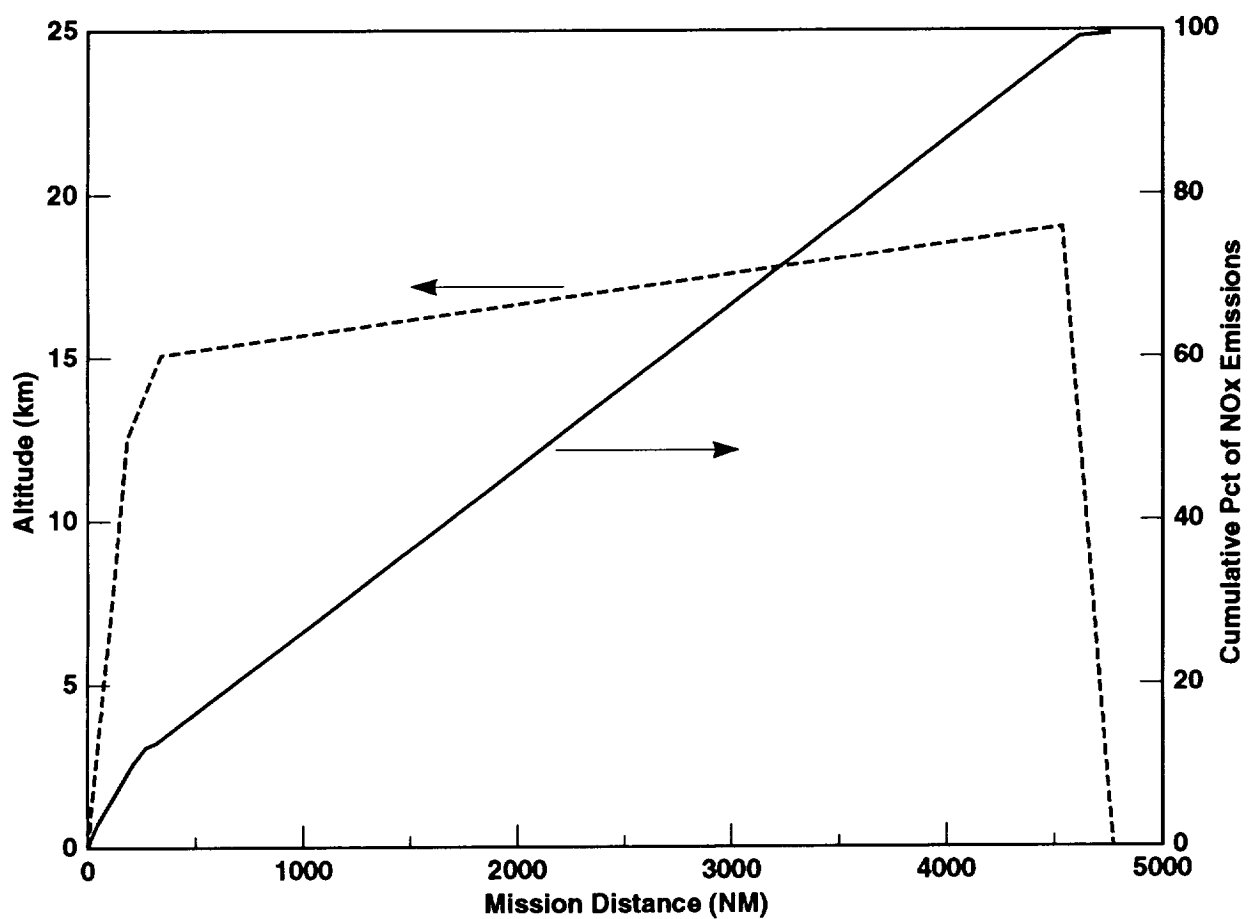


Figure 3-1.3. Mission profile for Mach 1.6 HSCT from Los Angeles to Tokyo.

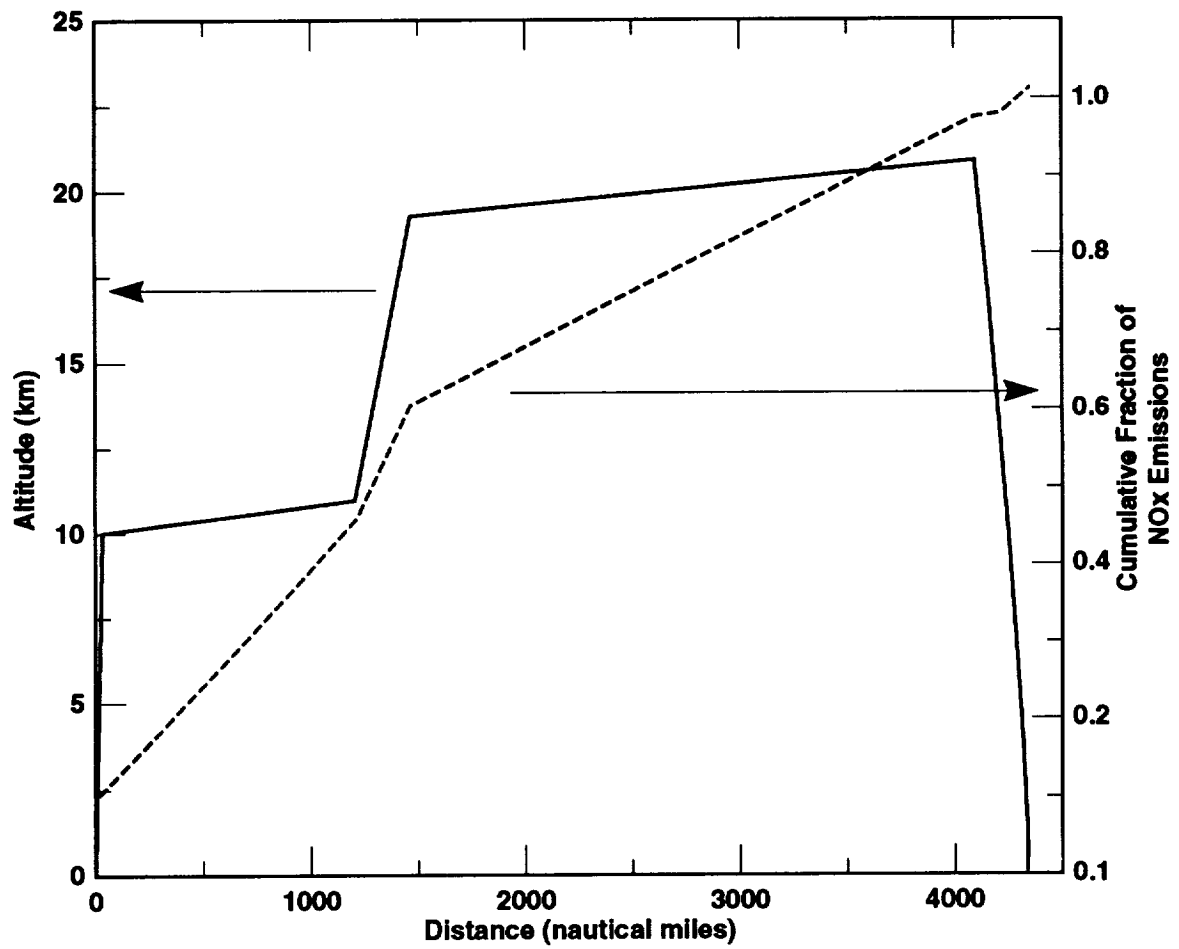


Figure 3-1.4. Mission profile for Mach 2.4 HSCT from Seattle to London.

REFERENCES

Boeing Commercial Airplane Group, *High-Speed Civil Transport Study Special Factors*, NASA Contractor Report No. 1811881, NASA, Washington, D.C., 1990.

Boeing Commercial Airplane Group, *1992 Current Market Outlook*, 1992.

McDonnell Douglas, *World Economics and Traffic Outlook*, Economics Research Department, Douglas Aircraft Company, Long Beach, CA, 1992.

Wuebbles, D. J., S. L. Baughcum, J. H. Gerstle, J. Edmonds, D. E. Kinnison, N. Krull, M. Metwally, A. Mortlock, and M. Prather, Designing a methodology for future air travel scenarios, in *The Atmospheric Effects of Stratospheric Aircraft: A First Program Report*, M. J. Prather and H. L. Wesoky, Eds., NASA Reference Publication 1272, National Technical Information Service, Springfield, VA, 1992.

Wuebbles, D. J., S. L. Baughcum, S. C. Henderson, R. Eckman, D. Maiden, M. Metwally, A. Mortlock, and F. Torres, Report of the Emissions Scenarios Committee: Preparations for the 1993 assessment, in *The Atmospheric Effects of Stratospheric Aircraft: A Second Program Report*, R. S. Stolarski and H. L. Wesoky, Eds., NASA Reference Publication 1293, National Technical Information Service, Springfield, VA, 1993.

Subchapter 3-2

Emissions Scenarios Development: Scheduled 1990 and Projected 2015 Subsonic, Mach 2.0, and Mach 2.4 Aircraft

Steven L. Baughcum
Dik M. Chan
Stephen M. Happenny
Stephen C. Henderson
Peter S. Hertel
Terry Higman
Debra R. Maggiora
Carlos A. Oncina

Boeing Commercial Airplane Group
Seattle, WA

PRECEDING PAGE BLANK NOT FILMED

INTRODUCTION

Three-dimensional (1 degree latitude \times 1 degree longitude \times 1 km altitude) distributions of fuel burned, nitrogen oxides (NO_x), carbon monoxide (CO), and hydrocarbons (HC) were calculated for the following components of the scenarios described in Subchapter 3-1:

- 1990 scheduled airliner, cargo, and turboprop aircraft
- Projected 2015 scheduled subsonic airliners (assuming no HSCT fleet exists)
- Projected 2015 scheduled subsonic airliners (assuming an HSCT fleet of 500 Mach 2.4 HSCTs were flying)
- Projected 2015 scheduled cargo aircraft
- Projected 2015 scheduled turboprop aircraft
- Projected 2015 HSCT traffic for 500 Mach 2.4 HSCTs with nominal NO_x emission indices of 5 and 15 gm NO_x /kg fuel burned at cruise.

The methods and the results are described below.

EMISSIONS CALCULATION METHODOLOGY

Boeing maintains an engineering database of aircraft performance and emissions characteristics for a number of subsonic passenger and cargo jets. For the work described here, 57 subsonic aircraft/engine configurations were used to calculate the emissions of the 1990 scenarios. Less detailed data were used for calculations of the Concorde aircraft and for turboprop aircraft. Using this database, technology modifications and improvements were projected to 2015 for subsonic jet aircraft. Calculations for the Mach 2.4 HSCT were based on the current Boeing preliminary design aircraft. The calculations will be described later in more detail for each component scenario. The general methodology is described below.

All aircraft were assumed to fly according to engineering design. Altitudes and mission profiles were calculated based on the performance of the aircraft and its mission weight. Air traffic control constraints were not considered. Flight schedules of departures for each aircraft type were based on Official Airline Guide (OAG) flight schedules for May 1990 and on projected schedules for 2015. For each aircraft type considered, a separate three-dimensional data set of fuel burned and emissions was calculated. Subsonic aircraft were flown along great circle routes between the cities. For the HSCT, routing between waypoints to avoid supersonic flight over land was used for many city-pairs. The HSCT was flown along great circle routes between these waypoints. For all flights, zero prevailing winds were assumed.

To calculate the global inventory of aircraft emissions, a computer model was developed which basically combines scheduling data (departures, aircraft type) with aircraft performance and emissions data. The Global Atmospheric Emissions Code (GAEC) computer model was used to calculate fuel burned and emissions from files of airplane performance and engine emissions data. The aircraft performance file contains detailed performance input data for a wide range of operating conditions. Each engine emission input file contains emission indices tabulated as a function of fuel flow rate.

For each route flown by the airplane/engine type, the takeoff gross weight was calculated as a function of the city-pair route distance. The fuel burned was calculated for the following flight segments:

- Taxi-out
- Climbout
- Subsonic Climb
- Subsonic Cruise

- Supersonic Climbout
- Supersonic Cruise
- Supersonic Descent
- Descent
- Approach and Land
- Taxi-in

For subsonic aircraft, emissions of NO_x, CO, and HC were calculated based on the measured ground level emission indices reported to the International Civil Aviation Organization (ICAO) for current aircraft. Normally, these measurements are reported at four thrust settings. For detailed calculations of a single mission, the normal process is to use the engine emission data, the engine performance data as provided by engine thermodynamic cycle models, and the airplane performance data. Thermodynamic cycle analyses are too computationally intensive for the calculation of a global inventory of emissions. A more simplified approach was used instead.

For the calculation of a global inventory of emissions, the ICAO emissions data were interpolated as a function of fuel flow rate and, corrected for temperature and pressure at altitude (based on U.S. Standard Atmosphere 1976). The results from this simplified approach will be compared with the detailed cycle deck analyses in a later section. Further details of the emissions calculations will be included in the contractor report to NASA. For the HSCT, where no hardware and thus no measurements exist, projected engine emissions data were provided by General Electric (GE) and Pratt & Whitney (P & W).

Distributions of fuel usage and emissions were done using 1 degree latitude × 1 degree longitude × 1 km altitude cells. The altitude corresponds to the geopotential altitudes of the U.S. Standard Atmosphere temperature and pressure profile and is thus pressure-gridded data. For each city-pair, the total route distance was calculated. The fuel burn rate and airplane gross weight were then calculated at discrete distances along the route path which corresponded to points where the airplane entered or left a cell (crossed any of the cells boundaries) or points where a transition in flight conditions occurred (climbout/climb, climb/cruise, cruise/descent, descent/approach and land, taxi-out/climbout, approach and land/taxi-in). The fuel burn rate would change dramatically at these transition points.

The emissions were calculated for each flight segment between the above described discrete points using the fuel burn rate within the segment. The total fuel burned in the segment was calculated as the difference in airplane gross weight at the segment end-points. The emissions were then assigned to a cell based on the coordinates of the endpoints.

Engineering Checks

The GAEC code was written to be a shortcut for the standard, computationally intensive Boeing emissions analysis process, and, as such, simplifying assumptions were made. In order to validate the GAEC code, a set of test cases were run using both GAEC and the standard Boeing Mission Analysis Program (BMAP-EMIT) process. Four routes for one aircraft/engine configuration were analyzed by both methods using the operating conditions assumed for the global emissions calculations (no winds, Standard Atmospheric conditions, 70% full passenger payload, 200 lb per passenger, etc.). Table 3-2.1 shows the total fuel burned and emissions generated for each portion of the flight segment as calculated by both codes.

In all of the test cases, the difference between total fuel or total emissions was less than 2% when the GAEC solution was compared to the BMAP-EMIT solution. The differences are the percentages relative to the BMAP-EMIT solutions. The most obvious discrepancy in the data is seen in the GAEC approach data where the HC and CO emissions were overestimated by 25% and NO_x was overestimated by 13%. This is most likely due to the approach performance averaging in

GAEC. The approach analysis in BMAP uses two thrust settings starting near idle and then increasing as the airplane gets closer to landing. GAEC assumes an average power setting for the entire approach-land segment, which results in higher overall emissions. However, only a small fraction of the fuel burned or emissions occur during approach. For calculations of global emissions where the primary interest is in accounting for the cruise emissions, the agreement was considered to be quite good, particularly for longer range missions.

Scenario Checks

A three-dimensional evaluation for the scheduled flights of each aircraft/engine configuration was calculated, and these were then summed to produce the various component scenarios described in Subchapter 3-1. Each three-dimensional aircraft database was checked out using the following procedure:

1. Fuel burned for the scenario was totaled over latitude, longitude, and altitude and then compared with reported global jet fuel consumption.
2. Global average emission indices were calculated for NO_x , CO, and hydrocarbons and compared with emission indices reported to ICAO to ensure the gridded emissions were reasonable.
3. The emissions were totaled over latitude and longitude, and then emission indices as a function of altitude were calculated. This is a test of the emission technology and the level of detail that went into the emission scenario calculation. Emission indices vary with power settings and thus vary at different stages of the flight. In general, NO_x emission indices should be greater during climbout than at cruise because a higher power setting is needed. Carbon monoxide and hydrocarbon emission indices will be largest at the lowest level because of low power settings during taxi operations (however, this is sensitive to the amount of time assumed during airport operations relative to takeoff).
4. The geographical distribution was checked using visual aids to ensure that it made sense for the scenario involved (Soviet Union traffic in the Soviet Union, HSCT high altitude flights only over water, etc.). Fuel burn and emissions as a function of latitude and longitude (superimposed on a map of the world) at each altitude level or summed into altitude bands were checked to ensure that routes were consistent with the type of aircraft shown and that airport locations were appropriate for each group of airplanes used in the scenario.

MACH 2.4 HSCT SCENARIOS

The Mach 2.4 HSCT scenarios were calculated using the Boeing preliminary design model 1080-924 with four Pratt & Whitney STJ989 turbine bypass engines with mixed compression translating center body (MCTCB2) inlets and two-dimensional semi-stowable (SS2D) nozzles. The aircraft has a double delta wing planform (see Figure 3-2.1) and a mostly composite structure. Overall body length is approximately 314 feet with a wing span of 139 feet. It was designed to carry over 300 passengers for a range of 5000 nautical miles.

Emissions data were provided by GE/P&W for a generic HSCT combustor with a nominal NO_x emission index at cruise of approximately 5 gm NO_x (as NO_2)/kg fuel. Nitrogen oxides, carbon monoxide, and hydrocarbon emission levels were calculated from these data as a function of power setting and altitude. A similar calculation was done to scale up to a nominal EI (NO_x)=15 scenario. For this scaling, the combustor was assumed to operate as a conventional combustor at low power settings and as an advanced low- NO_x combustor at higher settings. Based on discussions with both engine companies, the EI(NO_x) for this case was unchanged at low power settings and increased by a factor of 3 at higher thrust settings.

The basic HSCT mission profile was assumed as follows: 10 minute taxi out, all engine takeoff ground-roll and liftoff, climbout to 1500 feet and accelerate, climb to optimum cruise altitude (subsonic or supersonic, depending on whether over land or water), climbing supersonic cruise at constant Mach, descent to 1500 feet, approach and land, and 5 minute taxi in.

For a given HSCT model, fuel burned and emissions data were calculated for parametric mission cases: various takeoff weights (in increments of 50,000 pounds), two passenger-loading factors (100% and 65%), and with two cruise speeds (Mach 2.4 and Mach 0.9). These subsonic and supersonic mission profiles of varying range were used with a regression analysis to develop generalized performance for each HSCT mission segment as a function of weight.

HSCT flight profiles of fuel burn and emissions were calculated from this performance and emissions data for each HSCT mission. The departure network was described in Subchapter 3-1. These profiles with projected HSCT flight frequencies were then used to calculate the three-dimensional database, as described above.

Using the HSCT network developed in this study, 2192 HSCT departures per day were then modeled using 386 mission profiles. The average route distance flown was 3408 miles with a total daily HSCT mileage of 7,471,316 nautical miles. This corresponds to a daily HSCT passenger demand of 386,800 passengers, as was discussed in subchapter 3-1. The calculated fuel burned, emissions, and effective emission indices as a function of altitude (summed over latitude and longitude) are shown in Tables 3-2.2 and 3-2.3.

The three-dimensional character of the data set is illustrated in Figure 3-2.2, which shows NO_x emissions for the Mach 2.4 HSCT (nominal $\text{EI}(\text{NO}_x)=5$) case. Emissions at 18–21 km due to supersonic cruise are concentrated in the northern hemisphere, particularly between 40° and 50° N latitude. Flights above 13 km occur only over water.

The NO_x emissions as a function of altitude (summed over latitude and longitude) are shown more quantitatively in Figure 3-2.3 for the Mach 2.4, nominal $\text{EI}(\text{NO}_x)=5$ case. The peak NO_x emissions occur at 19–21 km altitudes with smaller peaks at 10–13 km altitude due to subsonic cruise. Figure 3-2.4a shows the cumulative fraction of NO_x emissions plotted as a function of altitude for the nominal $\text{EI}=5$ and $\text{EI}=15$ cases. Approximately 54% of the NO_x emissions from an HSCT fleet will occur above 17 km altitude. Figure 3-2.4b shows the cumulative fraction of fuel burn and emissions plotted as a function of altitude. This figure illustrates that 50–60% of the carbon monoxide and hydrocarbons emitted from an HSCT fleet are expected to occur above 17 km.

HSCT emissions are calculated to occur mostly at northern midlatitudes (Figure 3-2.5). Only 3% of the total fuel burned occurs north of 60° N latitude. No flights occur south of 40° S latitude. Approximately 32% of the fuel burned occurs between 30° S and 30° N latitude.

Emission indices for NO_x , CO, and hydrocarbons vary as a function of altitude (Figure 3-2.6). Nitrogen oxide levels are highest during times of high thrust requirements (i.e., climbout and supersonic climb), while CO and hydrocarbons are much lower at those times. During periods of low power, the CO and hydrocarbons are proportionally higher.

The effect of scaling the emission indices by treating the combustor as conventional at low power settings and as an advanced combustor at higher power settings results in NO_x emission indices for the nominal $\text{EI}=15$ case which vary significantly at different portions of the flight profile. This is shown graphically in Figure 3-2.7.

Mach 2.0 HSCT

A Mach 2.0 HSCT scenario is being developed by Boeing, based on the preliminary design model 1080-938 with four P&W STJ1016 turbine bypass engines with MCTCB2 inlets and SS2D nozzles. Combustor characteristics were provided by GE/P&W. The scenario is being calculated using the same methodology that was used for the Mach 2.4 scenario. The scenario development should be completed by the end of April 1993.

1990 SCHEDULED AIRLINER, CARGO, AND TURBOPROP SCENARIOS

Fuel burn and emissions (NO_x , CO, hydrocarbons) were calculated for scheduled 1990 turboprop, cargo, and airliner traffic. Flight frequencies and equipment types were taken from the May 1990 Official Airline Guide (OAG) as representative of the annual average. Aircraft performance data and emission characteristics were assembled for 57 subsonic jet aircraft/engine configurations, for the supersonic Concorde, and for three sizes of turboprop aircraft.

Airplanes known to function similarly and to have similar performance characteristics were combined under single airplane models. Airplanes for which Boeing does not have performance data were analyzed using performance data from airplanes estimated to have similar operating and performance characteristics.

1990 Scheduled Airliner and Cargo Scenario

The aircraft included in the 1990 airliner calculation are shown in Table 3-2.4. This table summarizes the fuel burned, emissions and globally averaged emission indices for each of the aircraft included in the compilation of the database. As the table illustrates, the emissions characteristics of the older aircraft (707, DC-8) are quite different from those of more modern aircraft (757, 767).

A three-dimensional database was calculated for each of the aircraft/engine configurations. These were then summed over all the aircraft types to produce a three-dimensional scenario of scheduled airliner and cargo aircraft. Table 3-2.5 summarizes as a function of altitude the calculated fuel burned and emissions for this case.

The emission indices vary significantly as a function of altitude as shown in Figure 3-2.8. Nitrogen oxide emission indices are higher during takeoff and climb and drop down during cruise. Most (60–65%) of the fuel burned and NO_x emissions occur between 9 and 12 km altitude (Figure 3-2.9a). Approximately 60–70% of the CO and hydrocarbons occur below 9 km. (Figure 3-2.9b)

Validation Test

In 1990, the U.S. airlines reported to the government on DOT-Form 41 their total jet fuel usage, number of departures, and average route distance flown for specific aircraft. Using the GAEC code, Boeing calculated the scheduled traffic for each of these airlines for selected aircraft reported (Boeing 727-200 and 747). The results are summarized in Table 3-2.6. The calculated total fuel burn for all the airlines taken together appears to be about 9% lower than reported. The model uses about 6% more departures than reported as the annual average by the airlines. The fuel/trip is calculated to be about 14–17% lower than reported.

In general, the agreement appears to be quite good and the differences arise both from simplified assumptions about the aircraft operation and the assumption that one week of departure data could be used to represent the annual average. The modeling calculation did not consider airport congestion, diversion due to weather, auxiliary power unit utilization, or air traffic control effects. It assumed that aircraft were flown according to engineering design with only the

necessary amount of fuel plus reserves; in reality however, aircraft do not refuel at every landing and may carry more extra fuel than required by the U.S. Federal Aviation Administration (FAA).

1990 Scheduled Turboprop

Three turboprops were selected to represent small, medium, and large categories of turboprops flying commercially in 1990. The results are tabulated in Table 3-2.7. Turboprop fuel was found to be a small fraction (1.1%) of the global jet fuel burn and will not be discussed in detail here.

1990 Generic Fleet Analysis

The engineering data files used in the calculation of the 1990 scheduled airliner and cargo scenario contain detailed information which is considered proprietary by the Boeing Company. In order to provide a paper trail of engineering data that could be used by NASA for their own tests, a 1990 generic database was constructed based on the performance curves of existing aircraft. The classification of airplanes and the performance characteristics of these generic airplanes were determined using fleet data from the Boeing marketing group and performance data from the predominant airplanes within the fleet classes. Eight generic classes of airplanes were identified. These classifications of 1990 fleet airplanes within the generic fleet are shown in Table 3-2.8.

The base performance data for the predominant airplane in each class were selected to represent the performance data of the generic class. The predominant airplane is defined as the airplane that had the greatest global fuel burn relative to all airplanes within that particular class during the year 1990. These base performance data were then adjusted using a weighting factor accounting for global and local performance characteristics of the airplanes within the generic classes. The local performance factors were determined by flying the aircraft of a given type on a mission typical of those flown by that aircraft class. Only the major contributors to total fuel burn within each class were included in the calculation of the weighting factors. The performance weighting factors were calculated as follows:

$$\text{factor} = \frac{(L1 * G1 + L2 * G2 + L3 * G3 + \dots + L_n * G_n)}{L_c * (G1 + G2 + G3 + \dots + G_n)}$$

where

L1, L2, ..., L_n are the local fuel, NO_x, HC, or CO values of each airplane within the generic class.

G1, G2, ..., G_n are the global fuel, NO_x, HC, or CO values of each airplane within the generic class.

L_c is the local fuel, NO_x, HC, or CO value of the base airplane representing the generic class.

Emissions were calculated for the complete generic 1990 fleet by "flying" each generic airplane on the OAG routes of all airplanes within the respective generic class using the generic airplane performance data and weighting factors.

As might be expected, representing the entire fleet of aircraft with only eight generic types is less accurate than using the actual aircraft types in service. A comparison of the calculated fuel burned and emissions calculated using the database of 58 jet airliners and the eight 1990 generic classes is shown in Table 3-2.9. For this calculation, the results for the detailed calculation using 58 jet aircraft types were summed into classes and used as the reference in the comparison with the generic calculation.

As Table 3-2.9 shows, the generic description does a good job of accounting for global fuel burned, but there are errors of 10–15% for some aircraft types. Similarly globally calculated NO_x

emissions appear to be accounted for to within about 10%. Hydrocarbon and carbon monoxide emissions are much more poorly accounted for in the generic calculations.

The generic description involves grouping aircraft of similar size and range together as a class. This means that both old and new technology aircraft are grouped together and treated as one. Improvements in combustor efficiency have resulted in significant changes in the CO and HC emissions of aircraft engines. Thus, the generic categories do not do a very good job of accounting for these emissions. Since the new and old technology aircraft are not uniformly distributed between countries, there will be errors introduced in the geographical distribution of the emissions when generic categories are used.

In general, while the 1990 generic aircraft may be useful for parametric studies, there are significant errors introduced by trying to represent the diverse global aircraft fleet by just a few generic aircraft types.

2015 SCHEDULED SUBSONIC AIRLINER, CARGO, AND TURBOPROP SCENARIOS

2015 Marketing Analysis

For year 2015, passenger demand was projected by averaging regional growth rates predicted by the Boeing and McDonnell Douglas market research groups. It was assumed that the airline networks will be the same in 2015 as in 1991 and that airlines will operate with the same average load factors.

In order to balance airplane size growth and airplane departures (flight frequency) growth, the initial calculations of 2015 scheduled available seats used the common growth rates, while the 2015 scheduled departures used 50% of the common growth rate (i.e., the airplanes are projected to get bigger on average). Future aircraft were grouped into 10 generic passenger and 5 generic cargo sizes (see Table 3-2.10).

Estimation of the airplane size and frequency requirements by city-pair market for the year 2015 requires that two elements be forecast:

- Total number of seats required by each city-pair market.
- Total number of departures required by each city-pair market.

Passenger Fleet Airplane Size Results

Figure 3-2.10 compares the available seat mile (ASM) distribution by generic size for the passenger airplane in the 1991 schedule data, for the year 2010 in Boeing's 1992 annual forecast, "Current Market Outlook" (based on Boeing growth rates only) and the NASA Emission Study Forecast for the year 2015 (based on the Boeing/McDonnell Douglas "common" growth rates, described in subchapter 3-1). The latter forecast is shown with and without the presence of a fleet of 500 M2.4 300-passenger HSCTs. Both forecasts show a trend towards increasing airplane size with time. This is more pronounced for the NASA emission study forecast due to the later time period and to the generally higher growth rates. A target HSCT fleet of 500 airplanes consumes about 11% of the subsonic ASM requirement. This comes mostly at the expense of the larger subsonic aircraft, because they are heavily used on the North Atlantic and Pacific/Oceania routes, prime HSCT routes.

Cargo Fleet Requirement

The process for estimating the frequencies and aircraft size for cargo airplanes was the same as for the passenger airplanes except:

- Tons were used as a measure of capacity.
- Tons required were assumed to increase at 6.3% per year for all markets.
- Frequencies were assumed to increase at 4.0% per year for all markets.

Figure 3-2.11 shows the resulting Available Ton Mile (ATM) distribution for the September 1991 schedule and the 2015 forecast results. As with the passenger fleet there is a shift to larger capacity airplanes. The growth in cargo demand plus the shift to larger airplanes result in a majority of the freighter departures being in aircraft of more than 40 ton capacity (DC-10/767 size airplanes).

2015 Aircraft Technology

Baseline 1990 airplane performance data and engine performance data were used in the analysis of each class of airplane in the 2015 fleet. One modern 1990 airplane was selected to represent each class of projected 2015 airplane. Technology improvement factors were applied to each airplane to account for estimated improvements in fuel burn and emissions for airplanes entering service between 1990 and 2015. Based on a Boeing marketing analysis, a 2015 fleet would be composed of 50% airplanes built before 2005 and 50% airplanes built after 2005. The technology improvement factors were calculated assuming that the entire fleet would be "state of the art" for the year 2005.

Estimating the fuel flow improvement factor was a two-step process. First, the baseline airplane fuel flow was corrected to 1990 technology and then corrected again to reflect 2005 technology. The 1990 correction is based on the assumption that turbofan engines of all thrust ratings and equal technology will have approximately equal fuel flow to thrust ratios at maximum power.

Engine emissions improvement factors were estimated based on known differences between older technology engines and new modern engines. The technology improvement factors used are summarized in Table 3-2.11.

2015 Scheduled Air Traffic

The results for the projected 2015 subsonic airliner scenario, assuming no HSCT fleet exists, are summarized by aircraft type in Table 3-2.12. The results, summed over latitude and longitude, are shown as a function of altitude in Table 3-2.13.

A fleet of 500 Mach 2.4 HSCTs has been calculated to carry 386,800 passengers/day. This passenger demand would then be satisfied by the HSCT fleet displacing it from the subsonic airliners; so a scenario of these modified subsonic airliner operations was calculated. The results for the projected 2015 subsonic scenario, assuming an HSCT fleet exists, are summarized in Tables 3-2.14 and 3-2.15.

The fuel burned and emissions for the projected 2015 scheduled cargo scenario are summarized in Tables 3-2.16 and 3-2.17. The calculations indicate that fuel burned by scheduled cargo aircraft will only be about 2.3% of that used by scheduled airliners.

The 2015 turboprop analysis was completed using the 1990 medium sized turboprop performance data for all turboprop routes in the projected 2015 OAG. No technology

improvement factors were applied to the data since it is uncertain how the fuel burn and emissions characteristics of these airplanes will change. A detailed analysis of future turboprop technology was not justified because the calculations for 1990 indicate that turboprops only consume 1.1% of the global jet fuel (see subchapter 3-4). Departures for turboprop aircraft were projected at 38,743 for 2015 with an average route distance of 149.9 nautical miles, for a total daily distance flown of 5,806,976 nautical miles. Global fuel usage by turboprops was calculated to be 4.14×10^9 kg/year, which is 1.7% of the fuel used by the projected 2015 airliners.

Discussion

The three-dimensional character of the data sets are illustrated in Figures 3-2.12 and 3-2.13, which show NO_x emissions as a function of altitude, latitude, and longitude for the 1990 and 2015 scheduled air traffic (airliner, cargo, and turboprop). These figures emphasize that much of the air traffic is expected to occur at northern midlatitudes with increased traffic in more southern latitudes by 2015.

NO_x emissions as a function of altitude are shown more quantitatively for the 1990 scheduled airliner and cargo scenario and the 2015 subsonic airliner and cargo (both with and without an HSCT fleet) scenarios in Figure 3-2.14. While NO_x emissions are expected to rise because of the increase in air traffic, only small changes in the altitude distribution are predicted.

Plots of fuel burned as a function of latitude (summed over altitude and longitude) (Figures 3-2.15 and 3-2.16) show that the largest relative increase is in the tropics and lower latitudes. In both 1990 and 2015, most air traffic is expected to occur in the northern hemisphere.

Fuel usage by scheduled airliner and cargo aircraft in 2015 is projected to be about 2.8–3.2 times larger than 1990 levels depending on whether an HSCT fleet exists or not. Global NO_x emissions from scheduled air traffic are projected to increase by about a factor of two from 1990 to 2015. By comparison, revenue passenger miles are projected to increase by a factor of 5.7, from 1203 billion in 1990 to 6883 billion in 2015 (based on the "common" forecast described in subchapter 3-1).

SUMMARY

A detailed database of 1990 and projected 2015 scheduled subsonic aircraft operations has been developed. The total emissions of each component are tabulated in subchapter 3-4, as well as a discussion of the calculated fuel burn relative to 1990 reported jet fuel consumptions.

A more detailed discussion of the methodology and results will be presented in a contractor report to NASA.

Table 3-2.1. Comparison of the Global Atmospheric Emission Code (GAEC)
Results with Detailed Engineering Model Calculations (BMAP/EMIT)
For Four Aircraft Missions Using One Aircraft/Engine Type

ROUTE	BMAP-EMIT				GAEC				Differences			
	fuel (lb)	CO (lb)	HC (lb)	NO _x (lb)	fuel (lb)	CO (lb)	HC (lb)	NO _x (lb)	fuel %	CO %	HC %	NO _x %
TPA-PBI	151	nmi										
taxi-out	432	18.1	1.5	1.5	432	18.2	1.5	1.6	0	-0.39	0	-8
takeoff	768	0.4	0	17.9	765.9	0.3	0	17.9	0.27	22.05	-2.5	0.22
climb	1912	0.9	0.1	45	1814.6	0.9	0.1	42.4	5.09	-7.16	-3.64	5.78
cruise	1916	4.9	0.4	22.7	2093.2	5.1	0.4	24.1	-9.25	-4.69	-9.19	-6.04
descent	387.5	30.2	2.5	1.3	396.6	30.5	2.5	1.3	-2.35	-0.83	-0.8	5.3
approach	400	7.1	0.6	2.7	400	5.3	0.4	2.3	0	25.63	24.91	13.21
taxi-in	239	10.1	0.8	0.9	240	10.1	0.8	0.9	-0.42	0.49	0.71	-2.27
Total	6115	71.7	6	92.2	6142.3	70.4	5.9	90.4	-0.45	1.83	1.88	2
LAX-DFW	1071	nmi										
taxi-out	431.9	18.1	1.5	1.5	432	18.1	1.5	1.6	-0.02	0	0	-6.67
takeoff	823	0.4	0	19	821	0.4	0.1	19.3	0.24	15.91	-2.27	-1.58
climb	5138	3.3	0.4	105.4	4967	3.2	0.4	100.9	3.33	3.32	2.5	4.27
cruise	16060	41.2	3.5	177.3	16148	42.1	3.6	177.9	-0.55	-2.18	-1.7	-0.34
descent	691.2	63.9	5.3	2	719.7	66	5.5	2.2	-4.12	-3.29	-3	-9.09
approach	400	7.1	0.6	2.7	400	5.3	0.4	2.3	0	26.06	24.56	12.83
taxi-in	239.1	10	0.8	0.9	240	10	0.8	0.9	-0.38	-0.4	1.19	-3.41
Total	23704	144.2	12.2	308.9	23728	145.1	12.3	305.1	-0.1	-0.64	-0.82	1.25
JFK-OSL	3198	nmi										
taxi-out	432	18.1	1.5	1.5	432	18.2	1.5	1.6	0	-0.55	0	-6.67
takeoff	976	0.4	0	22.9	975	0.4	0.1	23.1	0.1	0		-0.87
											20.41	
climb	5645.2	3.3	0.4	120.4	5682	3.5	0.4	118.9	-0.65	-5.74	-5	1.25
cruise	60965	129.4	11.6	717.6	60654	129.6	11.6	706.7	0.51	-0.15	0	1.52
descent	687.8	63.9	5.3	2	715.2	65.4	5.5	2.2	-3.98	-2.35	-2.64	-8.59
approach	400	7.1	0.6	2.7	400	5.2	0.4	2.3	0	26.76	24.56	12.45
taxi-in	239	9.9	0.8	0.9	240	10	0.8	0.9	-0.42	-0.81	-1.22	-3.41
Total	69346	232	20.3	868.2	69099	232.4	20.3	855.7	0.36	-0.17	0	1.44
SIN-VIE	5242	nmi										
taxi-out	431.9	18.1	1.5	1.5	432	18.1	1.5	1.6	-0.02	0	0	-8
takeoff	1087	0.4	0.1	25.8	1087	0.5	0.1	26	0	-11.36	10.61	-0.78
climb	6289.4	3.5	0.4	138	6596	3.9	0.5	141.4	-4.87	-10.8	-9.09	-2.46
cruise	111151	198	18.5	1387	110445	198.2	18.6	1365	0.64	-0.1	-0.05	1.53
descent	692.5	64.2	5.4	2	717.5	65.7	5.5	2.2	-3.61	-2.34	-2.05	-10
approach	400	7.1	0.6	2.7	400	5.3	0.4	2.3	0	25.53	24.56	12.83
taxi-in	239	9.9	0.8	0.9	240	10	0.8	0.9	-0.42	-1.01	-1.22	-2.27
Total	120290	301.4	27.3	1539	119918	301.8	27.3	1540	0.31	-0.13	0	-0.08

Table 3-2.2. Fuel Burned, Emissions, Cumulative (Label Cum) Fractions, and Emission Indices as a Function of Altitude (Computed Over Latitude and Longitude) for the Mach 2.4 (Nominal EI(NO_x)=5) HSCT Fleet Only*

Altitude Band (km)	Fuel (kg/year)	Cum Fuel [†] (%)	NO _x (kg/year)	Cum NO _x (%)	HC (kg/year)	Cum HC (%)	CO (kg/year)	Cum CO (%)	EI(NO _x)	EI(HC)	EI(CO)
0-1	2.24E+09	2.93	1.59E+07	3.19	2.92E+06	10.32	2.77E+07	11.85	7.12	1.31	12.37
1-2	7.65E+08	3.93	6.28E+06	4.45	4.47E+05	11.90	2.92E+06	13.10	8.21	0.59	3.82
2-3	7.65E+08	4.93	6.28E+06	5.70	4.47E+05	13.48	2.92E+06	14.35	8.21	0.59	3.82
3-4	7.65E+08	5.93	6.28E+06	6.96	4.47E+05	15.06	2.92E+06	15.60	8.21	0.59	3.82
4-5	7.65E+08	6.93	6.28E+06	8.21	4.47E+05	16.64	2.92E+06	16.86	8.21	0.59	3.82
5-6	7.65E+08	7.93	6.28E+06	9.47	4.47E+05	18.22	2.92E+06	18.11	8.21	0.59	3.82
6-7	7.65E+08	8.93	6.28E+06	10.73	4.47E+05	19.80	2.92E+06	19.36	8.21	0.59	3.82
7-8	7.65E+08	9.93	6.28E+06	11.98	4.47E+05	21.38	2.92E+06	20.61	8.21	0.59	3.82
8-9	7.65E+08	10.93	6.28E+06	13.24	4.47E+05	22.96	2.92E+06	21.86	8.21	0.59	3.82
9-10	1.64E+09	13.07	1.36E+07	15.96	8.00E+05	25.79	5.87E+06	24.38	8.30	0.49	3.59
10-11	3.13E+09	17.17	2.61E+07	21.18	1.41E+06	30.77	1.11E+07	29.11	8.34	0.45	3.53
11-12	2.61E+09	20.58	2.19E+07	25.56	1.14E+06	34.81	7.82E+06	32.46	8.38	0.44	3.00
12-13	4.75E+09	26.80	3.97E+07	33.52	2.05E+06	42.05	1.65E+07	39.55	8.36	0.43	3.48
13-14	1.52E+09	28.79	1.31E+07	36.13	4.83E+05	43.75	9.98E+05	39.97	8.61	0.32	0.66
14-15	1.52E+09	30.77	1.31E+07	38.75	4.83E+05	45.46	9.98E+05	40.40	8.61	0.32	0.66
15-16	1.52E+09	32.76	1.31E+07	41.36	4.83E+05	47.16	9.98E+05	40.83	8.61	0.32	0.66
16-17	1.52E+09	34.75	1.31E+07	43.98	4.83E+05	48.87	9.98E+05	41.26	8.61	0.32	0.66
17-18	1.56E+09	36.79	1.33E+07	46.64	4.95E+05	50.62	1.14E+06	41.74	8.51	0.32	0.73
18-19	7.40E+09	46.47	4.35E+07	55.35	2.17E+06	58.27	1.90E+07	49.87	5.88	0.29	2.56
19-20	1.86E+10	70.75	1.02E+08	75.72	5.36E+06	77.23	5.27E+07	72.43	5.48	0.29	2.84
20-21	2.23E+10	99.96	1.21E+08	99.97	6.44E+06	99.97	6.43E+07	99.96	5.43	0.29	2.88
21-22	2.97E+07	100.00	1.61E+05	100.00	8.58E+03	100.00	8.56E+04	100.00	5.42	0.29	2.88
Global Total	7.64E+10		5.00E+08		2.83E+07		2.33E+08		6.54	0.37	3.05

* 1.00E + 08 = 1.0 × 10⁸

Table 3-2.3. Fuel Burned, Emissions, Cumulative Fractions, and Emission Indices as a Function of Altitude (Computed Over Latitude and Longitude) for the Mach 2.4 (Nominal EI(NO_x)=15) HSCT Fleet Only*

Altitude Band (km)	Fuel (kg/year)	Cum Fuel (%)	NO _x (kg/year)	Cum NO _x (%)	HC (kg/year)	Cum HC (%)	CO (kg/year)	Cum CO (%)	EI(NO _x)	EI(HC)	EI(CO)
0 - 1	2.24E+09	2.93	3.32E+07	2.45	2.92E+06	10.32	2.77E+07	11.85	14.86	1.31	12.37
1 - 2	7.65E+08	3.93	1.74E+07	3.73	4.47E+05	11.90	2.92E+06	13.10	22.70	0.59	3.82
2 - 3	7.65E+08	4.93	1.74E+07	5.01	4.47E+05	13.48	2.92E+06	14.35	22.70	0.59	3.82
3 - 4	7.65E+08	5.93	1.74E+07	6.29	4.47E+05	15.06	2.92E+06	15.60	22.70	0.59	3.82
4 - 5	7.65E+08	6.93	1.74E+07	7.57	4.47E+05	16.64	2.92E+06	16.86	22.70	0.59	3.82
5 - 6	7.65E+08	7.93	1.74E+07	8.85	4.47E+05	18.22	2.92E+06	18.11	22.70	0.59	3.82
6 - 7	7.65E+08	8.93	1.74E+07	10.13	4.47E+05	19.80	2.92E+06	19.36	22.70	0.59	3.82
7 - 8	7.65E+08	9.93	1.74E+07	11.41	4.47E+05	21.38	2.92E+06	20.61	22.70	0.59	3.82
8 - 9	7.65E+08	10.93	1.74E+07	12.69	4.47E+05	22.96	2.92E+06	21.86	22.70	0.59	3.82
9 - 10	1.64E+09	13.07	2.86E+07	14.80	8.00E+05	25.79	5.87E+06	24.38	17.50	0.49	3.59
10 - 11	3.13E+09	17.17	4.74E+07	18.30	1.41E+06	30.77	1.11E+07	29.11	15.16	0.45	3.53
11 - 12	2.61E+09	20.58	4.69E+07	21.76	1.14E+06	34.81	7.82E+06	32.46	17.98	0.44	3.00
12 - 13	4.75E+09	26.80	6.74E+07	26.73	2.05E+06	42.05	1.65E+07	39.55	14.17	0.43	3.48
13 - 14	1.52E+09	28.79	3.89E+07	29.59	4.83E+05	43.75	9.98E+05	39.97	25.61	0.32	0.66
14 - 15	1.52E+09	30.77	3.89E+07	32.46	4.83E+05	45.46	9.98E+05	40.40	25.61	0.32	0.66
15 - 16	1.52E+09	32.76	3.89E+07	35.32	4.83E+05	47.16	9.98E+05	40.83	25.61	0.32	0.66
16 - 17	1.52E+09	34.75	3.89E+07	38.19	4.83E+05	48.87	9.98E+05	41.26	25.61	0.32	0.66
17 - 18	1.56E+09	36.79	3.96E+07	41.11	4.95E+05	50.62	1.14E+06	41.74	25.32	0.32	0.73
18 - 19	7.40E+09	46.47	1.30E+08	50.71	2.17E+06	58.27	1.90E+07	49.87	17.60	0.29	2.56
19 - 20	1.86E+10	70.75	3.05E+08	73.20	5.36E+06	77.23	5.27E+07	72.43	16.44	0.29	2.84
20 - 21	2.23E+10	99.96	3.63E+08	99.96	6.44E+06	99.97	6.43E+07	99.96	16.26	0.29	2.88
21 - 22	2.97E+07	100.00	4.83E+05	100.00	8.58E+03	100.00	8.56E+04	100.00	16.26	0.29	2.88
Global Total	7.64E+10		1.36E+09		2.83E+07		2.33E+08		17.75	0.37	3.05

* 1.00E+08 = 1x10⁸

Table 3-2.4. Globally Computed Fuel Burned, Emissions, and Emission Indices for Each Aircraft Included in the 1990 Scheduled Airline and Cargo Database*

File					Globally	Summed	Emission
	Fuel	NO _x	HC	CO	EI (NO _x)	Indices EI (HC)	EI (CO)
	(kg/year)	(kg/year)	(kg/year)	(kg/year)			
707-320B-C_JT3D-7	5.33E+08	3.00E+06	1.80E+07	1.96E+07	5.64	33.70	36.85
727-100_JT8D-9	2.71E+08	2.16E+06	5.62E+05	2.00E+06	7.98	2.08	7.39
727-200_JT8D-15	1.04E+10	1.01E+08	6.81E+06	3.85E+07	9.75	0.66	3.71
727-200_JT8D-9	1.97E+09	1.93E+07	1.79E+06	8.68E+06	9.76	0.91	4.39
737-200_JT8D-15	3.79E+09	3.51E+07	3.02E+06	1.84E+07	9.25	0.80	4.86
737-200_JT8D-9	2.43E+09	2.11E+07	2.72E+06	1.28E+07	8.67	1.12	5.26
737-300+400+500_CFM56	6.69E+09	7.11E+07	2.89E+06	5.58E+07	10.63	0.43	8.34
747-100+200_CFM56	5.49E+09	8.41E+07	5.56E+06	3.09E+07	15.34	1.01	5.62
747-100+200_JT9D-7A	5.43E+09	7.98E+07	9.48E+06	1.88E+07	14.70	1.75	3.47
747-200_JT9D-7J	8.14E+08	1.22E+07	1.48E+06	2.81E+06	14.98	1.82	3.46
747-200_JT9D-7Q	4.74E+09	5.49E+07	6.22E+06	1.77E+07	11.58	1.31	3.73
747-200_JT9D-7R4G2	4.08E+08	4.84E+06	1.62E+05	1.11E+06	11.86	0.40	2.73
747-200_RB211	3.52E+09	6.92E+07	1.65E+06	6.12E+06	19.62	0.47	1.74
747-300_CFM56	2.65E+08	4.15E+06	2.73E+05	1.44E+06	15.67	1.03	5.44
747-300_CFM56-80C2	2.49E+08	2.78E+06	2.24E+05	1.01E+06	11.16	0.90	4.04
747-300_JT9D-7R4G2	1.07E+09	1.34E+07	4.02E+05	2.68E+06	12.56	0.38	2.50
747-300_RB211	4.87E+08	1.00E+07	2.81E+05	1.03E+06	20.55	0.58	2.11
747-400_CFM56-80C2	4.27E+08	4.76E+06	5.18E+05	2.25E+06	11.15	1.21	5.27
747-400_PW4056	1.30E+09	1.69E+07	2.89E+05	3.76E+06	12.99	0.22	2.88
747-400_RB211	6.91E+08	9.94E+06	1.86E+06	1.80E+06	14.38	2.69	2.61
747SP_JT9D-7	9.45E+08	1.23E+07	2.20E+06	4.29E+06	12.99	2.33	4.54
747SP_RB211	1.74E+07	3.35E+05	3.81E+04	1.31E+05	19.26	2.19	7.55
757-200_PW2000	1.09E+09	1.45E+07	5.42E+05	5.33E+06	13.36	0.50	4.89
757-200_RB211	8.65E+08	1.03E+07	1.63E+06	5.73E+06	11.89	1.89	6.62
767-200+ER_CFM56-80A	1.39E+09	1.85E+07	1.58E+06	7.47E+06	13.27	1.13	5.37
767-200+ER_CFM56-80C2	2.60E+08	2.60E+06	4.53E+05	1.88E+06	10.00	1.74	7.25
767-200+ER_JT9D-7R4	1.13E+09	1.47E+07	3.70E+05	2.65E+06	13.08	0.33	2.35
767-200+ER_PW4000	3.13E+07	3.70E+05	9.45E+03	1.20E+05	11.83	0.30	3.84
767-300+ER_CFM56-80C2	5.29E+08	6.02E+06	1.24E+06	4.89E+06	11.38	2.35	9.24
767-300+ER_JT9D-7R4	1.32E+08	2.15E+06	5.52E+04	3.97E+05	16.25	0.42	3.00
767-300+ER_PW4060	3.82E+08	4.91E+06	1.68E+05	1.97E+06	12.86	0.44	5.15
767-300ER_RB211	4.18E+07	8.04E+05	1.15E+05	3.98E+05	19.25	2.75	9.54
A300-600+ER_CFM56-80C2	3.01E+08	3.51E+06	6.03E+05	2.29E+06	11.65	2.00	7.62
A300-B2+B4_CFM56-80C2	3.61E+09	6.42E+07	4.40E+06	2.36E+07	17.77	1.22	6.54
A310-200+300_CFM56-80A	1.65E+09	2.21E+07	1.75E+06	8.28E+06	13.34	1.06	5.00
A320-200+300_CFM56-5-A1	3.84E+08	5.34E+06	2.50E+05	2.15E+06	13.91	0.65	5.60
BAC111_SPEY-512	2.60E+08	2.62E+06	2.36E+05	1.84E+06	10.07	0.91	7.07
BAE146_ALF502	5.49E+08	5.09E+06	4.95E+06	1.33E+07	9.27	9.02	24.18
CARAVELLE-10B_JT8D	5.06E+07	4.21E+05	5.60E+04	2.66E+05	8.31	1.11	5.26
CONCORDE	1.47E+08	1.02E+06	1.20E+06	9.07E+06	6.94	8.14	61.53
DASSMR_JT8D-7	4.56E+07	3.63E+05	4.08E+05	8.88E+05	7.97	8.94	19.47

DC10-10_CF6-6D	9.73E+08	1.88E+07	6.11E+05	3.64E+06	19.36	0.63	3.74
DC10-30_CF6-50E2	6.77E+09	9.78E+07	6.22E+06	4.72E+07	14.44	0.92	6.97
DC8-63_JT3D	6.30E+08	3.82E+06	1.03E+07	1.13E+07	6.07	16.31	17.96
DC8-71_CFM56-B1	8.39E+08	8.61E+06	2.35E+05	4.04E+06	10.26	0.28	4.82
DC9-10+20+30_JT8D	3.61E+09	2.99E+07	5.46E+06	2.70E+07	8.29	1.51	7.48
DC9-40+50_JT8D	6.99E+08	6.94E+06	7.16E+05	3.99E+06	9.93	1.02	5.71
FOKKER-100_TAY-650	1.52E+08	1.19E+06	4.49E+05	4.42E+06	7.83	2.96	29.13
FOKKER-28_SPEY-555	7.70E+08	7.30E+06	5.37E+05	6.85E+06	9.48	0.70	8.90
IL-62_JT3D-7	5.65E+08	3.14E+06	9.51E+06	1.28E+07	5.55	16.82	22.62
IL-86_RB211	5.28E+08	9.54E+06	9.07E+05	3.03E+06	18.05	1.72	5.74
L1011_RB211	3.47E+09	6.22E+07	2.24E+06	9.36E+06	17.90	0.65	2.70
MD-82_JT8D-217	4.59E+09	5.55E+07	7.28E+06	2.29E+07	12.10	1.59	4.99
MD-87_JT8D-217	1.75E+08	1.91E+06	3.25E+05	9.88E+05	10.90	1.86	5.66
TRIDENT_JT8D-7	4.48E+07	3.58E+05	2.89E+05	5.83E+05	7.99	6.45	13.01
TU134_JT8D-7	2.86E+08	2.23E+06	1.40E+06	4.18E+06	7.79	4.91	14.63
TU154_JT8D-15	1.57E+09	1.48E+07	9.79E+05	5.26E+06	9.45	0.62	3.35
YAK-40+42_JT8D-7	3.61E+08	3.11E+06	2.76E+06	5.28E+06	8.60	7.63	14.60
Total	9.08E+10	1.14E+09	1.37E+08	5.17E+08	12.54	1.50	5.69

* 1.00E + 08 = 1.0×10^8

Table 3-2.5. Fuel Burned, Emissions, Cumulative Fractions, and Emission Indices as a Function of Altitude (Computed Over Latitude and Longitude) for the 1990 Scheduled Airline and Cargo Database*

Altitude Band (km)	Fuel (kg/year)	Cum Fuel (%)	NO _x (kg/year)	Cum NO _x (%)	HC (kg/year)	Cum HC (%)	CO (kg/year)	Cum CO (%)	EI(NO _x)	EI(HC)	EI(CO)
0 - 1	1.09E+10	12.03	1.32E+08	11.62	3.99E+07	29.21	1.54E+08	29.78	12.11	3.65	14.09
1 - 2	2.62E+09	14.92	4.14E+07	15.25	6.45E+06	33.93	2.38E+07	34.38	15.79	2.46	9.08
2 - 3	2.40E+09	17.57	4.01E+07	18.77	6.14E+06	38.42	2.12E+07	38.48	16.71	2.56	8.81
3 - 4	2.80E+09	20.65	5.04E+07	23.19	6.09E+06	42.88	2.00E+07	42.35	17.96	2.17	7.14
4 - 5	2.36E+09	23.25	3.92E+07	26.63	6.31E+06	47.50	1.94E+07	46.10	16.57	2.67	8.22
5 - 6	2.31E+09	25.80	3.68E+07	29.86	6.79E+06	52.47	2.06E+07	50.08	15.93	2.94	8.90
6 - 7	2.40E+09	28.45	3.73E+07	33.14	6.83E+06	57.47	2.01E+07	53.96	15.51	2.84	8.34
7 - 8	2.56E+09	31.26	3.67E+07	36.36	7.44E+06	62.92	2.15E+07	58.12	14.35	2.91	8.40
8 - 9	2.79E+09	34.34	3.65E+07	39.57	7.06E+06	68.09	2.05E+07	62.09	13.09	2.53	7.36
9 - 10	4.61E+09	39.41	5.93E+07	44.77	7.94E+06	73.91	2.28E+07	66.50	12.86	1.72	4.95
10 - 11	2.82E+10	70.49	3.05E+08	71.51	1.95E+07	88.15	8.41E+07	82.77	10.79	0.69	2.98
11 - 12	2.58E+10	98.94	3.14E+08	99.07	1.47E+07	98.91	7.96E+07	98.16	12.15	0.57	3.08
12 - 13	4.69E+08	99.46	5.10E+06	99.52	4.47E+05	99.23	1.26E+06	98.41	10.89	0.95	2.70
13 - 14	3.82E+08	99.88	4.83E+06	99.94	1.80E+05	99.36	6.89E+05	98.54	12.64	0.47	1.80
14 - 15	3.95E+06	99.88	3.65E+04	99.94	2.22E+04	99.38	1.59E+05	98.57	9.24	5.62	40.14
15 - 16	3.95E+06	99.89	3.65E+04	99.95	2.37E+04	99.40	1.69E+05	98.60	9.24	5.99	42.80
16 - 17	3.75E+07	99.93	2.28E+05	99.97	2.92E+05	99.61	2.55E+06	99.10	6.08	7.77	68.00
17 - 18	4.97E+07	99.98	2.98E+05	99.99	4.10E+05	99.91	3.60E+06	99.79	5.99	8.24	72.40
18 - 19	1.43E+07	100.00	8.58E+04	100.00	1.22E+05	100.00	1.07E+06	100.00	5.99	8.52	74.86
Global Total	9.08E+10		1.14E+09		1.37E+08		5.17E+08		12.54	1.50	5.69

* 1.00E+08 = 1x10⁸

Table 3-2.6. Comparison of Calculated 1990 Fuel Burned with Airline Reported Fuel Burned for Two Aircraft Types (Boeing 727-200 and 747)

[illegible]

Table 3-2.7. Summary of Fuel Burned and Emissions for 1990 Scheduled Turbo Prop Database*

Size	Fuel (kg/year)	Globally Averaged Emission Indices					
		NO _x (kg/year)	HC (kg/year)	CO (kg/year)	EI (NO _x)	EI (HC)	EI (CO)
Large turboprops	7.98E+08	9.65E+06	0.00E+00	3.73E+06	12.10	0.00	4.68
Medium turboprops	5.46E+08	5.96E+06	8.67E+05	3.09E+06	10.92	1.59	5.65
Small turboprops	6.42E+08	4.91E+06	2.44E+05	2.96E+06	7.65	0.38	4.60
Total	1.99E+09	2.05E+07	1.11E+06	9.77E+06	10.34	0.56	4.92

Altitude Band (km)	Fuel (kg/year)	Cum Fuel (%)	NO _x (kg/year)	Cum NO _x (%)	HC (kg/year)	Cum HC (%)	CO (kg/year)	Cum CO (%)	EI(NO _x)	EI(HC)	EI(CO)
0 - 1	4.42E+08	22.26	2.88E+06	14.04	3.78E+05	34.03	3.69E+06	37.80	6.52	0.86	8.35
1 - 2	2.28E+08	33.73	2.10E+06	24.26	1.50E+05	47.52	1.19E+06	49.94	9.21	0.66	5.21
2 - 3	2.71E+08	47.37	2.91E+06	38.45	1.29E+05	59.10	1.17E+06	61.90	10.76	0.48	4.32
3 - 4	3.23E+08	63.64	3.70E+06	56.45	1.57E+05	73.27	1.19E+06	74.07	11.43	0.49	3.68
4 - 5	3.91E+08	83.34	4.51E+06	78.44	1.96E+05	90.91	1.29E+06	87.28	11.54	0.50	3.30
5 - 6	2.72E+08	97.02	3.90E+06	97.42	8.83E+04	98.85	9.54E+05	97.04	14.34	0.33	3.51
6 - 7	4.48E+07	99.28	3.83E+05	99.29	9.45E+03	99.70	2.32E+05	99.41	8.55	0.21	5.17
7 - 8	1.43E+07	100.00	1.47E+05	100.00	3.31E+03	100.00	5.76E+04	100.00	10.26	0.23	4.03
Global Total	1.99E+09		2.05E+07		1.11E+06		9.77E+06		10.34	0.56	4.92

* 1.00E+08 = 1x10⁸

* 1.00E+08 = 1x10⁸

Table 3-2.8. Aircraft Types Included in the Construction of the 1990 "Generic" Database

Generic Class		Real Aircraft
1990 SST	Concorde	
P080	727-100_JT8D-9 BAC111_SPEY-512 BAE146_ALF502 CARAVELLE-10B_JT8D	DC9-10+20+30_JT8D FOKKER-100_TAY-650 FOKKER-28_SPEY-555 TU134_JT8D-7
P120	727-200_JT8D-9 737-200_JT8D-9 737-200_JT8D-15 737-300+400+500_CFM56 DASSMR_JT8D-7	DC9-40+50_JT8D MD-87_JT8D-217 TRIDENT_JT8D-7 YAK-40+42_JT8D-7
P180A	707-320B-C_JT3D-7 727-200_JT8D-15 IL-62_JT3D-7	MD-82_JT8D-217 TU154_JT8D-15
P180B	757-200_PW2000 757-200_RB211 A320-200+300_CFM56-5-A1	DC8-63_JT3D DC8-71_CFM56-B1
P250	747SP_JT9D-7 747SP_RB211 767-200+ER_CFM56-80A 767-200+ER_JT9D-7R4 767-200+ER_PW4000 767-200+ER_CFM56-80C2 767-300+ER_CFM56-80C2 767-300+ER_JT9D-7R4	767-300+ER_PW4060 767-300ER_RB211 A300-600+ER_CFM56-80C2 A300-B2+B4_CFM56-50C2 DC10-10_CFM56-6D DC10-30_CFM56-50E2 L1011_RB211 A310-200+300_CFM56-80A
P350	747-100+200_JT9D-7A 747-100+200_CFM56-50E2 747-200_JT9D-7J 747-200_JT9D-7Q	747-200_JT9D-7R4G2 747-200_RB211 IL-86_RB211
P500	747-300_CFM56-50E2 747-300_CFM56-80C2 747-300_JT9D-7R4G2 747-300_RB211	747-400_CFM56-80C2 747-400_PW4056 747-400_RB211

Table 3-2.9. Comparison of the Globally Computed Fuel Burned, Emissions, and Emission Indices for the 1990 Generic Database Relative to that Calculated Using Actual 1990 Aircraft

File	Fuel	NO _x	HC	CO	EI(NO _x)	EI(HC)	EI(CO)
1990.SST	0.00%	0.00%	0.00%	0.00%	0.00%	0.00%	0.00%
P080	0.52%	6.65%	-32.84%	-132.64%	6.17%	-33.53%	-133.85%
P120	11.85%	7.86%	50.61%	21.31%	-4.53%	43.98%	10.73%
P180A	-0.66%	7.31%	58.44%	34.85%	7.91%	58.71%	35.27%
P180B	15.01%	0.71%	64.02%	40.84%	-16.83%	57.67%	30.40%
P250	-13.58%	-11.57%	18.93%	10.73%	1.78%	28.62%	21.40%
P350	1.28%	-1.33%	-14.42%	-21.19%	-2.64%	-15.90%	-22.77%
P500	0.02%	-7.06%	-103.53%	-10.49%	-7.08%	-103.57%	-10.52%
Total	-0.29%	-1.55%	23.95%	-3.10%	-1.26%	24.17%	-2.80%

Table 3-2.10. Classes of "Generic" Subsonic Airliner and Cargo Aircraft Used in the 2015 Scenario Construction

Passenger Aircraft

Class	Seating Capacity	Average Seats
TBP (turboprop)	0 - 50	30
P060	50 - 70	60
P080	70 - 110	85
P120	110 - 140	120
P180	140 - 200	170
P250	200 - 300	250
P350	300 - 400	350
P500	400 - 600	500
P700	600 - 800	700
P900	> 800	900

YR 2015 "Generic" Cargo Airplane Sizes

Class	Capacity (Tons)	Average (Tons)
C005	0 - 5	3.0
C010	5 - 10	15.0
C040	20 - 40	30.0
C080	40 - 80	60.0
C160	> 80	120.0

Table 3-2.11. Technology Improvement Factors for 2015 Aircraft Relative to 1990 Technology

Generic Airplane	Fuel Flow Factor	NO_x factor	HC factor	CO factor
PTBP	1.00	1.00	1.00	1.00
P060	0.49	0.60	0.70	0.50
P080	0.69	0.70	0.60	0.70
P120	0.71	0.70	0.60	0.70
P180	0.75	0.70	0.60	0.70
P250A	0.87	0.60	1.00	1.00
P250B	0.86	0.70	0.60	0.70
P350	0.95	0.70	1.00	1.00
P500	0.86	0.70	0.60	0.70
P700	1.19	0.70	1.00	1.00
P900	1.28	0.70	1.00	1.00
C005	0.69	0.70	0.60	0.70
C010	0.75	0.70	0.60	0.70
C020	0.71	0.70	0.60	0.70
C040	0.87	0.60	1.00	1.00
C080	0.86	0.70	0.60	0.70
C160	0.86	0.70	0.60	0.70

Table 3-2.12. Globally Computed Fuel Burned, Emissions, and Emission Indices by Aircraft Type for 2015 Scheduled Subsonic Airliners if no HSCT Fleet Exists

File	Fuel (kg/year)	NO _x (kg/year)	HC (kg/year)	CO (kg/year)	Globally Averaged Emission Indices		
					EI (NO _x)	EI (HC)	EI (CO)
P060	2.63E+09	1.49E+07	1.47E+06	1.45E+07	5.66	0.56	5.50
P080	8.67E+09	6.84E+07	2.91E+06	6.59E+07	7.88	0.34	7.60
P120	1.42E+10	1.04E+08	8.02E+06	1.25E+08	7.37	0.57	8.85
P180	2.35E+10	1.73E+08	5.81E+06	1.23E+08	7.39	0.25	5.25
P250A	2.49E+10	2.15E+08	1.64E+07	1.63E+08	8.64	0.66	6.56
P250B	2.10E+10	1.54E+08	1.39E+07	7.59E+07	7.33	0.66	3.61
P350	4.32E+10	4.53E+08	1.52E+07	1.61E+08	10.49	0.35	3.72
P500	5.25E+10	4.88E+08	1.86E+07	2.23E+08	9.31	0.35	4.26
P700	3.15E+10	3.61E+08	5.11E+06	6.84E+07	11.48	0.16	2.17
P900	2.29E+10	2.06E+08	4.55E+06	6.52E+07	9.01	0.20	2.85
Total	2.45E+11	2.24E+09	9.20E+07	1.09E+09	9.14	0.38	4.43

Table 3-2.13. Altitude Distribution of Fuel Burned and Emissions (Computed Over Latitude and Longitude) for 2015 Scheduled Subsonic Airliners if no HSCT Fleet Exists.*

Altitude Band (km)	Fuel (kg/year)	Cum Fuel (%)	NO _x (kg/year)	Cum NO _x (%)	HC (kg/year)	Cum HC (%)	CO (kg/year)	Cum CO (%)	EI(NO _x)	EI(HC)	EI(CO)
0 - 1	2.63E+10	10.73	2.58E+08	11.51	2.97E+07	32.24	3.41E+08	31.37	9.81	1.13	12.97
1 - 2	6.54E+09	13.40	8.19E+07	15.17	5.44E+06	38.16	5.89E+07	36.80	12.53	0.83	9.01
2 - 3	5.65E+09	15.71	6.85E+07	18.23	4.67E+06	43.24	5.01E+07	41.41	12.12	0.83	8.86
3 - 4	7.37E+09	18.72	9.78E+07	22.60	4.04E+06	47.62	4.38E+07	45.45	13.27	0.55	5.95
4 - 5	6.06E+09	21.19	7.36E+07	25.89	4.20E+06	52.19	4.55E+07	49.64	12.14	0.69	7.51
5 - 6	5.76E+09	23.55	6.69E+07	28.88	4.29E+06	56.86	4.63E+07	53.91	11.62	0.75	8.05
6 - 7	5.19E+09	25.67	5.93E+07	31.53	3.80E+06	60.99	4.08E+07	57.67	11.43	0.73	7.86
7 - 8	5.62E+09	27.96	6.11E+07	34.26	4.20E+06	65.56	4.50E+07	61.82	10.89	0.75	8.02
8 - 9	6.29E+09	30.53	6.62E+07	37.21	4.46E+06	70.41	4.74E+07	66.19	10.53	0.71	7.55
9 - 10	7.38E+09	33.54	7.22E+07	40.44	4.44E+06	75.24	4.60E+07	70.43	9.78	0.60	6.24
10 - 11	5.04E+10	54.12	4.02E+08	58.41	7.29E+06	83.16	1.05E+08	80.14	7.99	0.14	2.09
11 - 12	1.12E+11	100.00	9.31E+08	100.00	1.55E+07	100.00	2.16E+08	100.00	8.29	0.14	1.92
Global Total	2.45E+11		2.24E+09		9.20E+07		1.09E+09		9.14	0.38	4.43

* 1.00E+08 = 1x10⁸

Table 3-2.14. Globally Computed Fuel Burned, Emissions, and Emission Indices by Aircraft Type for 2015 Scheduled Subsonic Airliners if 500 Mach 2.4 HSCTs were in Operation*

File	Fuel (kg/year)	NO _x (kg/year)	HC (kg/year)	CO (kg/year)	Globally Averaged Emission Indices		
					EI (NO _x)	EI (HC)	EI (CO)
P060	2.63E+09	1.49E+07	1.47E+06	1.45E+07	5.66	0.56	5.50
P080	8.67E+09	6.84E+07	2.91E+06	6.59E+07	7.88	0.34	7.60
P120	1.42E+10	1.04E+08	8.02E+06	1.25E+08	7.37	0.57	8.85
P180_with_hsct	2.34E+10	1.73E+08	5.81E+06	1.23E+08	7.39	0.25	5.26
P250A	2.49E+10	2.15E+08	1.64E+07	1.63E+08	8.64	0.66	6.56
P250B_with_hsct	1.64E+10	1.20E+08	1.16E+07	6.25E+07	7.32	0.71	3.82
P350_with_hsct	4.12E+10	4.33E+08	1.49E+07	1.57E+08	10.50	0.36	3.80
P500_with_hsct	4.97E+10	4.03E+08	4.97E+07	2.42E+08	8.11	1.00	4.86
P700_with_hsct	1.93E+10	2.27E+08	3.89E+06	5.02E+07	11.77	0.20	2.60
P900_with_hsct	9.43E+09	8.67E+07	2.43E+06	3.32E+07	9.19	0.26	3.52
Total	2.10E+11	1.85E+09	1.17E+08	1.04E+09	8.80	0.56	4.94

*1.00E + 08 = 1.0 × 10⁸

Table 3-2.15. Altitude Distribution of Fuel Burned and Emissions (Computed Over Latitude and Longitude) for 2015 Scheduled Subsonic Airliners if 500 Mach 2.4 HSCTs were in Operation.*

Altitude Band (km)	Fuel (kg/year)	Cum Fuel (%)	NO _x (kg/year)	Cum NO _x (%)	HC (kg/year)	Cum HC (%)	CO (kg/year)	Cum CO (%)	EI(NO _x)	EI(HC)	EI(CO)
0 - 1	2.49E+10	11.86	2.36E+08	12.77	3.97E+07	33.86	3.45E+08	33.32	9.47	1.59	13.88
1 - 2	6.28E+09	14.86	7.81E+07	17.00	8.57E+06	41.18	6.20E+07	39.31	12.43	1.36	9.88
2 - 3	5.42E+09	17.44	6.44E+07	20.49	6.57E+06	46.79	5.15E+07	44.27	11.90	1.21	9.50
3 - 4	7.00E+09	20.77	9.05E+07	25.40	5.46E+06	51.46	4.43E+07	48.55	12.94	0.78	6.33
4 - 5	5.81E+09	23.54	6.90E+07	29.14	5.81E+06	56.42	4.64E+07	53.02	11.88	1.00	7.98
5 - 6	5.51E+09	26.17	6.22E+07	32.51	6.03E+06	61.57	4.73E+07	57.59	11.28	1.09	8.59
6 - 7	4.94E+09	28.53	5.53E+07	35.51	4.47E+06	65.39	4.05E+07	61.50	11.19	0.90	8.19
7 - 8	5.35E+09	31.08	5.65E+07	38.57	5.18E+06	69.82	4.48E+07	65.82	10.56	0.97	8.38
8 - 9	5.99E+09	33.93	6.10E+07	41.87	6.05E+06	74.98	4.80E+07	70.45	10.19	1.01	8.01
9 - 10	6.53E+09	37.04	6.15E+07	45.20	5.94E+06	80.05	4.59E+07	74.88	9.41	0.91	7.02
10 - 11	4.07E+10	56.43	3.02E+08	61.58	7.99E+06	86.88	9.12E+07	83.68	7.43	0.20	2.24
11 - 12	9.14E+10	100.00	7.09E+08	100.00	1.54E+07	100.00	1.69E+08	100.00	7.76	0.17	1.85
Global Total	2.10E+11		1.85E+09		1.17E+08		1.04E+09		8.80	0.56	4.94

* 1.00E+08 = 1x10⁸

Table 3-2.16. Globally Computed Fuel Burned, Emissions, and Emission Indices for 2015 Scheduled Cargo Aircraft*

File	Fuel (kg/year)	NO _x (kg/year)	HC (kg/year)	CO (kg/year)	Globally Averaged Emission Indices		
					EI (NO _x)	EI (HC)	EI (CO)
C005	4.13E+07	3.28E+05	1.49E+04	3.38E+05	7.94	0.36	8.19
C010	1.16E+07	8.99E+04	4.04E+03	8.62E+04	7.72	0.35	7.41
C020	2.54E+07	1.95E+05	1.84E+04	2.76E+05	7.69	0.72	10.86
C040	4.57E+08	3.91E+06	2.91E+05	2.89E+06	8.56	0.64	6.34
C080	1.40E+09	1.10E+07	2.06E+06	9.87E+06	7.80	1.47	7.03
C160	3.71E+09	3.36E+07	1.17E+06	1.42E+07	9.07	0.32	3.84
Total	5.64E+09	4.91E+07	3.56E+06	2.77E+07	8.69	0.63	4.90

*1.00E + 08 = 1.0 × 10⁸

Table 3-2.17. Altitude Distribution of Fuel Burned and Emissions (Computed Over Latitude and Longitude) for 2015 Scheduled Cargo Aircraft.*

Altitude Band (km)	Fuel (kg/year)	Cum Fuel (%)	NO _x (kg/year)	Cum NO _x (%)	HC (kg/year)	Cum HC (%)	CO (kg/year)	Cum CO (%)	EI(NO _x)	EI(HC)	EI(CO)
0 - 1	4.24E+08	7.52	4.04E+06	8.23	1.05E+06	29.38	7.36E+06	26.59	9.52	2.47	17.35
1 - 2	1.04E+08	9.35	1.33E+06	10.94	1.84E+05	34.54	1.24E+06	31.07	12.81	1.77	11.97
2 - 3	1.02E+08	11.16	1.36E+06	13.72	1.95E+05	40.00	1.26E+06	35.64	13.32	1.90	12.36
3 - 4	1.30E+08	13.46	1.78E+06	17.34	1.64E+05	44.61	1.12E+06	39.69	13.71	1.27	8.65
4 - 5	9.27E+07	15.10	1.15E+06	19.68	1.71E+05	49.41	1.14E+06	43.81	12.36	1.84	12.30
5 - 6	9.62E+07	16.81	1.15E+06	22.03	1.78E+05	54.39	1.17E+06	48.03	11.99	1.85	12.16
6 - 7	9.69E+07	18.52	1.15E+06	24.37	1.76E+05	59.33	1.13E+06	52.13	11.83	1.82	11.70
7 - 8	1.05E+08	20.39	1.15E+06	26.72	1.93E+05	64.76	1.22E+06	56.53	10.97	1.84	11.59
8 - 9	1.12E+08	22.37	1.17E+06	29.11	1.91E+05	70.13	1.19E+06	60.84	10.52	1.71	10.68
9 - 10	1.11E+08	24.33	1.10E+06	31.36	2.00E+05	75.75	1.20E+06	65.19	9.94	1.81	10.86
10 - 11	6.54E+08	35.92	5.71E+06	42.99	2.38E+05	82.43	1.94E+06	72.22	8.72	0.36	2.97
11 - 12	3.62E+09	100.00	2.80E+07	100.00	6.26E+05	100.00	7.69E+06	100.00	7.73	0.17	2.13
Global Total	5.64E+09		4.91E+07		3.56E+06		2.77E+07		8.69	0.63	4.90

* 1.00E+08 = 1x10⁸

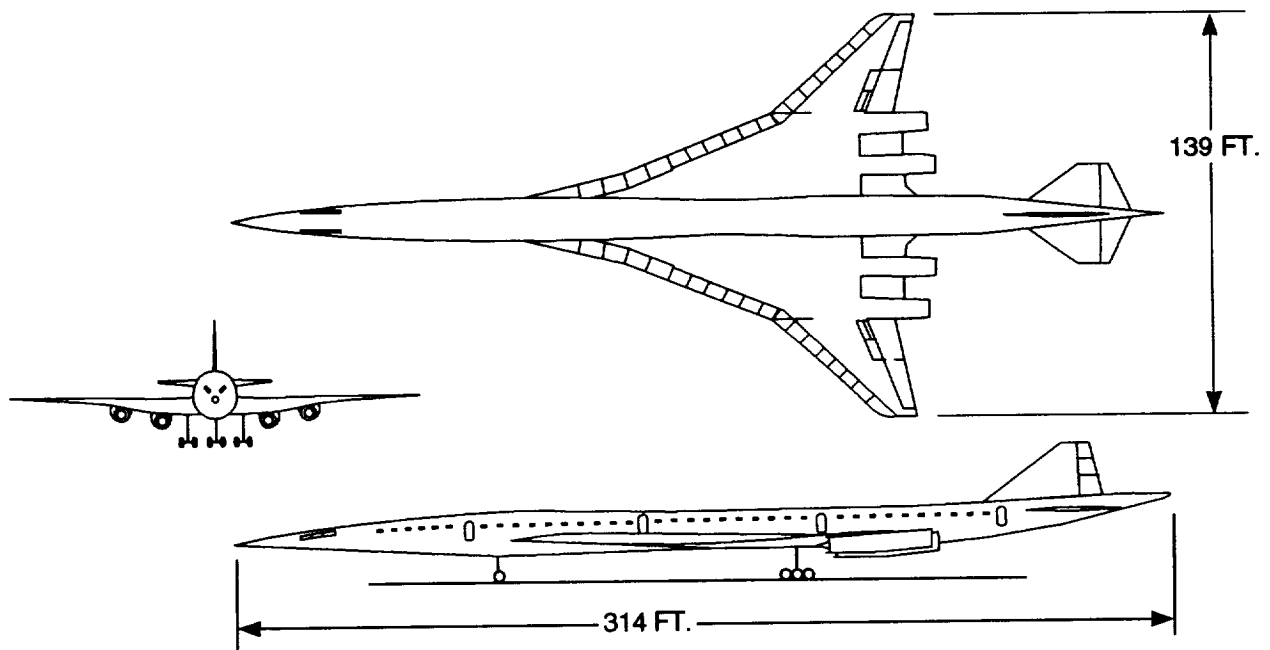


Figure 3-2.1. Drawing of Mach 2.4 HSCT configuration with dimensions.

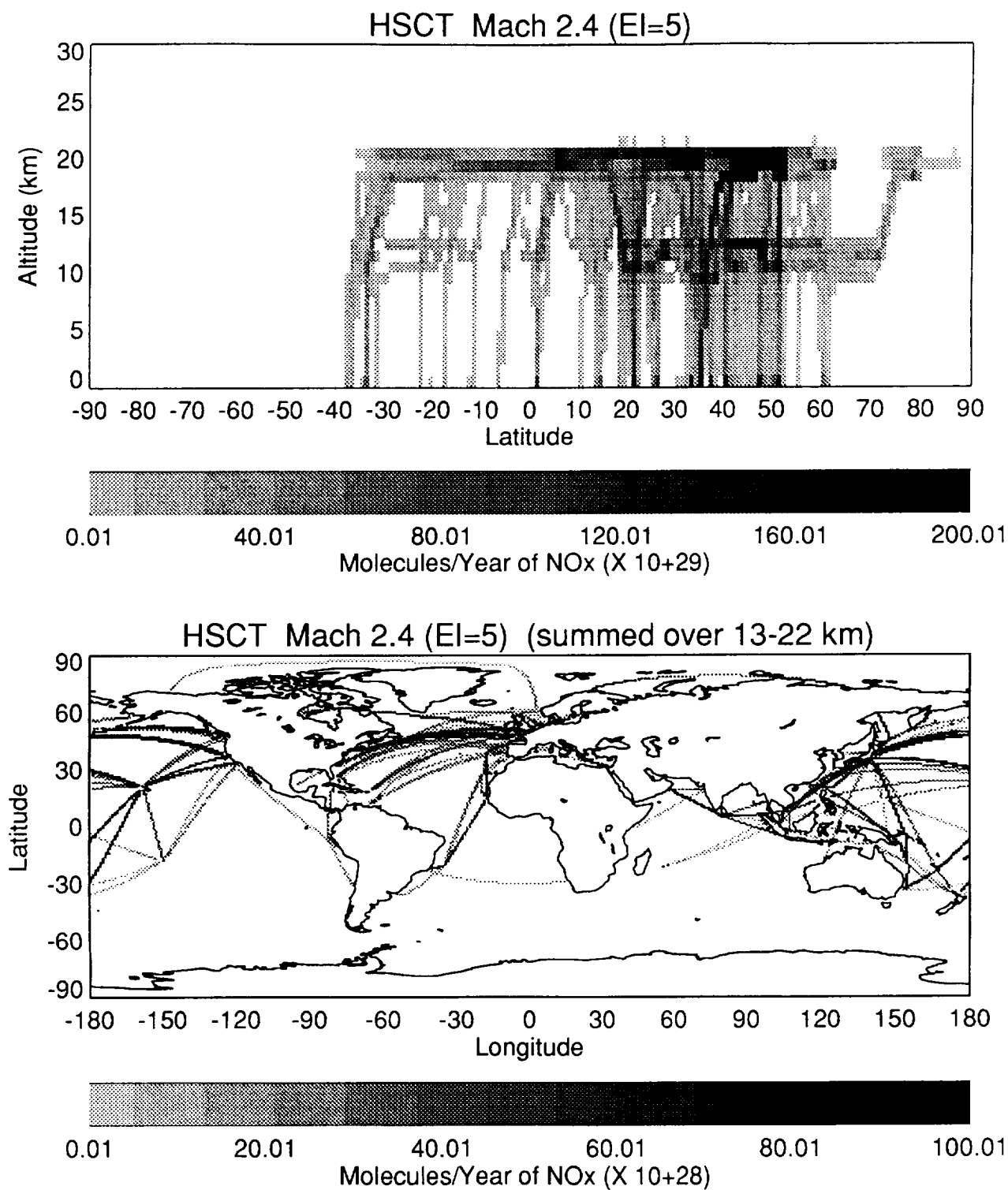


Figure 3-2.2. NO_x emissions for a fleet of 500 Mach 2.4 HSCTs as a function of altitude and latitude (upper panel) and as a function of latitude and longitude (lower panel), considering only the HSCT emissions.

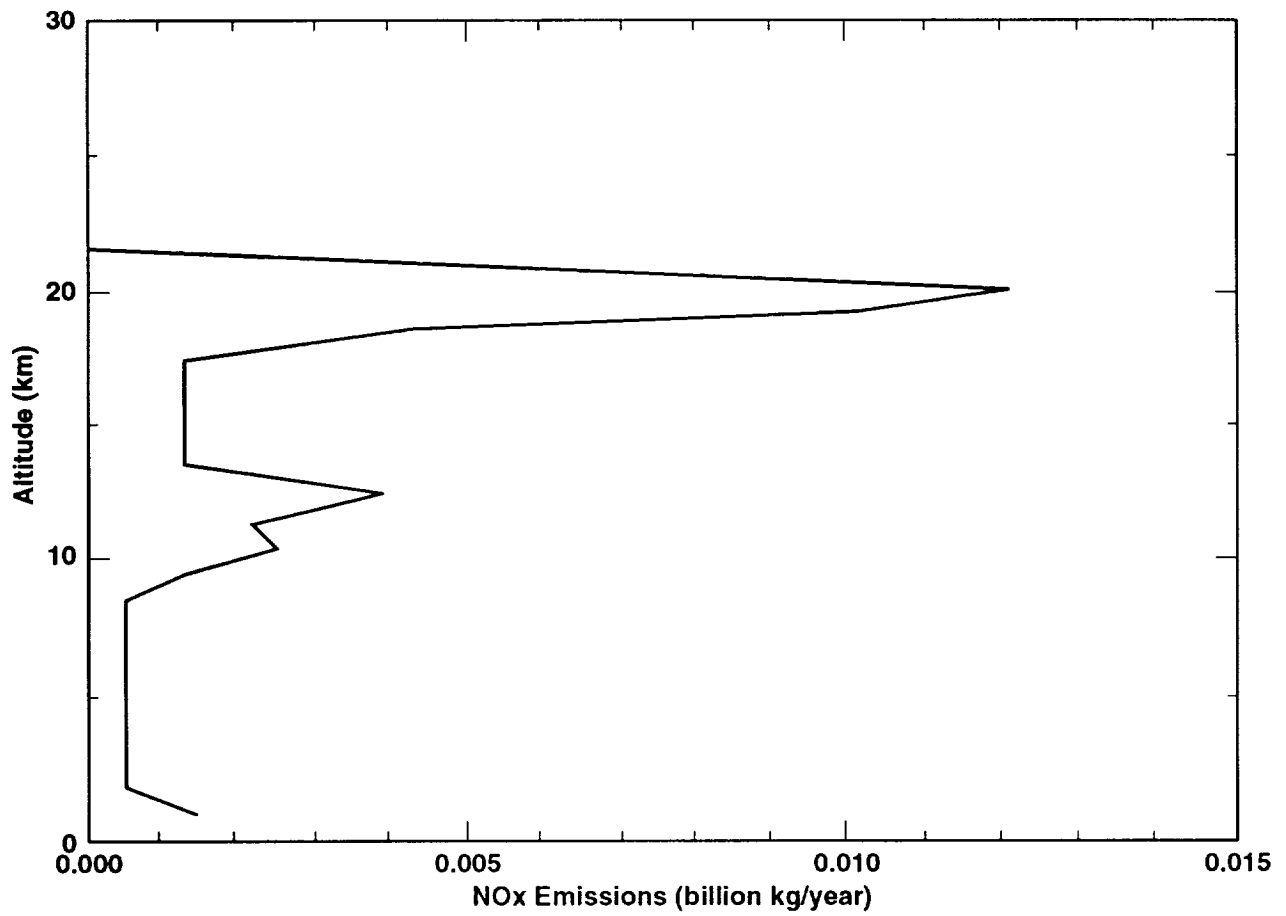


Figure 3-2.3. NO_x emissions as a function of altitude for Mach 2.4, nominal EI(NO_x)=5 (summed over latitude and longitude).

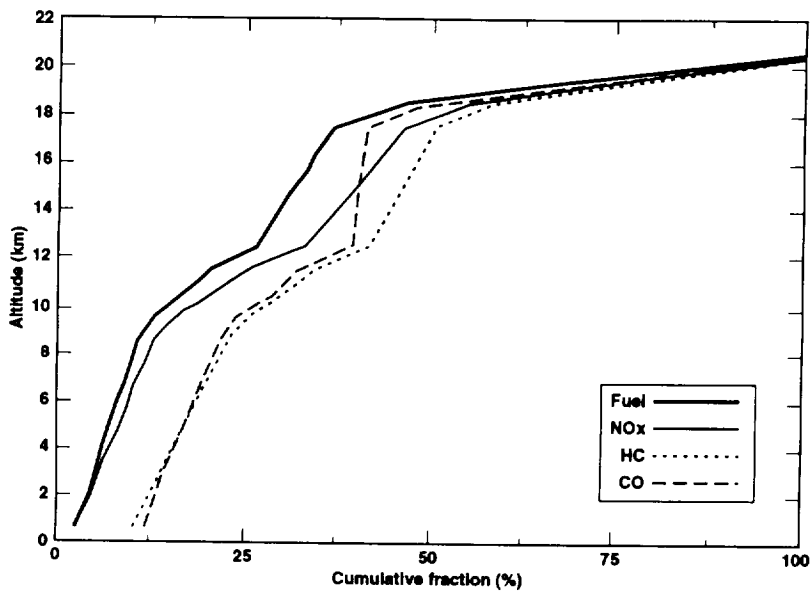
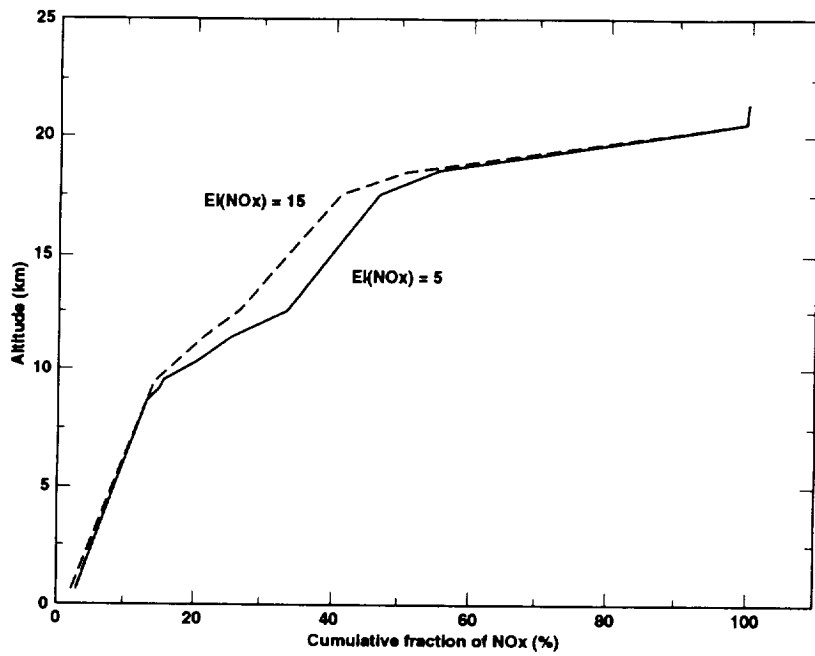


Figure 3-2.4. a) Cumulative fraction of NO_x emissions as a function of altitude for Mach 2.4, nominal $\text{EI}(\text{NO}_x)=5$ and 15. b) Cumulative fraction of fuel burned, NO_x , HC, and CO as a function of altitude for the Mach 2.4 HSCT, nominal $\text{EI}(\text{NO}_x)=5$ fleet only.

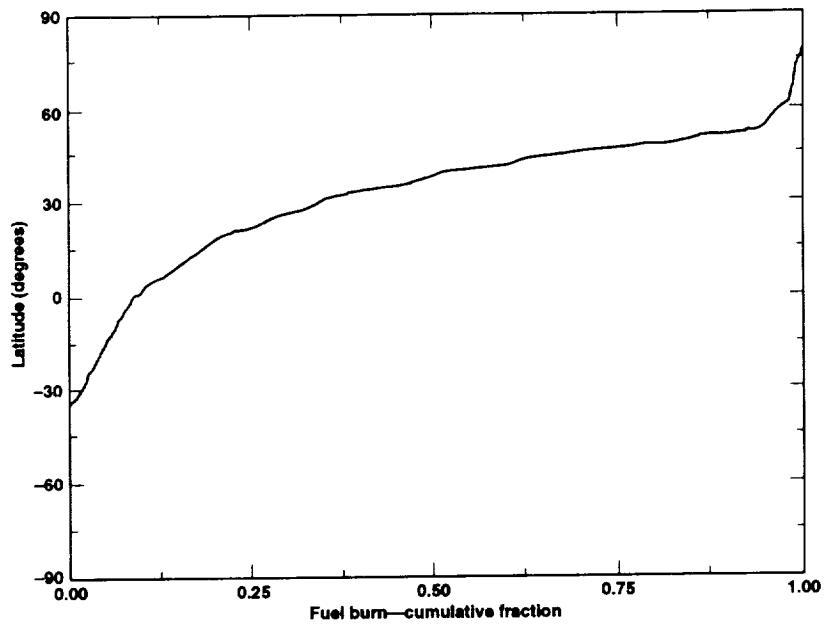
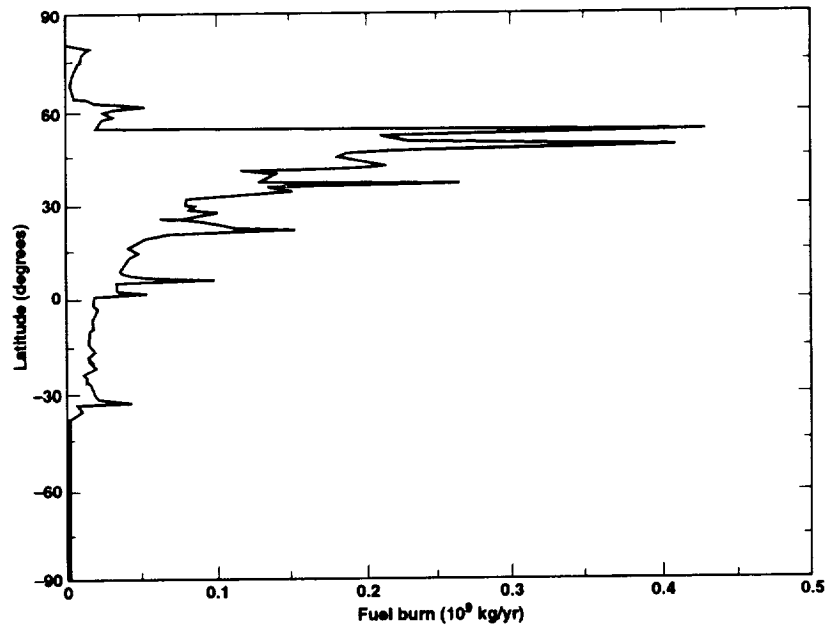


Figure 3-2.5. a) Fuel burn as a function of latitude, and b) cumulative fraction of fuel burn as a function of latitude for Mach 2.4 HSCT fleet only (summed over latitude and longitude).

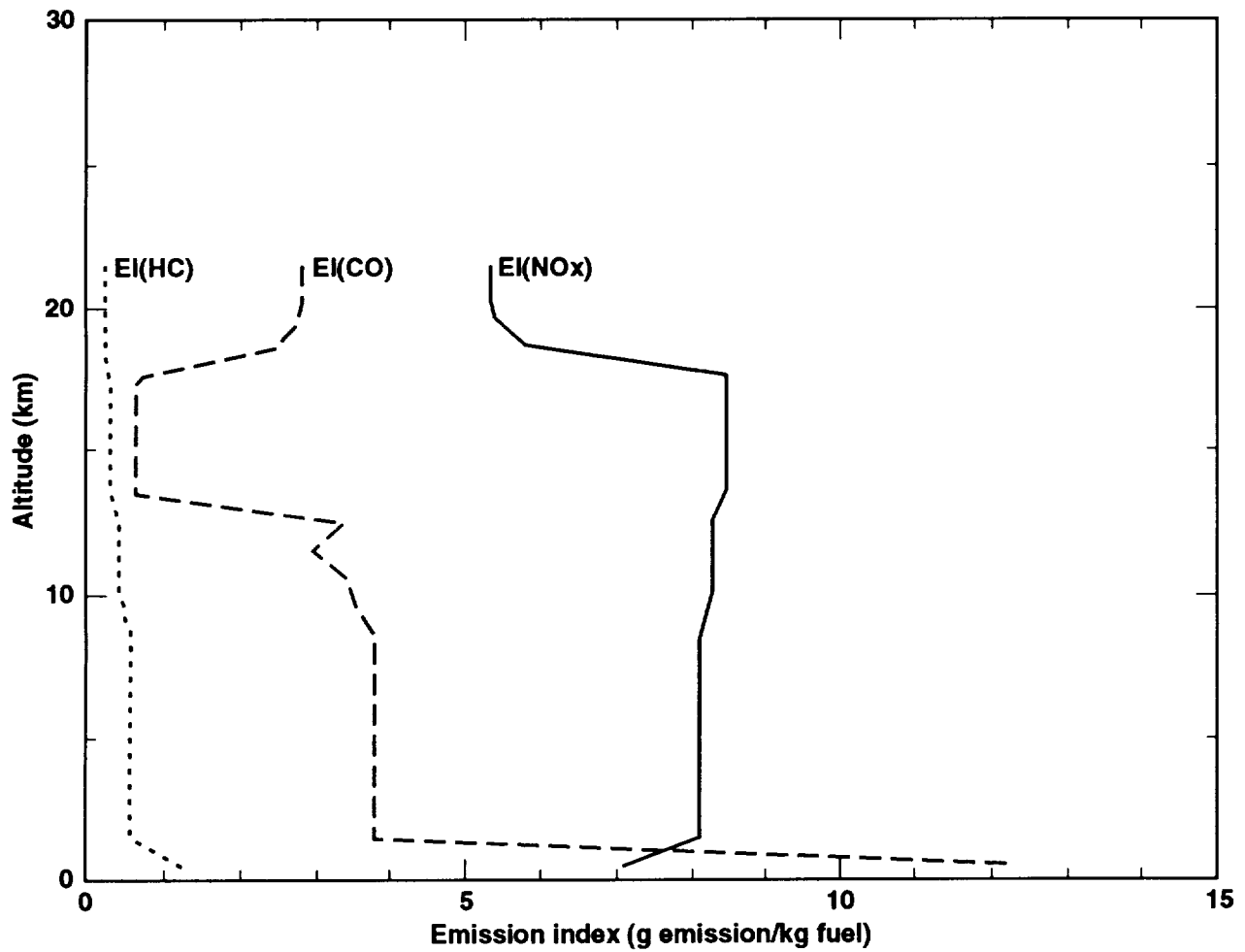


Figure 3-2.6. Emission indices for NO_x, HC, and CO as a function of altitude for the Mach 2.4, nominal EI(NO_x)=5 fleet only.

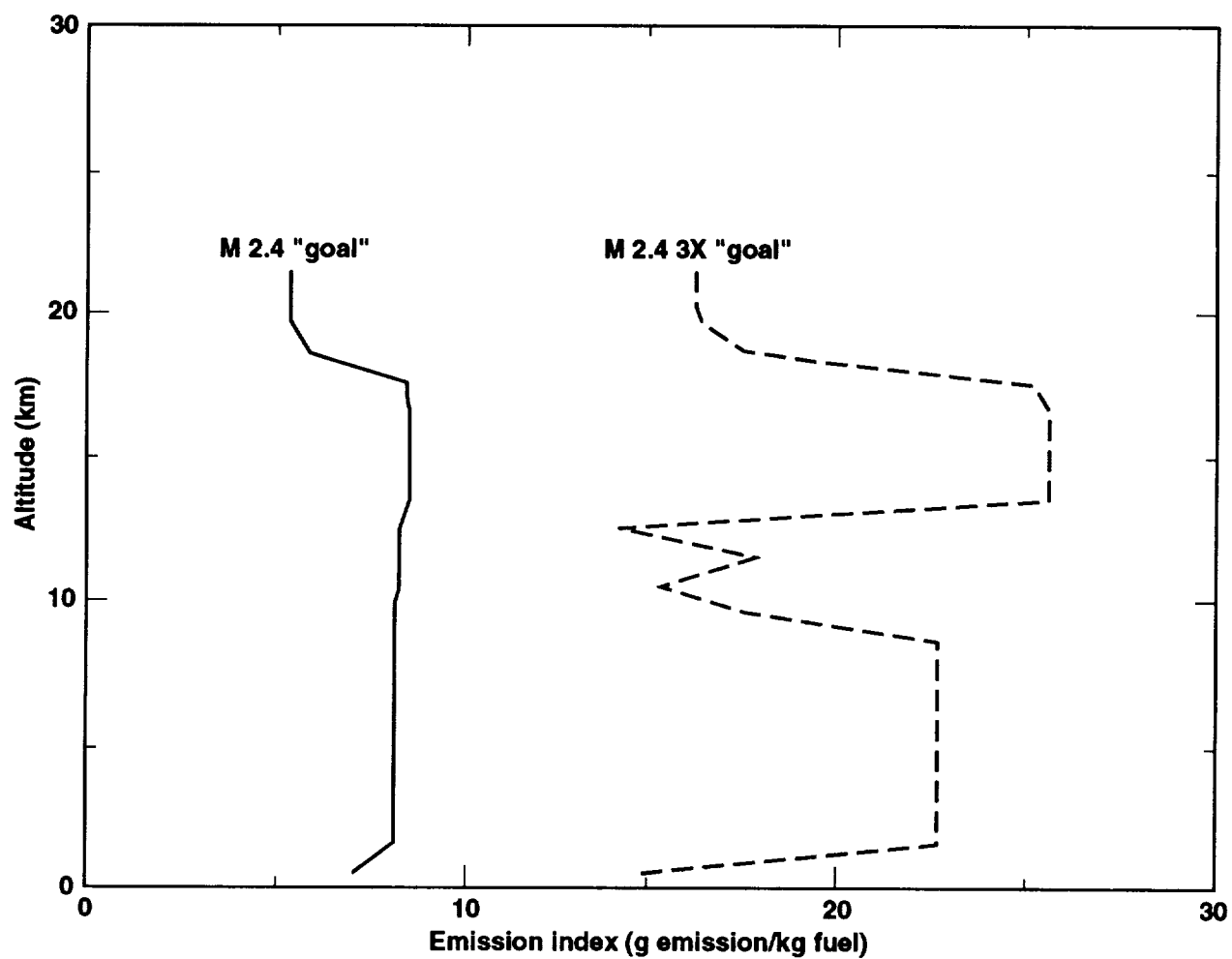


Figure 3-2.7. Emission index for NO_x as a function of altitude for the Mach 2.4 nominal EI (NO_x)=5 and 15 cases.

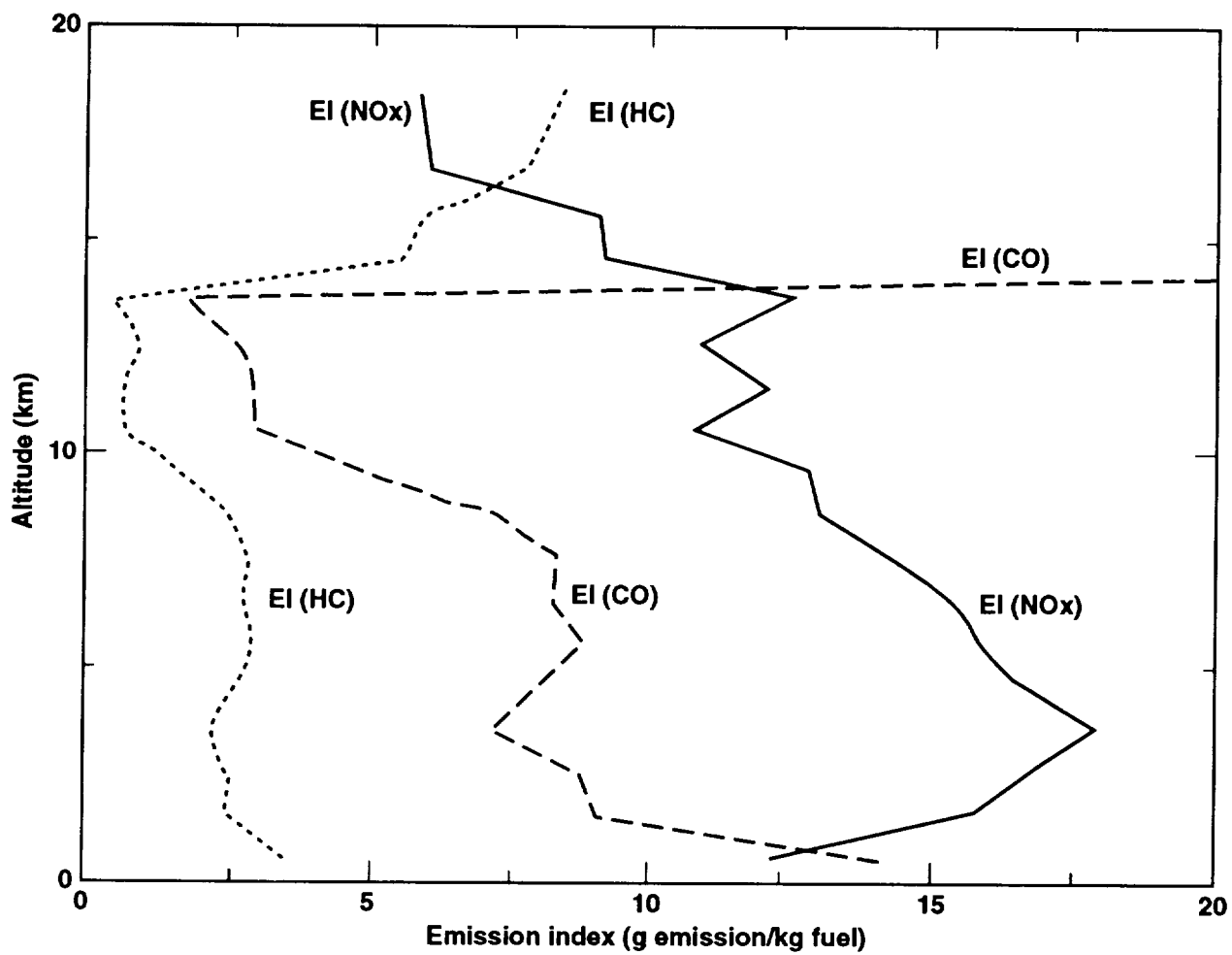


Figure 3-2.8. Emission indices for NO_x, CO, and HC as a function of altitude for the 1990 scheduled jet and cargo scenario.

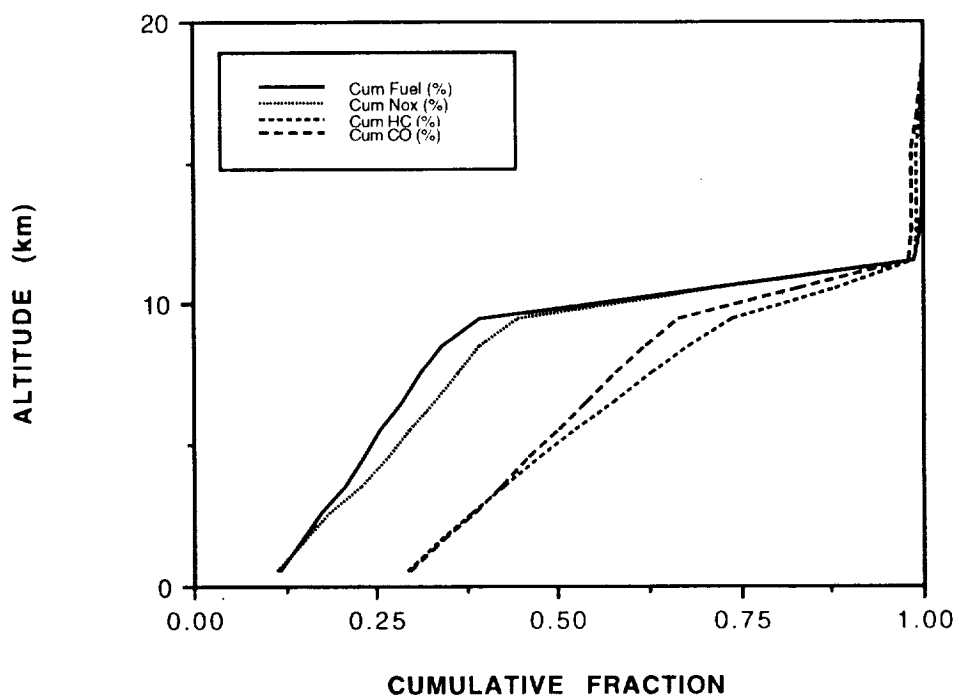
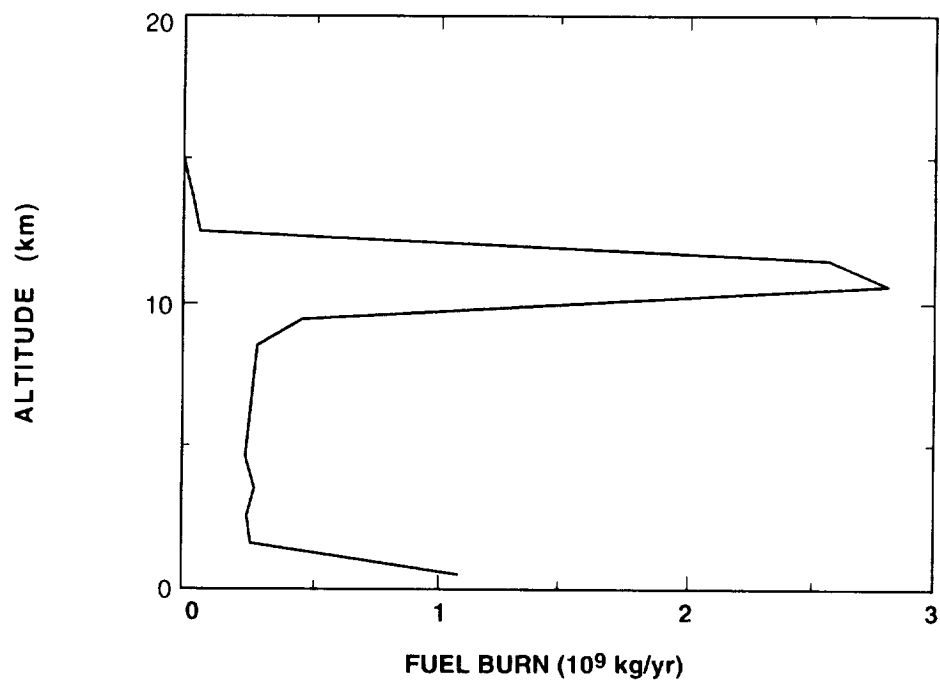


Figure 3-2.9. a) Fuel burned and b) cumulative fraction of fuel burned, NO_x , HC, and CO as a function of altitude (summed over latitude and longitude) for the 1990 scheduled jet and cargo.

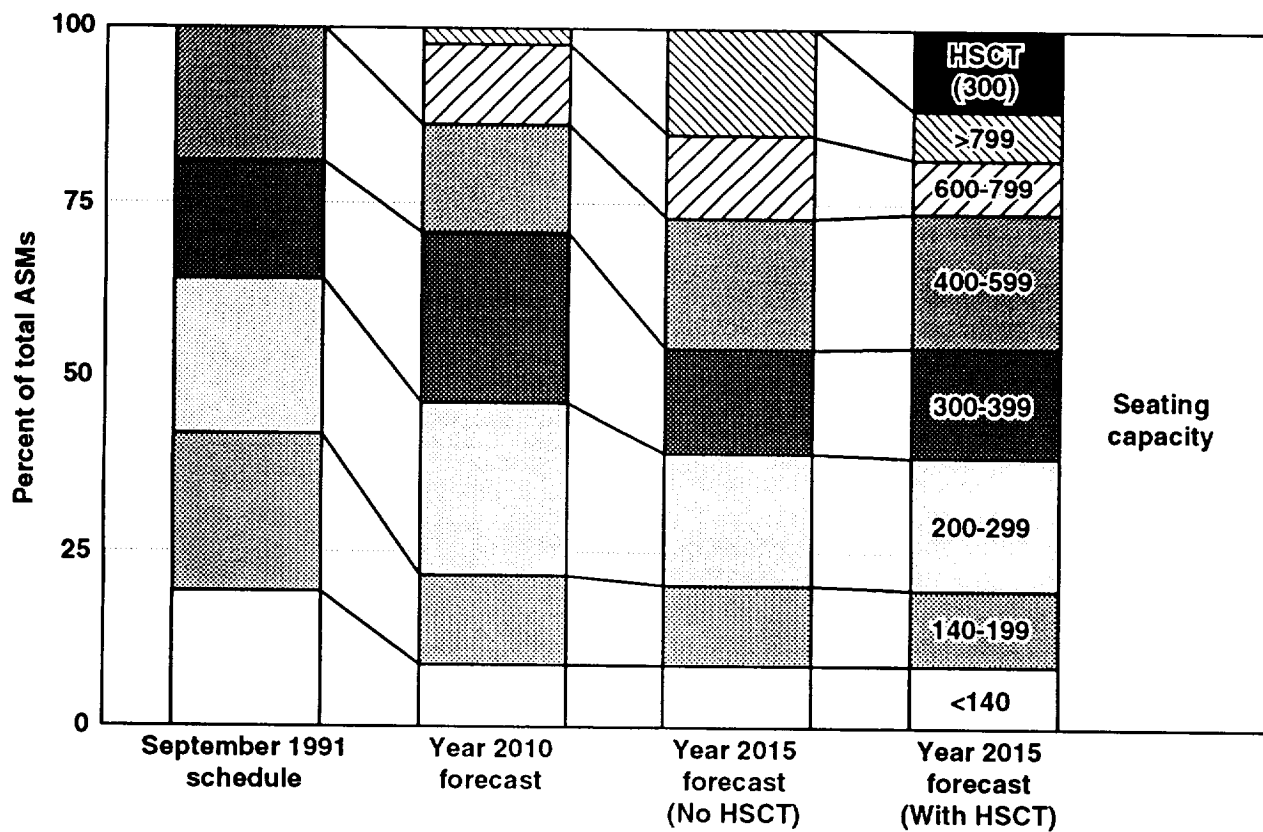


Figure 3-2.10. Passenger available seat mile distribution between different size aircraft for 1991, Boeing forecast for 2010, and the NASA study forecast for 2015 (with and without an HSCT fleet).

Emissions Study

Cargo Fleet ATM Distribution

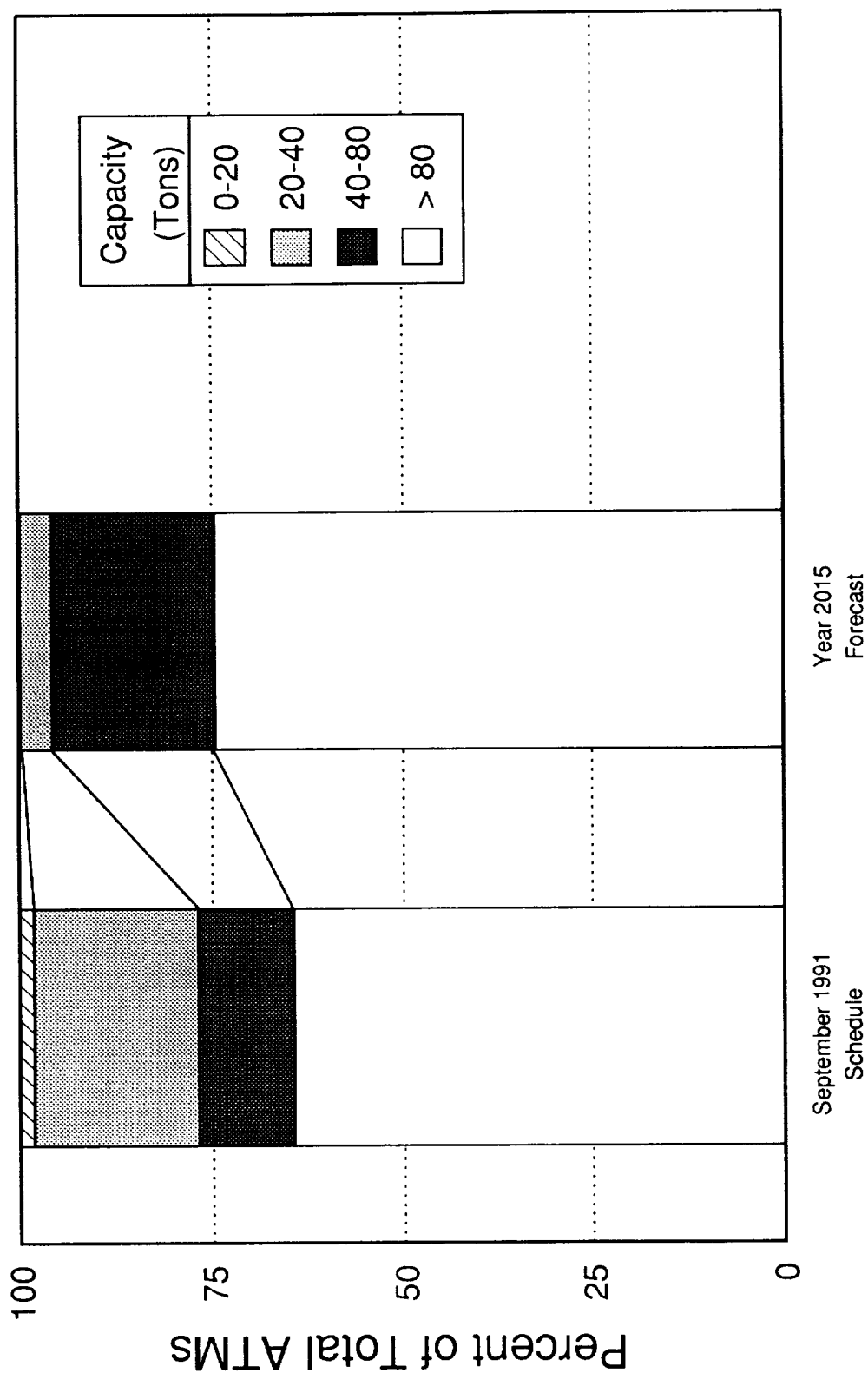


Figure 3-2.11. Cargo aircraft size distributions for 1991 and forecast for 2015.

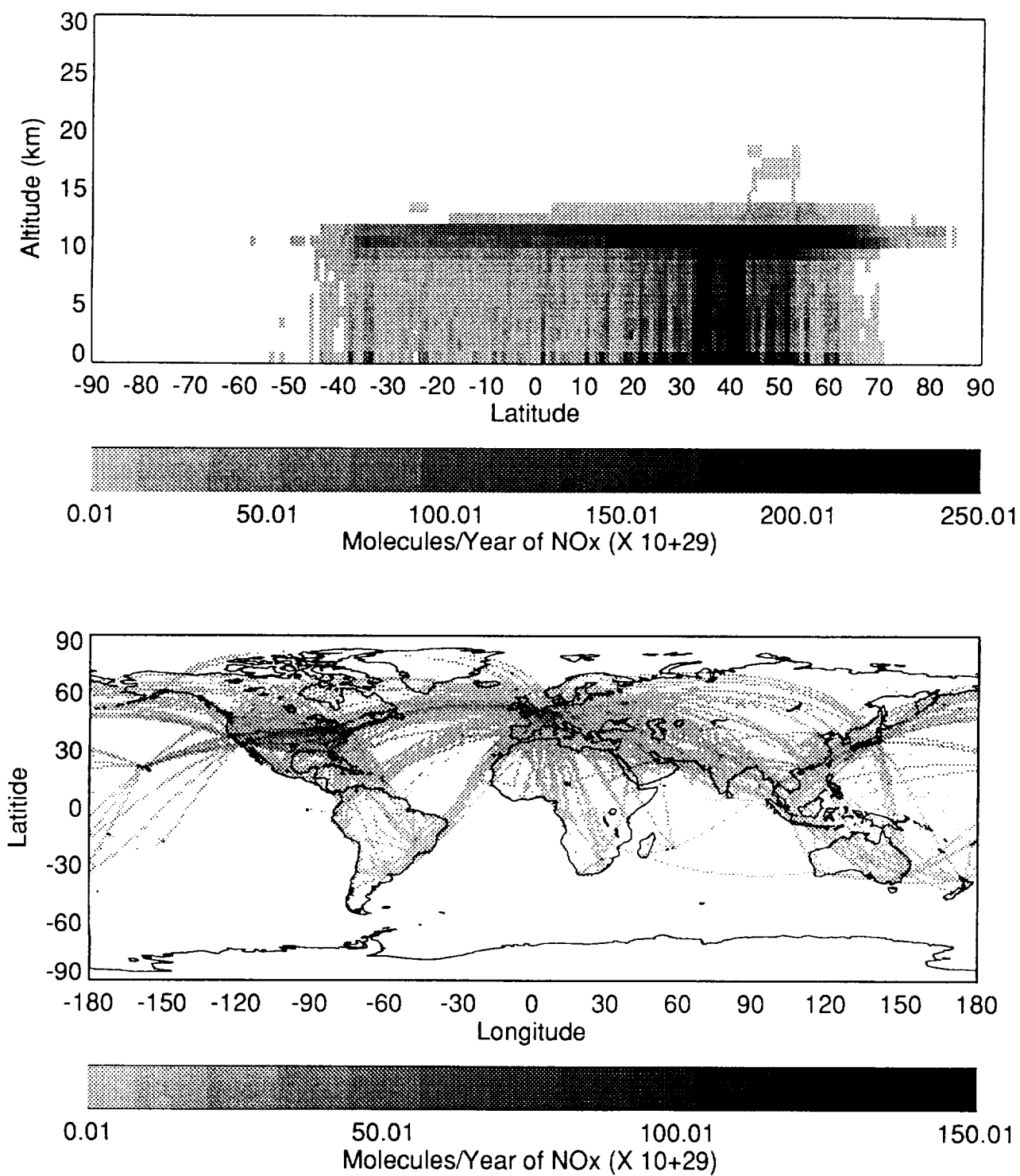


Figure 3-2.12. NO_x emissions for 1990 scheduled air traffic (airliner, cargo, and turboprop) as a function of altitude and latitude (summed over longitude) (top panel) and as a function of latitude and longitude (summed over altitude) (bottom panel).

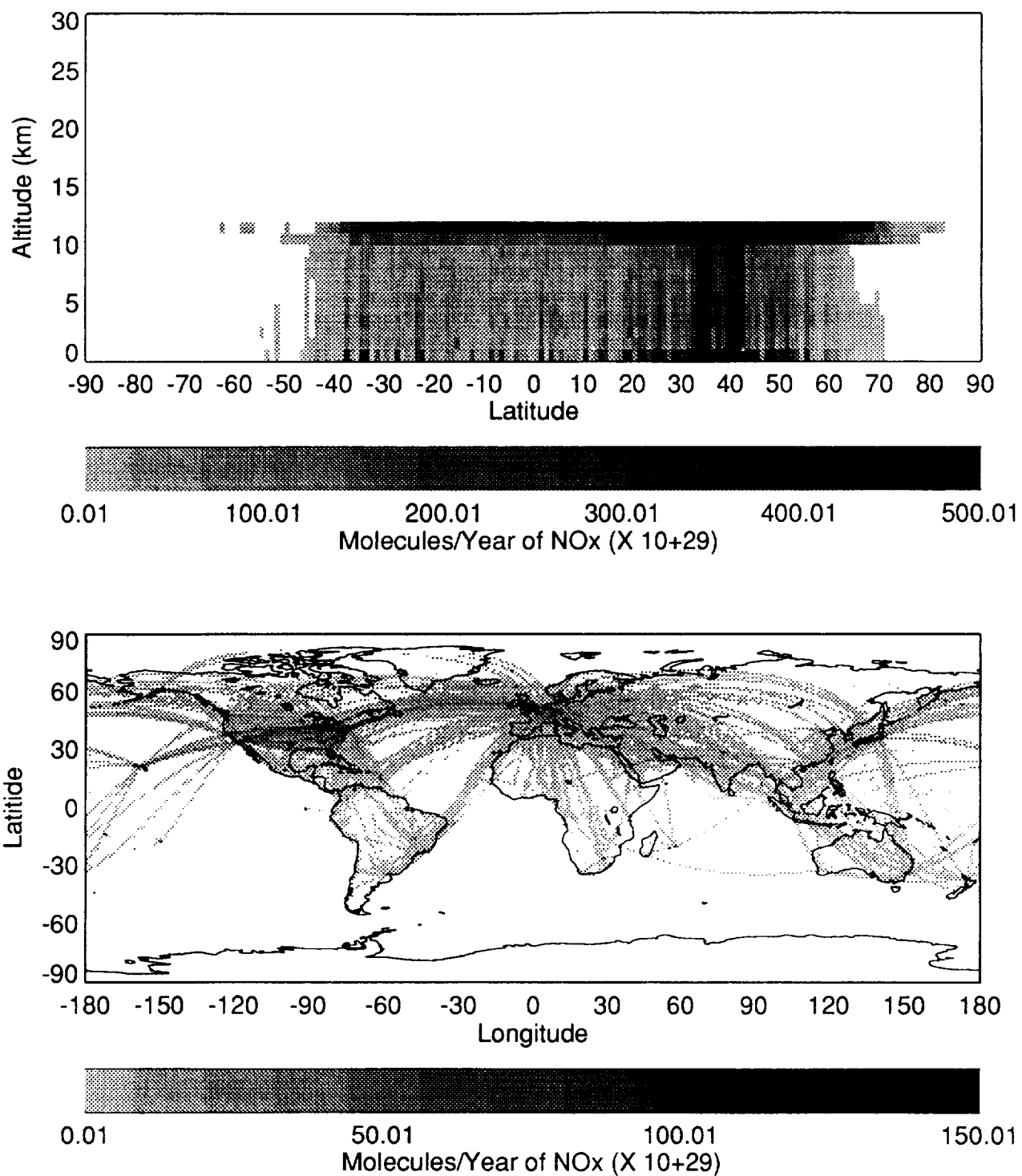


Figure 3-2.13. NO_x emissions for projected 2015 scheduled air traffic (airliner, cargo, and turboprop) as a function of altitude and latitude (summed over longitude)(top panel) and as a function of latitude and longitude (summed over altitude) (bottom panel) assuming no HSCT fleet exists.

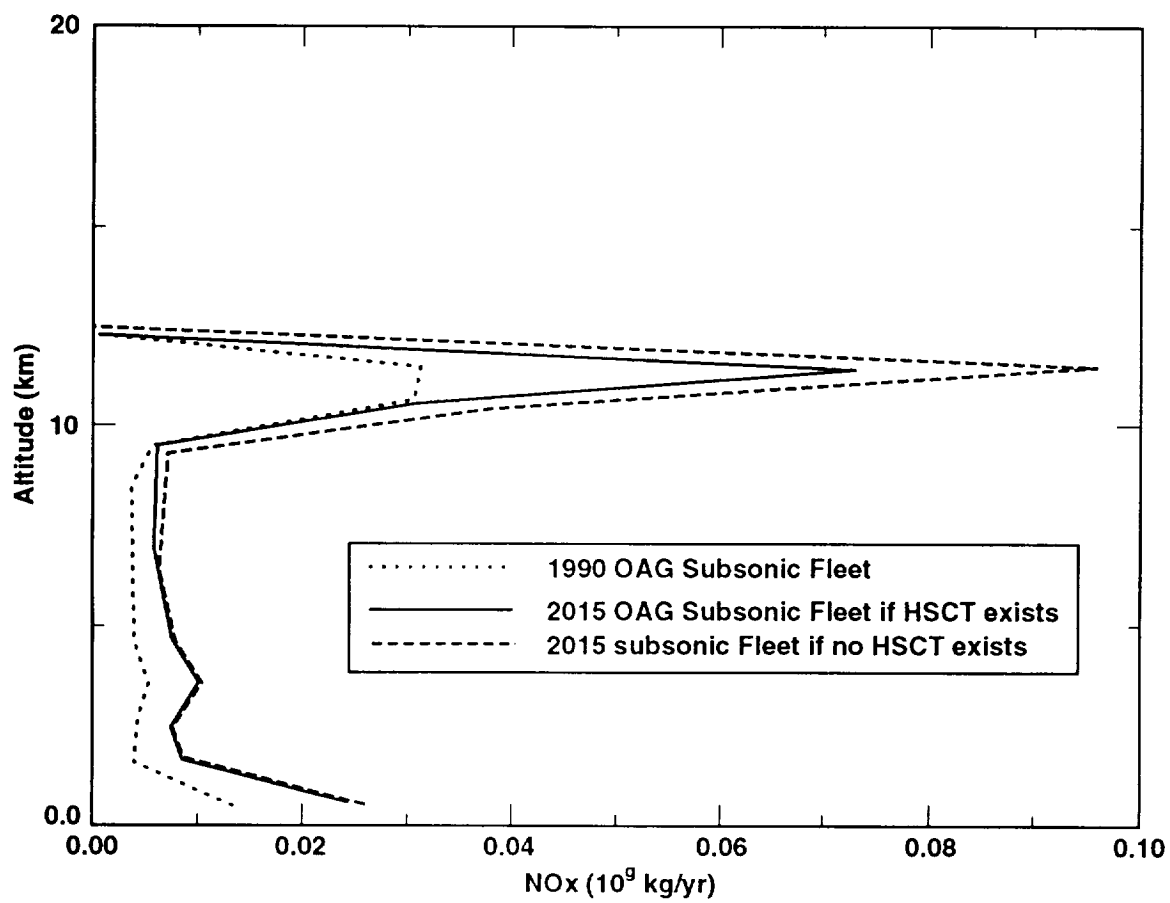


Figure 3-2.14. Altitude distributions of NO_x emissions for scheduled subsonic airliner and cargo aircraft in 1990 and 2015.

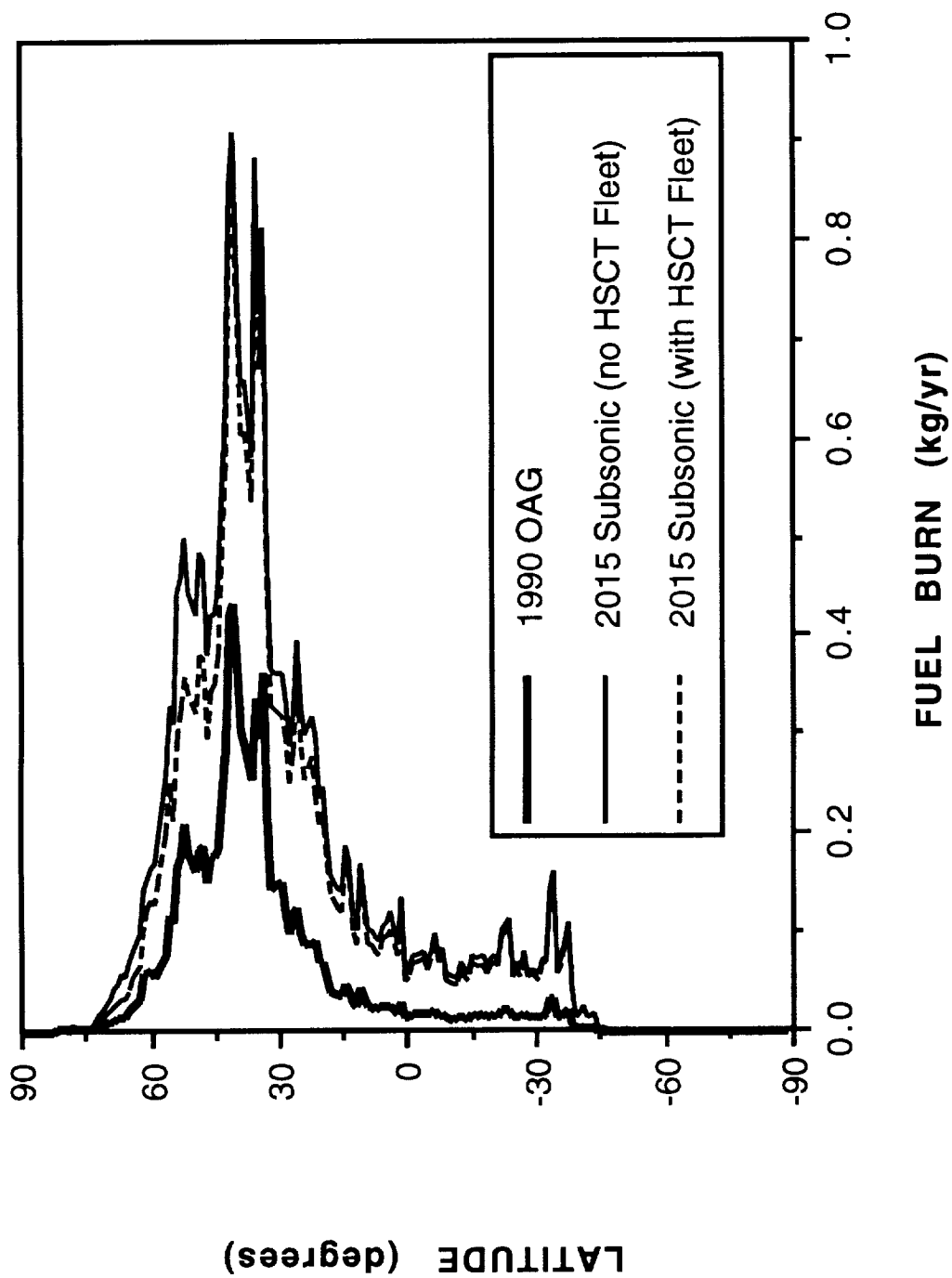


Figure 3-2.15. Latitude distribution of fuel burned for scheduled subsonic airliner and cargo aircraft in 1990 and 2015.

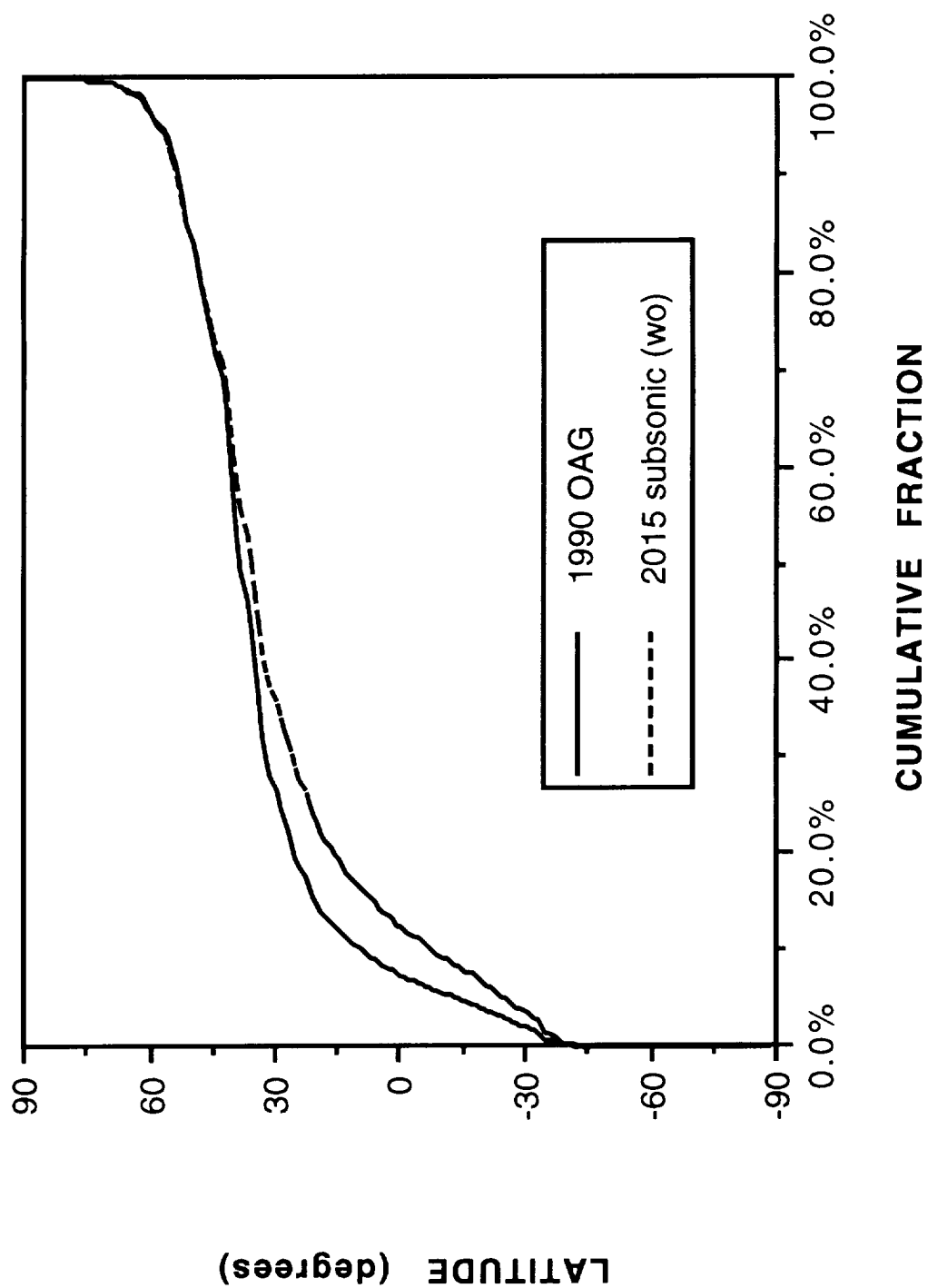


Figure 3-2.16. Cumulative fraction of fuel burned as a function of latitude for scheduled subsonic airliner and cargo aircraft in 1990 and 2015.

Subchapter 3-3

Emissions Scenarios Development: Scenario Database Development at McDonnell Douglas Corporation

Paul A. Barr
Andreas K. Grothues
Zvi H. Landau
Munir Metwally
John Morgenstern
Alan K. Mortlock
Richard Van Alstyne
Clay A. Ward

McDonnell Douglas Corporation
Long Beach, CA

INTRODUCTION

For over half a century, McDonnell Douglas (MDC) has been manufacturing many of the finest military and civilian aircraft that were ever built. During these years MDC has acquired an extensive traffic database and modeling capabilities that were used to support High Speed Research Program/Atmospheric Effects of Stratospheric Aircraft (HSRP/AESA) emission database requirements.

This chapter discusses the development of the emission database for military, charter, and nonscheduled Eastern Europe and Chinese air traffic. Two subsonic scenarios were developed, one focusing on the worldwide 1990 military, charter, and nonscheduled air traffic data and a similar scenario for year 2015. A supersonic scenario was also developed for Mach 1.6 HSCT using the supersonic network mentioned in Subchapter 3-1.

MILITARY AIR TRAFFIC DATABASE

1990 Emissions

Objective

The engineering database of worldwide military air traffic data for 1990 and a complementary database of associated engine emission indices were developed to be used in the AESA studies. The military air traffic data are composed of generic aircraft types, locations, flight routes, flight frequencies, and fuel burn profiles. For the purpose of this study, the emission constituents of interest are carbon monoxide (CO), oxides of nitrogen (NO_x), and total hydrocarbons (HC). Together, the military air traffic data and the emission data were processed to generate 1990 fuel burn and emissions grids with a resolution of 1 degree latitude × 1 degree longitude × 1 kilometer altitude.

Methodology

A. Inventory of Military Aircraft. Several data sources, both United States and international, were used to develop a worldwide inventory of military fixed-wing aircraft (see references, including Air Force Association, 1991; Forecast International, 1991; International Media Corporation, 1990; and International Institute for Strategic Studies, 1989). In general, the aircraft are grouped by country and then by the mission they perform. For each country, sovereign aircraft as well as foreign aircraft deployed in its territory are included. Foreign deployment assignments are also listed for the United States, Figure 3-3.1 shows 138 countries owning about 60,000 aircraft. Notably, three countries, the former Soviet Union, the United States, and China, account for 51% of the entire fleet. Once the country data are compiled, countries are aggregated into regions or alliances. Criteria are developed to include only pertinent aircraft. Single-engined piston aircraft were not considered because of a low cruise ceiling, low power, and small percentage of the global fleet (about 1%).

B. Aircraft and Mission Profiles. The aircraft in the 1990 worldwide inventory represent many unique aircraft designs and derivatives numbering in the hundreds. The variety of aircraft in the inventory range from high-technology, front-line fighter aircraft with state-of-the-art power plants to vintage transports of the 1940s equipped with radial engines. Many of these aircraft also have commercial applications; for example, the U.S. Air Force C-9A Nightingale, an aeromedical airlift transport, is a derivative of the popular DC-9 Series 30 commercial airliner. The approach undertaken in this study was to use generic aircraft to represent each aircraft type in the 1990 inventory; specifically, for each combination of military mission and region or alliance, a single notional aircraft was used for all aircraft in that combination.

Specific missions that were considered included fighter/ground attack, counterinsurgency, bomber, transport, tanker, trainer, maritime patrol, electronic warfare, and reconnaissance. Region and/or alliance categories included: United States, NATO (excluding United States) and non-Warsaw Pact Europe, former Soviet Union, the Warsaw Pact (excluding former Soviet Union), China, Caribbean and Latin America, Middle East and North Africa, Sub-Saharan Africa, and other Asian and Australasian countries.

Initially, each region or alliance was sampled such that the total quantity of aircraft possessed by the countries comprising the sampled constitute at least 50% of the total aircraft in the region. Then, the distribution of aircraft types for each mission was analyzed. Considerations in the analysis were given to aircraft characteristics found in Jane's (1990) and McGraw-Hill (1991), such as engine quantity, specific fuel consumption, rated power (thrust or horsepower), and type (turbofan, turbojet, turboprop, etc.); maximum gross weight; wing configuration; performance; and vintage. A region's generic aircraft for a particular mission reflect the characteristics of the region's predominant aircraft performing that mission. Figure 3-3.2 illustrates this generic aircraft development process.

Aircraft mission profiles used in the study were based on standard mission information contained either in USAF Guide 2 (U.S. Air Force, 1989), MIL-C-005011B (U.S. Air Force, 1977), or the aircraft's performance manual. Sea Power (Navy League of the U.S.A. 1988) and Air Force Regulation AFR 173-13 (U.S. Air Force, 1989) were also useful for this part of the analysis. All aircraft were assumed to fly radius missions; i.e., the aircraft flew a fixed distance along a great circle route and, depending on the mission, either landed and returned to the origin or returned to the origin without landing. Mission segment elapsed time and distance, altitude, and cumulative fuel burn were calculated using manufacturers' performance data. As an example, Figure 3-3.3 depicts a typical mission profile for the A-4 aircraft.

C. Engine Emission Indices. Numerous previous studies have examined the constituents contained in aircraft exhaust emissions. Therefore, a substantial database of emission indices exists in the literature. This effort relies primarily on reports for emission indices data including Pace (1977), Sears (1978), and ICAO Technical Issues Subcommittee (1989b).

This study collected data on three constituents: HC, CO, and NO_x, for the engines associated with the representative aircraft discussed above. For each engine and constituent there is a set of relevant emission indices. The emission index characteristically varies directly as a function of throttle setting for NO_x, and it varies inversely as a function of throttle setting for both HCs and CO. In essence, the emission indices measures combustor cleanliness for a given engine cycle. As an illustration, a set of indices is shown in Table 3.3.1 for the Allison TF-56 turboprop engine.

Much of the previous work on emission indices has focused on concentrations of emissions in proximity to airports. Therefore, a significant portion of the available data only addresses engine power settings common to the landing-takeoff cycle: taxi/idle, takeoff, climb, and approach. Interpolation was used in those cases where data are not available for an appropriate "cruise" power setting.

D. Aircraft Basing. The amount of detail that could be modeled for the military fleet was dependent on the limited time and effort available for this task. The amount of time it takes to base the aircraft in any given country is proportional to the number of aircraft in that country and the number of bases in that country. A trade study on aircraft basing has shown that it is not practical to base every military aircraft in the world in its exact location. Additionally, data required for such a task were not readily available. As a result, the concept of "centrally" basing aircraft has been adopted.

Centrally located basing is the selection of an airfield at or near the geographic center of a country and flying all of the aircraft, as represented by the generic aircraft, in the country from that

point. This solution was deemed adequate for the gross majority of countries having fixed-wing military aircraft. For a given country, the base was chosen by selecting from the National Geographic Society (1981) an airfield near its geographic center. The airfield coordinates were taken from McDonnell Douglas Corporation (1991). If the airfield is not listed in the report, the atlas served as the second source. However, because of their size, some countries require additional bases to more accurately describe their basing status. Three countries in particular, the former Soviet Union, the United States, and China were not based centrally because of fleet size and geographic considerations.

The former Soviet Union maintains the world's largest fleet of military aircraft, the total accounting for 21% of the entire global fleet. The former Soviet Union was divided into Theaters of Military Operations: a Central Reserve Theater and a Northern Front Theater. Both were further subdivided into Military Districts (MD). The aircraft are assumed to be based at or near the center of their district. Within a theater, the forces not assigned to a particular MD were evenly distributed between the districts in that theater. The strategic forces, including long-range bombers and reconnaissance aircraft, were based in this manner.

The U.S. fleet of military aircraft is the second largest in the world, accounting for 19% of the global military aircraft fleet. For this study, the United States is divided into five regions, as shown in Figure 3-4. Central basing of each region depends on the mix of operational missions of the region's bases. For example, if in the U.S. fleet all fighters and other tactical aircraft are represented by 5000 generic aircraft type F1, and region III has 10% of U.S. fighter bases, then 500 type F1 aircraft are based in region III. Naval aircraft are based at appropriate naval bases within four of the five regions, using basing data from Aviation Advisory Services (various years). The Marine Corps aircraft are included in the naval force total and distributed accordingly.

The Chinese military aircraft fleet represents roughly 10% of the world's air forces. The aircraft are mostly variants of dated Soviet designs. Their primary fighter, the J-6, is simply a Chinese variant of the late 1950s MIG-19. Available data allow for a basing scheme similar to that used for the former Soviet Union. For the 1990 emissions analysis, China was organized into seven Military Regions and within each region, sub-divided into military districts. Districts bordering the former Soviet Union and the coasts near Taiwan were assumed to require a higher concentration of aircraft than others due to political tension. Naval aircraft were based at naval headquarters within the Guangzhou, Nanjing, and Jinan Military Regions.

For each generic aircraft type, at least three directions of flight were randomly generated. However, where practical, flights were routed over indigenous territory and not over water. This depends on the mission range of the aircraft, the geographic location of the country, and the country's physical shape. Only the naval aircraft of the United States and China are intentionally directed over water.

1990 Global Fuel Burn Estimate

To estimate the military aircraft contribution to global fuel burn, it was first necessary to postulate a flight frequency, or utilization rate, for each country's inventory of military aircraft. Several assumptions were made in order to approximate aircraft utilization rates. Derivation of global utilization rates (in terms of Flying Hours per Year, or FH/YR) was based on U.S. Air Force experience.

In any given country, some of its military aircraft were assumed to be operational at some point during the course of a year. In the United States, maintenance requirements and the existence of backup or spare aircraft are two reasons why an aircraft may be deemed non-operational. Funds to support flying hours (and, indirectly, utilization rate) for U.S. Air Force aircraft were based on a unit's Primary Aircraft Authorization (PAA). According to U.S. Air Force Regulation 173-13,

(1989), PAA represents the number of aircraft "... authorized to a unit for performance of its operational mission." Typically, PAA were assumed to be some fraction of the total aircraft possessed by a unit. The remaining aircraft allow for "... scheduled and unscheduled maintenance, modifications, and inspections and repair without reduction of aircraft available for the operational mission." Examining the ratio of operational aircraft to total aircraft for the U.S. Air Force F-15 and F-16 fleet show roughly 75% of this fighter fleet are available to meet current flying requirements. This same percentage should apply to aircraft for which the primary role is pilot training. Higher cost aircraft such as the bombers, large transports, and electronic surveillance and/or reconnaissance platforms, tend to have a higher ratio of operational aircraft to total aircraft. For the purpose of this study, 90% has been assumed. U.S. utilization rates per PAA, based on a sample of representative aircraft programmed flying hours for 1989 from Air Force Regulation 173-13, are tabulated by mission in Table 3-3.2.

Other countries do not necessarily use their military aircraft at the same rate as the United States. No data have been located which would allow a comparison with the United States utilization rate; however, experts (at MDC) in the area of military operations and intelligence have been consulted and agree that the approximations used, as given in Table 3-3.3, are not unreasonable for the 1989-1990 time frame.

Combining the above scaled utilization rates with the ratio of operational aircraft to total aircraft yields an approximation of the annual flying hours by mission for each aircraft within each country's total fleet, as shown in Table 3-3.4. (the hours have been rounded to the nearest 25). The above data together with single sortie mission flight time (hours) yield estimates of the annual frequency of flights (trips/year) per aircraft, plus flight frequencies, mission profiles, and aircraft inventories can be combined to estimate fuel burn quantities.

2015 Military Scenario Projection

The forecast of military air traffic's contribution to global fuel burn in the year 2015 is influenced by many considerations. Of primary importance is the quantity and associated geographic distribution of aircraft present in the 2015 inventory. Any 25-year forecast of global military aircraft inventories, especially in light of recent world events, is speculative at best. Other considerations include relative changes in engine efficiency (fuel consumption), and to a lesser extent, new emission-reducing technologies incorporated into the military aircraft fleet.

To derive the 2015 inventory, the basis shifted from a 1990s country-by-country focus to a regional focus. The United States, the former Soviet Union, and China are still forecast individually; however, all remaining nations are included in one of five regions: Asia, Europe (includes Canada and former Warsaw Pact nations), Latin America, Middle East/North Africa, and Sub-Sahara Africa.

The forecast is based on a review and subsequent subjective amalgamation of many data sources including Correll (1991), Forecast International (1991), Lorell (1992), and Nation (1990, 1991, 1992). Some underlying themes appearing consistently among the varied sources of data include: the United States, NATO, and the former Soviet Union will see significant reductions in military aircraft force levels (on the order of 30%) by the year 2000; fewer new military aircraft programs will ever reach the production phase (and those that do will have experienced substantial schedule slips from original plans); and global war is now relatively unlikely, although regional conflicts will likely continue to pop-up and may even increase in frequency.

All military aircraft in the 2015 forecast were based in eight regions: United States, Europe, the former Soviet Union, Asia, Middle East/Northern Africa, China, Latin America, and Sub-Saharan Africa. The generic aircraft and standard mission profiles used to represent a region's military force structure in 2015 are similar to the 1990 generic aircraft with some adjustments for

improvements in fuel consumption. As in the 1990 fleet, headings are randomly generated; however, they are not restricted by water or hostile nation influences, and six headings per origin rather than three are used.

CHARTER AND UNREPORTED NONSCHEDULED TRAFFIC

Background

The database development for global distributions of exhaust emissions from two segments of commercial air traffic: charter and unreported nonscheduled traffic for Eastern Europe and China, are described in this section. Unreported in this context means that this traffic is not reported in the Official Airline Guide (OAG).

Commercial air traffic is composed of both scheduled and charter (nonscheduled) services. The scheduled services have evolved over time into fairly stable global distribution patterns. On the other hand, the charter services do not show such stability. The world traffic forecast of charter traffic, shown at Figure 3-3.5, identifies five domicile origin regions: Europe, Far East, Latin America, Middle East & Africa, and North America. Notably, the European and North American regions originate most of the traffic, with negligible traffic originating in the other regions. As a rule-of-thumb the charter traffic magnitude is about 10% of the total global scheduled traffic.

The unreported domestic scheduled traffic in the former Soviet Union, China, and the Eastern Europe nations (hereinafter collectively referred to as the Eastern Block) also needed to be included to complete the commercial air transport traffic coverage. Aeroflot is one of the world's largest airlines, and its domestic network is of transcontinental proportions and contributes a substantial amount of traffic to the global total.

This section describes the synthesis of representative models of the global charter traffic and the Eastern Block's unreported scheduled domestic traffic, the selection of generic aircraft, and the development of fuel burn and emission byproducts estimates. Objectives in the development of this database included: to assemble an origin-destination matrix representing a normalized global distribution of charter traffic; to determine the origin-destination pairs that reflect the most frequent actual combinations used by the charter operators; to develop model networks to simulate global charter traffic and the unreported scheduled domestic traffic of the Eastern Block for both 1990 and 2015 scenarios; to determine fuel consumed by appropriately selected generic aircraft when simulated on the model networks; and to develop estimates of both fuel burn and levels of emission byproducts, specifically CO, NO_x, and total HC.

Data on Charter and Nonscheduled Air Traffic

Since the Russian airline Aeroflot is the dominant carrier of the Eastern Block, its domestic network structure forms the kernel of the Eastern Block unreported scheduled domestic traffic model. The network structure derived from Aeroflot's July 1990 domestic passenger flight schedules yields 264 routes with a wide range of service frequencies and a relatively small equipment list. Analysis shows that the top 86 routes, by frequency of service, can adequately represent the geographical distribution of Aeroflot's domestic network. The final network model includes six additional routes to account for the remaining Eastern Block and China traffic. The total traffic for year 1990 equaled 149.73 billion annual seat miles (ASM).

Charter traffic data are usually presented in the aggregate form, which obscures the actual origin-destination information. There is no publication similar to the OAG that identifies charter origin-destination traffic. Since greater than 90% of the charter traffic originates in the European

and North American regions, the literature search focused on these two regions to identify relevant data sources.

ICAO (1990) reports annual statistics on charter traffic carried by 128 reporting airlines originating from 68 countries. The traffic statistics cover both passenger and system performance measures. These data form the basis for distributing the total regional data among the respective constituent countries.

Belet and de Daunant (1990) discuss the potential development of the European Charter operations under the umbrella of the emerging common market. The report presents distributions of passenger traffic from three major European charter traffic generators (Britain, Germany, and France) to 30 countries around the world. This information is the foundation for the European origin-destination traffic distribution matrix.

Statistics Canada (Canadian Government Publishing, 1989) presents detailed statistics for charter traffic from Canadian airports to all regions and specific destinations. The top four Canadian origins and the top three destination regions (composed of 23 specific destinations) constitute the Canadian portion of the North American origin-destination traffic distribution matrix.

Center for Transportation Information (1990) report is similar to the Canadian report. It shows the top charter traffic destinations, ordered by number of passengers. It also indicates that the top 15 United States airports originate 93% of the United States charter traffic. These 15 origins and the top 31 destinations make up the United States portion of the North American origin-destination traffic distribution matrix.

1990 Traffic Network Models

The global 1990 charter origin-destination traffic distribution matrix is obtained by first normalizing each regional traffic distribution matrix to account for regional 1990 traffic levels and then by merging the regional matrices. The normalization procedure provides the flexibility to adjust the global and regional traffic levels as necessary. For the network model, an OAG airport code and corresponding geographical coordinate identify each origin and destination. From the geographical coordinates, origin-destination great circle distances can be derived. Only 298 origin-destination pairs are active out of the 652 possible combinations. Figure 3-3.6 shows the resulting global distribution, by range, of these active combinations. The top 100 origin-destination pairs, in terms of Revenue Passenger Kilometers (RPK), appear to be a fair representation of the range distribution; thus, they form the basis for the charter traffic network model. The 1990 traffic level forecast, approximately 189 billion RPK, populates the 100 origin-destination pair network and results in a generic fleet size of 540 units to satisfy the network.

The 92 origin-destination pair network model for the Eastern Block's scheduled domestic traffic was populated with 87 billion ASM to account for 1990 levels of traffic.

2015 Traffic Network Model

The 100 origin-destination pair charter traffic model for the 2015 scenario shows 392 billion RPK. Forecasted regional growth factors were used to allocate the total traffic to appropriate regions. For the 2015 scenario, the scheduled domestic traffic of the Eastern Block was assumed to follow the same route patterns established in the 1990 model. The total traffic for this sector was projected at 166 billion ASM. Both the charter and Eastern Block traffic models for 2015 use the same generic aircraft as the respective 1990 scenarios.

Fleet Aircraft

Aircraft with many capacities, ranges, and vintages constitute the 1990 global charter fleet. The distribution of aircraft in the European charter fleet (Belet and de Daunant, 1990) provides a good indication of this aircraft mix. Figure 3-3.7 and Figure 3-3.8 show the composition of narrow-body and wide-body aircraft in this fleet, respectively.

McDonnell Douglas maintains an extensive database of generic aircraft used for modeling purposes. Six generic aircraft were selected from this database to represent the distribution of aircraft in the charter fleet: 2NBL, less than 1500 NM range and less than 136 passenger capacity; 3NBL, 1500–2500 NM range and less than 136 passenger capacity; 4NBS, 2500+ NM range and less than 136 passenger capacity; 4NBL, all ranges and 136–172 passenger capacity; 3WB, less than 2500 NM range and 172+ passenger capacity; and 4WB, 2500+ NM range and 172+ passenger capacity.

Similar to the above, three additional generic aircraft were chosen for the Eastern Block scheduled domestic traffic network model: the ILW, TU5, and TU3. There is no explicit range and/or capacity-driven assignment logic. In most cases, the generic aircraft assigned to a specific route has characteristics similar to the aircraft actually employed on the route. See Figure 3-3.9 for the relative distribution of aircraft types in the Eastern Bloc domestic scheduled fleet.

The same generic aircraft (and therefore fuel consumption rates and emission indices) were used in the year 2015 traffic network models as were used in the 1990 models. Historically, charter operators provide their services with equipment retired from service by the scheduled carriers. The generic aircraft in the 1990 charter scenario are not appreciably different from those aircraft in the 1990 scheduled carrier fleet. While there will of course be some charter fleet mix changes from 1990 to 2015 (1990 vintage equipment will replace some of the older charter aircraft), it is expected that the impact of these changes on global emissions will be relatively minor, especially when considering the fraction of total traffic that charter traffic represents. Forecasting changes to the Eastern Block fleet mix is difficult because of the large uncertainties that exist with respect to the existing fleet composition, changes to the existing ground transportation infrastructure, etc. Rather than introducing an additional source of variability, no changes were made to the 1990 aircraft for developing the 2015 Eastern Bloc scenario.

Fuel Burned

For each route defined by an origin-destination pair, the traffic model logic assigns a single generic aircraft type to absorb all annual traffic. The 1990 and forecast 2015 traffic between origin-destination pairs, generic aircraft capacity, and regional load factors defined the number of flights that must be completed annually to absorb all allocated traffic. Block fuel, and block time equations (both functions of great circle distance) were available for each generic aircraft. Block fuel is the sum of ground maneuver fuel, climb fuel, cruise fuel, descent fuel, and approach fuel. Block time is defined in a similar manner. These performance equations, together with the number of flights, provided annual estimates of fuel burn and aircraft hours for each route in the 1990 and 2015 traffic network models.

An aircraft's fuel burn on a route is not linear with distance. For the ground distance covered, an aircraft uses a relatively large amount of fuel in the initial climb. Similarly, an aircraft burns a relatively small amount of fuel while flying typical descent schedules. Taxi-out and takeoff operations concentrate fuel burn at the origin, while approach, landing, and taxi-in operations concentrate fuel burn at the destination. Although fuel consumed during the initial climb and descent phases of flight depends on factors such as initial cruise altitude, final cruise altitude, takeoff gross weight, and landing gross weight, constant amounts typical of each generic aircraft's class have been assumed for both the climb and descent phases of flight. Therefore, representative

values for engine start, taxi-out, takeoff, climb, descent, approach, land, and taxi-in fuel burns were subtracted from block fuel. Similarly, representative climb and descent distances are subtracted from the great circle distance. The remaining block (or cruise) fuel was then allocated over the remaining great circle distance. Next, the fuel burn is allocated to the appropriate altitude.

Several considerations influence an aircraft's cruise altitude including segment range, aircraft operating characteristics, type of cruise (step-climb, cruise-climb, constant altitude cruise, etc.), traffic, weather, and direction of flight. This analysis assumed that aircraft operate using either constant altitude cruise or cruise-climb profiles at altitudes representative of current operations. These altitudes range from 15,000 feet for short-range, twin-jet operations to 37,000 feet for long-range, wide-body operations. All cruise fuel was linearly allocated between the initial and final cruise altitudes.

Emission Indices

Conversion of pounds fuel consumed into estimates of emission byproducts require an emission index for each engine and constituent of interest. This study analyzed the emission byproducts CO, NO_x, and total HC. An emission index measures mass of constituent produced per mass of fuel burned and typically is depicted as a function of engine power setting, percent of takeoff thrust, or fuel flow rate. The NO_x index characteristically varies directly as a function of engine power setting, while the CO and HC indices vary inversely as a function of engine power setting. In essence, the emission indices measure combustor cleanliness for a given engine cycle.

Because block fuel and block time estimates are available, the average fuel flow rate is determinable for any route. Weighing this average fuel flow rate by the annual departures gives an annual weighted average fuel flow rate for each aircraft. This is the key into the emission indices tables. With fuel flow rate as a proxy for engine power setting, linear interpolation yields an estimate for the index values. Table 3-3.5 shows the emission indices used for both traffic scenarios.

MACH 1.6 EMISSION SCENARIO

The global atmospheric emissions from a future proposed Mach 1.6 High-Speed Civil Transport (HSCT) was developed using the supersonic network (market, routing, and fleet size) described earlier (in Subchapter 3-1). The Mach 1.6 scenario draws upon MDC configuration design studies, Pratt and Whitney/General Electric (P&W/GE) engine cycle data (STF-1015 Mixed Flow Turbo Fan), and the aforementioned supersonic network to provide predictions for the amount and distribution of exhaust emissions.

Configuration Design Studies

Configuration design studies provide the Mach 1.6 airplane performance predictions, including the amount, altitude, and down-range distance of engine emissions. MDC calculated the performance of the combined airframe and engine. Inlet conditions at the engine face were first provided to P&W and GE. Given the inlet conditions, P&W and GE provided uninstalled engine thrust, fuel burn, and nozzle exhaust emission constituents. MDC accounted for engine installation and operational effects on engine and airframe performance, which are integrated with the airframe design to create final HSCT performance predictions.

Previous Mach 1.6 design optimization studies developed the configuration shown in Figure 3-3.10. This configuration design was updated with the latest technology predictions, consistent with Douglas Mach 2.4 baseline studies. The design range was 5000 nautical miles with 15% subsonic over land. A new Mach 1.6 engine cycle was integrated into the design.

P&W/GE Engine Cycle Data

The Mach 1.6 engine cycle data were provided by P&W using the joint P&W/GE ground rules. P&W provided a Mixed Flow TurboFan (MFTF) cycle employing low NO_x combustor technology. The Mach 1.6 ground rules and combustor technology were consistent with Mach 2.0 and 2.4 technology.

Calculation of Exhaust Emissions

Once the configuration design and marketing/economic studies are completed, the final HSCT design was flown throughout the supersonic network, and exhaust emission constituents were distributed across the globe. Performance data from the configuration design studies were used to develop parametric formulas for calculating fuel burn and altitude during climb and cruise; and also, fuel burn constants for takeoff, landing, and descent. The parametric formulas and constants were assembled into an input file that describes the altitude and fuel burn as a function of distance between the cities and/or way points. The global fuel burn information was then converted to emission constituents with a second input file that describes the emission indices, EI, as a function of altitude. The fuel burn distribution for each route was calculated and then distributed in latitude and longitude across the global atmosphere, traveling in both directions. As the emissions of NO_x (as NO₂, at molecular weight 46.01), CO (at molecular weight 28.01), and HC (as methane, CH₄, at molecular weight 16.04) were calculated for each one kilometer altitude along the route, the emissions were assigned to the routed one degree latitude/longitude grids across the global atmosphere. In this manner, emission constituents were distributed in the same way the airplane actually flies each route. Additionally, different formula coefficients and constants can be calculated to assess other configurations (formula coefficients and constants are proprietary to MDC).

DEVELOPMENT OF EMISSION DATABASE

Method Summary

Formation of an emission grid database required development of a procedure that transformed fleet scenario data into a worldwide emission grid. The procedure consists of three basic steps: 1) assignment of fleet route description segments to grid latitude/longitude elements, 2) assignment of grid latitude/longitude fuel burn to grid altitude elements, and 3) calculation of resultant molecules from fuel burns within grid elements.

Each of these processing steps provides a unique product required during the development of the database. Specifically, Step 1 considers individual fleet routes and determines detailed mission descriptions within grid elements. Step 2 utilizes this product to compile fleet composite fuel burn at altitude profiles within grid elements. Finally, Step 3 employs these fleet fuel burn products to calculate total molecule production within grid elements.

Fleet scenario profiles provide the basis from which the emission processing evolves. The first step of the procedure assigns individual route segments to 1 degree × 1 degree worldwide grid elements. For a unique fleet type, each route assigned to the fleet is analyzed. The origin/destination coordinates of a route define a great circle. Using the great circle route, distances between 1 degree longitude bands are calculated. Similarly, within these calculated longitude bands, distances at 1 degree latitude intervals are subsequently calculated for each of these longitude/latitude subelements of the route. Routes that are not great circle routes (i.e., route diversions) are broken into their segmented route elements. Each of these segments forms a subroute (which is then treated as a great circle route) and is then re-analyzed as previously described. Each of these subroutes is then re-combined to its original segmented description for continuing processing.

Following calculation of elemental distances for an individual route, a re-evaluation of the route fuel/altitude profile is performed. The raw fleet input data for a route provides a gross fuel/ altitude profile, within which significant action points (i.e., departure, climb/descend, cruise, land) along the route are provided. Using the grid elemental distances, an interpolation of the gross profiles is performed to provide grid element fuel/altitude/range profiles. Once this interpolation is completed, the output product is sorted into ascending longitude grid elements for use in Step 2.

The two-dimensional fleet route/profile data file product from Step 1 is used in Step 2 for developing the worldwide fuel/altitude profiles for an individual fleet. Each grid element containing fleet route activity is analyzed to define total fuel usage between zero and 100,000 feet, at 2000-foot intervals.

For each grid element, all routes navigating an element have their fuel/altitude profiles interpolated throughout the altitude range. A composite total of the fuel burn within an altitude interval is maintained until all routes through the element are analyzed. The element's fuel/altitude profile is written to an intermediate output file for Step 3 processing. This procedure is repeated for all active grid elements.

The fleet scenario data in addition to the operational profiles, also provides engine emission indices assignable to the fleet's characteristic engine. The emission index, as provided, defines the number of pounds of emission product created per kilo pound of fuel burned. The fleet's engine indices are further described by the altitude levels of operation representative of composite engine operating levels (i.e., takeoff, climb, descent, cruise). These indices, in combination with the composite altitude/fuel burn profile developed from Step 2, are used in Step 3 to ultimately yield a worldwide assessment of CO₂, NO_x (in NO₂ equivalent), and total HC (represented as CH₄) emissions from aircraft fuel burns.

Using both the fuel burn/altitude profiles created in Step 2 for an aircraft fleet, and with the corresponding fleet's engine indices, the total molecule production of interest can be calculated from the following:

- Total Emission Product = Total Fuel Burn × Pounds of Emission Product/1000 pound Fuel Burn
- Total Molecules = Total Emission Product × Kilogram/Pounds × Molecular Weight × Molecules/Mole

This computation is performed for all active cells within a fleet's inventory. Once all individual fleet emissions are developed, a last pass through this processing step is performed. This computation cycle accumulates contributions of the individual fleets into a single worldwide distribution. This worldwide distribution, with a resolution of 1 degree × 1 degree × 1 kilometer, is written to the final output file for subsequent electronic transmission to NASA Langley.

Methodology Validation

During development of the emission grid database procedure, specific required tasks were identified within each of the processing steps. These specialized tasks are performed by software units. To ensure that each unit performed its assignment, each unit was tested in a stand alone environment prior to incorporation within a software processing module. This testing energized all branches within the unit and considered extremes of operation. In addition, it provided a level of detail from which direct comparisons to manual results were made. Following completion of unit testing, testing of the software processing module was performed. This testing verified both communications between units was correct, and overall performance was acceptable. This testing

used results from unit testing and comparisons to earlier two dimensional validated emission results.

Following completion of processing module tests, overall procedural testing was performed using 1990 study results. The objective of this testing was verification of communications between processing modules. Upon conclusion of these tests, 1992 MDC scenario data were processed. Comparisons were made of scenario fuel burns reported by the emission processor to those predicted via an independent procedure. In addition, comparisons were made between overall MDC and Boeing scenario data. This comparison did reveal an initial difference between molecular weights of constituents. The MDC scenario was subsequently updated to reflect the current constituent molecular weights.

Data Transmittal

The MDC data submittal for the 1990 and 2015 scenarios consisted of electronic transfer of 42 global emission files and 9 global fuel burn files. The 1990/2015 MDC scenarios described global emissions in a 1 degree latitude \times 1 degree longitude \times 1 kilometer grid. Three classes of files were developed describing emissions from worldwide military traffic, charter traffic, and from other scheduled traffic originating within both the former Soviet Union and China. A fourth data set, representing the composite of the above, was additionally generated. Within each of these classes, individual files (12 total) that describe global emissions for NO_x , HC, and CO were provided. For future analysis of other emission products, fuel burn distributions for each class (4 files) were also provided.

The MDC 2015 scenario consisted of generation of a parallel set of files (three classes and subsonic composite) and additionally contained a Mach 1.6 HSCT class of emissions. The HSCT was characterized as having three baseline NO_x cruise emissions (i.e., $\text{NO}_x = 5.0, 10.0, \text{ or } 15.0$). Consequently, nine emission files were provided for the HSCT class.

Data Overview

Tables 3-3.6 and 3-3.7 present a comprehensive summary of the fuel burns and contributions of each emission constituent for both the 1990 and 2015 scenarios. Figures 3-3.11 thru 3-3.18 depict geographic composite fuel distributions for both the 1990 and 2015 MDC scenarios. These figures show MDC scenario fuel usages occur primarily within the northern hemisphere, principally within the midlatitudes. This is not an unexpected consequence of the location of the three principal military powers (United States, the former Soviet Union and NATO/WARSAW Europe). The MDC 1990 scenario is dominated by the military class (64% of total fuel and 65% of NO_x). Although a substantial reduction in military flights in 2015 has been predicted, the military sector remains dominion for subsonic emissions (41% and 42% of total fuel and NO_x respectively). The MDC Mach 1.6 HSCT contributes over 66% to the combined 2015 fuel usage, and 56% of the total NO_x . In addition to the fuel growth for the northern hemisphere, the HSCT mission network also provides fuel growth into Oceania.

Figures 3-3.19 thru 3-3.21 present cumulative fuel burn versus altitude for each component (i.e., military, charter, other, and Mach 1.6 HSCT) for both the 1990 and 2015 scenarios. Three generic aircraft were used to model the Eastern Bloc domestic traffic not accounted for in the OAG. One generic aircraft in particular (Tu-5) dominates the scenario. The long-range routes and the cruise altitudes assumed, as well as the distribution of traffic in the network model, result in a relatively higher percentage of fuel being burned at high altitudes when compared to the charter and military scenarios where single aircraft or flight profiles do not dominate.

Similarly, Figures 3-3.22 thru 3-3.24 present cumulative emissions of NO_x versus altitude for both scenarios. Emissions of total HC and CO exhibit nearly identical profiles. Figures 3-3.25

thru 3-3.33 present average scenario emission indices at altitudes for each component. With respect to Figure 3-3.27 altitudes for supersonic climb and subsonic cruise overlap, so the climb EIs shown are averaged with the subsonic cruise EIs, where power settings are low. Additionally, supersonic cruise occurs at nearly maximum power setting.

Table 3-3.1. Emission Indices for the Allison TF-56 Turboprop Engine

Power Setting	Fuel Flow Rate (kg/hr)	Carbon Monoxide (gm/kg)	Oxides of Nitrogen* (gm/kg)	Hydrocarbons (gm/kg)
Idle	249	31.9	3.8	21.0
Approach	478	3.5	7.4	0.5
Intermediate	865	2.4	9.2	0.5
Military	943	2.1	9.3	0.5

*NO_x emission index in gm of NO_x as NO₂ emitted per kg of fuel.

Table 3-3.2. Representative U.S. Utilization Rates Per Primary Aircraft Authorized, by Mission Category

Mission	Annual Flying Hours
Fighter/Attack	332
Transport	676
Bomber	374
Trainer	546
Tanker/Reconnaissance/Other	335

Table 3-3.3. Assumed Utilization Rates of Military Aircraft as a Percentage of U.S. Utilization

Region/Alliance	Relative Utilization
NATO	100%
Warsaw Pact	75%
China	50%
Other	50%

Table 3-3.4. Annual Flying Hours Per Aircraft in Inventory by Mission and by Region or Alliance (Rounded to Nearest 25)

Mission	NATO	Warsaw pact	China/Other
Fighter/Attack	250	175	125
Transport	600	450	300
Bomber	325	250	175
Trainer	400	300	200
Tanker/Reconnaissance/ Other	300	225	150

Table 3-3.5. Charter and Eastern Block Scenarios Emission Indices

Generic Aircraft	Altitude Band (km)	Carbon Monoxide (gm/kg)	Oxides of Nitrogen (gm/kg)	Hydrocarbons (gm/kg)
2NBL	0 - 1	18.6	5.9	1.0
	1 - 9	3.4	8.6	0.1
	9 +	7.6	7.7	0.4
3NBL	0 - 1	4.2	6.9	0.7
	1 - 9	2.2	9.6	0.5
	9 +	2.9	6.9	0.6
3WB	0 - 1	7.0	9.1	0.7
	1 - 9	2.6	15.3	0.2
	9 +	13.3	7.0	1.4
4NBS	0 - 1	8.3	8.6	0.8
	1 - 9	2.0	12.8	0.2
	9 +	2.1	11.7	0.2
4NBL	0 - 1	12.3	7.8	2.6
	1 - 9	3.0	11.4	0.5
	9 +	4.6	9.9	0.8
4WB	0 - 1	28.8	5.3	6.5
	1 - 9	1.2	13.7	0.3
	9 +	9.4	7.1	2.1
TU3	0 - 1	4.9	8.6	2.8
	1 - 9	1.7	14.8	0.5
	9 +	2.3	11.1	1.1
TU5	0 - 1	22.0	3.6	8.8
	1 - 9	5.6	5.3	1.5
	9 +	11.6	4.2	3.3
ILW	0 - 1	16.3	7.9	1.6
	1 - 9	2.5	12.9	0.2
	9 +	8.6	10.1	0.8

Table 3-3.6. Results of 1990 Military, Eastern Block, and Charter scenarios
(Amounts Shown are Annual Totals)

Sceanrio	Fuel Burn (kg × 10⁹)	Carbon Monoxide (mol. × 10³³)	Oxides of Nitrogen (mol. × 10³³)	Hydrocarbons (mol. × 10³³)
Military	26.02	2.55	10.46	7.10
Eastern Block	8.28	0.65	1.77	0.82
Charter	6.65	0.79	0.74	0.15
Total	40.95	3.98	12.96	8.06

Table 3-3.7. Results of 2015 Military, Eastern Block, Charter, and Mach 1.6 HSCT scenarios (Amounts shown are annual totals)

Sceanrio	Fuel Burn (kg × 10⁹)	Carbon Monoxide (mol. × 10³³)	Oxides of Nitrogen (mol. × 10³³)	Hydrocarbons (mol. × 10³³)
Military	20.58	1.93	8.72	6.94
Eastern Block	15.79	1.23	3.36	1.55
Charter	13.49	1.60	1.56	0.34
Subtotal	49.86	4.76	13.64	8.83
Mach 1.6				
HCT*	99.13	5.99	6.20	1.12
Total	148.99	10.75	19.84	9.95

* Amounts are for scenario with NO_x emission index = 5.0.

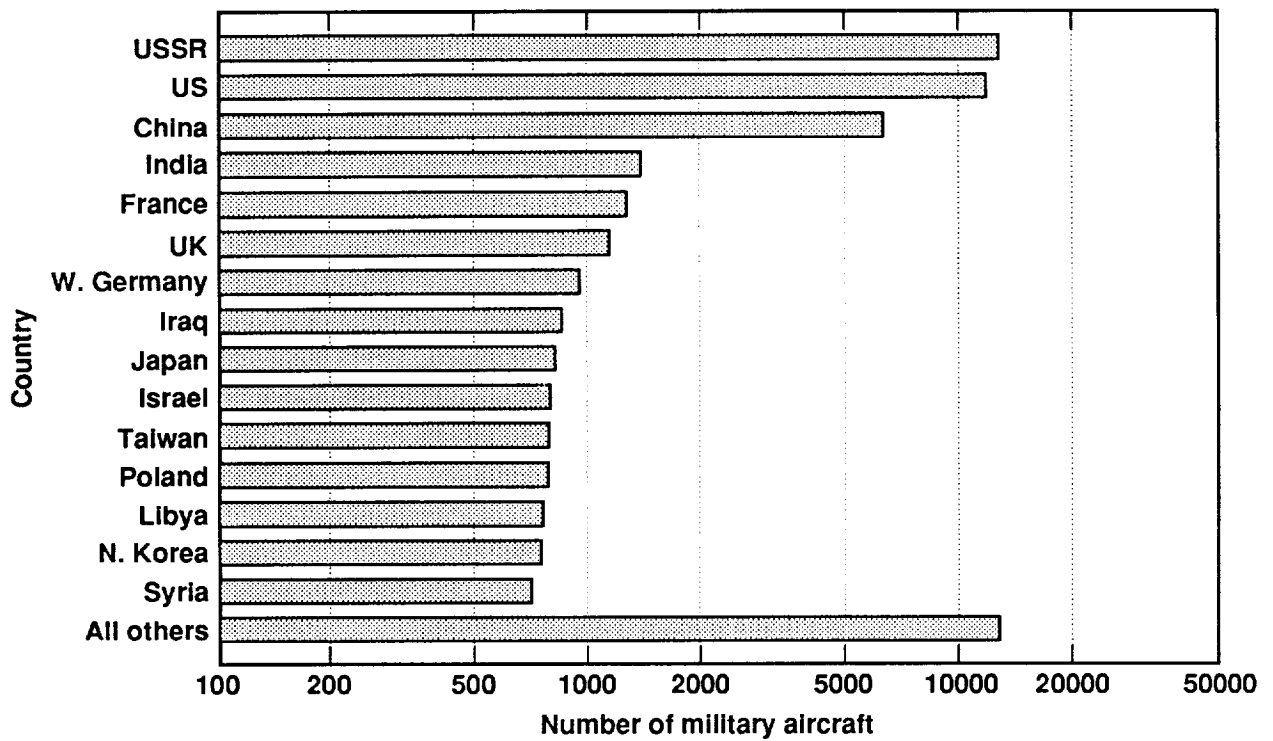


Figure 3-3.1. Distribution of military aircraft inventories. Approximately 60,000 fixed-wing aircraft counted for study. All Others category includes 123 countries.

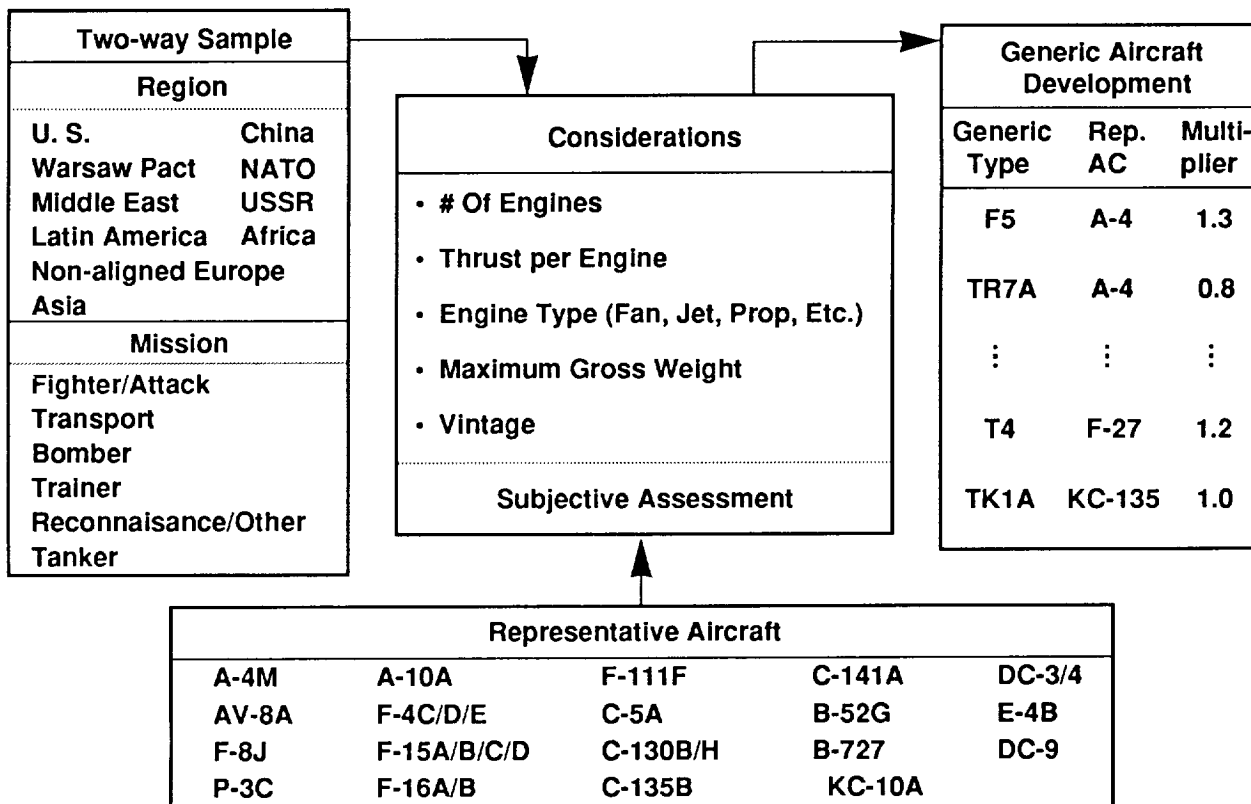


Figure 3-3.2. Generic aircraft development process.

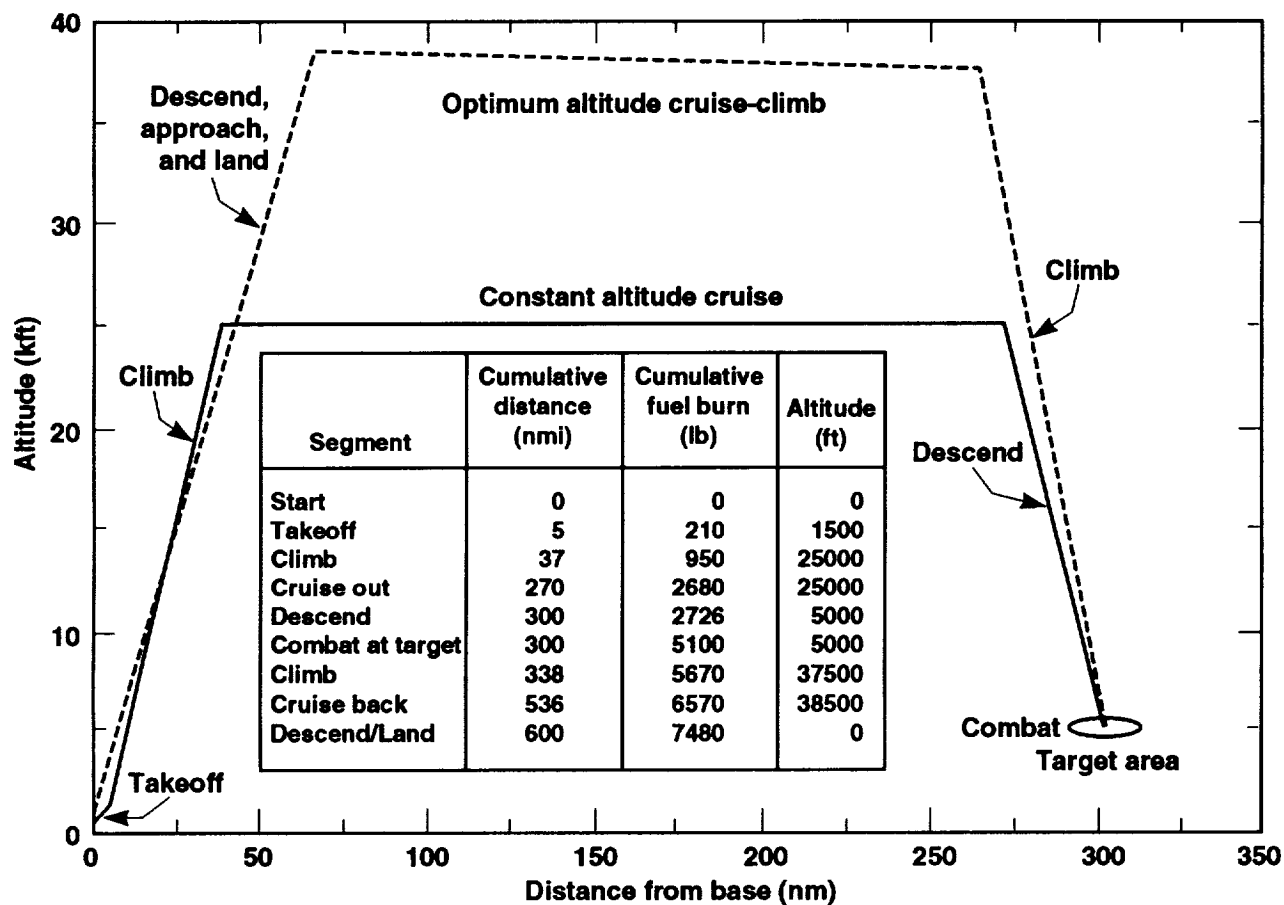


Figure 3-3.3. Representative mission profile for the A-4M military aircraft.

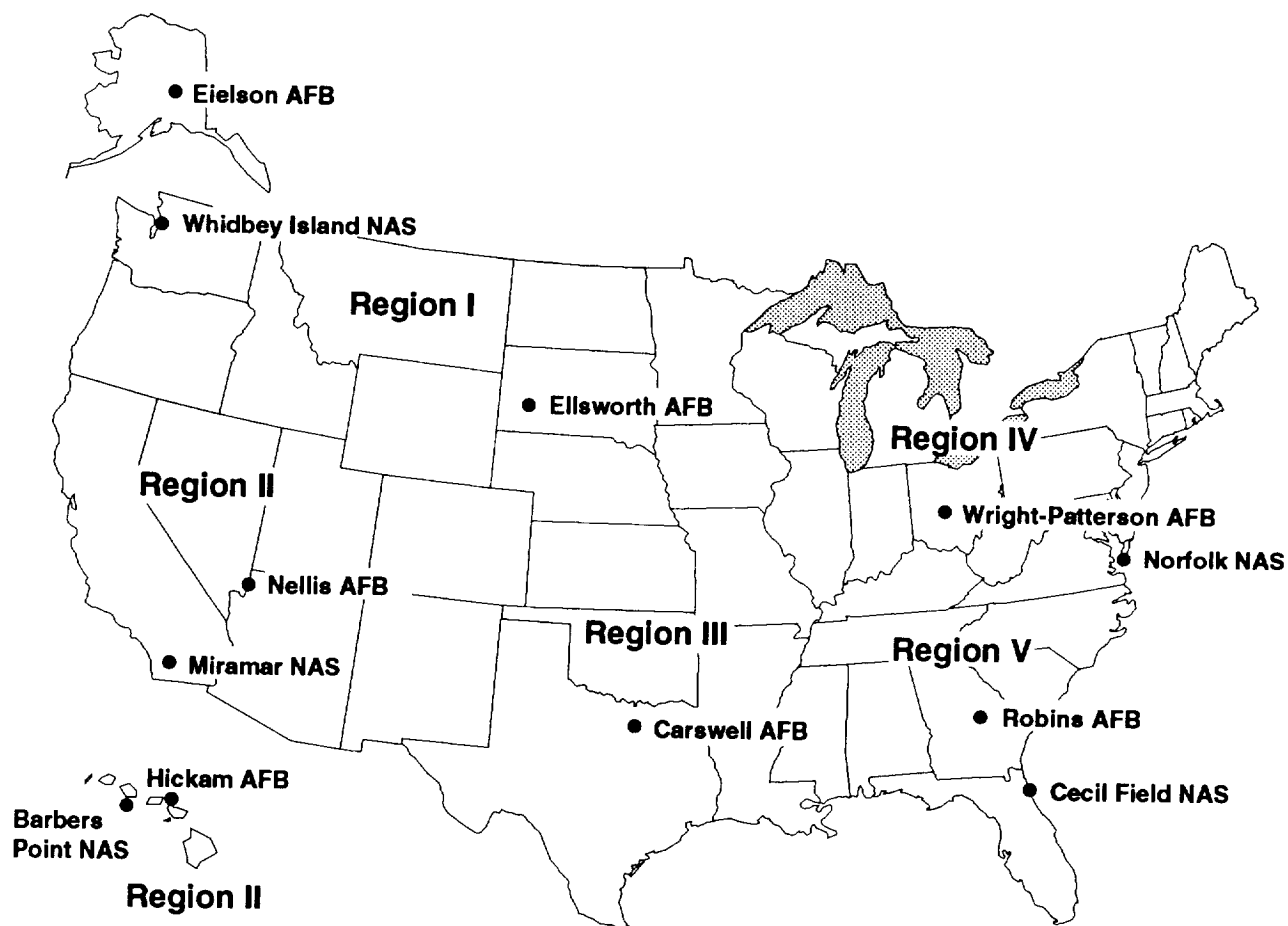


Figure 3-3.4. U.S. regions selected for basing of military aircraft fleet.

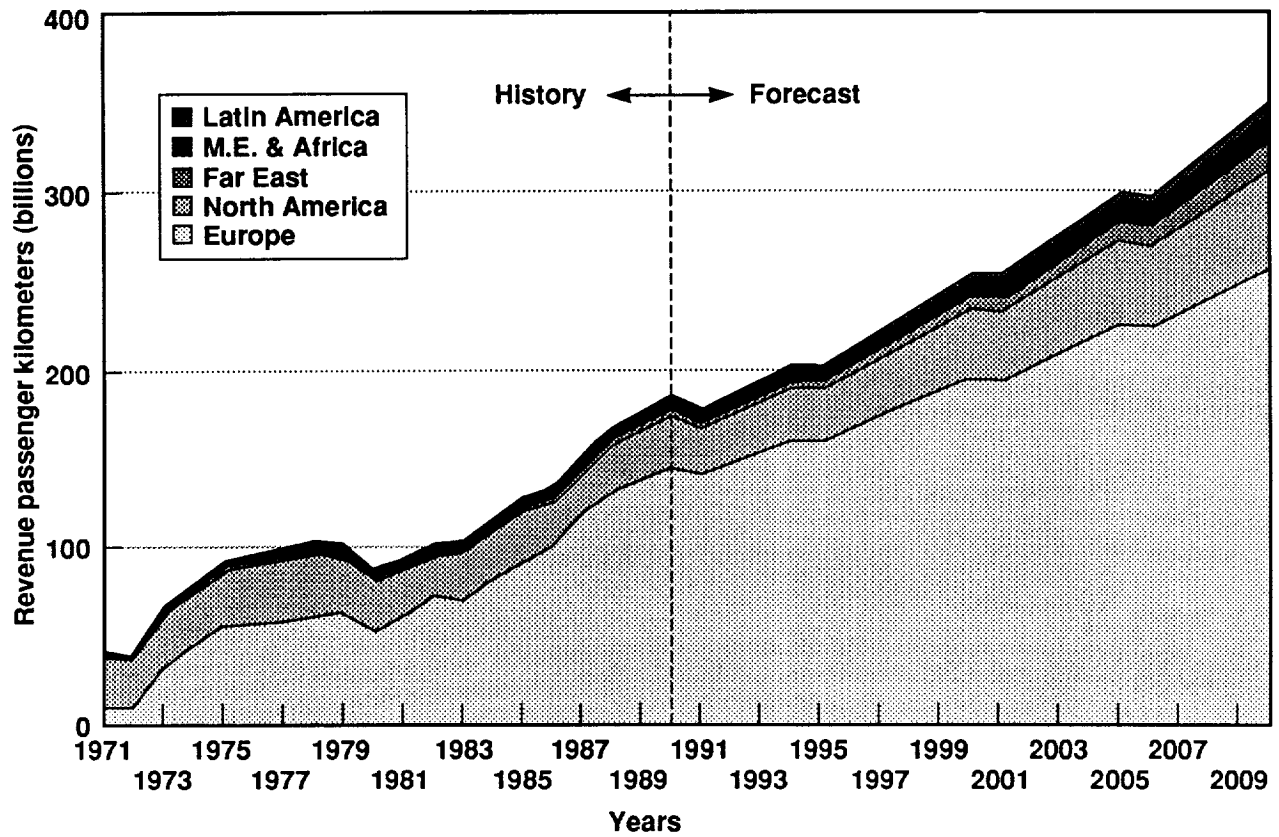


Figure 3-3.5. World traffic forecast by domicile regions of nonscheduled (charter) traffic based on ICAO data.

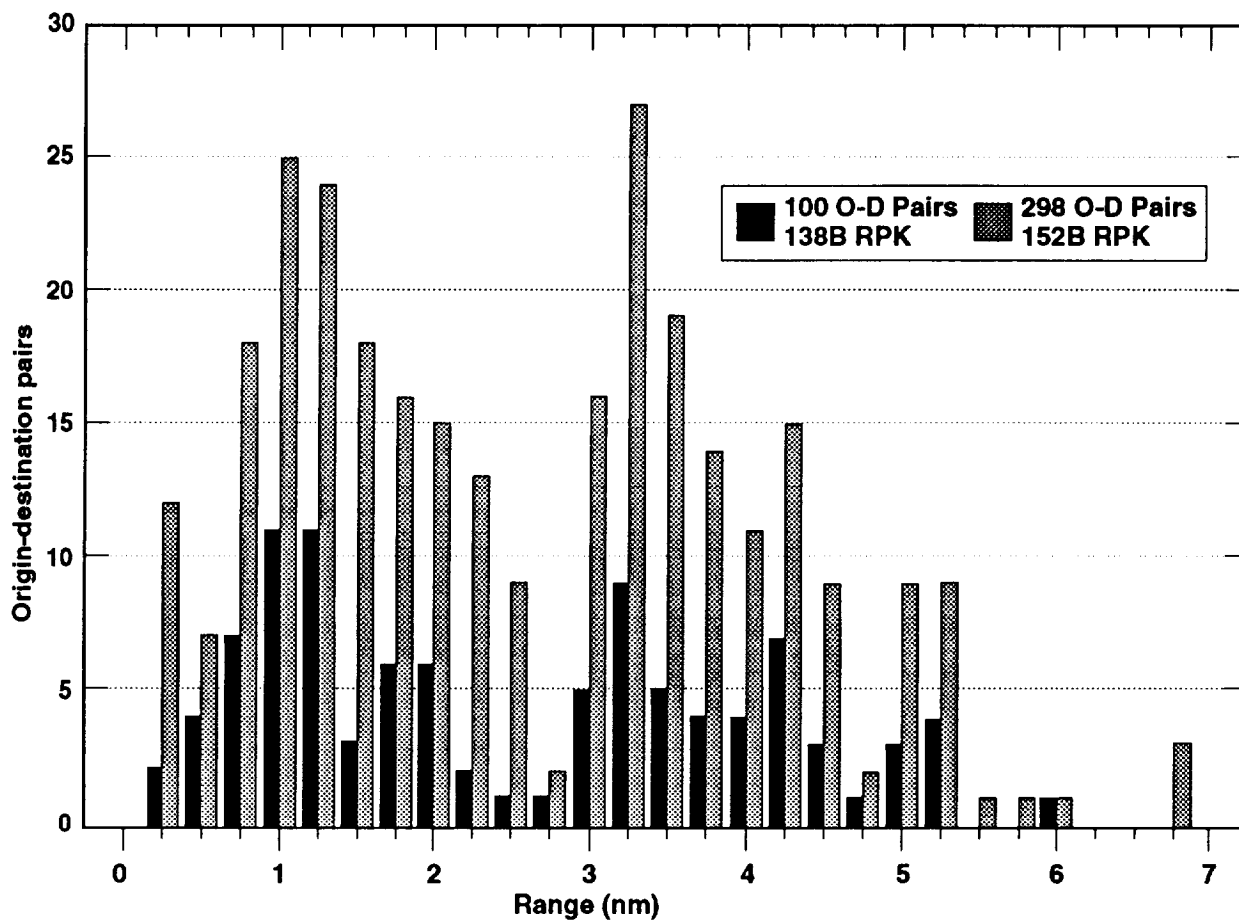


Figure 3-3.6. Global distribution by range of charter flights for various origin-destination (O-D) pairs. Shown in black are the top 100 pairs by RPK.

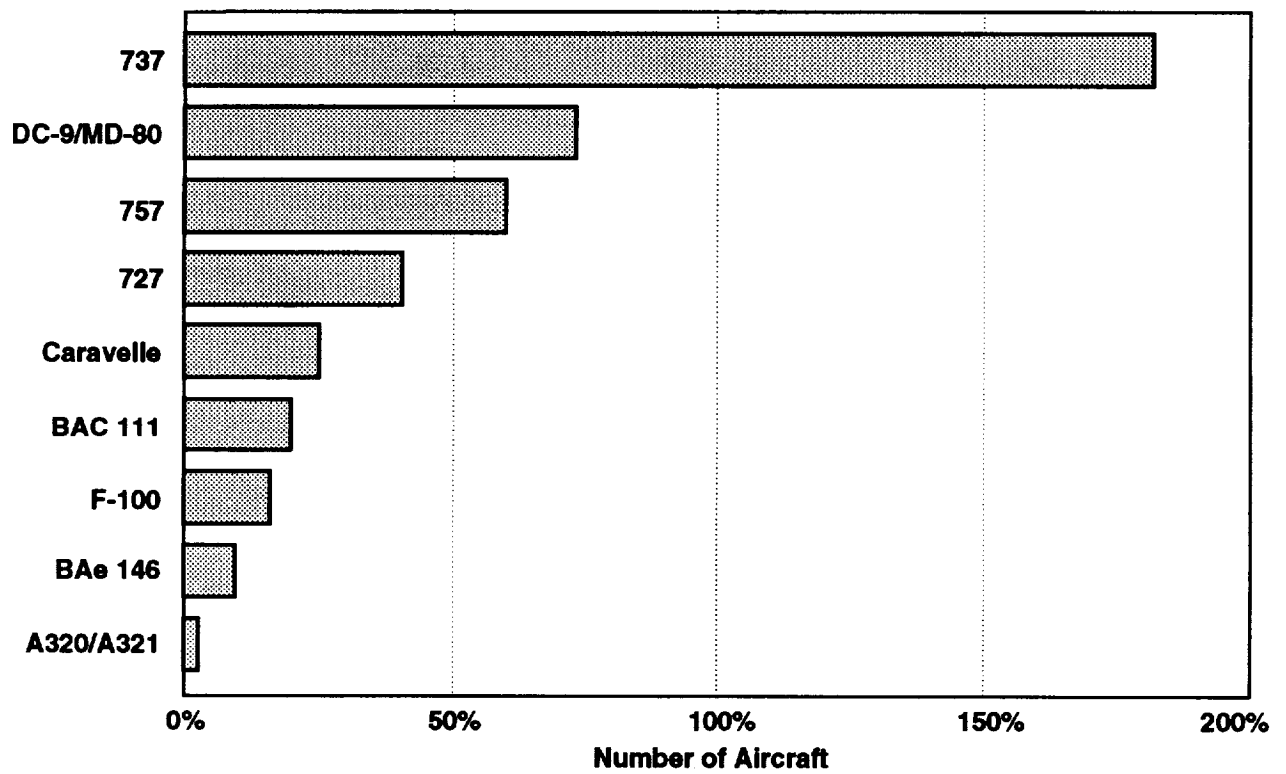


Figure 3-3.7. Distribution of 1990 European charter narrow-body fleet by aircraft type.

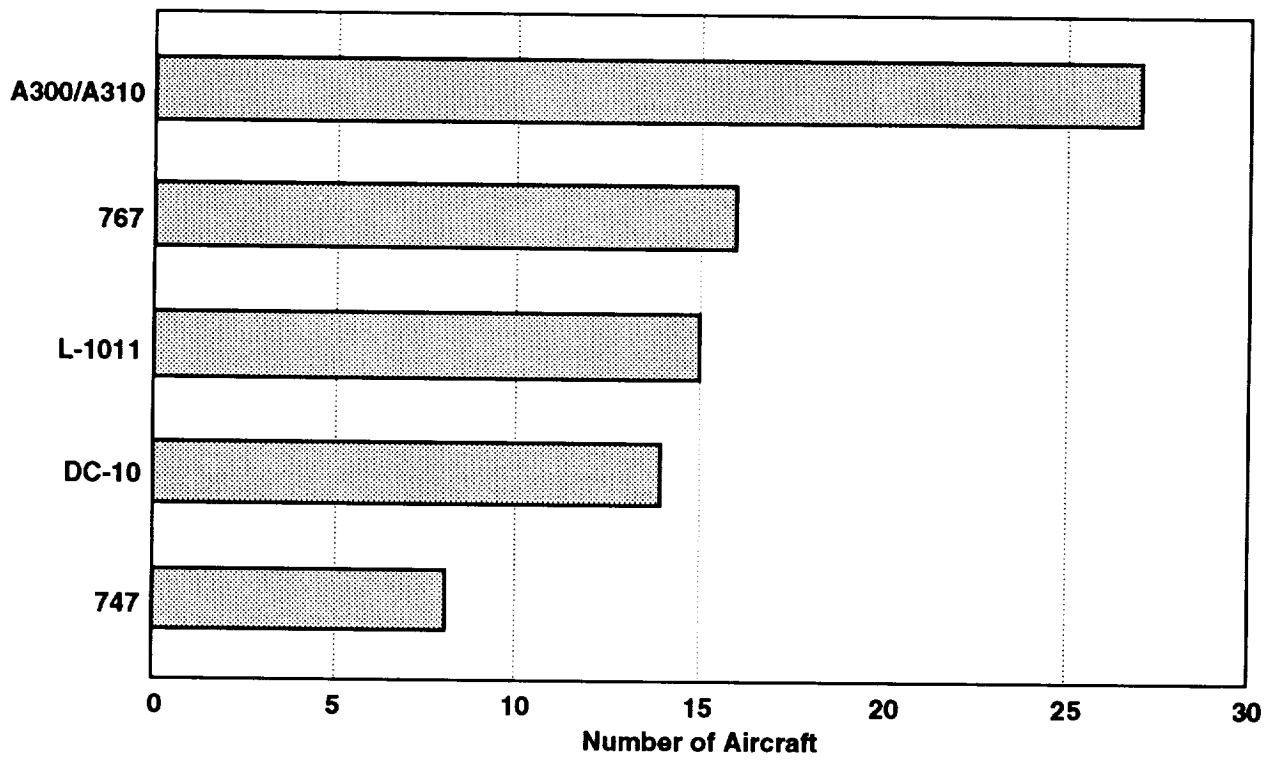


Figure 3-3.8. Distribution of 1990 European charter wide-body fleet by aircraft type.

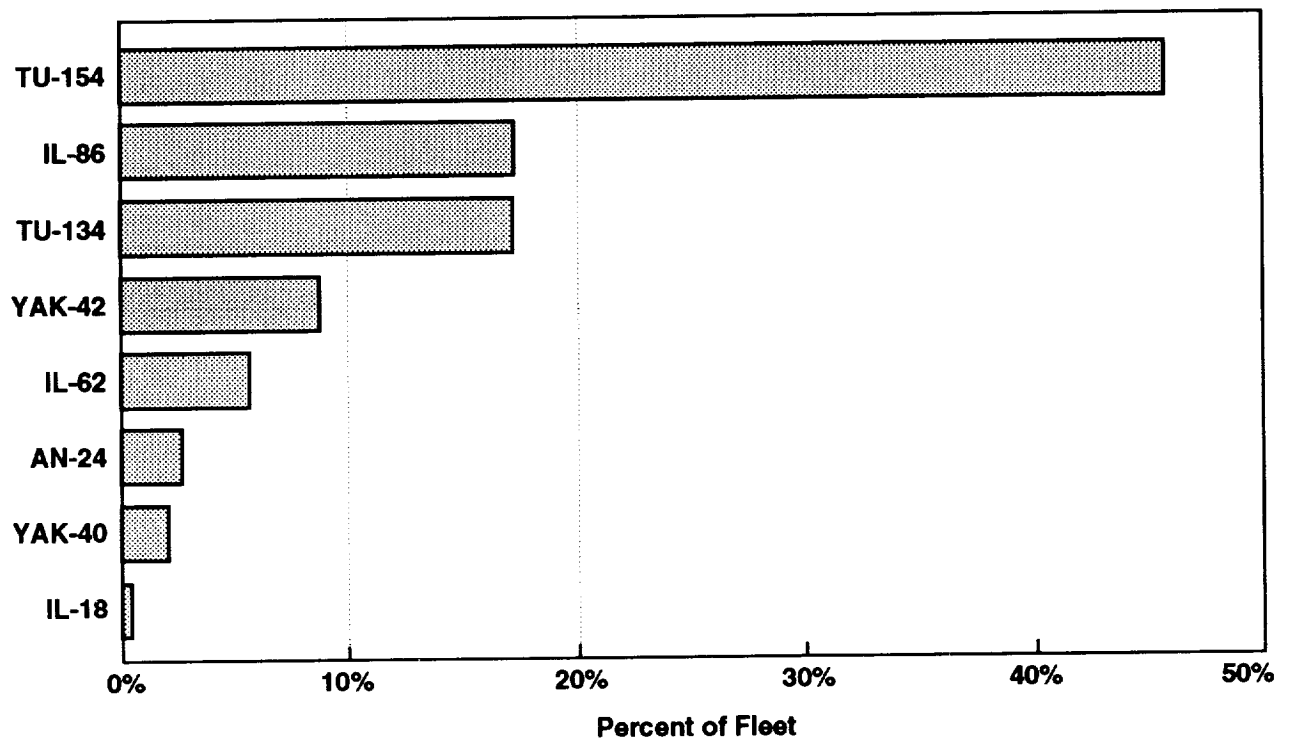


Figure 3-3.9. Distribution of Aeroflot 1990 domestic scheduled traffic fleet by aircraft type. The Eastern Block scenario generic aircraft are drawn from this distribution.

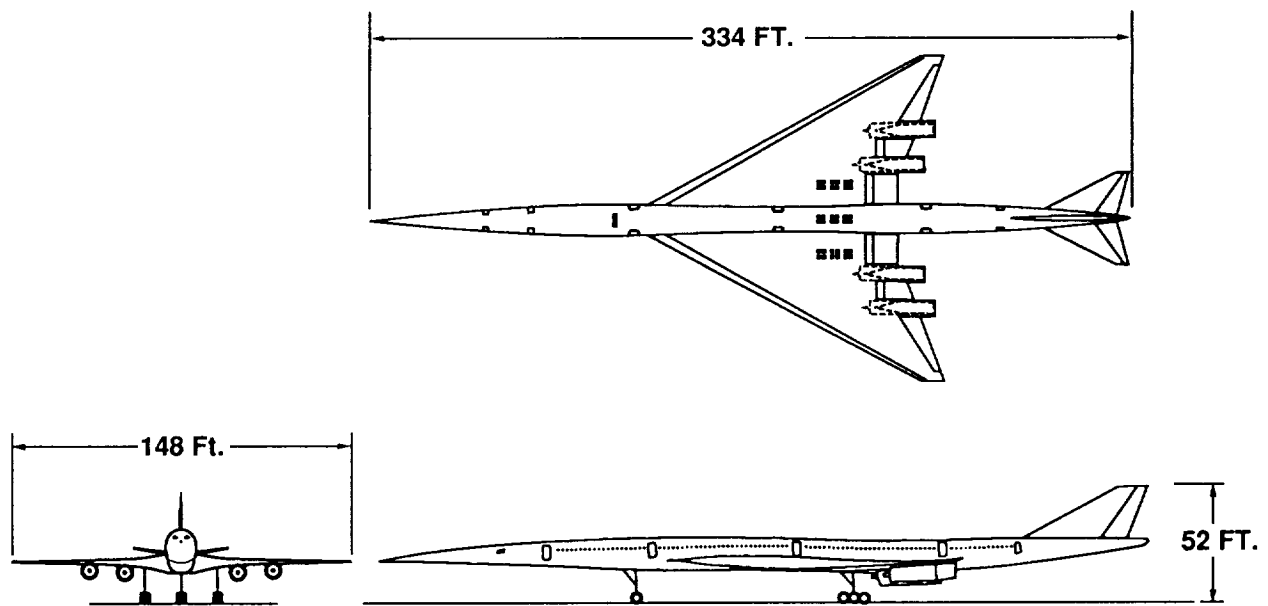


Figure 3-3.10. Configuration for a Mach 1.6 HSCT as updated in recent design optimization studies at McDonnell Douglas.

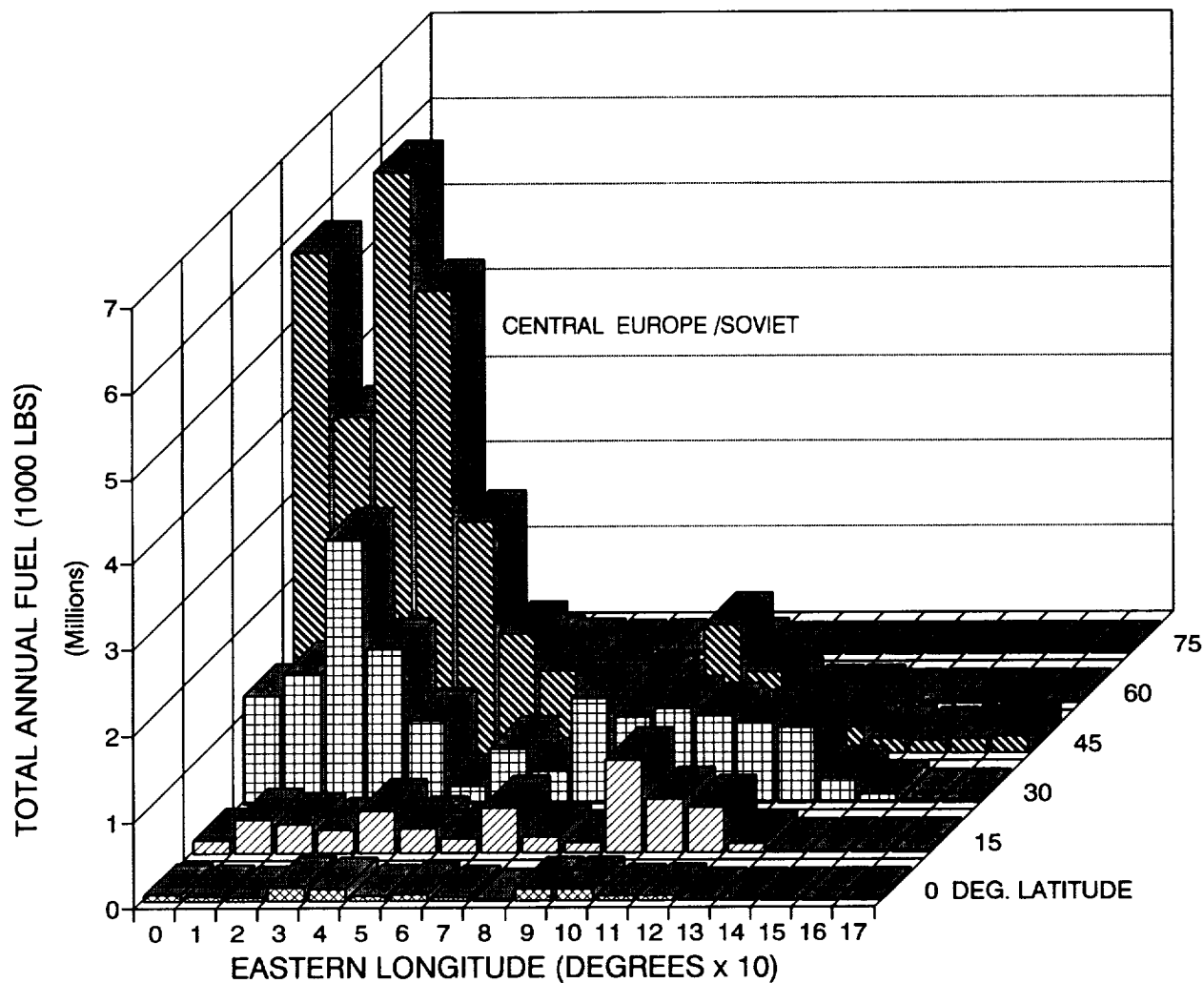


Figure 3-3.11. Total annual fuel distribution within the northern half of eastern hemisphere in 1990 for the military/charter/Soviet scenario.

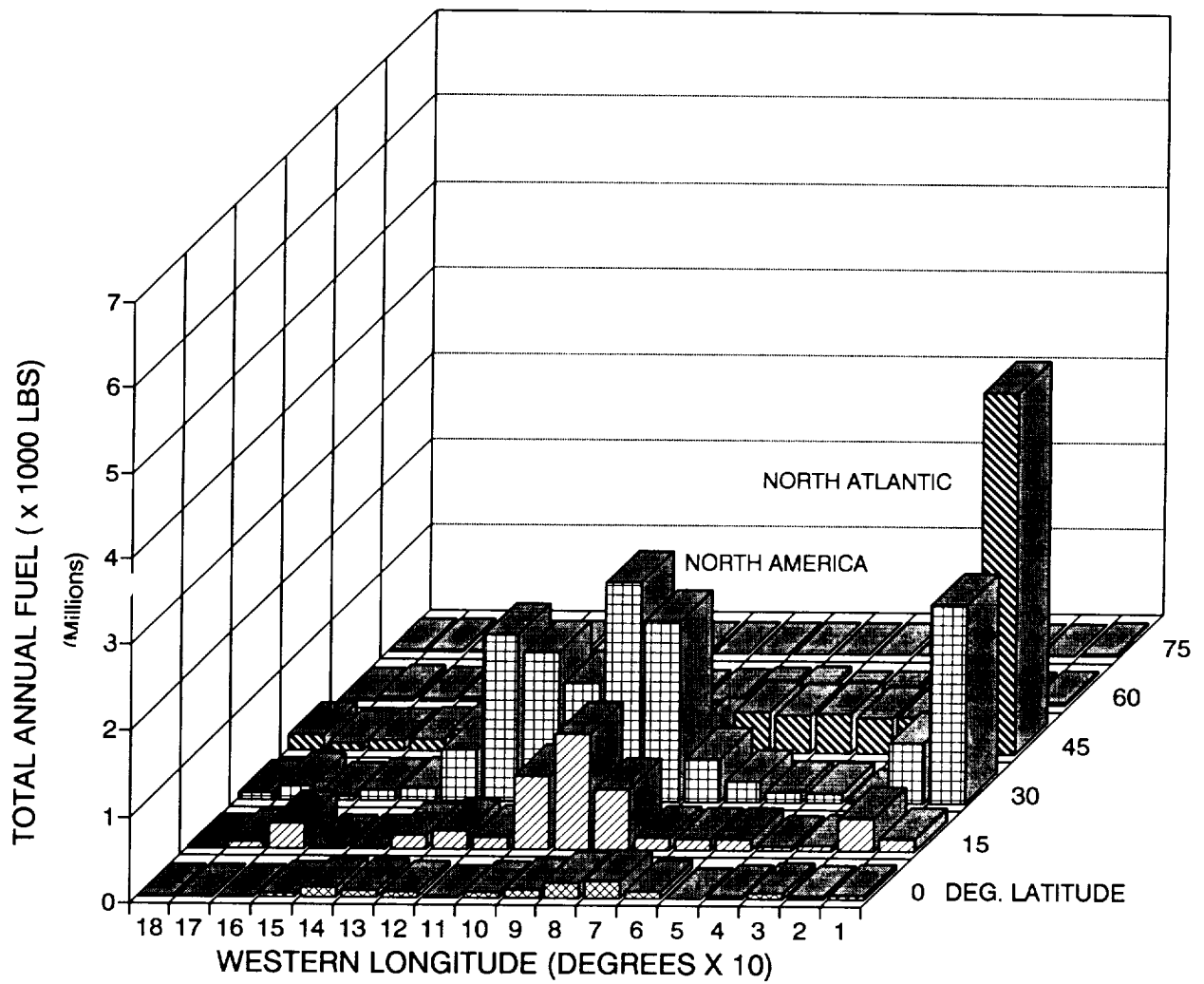


Figure 3-3.12. Total annual fuel distribution within the northern half of the western hemisphere in 1990 for the military/charter/Soviet scenario.

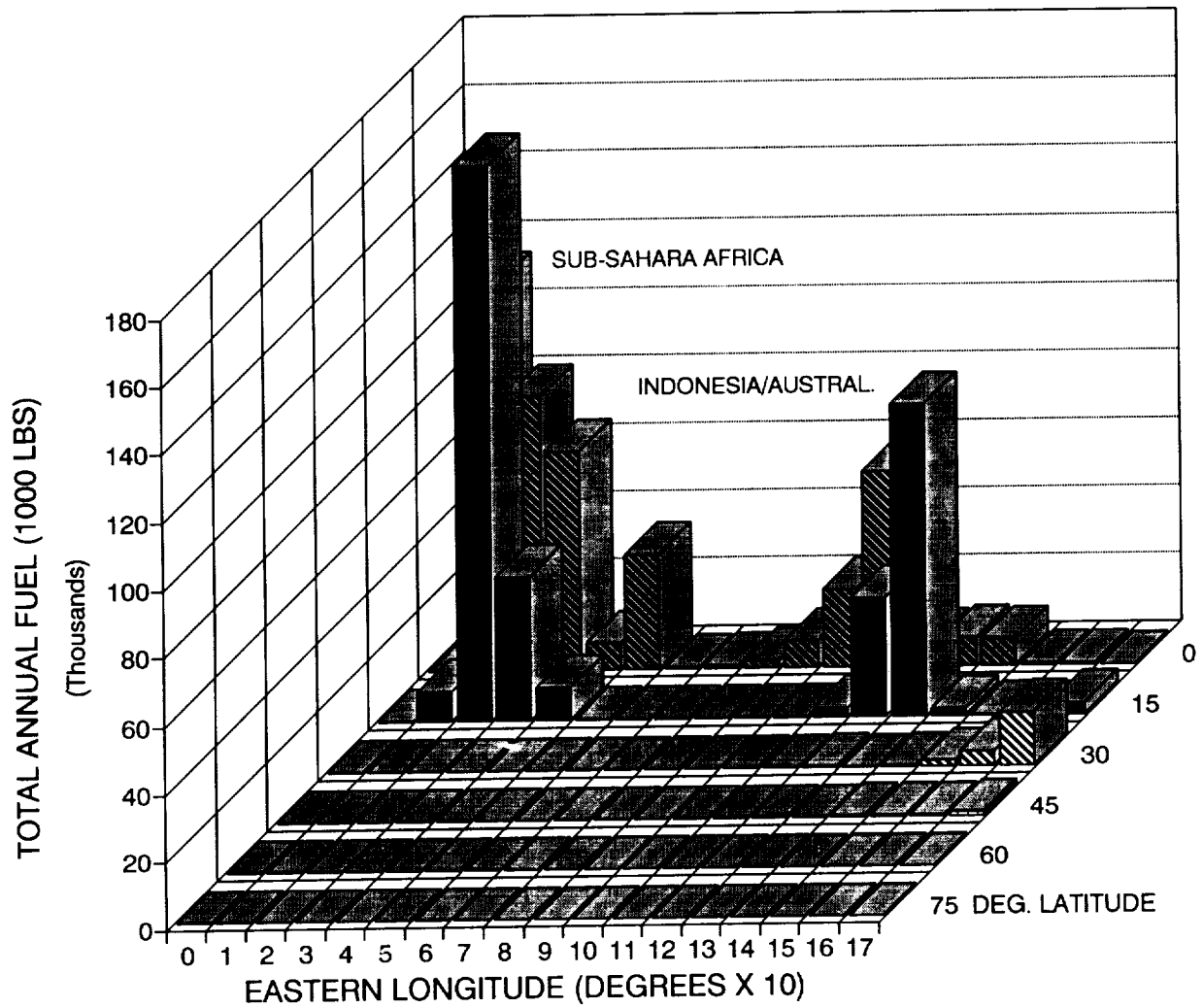


Figure 3-3.13. Total annual fuel distribution within the southern half of the eastern hemisphere in 1990 for the military/charter/Soviet scenario.

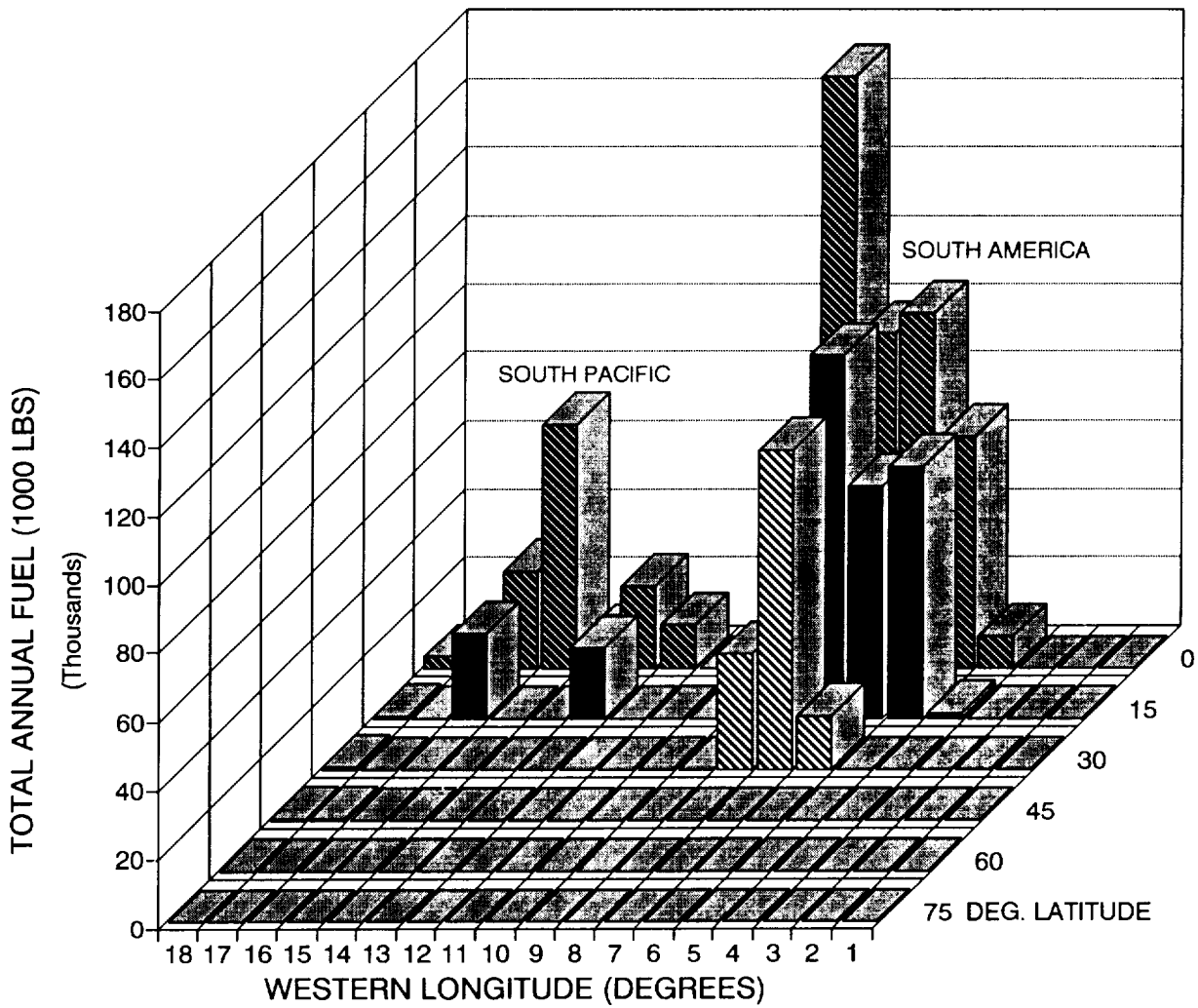


Figure 3-3.14. Total annual fuel distribution within the southern half of the western hemisphere in 1990 for the military/charter/Soviet scenario.

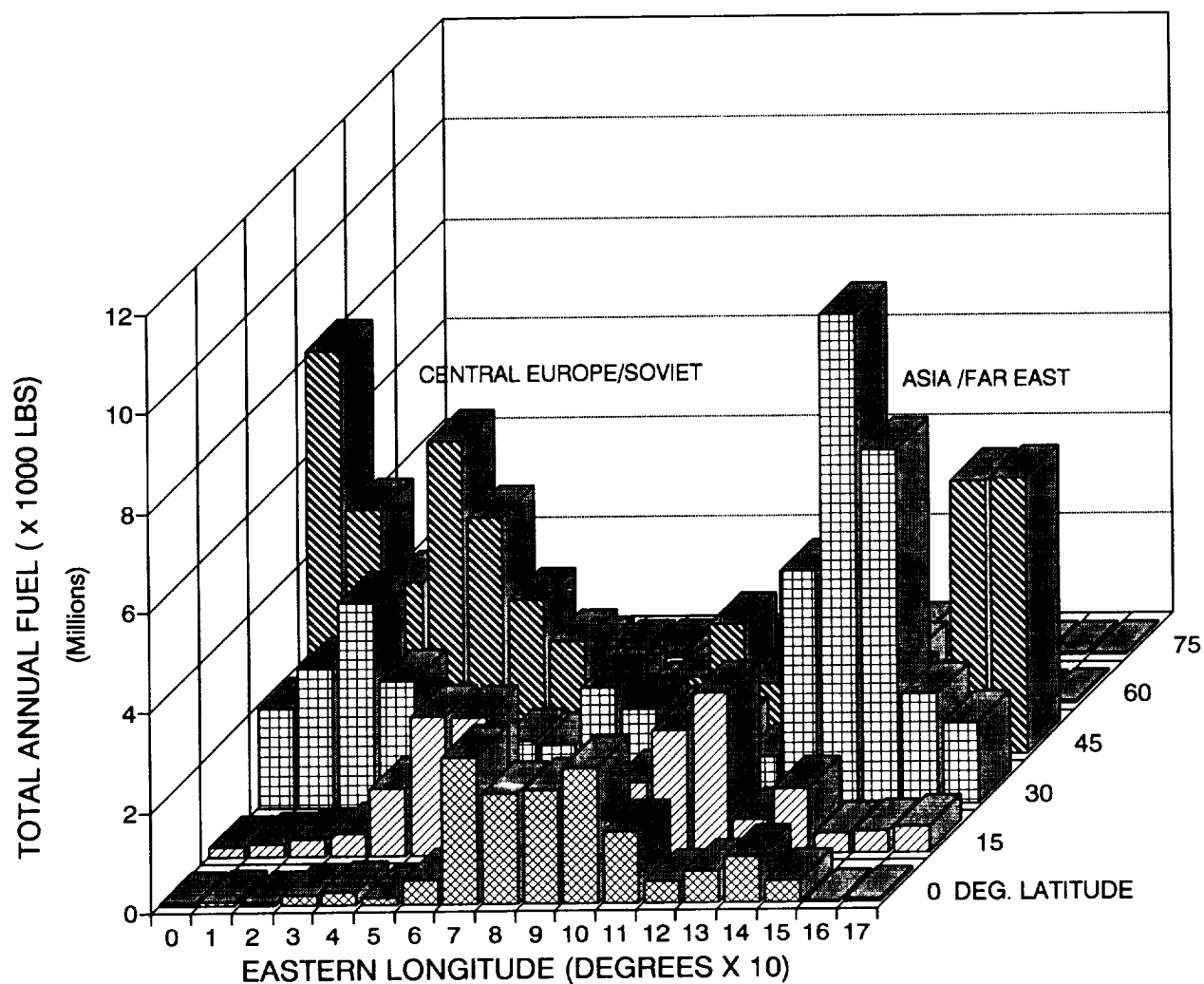


Figure 3-3.15. Total annual fuel distribution within the northern half of the eastern hemisphere in 2015 for the military/charter/Soviet/M1.6 HSCT scenario.

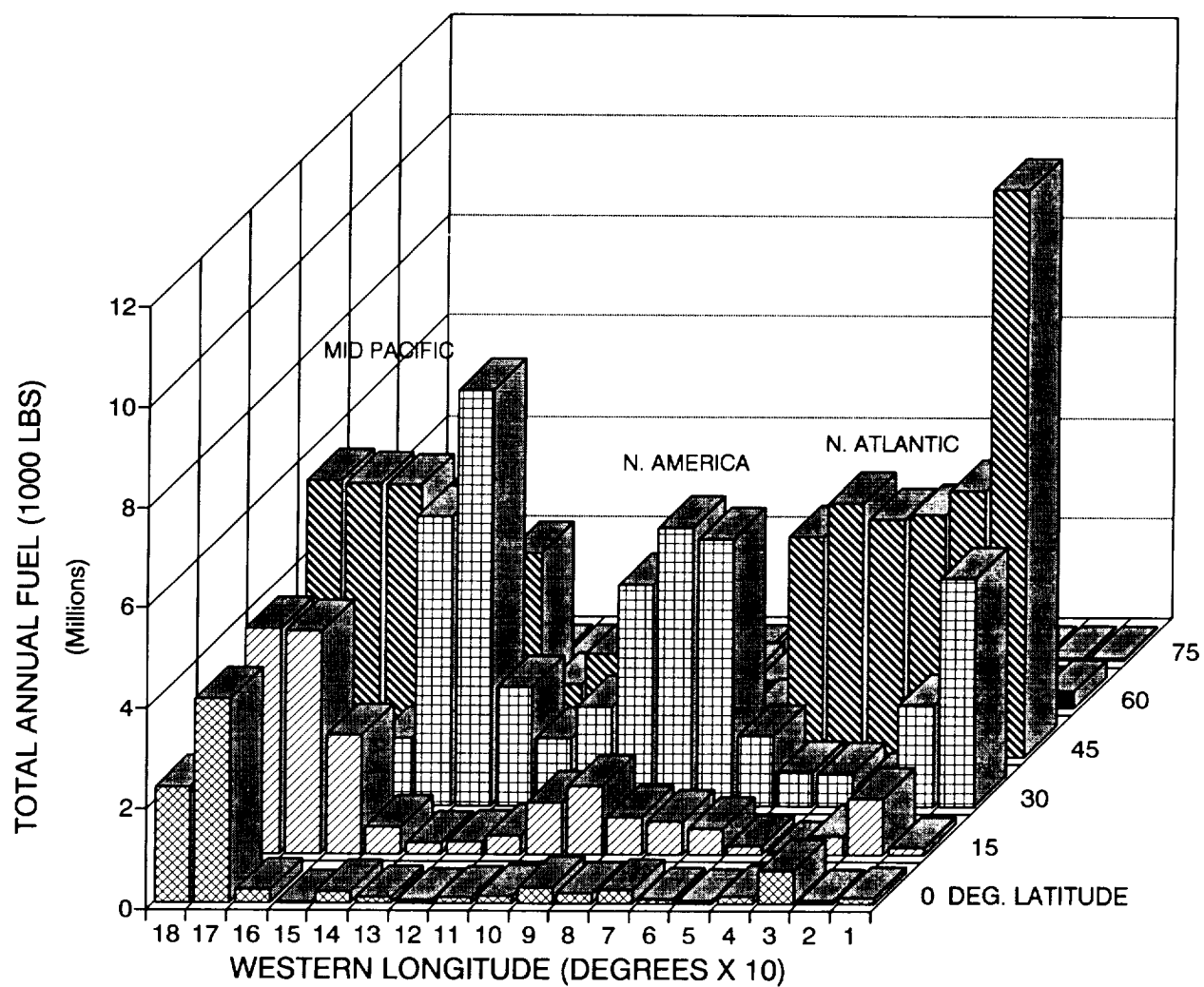


Figure 3-3.16. Total annual fuel distribution within the northern half of the western hemisphere in 2015 for the military/charter/Soviet/M1.6 HSCT scenario.

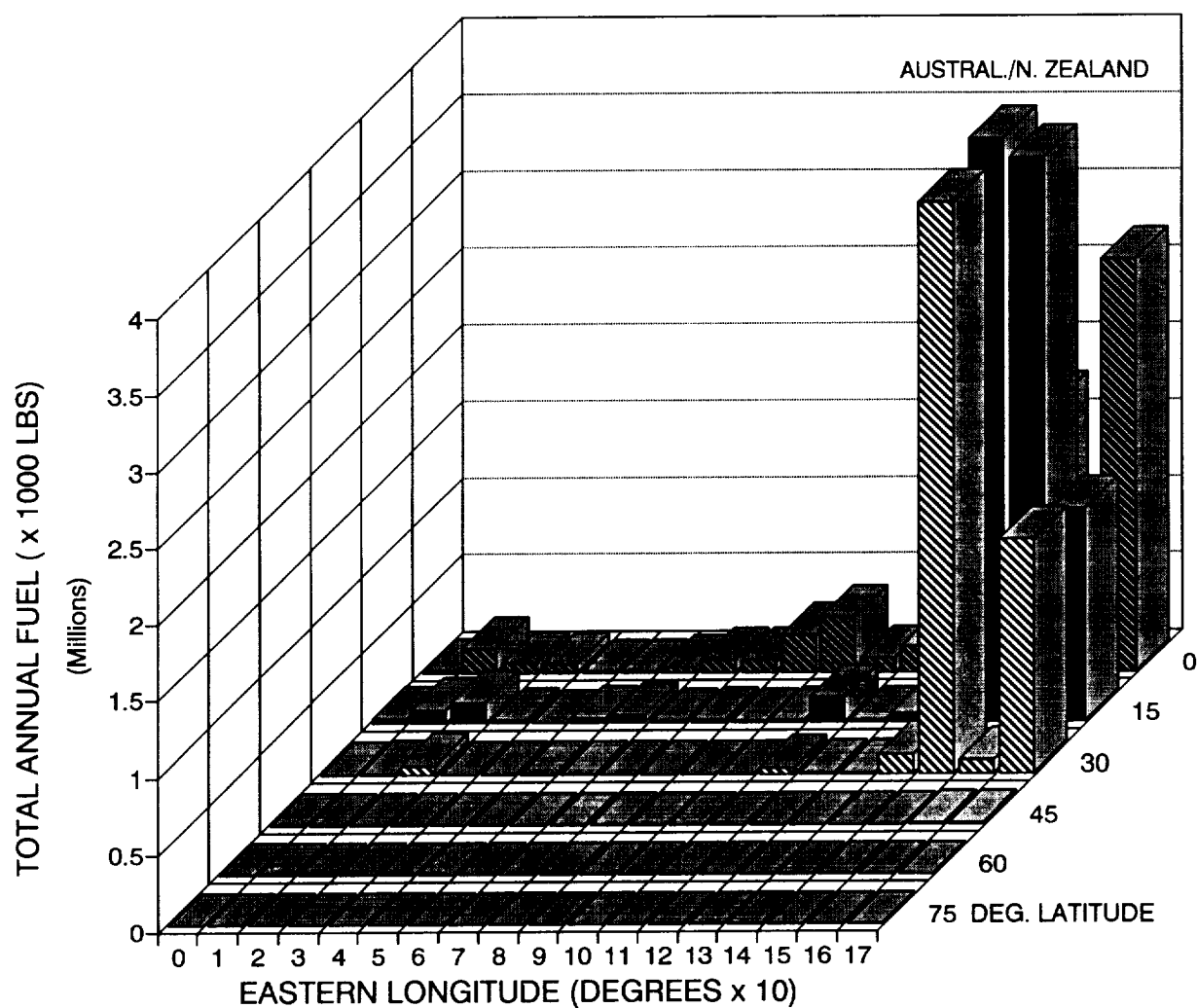
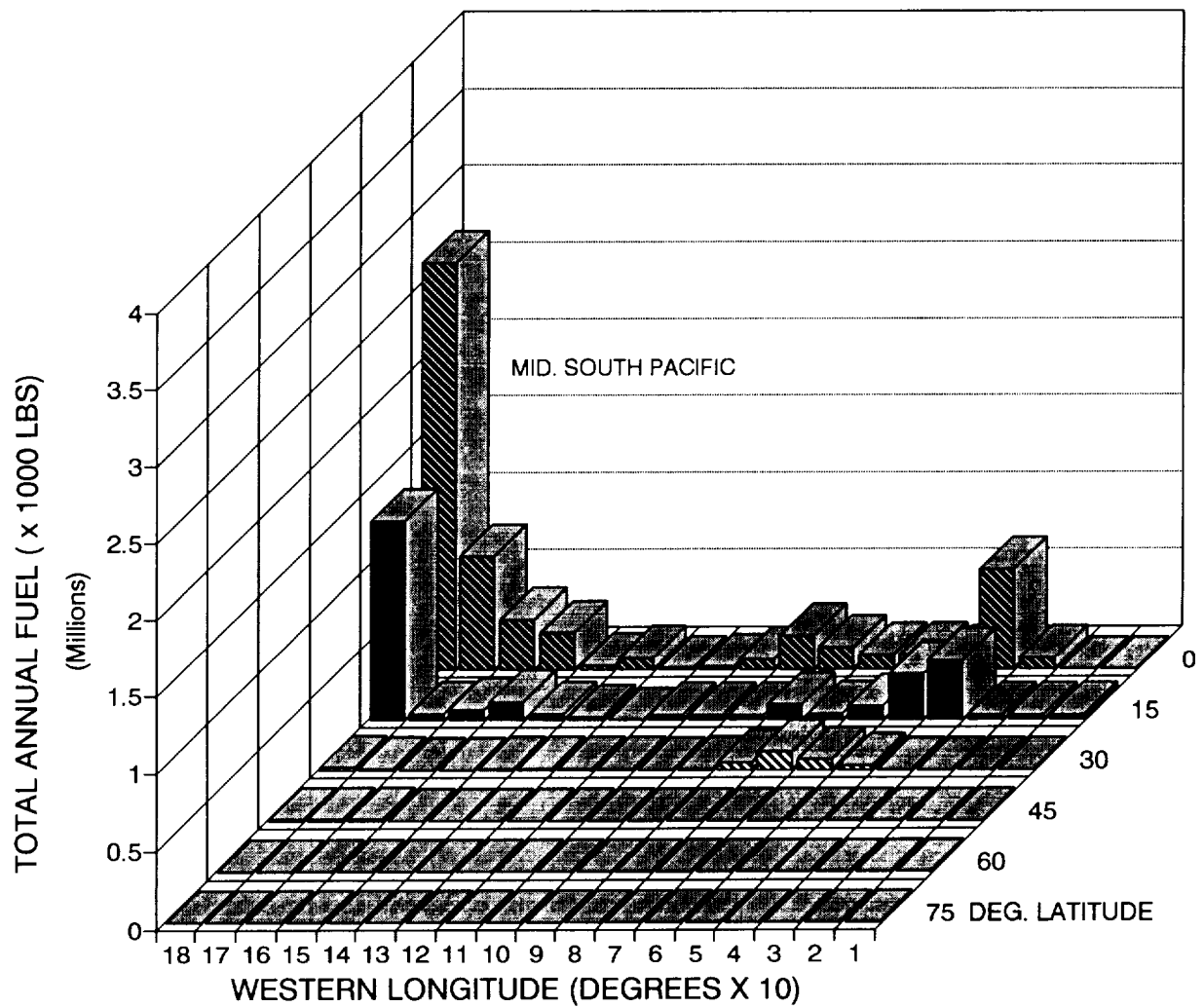


Figure 3-3.17. Total annual fuel distribution within the southern half of the eastern hemisphere in 2015 for the military/charter/Soviet/M1.6 HSCT scenario.



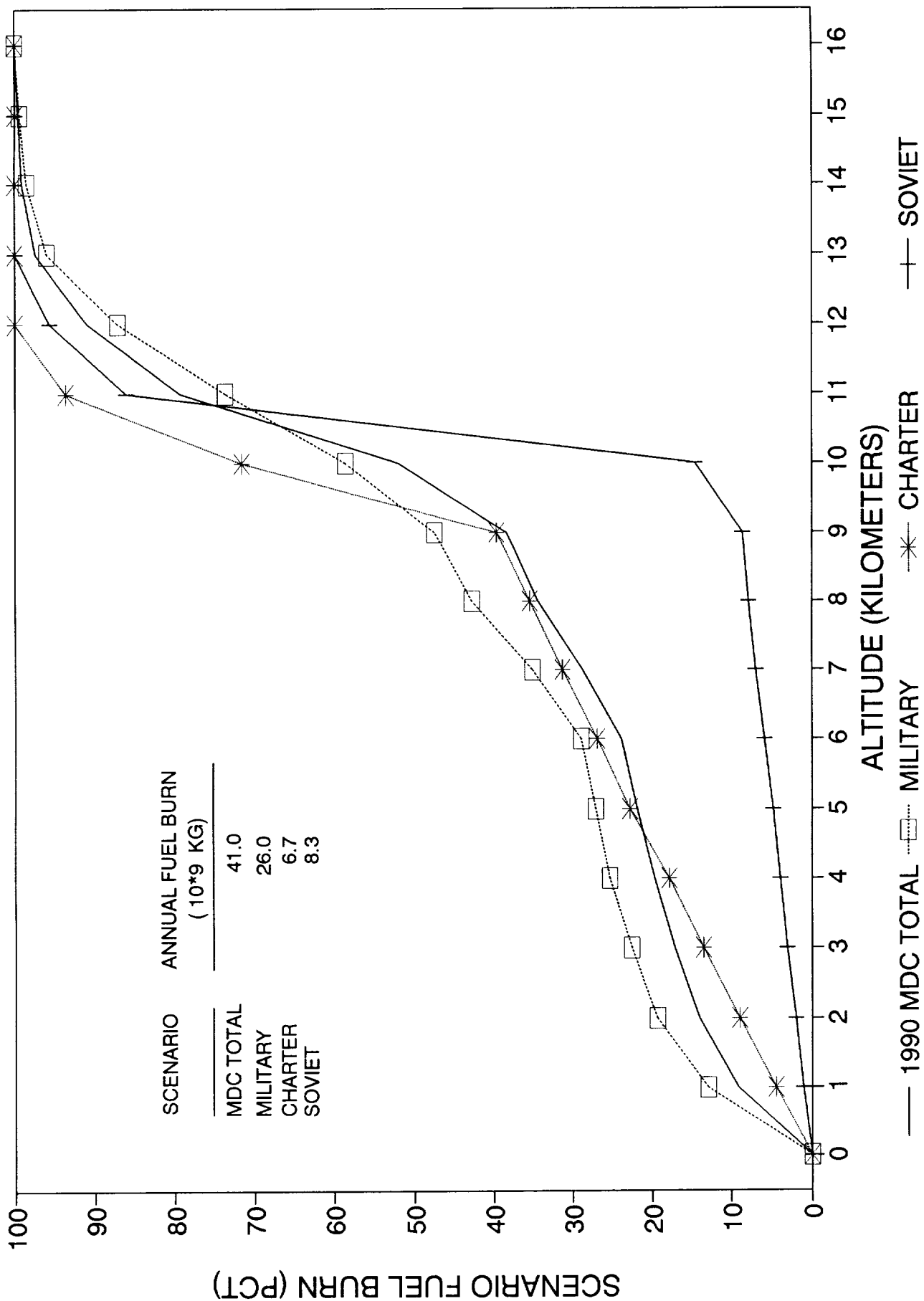


Figure 3-3.19. Cumulative fuel burn versus altitude for 1990 military, charter, and Soviet scenarios.

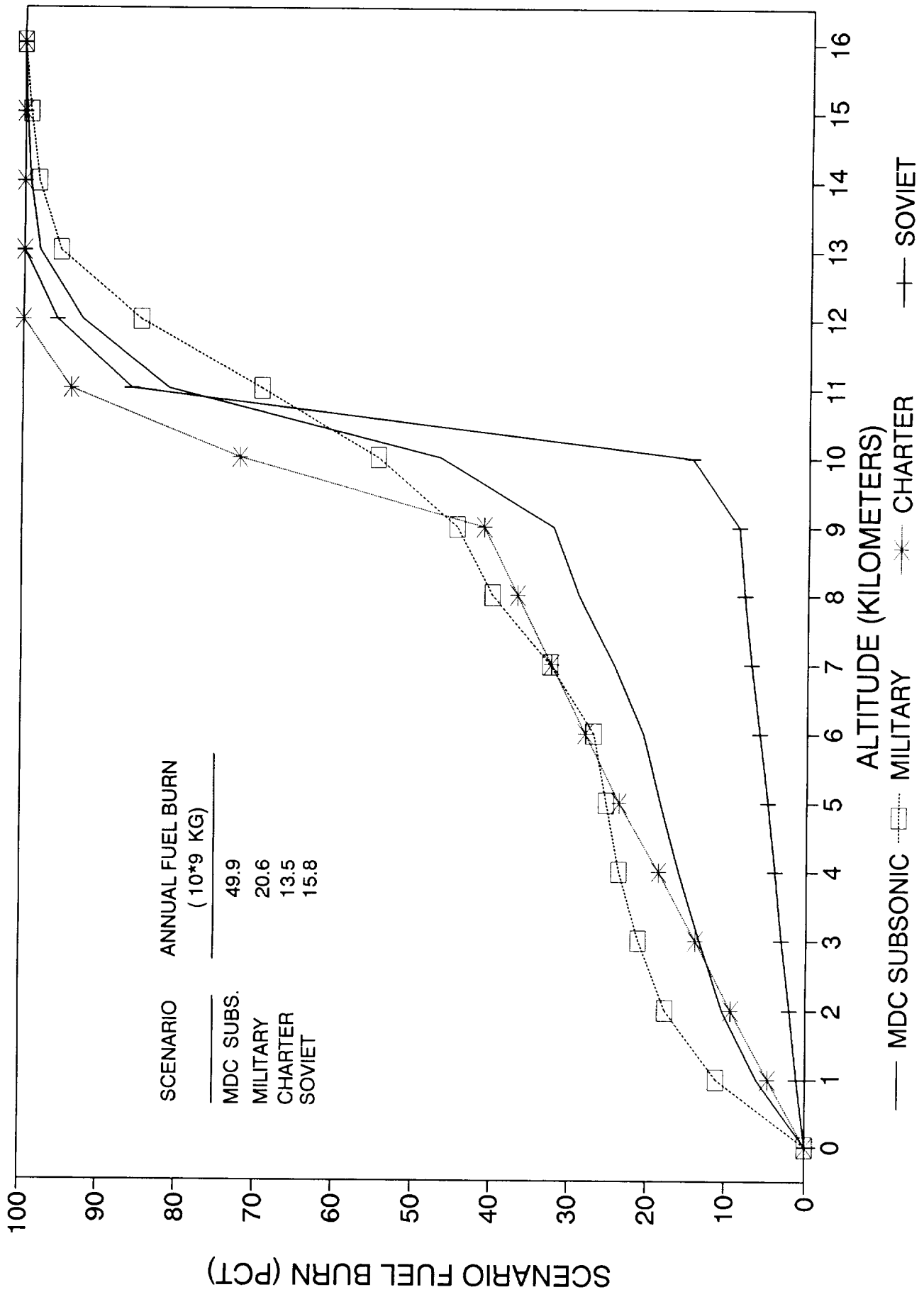


Figure 3-3.20. Cumulative fuel burn versus altitude for 2015 military, charter, and Soviet scenarios.

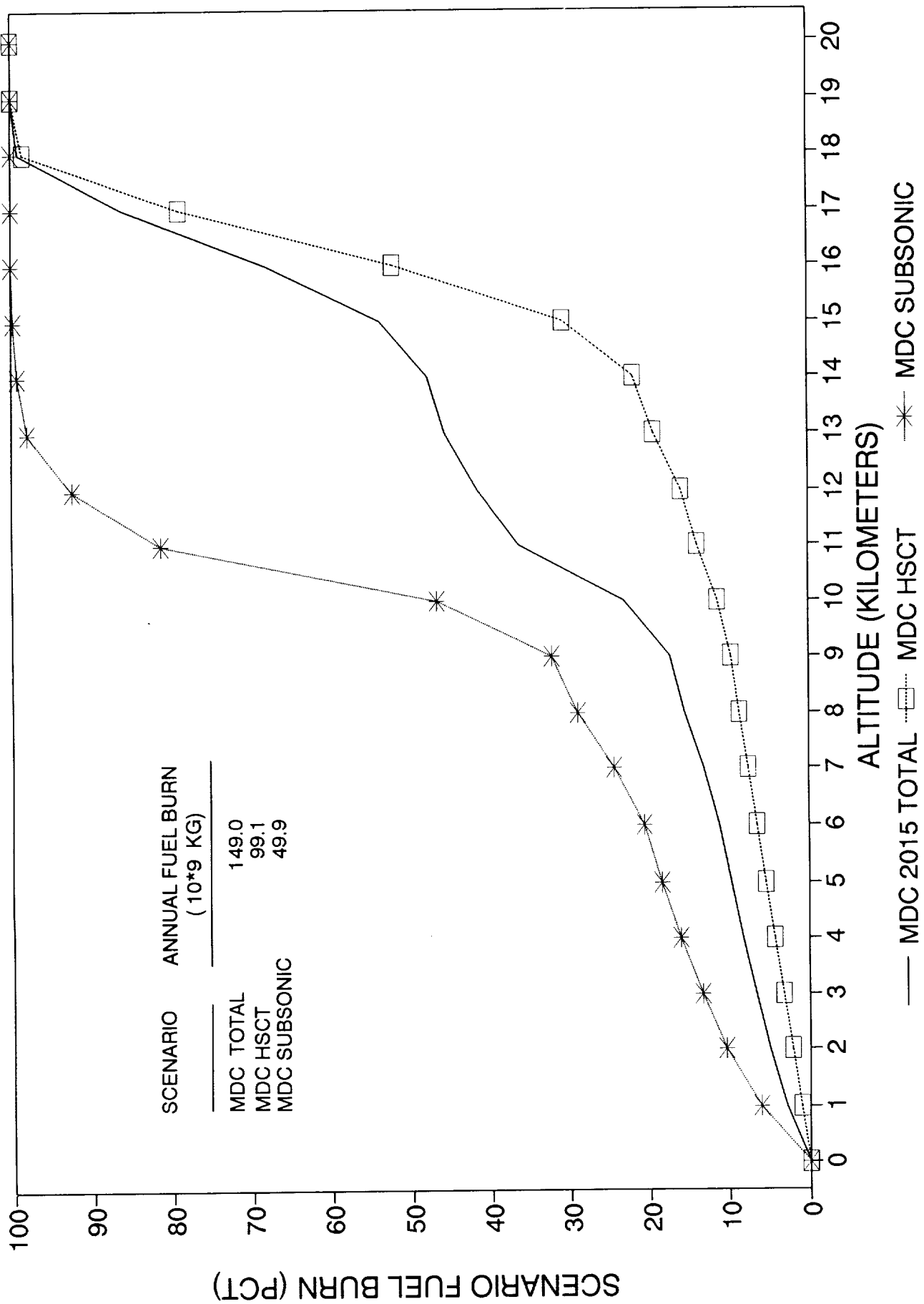


Figure 3-3.21. Cumulative fuel burn versus altitude for 2015 Mach 1.6 HSCT and subsonic scenarios.

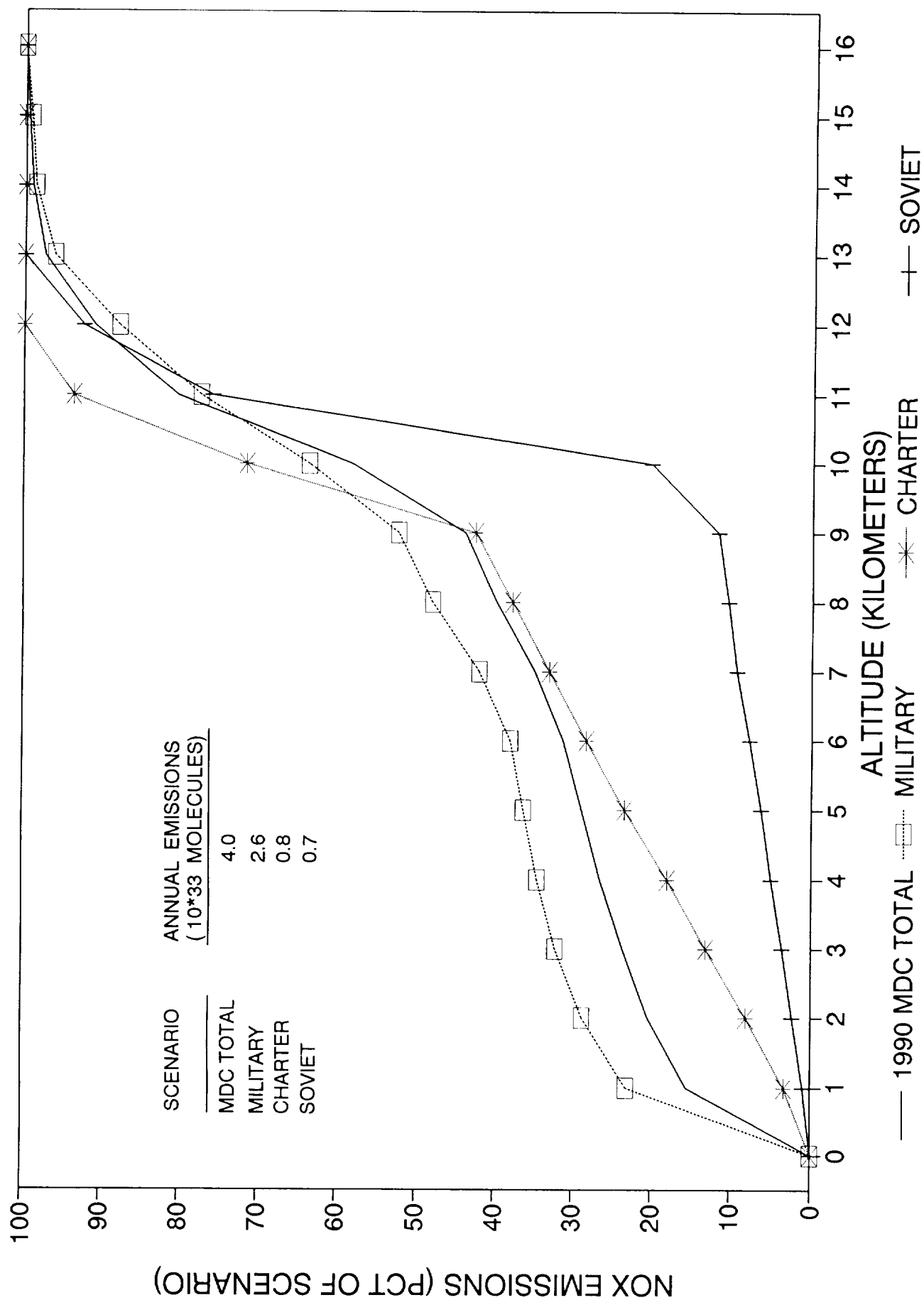


Figure 3-3.22. Cumulative NO_x emission versus altitude for 1990 military, charter, and Soviet scenarios.

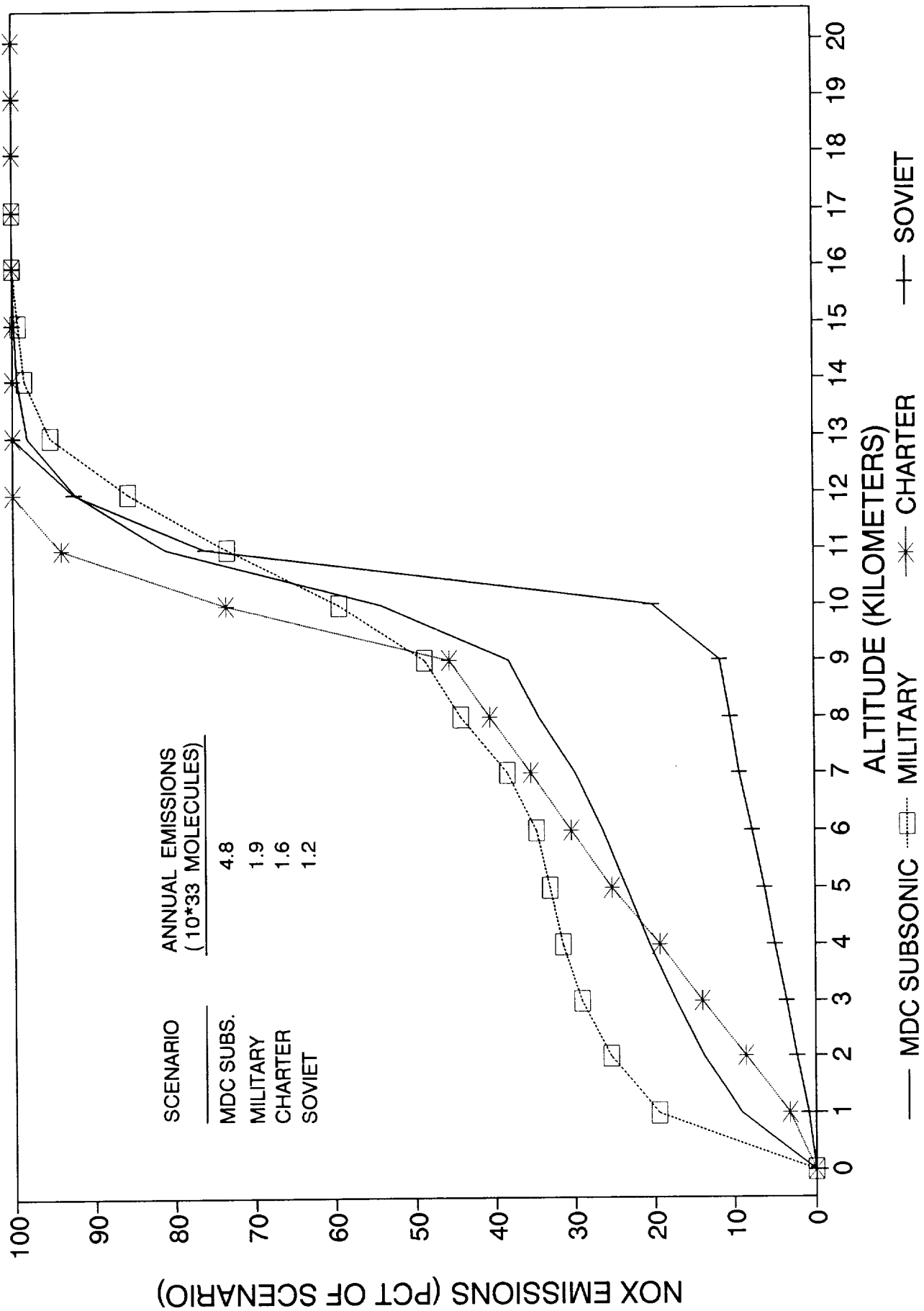


Figure 3-3.23. Cumulative NO_x emission versus altitude for 2015 military, charter, and Soviet scenarios.

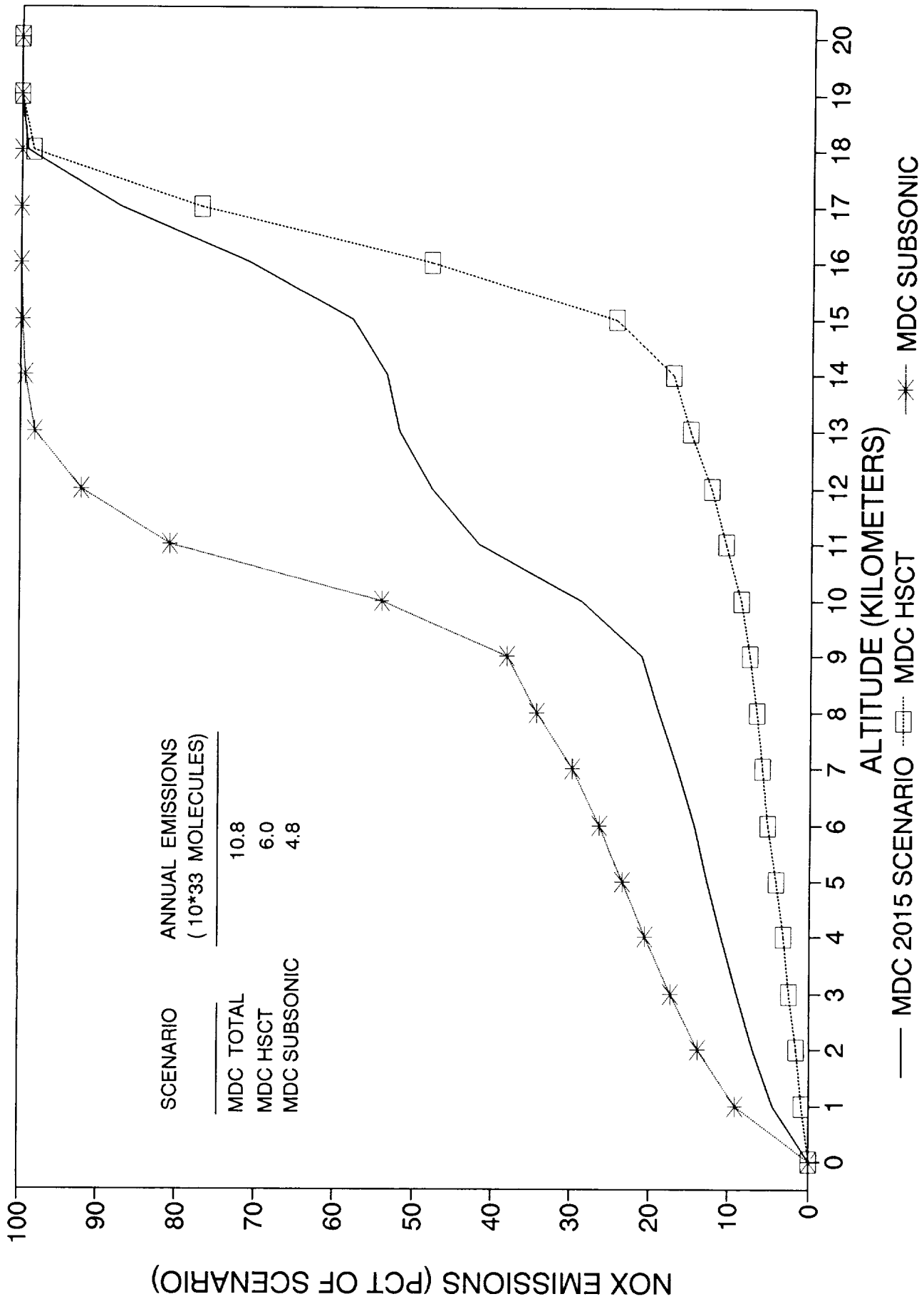


Figure 3-3.24. Cumulative NO_x emission versus altitude for 2015 Mach 1.6 HSCT and subsonic scenarios.

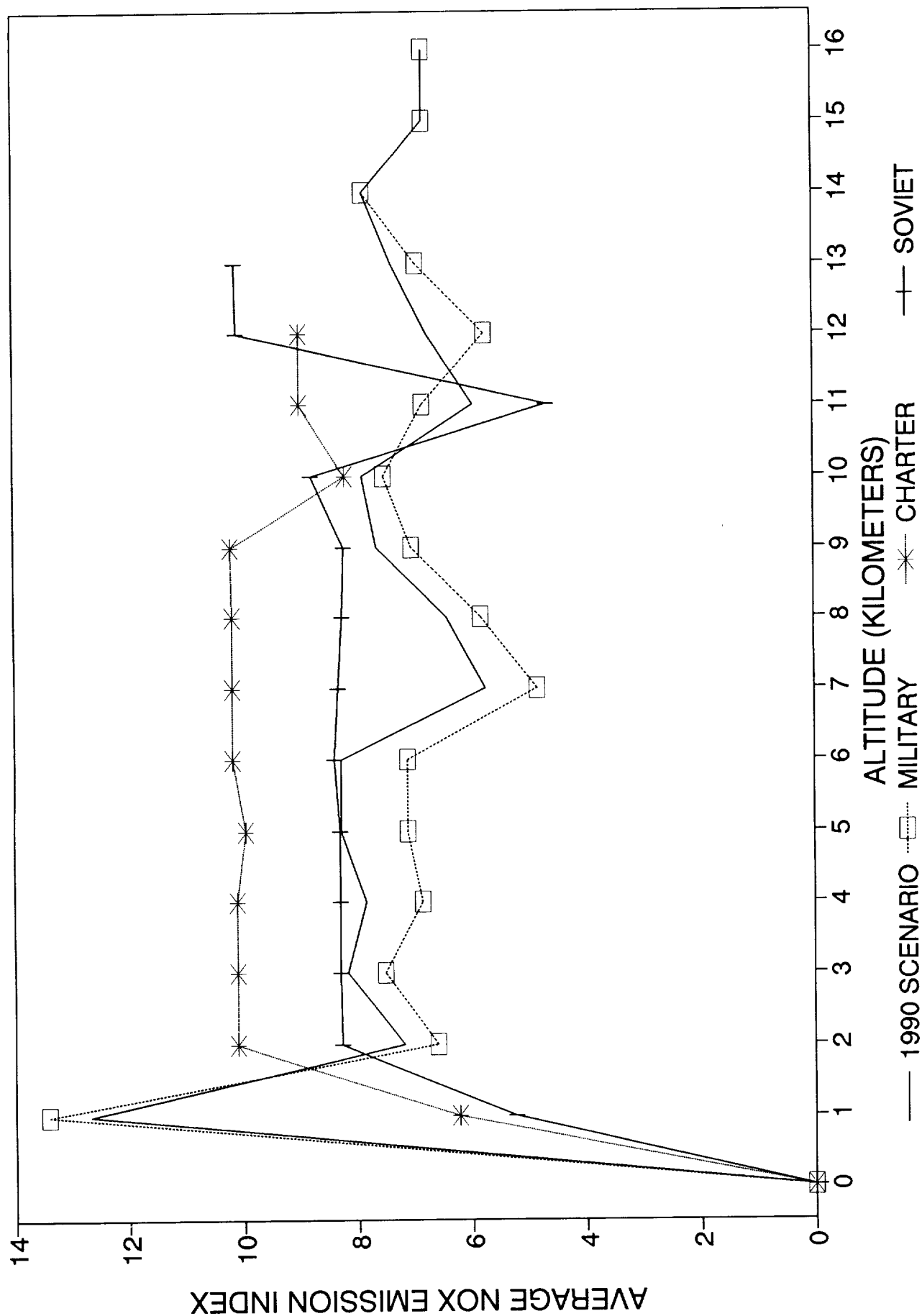


Figure 3-3.25. Emission index for NO_x versus altitude for 1990 military, charter, and Soviet scenarios.

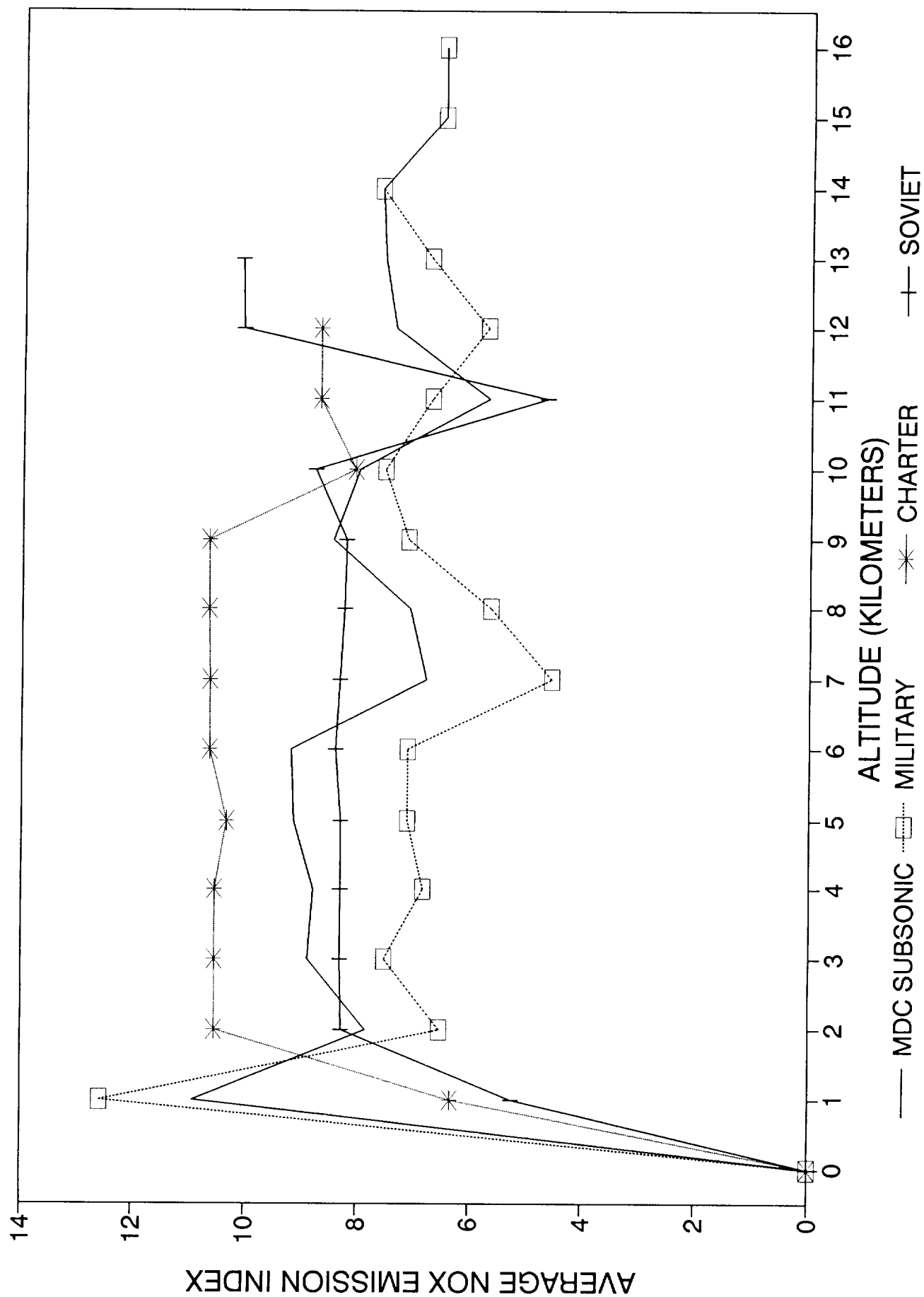


Figure 3-3.26. Emission index for NO_x versus altitude for 2015 military, charter, and Soviet scenarios.

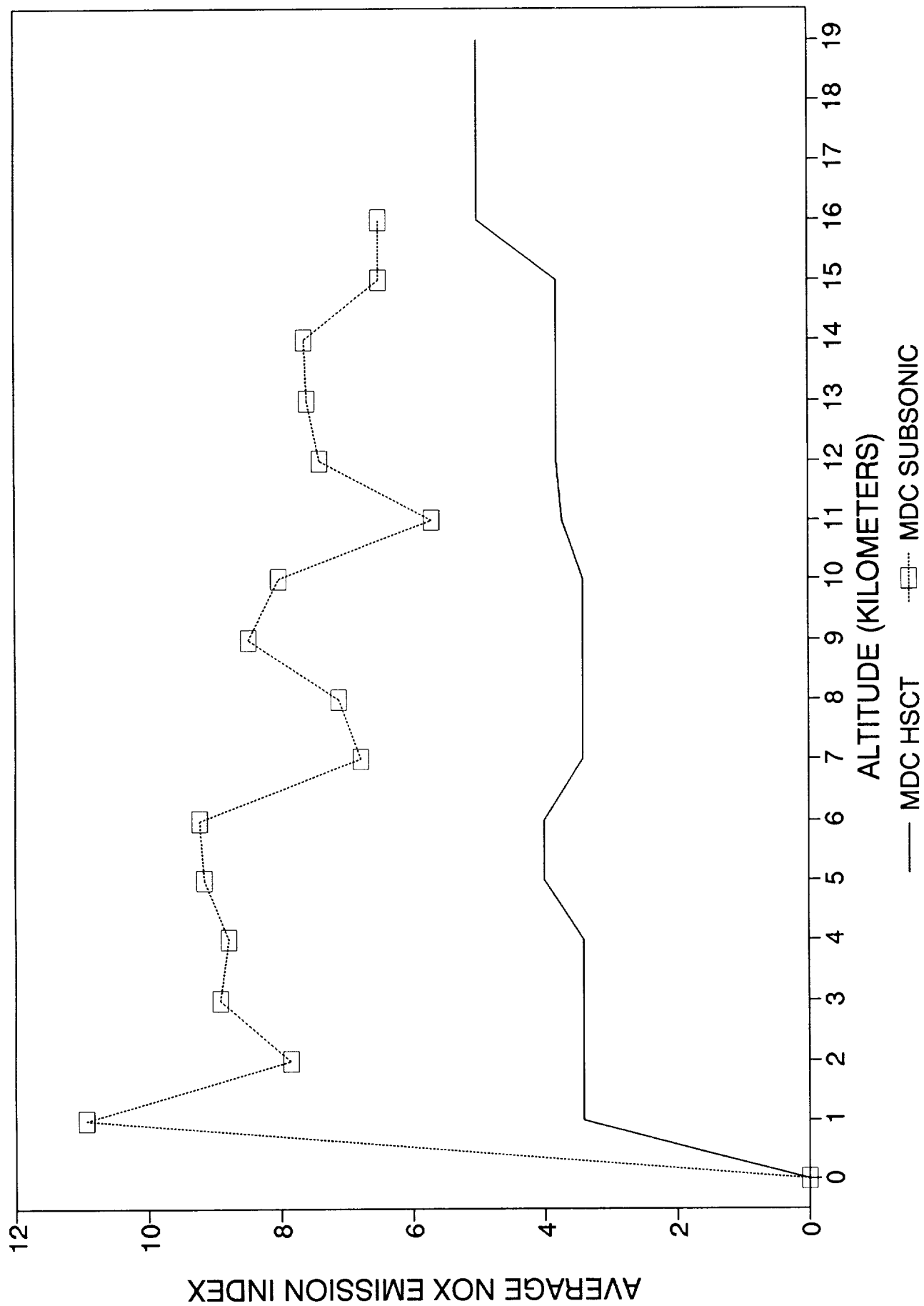


Figure 3-3.27. Emission index for NO_x versus altitude for 2015 Mach 1.6 HSCT and subsonic scenarios.

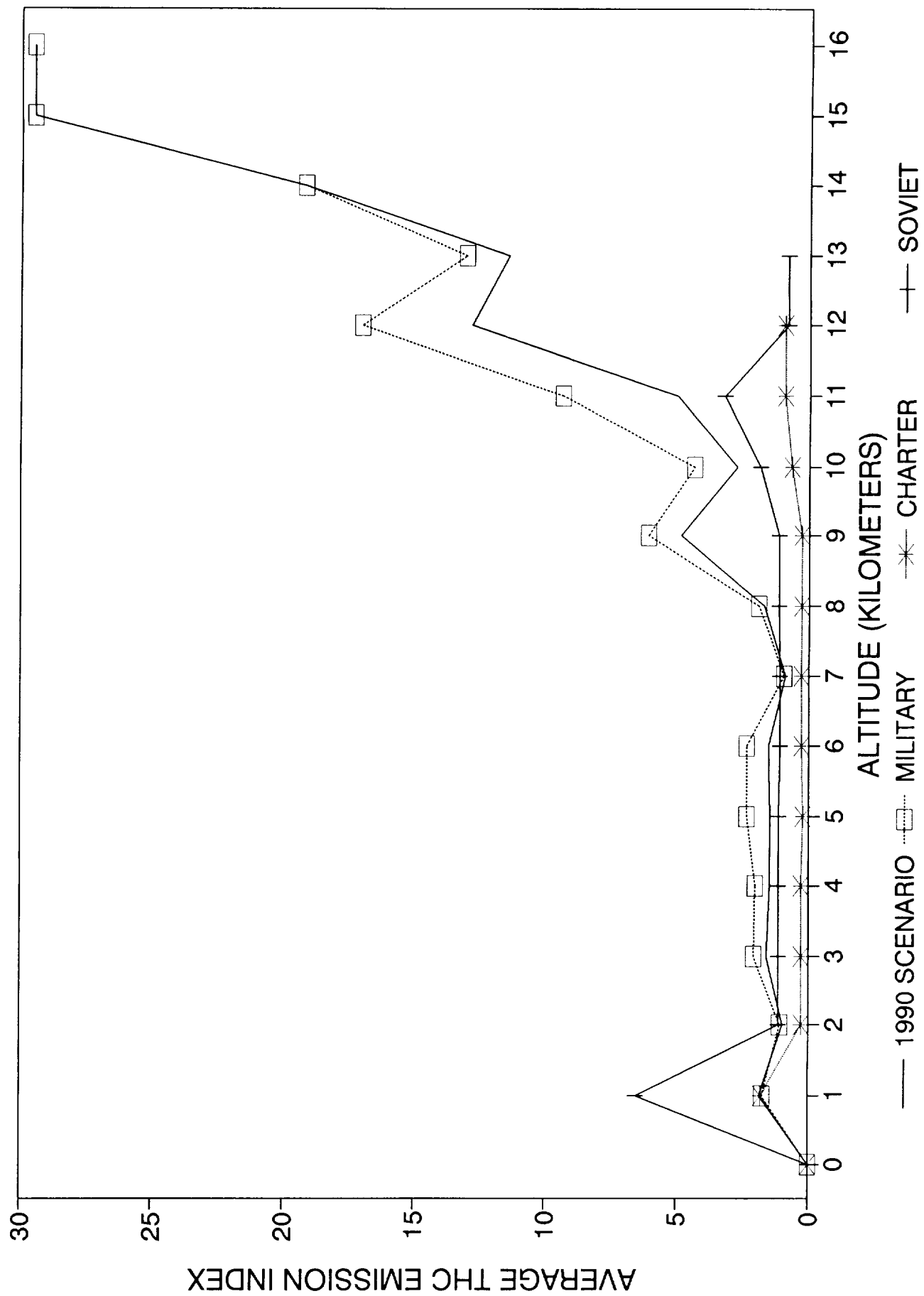


Figure 3-3.28. Emission index for total HC versus altitude for 1990 military, charter, and Soviet scenarios.

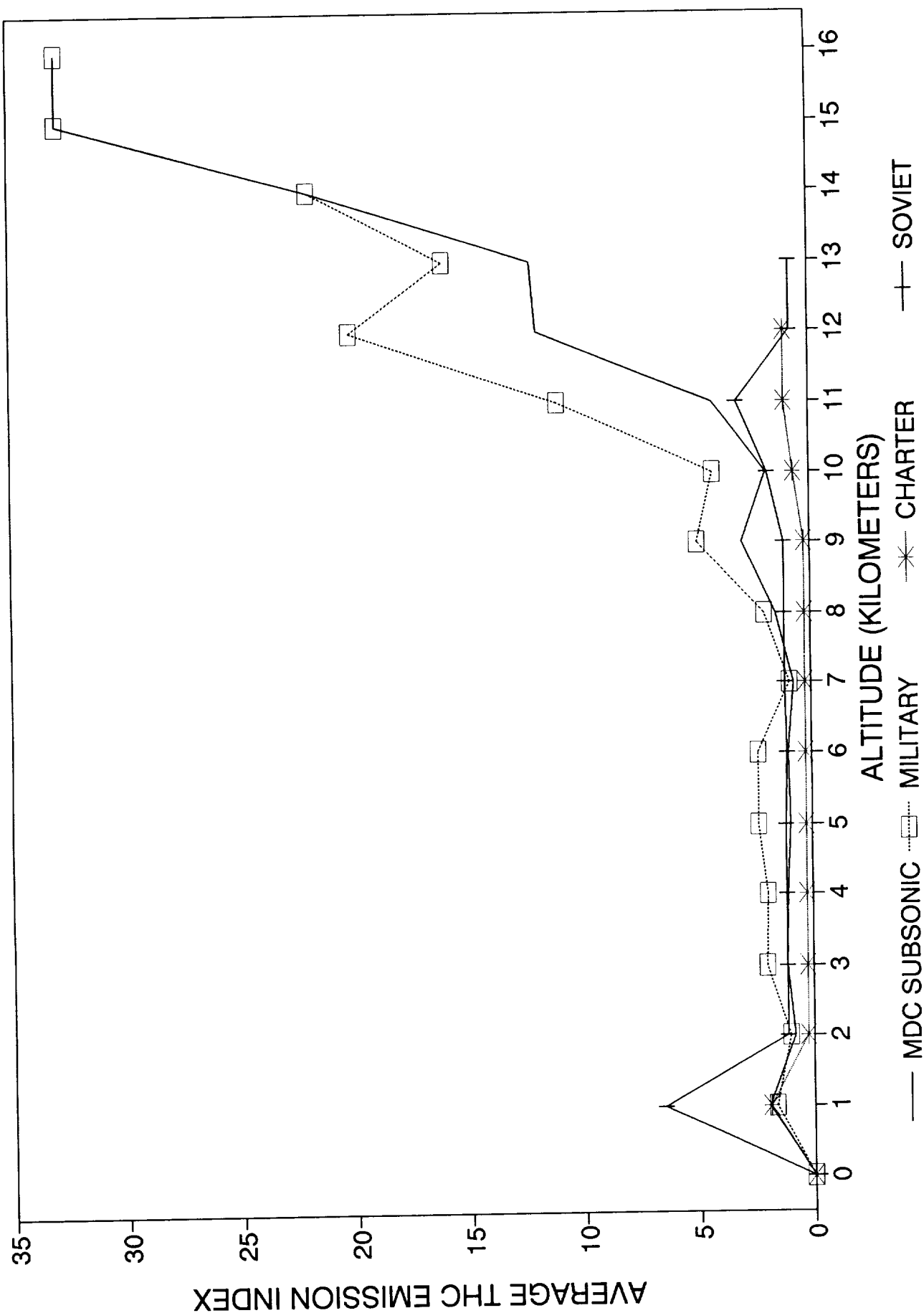


Figure 3-3.29. Emission index for total HC versus altitude for 2015 military, charter, and Soviet scenarios.

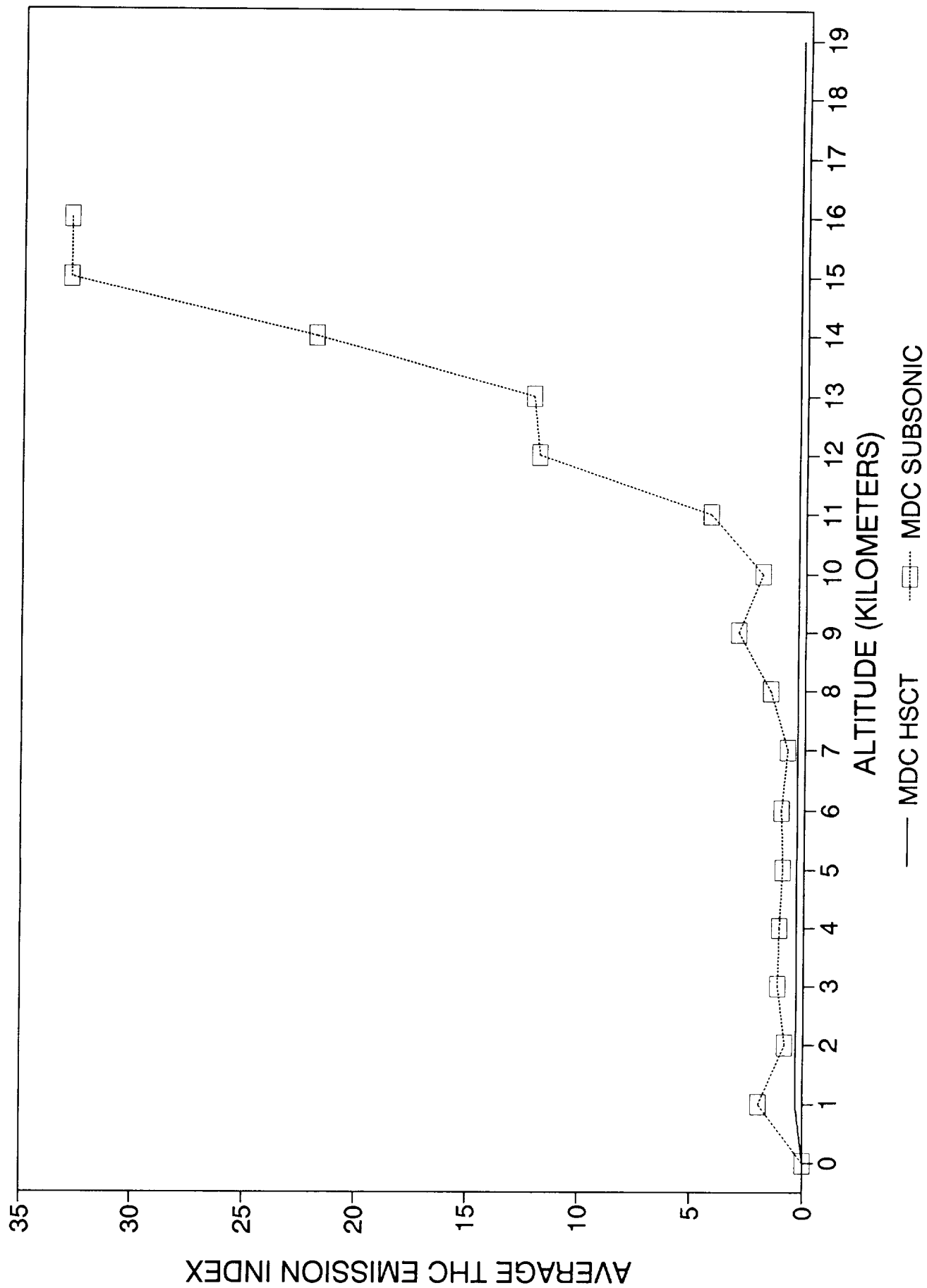


Figure 3-3.30. Emission index for total HC versus altitude for 2015 Mach 1.6 HSCT and subsonic scenarios.

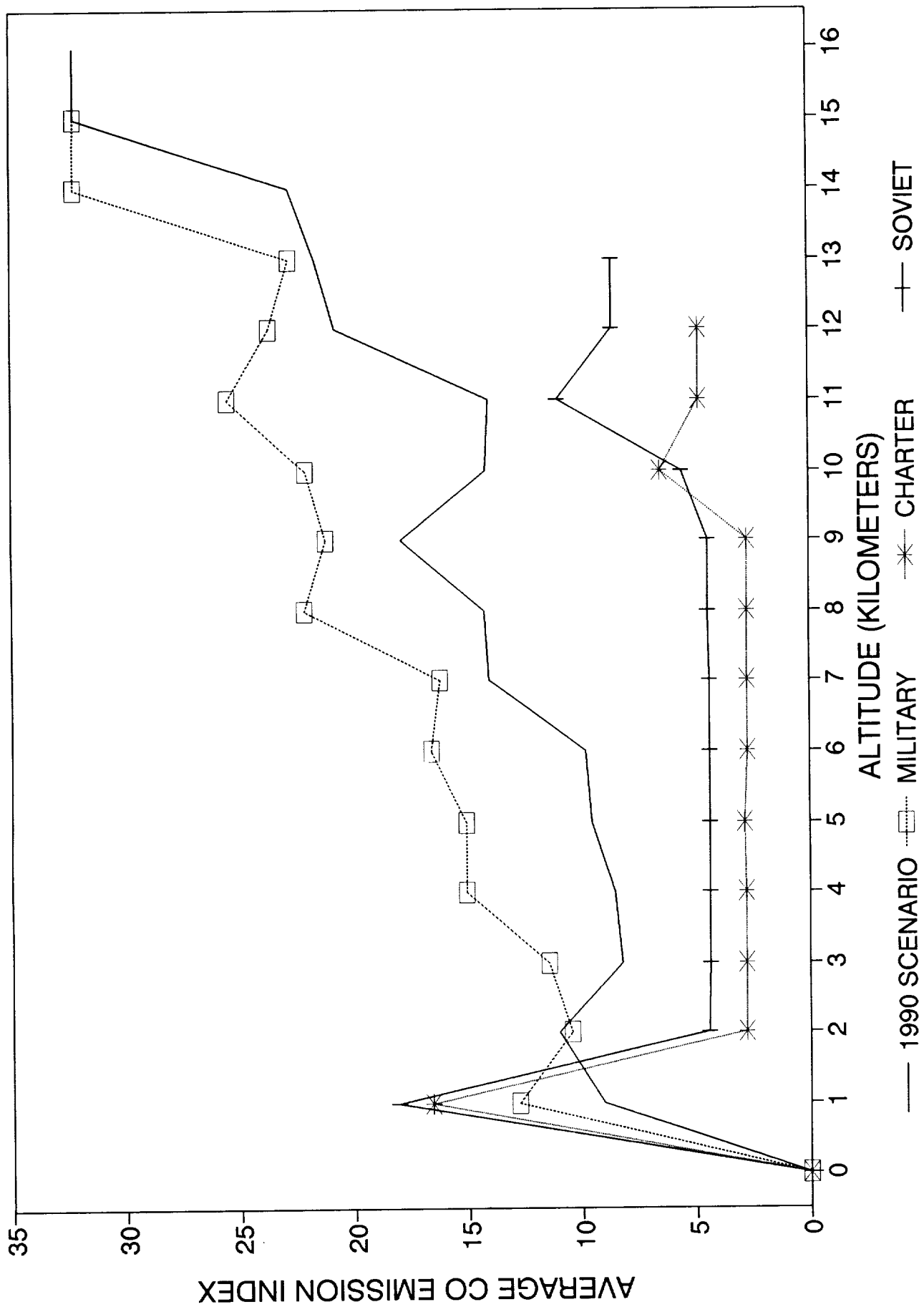


Figure 3-3.31. Emission index for CO versus altitude for 1990 military, charter, and Soviet scenarios.

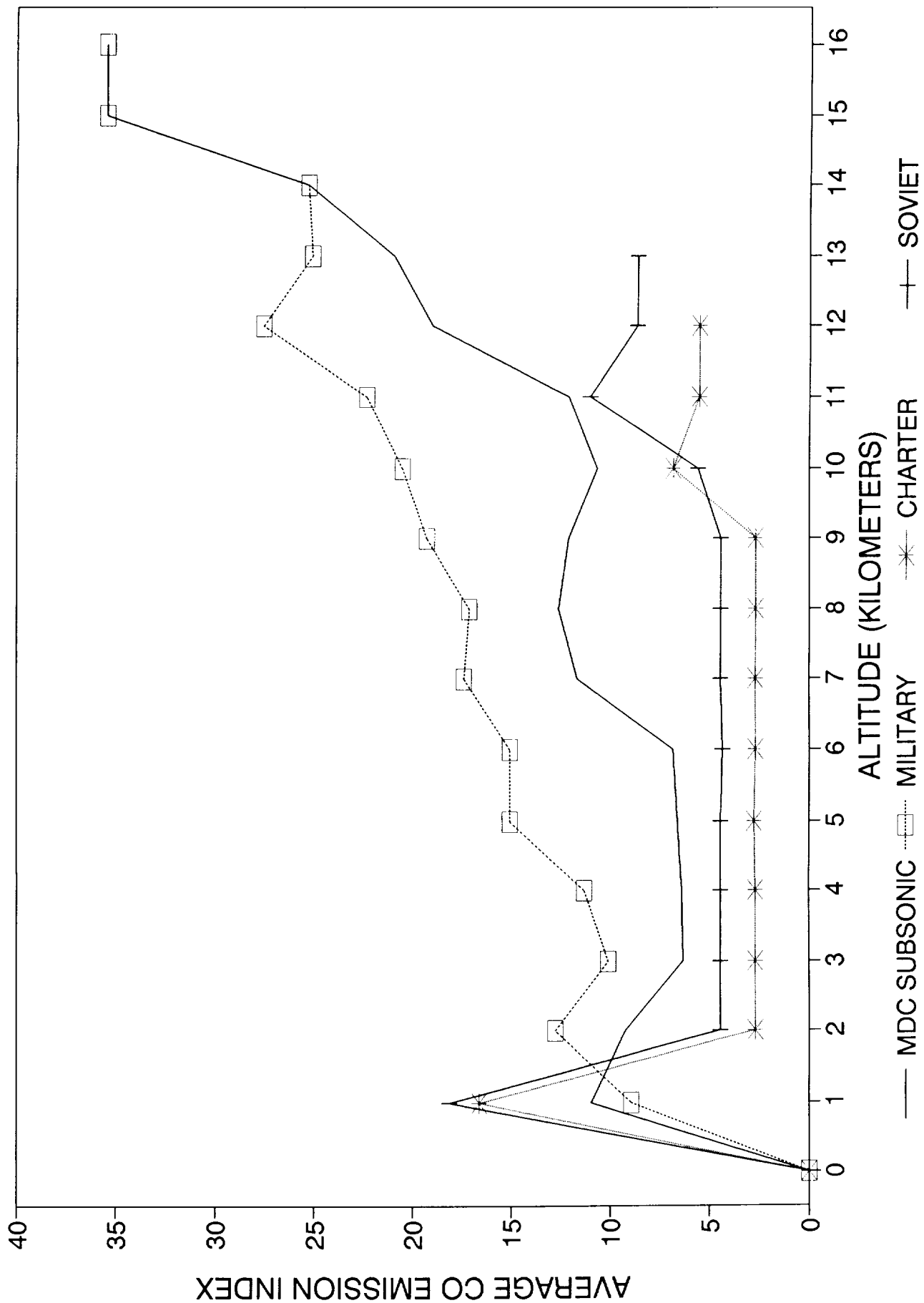


Figure 3-3.32. Emission index for CO versus altitude for 2015 military, charter, and Soviet scenarios.

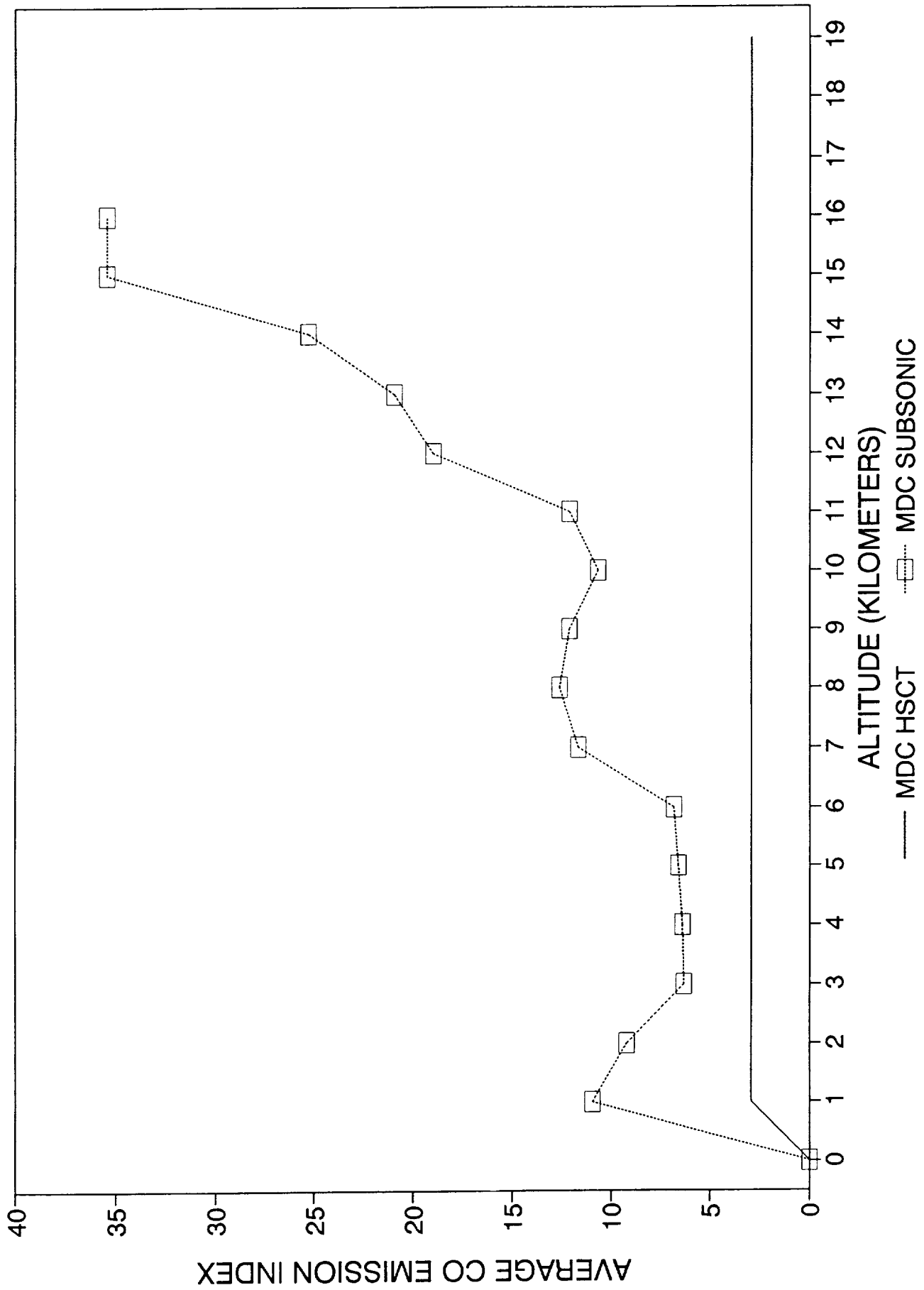


Figure 3-3.33. Emission index for CO versus altitude for 2015 Mach 1.6 HSCT and subsonic scenarios.

REFERENCES

- Air Force Association, *Air Force Magazine*, 74, Arlington, VA, May 1991.
- Aviation Advisory Services Limited, MILAV News, UK, various years.
- Belet, D., and L. C. de Daunant, *European Charter Airlines - Strategies For The 90s*, ITA Documents & Reports, Vol 22, Institute of Air Transport, 103 rue La Boetie-75008, Paris, France, 1990.
- Canadian Government Publishing Centre, Statistics Canada, *Air Charter Statistics*, Transportation Division, Aviation Statistic Center, Ottawa, Canada, 1987.
- Center For Transportation Information, *United States International Air Travel Statistics Calendar Year 1990*, (Table Id - Passenger Travel Between U.S. And Foreign Countries and Table IIId - Passenger Travel Between U.S. Ports And Foreign Countries), U.S. Department Of Transportation, Kendall Square, Cambridge, MA, 1990.
- Correll, J. T., Fifty Years of European Fighter Trends, *Air Force Magazine*, Air Force Association, Arlington, VA, Vol. 74, No. 2, February 1991.
- Forecast International/DMS Market Intelligence, *Military Aircraft Forecast*, Newton, CT, 1991-1992.
- ICAO Committee on Aviation Environmental Protection, *ICAO Engine Exhaust Emissions Databank*, presented by the Chairman, Technical Issues Sub Group, Montreal, Quebec, Canada, 1989b.
- ICAO, ICAO Digest Of Statistics, *Traffic - Commercial Air Carriers 1986-1990*, No. 379 Series T-No. 50, Montreal, Quebec, Canada H3A 2R2, 1990.
- International Media Corporation, *Defense and Foreign Affairs Handbook*, Alexandria, VA, 1990-1991.
- Jane's Information Group Limited, *Jane's All the World's Aircraft*, Surrey, UK, 1990.
- Lorell, M. A., The Future of Allied Tactical Fighter Forces in NATO's Central Region, RAND, R-4144-AF, 1992.
- McGraw-Hill Inc., Specifications, *Aviation Week and Space Technology*, New York, March 18, 1991.
- McDonnell Douglas Corporation, Military System Analysis Airfield Report, Long Beach, CA, July 1991.
- Nation, J. E., *British Military Requirements, Resources, and Conventional Arms Control*, RAND, R-3734-A/AF, January 1990.
- Nation, J. E., *West German Military Modernization Goals, Resources, and Conventional Arms Control*, RAND, R-3841-A/AF, 1991.
- Nation, J. E., *German, British, and French Military Resources/Requirements to 2015*, RAND, N2982-RGSD, May 1992.

National Geographic Society, *National Geographic Atlas of the World 5th Edition*, Washington DC. 1981.

Navy League of the U.S., *Sea Power*, 31, Arlington, VA, January 1988.

Pace, R. G., *Aircraft Emission Factors*, Office of Air and Waste Management, U.S. Environmental Protection Agency, Ann Arbor, MI, PB-275 067, March 1977.

Sears, D. R., *Air Pollutant Emission Factors for Military and Civil Aircraft*, Lockheed Missiles and Space Co., Contract No. 68-02-2614 for Office of Air Quality Planning and Standards, U.S. Environmental Protection Agency, Research Triangle Park, NC, 1978.

The International Institute for Strategic Studies, *The Military Balance 1989-1990*, Brassey's, London, 1989.

U.S. Air Force, "Standard Aircraft Characteristics and Performance, Piloted Aircraft (Fixed Wing)," MIL-C-005011B, Washington, DC, 1977.

U.S. Air Force, "U.S. Air Force Cost and Planning Factors," AFR-173-13, Washington, DC, 1989.

U.S. Air Force, USAF Standard Aircraft/Missile Characteristics, *U.S. Air Force Guide 2, 2*, Washington, DC, June 1989.

Subchapter 3-4

Emissions Scenarios Development: Completed Scenarios Database

Steven L. Baughcum
Boeing Commercial Airplane Group
Seattle, WA

Munir Metwally
McDonnell Douglas Corporation
Long Beach, CA

Robert K. Seals
Langley Research Center
National Aeronautics and Space Administration
Hampton, VA

Donald J. Wuebbles
Lawrence Livermore National Laboratory
Livermore, CA

INTRODUCTION

This subchapter describes the completed database for the 1993 HSRP/AESA Interim Assessment scenarios. The consistency checks and validation studies done on the completed database are also described, along with an evaluation of the strengths and weaknesses in the database. Finally, there is a description of future needs for improvements and further studies with the scenarios' development capabilities that have been developed.

COMPLETED EMISSIONS DATABASE

Individual components of the HSRP aircraft emissions database developed by Boeing and McDonnell Douglas Corp.(MDC) were delivered electronically to the Upper Atmosphere Data Program (UADP) system at the NASA Langley Research Center (LaRC). UADP personnel assembled the components into scenario data sets for use in the assessment modeling activities. The component data sets were on a standard 1 degree longitude \times 1 degree latitude \times 1 km geopotential altitude grid, and each data set included four basic parameters: fuel burn, NO_x emissions, HC emissions, and CO emissions. The processing steps involved in developing final scenario data sets are outlined below.

The component data sets were put into common units and file formats and then were used to develop standard two-dimensional scenario data sets comparable to the two-dimensional models being used in the HSRP interim assessment. An aggregation over longitude was done for each of the data components to transform them into 1 degree latitude \times 1 km altitude zonal files. At this point, the appropriate components were combined to provide seven basic scenario data sets (Scenarios A through G) as summarized in Table 3-1.1. These scenarios cover the range from a reference 1990 case composed of a subsonic fleet (Scenario A) to the 2015 case combining a subsonic fleet with a very high NO_x HSCT case (Scenario G). It should be noted that Scenario G is not produced from an engineering analysis of a high NO_x combustor, but is a scenario constructed for parametric studies by scaling NO_x emissions for the HSCT Mach 2.4, EI=15, case up by a factor of three.

Preparation of specific scenario data sets for input to the assessment models required transforming the standard two-dimensional scenario data onto the grid used by each particular model. To ensure uniformity, UADP personnel performed this transformation for each model. Transformations of the data were done first in the latitudinal direction and then in the vertical. In all cases, the model grid sizes were as large as or larger than the standard grid, and the transformation process was primarily one of summing. For example, latitude bin sizes for the six participating models were between 5 and 10 degrees as compared with the standard 1-degree grid. In cases where the standard grid did not line up with the boundaries of a model grid, linear interpolation was used to apportion emissions into the appropriate cells. The vertical dimension for the emission grid was geopotential altitude, based on the 1976 United States Standard Atmosphere, and most of the models use pressure for the vertical dimension. The 1976 Standard Atmosphere was used to relate the pressure levels of each model to the altitude grid of the emissions data.

SUMMARY OF COMPLETED DATABASE

A series of quality checks and validations were performed in developing the scenario data sets. Global sum values for each parameter and each component or scenario were checked at every processing step to ensure conservation of emissions. Maximum values of fuel burn and NO_x emissions for each scenario were examined for consistency. Table 3-4.1 shows the global sum values for each component and for the combined scenarios. For total emissions, the subsonic fleet is the largest contributor in 2015, except for the Mach 2.4, EI=45 case where HSCT emissions are larger than the subsonic component. The subsonic fleet is dominated in both 1990 and 2015 by the scheduled airline component. For the 2015 cases, the two largest emission contributors are the

196 187

PRECEDING PAGE BLANK NOT FILMED

scheduled airline and HSCT components, with HSCT emissions accounting for about 17% (EI=5), 37% (EI=15), or 64% (EI=45) of the total NO_x emissions for these scenarios. Scenario A, representing the 1990 subsonic fleet, and Scenario B, representing a 2015 subsonic fleet in the absence of HSCTs, have NO_x emissions of 1.46×10^9 kg/yr and 2.70×10^9 kg/yr, respectively. In comparison, Scenarios C and E include HSCT fleets achieving the nominal EI=5 NO_x emission goal and have NO_x emissions of about 2.8×10^9 kg/yr. Table 3-4.1 also illustrates the two different scheduled airline data sets used in developing 2015 scenarios. The first set, which assumed no HSCT fleet, was used for Scenario B and has a fuel burn of 245×10^9 kg/yr and NO_x emissions of 2.24×10^9 kg/yr. The second set, used in the 2015 HSCT cases (Scenarios C through G), accounts for a reduced subsonic fleet in the presence of an HSCT fleet and has a fuel burn of 210×10^9 kg/yr and NO_x emissions of 1.85×10^9 kg/yr. Thus, in the absence of an HSCT fleet, subsonic fleet NO_x emissions are projected to rise by about 85% over those in 1990. If an HSCT fleet is present, subsonic fleet NO_x emissions are still projected to rise by about 60% over 1990 levels.

Two kinds of graphical checks were made on the overall scenario datasets. Latitude-longitude cross section plots of fuel burn and of NO_x emissions, summed over altitude, were examined to ensure that route structures and global distributions were represented properly. Similarly, latitude-altitude cross sections, corresponding to the data sets used in the model assessment calculations, of fuel burn and NO_x were examined to ensure that vertical distributions looked reasonable.

Figures 3-4.1 and 3-4.2 illustrate the latitude-longitude distributions of NO_x emissions for three representative scenarios. In Figure 3-4.1, the top panel shows NO_x emission distributions, summed over altitude, for the 1990 fleet (Scenario A). The bottom panel shows NO_x emission distributions, summed over altitudes up to 13 km for Scenario F and can be viewed as representative of a 2015 subsonic fleet in the presence of an HSCT fleet. Comparison of the two panels shows qualitatively the projected increase in lower altitude emissions in 2015 relative to those in 1990. Figure 3-4.2 shows NO_x emissions summed above 13 km altitude for Scenarios D (upper panel) and F (lower panel) and illustrates the route structure assumed for an HSCT fleet. The distributions for the Mach 1.6 HSCT (Scenario D) and the Mach 2.4 (Scenario F) are essentially the same since they were assumed to be flying the same route structure and have, as seen from Table 3-4.1, similar total NO_x emissions. The HSCT network was developed with a ground rule that there be no supersonic flight over land, and Figure 3-4.2 illustrates this. In all cases, northern hemisphere routes dominate the network.

Figures 3-4.3 and 3-4.4 illustrate the two-dimensional (latitude and altitude) distributions of NO_x emissions for four scenarios. Figure 3-4.3 contrasts the 1990 subsonic fleet (upper panel) with the 2015 subsonic fleet assuming no HSCT fleet (lower panel). Figure 3-4.4 contrasts the 2015 scenario including a Mach 1.6, EI=15, HSCT (upper panel) to the similar Mach 2.4 HSCT scenario. In all cases, the largest amount of emissions are seen in the 30°N to 60°N latitude region. NO_x emissions peak in the 10 to 12 km altitude region, and Figure 3-4.3 clearly shows the projected increase in NO_x emissions in this altitude region by 2015. Figure 3-4.4 illustrates the secondary peak in emissions related to HSCT operations which occurs in the 15 to 17 km region for a Mach 1.6 HSCT (upper panel) and around 19 to 21 km for a Mach 2.4 HSCT. Figure 3-4.4 also illustrates that the HSCT peak emissions tend to be centered around 50°N while the subsonic peak emissions are centered more around 35°N to 40°N.

Figures 3-4.5, 3-4.6, and 3-4.7 focus specifically on the latitudinal distribution of NO_x emissions. Figure 3-4.5 shows the data of Figure 3-4.3 summed over all altitudes and illustrates the similar latitude distribution of emissions from the 1990 subsonic fleet (solid lines) and the 2015 subsonic fleet in the absence of an HSCT (dashed lines). The lower panel shows cumulative fraction of NO_x emissions going from southern to northern latitudes and indicates that the increased 2015 subsonic fleet does tend to push the distribution of emissions somewhat towards more southern latitudes. Figure 3-4.6 provides the latitude distribution of projected 2015

emissions for the Mach 1.6 scenarios for altitudes below 13 km (solid lines) and above 13 km (dashed lines). Figure 3-4.7 shows projected 2015 emissions for the Mach 2.4 scenarios in the same fashion. The tendency for HSCT peak emissions to occur at more northern latitudes than the peak subsonic emissions is shown in both figures. Contrasting the upper left and lower left panels in each figure illustrates the increase of NO_x emissions with increasing EI. The right panels in both figures show cumulative fraction of NO_x emissions. The latitudinal spread of HSCT emissions can be seen to be both toward 50°N to 60°N and toward the region between about 5°N and 30°N with a smaller fraction of the NO_x emissions occurring between 30°N to 45°N than is the case for the lower altitude subsonic emissions. In all cases, most of the emissions occur in northern midlatitudes.

Tables 3-4.2 through 3-4.7 and Figure 3-4.8 focus specifically on the altitude distribution of NO_x emissions which for ozone effects is the more critical aspect. Each of the tables shows detail for fuel burn as well as NO_x , hydrocarbon (HC), and carbon monoxide (CO) emissions as a function of altitude at the 1 km resolution of the standard scenario data sets. Tables 3-4.2 and 3-4.3 show the subsonic scenarios A and B. As illustrated in Figure 3-4.3, the subsonic emissions peak between 10 and 12 km with more than 99% of the emissions occurring below 13 km. Details are provided for the Mach 1.6 HSCT scenarios C and D in Tables 3-4.4 and 3-4.5 and for the Mach 2.4 HSCT scenarios E and F in Tables 3-4.6 and 3-4.7. For the Mach 1.6 cases, emissions above 13 km account for about 14% (EI=5) and 32% (EI=15) of total NO_x emissions. As illustrated earlier, the Mach 1.6 emissions are strongly peaked between 15 and 17 km with about 60% of the NO_x emissions above 13 km occurring in this 2-km region. For the Mach 2.4 HSCT scenarios, emissions above 13 km account for about 12% (EI=5) and 27% (EI=15) of total NO_x emissions. These emissions are strongly peaked in the 19 to 21 km altitude band with about 65% of the emissions above 13 km being found in this 2-km region.

Figure 3-4.8 provides a graphical illustration of the tabular data on altitude distribution of NO_x emissions for the subsonic fleets (panel c), the Mach 1.6 HSCT cases (panel a), and the Mach 2.4 HSCT cases (panel b). Panel c illustrates the growing amount of emissions projected from the 1990 fleet (solid line) to the 2015 fleet without an HSCT (dashed line) and then the reduced amount of emissions for a 2015 subsonic fleet (dotted line) in the presence of an HSCT fleet. In all three cases, the altitude distribution is very similar. In panels a and b, the projected NO_x emissions from the 2015 subsonic fleet with no HSCT fleet are contrasted with emissions from the 2015 HSCT cases for a nominal EI of 5 (dashed lines) and a nominal EI of 15 (dotted lines). The double emission peaks in 2015 resulting from subsonic and HSCT fleets are clearly seen as is the higher cruise altitude for a Mach 2.4 HSCT as compared to a Mach 1.6 HSCT.

Comparison of Calculated and Reported Jet Fuel Consumption

Total worldwide jet fuel consumption has been reported by the U.S. Department of Energy (DOE, 1991), as well as jet fuel consumption by civil aviation for 1990 (Balashov and Smith, 1992). The difference between the total reported jet fuel consumption and the total jet fuel use by civil aviation provides some estimate of the military fuel use. These results and those of the calculated 1990 fuel burn for each of the individual AESA component emission scenarios have been tabulated in Table 3-4.8.

Approximately 76% of the world jet fuel consumption has been accounted for in the calculated scenarios for 1990. General aviation was not considered in these calculations but is reported to account for only 2% of the world usage. The calculations of scheduled passenger airline, scheduled cargo, scheduled turboprop, charter, and former Soviet Union account for 81% of the jet fuel use reported by ICAO for commercial operations (Balashov and Smith, 1992). The military scenario is calculated to correspond to 66% of the non-civil jet fuel use (the difference between the total world jet fuel consumption and the reported world civil aviation fuel use).

This agreement is quite good considering the number of simplifying assumptions that have been made in order to make the problem computationally tractable. In all of the scenarios, the aircraft were assumed to fly according to engineering design along great circle routes between the city-pairs without accounting for diversions due to air traffic control, weather holds, airport congestion, and fuel use by auxiliary power units. Altitudes were calculated according to optimized performance rather than "step climbs" dictated by air traffic control. In addition, the calculations used May 1990 as representative of the annual average air traffic schedule for 1990.

Based on the comparisons reported in Subchapter 3-2 for scheduled airline operations, (Table 3-2.6), the scheduled airliner and cargo scenario may have a systematic error of about 9% in the fuel burned. It is much more difficult to evaluate the accuracy of the military, charter, and non-OAG-scheduled flights in the former Soviet Union. In addition to uncertainties about the fuel burn and emissions technologies for these nonscheduled operations, there are large uncertainties about the flight frequencies, utilizations, and the type of equipment utilized. In addition, for the nonscheduled air traffic, generic aircraft types were used. There can easily be systematic errors associated with using performance and emissions characteristics of generic aircraft in the calculations, particularly if there is large variability in the technology within a given class of aircraft. This was shown for the generic 1990 aircraft described in Subchapter 3-2, which were carefully constructed by linear combinations of actual aircraft performances. The errors may be even larger when such a detailed database is not available to guide the construction of the generic database. It is difficult to conclude at this time whether further refinements in these databases are needed or not, since the calculations have accounted for the majority of world jet fuel use.

It is difficult to assess the accuracy of the reported jet fuel consumption. These databases are compiled from a variety of sources in many countries. We believe that the DOE database for jet fuel is based on refinery product output. Jet fuel can be used in place of diesel fuel for both ground transportation and home heating. In countries where fuel is at a premium, jet fuel may be used for a variety of purposes other than aviation; thus, the DOE reports may overestimate the worldwide jet fuel use for aviation. Similarly, we believe the ICAO numbers are derived from airline reports, the completeness and accuracy of which vary. As a result, an estimate for military use derived from the difference between the DOE total jet fuel use and the ICAO report of civil aviation use may not be valid.

A comprehensive critique of the refinery production of jet fuel and of the ICAO database would be a major project. Since the calculated jet fuel amounts in the current emissions database account for about 80% of the reported usage, it is not clear that such a study is warranted at this time.

There are no measurements or other global inventories of aircraft emissions done with this level of detail with which to compare these scenarios. Recent estimates of subsonic emissions for 1987, considering only scheduled commercial traffic, were calculated for cruise altitudes only, summed over longitude, and presented at 10 degree latitude resolution. (Boeing, 1990). A recent three-dimensional calculation has been presented (McInnes and Walker, 1992) which considered six aircraft types operating on four characteristic mission profiles. Their database was calculated for 24 equal volume latitude cells with 7.5 degree longitude and 0.5 km altitude resolution. Their database initially accounted for only 50% of the reported fuel burn and was scaled to the reported value to attempt to account for military aviation, nonscheduled traffic, general aviation or charter traffic which were not explicitly calculated. The results presented here are much more comprehensive in terms of types of aircraft considered, level of detail included in the mission profile calculations, resolution of the data set, and in terms of the different components of global aviation included in the calculation. For the scheduled 1990 operations, the emission characteristics have been based on measured emission indices; but little experimental data exist to directly test the calculated emissions.

CONCLUSIONS AND FUTURE CONSIDERATIONS

The fuel burned and atmospheric emissions have been determined for 1990 aircraft and for several scenarios projected to the year 2015 that include both subsonic and projected HSCT fleets. HSCT scenarios were determined for several different cruise Mach numbers and different NO_x emission indices. The resulting data sets are the most realistic and most comprehensive ever developed. While other databases have been compiled in the past (e.g., Boeing, 1990), this is the first to generate the data on a high resolution three-dimensional grid which attempts to explicitly calculate not only scheduled operations but also military, charter, and flights in the former Eastern Bloc.

Nonetheless, there are still uncertainties associated with the existing data sets and needs for extending the existing analyses.

Possible Future Work

- The effects of HSCT emissions within the polar vortex can not be completely accounted for by two-dimensional stratospheric chemistry models. It may become important to route the aircraft to avoid a special atmospheric condition such as the polar vortex. An evaluation of the fraction of HSCT emissions emitted directly within the polar vortex would be valuable. Routes that make the largest contribution to HSCT emissions within the vortex should be identified. Scoping calculation to assess the possibility of waypoint routing to minimize these effects should be done for selected routes, with fuel, flight time, and connect time constraints.
- The engineering performance and emissions calculations are all based on a U.S. Standard Atmosphere temperature and pressure profile. Parametric studies to evaluate the effects of temperatures on the fuel burn and emissions for selected missions would be valuable.
- Evaluate HSCT seasonal variability and its impact on emission scenarios. While there are clearly seasonal variations in subsonic traffic, there is disagreement within the industry as to the similarity of HSCT seasonal traffic variations with comparable subsonic routes.
- Calculate the seasonal variability in the subsonic fleet scenarios for major airline schedule periods (summer and winter) using the 1990 OAG data.
- Conduct a preliminary evaluation of the effect of supersonic corridors (flights permitted over land in sparsely populated areas) on HSCT utilization, fuel use, and emission scenarios.

ACKNOWLEDGMENT

The support of Linda Hunt, Debra Maggiora, and Karen Sage in processing the data and providing graphical displays of the emission scenarios is gratefully acknowledged.

Table 3-4.1. Summary of Fuel Burn and Emissions From Each of the Component Databases and Scenarios*

File	Fuel (kg/yr)	NO _x (kg/yr)	HC (kg/yr)	CO (kg/yr)
<u>1990</u>				
Scheduled Airliner and Cargo	9.08E+10	1.14E+09	1.37E+08	5.17E+08
Scheduled Turboprop	1.99E+09	2.05E+07	1.11E+06	9.77E+06
Charter	6.65E+09	5.99E+07	4.08E+06	3.42E+07
Military	2.60E+10	1.94E+08	1.89E+08	4.86E+08
Former Soviet Union	8.28E+09	4.92E+07	2.17E+07	8.20E+07
Total (1990)	1.34E+11	1.46E+09	3.52E+08	1.13E+09
<u>2015</u>				
Scheduled Cargo	5.64E+09	4.91E+07	3.56E+06	2.77E+07
Scheduled Airliner (no HSCT fleet)	2.45E+11	2.24E+09	9.20E+07	1.09E+09
Scheduled Subsonic Airliner (HSCT fleet exists)	2.10E+11	1.85E+09	1.17E+08	1.04E+09
Scheduled Turboprop	4.14E+09	4.42E+07	7.27E+06	2.41E+07
Charter	1.35E+10	1.22E+08	8.91E+06	7.23E+07
Military	2.06E+10	1.47E+08	1.85E+08	4.05E+08
Former Soviet Union	1.58E+10	9.38E+07	4.13E+07	1.56E+08
HSCT M1.6 EI=5	9.91E+10	4.57E+08	2.98E+07	2.88E+08
HSCT M1.6 EI=15	9.91E+10	1.37E+09	2.98E+07	2.88E+08
HSCT M2.4 (EI=5)	7.64E+10	5.00E+08	2.83E+07	2.33E+08
HSCT M2.4(EI=15)	7.64E+10	1.36E+09	2.83E+07	2.33E+08
YR 2015 Total (no HSCT fleet)	3.04E+11	2.70E+09	3.38E+08	1.77E+09
YR 2015 Total (M1.6, EI15 fleet)	3.69E+11	2.76E+09	3.93E+08	2.01E+09
YR 2015 Total (M1.6, EI15 fleet)	3.69E+11	3.67E+09	3.93E+08	2.01E+09
YR 2015 Total (M2.4, EI15 fleet)	3.46E+11	2.80E+09	3.91E+08	1.96E+09
YR 2015 Total (M2.4, EI15 fleet)	3.46E+11	3.66E+09	3.91E+08	1.96E+09

* 1.0E + 08 = 1×10^8

Table 3-4.2. Fuel Burned, Emissions, Cumulative Fractions of Fuel Burned and Emissions, and Emission Indices as Function of Altitude for 1990 Aircraft Emissions (Scenario A)*

Altitude Band (km)	Fuel (kg/year)	Cum Fuel (%)	NO _x (kg/year)	Cum NO _x (%)	HC (kg/year)	Cum HC (%)	CO (kg/year)	Cum CO (%)	EI (NO _x)	EI (HC)	EI (CO)
0-1	1.51E+10	11.29	1.82E+08	12.47	4.70E+07	13.35	1.91E+08	16.93	12.08	3.12	12.67
1-2	4.89E+09	14.94	5.81E+07	16.44	8.50E+06	15.76	4.74E+07	21.13	11.89	1.74	9.70
2-3	3.92E+09	17.87	5.32E+07	20.07	8.18E+06	18.09	3.25E+07	24.01	13.59	2.09	8.30
3-4	4.20E+09	21.01	6.25E+07	24.35	7.78E+06	20.30	3.04E+07	26.70	14.87	1.85	7.23
4-5	3.63E+09	23.72	5.09E+07	27.83	7.74E+06	22.49	2.90E+07	29.27	14.04	2.14	8.00
5-6	3.42E+09	26.28	4.76E+07	31.08	8.11E+06	24.80	2.97E+07	31.90	13.94	2.38	8.69
6-7	4.41E+09	29.58	4.89E+07	34.42	8.45E+06	27.19	4.78E+07	36.13	11.09	1.91	10.84
7-8	4.91E+09	33.24	5.18E+07	37.97	1.13E+07	30.41	5.48E+07	40.98	10.56	2.31	11.16
8-9	4.37E+09	36.51	4.86E+07	41.29	1.47E+07	34.58	4.88E+07	45.31	11.12	3.36	11.18
9-10	1.02E+10	44.11	1.03E+08	48.34	2.28E+07	41.04	1.02E+08	54.31	10.15	2.24	10.00
10-11	3.95E+10	73.63	3.72E+08	73.74	7.57E+07	62.54	2.42E+08	75.76	9.41	1.92	6.13
11-12	3.06E+10	96.48	3.46E+08	97.38	7.49E+07	83.81	1.77E+08	91.47	11.32	2.45	5.81
12-13	3.18E+09	98.86	2.51E+07	99.10	3.13E+07	92.68	6.00E+07	96.78	7.88	9.83	18.85
13-14	1.01E+09	99.61	9.77E+06	99.77	1.22E+07	96.15	1.50E+07	98.11	9.67	12.09	14.84
14-15	2.29E+08	99.78	1.25E+06	99.85	1.01E+07	99.03	1.06E+07	99.05	5.47	44.37	46.17
15-16	1.91E+08	99.92	1.58E+06	99.96	2.59E+06	99.77	3.56E+06	99.36	8.26	13.60	18.68
16-17	3.75E+07	99.95	2.28E+05	99.97	2.92E+05	99.85	2.55E+06	99.59	6.08	7.77	68.00
17-18	4.97E+07	99.99	2.98E+05	99.99	4.10E+05	99.97	3.60E+06	99.91	5.99	8.24	72.40
18-19	1.43E+07	100.00	8.58E+04	100.00	1.22E+05	100.00	1.07E+06	100.00	5.99	8.52	74.86
Global Total	1.34E+11		1.46E+09		3.52E+08		1.13E+09		10.94	2.63	8.44

* 1.0E + 08 = 1.0 x 10⁸

Table 3-4.3. Fuel Burned, Emissions, Cumulative Fractions of Fuel Burned and Emissions, and Emission Indices as a Function of Altitude for 2015 Aircraft Emissions Assuming no HSCT Fleet Exists (Scenario B)*

Altitude Band (km)	Fuel (kg/year)	Cum Fuel (%)	NO _x (kg/year)	Cum NO _x (%)	HC (kg/year)	Cum HC (%)	CO (kg/year)	Cum CO (%)	EI (NO _x)	EI (HC)	EI (CO)
0-1	3.07E+10	10.10	3.03E+08	11.22	3.88E+07	11.49	3.90E+08	22.03	9.84	1.26	12.69
1-2	9.33E+09	13.16	1.06E+08	15.16	8.39E+06	13.97	8.26E+07	26.69	11.38	0.90	8.86
2-3	7.78E+09	15.72	8.95E+07	18.48	7.50E+06	16.19	6.33E+07	30.27	11.51	0.96	8.14
3-4	9.45E+09	18.82	1.19E+08	22.88	6.62E+06	18.15	5.61E+07	33.44	12.56	0.70	5.94
4-5	8.09E+09	21.48	9.43E+07	26.38	6.94E+06	20.21	5.75E+07	36.68	11.65	0.86	7.11
5-6	7.44E+09	23.92	8.47E+07	29.52	5.97E+06	21.97	5.73E+07	39.92	11.38	0.80	7.70
6-7	7.31E+09	26.32	7.43E+07	32.28	5.34E+06	23.55	6.51E+07	43.59	10.17	0.73	8.90
7-8	8.01E+09	28.95	7.86E+07	35.20	7.77E+06	25.85	7.47E+07	47.81	9.82	0.97	9.33
8-9	8.04E+09	31.59	8.13E+07	38.21	9.46E+06	28.65	6.85E+07	51.67	10.11	1.18	8.52
9-10	1.47E+10	36.43	1.31E+08	43.08	1.80E+07	33.97	1.24E+08	58.67	8.91	1.22	8.42
10-11	6.82E+10	58.84	5.06E+08	61.85	7.98E+07	57.59	3.15E+08	76.47	7.42	1.17	4.62
11-12	1.21E+11	98.75	1.00E+09	98.95	8.22E+07	81.94	3.28E+08	95.01	8.23	0.68	2.70
12-13	2.81E+09	99.67	2.13E+07	99.74	3.41E+07	92.03	5.86E+07	98.32	7.58	12.15	20.88
13-14	6.18E+08	99.88	4.70E+06	99.91	1.35E+07	96.04	1.56E+07	99.20	7.61	21.91	25.24
14-15	2.16E+08	99.95	1.08E+06	99.95	1.07E+07	99.20	1.09E+07	99.81	5.00	49.54	50.31
15-16	1.65E+08	100.00	1.33E+06	100.00	2.69E+06	100.00	3.38E+06	100.00	8.01	16.26	20.42
Global Total	3.04E+11		2.70E+09		3.38E+08		1.77E+09		8.85	1.11	5.82

* 1.0E + 08 = 1.0 × 10⁸

Table 3-4.4. Fuel Burned, Emissions, Cumulative Fractions of Fuel Burned and Emissions, and Emission Indices as a Function of Altitude for 2015 Aircraft Emissions with a Fleet of Mach 1.6 HSCTs with a Nominal EI(NO_x)=5 (Scenario C)*

Altitude Band (km)	Fuel (kg/year)	Cum Fuel (%)	NO _x (kg/year)	Cum NO _x (%)	HC (kg/year)	Cum HC (%)	CO (kg/year)	Cum CO (%)	EI (NO _x)	EI (HC)	EI (CO)
0-1	3.04E+10	8.26	2.84E+08	10.30	4.91E+07	12.51	3.98E+08	19.80	9.34	1.61	13.08
1-2	1.01E+10	11.01	1.06E+08	14.14	1.18E+07	15.52	8.89E+07	24.22	10.45	1.17	8.76
2-3	8.61E+09	13.35	8.91E+07	17.37	9.72E+06	18.00	6.78E+07	27.60	10.34	1.13	7.87
3-4	1.01E+10	16.10	1.15E+08	21.53	8.37E+06	20.13	5.97E+07	30.56	11.34	0.83	5.89
4-5	8.92E+09	18.52	9.41E+07	24.94	8.87E+06	22.39	6.15E+07	33.62	10.55	0.99	6.90
5-6	8.27E+09	20.76	8.43E+07	28.00	8.03E+06	24.43	6.14E+07	36.68	10.19	0.97	7.43
6-7	8.13E+09	22.97	7.39E+07	30.68	6.33E+06	26.05	6.78E+07	40.05	9.09	0.78	8.34
7-8	8.81E+09	25.36	7.76E+07	33.49	9.07E+06	28.36	7.76E+07	43.91	8.81	1.03	8.81
8-9	8.81E+09	27.75	7.97E+07	36.38	1.14E+07	31.25	7.21E+07	47.50	9.05	1.29	8.19
9-10	1.54E+10	31.92	1.26E+08	40.93	1.99E+07	36.32	1.28E+08	53.87	8.17	1.30	8.34
10-11	6.11E+10	48.49	4.15E+08	55.98	8.12E+07	57.01	3.08E+08	69.22	6.80	1.33	5.05
11-12	1.03E+11	76.34	7.86E+08	84.46	8.27E+07	78.08	2.88E+08	83.54	7.66	0.81	2.81
12-13	6.12E+09	78.00	3.39E+07	85.69	3.51E+07	87.01	6.82E+07	86.93	5.54	5.74	11.15
13-14	3.11E+09	78.85	1.42E+07	86.20	1.43E+07	90.65	2.29E+07	88.07	4.57	4.59	7.34
14-15	9.04E+09	81.30	3.47E+07	87.46	1.34E+07	94.05	3.65E+07	89.89	3.84	1.48	4.04
15-16	2.14E+10	87.11	1.08E+08	91.37	9.09E+06	96.36	6.52E+07	93.13	5.04	0.42	3.05
16-17	2.66E+10	94.32	1.33E+08	96.20	8.00E+06	98.40	7.73E+07	96.98	5.01	0.30	2.91
17-18	1.94E+10	99.60	9.75E+07	99.73	5.85E+06	99.89	5.65E+07	99.79	5.01	0.30	2.91
18-19	1.47E+09	100.00	7.38E+06	100.00	4.43E+05	100.00	4.28E+06	100.00	5.01	0.30	2.90
Global Total	3.69E+11		2.76E+09		3.93E+08		2.01E+09		7.49	1.07	5.46

* 1.0E + 08 = 1.0 x 10⁸

Table 3-4.5. Fuel Burned, Emissions, Cumulative Fractions of Fuel Burned and Emissions, and Emission Indices as a Function of Altitude for 2015 Aircraft Emissions with a Fleet of Mach 1.6 HSCTs with a Nominal EI(NO_x)=15 (Scenario D)*

Altitude Band (km)	Fuel (kg/year)	Cum Fuel (%)	NO _x (kg/year)	Cum NO _x (%)	HC (kg/year)	Cum HC (%)	CO (kg/year)	Cum CO (%)	EI (NO _x) (HC)	EI (CO)
0-1	3.04E+10	8.26	2.91E+08	7.93	4.91E+07	12.51	3.98E+08	19.80	9.58	1.61
1-2	1.01E+10	11.01	1.13E+08	11.02	1.18E+07	15.52	8.89E+07	24.22	11.16	1.17
2-3	8.61E+09	13.35	9.65E+07	13.64	9.72E+06	18.00	6.78E+07	27.60	11.21	1.13
3-4	1.01E+10	16.10	1.22E+08	16.97	8.37E+06	20.13	5.97E+07	30.56	12.05	0.83
4-5	8.92E+09	18.52	1.03E+08	19.76	8.87E+06	22.39	6.15E+07	33.62	11.52	0.99
5-6	8.27E+09	20.76	9.29E+07	22.29	8.03E+06	24.43	6.14E+07	36.68	11.23	0.97
6-7	8.13E+09	22.97	8.11E+07	24.50	6.33E+06	26.05	6.78E+07	40.05	9.98	0.78
7-8	8.81E+09	25.36	8.48E+07	26.81	9.07E+06	28.36	7.76E+07	43.91	9.62	1.03
8-9	8.81E+09	27.75	8.72E+07	29.18	1.14E+07	31.25	7.21E+07	47.50	9.89	1.29
9-10	1.54E+10	31.92	1.36E+08	32.88	1.99E+07	36.32	1.28E+08	53.87	8.84	1.30
10-11	6.11E+10	48.49	4.34E+08	44.70	8.12E+07	57.01	3.08E+08	69.22	7.11	1.33
11-12	1.03E+11	76.34	8.02E+08	66.52	8.27E+07	78.08	2.88E+08	83.54	7.81	0.81
12-13	6.12E+09	78.00	5.91E+07	68.13	3.51E+07	87.01	6.82E+07	86.93	9.66	5.74
13-14	3.11E+09	78.85	3.33E+07	69.03	1.43E+07	90.65	2.29E+07	88.07	10.68	4.59
14-15	9.04E+09	81.30	1.02E+08	71.81	1.34E+07	94.05	3.65E+07	89.89	11.28	1.48
15-16	2.14E+10	87.11	3.21E+08	80.55	9.09E+06	96.36	6.52E+07	93.13	15.00	0.42
16-17	2.66E+10	94.32	4.00E+08	91.44	8.00E+06	98.40	7.73E+07	96.98	15.04	0.30
17-18	1.94E+10	99.60	2.92E+08	99.40	5.85E+06	99.89	5.65E+07	99.79	15.04	0.30
18-19	1.47E+09	100.00	2.21E+07	100.00	4.43E+05	100.00	4.28E+06	100.00	15.02	0.30
Global Total	3.69E+11		3.67E+09		3.93E+08		2.01E+09		9.97	1.07
										5.46

* 1.0E + 08 = 1.0 x 10⁸

Table 3-4.6. Fuel Burned, Emissions, Cumulative Fractions of Fuel Burned and Emissions, and Emission Indices as a Function of Altitude for 2015 Aircraft Emissions with a Fleet of Mach 2.4 HSTs with a Nominal EI(NO_x)=5 (Scenario E)*

Altitude Band (km)	Fuel (kg/year)	Cum Fuel (%)	NO _x (kg/year)	Cum NO _x (%)	HC (kg/year)	Cum HC (%)	CO (kg/year)	Cum CO (%)	EI (NO _x)	EI (HC)	EI (CO)
0-1	3.16E+10	9.14	2.96E+08	10.58	5.17E+07	13.22	4.23E+08	21.61	9.38	1.64	13.38
1-2	9.84E+09	11.98	1.09E+08	14.45	1.20E+07	16.28	8.87E+07	26.15	11.04	1.22	9.02
2-3	8.31E+09	14.38	9.17E+07	17.73	9.85E+06	18.80	6.76E+07	29.60	11.04	1.19	8.14
3-4	9.83E+09	17.23	1.18E+08	21.93	8.49E+06	20.97	5.95E+07	32.65	11.96	0.86	6.05
4-5	8.61E+09	19.72	9.61E+07	25.35	9.00E+06	23.27	6.13E+07	35.78	11.16	1.05	7.12
5-6	7.96E+09	22.02	8.63E+07	28.43	8.16E+06	25.35	6.12E+07	38.91	10.84	1.02	7.69
6-7	7.82E+09	24.28	7.66E+07	31.16	6.45E+06	27.00	6.76E+07	42.37	9.79	0.82	8.64
7-8	8.51E+09	26.74	8.02E+07	34.03	9.20E+06	29.35	7.74E+07	46.33	9.43	1.08	9.10
8-9	8.50E+09	29.20	8.24E+07	36.97	1.15E+07	32.29	7.19E+07	50.01	9.68	1.35	8.46
9-10	1.55E+10	33.68	1.34E+08	41.75	2.03E+07	37.47	1.30E+08	56.64	8.64	1.31	8.36
10-11	6.17E+10	51.52	4.32E+08	57.17	8.19E+07	58.41	3.12E+08	72.60	7.01	1.33	5.06
11-12	1.03E+11	81.35	8.00E+08	85.72	8.33E+07	79.69	2.90E+08	87.42	7.75	0.81	2.81
12-13	7.56E+09	83.54	6.10E+07	87.89	3.61E+07	88.92	7.51E+07	91.26	8.07	4.78	9.94
13-14	2.14E+09	84.15	1.78E+07	88.53	1.40E+07	92.51	1.66E+07	92.11	8.32	6.57	7.77
14-15	1.73E+09	84.65	1.41E+07	89.03	1.12E+07	95.37	1.19E+07	92.71	8.16	6.45	6.84
15-16	1.68E+09	85.14	1.44E+07	89.55	3.17E+06	96.18	4.38E+06	92.94	8.55	1.89	2.60
16-17	1.52E+09	85.58	1.31E+07	90.01	4.83E+05	96.30	9.98E+05	92.99	8.61	0.32	0.66
17-18	1.56E+09	86.03	1.33E+07	90.49	4.95E+05	96.43	1.14E+06	93.05	8.51	0.32	0.73
18-19	7.40E+09	88.17	4.35E+07	92.04	2.17E+06	96.98	1.90E+07	94.02	5.88	0.29	2.56
19-20	1.86E+10	93.54	1.02E+08	95.67	5.36E+06	98.35	5.27E+07	96.71	5.48	0.29	2.84
20-21	2.23E+10	99.99	1.21E+08	99.99	6.44E+06	100.00	6.43E+07	100.00	5.43	0.29	2.88
21-22	2.97E+07	100.00	1.61E+05	100.00	8.58E+03	100.00	8.56E+04	100.00	5.42	0.29	2.88
Global Total	3.46E+11		2.80E+09		3.91E+08		1.96E+09		8.10	1.13	5.66

* 1.0E + 08 = 1.0 x 10⁸

Table 3-4.7. Fuel Burned, Emissions, Cumulative Fractions of Fuel Burned and Emissions, and Emission Indices as a Function of Altitude for 2015 Aircraft Emissions with a Fleet of Mach 2.4 HSCTs with a Nominal EI(NO_x)=15 (Scenario F)*

Altitude Band (km)	Fuel (kg/year)	Cum Fuel (%)	NO _x (kg/year)	Cum NO _x (%)	HC (kg/year)	Cum HC (%)	CO (kg/year)	Cum CO (%)	EI (NO _x)	EI (HC)	EI (CO)
0-1	3.16E+10	9.14	3.14E+08	8.57	5.17E+07	13.22	4.23E+08	21.61	9.93	1.64	13.38
1-2	9.84E+09	11.98	1.20E+08	11.85	1.20E+07	16.28	8.87E+07	26.15	12.17	1.22	9.02
2-3	8.31E+09	14.38	1.03E+08	14.66	9.85E+06	18.80	6.76E+07	29.60	12.38	1.19	8.14
3-4	9.83E+09	17.23	1.29E+08	18.17	8.49E+06	20.97	5.95E+07	32.65	13.09	0.86	6.05
4-5	8.61E+09	19.72	1.07E+08	21.10	9.00E+06	23.27	6.13E+07	35.78	12.45	1.05	7.12
5-6	7.96E+09	22.02	9.73E+07	23.76	8.16E+06	25.35	6.12E+07	38.91	12.23	1.02	7.69
6-7	7.82E+09	24.28	8.76E+07	26.16	6.45E+06	27.00	6.76E+07	42.37	11.20	0.82	8.64
7-8	8.51E+09	26.74	9.13E+07	28.65	9.20E+06	29.35	7.74E+07	46.33	10.74	1.08	9.10
8-9	8.50E+09	29.20	9.34E+07	31.21	1.15E+07	32.29	7.19E+07	50.01	10.99	1.35	8.46
9-10	1.55E+10	33.68	1.49E+08	35.28	2.03E+07	37.47	1.30E+08	56.64	9.61	1.31	8.36
10-11	6.17E+10	51.52	4.53E+08	47.68	8.19E+07	58.41	3.12E+08	72.60	7.35	1.33	5.06
11-12	1.03E+11	81.35	8.25E+08	70.22	8.33E+07	79.69	2.90E+08	87.42	7.99	0.81	2.81
12-13	7.56E+09	83.54	8.86E+07	72.64	3.61E+07	88.92	7.51E+07	91.26	11.73	4.78	9.94
13-14	2.14E+09	84.15	4.36E+07	73.83	1.40E+07	92.51	1.66E+07	92.11	20.40	6.57	7.77
14-15	1.73E+09	84.65	3.99E+07	74.93	1.12E+07	95.37	1.19E+07	92.71	23.04	6.45	6.84
15-16	1.68E+09	85.14	4.02E+07	76.02	3.17E+06	96.18	4.38E+06	92.94	23.88	1.89	2.60
16-17	1.52E+09	85.58	3.89E+07	77.09	4.83E+05	96.30	9.98E+05	92.99	25.61	0.32	0.66
17-18	1.56E+09	86.03	3.96E+07	78.17	4.95E+05	96.43	1.14E+06	93.05	25.32	0.32	0.73
18-19	7.40E+09	88.17	1.30E+08	81.73	2.17E+06	96.98	1.90E+07	94.02	17.60	0.29	2.56
19-20	1.86E+10	93.54	3.05E+08	90.06	5.36E+06	98.35	5.27E+07	96.71	16.44	0.29	2.84
20-21	2.23E+10	99.99	3.63E+08	99.99	6.44E+06	100.00	6.43E+07	100.00	16.26	0.29	2.88
21-22	2.97E+07	100.00	4.83E+05	100.00	8.58E+03	100.00	8.56E+04	100.00	16.26	0.29	2.88
Global Total	3.46E+11		3.66E+09		3.91E+08		1.96E+09		10.58	1.13	5.66

* 1.0E + 08 = 1.0 x 10⁸

Table 3-4.8. Comparison of Calculated 1990 Jet Fuel Usage with Reported Jet Fuel Use

	1990		Calculated Scenarios	
	Reported Fuel Use		Fraction of	
	(kg/year)	Total (%)	(kg/year)	Total (%)
Total World Jet Fuel Consumption (Ref. 1)	1.76E+11		1.34E+11	75.98
World Civil Aviation Fuel Use (Ref. 2)	1.37E+11			
General Aviation (Ref. 2)	3.50E+09	1.99		
Commercial Airlines (Ref. 2)	1.33E+11	75.57	1.08E+11	61.20
Scheduled Airliner and Cargo			9.08E+10	51.59
Scheduled Turboprop			1.99E+09	1.13
Charter			6.65E+09	3.78
Nonscheduled Former Soviet Union			8.28E+09	4.70
Non-Civil Usage (Military)	3.95E+10	22.44	2.60E+10	14.77

Reference 1: Department of Energy, 1991.
Reference 2: B. Balashov and A. Smith, 1992.

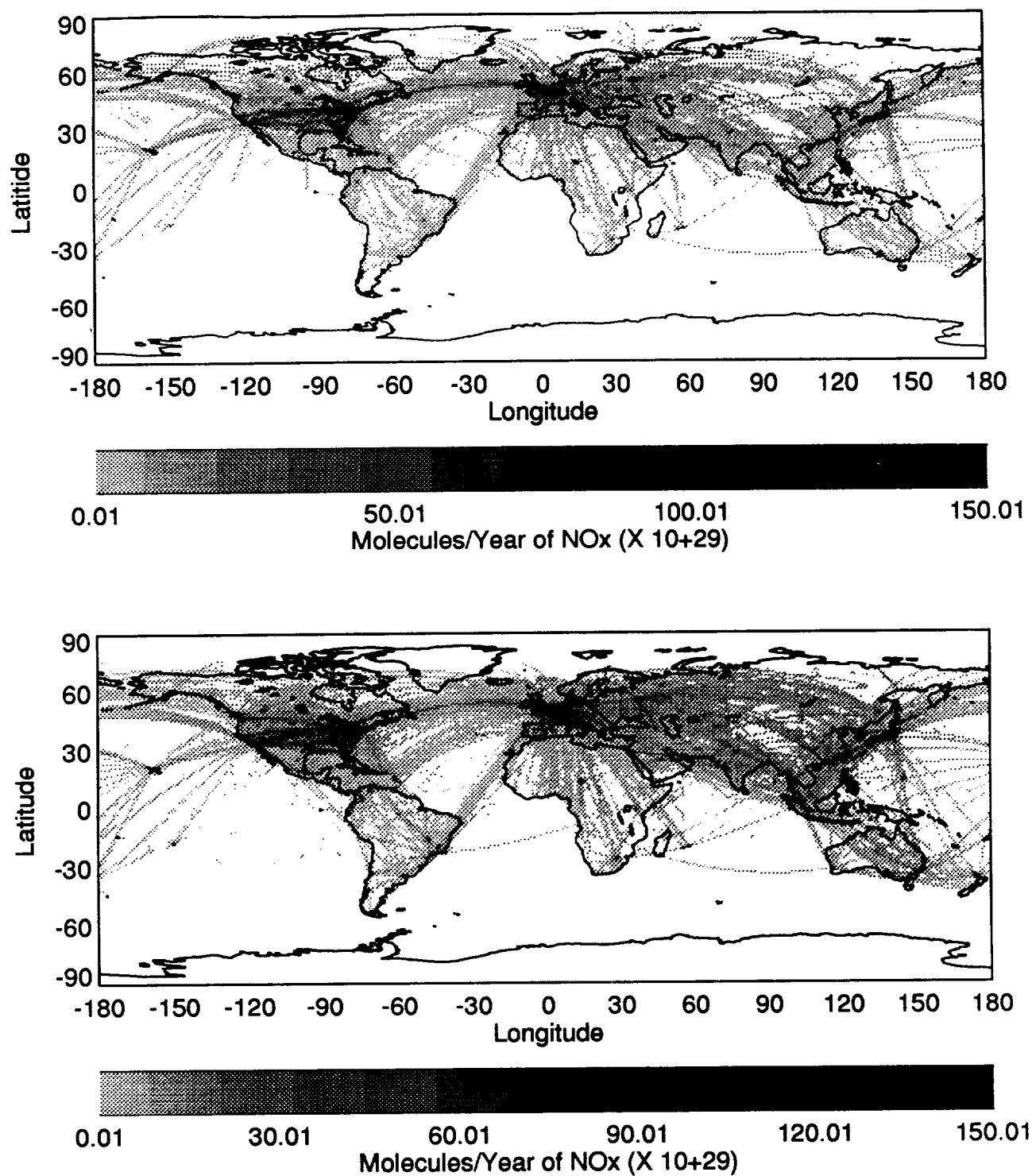


Figure 3-4.1. Annual NO_x emissions for the 1990 subsonic fleet (Scenario A, top panel) and for the proposed 2015 Mach 2.4 (EI=15) HSCT case (Scenario F, bottom panel) as a function of latitude and longitude. Scenario F results shown are computed over altitudes below 13 km to emphasize the subsonic fleet.

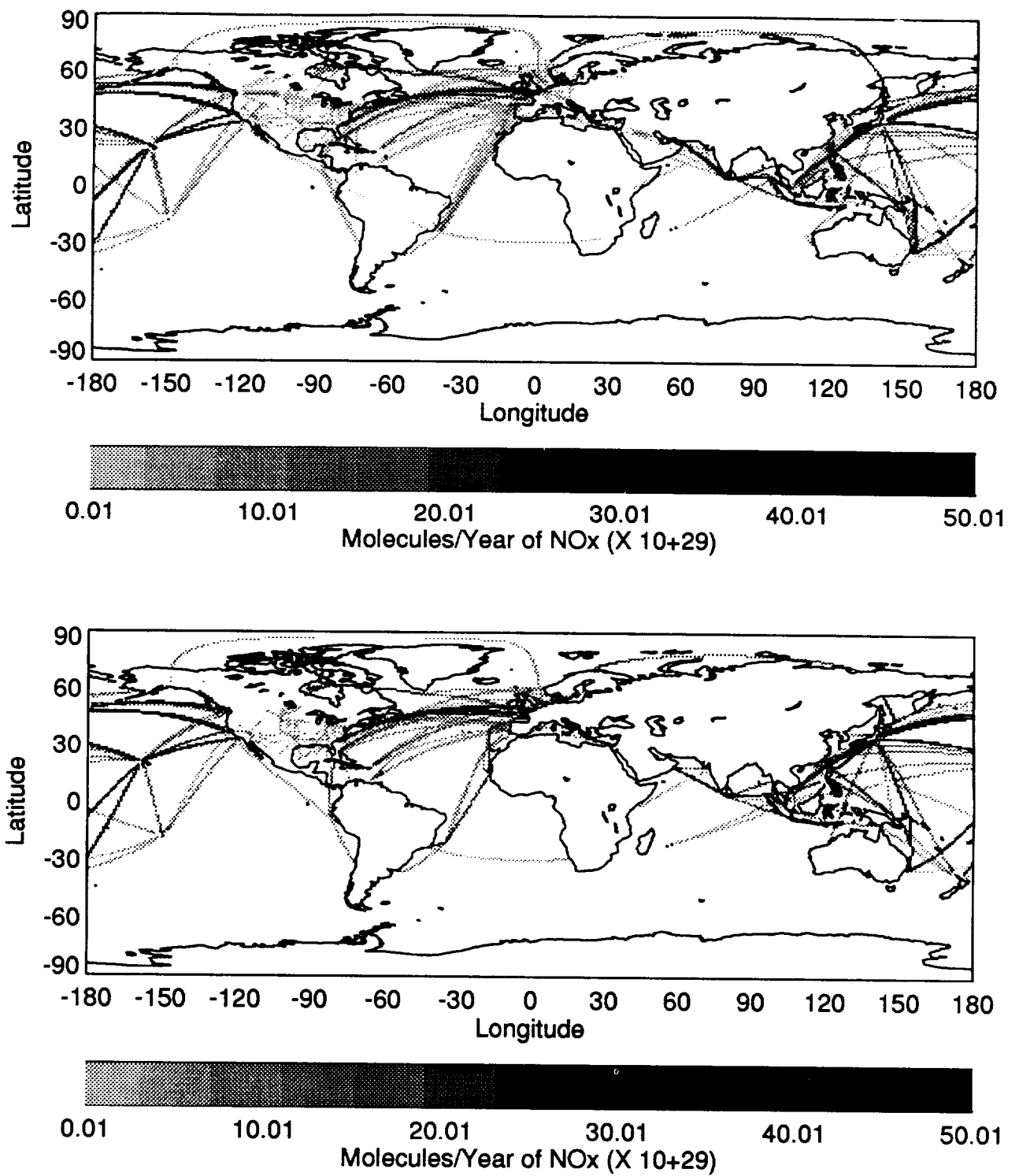


Figure 3-4.2. Annual NO_x emissions above 13 km for the proposed 2015 Mach 1.6 (EI=15) HSC case (Scenario D, upper panel) and the proposed Mach 2.4 (EI=15) HSC case (Scenario F, bottom panel).

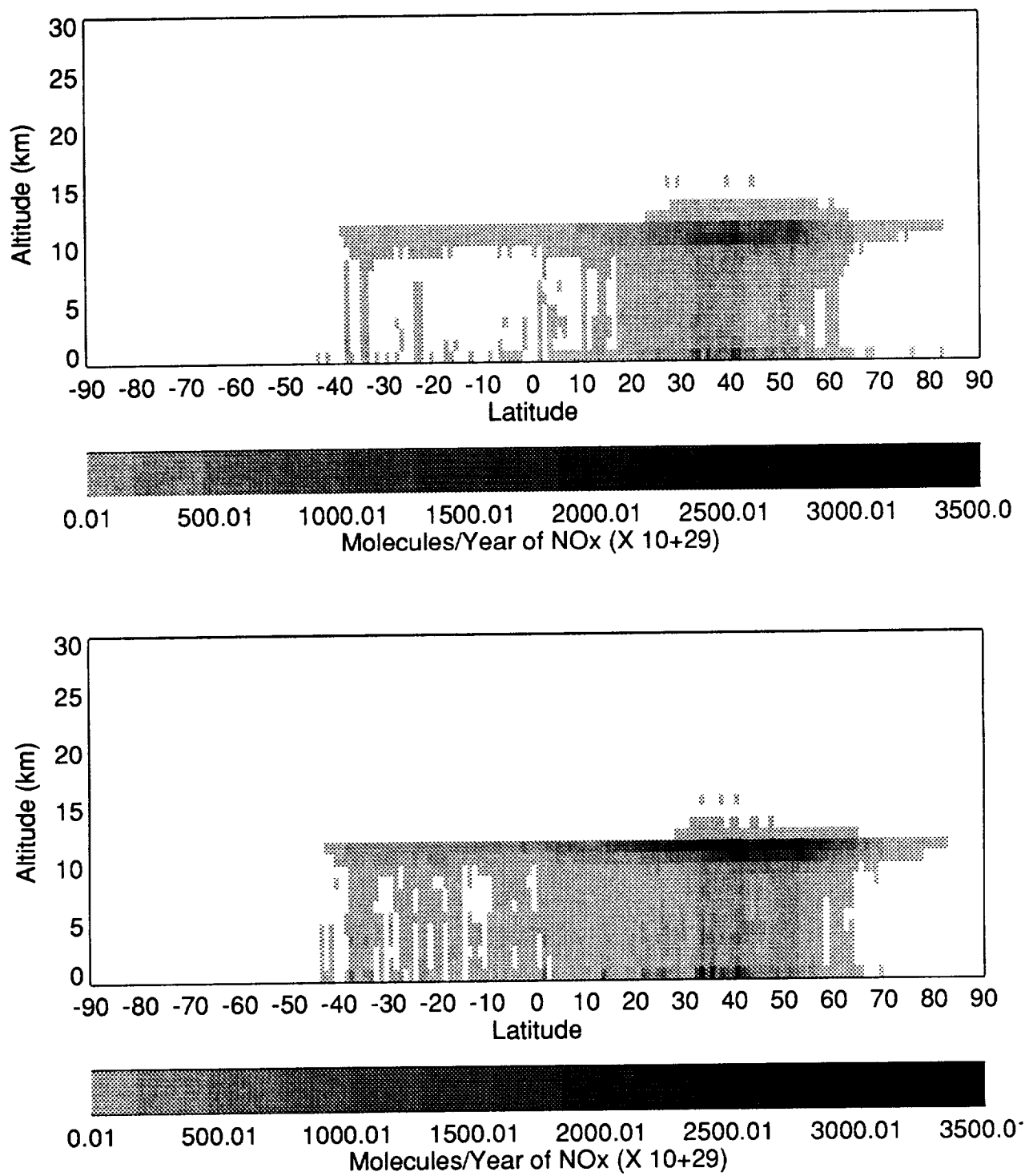


Figure 3-4.3. Annual NO_x emissions for the 1990 subsonic fleet (Scenario A, top panel) and for the 2015 subsonic fleet in the absence of an HSCT fleet (Scenario B, bottom panel) as a function of geopotential altitude and latitude.

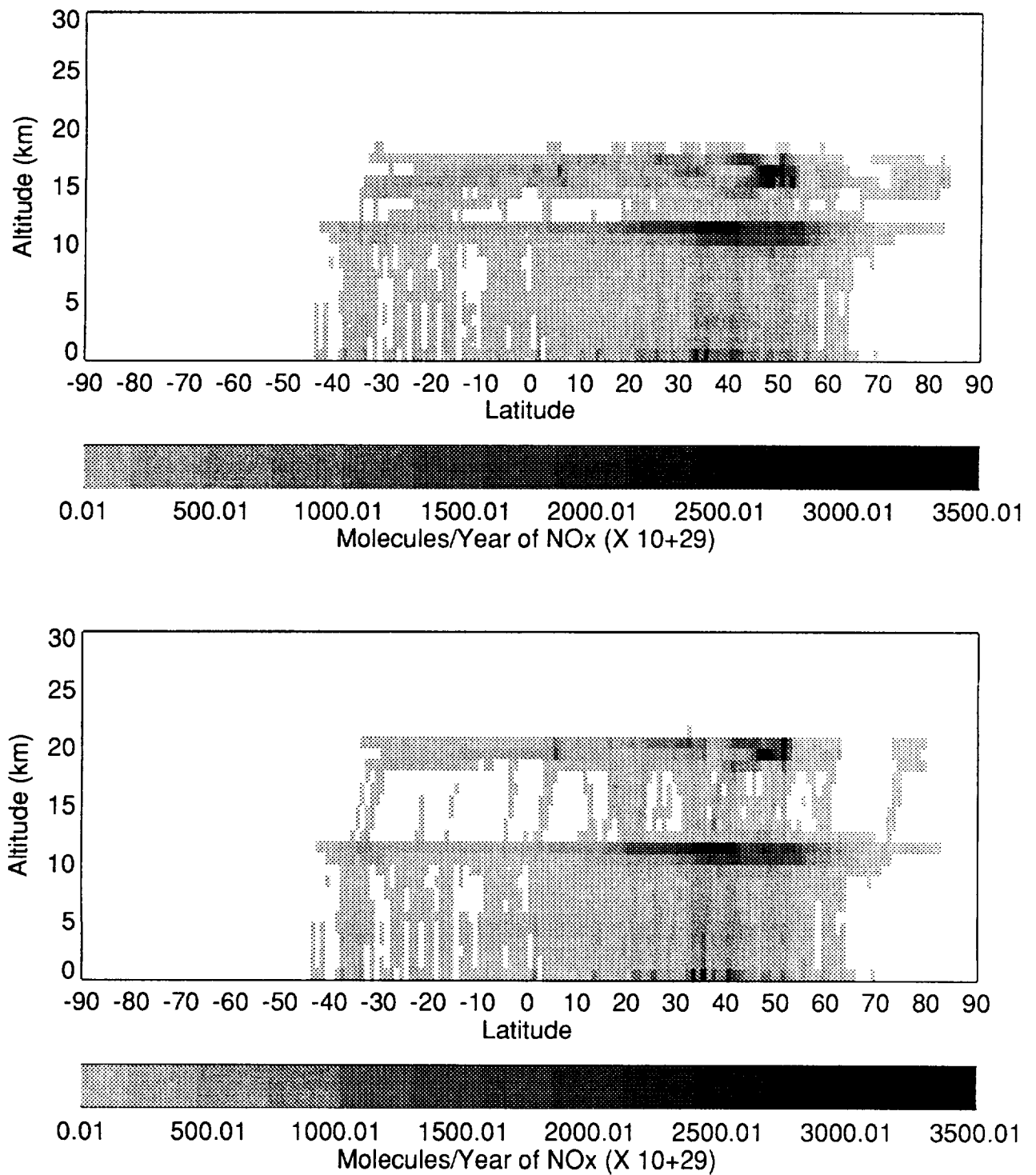


Figure 3-4.4. Annual NO_x emissions for the proposed 2015 Mach 1.6 (EI=15) HSCT case (Scenario D, top panel) and for the proposed 2015 Mach 2.4 (EI=15) HSCT (Scenario F, bottom panel) as a function of geopotential altitude and latitude.

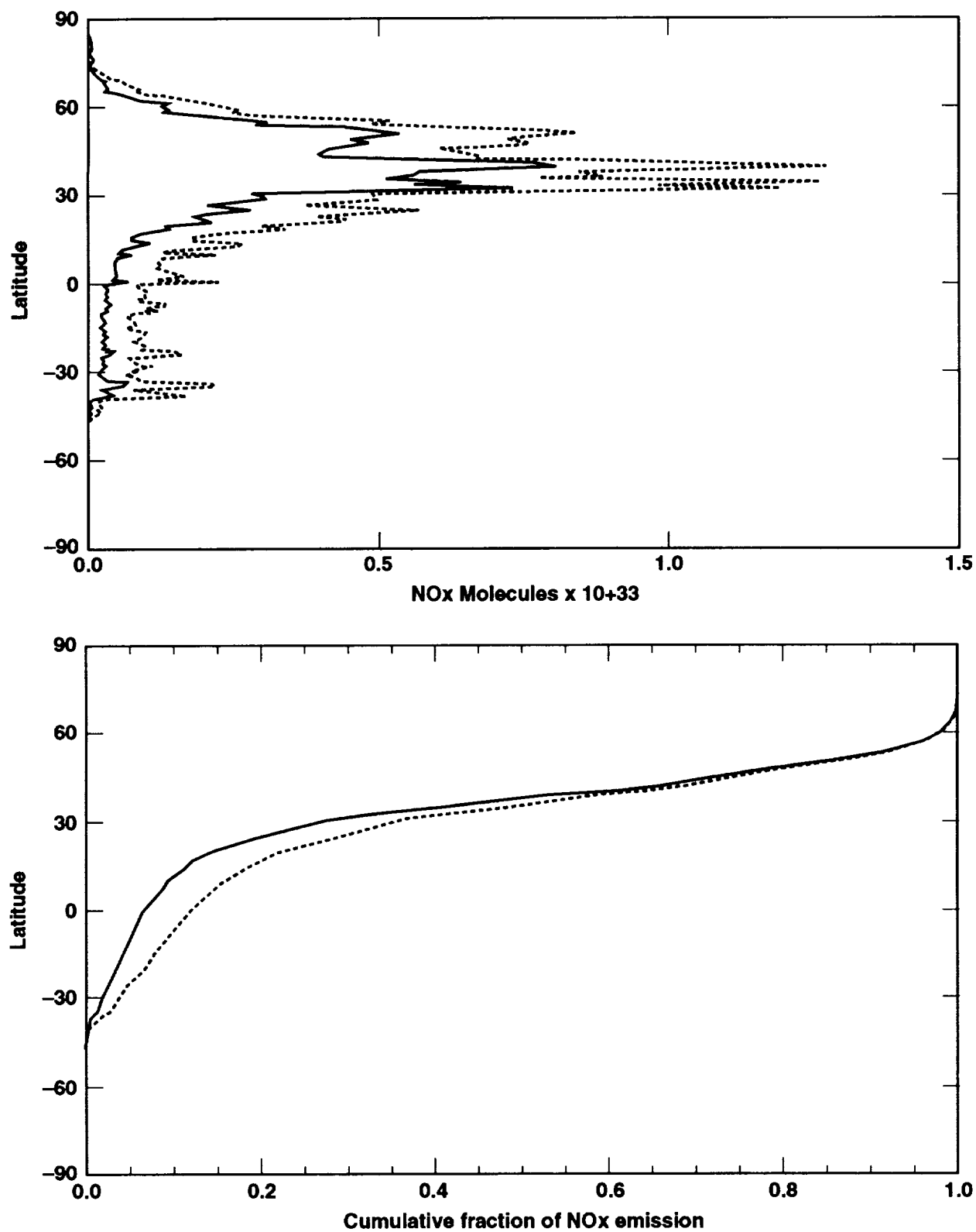


Figure 3-4.5. Annual NO_x emissions and cumulative fraction of NO_x emissions as a function of latitude for the 1990 subsonic fleet (Scenario A, solid lines) and for the 2015 subsonic fleet in the absence of an HSCT fleet (Scenario B, dotted lines).

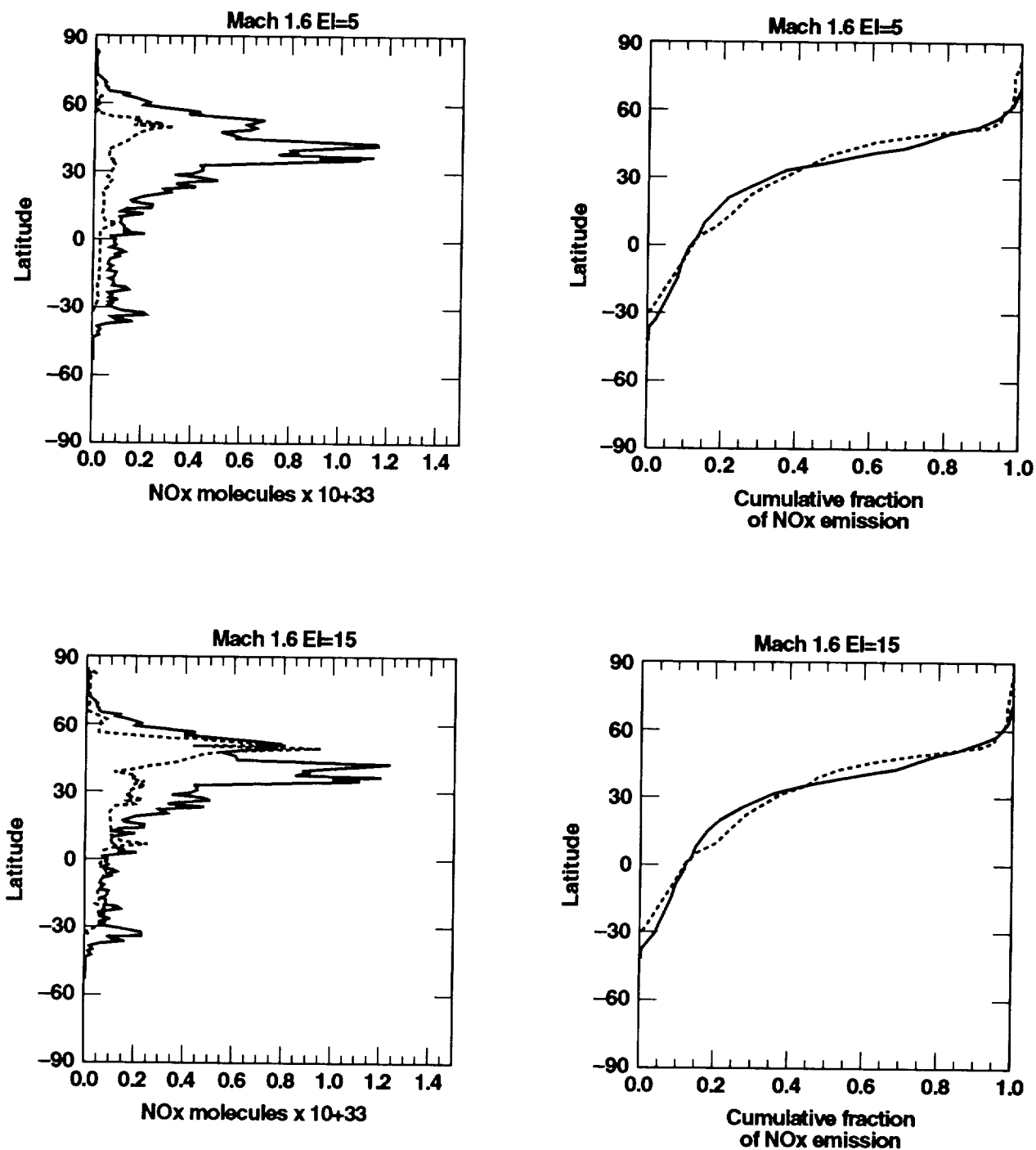


Figure 3-4.6. Annual NO_x emissions and cumulative fraction of NO_x emissions as a function of latitude for Scenario C (proposed 2015 Mach 1.6, EI=5 HSCT case) and for Scenario D (proposed 2015 Mach 1.6, EI=15 HSCT case). Solid lines indicate emissions summed below 13 km while dotted lines indicate emissions computed above 13 km.

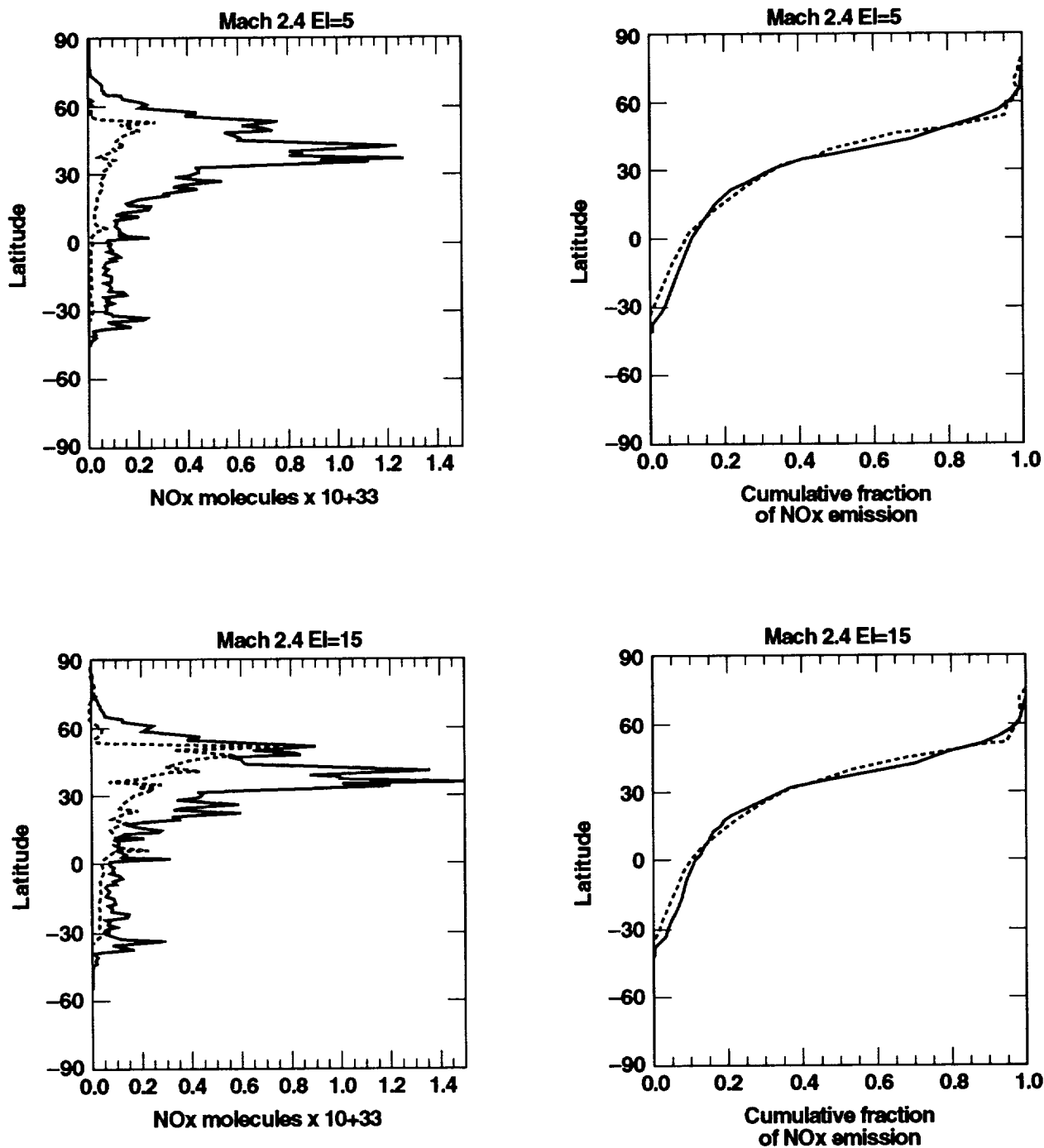


Figure 3-4.7. Annual NO_x emissions and cumulative fraction of NO_x emissions as a function of latitude for Scenario E (proposed 2015 Mach 2.4, EI=5 HSCT case) and for Scenario F (proposed 2015 Mach 2.4, EI=15 HSCT case). Solid lines indicate emissions computed below 13 km while dotted lines indicate emissions summed above 13 km.

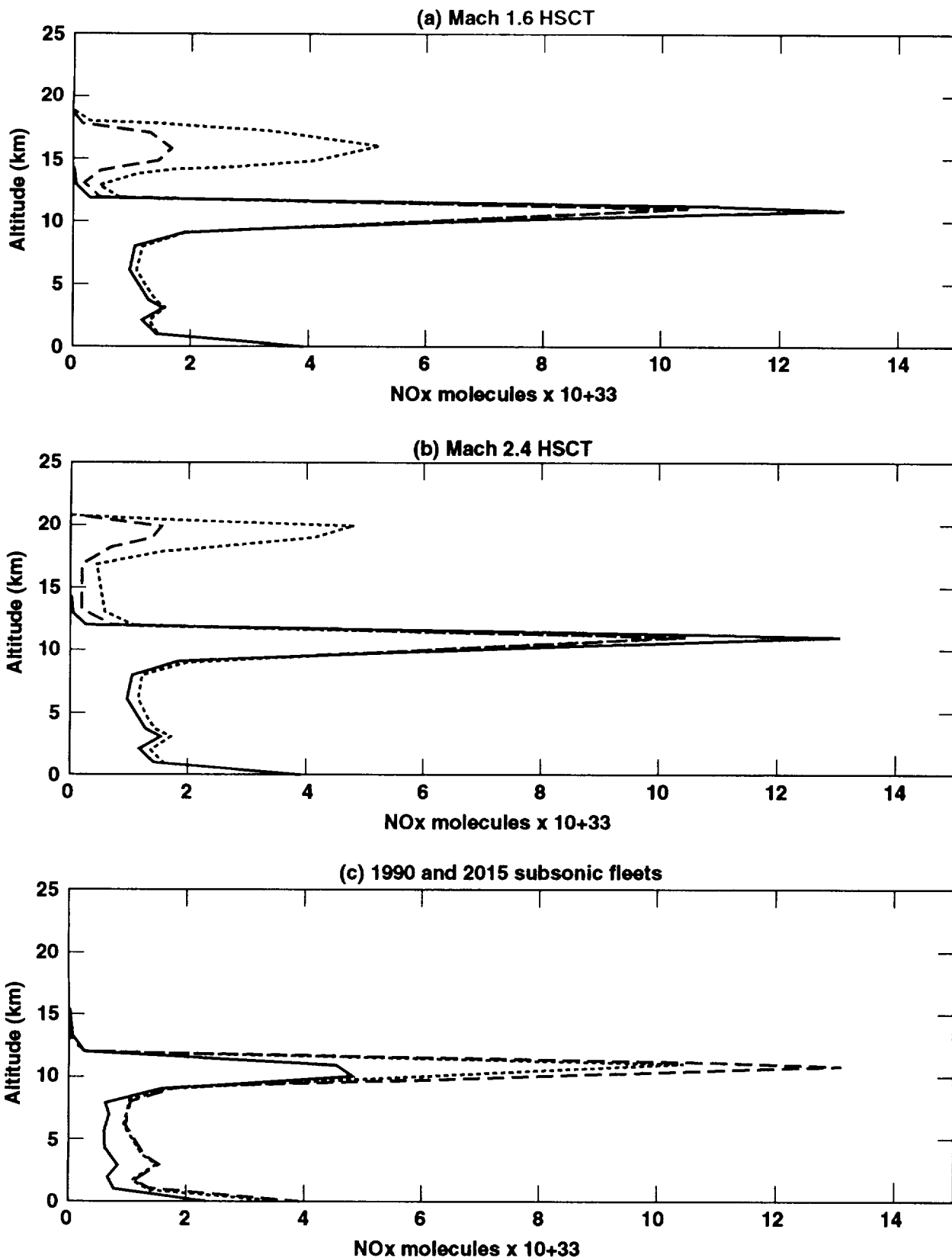


Figure 3-4.8. Annual NO_x emissions as a function of geopotential altitude for the Mach 1.6 HSCT cases (panel a), for the Mach 2.4 HSCT cases (panel b), and for the 1990 and 2015 subsonic fleets (panel c). In panels a and b, the solid line indicates the 2015 subsonic fleet without an HSCT, the dashed line indicates the EI=5 HSCT cases, and the dotted line indicates the EI=15 HSCT cases. In panel c, the solid line indicates the 1990 subsonic fleet, the dashed line the 2015 subsonic fleet without an HSCT, and the dotted line the revised 2015 subsonic fleet with an HSCT.

REFERENCES

- Balashov, B., and A. Smith, *ICAO Journal*, August, 18–21, 1992.
- Boeing Commercial Airplane Group, *High Speed Civil Transport Study: Special Factors*, NASA Contractor Report 181881, NASA, Washington, D.C., 1990.
- Department of Energy, *International Energy Annual 1991*, DOE/EIA-021, Washington, D.C., 1991.
- McInnes, G., and C. T. Walker, *The Global Distribution of Aircraft Air Pollutant Emissions*, Warren Spring Laboratory Report 872, 1992.

Chapter 4

Update of Model Simulations for the Effects of Stratospheric Aircraft

Malcolm K. W. Ko
Atmospheric and Environmental Research Inc.
Cambridge, MA

Anne R. Douglass
Goddard Space Flight Center
National Aeronautics and Space Administration
Greenbelt, MD

Contributors

Guy V. Brasseur, XueXi Tie
National Center for Atmospheric Research

David B. Considine, Charles H. Jackman, Eric L. Fleming
Goddard Space Flight Center
National Aeronautics and Space Administration

Robert S. Harwood, Jonathan Kinnersley
University of Edinburgh

Ivar S. A. Isaksen
University of Oslo

Douglas E. Kinnison, Donald J. Wuebbles
Lawrence Livermore National Laboratory

John A. Pyle
University of Cambridge

Debra K. Weisenstein
Atmospheric and Environmental Research Inc.

INTRODUCTION

The results presented in this chapter are from six two-dimensional zonal-mean models (AER, CAMED, GSFC, LLNL, NCAR, and OSLO, see Table 1). The purpose of this chapter is to present results from calculations using the emissions data presented in Chapter 3 of the program report (1993) and discuss the factors that affect the uncertainties in the calculated results. While the discussion will focus on the recent results obtained using the latest emissions scenarios and parameterization of heterogeneous chemistry, it also draws on the results obtained over the previous years.

MODEL FEATURES, SIMILARITIES, AND DIFFERENCES

The models that provided results for this document are representative of the models being used for ozone assessment studies connected with the chlorine/ozone problem (WMO, 1992). The results for aircraft assessment may be sensitive to model features that have not been tested previously. Previous model validations have concentrated on the effect of increased chlorine in which the source for chlorine is more or less uniformly distributed through the middle and upper stratosphere. Aircraft emissions are deposited close to the tropopause. The results should depend on the ability of the model to simulate the dynamics of the lower stratosphere and upper troposphere with respect to synoptic-scale motions and the exchange of mass between the stratosphere and the troposphere. Increases in NO_y in the lower stratosphere lead to large adjustments of the HO_x and ClO_x chemical cycles. Validation of various mechanisms is also more difficult, since the changes in each cycle are likely to be small compared with those observed in the polar regions.

There are common features among the models because of similarity in the basic approach, and because improvements to the models were made as a result of several model intercomparison workshops (Jackman et al., 1989b; Prather and Remsberg, 1993). However, differences still exist among the models. We will try to make use of these different approaches to get a better idea of the uncertainties associated with the model predictions.

Treatment of Photochemistry

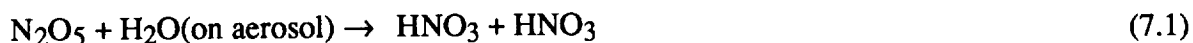
Reaction rates and photolysis cross sections used in the calculations are taken from JPL-92 (De More et al., 1992). The radiative transfer calculations in the models differ in their treatment of multiple scattering. There are also significant differences in photolysis rates which have a significant contribution from the spectral interval containing the Schumann-Runge bands (see Prather and Remsberg, 1993). However, these have only a small impact on the calculated ozone changes.

For a test case in which the long-lived species such as ozone and total odd nitrogen are held fixed, the calculated radical concentrations in three of the models (AER, GSFC, and LLNL) are in good agreement with each other and with ATMOS sunset measurements (see Prather and Remsberg, 1993, section M.).

The models also differ in the diurnal treatments used to calculate the long-lived trace gases. The AER model uses an explicit diurnal integration. The other models use diurnally averaged production and loss rates to calculate daytime average constituent concentrations. In some cases, precalculated factors computed off-line with a diurnal model are used in this calculation. The diurnal treatment is particularly important for determining the rate of heterogeneous reaction of N_2O_5 with H_2O , because N_2O_5 exhibits a large diurnal variation. The similarity among the model calculated results on ozone changes would suggest that this is treated in an adequate manner.

Heterogeneous Reactions

Previous assessments of the impact of a fleet of supersonic aircraft flying in the lower stratosphere considered only gas-phase photochemical reactions (Johnston et al., 1989 Prather and Wesoky, 1992, Chapter 5). The importance of the reaction $\text{N}_2\text{O}_5 + \text{H}_2\text{O}$ on background sulfate aerosols to this calculation had been demonstrated by Weisenstein et al. (1991) and Bekki et al. (1991). Laboratory measurements and atmospheric observations indicate that this reaction is important to the chemical balance controlling the photochemical removal of ozone in the lower stratosphere. Because this reaction appears to proceed on sulfate aerosols independent of their composition (see Chapter 5), its incorporation in a two-dimensional model appears to be straightforward. The two reactions on sulfate aerosols included in the calculations are



In both cases, it is assumed that the products are immediately released in gas phase.

The reaction rate is parameterized as first-order rate equal to the product of a reaction probability and collision frequency with the aerosol corresponding to clean conditions (i.e., several years after any significant volcanic injection of sulphur). The surface area are fixed at recommended values as functions of latitude (WMO, 1992, Chapter 8). Note that the median value over the past two decades is a factor of 4 larger than this value.

The reaction probability for (7.1) is taken to be 0.1 independent of aerosol composition. For (7.2), a temperature-dependent expression $[(0.06 \exp(-0.15(T-200)))]$ is used to simulate the dependence on aerosol composition. A more realistic parameterization involving the water content of the sulfate particle (Hanson and Ravishankara, 1991) was not used in this set of calculations. However, the effect from (7.2) is small at background condition. Since the zonal-mean temperatures and the water vapor concentrations in the models are different (see Prather and Remsberg, 1993, Section A and B), parameterized rates for (7.2) are expected to be different in the models.

Heterogeneous reactions occurring on polar stratospheric clouds (PSCs) could be important. However, 2-D models are not well suited for evaluating the effects of polar chemistry. It is difficult to represent the isolation of the polar vortex in a 2-D model. The effect of the displacement of the north polar vortex away from the pole may only be included through parameterization. Also, polar processes can affect species at midlatitudes through mechanisms that are not well-simulated in two-dimensional models. None of the simulations performed for the prescribed scenarios includes PSC chemistry.

Dynamics

All of the models employ either a residual or diabatic circulation and an "eddy transport" parameterized by eddy diffusion coefficients to represent the transport by planetary wave motions. Details concerning 2-D representations of stratospheric transport are discussed in Chapter 6 of WMO (1986) and are not considered further here. Two of the models (CAMED, NCAR) include interactive dynamics. The LLNL model uses a specified temperature field and the model-calculated ozone concentrations to calculate the local diabatic heating rate, which is used to derive the diabatic circulation. The other models (AER and GSFC) use specified seasonally varying winds and temperatures that are fixed for all simulations. In the GSFC model, the horizontal diffusion is calculated to be consistent with the circulation.

How the ozone distribution calculated in a fixed-circulation model is affected by the choice of circulation is discussed by Jackman et al. (1989a). Studies of the interannual variability of ozone calculated using circulations derived from successive year observations of temperature and ozone have been reported by Schneider et al. (1991) and Jackman et al. (1991). In both studies, the calculated interannual variation of the column ozone are of the same order as seen in the TOMS data.

Although there are similarities in the features of the large-scale transport used in each model, there are differences in the details of the transport as seen in the prescribed calculations of the Models and Measurements comparisons. For example, the models are not uniform in such features as the latitude range of the region of upward motion in the tropics and in the strength of the circulation as evidenced by the wide variation in the model lifetimes calculated by different models for tracers with prescribed removal rates (see Prather and Remsberg, 1993, Section O).

Representation of the Tropopause

Since the aircraft emissions are deposited close to the tropopause, the vertical resolution, the choice of coordinate system, and the treatment of tropopause height are important to these assessments. All models use pressure or log pressure as the vertical coordinate, with the exception of the CAMED model, which uses isentropic coordinates. The vertical resolution is 1 km for the AER, LLNL, and NCAR models, 2 km for the GSFC model, and about 3.5 km for the CAMED model. The tropopause height is specified as a function of latitudes and seasons and is typically defined in the model as the boundary where the values of K_{yy} and K_{zz} change from their large tropospheric values to their smaller stratospheric values.

Carbon-14 (^{14}C) atoms deposited in the stratosphere from atmospheric nuclear explosions are removed by strat/trop exchange. The observed concentrations of ^{14}C can be used to calibrate the transport rate in the models (Johnston et al., 1976 Johnston, 1989). This test is one of the exercises in the M & M Intercomparison (Prather and Remsberg, 1993, section I). Although such tests show that the models calculated residence times correspond to the correct magnitude, they do not provide any indication for the validity of the mechanisms. Cross-tropopause transport in the models is represented by advection and eddy flux across the boundary. At the model grid boxes where the tropopause height changes with latitude, the side of the grid box becomes part of the boundary. The horizontal diffusion across this boundary can be a substantial component of strat/trop exchange in some models (see Shia et al., 1993). However, this mechanism is probably not realistic.

DESCRIPTION OF PRESCRIBED SCENARIOS

A fleet of subsonic aircraft is assumed to be in operation prior to the introduction of the HSCT fleet. The scenarios used in the calculations assume that the size of the subsonic fleet will be slightly reduced when the HSCT fleet is deployed. The sizes of the two subsonic fleets are based on market research performed for the HSRP program. The ozone changes reported in this chapter correspond to the difference between the case when the HSCT fleet is operating with the modified subsonic fleet and the case with the unmodified subsonic fleet, but all other boundary conditions are the same. The reported changes are the steady-state responses of ozone to the continuous operation of a fleet of HSCT in the 2015 atmosphere. Given the residence time of the injected emissions and the photochemical lifetime of ozone in the lower stratosphere, the atmosphere should approach steady state after 3 to 5 years.

The boundary conditions for the 1990 and the 2015 atmospheres are given in Table 2. The chlorine loading for 2015 is 3.7 ppbv. Additional simulations are made in which the chlorine

level is reduced to 2.0 ppbv, a value expected by about 2060. In all simulations, it is assumed that the aerosol surface area remains the same at the prescribed background level.

The scenarios considered here are given in Table 3. The emissions from the aircraft (HSCT and subsonic) are as described in Chapter 3. In the simulations, they are deposited along the flight path and assumed to be zonally mixed instantaneously and distributed uniformly within the model grid box. Features with spatial scale smaller than the grid box are not resolved. No attempt is made to simulate the sub-grid processes.

Emissions from the aircraft include oxides of nitrogen, carbon dioxide, carbon monoxide, water vapor, unburned hydrocarbons, and sulfur oxides from sulfur in the fuel. The amount emitted is given as an emission index (EI), which is the amount emitted in grams per kilogram of fuel burned. These values are summarized in Table 4.

The model simulations include injections of NO_x , H_2O , CO , and unburned hydrocarbons as CH_4 . The emission of CO_2 is not included in the simulation. The effects of the CO_2 emitted by aircraft are likely to be no different from CO_2 emitted at the ground. Thus, the contribution to greenhouse warming can be estimated from the ratio of jet fuel to other fossil fuel. The effect of sulfur is also excluded. The amount of SO_2 emitted is unlikely to give large perturbations to the HO_x chemistry. None of the six models has incorporated the relevant microphysics model to calculate the aerosol distribution from gas sulfate. Recent analyses by Pitari et al. (1993) and Bekki and Pyle (1993) indicate that operation of a HSCT fleet may lead to up to a factor of 2 increase in aerosol loading in the northern hemisphere. The effect of aerosol increase will be discussed in the last section of this chapter.

CHANGES IN BACKGROUND CONCENTRATIONS OF THE EMITTED TRACE GASES

The residence time of the emitted species plays a role in determining the magnitude of the perturbation for any species in the aircraft exhaust. The residence time is determined by the photochemical lifetime if the species is photochemically active. Otherwise, the residence time is determined by transport in the lower stratosphere. As shown previously (Chapter 3A, Prather and Wesoky, 1991 Chapter 3, this report), large perturbations are expected for total odd nitrogen (NO_y) and H_2O . The magnitude of the changes in H_2O and NO_y are controlled by transport, since there are no significant photochemical removal processes in the lower stratosphere. The differences in the model-calculated changes in NO_y and H_2O result directly from the differences in the transport formulation in the different models.

NO_y and H_2O

Previous intercomparison studies (Chapter 5, Prather and Wesoky, 1991) showed that the residence time of the injected NO_y is a function of the cruise altitude; material injected at higher cruise altitudes has a longer residence time. The model-calculated residence time ranges from 0.5-0.8 years for the Mach 1.6 case and 1.1-1.5 years for the Mach 2.4 case.

The calculated changes in NO_y are shown in Figure 1a and 1b for the Mach 2.4, EI=15 and the Mach 1.6, EI=15 cases, respectively. For the most part, the models show similar behavior to each other. For NO_y , the largest absolute changes are seen in the lower stratosphere, near the flight altitude poleward of 30°N . For the purpose of analyzing the ozone response, it is also useful to examine the percent changes in NO_y concentration. The calculated percent change in NO_y for the Mach 1.6 and Mach 2.4, NO_x EI=15 cases are given as functions of height at 45°N for the two cases in Figures 2a and 2b, and as functions of latitude at cruise altitudes in Figures 2c and 2d. The cruise altitudes are 18-20 km for the Mach 2.4 fleet and 16-18 km for the Mach 1.6 case. Figures 2a and 2b show a much larger spread among the models below the injection

height. For the Mach 2.4 case, the model-calculated changes at 18 km (Figure 2c) range from 40% to 60% in the northern latitudes; 10% to 50% in the tropics; and a few percent to 20% in the southern latitudes. There is more spread in the tropics for the Mach 1.6 case (Figure 2d). Although the large percent change in the tropics is not expected to affect the calculated ozone, the cause for the large discrepancy among the models should be resolved.

The results for H₂O are shown in Figure 3. The corresponding percentage changes are shown in Figure 4. The difference between the NO_y response and the H₂O responses illustrates the dependence on the background concentrations adopted in the models (see Prather and Remsburg, 1993, section B).

The similarity of the behavior of the 2-D models does not necessarily indicate that these transport-controlled changes are modeled correctly. Three-dimensional models (Douglass et al., 1993) indicate the importance of middle latitude synoptic scale events to strat/trop exchange processes. Similar tracer calculations with 2-D and 3-D models show that the advective part of 2-D strat/trop exchange is placed poleward of 45°N, in contrast to 3-D calculations, which place strat/trop exchange at middle latitudes. For a tracer injected at middle latitudes, the strat/trop exchange is more rapid in the 3-D calculations than in 2-D calculations. This difference could result in substantially smaller perturbations to species such as NO_y and H₂O in the lower stratosphere than are currently calculated in a 2-D model.

CH₄ and CO

The increases in the concentrations of CH₄ and CO due to the emissions are much smaller compared with their background values than the changes in H₂O and NO_y (Chapter 3A, Prather and Wesoky, 1992 Chapter 3, this report). Both of these constituents also respond to the changes in OH concentration caused by injection of H₂O and NO_y. Their impact on ozone is calculated to be small.

CHANGES IN PHOTOCHEMICAL RATE

Changes in Radical Concentrations

Previous studies have established that the first-order effect from aircraft emissions is the increase in the local concentration of NO_y (Johnston, 1971). In the absence of repartitioning, the increase in NO_y should lead to proportional increases in the concentrations of the active nitrogen species, thus enhancing the ozone removal rate associated with the NO_x cycle. However, there may be adjustment of the other cycles. Previous calculations using gas-phase chemistry showed that the adjustments in the other cycles had a small effect on the ozone removal rate, because reactions with NO_x radicals constituted about 60% of the local removal in the lower stratosphere (see Weisenstein et al., 1991). The calculated ozone response was almost linearly related to the change in NO_y in the lower stratosphere. With the inclusion of the heterogeneous reaction N₂O₅+H₂O, reactions with HO_x radicals become the major ozone removal process. As a result, injected H₂O plays a larger role than in the gas-phase chemistry case. In addition, adjustments in other radicals as a result of the NO_y increase has a significant impact on the ozone removal rate.

The model-calculated changes in NO₂ for the Mach 2.4, EI=15 case are shown in Figure 5. The model results show that the NO₂/NO_y ratio changes by less than 8% in all the cases considered. Thus, the increase in NO₂ is expected to be the same as the increase in NO_y, i.e., about 60% for the mach 2.4, NO_x EI=15 case.

The response for OH and HO₂ is more complicated. The 20% increase in H₂O is expected to lead to increases in OH and HO₂. However, the added NO_y also enhances the local removal rate of OH through the reactions of OH + HNO₃ and OH + HNO₄. In addition, OH removed by the

reaction of OH + NO₂ can be regenerated through photolysis of HNO₃, this could affect the OH concentration on a seasonal basis. Finally, photolysis of HNO₃ formed from the heterogeneous reactions also constitutes a net source for OH. The model-calculated percent change for HO₂ and OH are shown in Figures 6 and 7. The model calculations showed decreases in HO₂ (up to 30%) and in OH (up to 10%) in the lower stratosphere at middle and high latitudes.

Decreases ranging from 20% to 40% are calculated for ClO for both the 3.5 ppbv (see Figure 8) and 2.0 ppbv cases for total chlorine. The decrease in ClO is due to formation of ClONO₂. There is little change in the HCl reservoir.

Changes in Ozone Removal Rates

Figures 9a and 9b show the calculated changes in the local removal rate of ozone at 47°N for the different scenarios for June and December, respectively. The results are from the AER model. As discussed in Weisenstein et al., 1991 the removal rates around 20 km correspond to ozone lifetimes of 4 years in winter and 0.7 years in summer. Thus, the ozone concentration in the lower stratosphere is not expected to exhibit photochemical response and decrease in proportion to the calculated changes in the removal rate.

The results in Figure 5 and the discussion above showed that there is a 60% increase in NO₂ for the Mach 2.4, NO_x EI=15 case around 20 km. Yet, the ozone removal rate only increases by 5% in winter and 15% in summer at the same altitude. This is due to the adjustments in the other chemical cycles. Figure 10 shows a breakdown of the removal rate by cycles for the 2015 atmosphere with the modified subsonic fleet (Experiment 2). In summer, the NO_x cycle and HO_x cycle contribute about equally (35% each) to the ozone removal rate at 20 km. In winter, the role of NO_x is greatly diminished to about 10%. Figure 11 shows absolute (not percentage) changes in each cycle for the Mach 2.4, EI-15 case. In summer, the increase in the NO_x cycle is more than compensated by the decrease in the HO_x cycle below 16 km. As a result there is a decrease in the ozone removal rate. At 20 km, the net increase in the ozone removal rate is about 20% smaller than the changes due to the NO_x cycles because of compensation from the HO_x and ClO_x cycles. The change in the ozone removal rate is much smaller in winter than in summer with the ClO_x cycle playing a larger role.

CHANGES IN OZONE

Role of Transport

The local concentration of ozone ([O₃]) in a region can be written in the form

$$\frac{d[O_3]}{dt} = P + I - (L + T)[O_3]$$

where P is the local photochemical production rate, I is the rate ozone is transported into the region, L[O₃] is the local photochemical removal rate, and T[O₃] is the rate ozone is exported out of the region. If we annually average the above equation, we obtain the approximate expression that

$$[O_3] = \frac{P+I}{L+T} \text{ and } \frac{\Delta[O_3]}{[O_3]} = \frac{\Delta L}{L} \frac{L}{L+T}$$

where ΔL is the change in the photochemical removal rate and Δ[O₃] is the change in local concentration in response to ΔL. In the midlatitude lower stratosphere, L is the same order of magnitude as T so that we expect $\frac{L}{L+T}$ to be about 1/3 to 1/2.

Model Results for the Prescribed Scenarios

The calculated changes in the column abundance of ozone are summarized in Tables 5a and 5b. The results show a systematic ordering within each model. For the same emission, a fleet flying at higher altitude has a larger effect on ozone. For the Mach 2.4 fleet, a fleet with larger EI for NO_x also depletes more ozone. The response in column ozone is a result of the decrease in the middle and lower stratosphere coupled with an increase in the upper troposphere. For the Mach 1.6 fleet, the emissions are deposited close to the tropopause. Depending on the treatment of the injected H_2O and NO_x , the calculated tropospheric increase may overwhelm the calculated stratospheric decrease. As a result, fleets with larger EI may have smaller decrease or larger increase in ozone. This appears to be the case for the OSLO model. The GSFC and AER models show similar effect although the calculated changes in ozone are sufficiently small so that the number may not be significant.

Figure 12 shows the calculated local changes in ozone for the Mach 2.4, NO_x EI=15 case. The calculated ozone depletions in the lower stratosphere are typically between 1% to 2% in the southern hemisphere. The calculated decrease in the CAMED model is small, consistent with the results that the increase in NO_y is also small. The calculated maximum change at the northern polar region ranges from 2% in the AER, GSFC, and OSLO models to 5% in the LLNL and NCAR model. Note that the calculated percent decrease reaches a maximum near 30 km in most models. This indicates that the amount of NO_x transported out of the region dominated by heterogeneous chemistry will have a large impact on the calculated ozone changes.

The calculated changes in the troposphere also show some differences among the models. The region of ozone increase is indicative of the position of the tropopause and the rate of strat/trop transport. However, it should be noted that the 2-D models do not contain all the necessary mechanisms for calculating the NO_x budget, the hydrocarbon budget, and the ozone budget in the troposphere.

The calculated changes in column ozone are shown in Figure 13 for the scenarios. The calculated ozone decrease in Scenario D is about 1% to 2% at 60°N, 0.5% at the equator and southern hemisphere. The positive column change in the CAMED model indicate that the tropospheric O_3 increases outweigh the stratospheric losses. For the Mach 1.6, EI=15, case (Figure 13b) an ozone decrease of less than -1% at 60°N is found in most models. The changes in the tropics range from -0.4% to +0.4%. In the southern hemisphere it ranges from -0.6% to +0.4%.

The results presented here are similar to those obtained using the old emission data (see Prather and Wesoky, 1991; Stolarski and Wesoky, 1993). Based on the set of calculations reported there, the calculated ozone depletion for gas-phase chemistry should be about a factor of 3 larger than the heterogeneous case for the Mach 2.4, EI=15 case. Discussion in Chapter 6 indicated that there are indications that reaction (7.1) may be occurring slower than what is assumed in the calculations. If that is the case, the ozone depletion would be larger than what is presented here.

Sensitivity to Chlorine Background

The results for the Mach 2.4 EI=15 case relative to the 2.0 ppbv chlorine background are shown in Figure 14. All models show larger calculated depletion than the 3.7 ppbv chlorine background case, indicating that compensation from the chlorine cycle is less effective. Results from the AER model show that the percent compensation in the ClO_x cycle is the same in both cases. However, with the chlorine cycle playing a much smaller role in the 2-ppbv background, the effect on the ozone removal rate is much smaller.

Sensitivity to Transport Feedback

The CAMED model calculates the circulation for each experiment. The results show an ozone increase in the tropics for all the cases. This region of increased ozone is particularly noticeable in the spring just south of 30°N. It is not clear if this ozone increase is an effect of the change in circulation or some other model difference. Note that all other models produce a positive ozone change in the tropics; it is only in the CAMED model that this increase is larger than the decrease calculated at higher altitudes.

Role of Emitted CH₄ and CO

Previous simulations using gas-phase chemistry indicated that the ozone response is controlled by NO_x and that the H₂O with CO and hydrocarbons do little to modify the ozone response. With inclusion of heterogeneous chemistry, the effect of H₂O emission is enhanced. Additional simulations performed using the AER model and the GSFC model indicate that the calculated ozone depletion would be about 20% smaller if only the NO_y emission were used. The effects from CO and the unburned hydrocarbons are still minimal.

OTHER UNCERTAINTIES

Change in Aerosol Surface

It has been pointed out that since jet fuel contains traces of sulfur, SO₂ is emitted during engine operation. Operation of both the subsonic and HSCT fleets may increase the loading and size distribution in the sulfate layer. This could have an effect on ozone because of the changes in the heterogeneous conversion rate and changes in the circulation in the atmosphere.

Recent model studies indicate that there will be a 50% increase in the aerosol loading relative to the model-calculated background for a sulfur EI of 1 (Pitari et al., 1993) and up to a factor of 2 assuming a sulfur EI of 2 (Bekki and Pyle, 1993). The effect of the simultaneous increase in aerosol on calculated ozone depletion is within 20% of the case calculated with fixed aerosol. Although the effects from the emitted NO_x is smaller with the simultaneous increase of the aerosol, there is an increase in the chlorine-related ozone removal. The results are consistent with the findings of Weisenstein et al. (1993) which show the effect from an assumed factor of 4 increase in aerosol. The work of Weisenstein et al (1993) examines only the effect of aerosol on the heterogeneous conversion rate. The work of Bekki et al. (1993) and Pitari et al. (1993) also take into account the effect of changes in circulation.

PSC Chemistry

The results reported in Tables 5a and 5b do not include the effect of PSC chemistry in the polar regions. How this omission may affect the calculated ozone depletion depends on whether the added NO_x and H₂O change the occurrence of PSCs. If there is no change in PSC occurrence, operation of the HSCT fleet would alleviate the ozone depletion in the polar region, as some of the ClO produced by heterogeneous reactions on PSC surfaces would combine with the added NO_x to form ClONO₂.

On the other hand, increases in NO_x and H₂O may result in more frequent formation of PSCs and may even make possible formation of NAT in polluted midlatitude corridors or in the tropics. A key difference in the ozone behavior in the polar vortices (north versus south) is the broadscale denitrification (permanent removal of odd nitrogen species from the stratosphere) that takes place in the Antarctic. It is not clear whether increases in H₂O and NO_x, as well as

possible increases in the number of condensation nuclei, could trigger denitrification in the Arctic. In this case, there may be more chlorine activation leading to larger ozone depletion in the vortices.

Estimates of the potential increases in both Type I and Type II PSC formation due to stratospheric aircraft emissions have been made by Peter et al. (1991). This study considers the increase resulting from increases in HNO_3 and H_2O in both Type I and Type II PSC formation at 70°N at 30 mb and 50 mb, for all months. The study concludes that the introduction of a HSCT fleet could substantially increase the probability of both Type I and Type II PSC formation.

Estimates of the increase in Type I PSC incidence and the impact on stratospheric ozone levels have been made by Considine et al. (1993). This study calculates the potential increases in Type I PSCs from a stratospheric aircraft perturbation and uses a 2-D photochemical model to calculate the subsequent chemical effects on ozone. The effects of the increased PSC formation on predictions of HSCT-induced ozone depletion are calculated to be minor.

PSC chemistry is treated in a version of the NCAR model. Type I and Type II PSCs are formed when the calculated zonal-mean temperature falls below 195 K and 191 K, respectively. In the presence of PSCs, all HCl and ClONO_2 are converted to active chlorine. With Type I PSCs, there is also denitrification with a time constant of 30 days. With Type II PSCs, dehydration and denitrification occurs with a time constant of 5 days. Additional calculations from NCAR indicate that the increase in H_2O and the ozone change from the HSCT emissions could cause a cooling of 0.5 K to 1 K in the lower stratosphere at northern latitudes. Using available data, they estimated that the threshold temperature for PSC formation may increase by up to 0.3 K.

The results presented by Pitari et al. (1993) show that NAT formation is enhanced when the sulfate loading increases. Their results show that the residence time of the injected NO_y can be 40% shorter due to removal of NO_y by denitrification and sedimentation of ice particles. As a result, the calculated ozone decrease is also 40% smaller.

Large uncertainties remain for estimates of the effect of PSC chemistry. More definitive conclusions must await better understandings of the microphysics of cloud formation, how processes in the polar region affect O_3 at midlatitudes, and the importance of heterogeneous reactions involving chlorine species if NAT occurs at middle and tropical latitudes.

Details of Plume Evolution

The source function for the emitted materials used in the calculations is assumed to have the same latitude-height distribution as the flight paths, and the chemical composition is assumed to be identical to that of the emission at the tail pipe. Chemical transformation, occurring via homogeneous and heterogeneous reactions, may alter the composition of the materials (see discussion in Chapter 3). However, the effect on calculated ozone changes is expected to be small unless a significant amount of NO_y is removed in the plume by the denitrification process. Plume subsidence and subsequent dispersion in the first few weeks before the emitted materials become zonally mixed could provide an effective distribution of sources that differs from the flight paths.

The possibility that the emitted material may not be well mixed zonally raised the question of the importance of the proper treatment of nonlinear chemistry (Tuck, 1979) and chemical eddies (Pyle and Rogers, 1980). Recent results from Jadin and Bromberg (1991) showed their treatment of chemical eddies resulted in a decrease in calculated ozone loss due to more efficient removal of NO_x in the lower stratosphere.

ACKNOWLEDGMENTS

Numerous persons contributed to the success of this effort. We would like to thank the modeling groups that delivered the model results in a timely fashion, the support of the Upper Atmosphere Data Program at NASA Langley, and all those that helped to prepare and review this chapter. Special thanks go to Linda Hunt and Karen Sage from NASA Langley who generated the numbers for the tables and the graphics in this chapter.

Table 1. Models Providing Results in the Assessment

AER	Atmospheric and Environmental Research Inc.,	M. Ko and D. Weisenstein
CAMED-ø	University of Cambridge and University of Edinburgh	J. Pyle, R. Harwood, and J. Kinnnersley
GSFC	NASA Goddard Space Flight Center	C. Jackman, A. Douglass, E. Fleming, and D. Considine
LLNL	Lawrence Livermore Laboratory	D. Wuebbles and D. Kinnison
NCAR	National Center for Atmospheric Research	G. Brasseur and X. Tie
OSLO	University of Oslo	I. Isaksen

Table 2. Boundary Conditions for Background Atmospheres

Species	Concentration in "1990"- 3.3 ppb Chlorine	Concentration in "2015"-3.7 ppb Chlorine	Concentration in "2015"-2.0 ppb Chlorine
CFC-11	253 ppt	260 ppt	124 ppt
CFC-12	434 ppt	510 ppt	359 ppt
CFC-113	44 ppt	70 ppt	49 ppt
CFC-114	7 ppt	10 ppt	7.8 ppt
CFC-115	5 ppt	8 ppt	7.2 ppt
CCl ₄	103 ppt	100 ppt	34 ppt
HCFC-22	92 ppt	200 ppt	3.7 ppt
CH ₃ CCl ₃	145 ppt	150 ppt	0 ppt
Halon-1301	2.6 ppt	6 ppt	2.6 ppt
Halon-1211	2.0 ppt	2 ppt	0.2 ppt
CH ₃ Cl	600 ppt	600 ppt	600 ppt
CH ₃ Br	15 ppt	15 ppt	15 ppt
N ₂ O	308 ppb	330 ppb	330 ppb
CH ₄	1685 ppb	2050 ppb	2050 ppb
CO ₂	350 ppm	390 ppm	390 ppm

Note:

Units, mixing ratio by volume : 1 ppt = 1 part per trillion, 1 ppb = 1 part per billion, 1 ppm = 1 part per million.

The total chlorine content is about 3.7 ppb in the "2015" atmosphere.

While it is recognized that other boundary conditions affecting tropospheric chemistry such as CO and NO_x will change with time, it is recommended that each model keeps its present day reference troposphere unchanged in the simulations.

Table 3. Summary of Assessment Scenarios

Experiment	Aircraft [†]	Mach number & NO _x EI for HSCT	Chlorine Background
I	Modified subsonic + HSCT, scenario C	Mach 1.6, EI=5	3.7 ppbv
II	Modified subsonic + HSCT, scenario D	Mach 1.6, EI=15	3.7 ppbv
III	Modified subsonic + HSCT, scenario E	Mach 2.4, EI=5	3.7 ppbv
IV	Modified subsonic + HSCT, scenario F	Mach 2.4, EI=15	3.7 ppbv
V	Modified subsonic + HSCT, scenario D	Mach 2.4, EI=15	2.0 ppbv
VI	Modified subsonic + HSCT, scenario G	Mach 2.4, EI=45	3.7 ppbv

*Change in ozone is calculated relative to the background atmosphere with a subsonic fleet as described in scenario B in Chapter 3, subchapter 3-1.

†Scenarios are defined in Chapter 3, subchapter 3-1.

Table 4. Emission Indices

Emission Indices gm/kg Fuel		
Species	Subsonic	HSCT
NO _x	As specified	As specified
H ₂ O	1230	1230
CO	1.1	1.5 (1.2-3.0)
HC (as CH ₄)	0.2	0.2 (0.02-0.5)
SO ₂	1.1	1.0
CO ₂	3160	3160

Table 5a. Calculated Percent Change in the Annual Averaged Column Content of Ozone Between 40°N and 50°N

Scenarios	AER	GSFC	LLNL	OSLO	CAMED	NCAR
I: Mach 1.6, NOX EI=5*	-0.04	-0.11	-0.22	0.04	0.69	-0.01
II: Mach 1.6, NOX EI=15*	-0.02	-0.07	-0.57	0.15	0.48	-0.60
III: Mach 2.4, NOX EI=5*	-0.47	-0.29	-0.58	-0.47	0.38	-0.26
IV: Mach 2.4, NOX EI=15*	-1.2	-0.86	-2.1	-1.3	-0.45	-1.8
V: Mach 2.4, NOX EI=15†	-2.0	-1.3	-2.7	-0.42	-1.1	-2.3
VI: Mach 2.4, NOX EI=45*	-5.5	-4.1	-8.3	-3.5	-2.8	-6.9

Table 5b. Calculated Percent Change in the Annual Averaged Content of Ozone in the Northern Hemisphere

Scenarios	AER	GSFC	LLNL	OSLO	CAMED	NCAR
I: Mach 1.6, NOX EI=5*	-0.04	-0.12	-0.18	0.02	0.63	-0.04
II: Mach 1.6, NOX EI=15*	-0.02	-0.14	-0.48	0.10	0.63	-0.54
III: Mach 2.4, NOX EI=5*	-0.42	-0.27	-0.50	-0.39	0.25	-0.25
IV: Mach 2.4, NOX EI=15*	-1.0	-0.80	-1.8	-1.0	-0.26	-1.5
V: Mach 2.4, NOX EI=15†	-1.7	-1.2	-2.3	-0.43	-0.80	-1.9
VI: Mach 2.4, NOX EI=45*	-4.6	-3.6	-7.0	-3.1	-2.1	-5.1

*Relative to a background atmosphere with chlorine loading of 3.7 ppbv, corresponding to the year 2015.

†Relative to a background atmosphere with chlorine loading of 2.0 ppbv, corresponding to the year 2060.

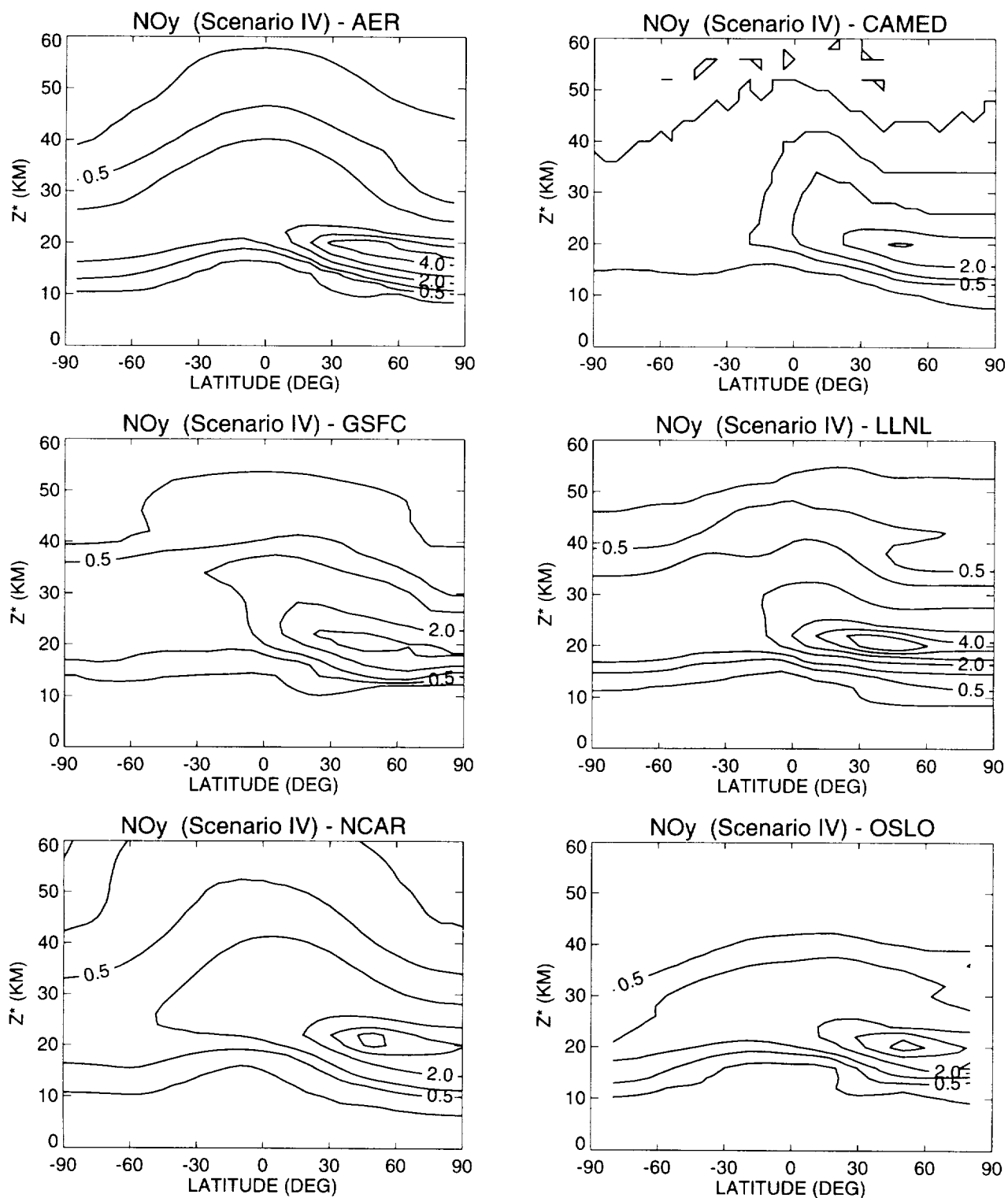


Figure 1a. Calculated changes in the local concentration of NO_y (ppbv) in June for the Mach 2.4 (EI=15) case. The contour intervals are 1 ppbv, 2 ppbv, 3ppbv, 4 ppbv and 5 ppbv.

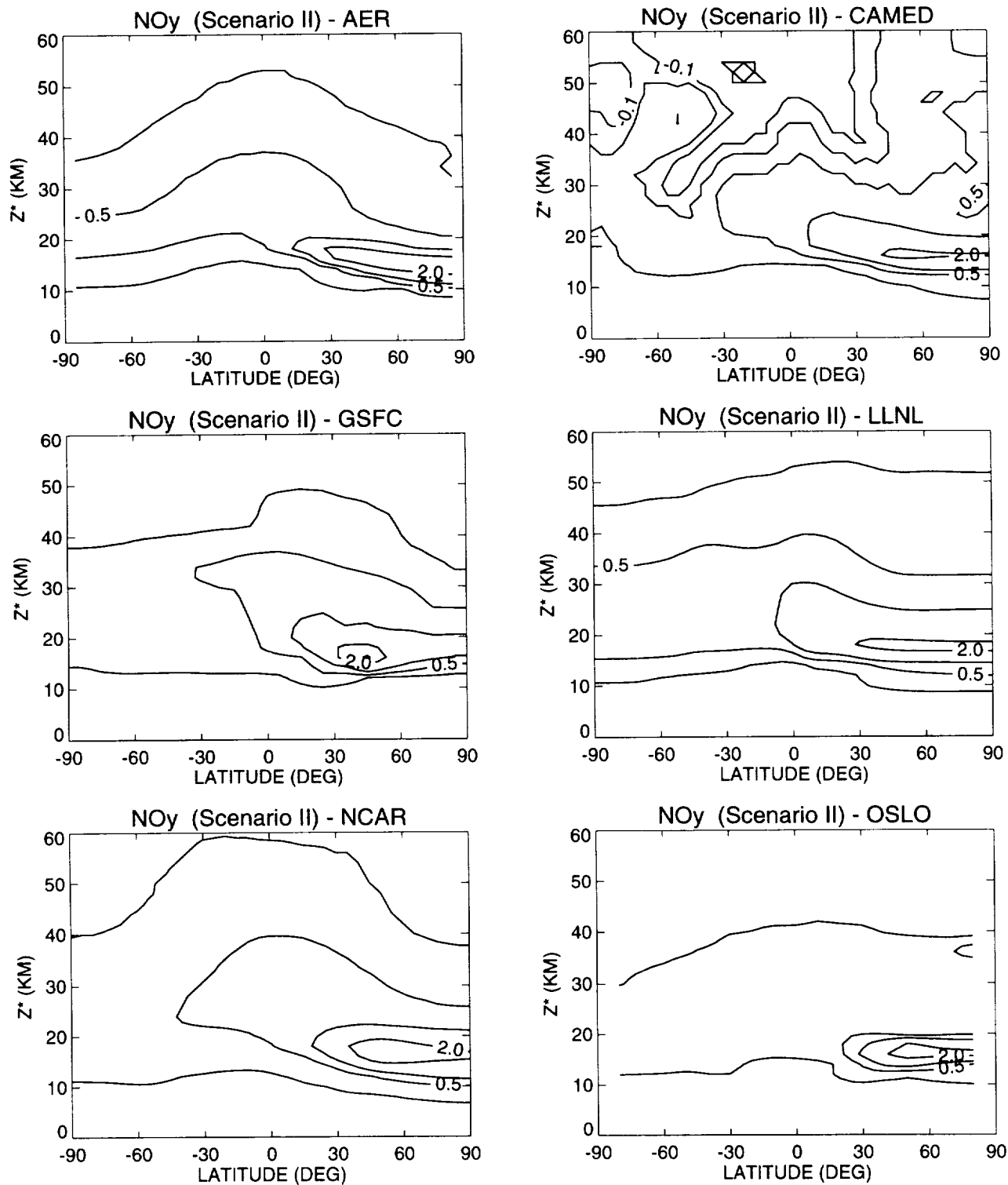


Figure 1b. Calculated changes in the local concentration of NO_y (ppbv) in June for the Mach 1.6 (EI=15) case. The contour intervals are 1 ppbv, 2 ppbv, 3ppbv, 4 ppbv and 5 ppbv.

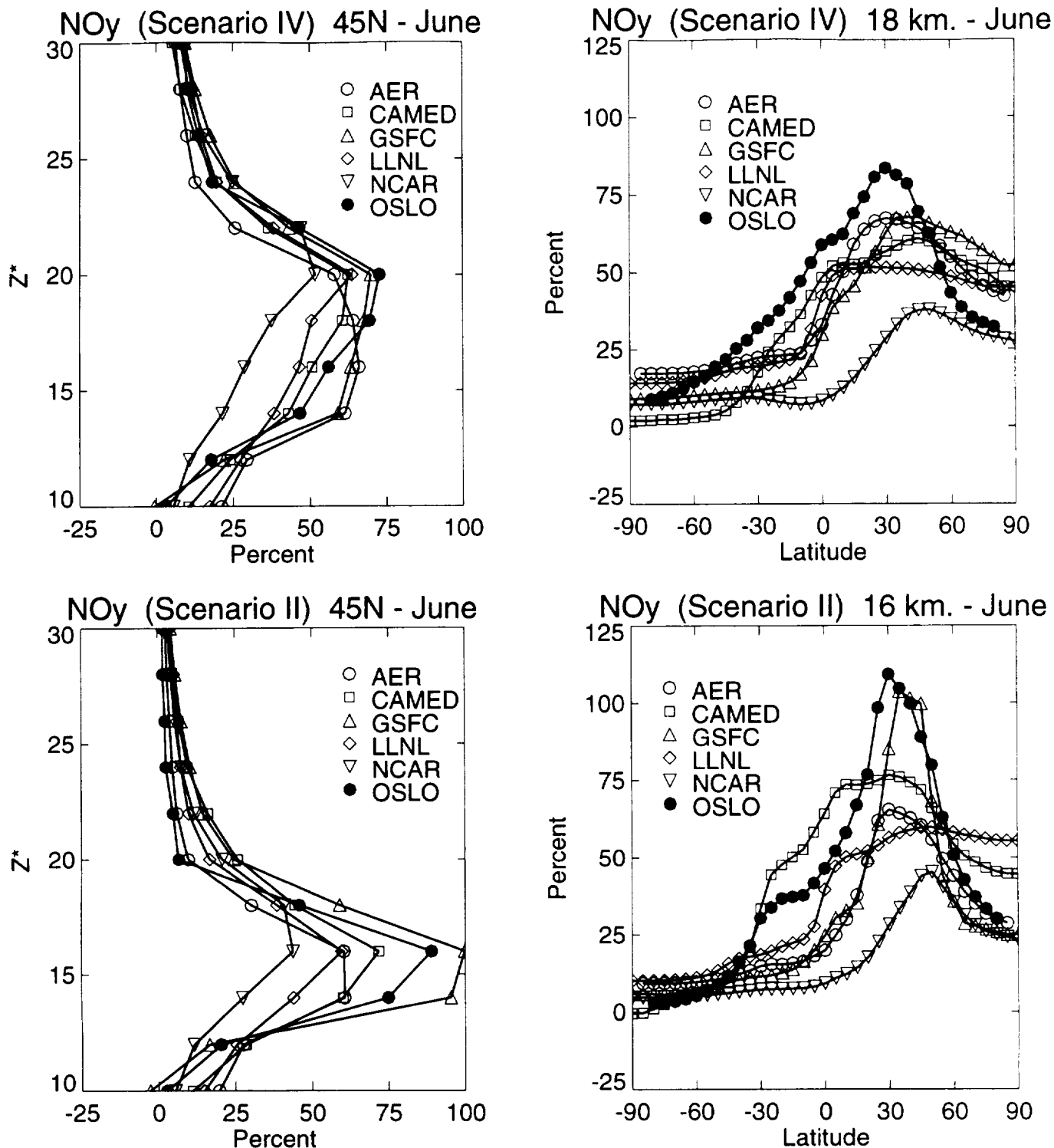


Figure 2. Model calculated percent change in concentrations of NO_y : Panel (a) Calculated altitude profile for the percent change of NO_y for the Mach 2.4, NO_x EI=15 case at 45°N for June. Panel (b) Calculated altitude profile for the percent change of NO_y for the Mach 1.6, NO_x EI=15 case at 45°N for June. Panel (c) Calculated latitude profile for the percent change of NO_y for the Mach 2.4, NO_x EI=15 case at 18 km for June. Panel (d) Calculated latitude profile for the percent change of NO_y for the Mach 1.6, NO_x EI=15 case at 16 km for June.

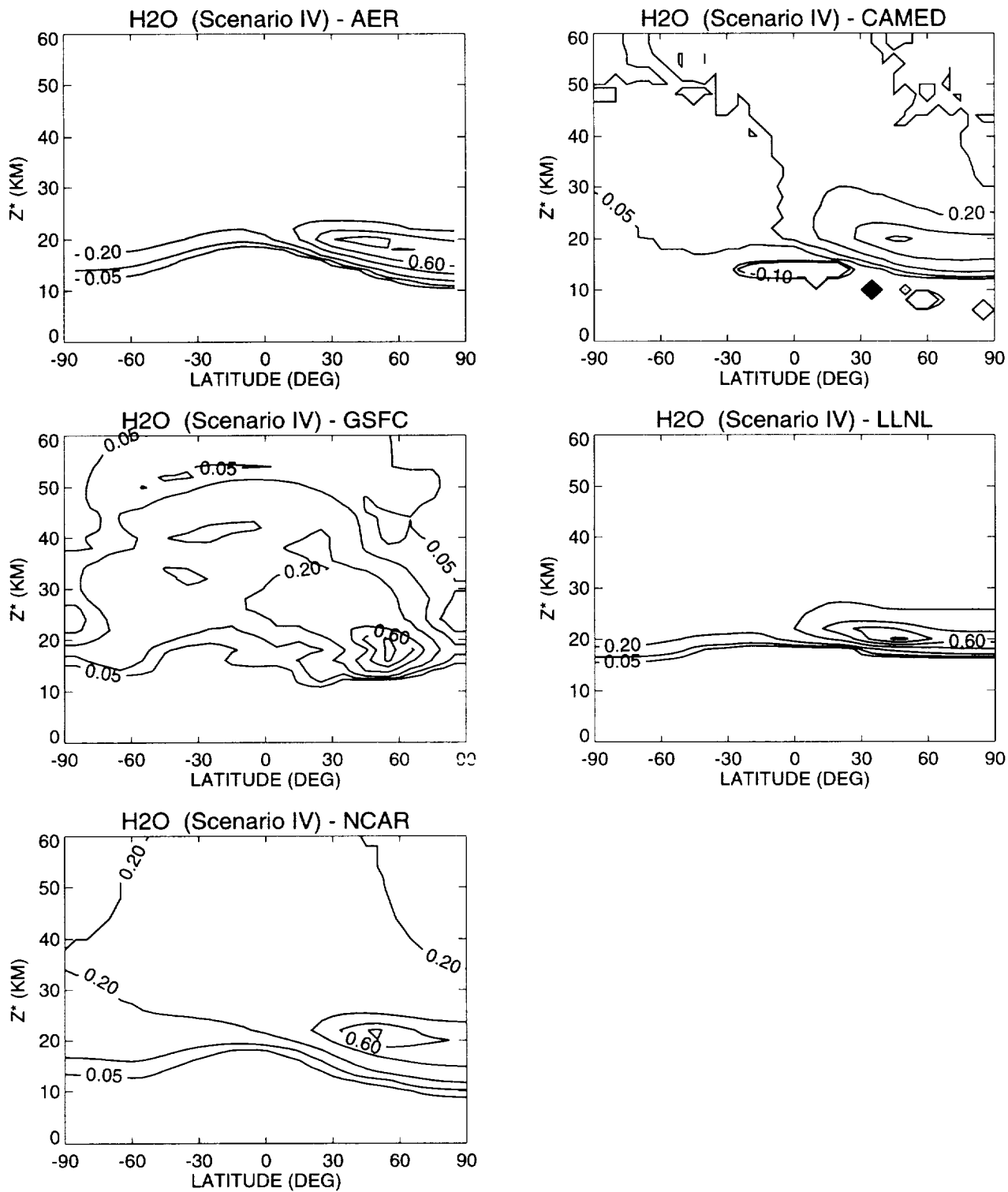


Figure 3a. Calculated changes in the local concentration of H_2O (ppmv) in June for the Mach 2.4 (EI=15) case. The contour intervals are 0.1 ppmv, 0.2 ppmv, 0.4 ppmv, 0.6 ppmv, 0.8 ppmv, 1 ppmv.

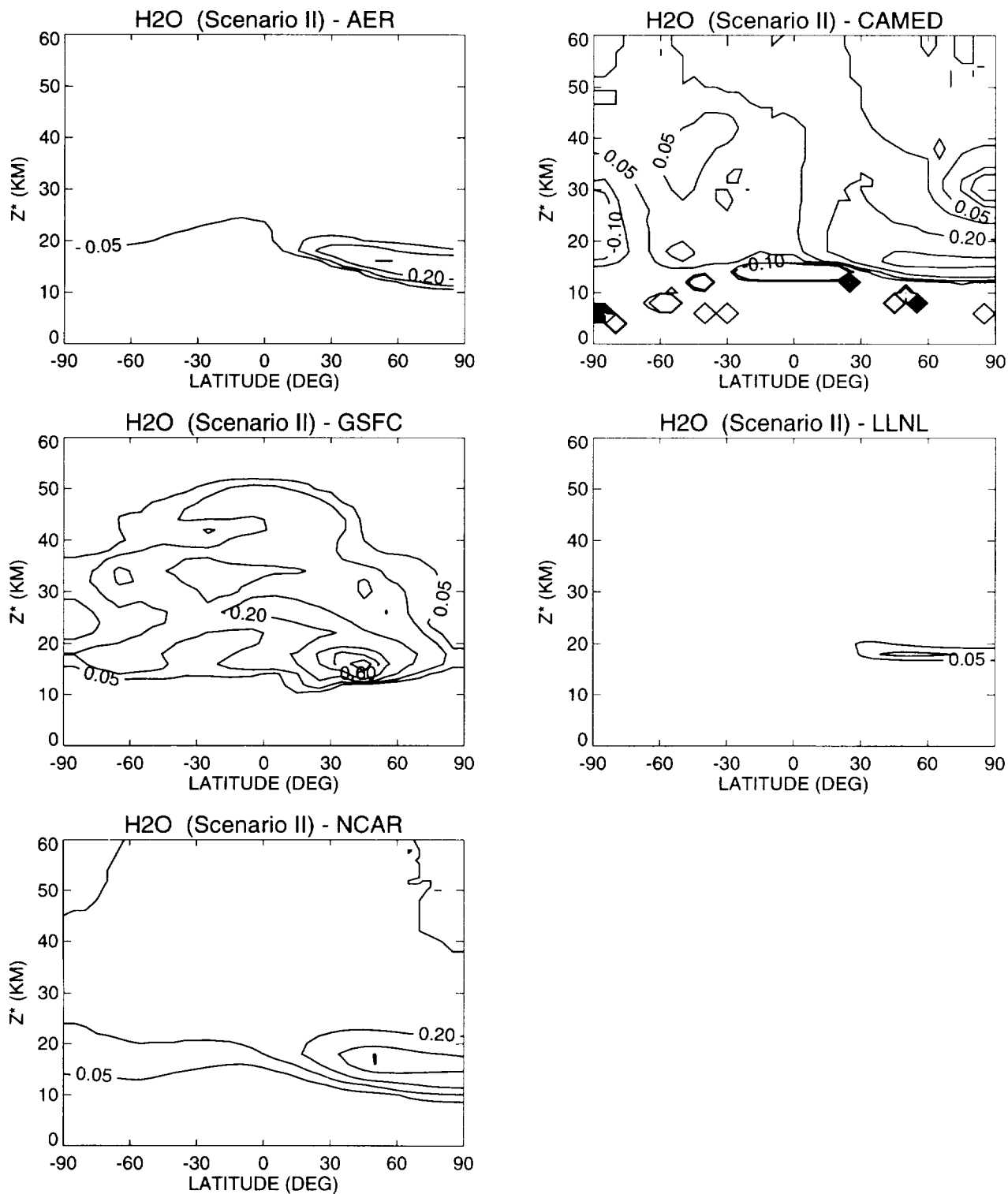


Figure 3b. Calculated changes in the local concentration of H_2O (ppmv) in June for the Mach 1.6 (EI=15) case. The contour intervals are 0.1 ppmv, 0.2 ppmv, 0.4 ppmv, 0.6 ppmv, 0.8 ppmv, 1 ppmv.

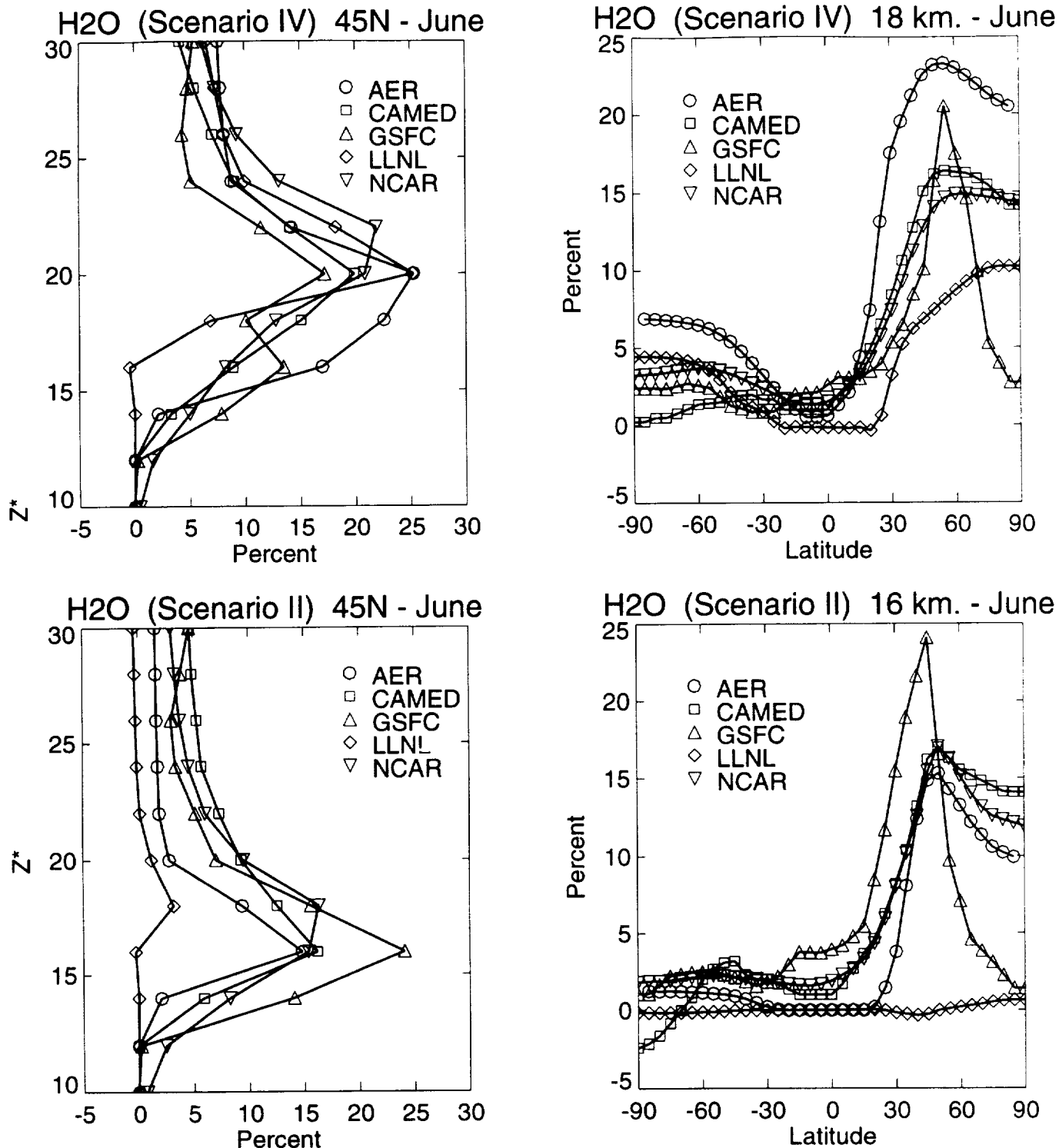


Figure 4. Model calculated percent change in concentrations of H_2O : Panel (a) Calculated altitude profile for the percent change of H_2O for the Mach 2.4 case at $45^\circ N$ for June. Panel (b) Calculated altitude profile for the percent change of H_2O for the Mach 1.6 case at $45^\circ N$ for June. Panel (c) Calculated latitude profile for the percent change of H_2O for the Mach 2.4 case at 18 km for June. Panel (d) Calculated latitude profile for the percent change of H_2O for the Mach 1.6 case at 16 km for June.

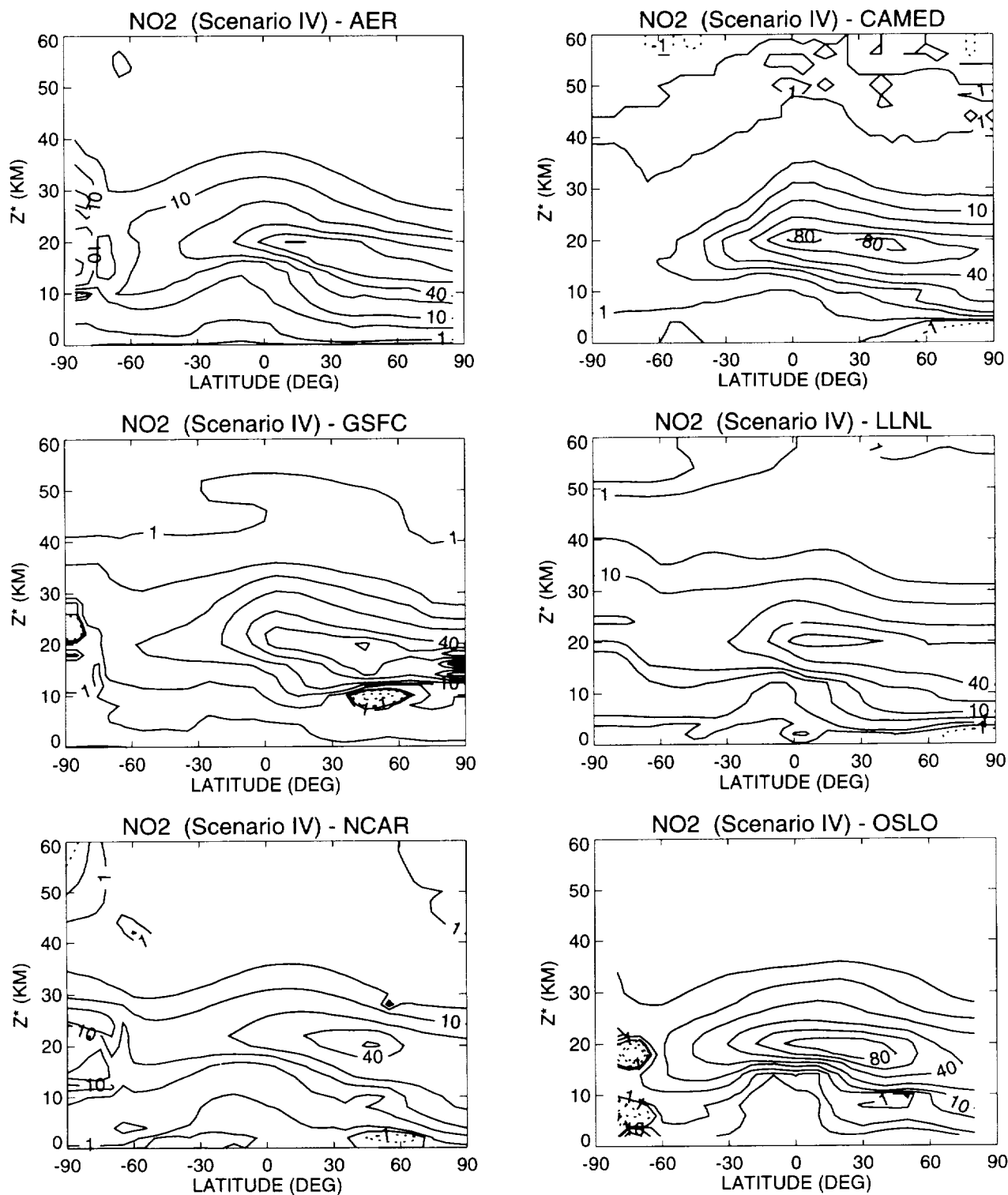


Figure 5. Calculated percent changes in the local concentration of NO₂ in June for the Mach 2.4 (El=15) case. The contour levels are 0%, 1%, 5%, 10%, 20%, 40%, 60%, 80%, 100%.

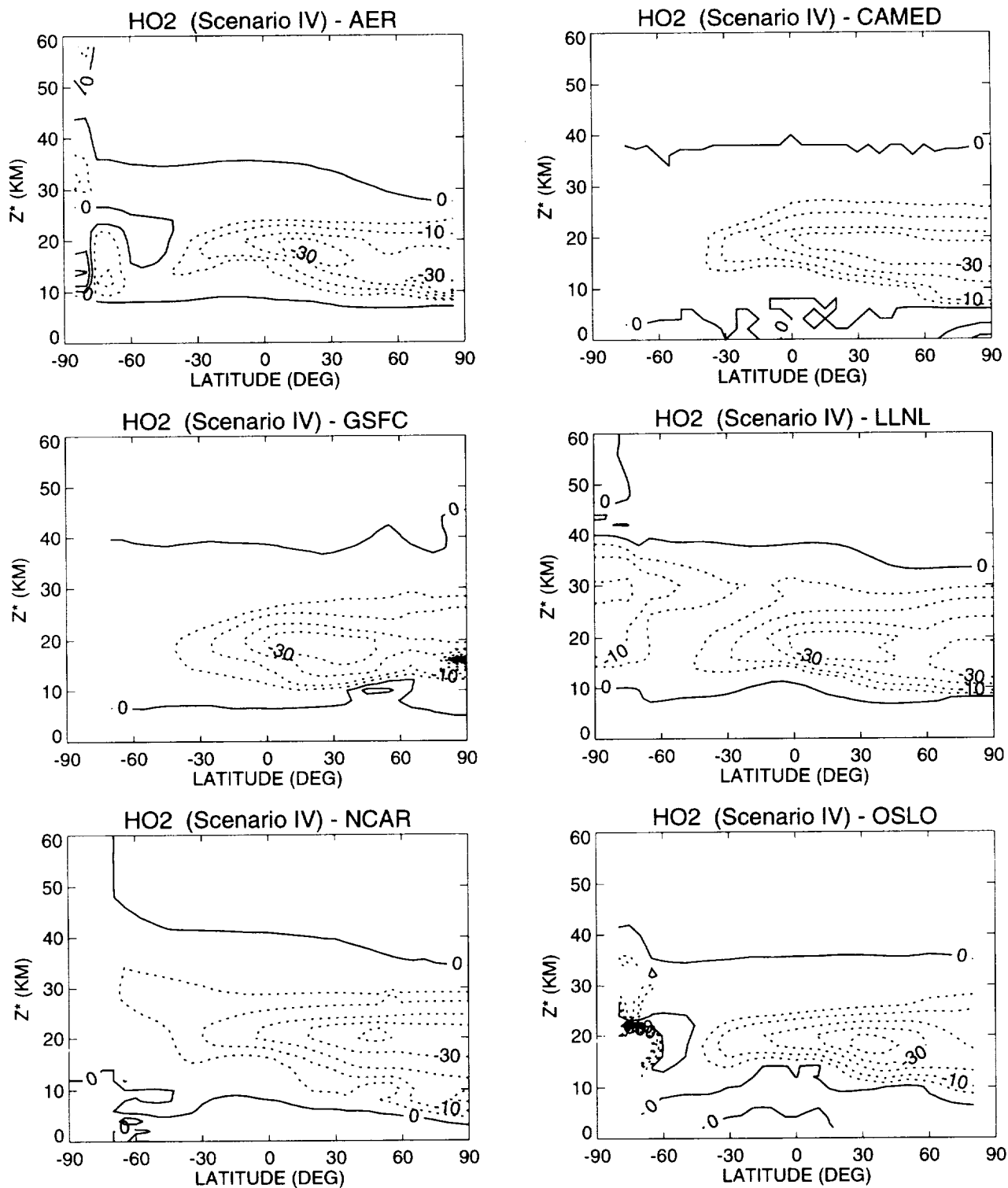


Figure 6. Calculated percent changes in the local concentration of HO_2 in June for the Mach 2.4 ($\text{EI}=15$) case. The contour levels are -50%, -40%, -20%, -10%, -5%, 0%.

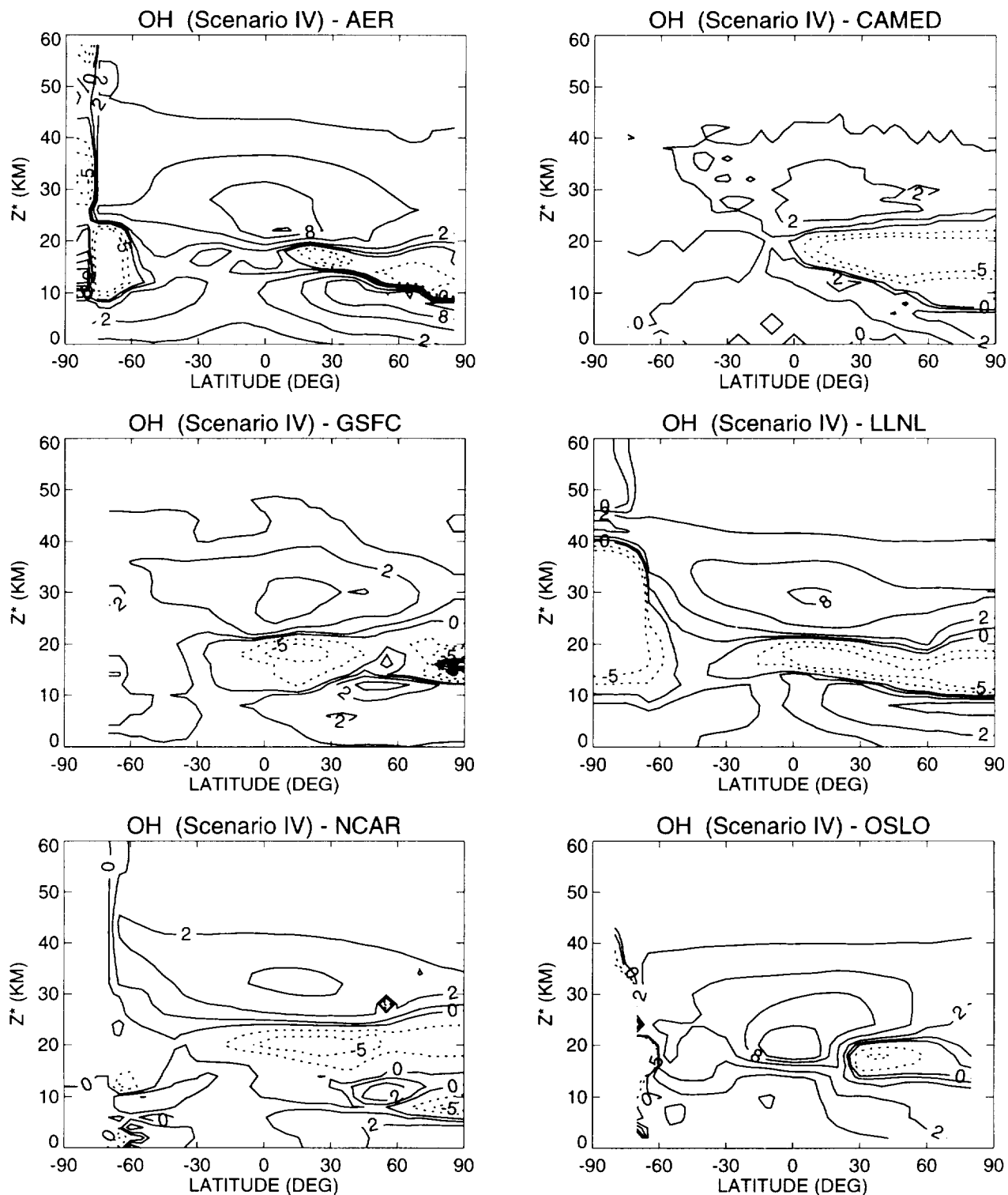


Figure 7. Calculated percent changes in the local concentration of OH in June for the Mach 2.4 (EI=15) case. The contour levels are -5%, -2.5%, 0%, 1%, 2.5%, 5%, 7.5%, 10%.

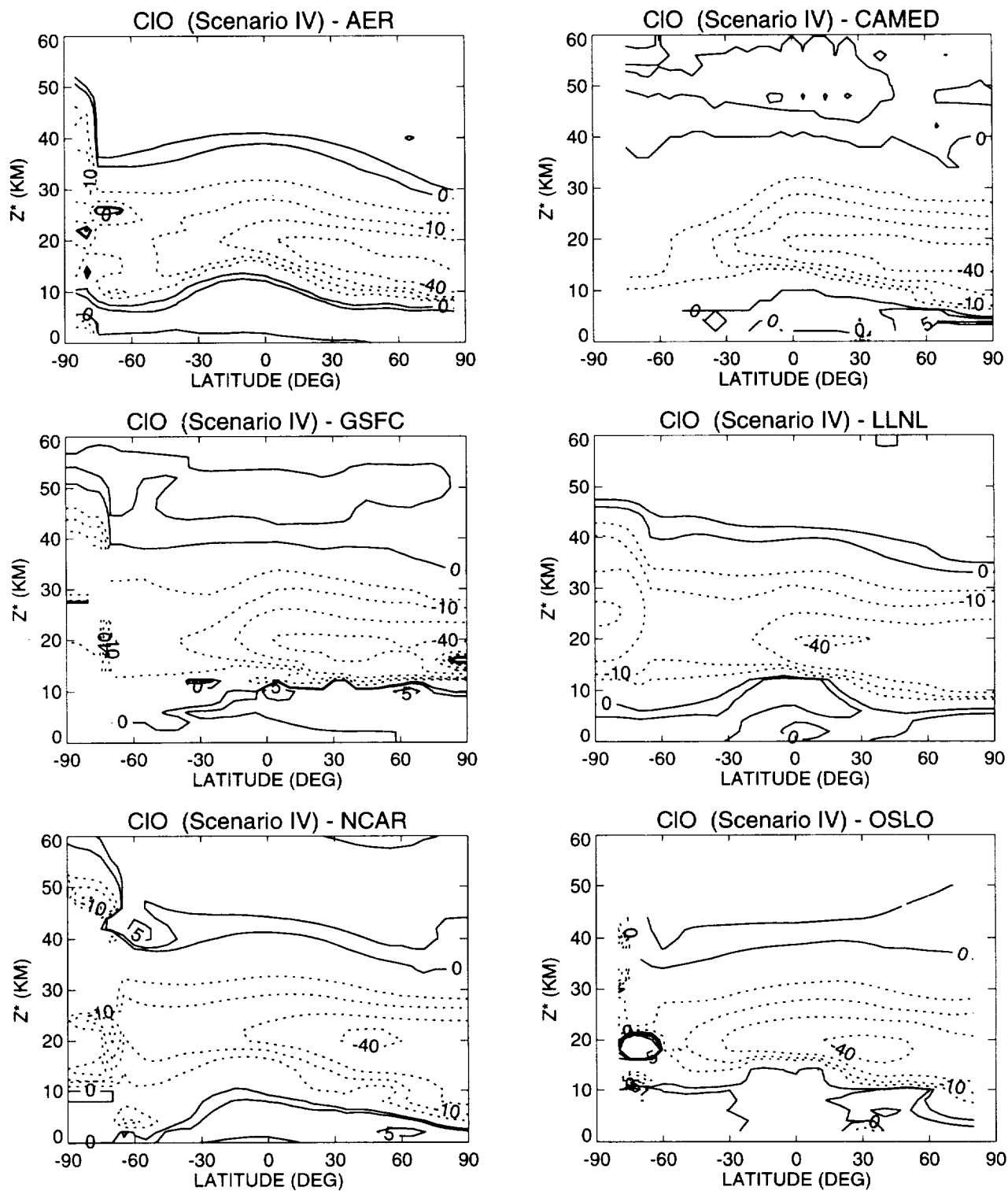


Figure 8. Calculated percent changes in the local concentration of CIO in June for the Mach 2.4 (EI=15) case. The contour levels are -80%, -60%, -40%, -20%, -10%, -5%, 0%.

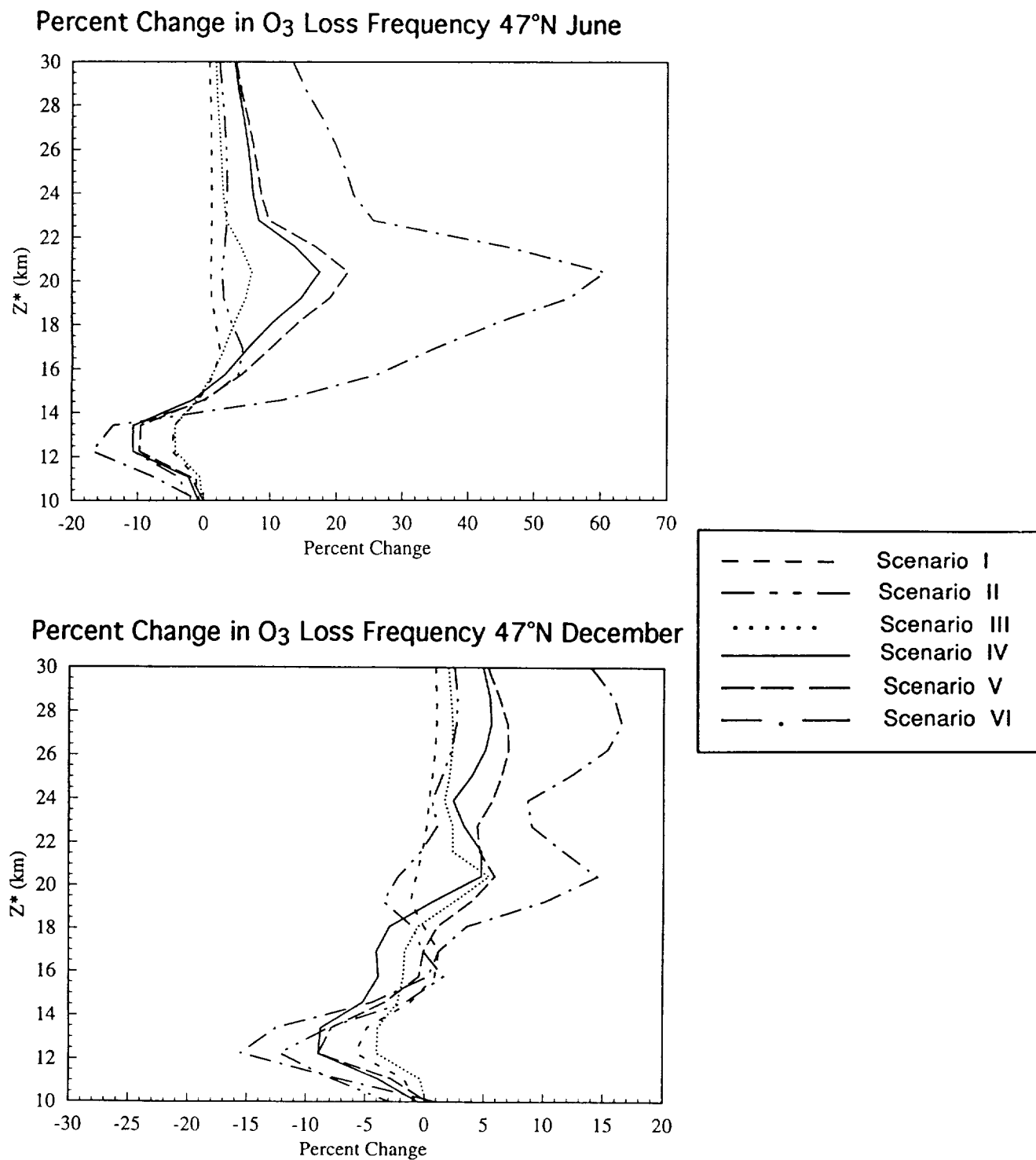


Figure 9. Calculated percent change in the photochemical removal rate of ozone at 47°N for Summer (panel a) and Winter (panel b) for different scenarios. The results are from the AER model.

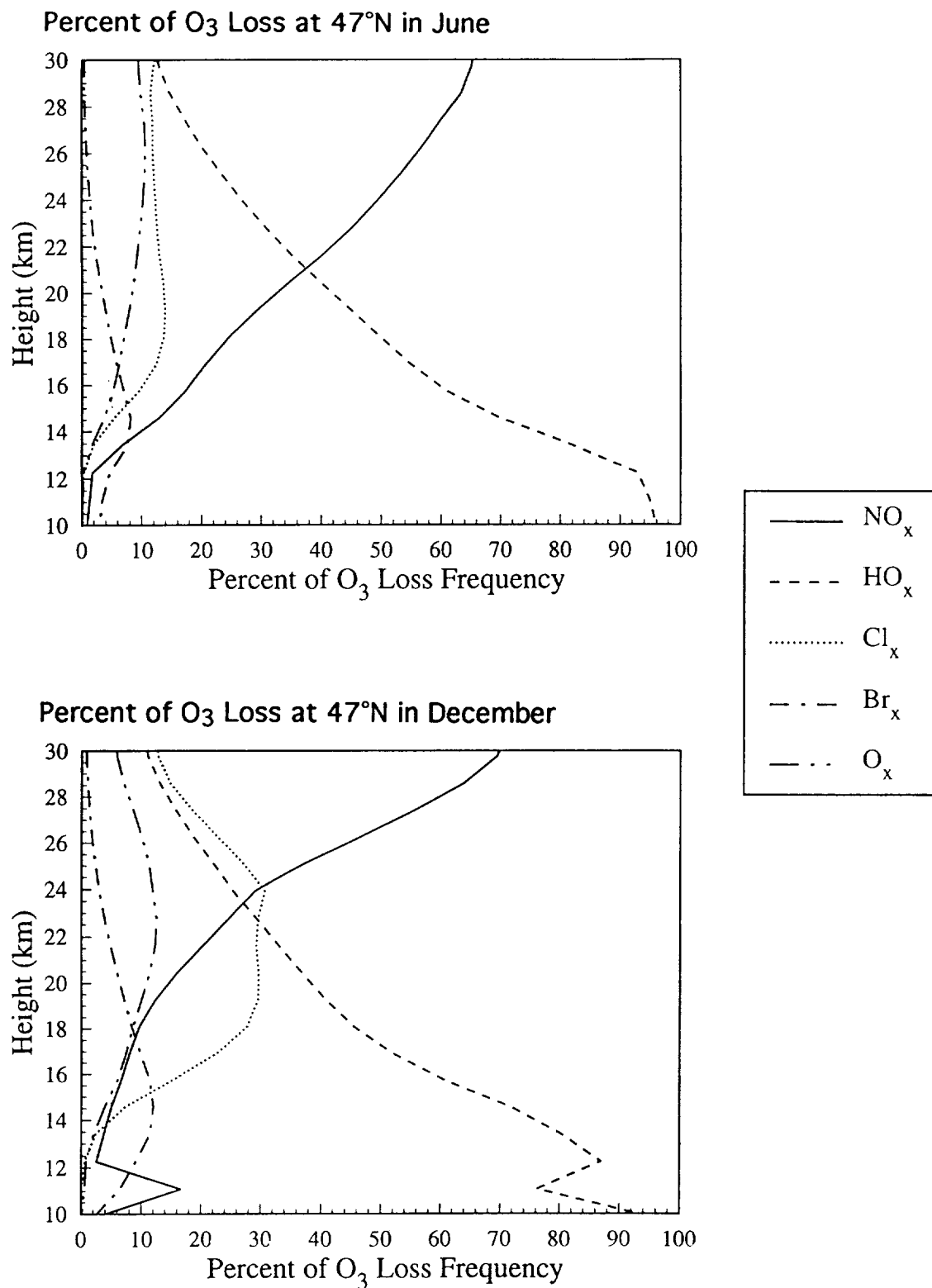


Figure 10. The percent contribution from the different cycles to the local photochemical removal rate of ozone. The results are from the AER model for the 2015 atmosphere with subsonic aircraft.

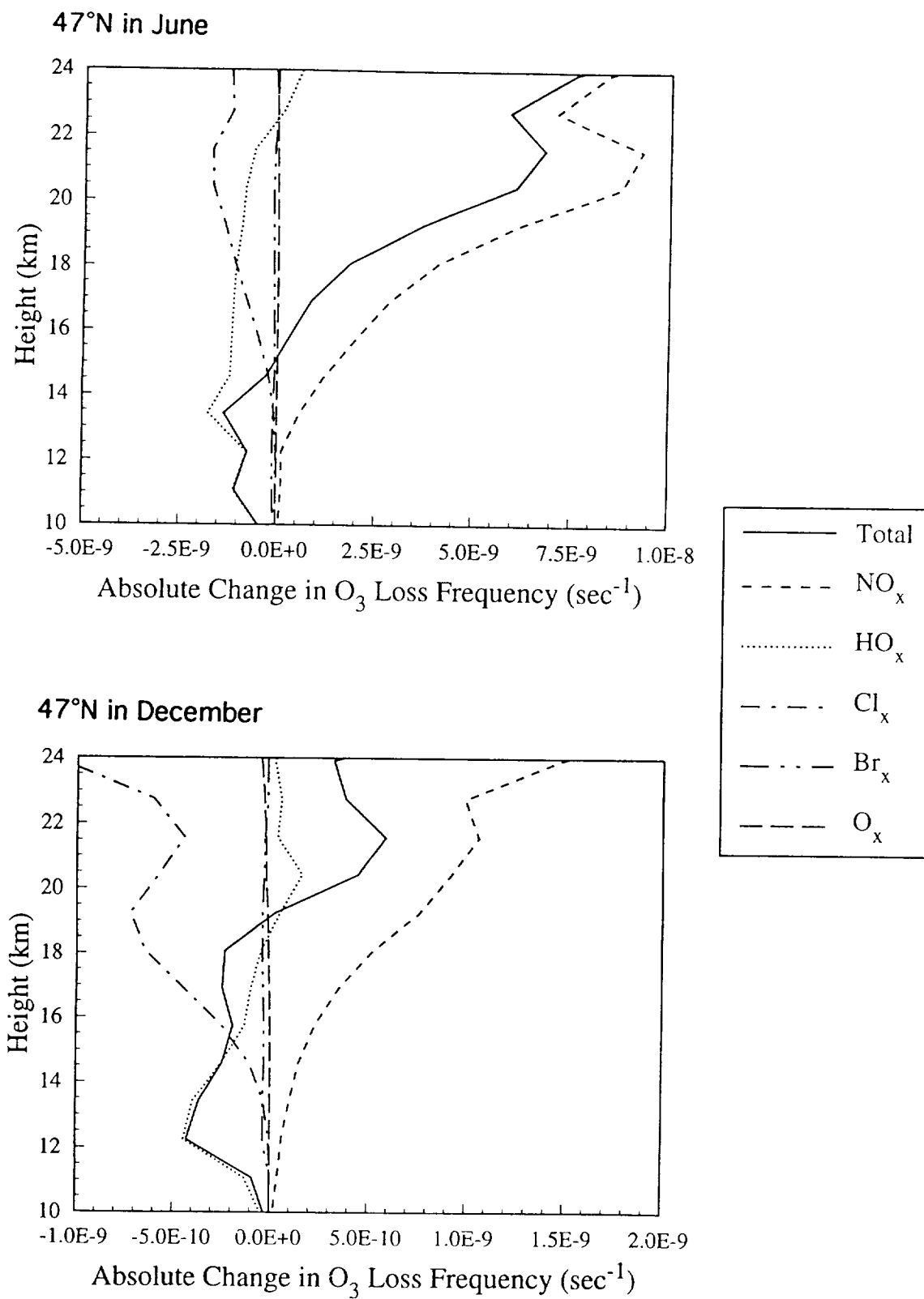


Figure 11. The model-calculated change in each of the chemical cycles. The results are from the AER model for the Mach 2.4, NO_x EI=15 fleet in the 2015 atmosphere.

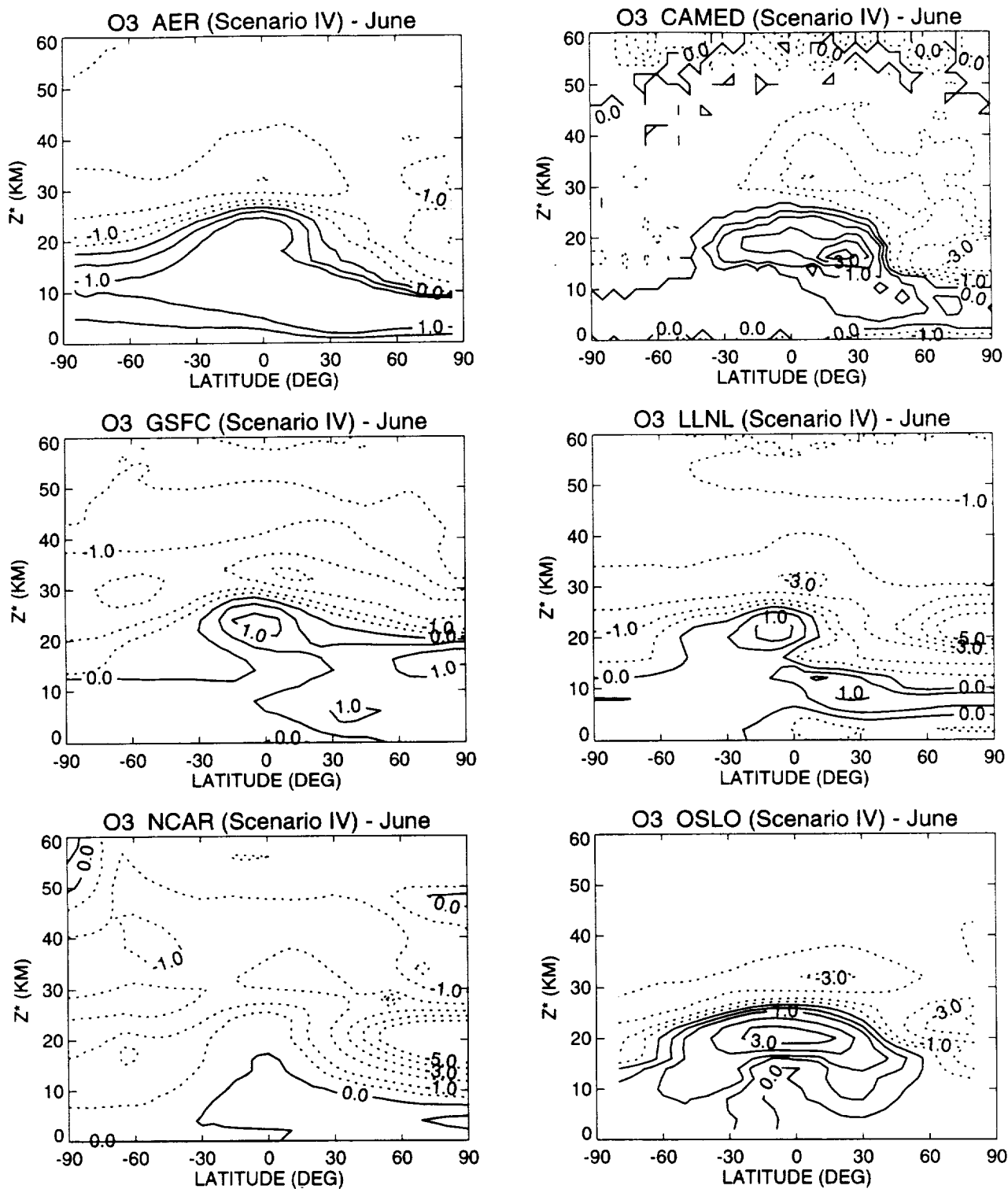


Figure 12. Model-calculated percent change in local ozone for June for the Mach 2.4, NO_x EI=15 fleet in the 2015 atmosphere. The contour intervals are -4%, -3%, -2%-1%, -0.5%, 0%, 0.5%, 1%, 2%, 3%, 4%.

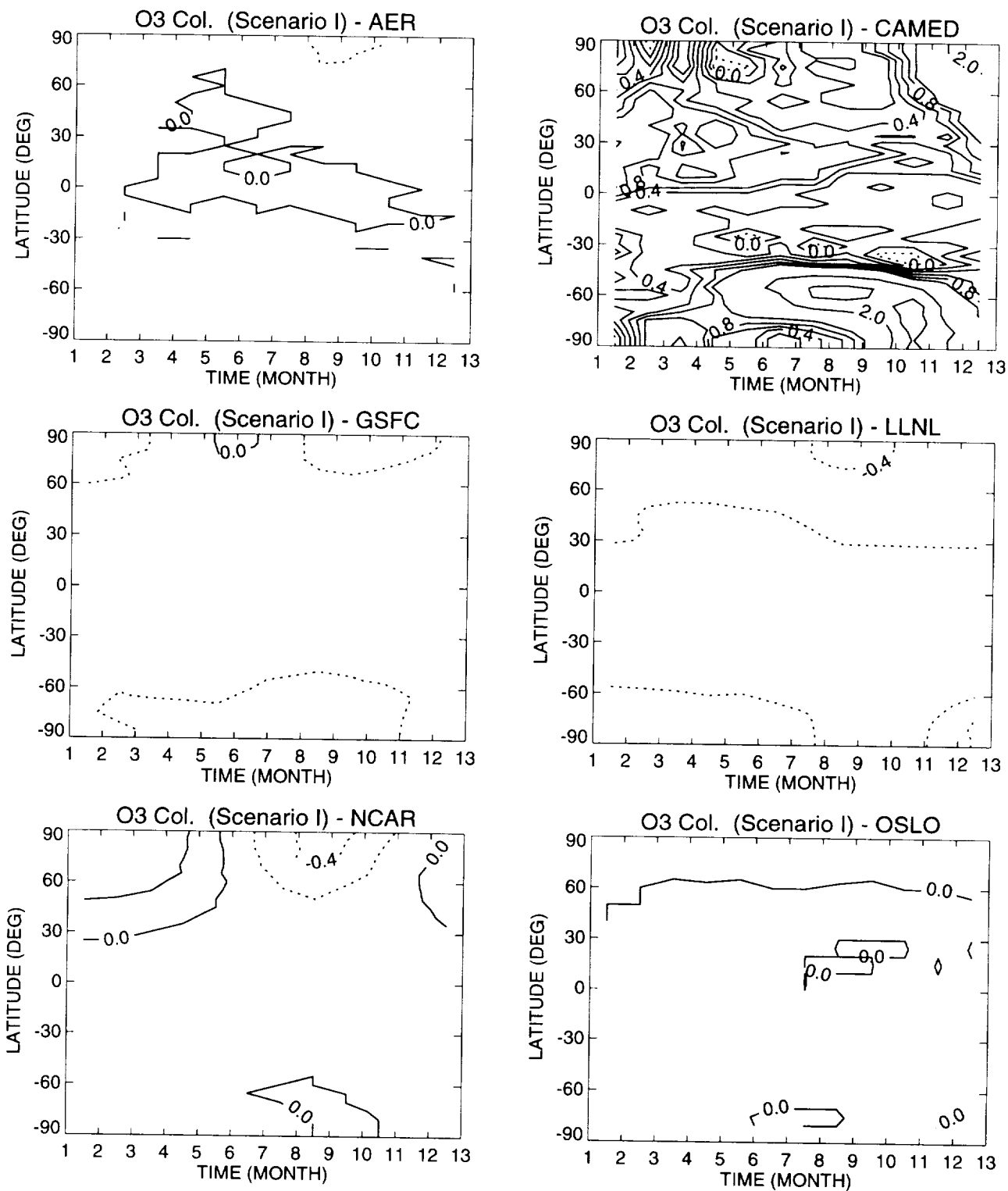


Figure 13a. Model-calculated change in the column abundance of ozone for the Mach 1.6 (EI=5) case in the 2015 atmosphere. The contour intervals are -6%, -5%, -4%, -3%, -2%, -1%, -0.8%, -0.6%, -0.4%, -0.2%, 0%, 0.2%, 0.4%, 0.6%, 0.8%, 1%, 2%.

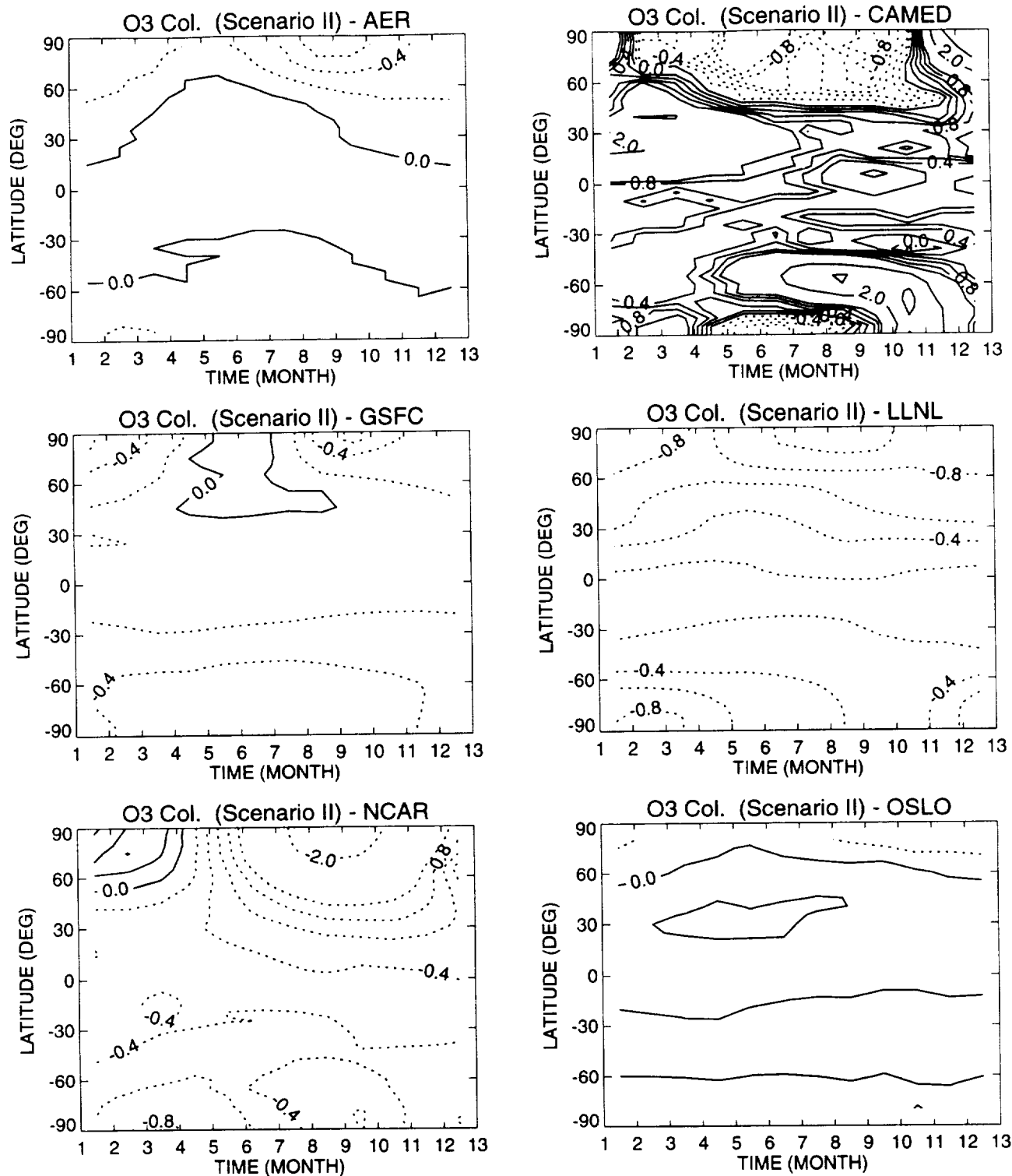


Figure 13b. Model-calculated change in the column abundance of ozone for the Mach 1.6 (El=15) case in the 2015 atmosphere. The contour intervals are -6%, -5%, -4%, -3%, -2%, -1%, -0.8%, -0.6%, -0.4%, -0.2%, 0%, 0.2%, 0.4%, 0.6%, 0.8%, 1%, 2%.

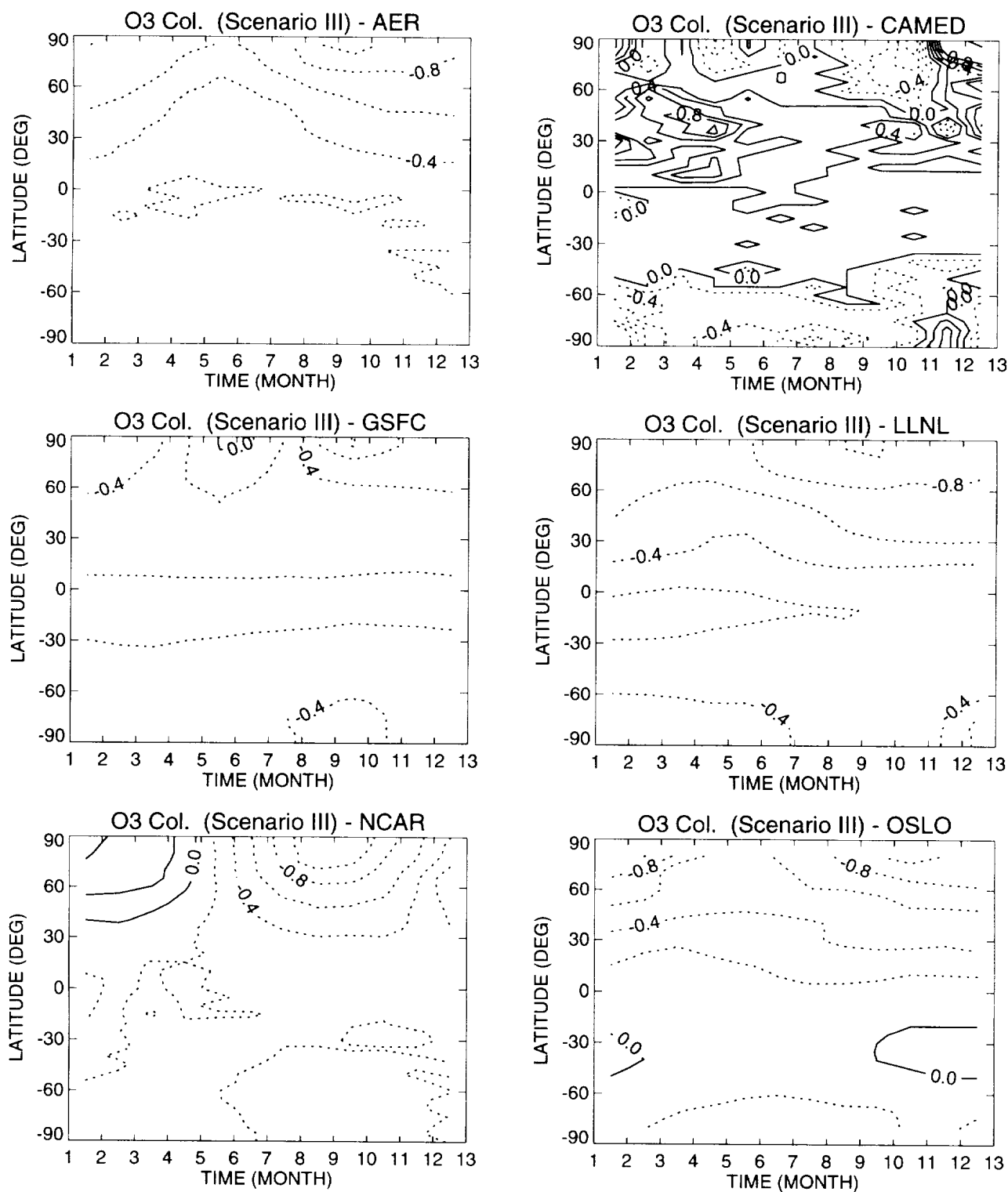


Figure 13c. The model-calculated change in the column abundance of ozone for the Mach 2.4 (EI=5) case in the 2015 atmosphere. The contour intervals are -6%, -5%, -4%, -3%, -2%, -1%, -0.8%, -0.6%, -0.4%, -0.2%, 0%, 0.2%, 0.4%, 0.6%, 0.8%, 1%, 2%.

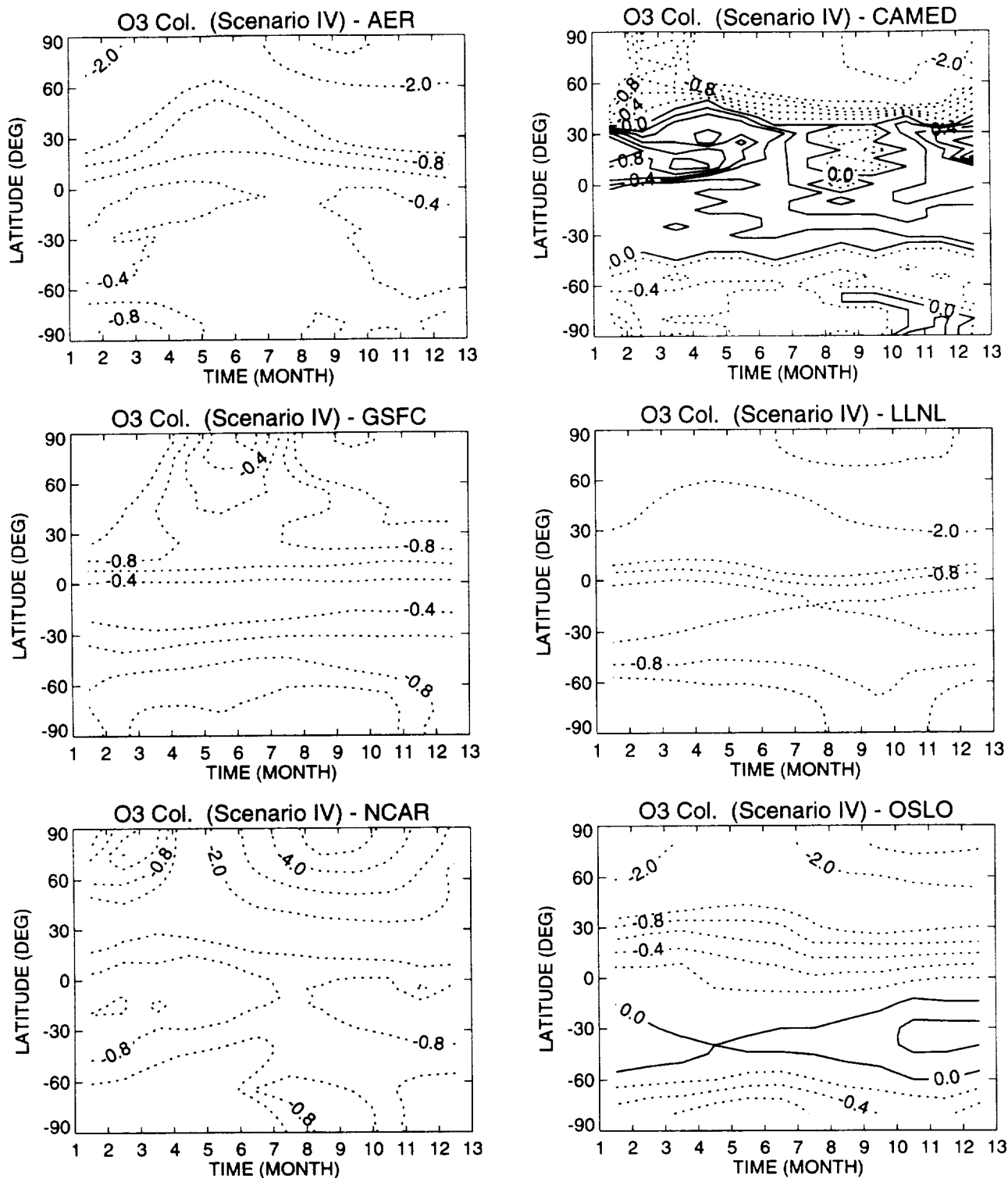


Figure 13d. The model-calculated change in the column abundance of ozone for the Mach 2.4 (EI=15) case in the 2015 atmosphere. The contour intervals are -6%, -5%, -4%, -3%, -2%, -1%, -0.8%, -0.6%, -0.4%, -0.2%, 0%, 0.2%, 0.4%, 0.6%, 0.8%, 1%, 2%.

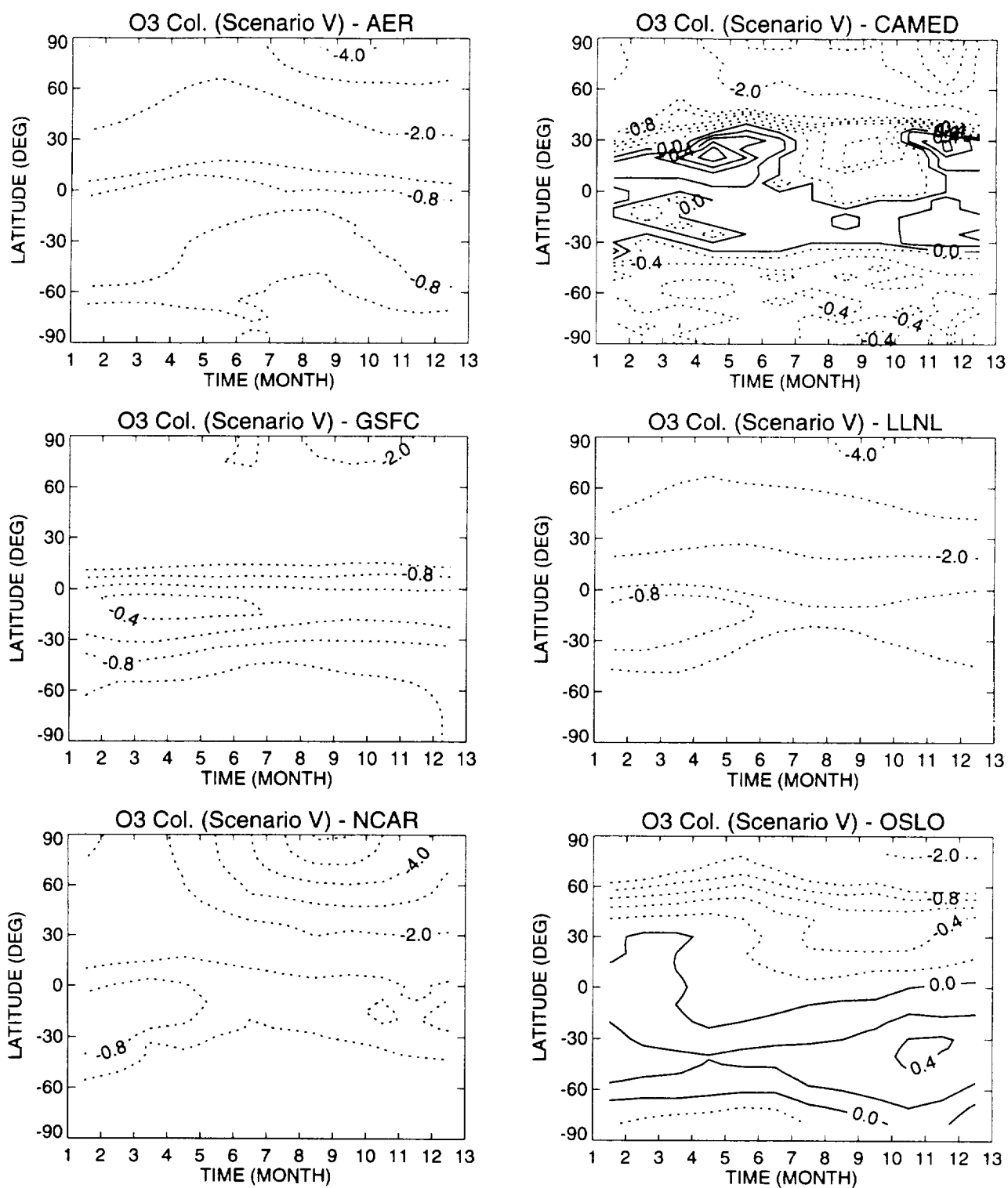


Figure 14. Model-calculated change in the column abundance of ozone for the Mach 2.4, NO_y EI=15 fleet in the 2.0 ppbv chlorine background. The contour intervals are -6%, -5%, -4%, -3%, -2%, -1%, -0.8%, -0.6%, -0.4%, -0.2%, 0%, 0.2%, 0.4%, 0.6%, 0.8%, 1%, 2%.

REFERENCES

- Bekki, S., and J. A. Pyle, Potential impact of combined NO_x and SO_x emissions from high speed civil transport aircraft on stratospheric aerosols and ozone, *Geophys. Res. Lett.*, 20, 723-726, 1993.
- Bekki, S., R. Toumi, J. A. Pyle, and A. E. Jones, Future aircraft and global ozone, *Nature*, 354, 193-194, 1991.
- Considine D. B., A. R. Douglass, and C. H. Jackman, Effects of a parameterization of nitric acid trihydrate cloud formation on 2D model predictions of stratospheric ozone depletion due to stratospheric aircraft, submitted to *J. Geophys. Res.*, 1993.
- DeMore, W. B., D. M. Golden, R. F. Hampson, M. J. Kurylo, C. J. Howard, A. R. Ravishankara, C. E. Kolb, and M. J. Molina (1992) *Chemical Kinetics and Photochemical Data for Use in Stratospheric Modeling*. Evaluation No. 10, JPL Publication 92-20, Pasadena, CA.
- Douglass A. R., R. B. Rood, C. J. Weaver, M. Cerniglia, and K. Brueske, Implication of three-dimensional tracer studies for two-dimensional assessments of the impact of supersonic aircraft on stratospheric ozone, *J. Geophys. Res.*, in press, 1993.
- Hanson, D. R., and A. R. Ravishankara, The reaction probabilities of ClONO_2 and N_2O_5 on 40 to 75% sulfuric acid solutions, *J. Geophys. Res.*, 96, 17,307-17,314, 1991.
- Jackman C. H., A. R. Douglass, S. Chandra, R. S. Stolarski, J. E. Rosenfield, J. A. Kaye, and E. R. Nash, Impact of interannual variability (1979-1986) of transport and temperature on ozone as computed using a two-dimensional photochemical model, *J. Geophys. Res.*, 96, 5073-5079, 1991.
- Jackman, C. H., A. R. Douglass, P. D. Guthrie, and R. S. Stolarski, The sensitivity of total ozone and ozone perturbation scenarios in a two-dimensional model due to dynamics input, *J. Geophys. Res.*, 94, 9873-9887, 1989a.
- Jackman, C. H., R. K. Seals, and M. J. Prather, Eds., *Two-Dimensional Intercomparison of Stratospheric Models*. NASA Conference Publication 3042, Proceedings of a workshop sponsored by the National Aeronautics and Space Administration, Washington, D.C., Upper Atmosphere Theory and Data Analysis Program held Sept. 11-16, 1988, in Virginia Beach, VA, 1989b.
- Jadin, F. A., and D. V. Bromberg, The numerical assessments of ozone reduction by stratospheric aircraft in the 2-D model including chemical eddies, *J. Meteor. Hydrol.*, 1991.
- Johnston, H. S., Evaluation of excess carbon-14 and strontium-90 data for suitability to test two-dimensional stratospheric models, *J. Geophys. Res.*, 94, 18485-18493, 1989.
- Johnston, H. S., Reduction of stratospheric ozone by nitrogen oxide catalysts from supersonic transport exhaust, *Science*, 73, 517-522, 1971.
- Johnston, H. S., D. Kattenhorn, and G. Whitten, Use of excess carbon-14 data to calibrate models of stratospheric ozone depletion by supersonic transports, *J. Geophys. Res.*, 81, 368-380, 1976.
- Johnston, H. S., D. Kinnison, and D. J. Wuebbles, Nitrogen oxides from high altitude aircraft: An update of the potential effect on ozone, *J. Geophys. Res.*, 94, 16351-16363, 1989.

- Peter, T., C. Bruehl, and P. J. Crutzen, Increase in the PSC-formation probability caused by high-flying aircraft, *Geophys. Res. Lett.*, 18, 1465-1468, 1991.
- Pitari, G., V. Rizi, L. Ricciardulli and G. Visconti, HSCT impact: the role of sulfate, NAT and ice aerosols studied with a 2-D model including aerosol physics, submitted to *J. Geophys. Res.*
- Prather M. J., and H. L. Wesoky, Eds., *The Atmospheric Effects of Stratospheric Aircraft: A First Program Report*. NASA Reference Publication 1272, National Technical Information Service, Springfield VA., 1992.
- Prather, M. J., and E. E. Remsberg, *The Atmospheric Effects of Stratospheric Aircraft : Report of the 1992 models and measurements workshop*, NASA Reference Publication 1292, NASA, Washington, D.C., 1993.
- Pyle, J. A., and C. F. Rogers, Stratospheric transport by stationary planetary waves: The importance of chemical processes, *Quart. J. Roy. Meteorol. Soc.* 106, 421-446, 1980.
- Schneider, H. R., M. K. W. Ko, C. A. Peterson, and E. Nash, Interannual variations of ozone: interpretation of 4 years of satellite observations of total ozone, *J. Geophys. Res.*, 96, 2889-2896, 1991.
- Shia, R-L, M. K.W. Ko, M. Zou, and V. Rao Kotamarthi, Cross tropopause transport of excess ^{14}C in a two-dimensional model, submitted to *J. Geophys. Res.*, 1993.
- Tuck, A. F., A comparison of one- two- and three-dimensional model representations of stratospheric gases, *Phil Trans. Roy. Soc. London*, A290, 477-494, 1979.
- Weisenstein D., M. K. W. Ko, J. Rodriguez and N.D. Sze, Ozone impact of High Speed Civil Transport and sensitivity to stratospheric aerosol loading, submitted to *J. Geophys. Res.*, 1993
- Weisenstein, D. K., M. K.W. Ko, J. M. Rodriguez, and N.-D. Sze, Impact of heterogeneous chemistry on model-calculated ozone change due to high speed civil transport aircraft, *Geophys. Res. Lett.*, 18, 1991-1994, 1991.
- World Meteorological Organization (WMO), *Atmospheric Ozone 1985, Assessment of Our Understanding of the Processes Controlling its Present Distribution and Change*, World Meteorological Organization, Global Ozone Research and Monitoring Project Report No. 16., WMO, Geneva, 1986.
- World Meteorological Organization (WMO), *Scientific Assessment of Stratospheric Ozone : 1991*, World Meteorological Organization, Global Ozone Research and Monitoring Project Report No. 25, WMO, Geneva, 1992.

Chapter 5

Engine Trace Constituent Measurements Recommended for the Assessment of the Atmospheric Effects of Stratospheric Aircraft

Frederick L. Dryer
Princeton University
Princeton, NJ

Charles E. Kolb
Richard C. Miake-Lye
Aerodyne Research, Inc.
Billerica, MA

Willard J. Dodds
General Electric Aircraft Engines
Cincinnati, OH

David W. Fahey
Aeronomy Laboratory
National Oceanic and Atmospheric Administration
Boulder, CO

Stephen R. Langhoff
Ames Research Center
National Aeronautics and Space Administration
Moffett Field, CA

Engine Exhaust Trace Chemistry
Committee Membership

F. Dryer; Princeton University (Chair); Princeton, NJ
J. Facey; NASA Headquarters; Washington, DC
D. Fahey; NOAA Aeronomy Laboratory; Boulder, CO
A. Hansen; Lawrence Berkeley Laboratory; Berkeley, CA
P. Heberling; General Electric Aircraft Engines; Cincinnati, OH
S. Langhoff; NASA Ames Research Center; Moffett Field, CA
E. Lezberg; NASA Lewis Research Center; Cleveland, OH
R. Lohmann; Pratt & Whitney; East Hartford, CT
R. Miake-Lye; Aerodyne Research; Inc.; Billerica, MA
R. Niedzwiecki; NASA Lewis Research Center; Cleveland, OH
R. Oliver; Institute for Defense Analyses; Alexandria, VA
K. Wolfe; ARC Professional Services (Exec. Sec.); Washington, DC

PREFACE

In 1992, the Engine Exhaust Trace Chemistry (EETC) Committee was organized to provide guidance and recommendations to the HSRP/AESA in developing a future engine emissions measurement and assessment program. Such a program is needed to provide evidence that the actual emissions characteristics of high-speed civil transport aircraft are indeed consistent with those characteristics used in the stratospheric modeling segments of the program. Two major challenges in such an effort are 1) as advances are made in understanding atmospheric effects, the specific emissions that need to be quantified may change, and 2) HSCT engine development will not reach full systems testing, under either ground or flight conditions, until some time after 1998. Thus, the EETC Committee must deduce exhaust emissions levels for aircraft engines well before they have been prototyped and tested.

The initial efforts of this committee have therefore concentrated on prioritizing what emissions characterizations should be performed, assessing alternative and/or emerging diagnostic methods for performing these characterizations, and defining the various venues which might exist both for gaining experience in using these diagnostics on simulated HSCT engine components and existing engines in order to provide more precise estimates of future full system HSCT emissions. While all of the committee members were intensely involved in shaping and carrying forth the various sub-elements of the study that resulted in this report, special recognition is given to lead authors R. C. Miake-Lye, D. W. Dodds, D. W. Fahey, C. E. Kolb, S. R. Langhoff, and to Aerodyne Research, Inc. for the report's preparation (ARI Report No. RR-947). This chapter is an edited version of the consensus report of the EETC Committee.

On the basis of this report, and as part of a NASA research initiative in the fall of 1992, two new instrument development programs were added to the HSRP/AESA program. Aerodyne Research, Inc. is presently developing a tunable diode laser differential infrared absorption system to provide nonintrusive and extractive sampling measurements. This effort will provide redundant measurements on NO_x , as well as a full characterization of all NO_y emissions species, with advanced versions providing measurements of SO_2 , SO_3 , CO_2 , CO , and OH . University of Missouri-Rolla will complete development of and utilize a mobile aerosol classifier technology with nuclei counters to measure the exhaust particulate number density, size distribution, and hydration properties. Additional analyses will also be performed by this group to characterize the chemical composition and morphology of exhaust particulate. Each of these instruments will be used to provide measurements in fundamental combustion, engine development, and engine prototype venues.

The instrument programs described above have only recently been initiated and results will be reported in future Program reports. The EETC Committee will continue to provide interpretive and guiding support to the community as measurement studies proceed.

Fred Dryer
May 1993

INTRODUCTION

The Engine Exhaust Trace Chemistry (EETC) Committee has been established to provide guidance and recommendations for a future engine measurement program in the NASA High Speed Research Program's study of the Atmospheric Effects of Stratospheric Aircraft (AESA). This engine measurement program will obtain experimental data on the emissions expected from a proposed fleet of high-speed civil transports (HSCTs). Such data are crucial to the HSRP's efforts to understand the impact of HSCT flights in the stratosphere.

The committee is composed of representatives from the range of disciplines that will contribute to this measurement effort. Combustor development researchers from NASA and from both members of the General Electric Aircraft Engines/Pratt & Whitney partnership are joined by representatives with specific interests pertinent to these engine measurements or their assessment. Additional members include those with backgrounds in combustion research, atmospheric measurement, and particulate measurement, and those with relevant aerodynamic or engine expertise.

Since fully developed engines of the proposed HSCT fleet will not be built before the end of the AESA study, a variety of developmental prototype engine components or surrogate engine measurements will be used to obtain relevant emissions data. It is the committee's charge to recommend measurements of trace chemical species by prioritizing a list of required species, assessing possible measurement venues available to the program, and identifying measurement techniques.

This report is based on the conclusions reached in the first committee meeting held at Aerodyne Research, Inc. on 21 April 1992, which were refined and expanded upon in a NASA Lewis Research Center sponsored Engine Exhaust Emissions Workshop held 22-23 June 1992. The objectives of the initial committee meeting were to 1) establish a prioritized list of engine trace species and 2) identify measurement venues available to the measurement program. The species measurements were grouped into two priority classes, with relevance to reported global chemical effects determining the top priority. Measurement venues for the various recommended species measurements were identified, and detailed measurement opportunities and constraints were slated for discussion in the subsequent Engine Exhaust Emissions Workshop.

The objectives of the HSR Engine Exhaust Emissions Workshop were:

1. To further define and prioritize engine exhaust gas constituents of greatest atmospheric concern in order to stimulate discussion in the larger community and to gain a broader consensus on the recommended measurement program.
2. To define measurement venues by identifying measurement opportunities and determining experimental constraints for studies on fundamental laboratory combustion apparatuses, combustion flame tubes, combustor rigs, and full-scale engine tests potentially available for AESA studies. Discussions of combustion apparatus operating characteristics and their relationship to full-scale HSCT engines were scheduled and information related to availability and characteristics of existing instrumentation and limitations on instrument access was requested.
3. To compare instrumentation capabilities and identify measurement needs for prioritized constituents, considering both existing measurement techniques and promising state-of-the-art technologies. Discussion was directed toward specifying accuracies and constraints on the application of candidate instruments in order to initiate ranking possible techniques, while still recognizing the need for redundant measurements for important constituents.

The initial EETC Committee definition of AESA measurement needs was presented at the AESA Annual Meeting in May 1992 and again as part of the background and introduction to the June workshop. Including the substantial conclusions of the workshop, the following sections summarize the needs and motivations for the recommended measurement program, provide a prioritized list of species to be measured, discuss where the measurements should be performed and what measurement venues could be made available to the AESA program, and identify candidate measurement techniques, listing their accuracies and potential application at relevant measurement venues.

BACKGROUND

Criteria for Prioritization

Accurate measurements of the gaseous trace chemical species concentrations and the particulate composition of jet engine exhaust flows is a challenging task. A clear set of measurement priorities is necessary in order to motivate the effort required to achieve the program's measurement goals and to clearly focus the required instrument development and measurement planning activities.

To date the committee's deliberations have identified three levels of motivation for performing jet engine and jet engine component exhaust measurements under the HSRP/AESA program's charter. These are:

1. To quantify the impact that an HSCT fleet's exhaust deposition will have on both the concentrations of key chemical species (and/or species families) and the particulate/aerosol loading levels on stratospheric chemistry and climatic phenomena. Chemical and radiative effects can occur both on the global scale and within impacted latitudinal regions containing significant flight routes (e.g. 30° - 60°N) at the lower stratospheric altitudes (10 - 25 km) affected by potential HSCT operations.
2. To identify and quantify exhaust components driving plume/wake chemical and condensation processes in the region immediately behind an aircraft. These processes have the potential to modify either the exhaust chemical speciation or the altitude of deposition in ways that significantly affect the impact of deposited exhaust species on stratospheric chemistry within latitudinal flight corridors.
3. To identify and quantify exhaust species that may serve as indicators of the effectiveness of new jet engine or jet engine component designs and thus help evaluate the efficiency of design options in minimizing the production of undesirable exhaust components while maximizing the fuel efficiency, reliability and durability of advanced engines.

It is the committee's judgment that the first level of motivation, as defined above, is the overriding criterion for selecting both prospective exhaust species measurement targets and engines and/or engine components for testing. To evaluate which gaseous exhaust species have the potential to significantly impact global and/or latitudinal stratospheric chemistry, the committee has communicated with the HSRP/AESA Models and Measurements Committee (see letter to M. K. W. Ko, Appendix A) to request help in confirming the anticipated impact of total nitrogen oxide (NO_y) deposition and in evaluating the possible impact of non-methane hydrocarbon (NMHC) exhaust levels. Furthermore, to assess the potential global and latitudinal impact of exhaust particulates (soot, sulfate, etc.) on both the direct stratospheric particle albedo and on the availability of condensation nuclei for sulfuric acid aerosols (SAA) and polar stratospheric cloud (PSC) formation, we have requested additional input from the Stratospheric Aerosol Science Committee (see letter to R.P. Turco, Appendix A).

The second level of motivation for setting exhaust measurement priorities is to measure exhaust species that may participate in plume/wake chemistry or in condensation processes which affect either the chemical speciation or altitude profile of the deposited gases in a manner that is significant at the global or latitudinal corridor level. To date several potentially important plume/wake phenomena have been identified (Miake-Lye et al., 1991), but none has been shown conclusively to affect the larger scale phenomena. While work continues on these potential effects under the direction of the Exhaust Plume/Aircraft Wake Vortex Committee, possible plume/wake effects must play a secondary role in setting exhaust measurement priorities at this point.

The third level of priority is how well the exhaust measurements to provide feedback information to the engine combustor designers. For instance, while the engine research community already routinely utilizes NO_x and Society of Automotive Engineers (SAE) smoke number measurements to characterize exhaust properties, it is conceivable that real-time total NO_y , NO_y speciation, or detailed particle characterization measurement technology, which may be developed and deployed as part of the HSRP/AESA exhaust measurement programs would produce information useful for fine-tuning engine or engine component design or for selecting between alternative design approaches. The engine design and testing community has not yet determined if such measurements would indeed be useful. The committee will keep this question before the engine designers and will use any positive response as a third level of priority for setting HSRP/AESA exhaust properties' measurements.

The focus of the AESA study is the potential effects of these emissions on the stratosphere. As such, measurements and estimates of engine emissions under stratospheric cruise conditions are most pertinent to the needs of AESA. However, stratospheric aircraft will climb out of the troposphere with engines operating under higher thrust conditions relative to cruise and begin to descend out of the stratosphere again with different power settings. The Emissions Scenarios Committee (D.J. Wuebbles, chair) is considering such detailed flight profiles, and emissions estimates will be required for all engine conditions during which emissions are deposited in the stratosphere. Particularly NO_y emissions, and perhaps total hydrocarbons (THC) and soot, will depend on the combustor operating pressure and temperature. Although not directly relevant to stratospheric effects, emissions during takeoff, climb out, and the perhaps lengthy required overland subsonic cruise could also vary considerably. Clearly, the measurements discussed in this report will need to be carried out for a range of experimental parameters corresponding to relevant engine operating conditions.

Stratospheric Chemical Families and Jet Engine Exhaust Components

Atmospheric chemists engaged in analyzing the chemistry of stratospheric ozone have discovered that the concept of "chemical families" or closely connected classes of chemical species is very useful in understanding the photochemistry of the stratosphere. For instance, while much of their concern is focused on ozone, O_3 , the stratospheric chemistry community has learned that they need to consider the odd oxygen ($\text{O} + \text{O}_3$) chemical family. This is because O and O_3 interconvert so rapidly that a sink for atomic oxygen, O , leads directly to a loss of O_3 .

Other chemical families of critical importance in the stratosphere are NO_x ($\text{NO} + \text{NO}_2$), NO_y ($\text{NO} + \text{NO}_2 + \text{NO}_3 + \text{N}_2\text{O}_5 + \text{HNO}_3 + \text{HOONO}_2 + \text{ClONO}_2 + \text{organic nitrates}$), ClO_x ($\text{Cl} + \text{ClO} + \text{ClOO} + \text{OCIO}$), BrO_x ($\text{Br} + \text{BrO} + \text{OBrO}$), HO_x ($\text{H} + \text{OH} + \text{HO}_2$), CO_x ($\text{CO} + \text{CO}_2$) and SO_x ($\text{SO} + \text{SO}_2 + \text{SO}_3 + \text{HSO}_3 + \text{H}_2\text{SO}_4$). Of course there are some "intermarriages" which connect families, i.e., ClONO_2 connects NO_x and ClO_x and HOCl connects HO_x and ClO_x . Water vapor, H_2O , and hydrogen peroxide, H_2O_2 , can be viewed as sources and/or reservoirs of HO_x species. Another common family identified in atmospheric chemistry studies, the non-methane hydrocarbons (NMHC), is composed of all hydrocarbon compounds with two or more carbon atoms and their partially oxidized degradation products.

Not all potential members of a given family will be emitted at significant levels by HSCT engines. For instance, the hot HSCT exhaust will supply a limited number of NO_y compounds: NO , NO_2 , and possibly HNO_3 . However, the other NO_y compounds will evolve as the exhaust mixes with stratospheric air and is exposed to photochemical oxidation processes. While not strictly a chemical family, condensed phase particulates and aerosols are now known to play a major role in stratospheric chemistry and the potential impact of HSCT exhaust particles on stratospheric properties must also be considered.

The lower stratospheric chemical families for which significant levels of potential HSCT exhaust emissions may be expected and a discussion of their possible impact on stratospheric chemistry are presented below.

Nitrogen Oxides (NO_x , NO_y)

The principal documented perturbation of a projected HSCT fleet at global or latitudinal corridor scales is to the lower stratospheric NO_y content (Johnston, et al., 1989; Johnston, et al., 1991; Douglass, et al., 1991). Whether or not this additional NO_y causes a significant reduction in the O_x ($\text{O} + \text{O}_3$) content of the lower stratosphere depends strongly on the chemical model utilized. Traditional homogeneous gas-phase photochemistry models (Johnston, et al., 1989; Douglass, et al., 1991) indicated a significant O_3 reduction for large HSCT fleets, while models that include heterogeneous conversion of N_2O_5 to HNO_3 on sulfuric acid aerosols (SAA) (Weissenstein et al., 1991; Bekki et al., 1991) indicate no major O_x loss. Peter et al., (1991) do, however, present model results that indicate that a 600-plane HSCT fleet operating at 22 km in typical northern hemisphere aviation routes could lead to a doubling of polar stratospheric cloud (PSC) levels above the Arctic during the December to March polar ozone depletion season. This effect is due to the increase in NO_y , specifically HNO_3 , generated by emissions from this hypothetical fleet and could significantly increase ozone depletion because of the consequential increases in active chlorine levels. Thus, the most obvious and highest priority for the HSRP/AESA exhaust measurement program is to ensure that total projected HSCT engine NO_y output is carefully measured.

Thermochemical and chemical kinetic considerations limit significant potential nitrogen oxide engine exhaust exit plane species to NO_x ($\text{NO} + \text{NO}_2$) plus a possibility of minor levels of HNO_3 . Nitric oxide is likely to comprise 90+ %, NO_2 0.1 to ~10 % and HNO_3 < 0.1 % of a typical HSCT exhaust at the nozzle exit plane. However, chemistry inside traditional sampling probes may convert significant amounts of NO to NO_2 and NO_2 to HNO_3 . Thus, great care must be exercised to ensure all NO_y is properly measured. For example, conventional catalytic or photolytic NO_2 converters used in chemiluminescence systems will not convert HNO_3 to NO . Proven total NO_y and/or reliable individual measurements of NO , NO_2 , and HNO_3 are judged to be necessary to ensure the NO_y output of prototype HSCT engines or engine components is well characterized.

Particulates

Particulates from the HSCT fleet exhaust may add significantly to the total particle burden of affected portions of the stratosphere, particularly in the periods between major volcanic eruptions. The emitted particulates are primarily submicron soot particles. Some particulate sulfate (either formed from the fuel sulfur content or entrained with the combustion/bypass airstream) is also thought to be present, but whether this is deposited on the surface of the soot or formed into separate sulfate particles is unknown at this time. The same uncertainty applies to any condensed metal oxides formed by oxidation of either engine components or the fuel's trace metal content (primarily from fuel processing and handling since no metal additives are expected in HSCT fuels). As noted above, two possible particulate related effects from HSCT exhaust are possible: 1) the scattering/absorption properties of the normal background sulfate aerosol are modified by the addition of the HSCT soot, most of which may eventually be incorporated into ambient sulfate

aerosol; 2) the HSCT exhaust particles may supply additional condensation nuclei which lead to significant new aerosol formation in the affected portions of the stratosphere (including the aircraft wake), in turn affecting both the number density of aerosols and their size distribution. Gaseous SO_x emissions will also contribute to the aerosol loading of the stratosphere, once converted to condensed sulfate (see Sulfur Oxides SO_x below).

In reference to this second effect, we do know that apparently only 1 - 2% of freshly produced soot from jet fuel combustion can nucleate water vapor at levels of supersaturation ($\sim 1\%$) typical of the atmosphere (Hallett et al., 1989; Hudson et al., 1991; Pitchford et al., 1991). However, we do not know what fraction can nucleate SAAs or PSCs under stratospheric conditions, or how chemical reactions in the plume and wake or the stratosphere itself affect the level of active condensation nuclei.

It is apparent that the stratospheric chemistry and aerosol physics community is not yet prepared to specify what level of HSCT exhaust particulate might significantly perturb the impacted portions of the lower stratosphere. It may be necessary to provide a much more complete characterization of prospective HSCT exhaust particulates (mass loading, size distributions, surface composition and reactivity, bulk composition, water, and acid nucleation properties---see Stratospheric Aerosol Science Committee Report, Appendix A) before that community is able to predict the deposition level that would trigger a significant stratospheric response.

Sulfur Oxides (SO_x)

The stratosphere contains a great deal of SO_x , some in the gas phase, primarily as SO_2 or H_2SO_4 vapor, and more in the condensed phase as sulfuric acid aerosol. The lower stratospheric SO_x burden is periodically increased dramatically by a major volcanic eruption such as El Chichon or Mount Pinatubo. The SO_x added by an HSCT fleet is not expected to dramatically increase ambient stratospheric SO_x levels; however, Hofmann (1991) has suggested that the current commercial aircraft fleet may be adding measurable levels of SO_x to the lower stratosphere's intervolcanic background, which eventually contributes to the sulfate aerosol loading.

Even if this global stratospheric SO_x impact is real and exacerbated by the HSCT fleet, it does not necessarily dictate exhaust SO_x (SO_2 , SO_3 , H_2SO_4) measurements, since the total level of exhaust SO_x output can be predicted from fuel sulfur content, and since all SO_x emitted to the stratosphere forms H_2SO_4 on a reasonably short time scale. On the other hand, SO_x speciation in the exhaust and wake may well impact the plume and wake conversion of inactive soot particles to active condensation nuclei (Miake-Lye et al., 1991), while H_2SO_4 vapor may induce new particle formation in the plume via $\text{H}_2\text{SO}_4/\text{H}_2\text{O}$ binary homogeneous nucleation (Turco, R.P., private communication, 1992).

Non-Methane Hydrocarbons (NMHC)

Non-methane hydrocarbons in HSCT exhaust would arise from unburned or partially oxidized fuel and lubricant compounds. Their potential impact on lower stratospheric chemistry arises from the possible formation of organic nitrate or peroxyxynitrate compounds, R-O NO_2 , R-OO NO_2 or R-C(O)OO NO_2 , where R is a hydrocarbon fragment. These compounds are known to sequester a significant level of NO_y in some regions of the troposphere and would be much more stable against thermochemical decomposition in the colder stratosphere. However, it is unlikely that advanced HSCT engines will emit large enough levels of NMHC to significantly perturb stratospheric NO_y speciation. Preliminary results using the AER model (see Appendix A) indicate that estimates of NMHC impact on ozone depletion through peroxyacetyl nitrate (PAN) chemistry are negligible. Some exhaust emission measurements may need to be performed on HSCT combustors in order to conclusively demonstrate that the expected range of NMHC emissions falls below the threshold of significant effects.

Hydrogen Oxides (HO_x) and Related Species

Water vapor, H₂O, will be a major exhaust component added to the stratosphere by an HSCT fleet. The level of H₂O in the plume and wake will be much higher than the ambient stratosphere, leading to condensation (contrail formation) under some conditions. Exhaust water vapor does not need to be measured, since it can be accurately calculated from fuel consumption.

Exhaust hydroxyl levels (OH) are not high enough and the lifetime of OH is too short to affect the bulk stratosphere, but plume and wake levels of NO₂, HNO₃, SO₃, and H₂SO₄ are determined by OH-induced chemistry (Miake-Lye et al., 1991). These species, in turn, may affect soot condensation nucleation processes. Exhaust OH will also drive NO₂ to HNO₃ conversion in exhaust sampling probes. Such issues motivate the measurement of exhaust OH levels. High levels of exhaust HO_x may lead to significant amounts of hydrogen peroxide (H₂O₂). H₂O₂ is a powerful oxidant in condensed phase systems and may cause substantial oxidative activation of soot CCN or enhanced oxidation of SO₂ to sulfuric acid. Hydrogen peroxide can also trigger heterogeneous HO_x chemistry, which can oxidize NO to NO₂ and HONO, and NO₂ to HNO₃, (Gradel and Weschler, 1981). Furthermore, dissolved H₂O₂ directly converts HNO₂ to HNO₃ (Lee and Lind, 1986).

Other Exhaust Pollutant Species

Other significant exhaust pollutant species include CO_x (CO + CO₂), methane (CH₄), and nitrous oxide (N₂O). There are such large fluxes of CH₄, CO₂, and N₂O into the stratosphere from the troposphere that prospective HSCT exhaust additions are negligible. Carbon monoxide is transported into the stratosphere from the troposphere and produced in situ (along with CO₂) from methane and NMHC oxidation at much higher levels than that expected from HSCT exhaust deposition. None of these HSCT exhaust emissions are currently expected to significantly impact the chemistry of the plume/wake or the bulk stratosphere.

There is some interest in measuring CO₂ as an internal exhaust concentration standard, so that measurements of individual species can be better referenced to combustion fuel burn, supporting a representative measurement of the total emissions. Like H₂O, accurate CO₂ levels can be predicted from fuel consumption. Measurements of total hydrocarbons (THC) may be a surrogate for NMHC measurements if the methane component can be separately accounted for.

The motivations for measuring species in relevant chemical families are summarized in Table 1, where estimated emission levels or estimated perturbations to the atmospheric composition are compared with background levels when these are known.

SPECIES MEASUREMENT RECOMMENDATIONS

Based on the preceding criteria and discussion of chemical families, a set of priorities for species measurements can be formulated. The global or latitudinal impact (criterion 1) is given the highest priority, since significant stratospheric effects are expected to follow directly from such perturbations. Plume and wake effects (criterion 2) are given second priority until global implications of these effects are better understood. Engine development criteria (criterion 3) do not motivate additional measurements at present, but the current list of measurements may prove useful to this end.

First Priority - The first priority species measurements include NO_y and particulate measurements.

NO_y. NO_y has been the emission of central concern because of its potential catalytic destruction of ozone, and a definite, conclusive measurement of the total amount of NO_y emitted

from engine developmental rigs is required. An absolute measurement of NO_y is essential to quantify its emission level to 20% using existing chemiluminescence techniques, which convert NO_y to NO followed by titration with O_3 . In doing so, it is essential to resolve any outstanding questions involving the sampling technique, such as partial conversion of NO_2 to HNO_3 by reaction with OH in the sampling system. It is anticipated that the chemiluminescent technique, with any improvements, will become a "gold standard" to judge other methods. The recommended emissions measurements must implement this chemiluminescence method in a way consistent with that used by the atmospheric community so that direct correspondences can be made between engine emission measurements and atmospheric measurements.

The measurement of NO_y is considered sufficiently critical that the committee felt that a second independent redundant measurement must be employed. The species in the NO_y family expected in the engine exhaust (NO , NO_2 , and HNO_3) must be measured redundantly to account for the complete NO_y emission. By making correspondences between the measured values obtained using distinct techniques, a complete and accurate NO_y emission measurement will be ensured. Redundant measurement techniques would not have to be as accurate as the chemiluminescent "gold standard," but it would have to be sufficiently accurate to validate the chemiluminescent technique. It was felt that this measurement should be spectroscopic, probably differential absorption, to avoid processes competing with fluorescence.

In making these redundant measurements, the temporal and spatial averaging inherent to the different techniques will not necessarily be the same. An important part of the reduction and analysis of such data will be to account for effects due to different temporal and spatial responses. This will be required to reconcile redundant measurements and, perhaps most importantly, provide a representative measure of the total emissions. Reconciling line-of-sight optical measurements with point extractive probe sampling is particularly difficult due to their extreme spatial averaging disparity.

Particulates. Particulate measurements are motivated by the role of heterogeneous chemistry on the chemical balance in the stratosphere. While heterogeneous effects are expected to be major, understanding of these processes is still evolving and the role of aircraft engine particulate emissions, in particular, has yet to be well defined. To bound the potential impact, a soot emission index and total particle number densities are required. This must be done for the new combustor concepts, (lean-premixed-prevaporized, LPP, and rich-burn/quick-quench/lean-burn, RQL), because the number density and size distribution of carbonaceous (soot) particulates could be very different for these two concepts, with both differing from conventional combustors. Thus, it would be difficult to infer the emissions from measurements from current combustors. The total number density is considered the most critical factor, since the residence time in the stratosphere is sufficiently long that most particles would eventually become active aerosol condensation nuclei.

A measurement of the total mass of particulates is recommended at a high priority. This straightforward measurement will provide the total atmospheric burden of particulates. Such a measurement would provide a check on experiments that simultaneously determine the size distribution and total number density (see later discussion). The Stratospheric Aerosol Science Committee (see Appendix A) recommends that trace metal emissions also be measured at a high priority. However, the Engine Exhaust Emissions Measurement Committee assigns a second priority to these and other more detailed characterizations of the particulate emissions, based on the need for a better bounding of their global impact.

Second Priority - Speciation of the NO_y and SO_x families, detailed characterization of particulates, measurement of OH , and calibration using CO_2 measurements are ranked as the next highest priority.

NO_y Speciation. The complete and accurate measurement of NO_y requires quantifying the contributions from all non-negligible species in the chemical family. The detailed NO_y speciation, i.e., partitioning into NO, NO₂, and HNO₃ once measured and summed to give the total emission, is generally not important as input to global models, since photochemical equilibrium will be established based on the total NO_y emission if there are no other chemical changes. Such other changes may occur, however, through condensation and heterogeneous processes in the plume and wake. Thus, the detailed speciation, potentially extractable from the measurements required for global impact, is recommended to provide data for understanding the evolution behind the aircraft, which may depend on operating conditions (e.g., supersonic cruise vs subsonic climb or cruise). Ideally this will be done with the same spectroscopic technique that gives the redundant total NO_y measurements.

Particulates. The detailed characterization of the particulate emissions includes measurement of particle size distributions, as well as cloud condensation nuclei (CCN) and ice nuclei (IN) activities. These properties may change due to chemical processing in the atmosphere, both in the plume and wake and later as the emissions are mixed to global scales. The particle size distribution is potentially important for modeling the plume and for determining the fraction of particles that are removed from the stratosphere. A measurement of the size distribution in conjunction with the total number density can be compared with the independent experiment that measures total mass.

A measurement of the reactivity of particulates is considered more difficult, but sufficiently important to warrant further study. An important question is what fraction of the soot and sulfate particulates become active CCN and/or IN. There is a need for both characterization of the emissions from engine developmental rigs and fundamental experiments to understand the chemical evolution processes.

SO_x Speciation. Condensation and heterogeneous chemistry is intimately linked to sulfate aerosol and gaseous SO_x concentrations. The AESA Stratospheric Aerosol Science Committee (R. Turco, chair) has specifically requested measurements to determine SO_x partitioning into SO₂ and SO₃/H₂SO₄ (see Appendix A). Since all the fuel sulfur is emitted as some SO_x species, the total SO_x emission can be quantified by measuring the fuel sulfur. However, if condensation and heterogeneous chemistry is to be followed, particularly immediately behind the aircraft in the wake or in flight corridors, the individual constituents must be measured separately at the engine exit plane to account for their chemical effects. A measurement of SO₃ to 0.1 ppm would allow validation of models that predict the SO_x speciation at the exit plane.

Non-Methane Hydrocarbons. The measurement of this class of species is given second priority because these species emission rates are small and relatively well known. On the other hand, the background concentration of these species is negligible, so they represent a large perturbation. Non-methane hydrocarbons are not expected to significantly affect the gas-phase or heterogeneous processes implicated in ozone destruction for the anticipated THC emissions of EI(CH₄) = 0.2. A measurement of this EI is necessary to be sure NMHC's role is negligible.

The methane component of THC is typically larger than the NMHC component (Spicer et al., 1992). The largest NMHC emissions are in the form of ethene, propene, acetylene, formaldehyde, and acetaldehyde. Thus, a bound can be placed on the NMHC concentrations by measuring THC accurately using a flame ionization detector (FID). It was recommended that the measurement of THC be undertaken to 1 ppm C to place a bound on the NMHC.

OH Radical Concentration. The hydroxyl radical present at the engine exit plane drives the oxidative processing of NO_y and SO_x in the engine plume and the aircraft wake. Its concentration and lifetime are too small to influence global stratospheric chemistry directly, so its potential impact is through local effects in the plume and wake that modify the net emissions deposited in the atmosphere. Its measurement is recommended at the engine exit plane at the 0.1 ppm level.

CO₂ Calibration. As a major combustion product, the CO₂ concentration is well known from the stoichiometry of the combustion process in a combustor optimized for efficient fuel use. Thus, measurement of CO₂ is not necessary for its own sake but it provides a valuable calibration measurement which can serve as an internal reference for other trace gas emissions. Calibration and establishing correspondences between measurements made with different techniques will be a major part of the recommended measurement program, and CO₂ is included here as a second priority measurement to help ensure that a representative total emission measurement is made.

SPECIES MEASUREMENTS AND MEASUREMENT VENUES

While flame tube experiments are showing promising results and combustor and engine cycle development is advancing under NASA's HSR Program, complete HSCT engines will not be available during the lifetime of the AESA studies. Thus, the best estimates of the emissions performance of the engines for this proposed supersonic stratospheric fleet will be obtained from 1) experiments in fundamental combustion apparatuses at the planned operating conditions, 2) developmental flame tube and combustor rigs at NASA and its industrial HSRP partners' facilities, and 3) surrogate advanced cycle engines that have thermodynamic behavior similar to that planned for the HSCT engines, even though their combustors may not be optimized for low emission performance as the future engines will. Measurements using these surrogate engines will be useful for following the chemical evolution of the emissions after they leave the combustor, as they flow toward the exit plane of the engine. Their utility to HSRP depends on knowing the emissions performance of their combustors, as compared to the HSRP combustors, and being able to reliably account for turbine/nozzle processes as the emissions are scaled from current technology to that being developed under HSRP.

The species measurements recommended above are not necessarily appropriately measured at all of the measurement venue types. Chemistry continues in the hot exhaust gases as they pass through the turbine sections and nozzle, so that chemical families' speciation and particulate properties may be significantly different at the combustor exit versus the engine exit and may depend sensitively on engine operation conditions. On the other hand, neither NO_y, soot, nor SO_x are produced downstream of the combustor so combustor or flame tube measurements of total chemical family emissions are meaningful—particularly since these facilities are currently available and represent the technology planned for the proposed engines.

NO_y. The absolute measurement of the total NO_y emission is appropriately made at all of the measurement venue types. Multiple measurements of the total NO_y emission index would increase confidence in its accuracy. Speciation of the NO_y may evolve as oxidation of NO produces NO₂ and perhaps HNO₃. Thus, to provide initial conditions for plume and wake modeling, measurement of individual NO_y species is necessarily done at the engine exit plane. Fundamental experiments to understand the chemical evolution in the engine and in any measurement device (e.g., sampling probe) are also important to an accurate absolute NO_y measurement.

Particulates. While particle oxidation may proceed after the combustor and agglomeration may change particle size distributions, total particulate masses and number densities at the combustor exit need to be quantified. Cloud condensation nuclei and ice nuclei properties are appropriately measured at the engine exit or by simulating their chemical history to that point or beyond in fundamental experiments.

SO_x Speciation. A measurement of the individual SO_x species must be done after the chemical processing occurring in the turbine and nozzle is complete. A comparison of the total SO_x and the fuel sulfur would provide verification that the total sulfur emission is being accounted for.

NMHC. Since the measurement of NMHC is simply to place an upper bound on the EI, measurement at any and all of the measurement venue types is called for.

OH Radical Concentration. This reactive radical's concentration will be changing quickly as the gases flow through the engine, so measurement at the engine exit is needed to provide initial conditions for subsequent chemical processing. (OH levels at the combustor exit would allow quantitative estimation of the chemical processing occurring in the engine, but this is a much lower priority measurement to be considered only if the instrumentation developed for an engine exit measurement is available.)

CO₂ Calibration. Calibration is essential for all measurement venues so, when CO₂ measurement can aid in this task, it should be measured.

This discussion of measurement venues and the species measurements that are appropriate for each of them is summarized in Table 2. The first priority measurements are highlighted in boldface, while the next most important class of measurements is italicized.

DIRECTORY OF MEASUREMENT VENUES

Background

The Engine Exhaust Emissions Workshop included a session on measurement venues. The objective of this session was to assemble information on measurement venues such as flame tubes, combustor rigs, and gas turbine engines, where measurements of important exhaust gas constituents could be made over the next several years. Specific documents that were generated include:

- A brief description of each of the candidate venues with discussion of its advantages and disadvantages.
- A catalog of available venues at several test facilities.

Additionally, recommended measurement venues for near-term research programs and test issues were discussed.

Descriptions of Test Venues

Test venues are divided into six categories:

- Flame Tubes
- Sector Combustor Rig
- Annular Combustor Rig
- Current Engine
- Advanced Engine
- HSCT Engine

As of mid-1992, all HSCT combustor development is being done in flame tube rigs. Testing of larger sector combustors is starting in early 1993, and annular testing will not occur before 1995. These venues are described below.

Flame Tubes

A flame tube is a small-scale, simplified prototype combustor that simulates the salient features of an actual gas turbine combustor. Flame tubes are being used for early development of new

combustor concepts such as the rich-burn/quick-quench/lean-burn (RQL) and lean-premixed-prevaporized (LPP) combustors being developed for future HSCT aircraft.

The flame tube consists of a small burner, typically mounted in a 6 in. to 10 in. pipe, as shown in Figure 1. High-pressure combustion air supplied from a remote compressor facility is preheated to realistic combustor inlet temperatures by indirect-fixed or electrical heaters. For a realistic simulation of projected HSCT engine combustor inlet conditions at supersonic cruise, inlet temperature should be 1200°F, pressure should be 150 to 200 psia, and exit temperature should be between 2800°F and 3500°F. Primary measurements made in flame tubes include gas samples to evaluate combustion efficiency, carbon monoxide and carbon dioxide (using nondispersive infrared, NDIR), unburned hydrocarbons (using flame ionization detection, FID), and NO_x (using chemiluminescence). Metal temperatures (thermocouples) and pressure distributions are also measured routinely.

The flame tube provides a small, relatively low cost vehicle to conduct initial development tests of new combustor concepts. The simplified flowfield and small size of the flame tube simplify measurement of emissions.

On the other hand, optical access to the combustor is difficult to obtain due to the high test pressures and temperatures. Flame tube test facilities are often cramped, dusty, hot, and noisy. Another concern is that flame tubes do not accurately simulate practical combustor cooling and piloting design features that could affect emissions from an engine combustor. Further, the effects of combustor products expansion, which occurs in the turbine of an actual engine, are not properly simulated. These effects could include particle burnout and change in, for example, distribution of NO_x species.

Sector Combustor Rig

A gas turbine combustor typically consists of a 360 degree ring containing 18 to 30 fuel injectors, as shown in Figure 2. A sector combustor is a full-scale portion of the combustor containing three to six fuel injectors, as shown in Figure 3. The sector combustor rig uses compressor facilities and air heaters similar to those used with flame tubes, except that higher airflow capability is required. Representative inlet and exit temperatures and pressures are used. Sector tests are used for early combustion system development. Use of sectors reduces hardware and test costs for early development. Sectors are also used for very high pressure combustor tests (up to 600 psia) to reduce airflow requirements, which affect compressor facility costs.

Sector combustors are more representative than flame tubes in that they accurately simulate all important combustor design features. However, test costs are significantly higher and more detailed measurements may be required to adequately represent the more complex sector combustor flowfield. As with the flame tube, turbine effects are not properly simulated.

Annular Combustor Rig

An annular combustor rig (Figure 4) is designed to accommodate an actual engine combustor. The annular rig provides essentially the same information as the sector. The primary advantages of the annular rig are that it exactly duplicates the engine flowpath, eliminates concerns about the effects of secondary flows, which occur adjacent to the section sidewalls, and provides a larger statistical sample.

Disadvantages of annular rig tests are that they are expensive, and operating pressures are often limited due to air supply facility limitations.

Tests of Current Engines

In all rig tests, the combustor is operated without an engine compressor and turbine. This provides capability to independently vary airflow, fuel flow, pressure, and temperature to the combustor in order to easily simulate a wide range of engine operating conditions. However, none of the rig tests reproduce the time-temperature history of combustion products as they pass through the turbine. To adequately assess effects of chemical reactions that may occur in the turbine, it is necessary to conduct a full engine test.

Factory engine tests also are conducted in large test cells such as the one illustrated in Figure 5. Test cells are generally designed to provide ambient temperature and pressure inlet conditions. However, several test cells are available that can also simulate the reduced pressures and temperatures encountered during high-altitude cruise. Current engines which operate at inlet temperatures of up to 1100°F and pressures up to 450 psia, and turbine inlet temperatures up to 2700°F are routinely tested by engine manufacturers. Provisions are available for mounting gas sampling rakes at the engine exhaust (Figure 6).

Advantages of current engines is that they are widely available and they do reproduce turbine effects on exhaust gases reactions. However, the combustion systems in current engines are not representative of future HSCT engines, and combustor inlet and exit temperatures are generally 100°F to 200°F lower than HSCT values. Engine tests are also considerably more expensive than rig tests.

Advanced High Temperature Engine Tests

A few advanced military product and demonstrator engines operate at combustor temperatures comparable with projected HSCT engines. These engines would properly represent the HSCT turbine conditions. However, these engines do not have combustors representative of an HSCT, and tests are expensive and are not conducted frequently.

HSCT Engine

First tests of an HSCT-type engine having the correct combustion system and operating temperatures are not scheduled until 1998.

Catalog of Test Venues

Appendix B lists available test venues based on input from participants at the workshop. This information is meant to serve as a resource for atmospheric scientists who are planning programs that would benefit from combustion rig or engine measurements. The catalog is only a guide to help identify test opportunities. The test organization must be contacted to discuss specific programs.

Generally, costs will be lower if programs can "piggy-back" on existing test programs. Ideally, measurements taken on a noninterference basis could be obtained at no cost to the proposed programs. However, experience has shown that true piggy-back tests are very difficult to achieve. As a minimum, one man-month of engineering support from the test organization will be required for coordination of measurements with planned test activities. Delay of tests to set up instrumentation and increased test time to take measurements will lead to additional costs. The level of costs is indicated qualitatively in the catalog. For rough estimates, "low" is less than \$5,000, "medium" is \$5,000 to \$25,000, and "high" is up to \$70,000.

The catalog also contains remarks with regard to instrumentation access and other special considerations.

Contacts for each of the venues are provided. If tests are to be conducted at one of the facilities listed, it is imperative that contact is made to agree on the scope of testing and to develop firm cost estimates before a proposal is submitted.

Recommended Test Venues

The consensus of the workshop participants was that simple laboratory burners operated at inlet pressures and temperatures representative of HSCT combustor inlet conditions should be used for instrument development, evaluation of sampling probe influence on sample composition, and redundant measurements of species using different instruments. Flame tube rigs should be used to compare advanced combustor concept NO_x and particulate characteristics with those of current combustors at HSCT combustor operating conditions.

Understanding effects of chemical reactions in the turbine and nozzle was given as lower priority. Turbine effects at representative conditions could be evaluated independently by comparing annular rig test results with advanced engine test results, but such a program would be expensive and difficult to coordinate. Analysis of particle burning and continued gas-phase reactions in the turbine and nozzle would be more cost-effective than tests for this purpose.

Issues

Specific issues that were raised at the workshop included the following:

- Even with piggy-back tests, costs for setup, test coordination, and test delays could be substantial.
- The catalog of venues is not all-inclusive. Flame tubes are available at many universities and industrial laboratories. The catalog only lists data provided by participants of the workshop.
- The only truly valid test venue is the HSCT demonstrator engine. However, that engine will not run until 1998.
- Optical access for flame tube tests is not routinely available. The effort of designing for optical access, if required, should be considered carefully in planning programs.
- Reconciliation of line-of-sight measurements with point measurements in the complex, highly turbulent combustor flowfield is not straightforward and should be considered in comparing different measurement techniques.
- Reconciliation of sample averaging effects (temporal as well as spatial) between various optical methods and sample probe (extractive) measurements in complex, highly turbulent, reacting flows is not straightforward and should be considered in comparing different measurement techniques.

MEASUREMENT TECHNIQUES

Overview

Measurement instrumentation for the priority exhaust species identified in the Species Measurements and Measurement Venues section must function over a wide range of exhaust flow temperatures and pressures associated with the range of likely measurement venues as identified

there and in Directory of Measurement Venues section. Furthermore, for the first priority exhaust species designated in the June workshop, the committee has recommended that two redundant techniques, based on different measurement principles, be deployed during initial measurement campaigns in order to ensure the reliable quantification of exhaust species with the greatest anticipated atmospheric impact.

This section presents recommendations from the June workshop on both measurement accuracy requirements and potential measurement techniques capable of meeting these requirements for exhaust flows from venues such as flame tubes, combustor rigs, and surrogate engines. For several classes of priority species, the combustor development community has previously established and regularly utilizes measurement techniques based on extractive probes followed by exhaust species analysis schemes. As discussed below, these existing techniques are generally recognized to be based on sound measurement principles and are generally recommended for continued use. However, for the most critical first priority measurements the committee also recommends options for redundant new measurement techniques which can validate the existing techniques and, in many cases, expand the information gathered in ways valuable to the HSRP/AESA effort. It should be noted that the recommended new measurement techniques are not really novel or untested. In all cases they have been successfully utilized to measure the various target species in laboratory and/or atmospheric experimental programs, sometimes for years. However, they are new in the sense that they are not routinely applied in gas turbine combustor or engine exhaust measurement programs.

First Priority Measurement of NO_y

As discussed earlier, NO_y denotes the sum of all nitrogen oxide species, excepting nitrous oxide (N₂O), produced in the combustor and exhaust flow. On thermochemical grounds NO_y is expected to encompass only NO and NO₂ at combustor or flame tube outlets, but may include some HNO₃ at the engine exhaust plane. Furthermore, chemistry inside sampling probes may convert additional NO to NO₂ and NO₂ to HNO₃. The standard technique for measuring exhaust NO_y assumes only NO and NO₂ (NO_x) are present in important quantities. After probe sampling, NO₂ is catalytically reduced to NO. Nitrogen oxide is quantified via its chemiluminescent (CL) reaction with O₃ (SAE, 1980a, EPA, 1973, 1972, and 1978). Several commercial instruments operating on these principles are utilized by the gas turbine combustor community.

The committee's major concern is to ensure that the standard chemiluminescent techniques for NO_x is both accurate and inclusive, i.e., that no significant fraction of the NO_y is missed due to conversion to HNO₃ or other NO_y species in either the exhaust flow or sampling probe. Historically, some attempts have been made to validate probe-sampled NO_x measurements with simultaneous optical (UV absorption) measurements of NO (McGregor et al., 1973; Few and Lowry, 1981; Meinel and Krauss, 1978; Zabielski, et al., 1981). These studies have emphasized the necessity of proper probe design in order to minimize NO chemical conversion during sampling as well as the necessity of proper spectroscopic data analysis if an accurate intercomparison is to be achieved. Agreement between the two techniques for laboratory burners can reach the 20-30% level if care is taken with both techniques (Meinel and Krauss, 1978; Zabielski et al., 1981).

Based on the Engine Exhaust Emissions Workshop session on measurement techniques at the June Workshop, the following recommendations are offered for the measurement of NO_y emissions:

1. Improve the performance of the chemiluminescence technique by: a) establishing conversion and specificity for NO₂ and HNO₃ (possibly using the photolysis of these species to NO), b) measure probe loss of specific NO_y species (NO₂, HNO₃) or interconversion among them that would affect measurements in engine or combustor tests, and c) certify calibration standards.

2. Use a redundant, independent optical technique to verify chemiluminescence performance in a dedicated test series. Candidate techniques include tunable diode laser (TDL) absorption, Fourier transform infrared (FTIR) spectroscopy, and laser-induced fluorescence (LIF).
3. Establish limits on the amount of HNO_3 that could be produced at HSCT engine operating conditions before reaching the nozzle exit plane through measurements in well-documented reacting flow environments with NO_x present. Either TDL or FTIR optical techniques or wet chemistry/filters could be employed to establish such a limit.

A comparison of the estimated measurement requirements for NO_y species and the detection capabilities of the established chemiluminescent technique as well as candidate new techniques for confirming measurements are shown in Table 3a.

First and Second Priority Particulate Measurements

As discussed earlier, the potential impact of soot and related exhaust particulate emissions on the stratosphere and in the exhaust plume and wake are not yet fully defined but may be significant. Based on these concerns, measurement of the total particulate EI and number density have been assigned a first priority, while the particulate size distribution and condensation nucleation capabilities have been assigned a second priority.

The established particulate measurement technique, quantification of an SAE smoke number (SAE, 1980b), can be related to a total particulate EI. A recently developed aethalometer (Hanson et al., 1982) promises to put measurement of soot-dominated particulate EIs on a more reproducible basis. Soot emission number densities and size distributions can also be measured using cloud chamber detection techniques, with the University of Missouri at Rolla's differential mobility analyzer representing a state-of-the-art instrument for separating and detecting various soot size fractions as well as investigating their water nucleation properties (Hagen et al., 1989). While particle size distribution and condensation nucleation property measurements are a second priority, it is encouraging to note that an integrated instrument such as the University of Missouri apparatus can obtain this information in addition to measuring the first priority EI and number density requirements.

In summary, the recommendations for first and second priority particulate measurements from the measurement techniques section at the June Workshop are:

1. Compare the established smoke meter measurements with the aethalometer.
2. Compare the smoke meter and aethalometer with the differential mobility analyzer, considering the possibility of any loss or conversion in the sampling probe in detail.
3. Evaluate the use of wire impactor analysis embedded in the exhaust flow to resolve probe sampling issues.
4. Make routine measurement of the total particulate number density with a standard condensation nuclei (CN) counter.
5. Perform condensation nucleation efficiency tests on exhaust particles using low supersaturation ratio cloud chamber detectors in conjunction with CN counter measurements of number density.

The expected particulate loadings for both the RQL and LPP options for the HSCT gas turbine combustor are also shown in Table 3a along with the capabilities of the measurement techniques discussed above.

Second Priority Gaseous Species Measurements

While the measurement techniques working group at the June Workshop concentrated on instrumentation for the first priority NO_y and particulate measurements, it did consider measurement options for second priority gaseous species including SO_x (SO_2 , SO_3), HC, OH, and CO_2 as a gaseous species internal calibration.

The alternate techniques considered are primarily optical and most have the option of being applied either in an in situ manner without probe sampling or in an "extractive" mode, in line with established probe sampling systems for NO_x and other trace gases. If used in an in situ mode most techniques are somewhat less sensitive and are dependent on adequate optical access to the combustor test rig. Used in an extractive mode, care must be taken to avoid wall or other chemical loss for the most reactive species including SO_3 and OH.

Detection requirements in both surrogate engines and combustor/flame tube rigs are shown in Table 3b along with estimated detection precisions for both established and new measurement techniques. The most versatile new techniques would appear to be those based on infrared spectroscopy, including tunable diode laser differential spectroscopy and Fourier transform infrared spectroscopy.

SUMMARY OF RECOMMENDATIONS

The measurement of trace species emitted from HSRP engine developmental rigs is an essential part of the AESA study. Because the engines used to power the proposed HSCTs will not be available during the course of AESA, these developmental rigs and available surrogate engines will provide the only experimental basis for estimates of the expected emissions of these proposed stratospheric vehicles. Priorities for exhaust trace species emissions measurements have been established based on current understanding of homogeneous and heterogeneous stratospheric chemistry and the following criteria, in order of importance:

1. Impact on key species or chemical families at global scales, including latitudinal regions.
2. Impact on chemistry, condensation, or altitude of deposition due to plume and wake processes.
3. Evaluation of component design or criteria for design choices in HSRP combustor development.

NO_y plays a central role in the homogeneous and heterogeneous processes associated with ozone destruction in the stratosphere and, as a significant trace constituent of engine exhaust, becomes the prime species family for measurement. Its importance is considered so paramount that redundant measurements are recommended particularly for this chemical family to ensure that it is measured accurately and completely across the expected species (NO , NO_2 , and HNO_3). The detailed distribution among these species is important in understanding the initial chemical and physical evolution of the wake, and the measurement of the NO_y chemical speciation is given the second highest priority.

Perturbations of the stratospheric aerosol loading have the potential to affect heterogeneous chemistry, and the estimated impact of heterogeneous processes on stratospheric ozone grows

larger as our understanding increases. Particulate emissions need to be quantified to model potential HSCT effects on heterogeneous chemistry. For this reason, the total particle mass and particle number density measurements are given a top priority. The more detailed characterization of the particulate emissions, including a complete particle size distribution and the particulate cloud condensation nuclei (CCN) and ice nuclei (IN) activities, is given second priority.

The sulfuric acid aerosol (SAA) and sulfate aerosol contributions to the stratospheric aerosol loading due to HSCTs will result from condensation of SO_x emissions. The initial condensation kinetics will be determined by the oxidation of the fuel sulfur and its interaction with water vapor and condensation nuclei emitted from the engine or entrained from the ambient atmosphere. Thus, the speciation of the SO_x family is also placed in the second priority class. Similarly, OH measurements are recommended at this level since, as a reactive radical, OH participates in the plume/wake oxidation of SO_x and NO_y and helps to determine their speciation immediately behind an aircraft. Non-methane hydrocarbons (NMHC) do not appear to play a major role in ozone destruction at currently expected emission levels, but measurements are needed to place an upper bound on their level of emission from developmental rigs, since much higher levels can interact with NO_y chemistry through organic nitrates. Carbon dioxide provides a useful reference as a major combustion product, which can help to ensure that representative measurements of the total emission of a given species can be made reliably.

For each of these recommended species measurements, measurement venue types are recommended in Table 2. Species that continue to react as they flow from the combustor to the engine exit are best measured on complete engines. Conserved chemical families can be measured in combustor tests or in engines, even though their speciation may continue to evolve. Fundamental laboratory experiments are recommended when they can be used to provide additional insight on specific chemistry or to aid in diagnostic development.

Measurement venues are cataloged in Appendix B and include entries on flame tubes, combustor sector rigs, full annular combustor rigs, and current engines provided by workshop participants. The catalog is not all-inclusive and, for flame tubes in particular, other university and industry measurements may be available. Simple laboratory combustion apparatuses are recommended for instrument development, resolving questions on the influence of gas sampling on measurements, and calibrating species concentrations with redundant measurements. Measurements of NO_x/NO_y levels and particulate characteristics from advanced-concept combustors should be made in flame tube rigs for comparison with emission from current combustors operating at HSCT combustor conditions.

Second priority speciation measurements (NO_y , SO_x) and characterization of chemical-evolving emissions (OH and particulate reactivity, CCN, IN activities) can be evaluated by comparing annular rig test results with those from advanced engine tests in lieu of full HSCT engines. The costs and complexity of such a measurement program suggest that analysis or laboratory studies of turbine/nozzle gas-phase chemistry and particle chemical processing would be more cost-effective and should be tackled first.

Measurement requirements and suggested measurement techniques have been tabulated for both first and second priority species. Both currently established techniques (chemiluminescence, CL, flame ionization detection, FID, etc) and additional, new applications of optical measurements are recommended for the gaseous species. The additional techniques will allow redundant measurements of NO_y as a first priority species and more detailed quantification of the partitioning of the exhaust emissions among second priority species. Particulate measurement techniques are recommended which provide at least total mass and number density of soot emissions, and additional characterization of second priority soot properties using a given technique is considered advantageous.

Redundant measurement of first priority species and the more detailed exhaust gas characterization possible with the recommended second priority measurements will provide the basis for accurate and reliable estimates of the emissions from the proposed HSCT aircraft. Subsequent AESA assessment model calculations can then be based on the most complete emission information available and thus will accurately reflect the chemical perturbation to the atmosphere potentially caused by future supersonic stratospheric aircraft.

Table 1. Important Chemical and Particulate Jet Exhaust Emissions

Species	EI(a)	Exhaust Exit Molar Fraction(b)	Perturbation Level(c)	Background Level(d)	Significance of Problem	Measurement Priority
NO_x, NO_y						
NO _x	5-50(e)	5-50 x 10 ⁻⁵	3-5 ppbv(f)	2 - 16 ppbv(f)	About 90% of the exhaust NO _y is NO- rapidly oxidized to NO ₂ and other NO _y species in the stratosphere. NO _y accounts for 50% of the ozone depletion below 40 km	First priority- standard titration plus redundant spectroscopic
NO	4.5-45(e) (as NO ₂)	4-40 x 10 ⁻⁵			About 90% of the NO _y exhaust is NO- rapidly oxidized to NO ₂ in the stratosphere	First priority- standard titration plus redundant spectroscopic
NO ₂	0.5-5(e)	5-50 x 10 ⁻⁶	--	see (f)		First priority- standard titration plus redundant spectroscopic
HNO ₃	0.006	4.0 x 10 ⁻⁸ (g)	--	see (f)	Nitric acid can contribute to PSC, NAT formation at sufficiently cold temperatures	Second priority- important for chemistry in plume
Particulates						
Soot	0.02(e)	--	~.007 ppbm ^(h)	~.007 ppbm ^(h)	Particulate emissions can potentially increase the mass and/or chemical reactivity of the global background sulfate aerosol layer- stratospheric particulates could conceivably change the global radiative energy balance, thereby affecting global climate change	First priority to measure number density and total mass; second priority to measure size distribution and reactivity

Table 1. Important Chemical and Particulate Jet Exhaust Emissions (Cont'd)

Species	EI(a)	Exhaust Exit Molar Fraction(b)	Perturbation Level(c)	Background Level(d)	Significance of Problem	Measurement Priority
SO_x						
SO ₂	0-1(e)	$0-7 \times 10^{-6}$.01 - .02 ppbv(i)	0.05 - 0.1 ppbv(i)	Speciation could affect plume and wake chemistry and sulfate aerosol condensation. Sulfate aerosols can have the effects listed above for particulates and, at their expected higher levels, could be the dominant particulate perturbation	Second priority
SO ₃	<0.1	$<5 \times 10^{-7}(g)$	---	--		
H ₂ SO ₄	--	--	.11 - .22 ppbv(i)	1.13 ppbv(k)		
CO_x						
CO ₂	3160(e)	3.2×10^{-2}	0.7 - 1.2 ppmv(f)	350 ppmv(f)	Not expected to be significant compared with background, but could contribute very slightly to global warming	Second priority- can be a useful calibration for other measurements
CO	1-6(e)	$2-10 \times 10^{-5}$	1.7-1.8 ppbv(f)	10 - 50 ppbv(f)	Does not contribute to O ₃ loss; no appreciable global effect expected	Low priority
HO_x Reservoirs						
H ₂ O	1240(e)	3.0×10^{-2}	0.2 - 0.8 ppmv(l)	4 - 15 ppmv(l)	Global impact- major source of odd hydrogen radicals, which contribute to O ₃ depletion through HO _x cycle- modify ClO _x and NO _x cycles- may contribute to PSC formation and also to global warming.	Low priority - can be determined from fuel consumption
OH	0.4	$1.0 \times 10^{-5}(g)$	Insignificant	0.5 - 1 pptv(m)	Rapidly depleted in plume- affects NO _y and SO _x speciation	Second priority-affects speciation in plume

Table 1. Important Chemical and Particulate Jet Exhaust Emissions (Cont'd)

Species	El(a)	Exhaust Exit Molar Fraction(b)	Perturbation Level(c)	Background Level(d)	Significance of Problem	Measurement Priority
HO_x Reservoirs (continued)						
HO ₂	0.007	1.0 x 10 ^{-7(g)}	Negligible	2 - 10 pptv(m)	No appreciable affect	Low priority
H ₂ O ₂	0.002	2.4 x 10 ^{-8(g)}	Negligible	≤ 10 pptv(n)	No appreciable affect	Low priority
CH₄ and NMHC						
THC (total hydro- carbon)	0.1-0.2(e) (as CH ₄)	3-6 x 10 ⁻⁶	--	>1600 ppbv(l)	The THC emissions are small; however, some NMHC emissions are large compared with the zero background. Chemistry of these species in the stratosphere is not well understood, but they may act as reservoirs such as PAN	Second priority- obtain bound
CH ₄	0.04	1 x 10 ^{-6(o)}	--	1600 ppbv(l)	No global impact as CH ₄ concentrations not significantly changed	Low priority
Major NMHC	0.001-0.01 (as CH ₄)	1-10 x 10 ^{-8(o)}	--	0.2 ppbv ethane,(f) 0.6 ppbv propane(f) 0.2 ppbv acetylene(f)	Probably not significant; may warrant further research (see Appendix A)	Low priority
Cl_y						
Cl _y	0.01(p)	1 x 10 ⁻⁷	--	1 ppbv(l)	Cl _y has significant implications for ozone depletion. However, an insignificant amount of Cl _y will be emitted from the engines	Low priority

Table 1. Important Chemical and Particulate Jet Exhaust Emissions (Cont'd)

Species	EI(a)	Exhaust Exit Molar Fraction(b)	Perturbation Level(c)	Background Level(d)	Significance of Problem	Measurement Priority
Metals/Metal Oxides						
Al, Mn, Cr, Fe, Pb, V	0.0001-0.001	1-10 x 10 ⁻⁹ (q)		> 1.7 particles (> 1 µm)/m ³ (r)	Could serve as cloud/aerosol condensation nuclei, probably negligible compared to meteor metal oxide background and spacecraft debris/rocket exhaust particle levels	Low priority

(a)Emission index, $EI(Y)X = (g/s \text{ species } X) / (kg/s \text{ fuel})$, where the preceding subscript (Y) indicates that the EI of species X is being reported in terms of the mass of an equivalent molar quantity of species Y. E.g. $EI(NO_2) NO_x$, $EI(CH_4) THC$ allow the EIs of the components comprising NO_x (NO , NO_2) and THC (C_nH_m , ...) to be directly added when their EIs are all based on molecular weights of NO_2 and CH_4 , respectively.

(b)Molar fraction is computed from the EI assuming an overall fuel to air mass ratio of 0.0155 and depends linearly on this ratio. (Molar fraction = $EI/1000 \times 29/MW \times 0.0155$, where MW is the reference molecular weight.) The molar fraction of trace species such as OH, HO_2 , HNO_3 , SO_3 , etc. were computed from the Aerodyne model chemistry code(g) and EIs were back-calculated from these molar fractions. These species concentrations and EIs depend sensitively on the temperatures and pressures within the engine.

(c)The perturbations are based on fuel usage of 7.7×10^{10} kg/yr (Douglass et al. in Prather et al., 1992) or 7.0×10^{10} kg/yr and model calculations (Ko et al., in Prather et al., 1992) or other estimates as noted.

(d)Backgrounds are based on model calculations (Ko et al., in Prather et al., 1992) or reported measured background levels (Ko and Douglass et al., in Prather et al., 1992 and others as noted).

(e)Estimates for HSCT engines provided to the HSR program by engine developers (Miake-Lye in Prather et al., 1992).

(f)Douglass et al., in Prather et al., 1992

(g)Estimates calculated using Aerodyne chemical kinetics model (Miake-Lye et al., 1991).

(h)Pueschel et al., 1992 measured current mass mixing ratio of stratospheric soot particles and estimated doubling due to HSCT emissions.

(i)Turco, R.P. in Appendix A estimates SO_x perturbations to be 10 - 20% of background.

(j)Turco et al., 1982; non-volcanically perturbed measured SO_2 background 15 - 22 km.

Table 1. Important Chemical and Particulate Jet Exhaust Emissions (Cont'd)

-
- (k) Hofmann 1990; 1989 "pre-Pinatubo" background mass mixing ratio for sulfuric acid aerosol 18 - 22 km.
 - (l) Ko et al., 1992 in Prather et al., 1992; note that NO_x will photochemically evolve after emission to significantly enhance each NO_y species, including NO_2 and HNO_3 .
 - (m) Stimpfle et al., 1990.
 - (n) Park and Carli, 1991 and references therein.
 - (o) For non-HSCT engine. Major NMHCs include ethene, propene, formaldehyde, acetone (Spicer et al., 1992).
 - (p) Based on Cl content measurements of crude oils, before refining and not from an exit-plane measurement (Table 2.2 CIAP Monograph 2, 1975).
 - (q) Based on measurements of the exhaust of an auxiliary power unit turbine operating at high temperatures (Table 2.4 CIAP Monograph 2). Correspondences to HSCT engines very tenuous; much of metal due to engine erosion, which may be time dependent, and HSCT engine materials are likely to differ dramatically. Crude oils' metal contents (Table 2.2, CIAP, 1975) would result in lower EI's and molar fractions.
 - (r) Zolensky et al., 1989, measured 1.7 particles greater than 1 μm particles/ m^3 in 1985. Hunten et al., 1980 calculate significant stratospheric metal oxide flux from mesospheric meteor ablation.

Table 2. Measurement Venue Types

Engines	Combustors/Flame Tubes	Fundamental Combustion
1. NO, NO₂, HNO₃ total NO_y (absolute measurement) <i>speciation</i>	NO, NO₂, NO_x total NO_x (absolute measurement)	NO, NO₂, HNO₃
2. particulates total mass <i>properties</i> <i>Size distribution</i> <i>reactivity</i>	particulates total mass <i>Size distribution</i>	particulates <i>CCN, IN</i> <i>Reactivity</i>
3. <i>SO₂/SO₃, H₂SO₄</i>		
4. <i>OH</i>		
5. <i>NMHC</i>	<i>NMHC?</i>	
6. <i>CO₂</i>	<i>CO₂</i>	<i>CO₂</i>

Bold face = First Priority*Italics = Second Priority*

Table 3a. First Priority Species Measurement Techniques

Species	Detection Requirements (ppmv) Engine Combustor/Flame Tube	Established Techniques (Precision ppmv)	New Techniques (Precision ppmv)
NO	40-300 (± 2) 80-600 (± 2)	Chemiluminescence $\pm 0.1 - 1.0$ using recommended standard probe design for cooling, materials, etc.	TDL ($\pm < 1$ ppmv) FTIR ($\pm < 1$ ppmv?) LIF ($\pm < 1$ ppmv) UV absorption ?
NO ₂	40-300 (± 2) 80-300 (± 2)	Chemiluminescence/catalytic conversion ($\pm < 2$ ppmv) conversion efficiency must be demonstrated w/o demonstration of specificity, measurement is <u>upper limit</u> for NO ₂	Chemiluminescence/ photolytic conversion ($\pm < 1$ ppmv) TDL ($\pm < 1$ ppmv) FTIR ($\pm < 1$ ppmv?) LIF ($\pm < 10$ ppmv)
HNO ₃	2 ± 2 N/A	None	TDL ($\pm < 2$ ppmv) FTIR ($\pm < 2$ ppmv?) Wet Chemistry/filter techniques ?
NO _y	40-300 (± 2) 80-600 (± 2)	None	Chemiluminescence/ catalytic conversion ($\pm < 1$ ppmv) catalytic performance needs to be demonstrated TDL (NO _x + HNO ₃) ($\pm < 1$ ppmv) FTIR (NO _x + HNO ₃) ($\pm < 1$ ppmv)
Particulates	RQL ~0.02 g/kg fuel/burned LPP ~0 g/kg fuel/burned (immeasurably small using smoke meter)	Smoke meter (filter-based, 40-sec response) (< 0.02 g/kg)	Aethalometer ($< 2 \times 10^{-5}$ g/kg) (real time, 1 - 10 sec response) Mobile Aerosol Sampling System (MASS) (diff mobility analyzer) options: - mass, number density, size dist (0.01 μ m - 1 μ m diam.), CN/CCN activity properties, delayed analysis of composition, etc., flight worthy design Total CN, Impactor (surface, No., vol, chem comp)

Table 3b. Second Priority Gaseous Species Measurement Techniques

Species	Detection Requirements (ppmv) Engine	Combustor/Flame Tube	Established Techniques (Precision ppmv)	New Techniques (Precision ppmv)
SO _x	7 ± 1 SO ₂ 1 ± 1 SO ₃	7 ± 1 SO ₂ 1 ± 0.1 SO ₃	(Non-dispersive UV) Electrochemical	LIF (1-10 ppmv SO ₂) TDL (in situ 1 ppmv SO ₂ , 0.4 ppmv SO ₃ ; extractive 0.03 ppmv SO ₂ , 0.1 ppmv SO ₃) FTIR (1 ppm SO ₂) MS (~1 ppmv, possibly SO ₂ /SO ₃ Isotope dilution/MS (<< 1 ppmv) (MS = Mass Spectrometry)
HC	1-6 ± 1 (± 1)		FID (THC) (< 1) GC/FID (CH ₄ + NMHC) GC = Gas Chromatography FID = Flame Ionization Detection	TDL (CH ₄) in situ ± 0.2 ppmv use for (THC-CH ₄), extractive ± 0.01 ppmv
OH	10 ± 1	± 200	UV absorption (line) ± 0.1	TDL* (line) in situ ± 0.2 ppmv (engines), extractive ± 0.1 ppmv LIF* (point) (<1 ppmv) in situ UV laser differential absorption* (0.003 ppmv in situ)
CO ₂	32000 (± 2% reading)	64000 (± 2% reading)	(Non-dispersive IR) (± 2% reading)	TDL ± 1% extractive, in situ FTIR ± 1% extractive?

* Special Concerns: 1) need to establish representativeness of optical measurements for chemical flux determination, especially for point measurements; 2) need to establish sampling integrity for extractive sample probes; 3) possible need for fundamental lab experiments to evaluate sampling.

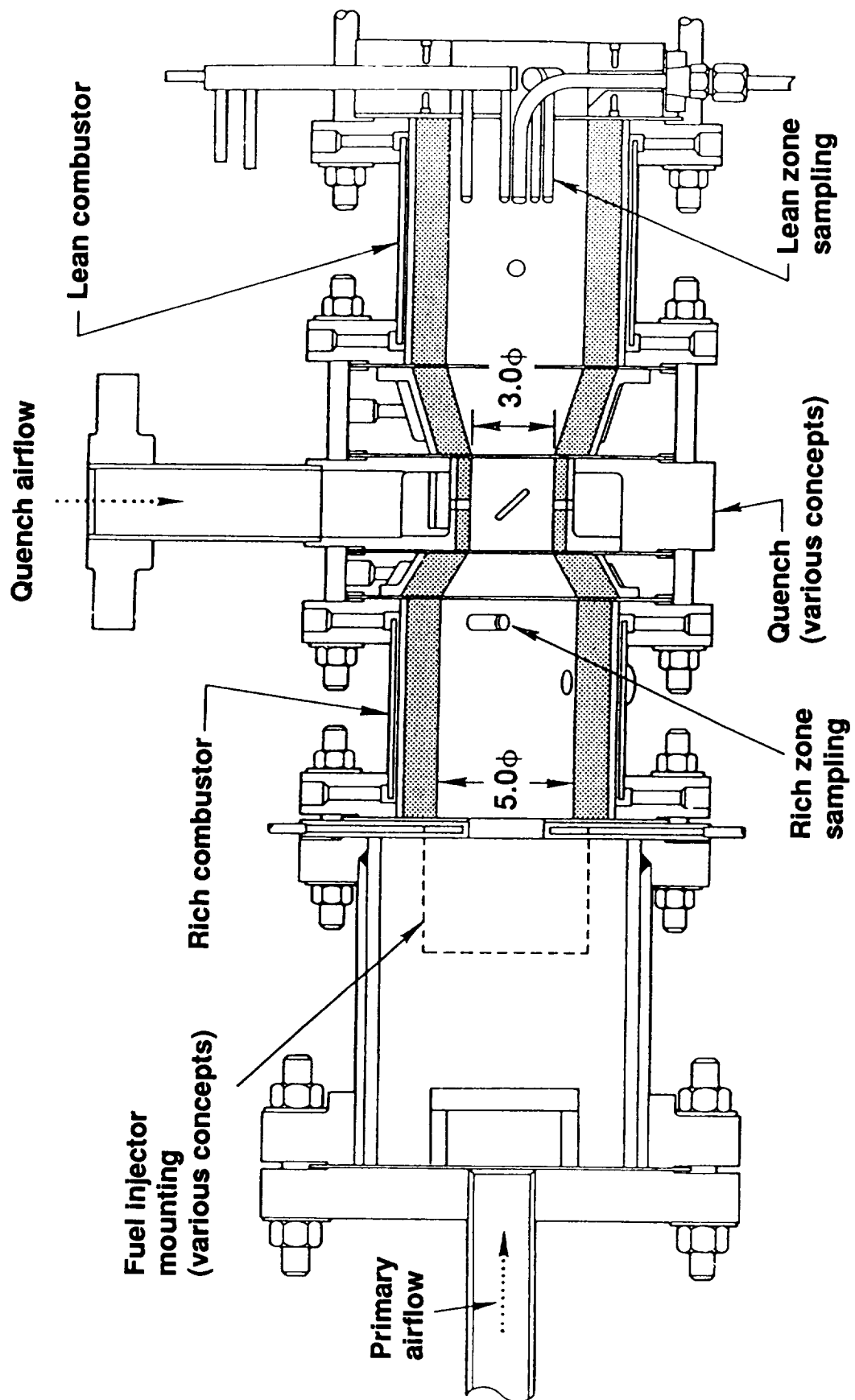


Figure 1. Flame tube for RQL combustor development.

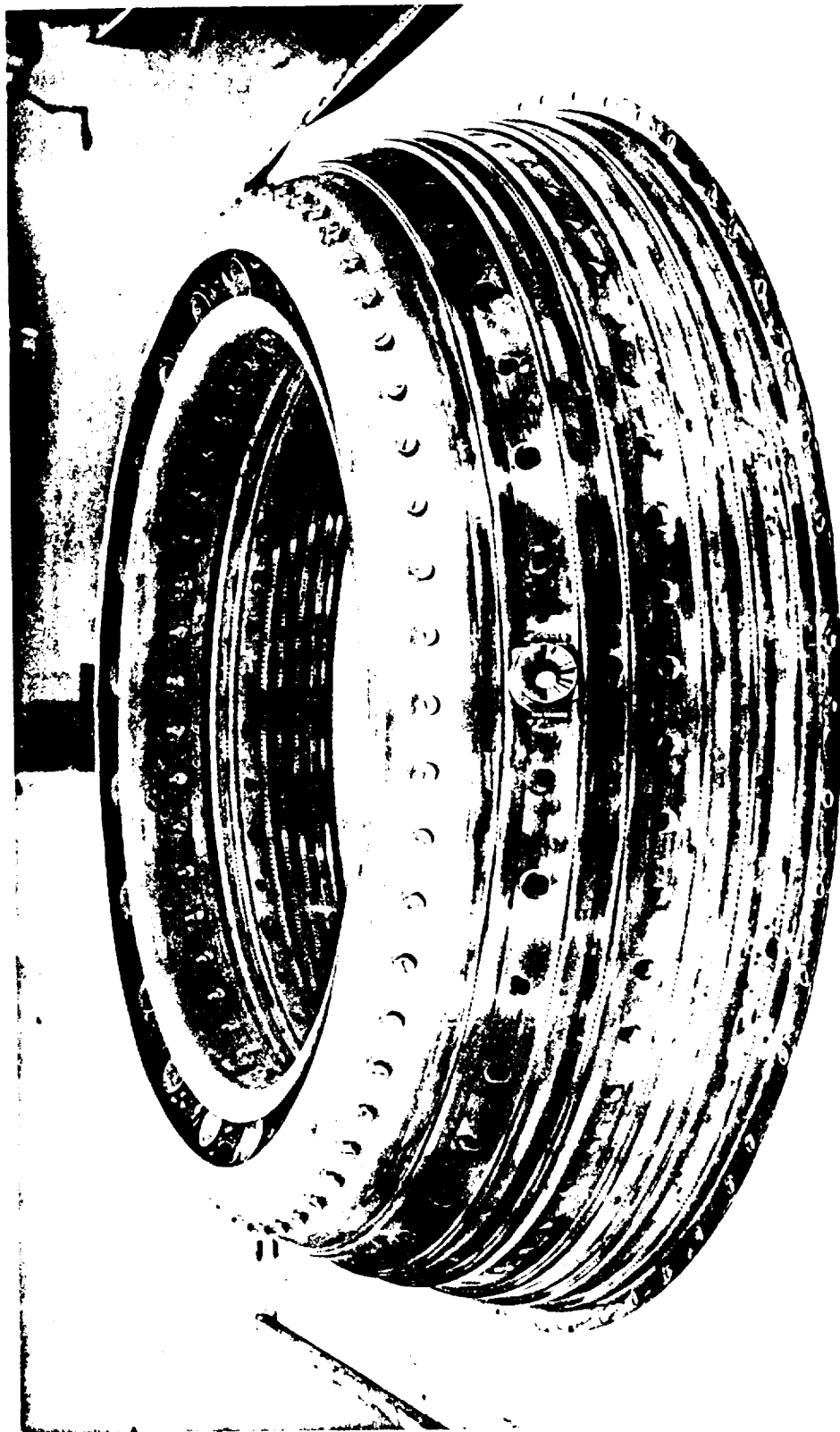


Figure 2. CF6-50 combustor assembly.



Figure 3. CF6-80 combustor exit instrumentation rakes mounted in five-cup sector-combustor test rig.

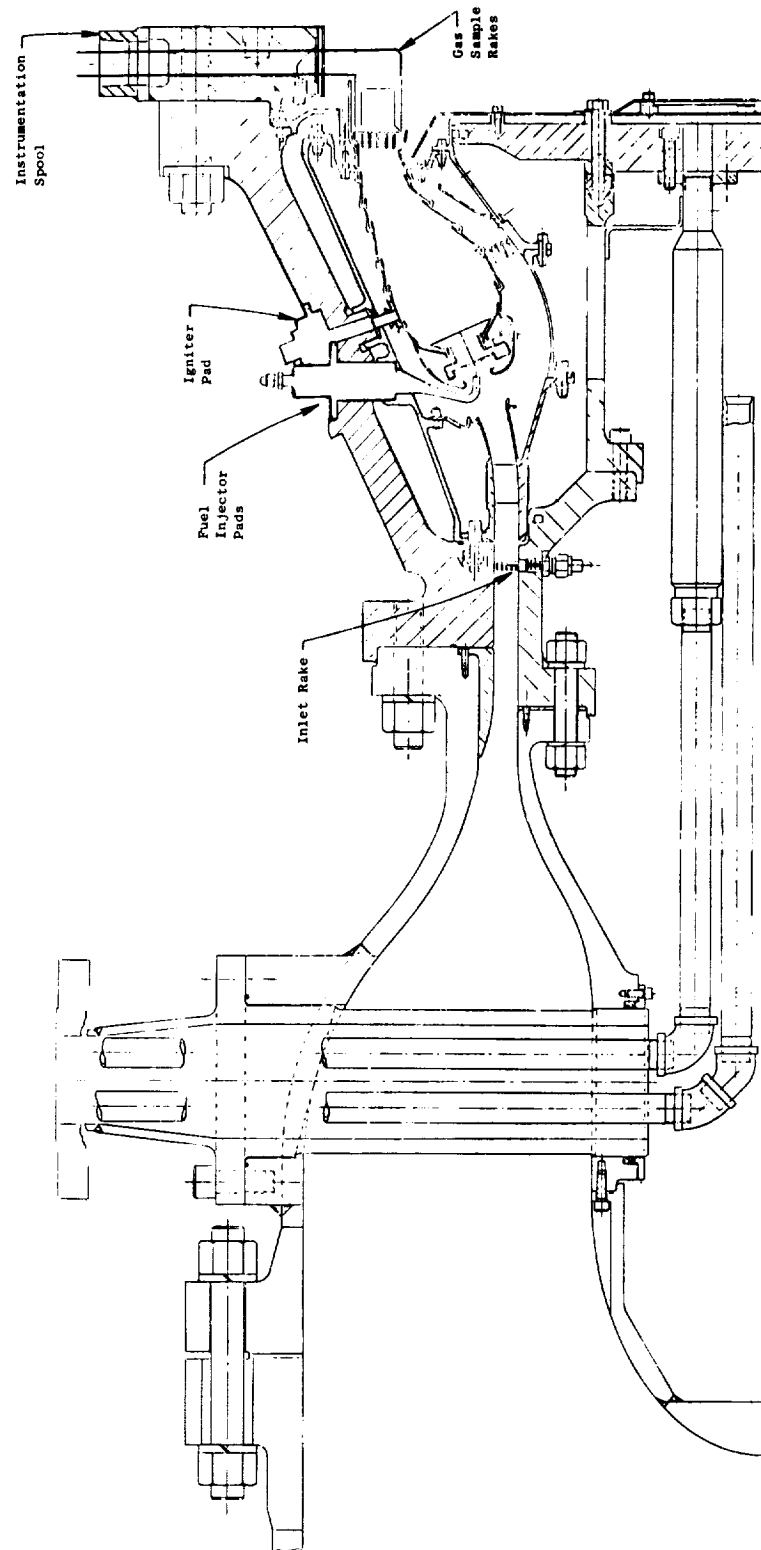


Figure 4. Combustor test rig cross section.

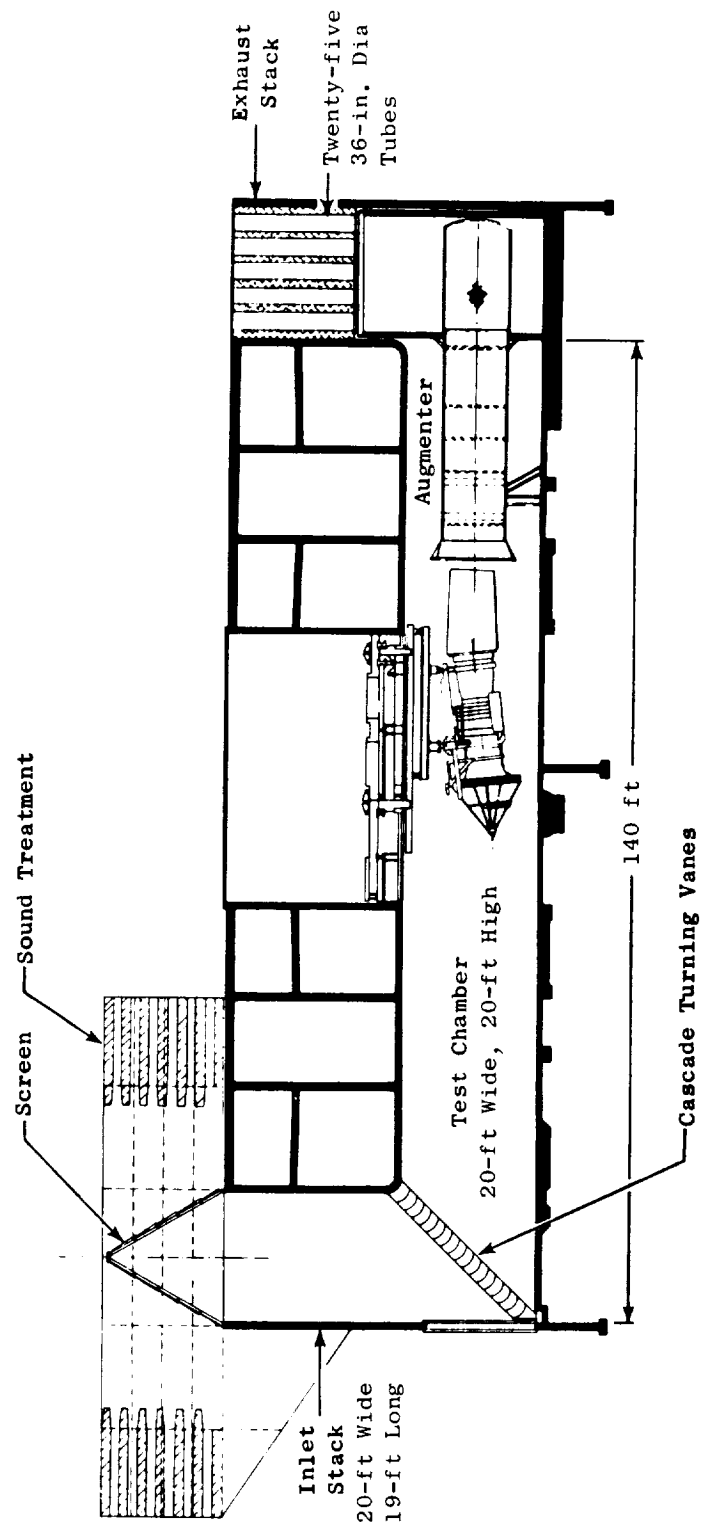


Figure 5. Development engine test cell cross section.

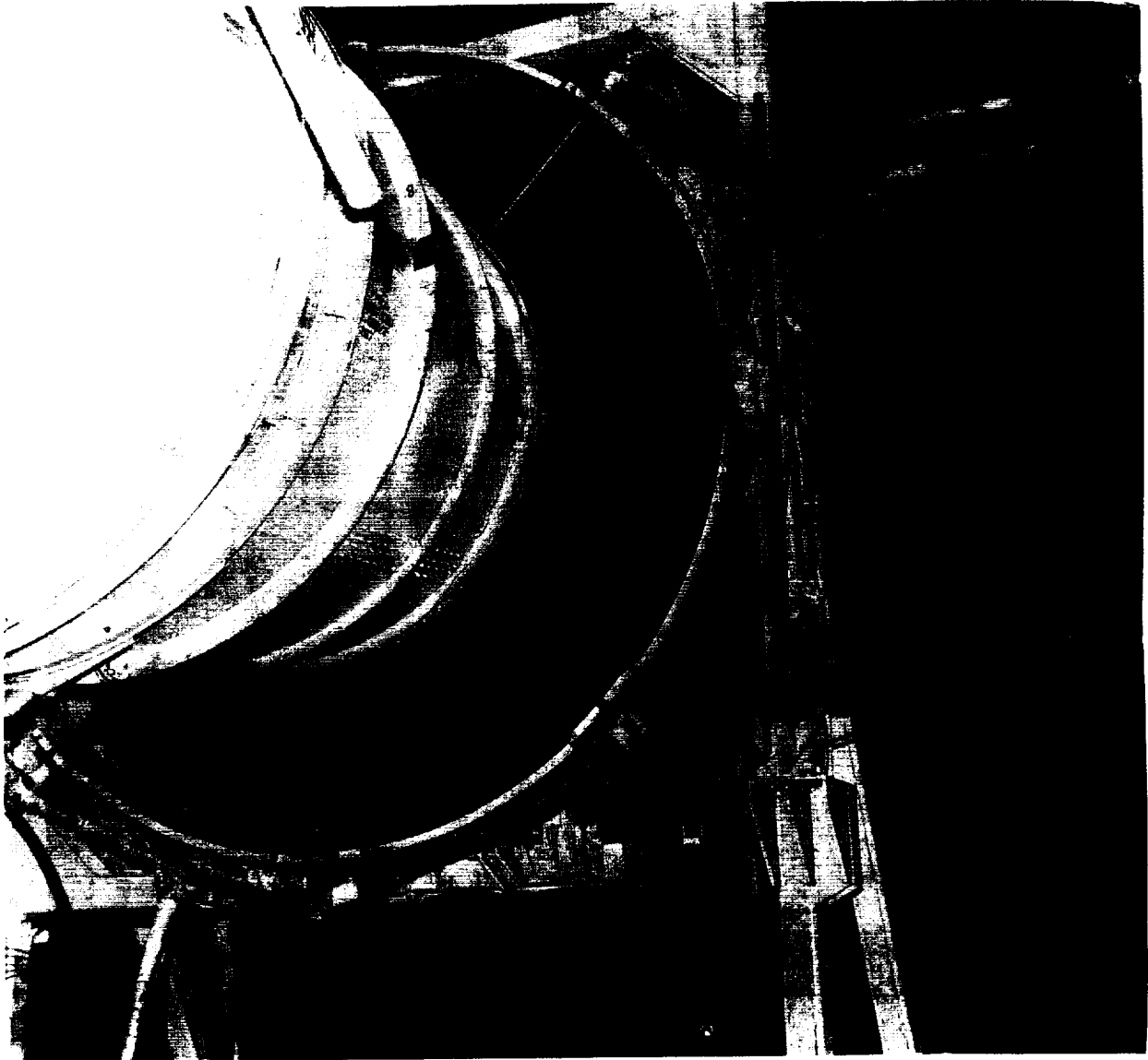


Figure 6. Rake system mounted behind CFM56 engine.

APPENDIX A

CORRESPONDENCE WITH STRATOSPHERIC AEROSOL SCIENCE AND MODELS & MEASUREMENTS COMMITTEES

AERODYNE RESEARCH, Inc.

45 Manning Road
Billerica, Massachusetts 01821-3976
(508) 663-9500 Fax (508) 663-4918

ARI File No. 3806-001

29 April 1992

Prof. Richard P. Turco
University of California, Los Angeles
Los Angeles, CA 90024-1565

Re: Aerosol data for EETC Committee

Dear Prof. Turco:

The Engine Exhaust Trace Chemistry Committee of the NASA HSRP/AESA met last week to discuss priorities for new or additional engine measurements to be recommended to the AESA. While the committee made considerable progress toward putting together a set of recommendations—I will present a summary at the annual meeting in May—it became apparent that additional input from your committee on Stratospheric Aerosol Science is required.

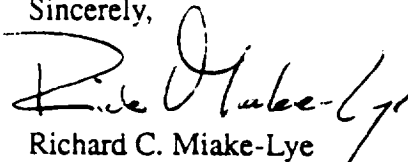
More specifically, justification of particulate measurements in engine or engine component exhaust flows depends on identifying their most significant impact on stratospheric chemistry and/or radiation transport. The EETC Committee would appreciate your comments on the following issues, based on current understanding of aerosol chemistry:

1. How do engine exhaust aerosols affect the radiation/chemical balance most significantly:
 - a. Direct scattering effects?
 - b. Aerosol-forming (CCN) properties?
2. At what level of emissions do engine particulates become important?
 - a. Is the significant emissions level measured in number density, total mass loading, or in terms of the total particle size distribution?
 - b. What background/ambient levels represent the threshold criteria?
3. What characterization of particulates is required?
 - a. Is soot the only important particulate emission (vs. metals, condensates, *etc.*)
 - b. What information is required about surface reactivity, CCN-activity, *etc.* for incorporation into existing models of particulate effects?

29 April 1992

We are beginning to plan for a workshop on emissions measurements to be held at LeRC on 24-25 June to which your committee will be expected to contribute. However, on a more immediate time-scale, we would hope that you could address these questions in your committee's meeting at Virginia Beach and provide EETC with some direction for planning that workshop. In fact, if any existing materials could help to refine our thinking before May 17th, please bring them to my attention. I will give you a call in a few days to hear your thoughts on this interaction.

Sincerely,



Richard C. Miake-Lye
Senior Systems Scientist

xc: F.L. Dryer, Princeton
R.W. Niedzwiecki, NASA LeRC
H.L. Wesoky, NASA Hq



DEPARTMENT OF ATMOSPHERIC SCIENCES
405 HILGARD AVENUE
LOS ANGELES, CALIFORNIA 90024

Dr. Richard Stolarski
Laboratory for Planetary Atmospheres
Mail Stop 916
NASA Goddard Space Flight Center
Greenbelt, MD 20771

June 1, 1992

Dear Rich,

Attached is the summary report of the Stratospheric Aerosol Science Committee (SASC) held at the second annual HSRP review meeting in Virginia Beach. The committee discussions covered a number of topics related to the HSRP program, including possible new aerosol instrumentation, interactions between SASC and the engine test group, and the development of heterogeneous chemistry parameterizations for the atmospheric modeling teams. To summarize, the following recommendations arose from the meeting:

1. The definition of soot emission rates, properties and distributions in the stratosphere should be pursued. We suggest that the wire impactor archive at Ames be analyzed for soot quantities, size distributions and trends. The impaction efficiency of soot on the wires should be calibrated through appropriate laboratory simulations.
2. In the upcoming engine tests, the following parameters should be measured (the parameters are roughly ordered according to priority within this subset):
 - Soot emission factor
 - Soot particle number (per gram of soot emitted, or CN/g)
 - Engine-soot trace metal signature
 - Sulfur oxide partitioning into SO_2 , and $\text{SO}_3/\text{H}_2\text{SO}_4$.If other resources are available, the following parameters could also be measured:
 - Soot size distribution ($\#/\text{cm}^3$ -micrometer)
 - Cloud condensation nuclei (CCN) and ice nuclei (IN) activity of the soot particles.

The soot mass emission measurements are relatively easy to make, and soot is a unique product of aircraft activity that may be useful as a tracer of dynamical processes. The sulfur oxide abundances are important in determining the initial microphysical development of the contrail, which

in turn may affect the longer term chemical impacts of the exhaust gases and particulates.

3. Measurements of the composition of stratospheric particles are needed to confirm existing theories of heterogeneous chemical processing on these aerosols, and to apply laboratory data in an appropriate way to the aircraft impact assessment. The committee was briefed on a new measurement concept based on infrared spectroscopy, which offers a possible real-time aircraft-borne size-discriminating capability for quantitatively determining the principal components of stratospheric aerosols. We suggest that a proposal be solicited from the research team involved. A subcommittee of SASC can review this and any other instrumentation proposals received by your office and make a recommendation for action.

4. The evolving Mt. Pinatubo aerosols in the lower stratosphere provide an enhanced analog of the sulfate aerosols produced by aircraft exhaust, and thus offer the possibility for delimiting the potential chemical effects of aircraft emissions. Accordingly, the volcanic aerosols should be monitored in the following ways: i) periodic latitude transects with an airborne lidar — Browell's lidar is ideal for this purpose; ii) satellite horizontal and vertical distribution maps of aerosol extinction or other parameters — the SAGE system should be able to provide some of this data operationally, particularly as the aerosols thin out, and nimbus or other systems may yield important additional information; iii) ER-2 flight data to complement the lidar and satellite observations. The HSRP could maintain a low profile in this regard, simply encouraging planned field projects to collect relevant data. For studying the chemical effects of Pinatubo aerosols, the SPADE mission is ideally suited. The HSRP might also wish to co-sponsor a limited number of lidar flights and satellite data analyses.

The volcanic aerosol data may be useful for defining the residence times in, and transport rates between, the different regions of the stratosphere (tropical, midlatitude, and polar), and for calibrating the lifetimes of materials in the lower stratosphere. The enhanced heterogeneous chemistry that may be occurring on the Pinatubo aerosols can be investigated to calibrate potential aircraft effects, and to constrain chemistry models. The volcanic aerosol enhancement is 10-100 times the ambient level, which is large enough to speed up the sulfate aerosol reactions to detectable rates even at low and middle latitudes; by comparison, the aircraft sulfate aerosol perturbation is likely to be only about 10-20% above ambient. Such in situ measurements should provide an acid test of the chemical models being employed in the HSRP, and of the applicability of laboratory data directly to stratospheric conditions.

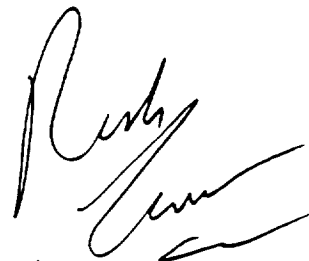
5. The SASC can interact with the HSRP modeling assessment community in the following possible ways: by evaluating the heterogeneous reaction rates presently adopted in photochemical models;

by providing guidance on the use of laboratory data to define stratospheric heterogeneous reaction rates; by specifying appropriate parameterizations for heterogeneous reactions, including PSC properties (appearance temperatures, surface areas and physical effects) and reaction sticking coefficients under various conditions. The SASC can participate in other related activities such as NASA's chemical kinetics evaluation panel and the heterogeneous chemistry modeling initiative out of Jack Kaye's office.

Attached is additional information on the SASC meeting, with a statement pointing out the significance of aerosol-related research to the HSRP, and a preliminary brief on the properties and effects of soot in the stratosphere.

Sincerely,

Richard Turco
(for the Committee)

A handwritten signature in dark ink, appearing to read 'Richard Turco', with a stylized flourish at the end.

Cc: Committee Members, and Ex-Officio Members

P.S. I have attached a copy of a letter I received from Tony Hansen that contains a more detailed description of soot measurement techniques that might be used in the engine tests. Again, the priority of the measurements is given in item 2 above.

Report of the Stratospheric Aerosol Science Committee (SASC) May 19, 1992, Virginia Beach, VA

The second meeting of SASC was held at the annual HSRP conference in Virginia Beach. The following committee members were present: D. Baumgardner, D. Blake, J. Dye, P. Hamill, A. Hansen, D. Murphy, R. Pueschel, P. Whitefield, C. Wilson, and G. Yue. M. Prather, R. Niedzwiecki, R. Oliver and R. Stolarski sat in, and a number of other conference attendees participated in the discussions. Because of the large attendance, the deliberations were less focused. A good part of the discussion covered topics already resolved at the first SASC meeting, as summarized in an earlier report of that meeting. The major recommendations that followed from the second meeting are summarized in the preceding letter to Rich Stolarski. Several general issues that arose concerning soot and other aerosols are addressed below. For example, a focus on aerosols and aerosol measurements in the HSRP needs to be justified quantitatively. The significance of aerosol processes is described below.

Rationale for Aerosol Measurements

The aerosol science committee discussed the reasons for carrying out detailed measurements of the stratospheric aerosols in the High Speed Research Program. The study of atmospheric chemistry and microphysics has a well-established history of synergistic interactions between laboratory studies, field experiments and modeling analyses. Laboratory measurements provide fundamental data that define the basic processes that may occur. Field experiments identify the key processes and interactions that actually occur in the atmospheric environment, including the variability introduced naturally. Models provide a quantitative framework for integrating these key processes — with laboratory data to establish the basic physics and chemistry, and field data to validate the process interactions. A fully integrated model can be used to predict effects that might occur as a result of an expected or unexpected external or internal forcing, and to analyze incomplete data sets to extend their useful application.

It has recently been recognized that heterogeneous chemical reactions catalyzed by stratospheric particles lead to fundamental changes in stratospheric composition. The most obvious manifestation of heterogeneous effects is seen in the annual formation of the "ozone hole" over Antarctica. The ozone hole chemistry involves polar stratospheric clouds (PSCs) composed of nitric acid and water ices. More recently, it has been found that the background sulfate aerosols, and the related volcanic sulfate particles, also participate in important heterogeneous reactions of nitrogen oxides leading to denoxification. Both the ice clouds causing the ozone hole and the sulfates causing denoxification are relevant to the impacts of aircraft exhaust on stratospheric composition.

The engine emissions of the proposed HSCT include water vapor, nitrogen oxides and sulfur oxides, all of which contribute to aerosol formation. The expected aerosol perturbations on a global scale are expected to be small (see the summary, Stratospheric Soot: Sources, Quantities and Effects, below). However, in many regions, the accumulation of water and NO_x could enhance the probability of PSC formation and chlorine activation. Concern centers on the Northern Hemisphere high latitudes, where aircraft traffic will be particularly heavy and the potential for anomalous chemistry is high. Both enhanced sulfate aerosols and PSCs could contribute to the accelerating depletion of ozone by chlorofluorocarbons detected recently, and which is expected to persist for decades despite the Montreal Treaty to limit chlorofluorocarbon production. Preliminary chemical modeling by several groups demonstrates a substantial possible impact on the stratosphere due to aerosol enhancement by the HSCT. However, the treatment of heterogeneous chemistry in these models is exceedingly crude, and must be improved if credible assessments are to be carried out.

The emission of soot into the stratosphere is apparently unique to aircraft engines, and may have potentially important environmental implications. The soot particles may act as freezing nuclei within sulfate aerosols, hastening the onset of freezing of sulfate droplets in fall and winter, accelerating the formation of PSCs, and enhancing the chlorine activation and ozone depletions associated with these ice clouds. Soot may also prove to be a useful tracer of the dynamics of the lower stratosphere, leading to a clearer picture of the stratospheric lifetimes and removal processes of aircraft exhaust products.

Previous studies of the stratospheric impact of high-altitude aircraft were based almost exclusively on photochemical considerations. Potential hazards to the ozone layer, although serious, were found to be manageable. However, the suggestions of potentially important heterogeneous chemical effects of aircraft remain largely unexplored, and thus represent a major threat to any plan to deploy an HSCT fleet. The HSRP is supporting laboratory research, field experimentation and modeling analyses related to heterogeneous stratospheric chemistry. This support is appropriate and judicious. The Stratospheric Aerosol Science Committee (SASC), established by the HSRP, can contribute to a sensible, focused aerosol research program.

Stratospheric Soot: Sources, Quantities and Effects

The effects of soot on the atmosphere were estimated during the CIAP program in the early 1970's. In a subsequent paper, Turco et al. (J. Appl. Meteorol., 19, 78, 1980; see also Toon et al., NASA Ref. Publ. 1058, 1980) applied a more detailed microphysical model to quantify the compositional and climatic effects of continuous high-altitude aircraft flights. Turco et al. considered only the global-average effects, using a sulfur dioxide emission factor of 1g/kg, and a soot emission factor of 0.3

g/kg with a total soot emission of 0.009 teragrams/year. By comparison, the soot emission factor for the advanced HSCT is around 0.02 g/kg. In recent measurements of background soot concentrations, abundances of between 1-2 nanograms/m³ have been found in the stratosphere. This amount of soot is consistent with an overall aerosol single scatter albedo of about 0.99-0.98, which was observed independently. The estimated emissions of soot by the proposed HSCT would likely double this amount, averaged over the hemisphere. In flight corridors, the increase could be as large as a factor of ten. A significant increase in the total number of aerosol particles of all sizes could also occur. Because the HSCT flies well into the stratosphere, compared to present commercial aircraft, which cruise near the tropopause, the stratospheric accumulation of soot per unit mass emitted would be greater for the HSCT.

The possible sources of stratospheric soot include commercial subsonic aircraft, high-altitude military aircraft, tropospheric soot from forest fires and air pollution, and extraterrestrial elemental carbon. In the first HSRP report (Prather et al., NASA Ref. Publ. 1272, 1992), Turco reviewed the sources, amounts and effects of several stratospheric aerosol materials. The total soot source for the stratosphere was estimated as 0.001 teragrams/year. The most likely source was assumed to be commercial air traffic, although confirming data are absent. This conclusion follows from the amount of soot measured — which is consistent with transport from near the tropopause level — and the presence of eternally-mixed soot particles — which implies relatively fresh particles unprocessed by convective clouds. The fact is that little quantitative information is currently available to define the stratospheric cycle of soot.

Possibly important stratospheric effects of soot and sulfur emissions from high-altitude aircraft operations include:

1. Optical and radiative perturbations caused by enhanced aerosols (these have been estimated to be quite small by Turco et al. and others).
2. Soot particles entrained into sulfate aerosols subsequently acting as freezing sites for PSC formation, extending the period and range of PSC occurrence.
3. Enhanced heterogeneous chemical processing on increased aerosol surface areas in the wakes of HSCTs; specifically, the conversion of emitted nitrogen oxides to nitric acid, and the activation of chlorine for ozone attack.
4. Persistent contrails formed under cold stratospheric conditions leading to a local augmentation of heterogeneous processing.
5. A decrease in the threshold for PSC formation over large areas of the globe due to the accumulation of nitric acid and water vapors in aircraft corridors, with possible heterogeneous chemical effects.

Of these specific issues, items 2, 4 and 5 may be the most critical. A comprehensive research program can reduce many of the uncertainties associated with the soot and aerosol effects of high-altitude flight.

AERODYNE RESEARCH, Inc.

45 Manning Road
Billerica, Massachusetts 01821-3976
(508) 663-9500 Fax (508) 663-4918

ARI File No. 3806-001

29 April 1992

Dr. Malcolm K.W. Ko
Atmospheric and Environmental Research, Inc.
840 Memorial Drive
Cambridge, MA 02139

Re: NMHC data for EETC Committee

Dear Malcolm:

The Engine Exhaust Trace Chemistry Committee of the NASA HSRP/AESA met last week to discuss priorities for new or additional engine measurements to be recommended to the AESA. While the committee made considerable progress toward putting together a set of recommendations—I will present a summary at the annual meeting in May—it became apparent that additional input from the global modeling community is required.

It is clear that NO_y is of primary concern and its careful quantitation motivates detailed and, in some cases, redundant measurements to complement the standard NO_x measurement techniques currently used routinely. For the purpose of establishing measurement criteria based on the impact of expected emission levels, can you provide me with the fraction of the NO_y budget emitted by model HSCT fleets for the current AESA scenarios with NO_x EIs of 5 and 15?

The non-methane hydrocarbons (NMHCs) emitted in the exhaust represent a more minor set of species and the EETC Committee needs some guidance on how to establish criteria for measuring them either as a class or by species. I understand that you and Chuck Kolb have discussed possible estimates that could provide insight on this question. Input from the modeling community is requested to ascertain:

1. At what level of emissions does engine NMHC chemistry become important?
2. Is the distribution among the various species important? Or can the behavior of the class be bounded by modeling a single more active species?

Whether NMHCs even need measurement depends on whether emissions at EIs less than 0.1 (or, more generously, 1) can significantly perturb the NO_y chemistry occurring with NO_x EIs of 5 to 15.

We are beginning to plan for a workshop on emission measurements to be held at LeRC on 24-25 June, at which this information will be important. However, on a more immediate time-scale, we would hope that you could address these questions in time for the Virginia Beach meeting and provide EETC with some direction for planning that workshop. Please keep us posted on your thoughts and efforts on these measurement issues.

Best Regards,



Richard C. Miake-Lye
Senior Systems Scientist

xc: F.L. Dryer, Princeton
R.W. Niedzwiecki, NASA LeRC
H.L. Wesoky, NASA Hq

M.K.W. Ko and D.K. Weisenstein of Atmospheric and Environmental Research, Inc. have provided the results of calculations using the AER model to test the sensitivity of ozone depletion to NMHC emissions. While the standard HSRP model scenarios are currently representing hydrocarbon emissions as though the entire mass of hydrocarbon were emitted as methane (CH_4), these calculations were performed with the entire emitted hydrocarbon mass as ethane (C_2H_6). C_2H_6 was chosen to represent the NMHCs since the existing chemical models include PAN chemistry that arises through C_2H_6 , but not longer-chain hydrocarbon molecules. This is viewed as a conservative estimate, however, since C_2H_6 should be at least as effective in forming organic nitrates and sequestering NO_y as other NMHC emissions. Emission levels 10 and 100 times the standard scenario CH_4 EI were also calculated to provide estimates of a level of NMHC emissions that could have non-negligible impact on O_3 depletion.

The basic scenario used (Case A, Fig. A.1) was the standard Mach 2.4 case with $\text{EI}(\text{NO}_2)\text{NO}_x = 15$ which has a CH_4 emission index of 0.2. For these calculations, C_2H_6 EI's of 0.2 (Fig. A.2), 2 (Fig. A.3) and 20 (Fig. A.4) were used to explore the sensitivity of O_3 changes to the introduction of NMHCs. Note that the total mass is used in the EI, so that a C_2H_6 EI of 0.2 represents roughly half as many moles as a CH_4 EI of 0.2 but the carbon atoms are approximately the same in each case. These calculations were compared with the standard Case A scenario ($\text{EI CH}_4 = 0.2$) as well as a Case A scenario with EI CH_4 increased to 20 (Fig. A.5). The latter, increased CH_4 calculation differentiates between increasing the THC emission as CH_4 versus increased levels of C_2H_6 .

These results indicate that, for C_2H_6 EI = 0.2, no appreciable changes in the ozone depletion are calculated. Non-negligible effects are calculated when $\text{EI C}_2\text{H}_6 = 2$ (20% smaller O_3 loss) and, for $\text{EI C}_2\text{H}_6 = 20$ which is two orders of magnitude greater than the expected levels, the O_3 loss is dramatically reduced. This is due to 10 - 20% reductions in the amount of NO_x (active NO_y) relative to $\text{EI C}_2\text{H}_6 = 0.2$, as PAN increases at the expense of HNO_3 . (The $\text{EI C}_2\text{H}_6 = 20$ changes are markedly different from the $\text{EI CH}_4 = 20$ calculation.)

These C_2H_6 calculations indicate that the expected levels of NMHC emissions have little effect on the model calculation of ozone depletion. The lack of significant effects at this emission level is strengthened by the fact that the substitution of the entire hydrocarbon emission with C_2H_6 is a conservative estimate of the effects of NMHC since 1) the actual NMHC emissions will be distributed among a variety of less active PAN precursors and 2) the hydrocarbons emitted as CH_4 in actual engines are typically a significant fraction of the total, reducing the amount of hydrocarbons emitted as NMHC. Thus a measurement of THCs that can bound the NMHC emissions below $\text{EI} = 1$ would obviate the need for detailed measurement of the hydrocarbon composition of the engine exhaust stream.

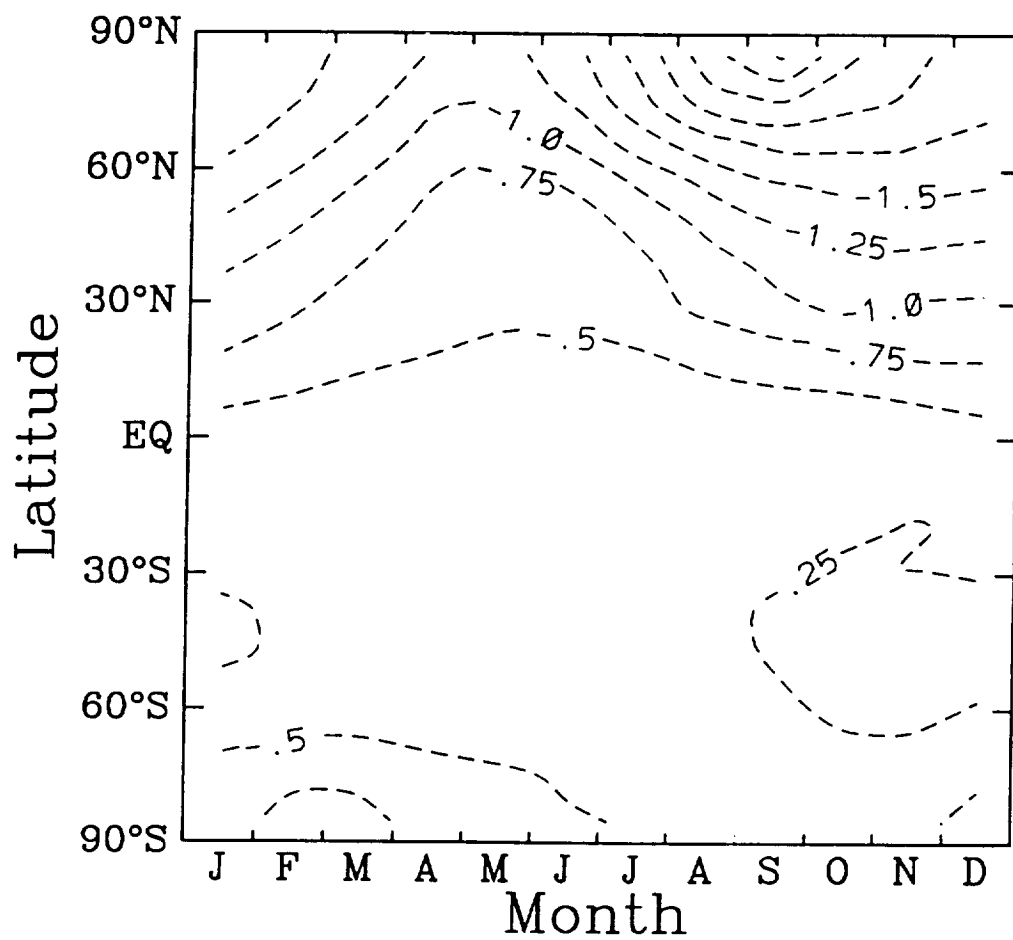


Figure A.1. AER model calculated percent change in the column abundance of ozone using the HSRP/AESA basic sceanrio (Case A) for a Mach 2.4 aircraft with $EI_{(NO_2)}NO_x = 15$ and $EI_{(CH_4)}HC = 0.2$.

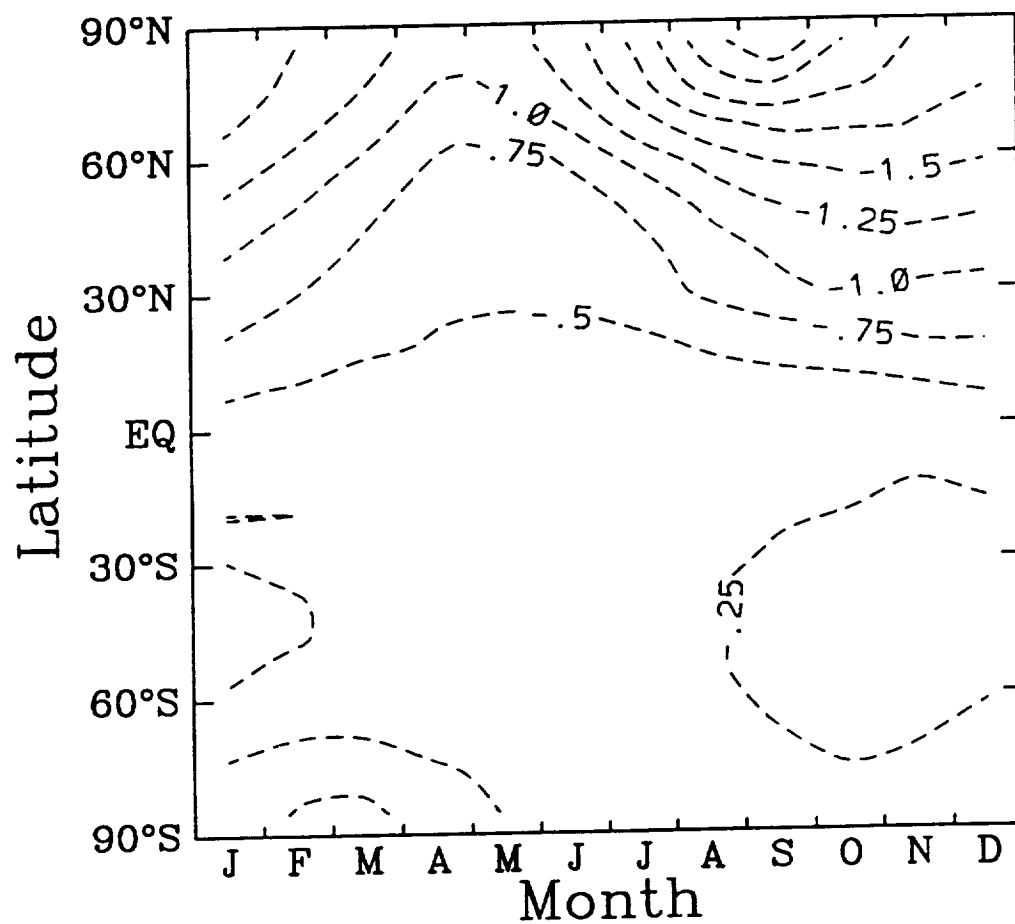


Figure A.2. Same figure as Figure A.1. except that $El_{(CH_4)HC} = 0.2$ is replaced by $El_{(C_2H_6)HC} = 0.2$. Note that the result is very similar to Figure A.1.

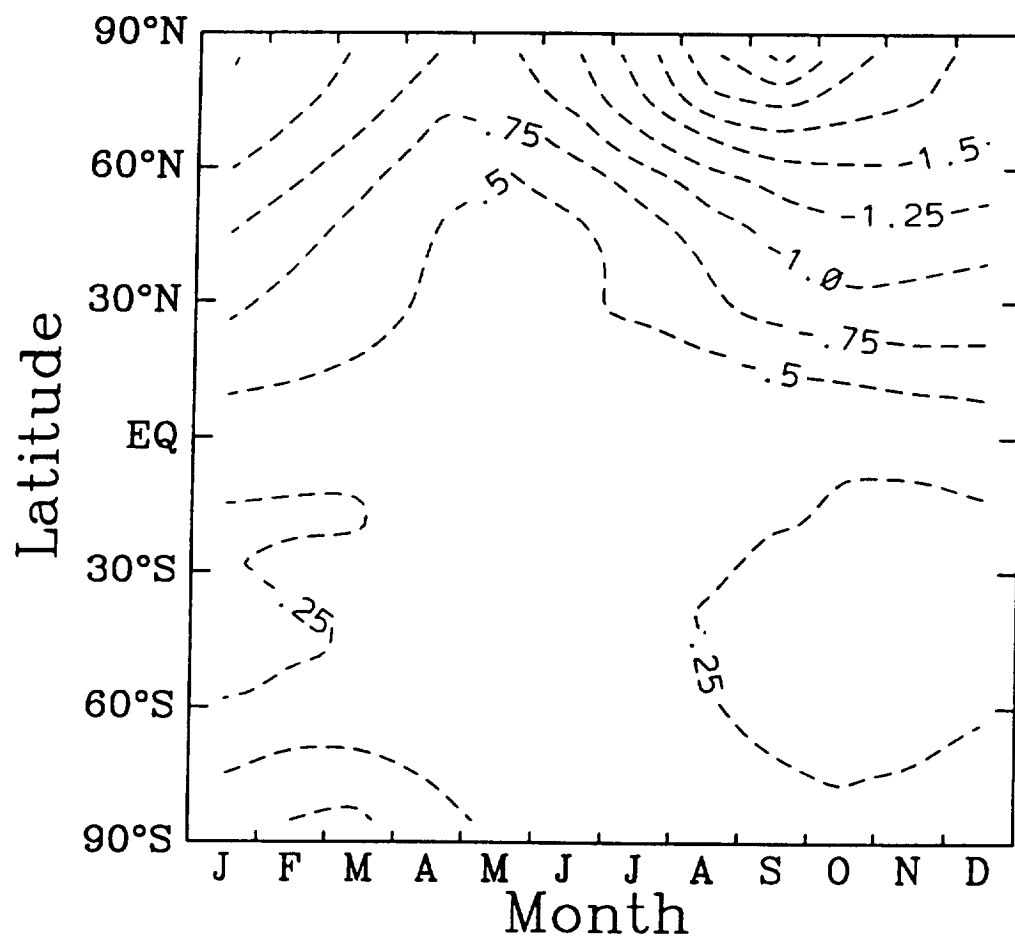


Figure A.3. As Figure A.1 with $El(C_2H_6)_{HC} = 0.2$ showing modest decreases in ozone loss relative to A.1 and A.2.

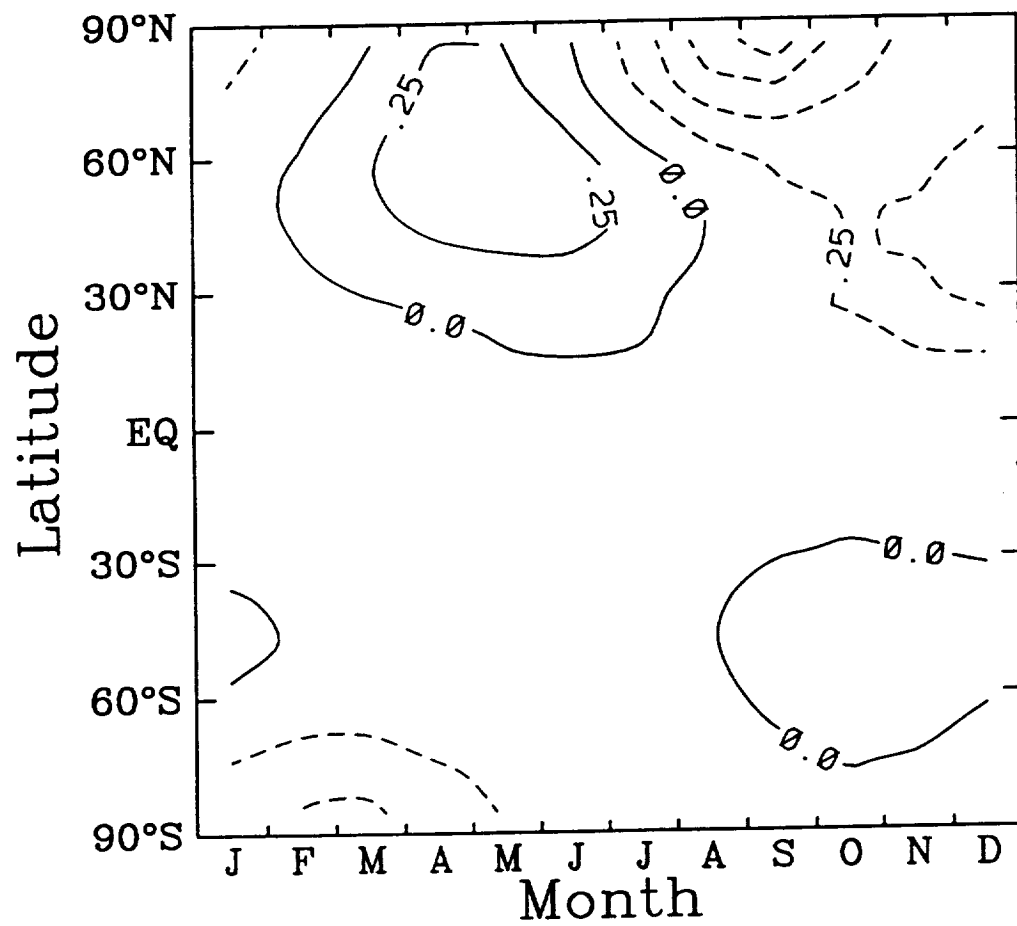


Figure A.4. As Figure A.2 with $El(C_2H_6)HC = 0.2$ showing substantial decreases in ozone loss (and actually showing ozone increases).

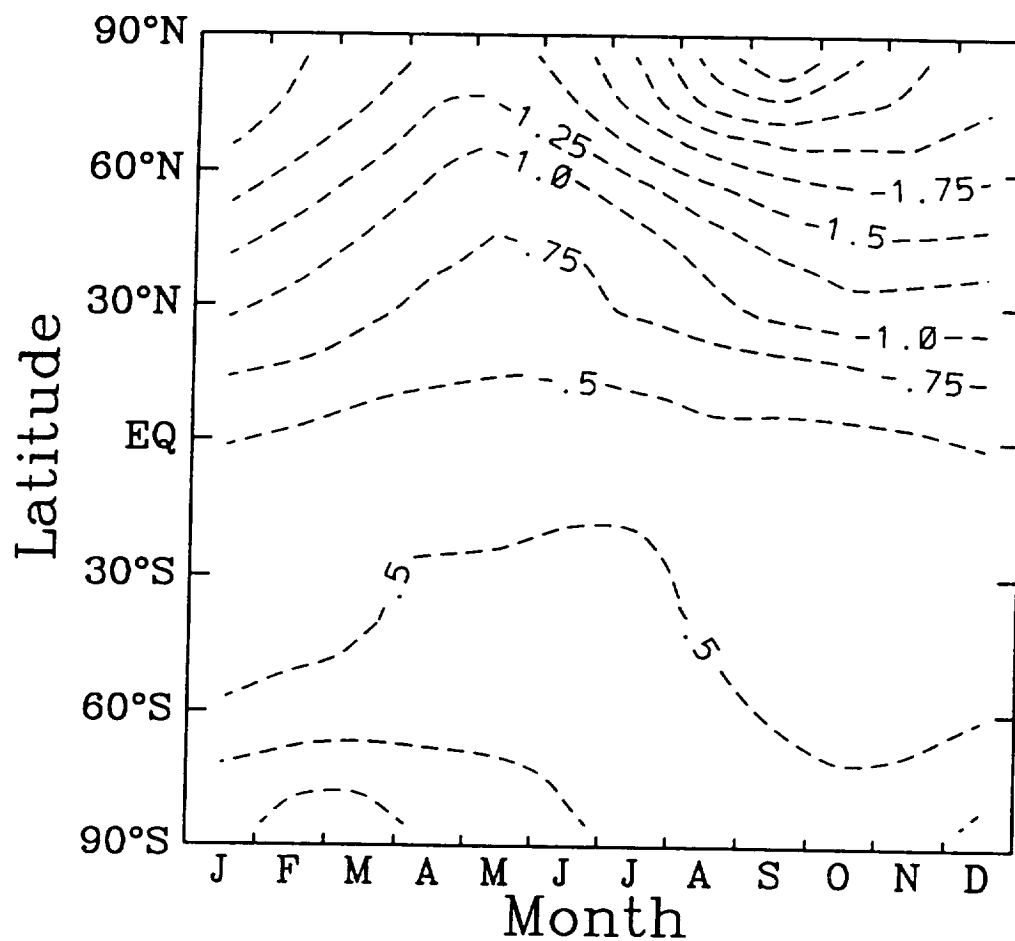


Figure A.5. As Figure A.4 but replacing $El_{(C_2H_6)HC} = 0.2$ with $El_{(CH_4)HC} = 20$, demonstrating that the suppression of ozone destruction seen in A.4 due to very high emissions of C_2H_6 is dependent on the hydrocarbon type (and subsequent PAN chemistry); and is absent for the high CH_4 levels used in the calculation illustrated here.

APPENDIX B
CATALOG OF MEASUREMENT VENUES

VEHICLE: FLAME TUBE

ORGANIZATION:	MASA LEWIS, CLEVELAND, OH	GEAE/COMB. LAB, CINCINNATI, OH	GEAE/CELL A5, CINCINNATI, OH
TEST CONDITIONS:	1100°F/20 ATM	1100°F/75 psia	1200°F/300 psia
AVAILABILITY:	1992-2000	7/92-6/95	1992-1995
TEST FREQUENCY:	WEEKLY	WEEKLY	MONTHLY
COST: (\$/DAY)	NEGOTIABLE	LOW	MEDIUM
SETUP/COORDINATION COST:	NEGOTIABLE	LOW	MEDIUM
INSTRUMENTATION AVAILABLE:	<p>GAS SAMPLE PROBES AND GAS ANALYZERS:</p> <p>CO/CO₂, NO/NOx, HC, SMOKE, TMC, OXYGEN: LASER DIAGNOSTICS</p> <p>- LASER INDUCED FLUORESCENCE</p> <p>- FLOW VISUALIZATION</p>	CO/CO ₂ , NO/NOx, HC, SMOKE	CO/CO ₂ , NO/NOx, HC, SMOKE
INSTRUMENTATION ACCESS:	<p>Windowed access (2 1/2" dia.) to 3" square cross-section, premix section and (1 1/2" x 1" rect.) in combustion zone located at 4 axial positions. 6 probes located at 3 axial locations in combustion zone.</p>	<p>Traversing water-cooled gas sample probes. No optical access except for atmospheric pressure tests.</p>	<p>Fixed Gas sample rake. No optical access. No personnel access during tests.</p>
OTHER REMARKS:	<p>Rich/Quench/Lean and Lean-Premixing-Prevaporizing combustors.</p> <p>Joint programs require Space Act agreements and must be worked out in advance before anyone can propose using NASA facilities.</p>	<p>Rig is an 8" diameter Lean Premixing-Prevaporizing combustor. Multiple experiments in test bay. Tight clearances. No personnel access during test at elevated pressure.</p>	<p>Rig is an 8" diameter Lean Premixing-Prevaporizing combustor.</p>
CONTACT:	VALLERIE LYONS - 216/433-5970	WILL DODDS - 513/774-4560	WILL DODDS - 513/774 4560

VEHICLE: FLAME TUBE (CONTINUED)

ORGANIZATION:	ALLISON, INDIANAPOLIS, IN	ALLISON, INDIANAPOLIS, IN	UTRC, E. HARTFORD, CT
TEST CONDITIONS:	1000°F/300 psia	1300°F/300 psia	1400°F/150 psia
AVAILABILITY:	1993	1993	1992-1994
TEST FREQUENCY:	WEEKLY	WEEKLY	WEEKLY
COST: (\$/DAY)	LOW	LOW	LOW
SETUP/COORDINATION COST:	LOW	LOW	LOW
INSTRUMENTATION AVAILABLE:	CO/CO ₂ , NO/NOx, HC, SMOKE	CO/CO ₂ , NO/NOx, HC, SMOKE	CO/CO ₂ , NO/NOx, HC, SMOKE
INSTRUMENTATION ACCESS:	Three single point translating emissions racks.	NONE	Optical access is feasible. Modular rig construction may permit easy adaptation of instrumentation sections.
OWNER REMARKS:	Sector of Allison Advanced Low NOx combustor tested in 4"x 4" flame tube at Allison. Emissions correlation to be done under MSR Task Order Contract.	Sector of Allison Accelerating Swirl Passage (ASP) combustor tested in 3"x 3" flame tube at NASA LeRC. Emissions correlation to be done at Allison under MSR Task Order Contract.	Rig is a single segment 5" dia. rich/quench/lean combustor rig. Limited room is available in immediate vicinity of rig. May pose a problem for bulky equipment.
CONTACT:	JOEL TOOF - 317/238-3836	JOEL TOOF - 317/230-3836	BOB LOWMAN - 203/565-7778 DAVE KADKA - 203/565-4581 TON ROSEJOHN - 203/727-7418

VENUE: SECTOR

ORGANIZATION:	PRATT & WHITNEY, MIDDLETOWN, CT	GEAE/CELL A3, CINCINNATI, OH	GEAE/CELL A18, CINCINNATI, OH
TEST CONDITIONS:	1200°F/500 psia	1100°F/600 psia	1400°F/600 psia
AVAILABILITY:	1993-1995	1993	1994-1996
TEST FREQUENCY:	MONTHLY	QUARTERLY	QUARTERLY
COST: (\$/DAY)	HIGH	HIGH	HIGH
SETUP/COORDINATION COST:	HIGH	HIGH	HIGH
INSTRUMENTATION AVAILABLE:	CO/CO ₂ , NO/NOx, HC, SMOKE	CO/CO ₂ , NO/NOx, HC, SMOKE	CO/CO ₂ , NO/NOx, HC, SMOKE
INSTRUMENTATION ACCESS:	Optical access is extremely difficult due to double walled, pressure vessel construction.	Gas sample probes only.	Gas Sample Probe only.
OTHER REMARKS:	Rig is a 60° sector of a rich/quench/lean combustor. Traversing exhaust rake available for detailed circumferential gas sampling and temperature surveys.	Rig is a 60° sector of a Lean Premixing-Prevaporizing combustor.	Rig is a 60° sector of a Lean Premixing-Prevaporizing combustor.
CONTACT:	BOB LOWMAN - 203/565-7778 DAVE KUZKA - 203/565-4501	WILL DODDS - 513/774-4560	WILL DODDS - 513/774-4560

VENUE: SECTION (CONTINUED)

ORGANIZATION:	CALSPAN, BUFFALO, NY
TEST CONDITIONS:	WEAR/-100 psi
AVAILABILITY:	1992-1999
TEST FREQUENCY:	SEE NOTE (2)
COST: (\$/DAY)	VERY HIGH - SEE NOTE (3)
SETUP/COORDINATION COST:	VERY HIGH - SEE NOTE (3)
INSTRUMENTATION AVAILABLE:	CO/CO ₂ , MO/NOM, MC OTHER-SEE NOTE (4)
INSTRUMENTATION ACCESS:	SEE FIGURES 1 AND 2
OTHER REMARKS:	SEE NOTES (1) AND (5)
CONTACT:	TOMAS ALBRECHTINSKI 716/631-6764

Calspan Advanced Technology Center

Notes:

- (1) 1/4 Sector F100 and Allison T56 Combustor Rigs available. Air supplied by external compressors (rented) and heated to nominal combustor inlet operating temperature. Inlet pressure nominally ~100 psi.**
- (2) Testing performed on contract basis for sponsoring agency. Frequency dependant on contract requirements.**
- (3) Basic operating costs include fuel, compressor rental and manpower to operate zone facility. ((Manpower costs ~\$10K/week). No facility usage fees.**
Set-up costs include materials and manpower to support collaborative efforts, TBD.
- (4) Conventional NO/NO_x, CO/CO₂ , THC instrumentation available. Other diagnostic support, i.e., non-intrusive laser and optical measurements can be supported/developed on a collaborative basis.**
- (5) Calspan open to discussions regarding teaming arrangements and collaborative combustor rig measurement programs.**

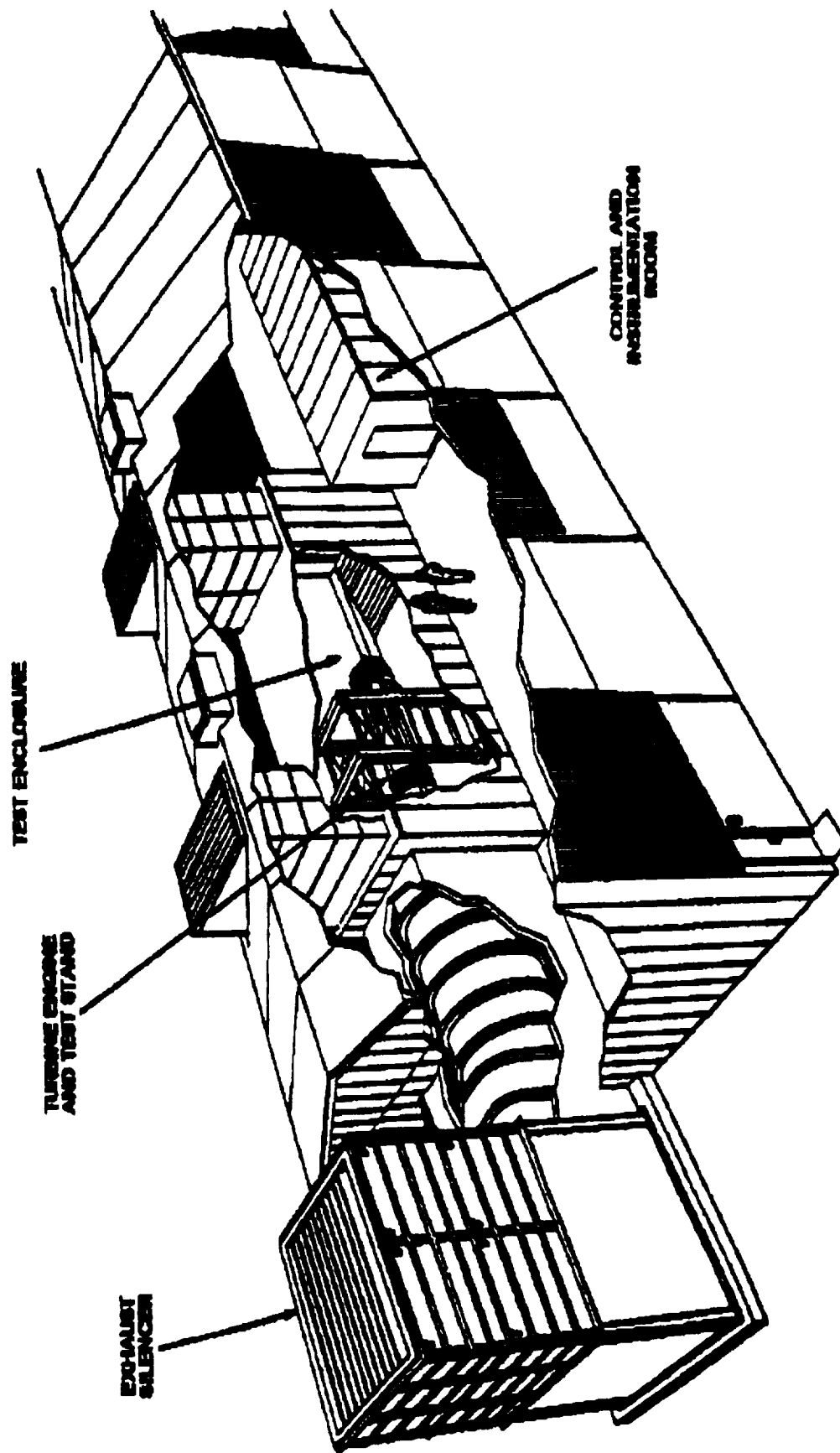


Figure 1 LARGE ENGINE RESEARCH CELL (LERC)

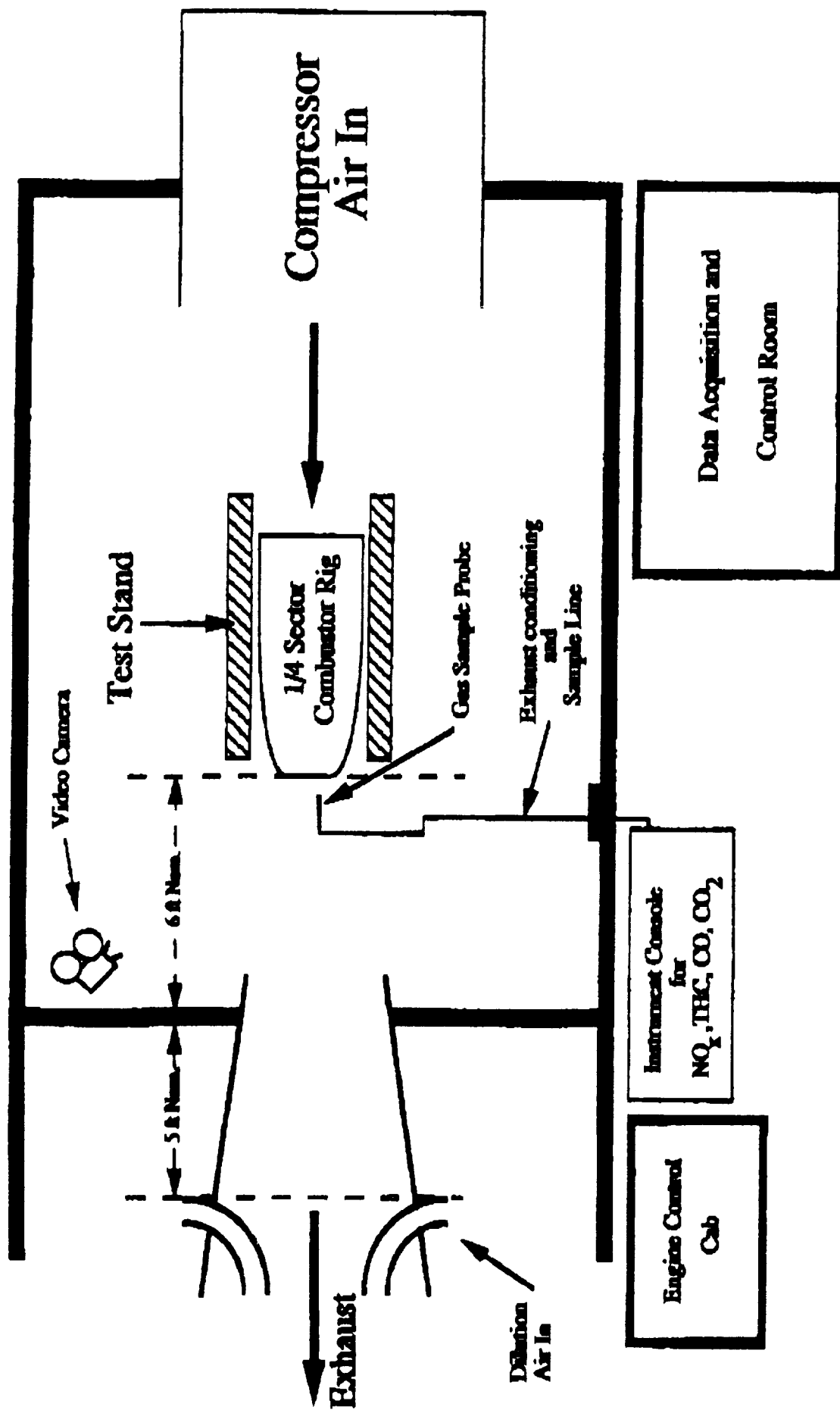


Figure 2 Schematic Diagram of the Engine Research Cell

VEHICLE: FULL ANNULAR

ORGANIZATION:	ALLISON, INDIANAPOLIS, IN	ALLISON, INDIANAPOLIS, IN	PRATT & WHITNEY, MIDDLETOWN, CT
TEST CONDITIONS:	660°F/275 psia	1100°F/300 psia	1200°F/308 psia
AVAILABILITY:	1992	1995-1996	1995-1996
TEST FREQUENCY:	MONTHLY	WEEKLY	MONTHLY
COST: (\$/DAY)	LOW	LOW	HIGH
SETUP/COMBINATION COST:	LOW	LOW	VERY HIGH
INSTRUMENTATION AVAILABLE:	CO/CO ₂ , NO/NOx, HC, SMOKE	CO/CO ₂ , NO/NOx, HC, SMOKE	CO/CO ₂ , NO/NOx, HC, SMOKE
INSTRUMENTATION ACCESS:	Fixed probe, burner outlet.	Rotating multi-point emissions probe.	Optical access is extremely difficult due to double walled, pressure vessel construction.
OTHER REMARKS:	Propose to make rig measurements at sea level and altitude and engine measurements at sea level. Under NASA Task Order Contract we will use Allison's semi-analytical and hybrid modeling technique to obtain rig to engine emissions correlations. Use validated correlations to predict engine emissions over specified mission profiles.	NONE	Rig is a full annular (360°) of a rich/quench/lean combustor. Traversing exhaust rake available for a detailed circumferential gas sampling and temperature surveys.
CONTACT:	JOEL TOOF - 317/230-3836	JOEL TOOF - 317/230-3836	BOB LOHMAN - 203/565 7778 DAVE KUMKA - 203/565-4581

VEHICLE: CURRENT ENGINE

ORGANIZATION:	ALLISON, INDIANAPOLIS, IN	PRATT & WHITNEY (SEE BELOW)	GE AIRCRAFT ENGINES (SEE BELOW)
TEST CONDITIONS:	880°F/275 psia	1100°F/450 psia	1100°F/450 psia
AVAILABILITY:	1992-1993	1992-1999	1992-1999
TEST FREQUENCY:	QUARTERLY	AS REQUIRED BY ENGINE PROGRAMS	DAILY
COST: (\$/DAY)	LOW	HIGH	HIGH
SETUP/COORDINATION COST:	LOW	HIGH	HIGH
INSTRUMENTATION AVAILABLE:	CO/CO ₂ , NO/NOx, HC, SMOKE	CO/CO ₂ , NO/NOx, HC, SMOKE	
INSTRUMENTATION ACCESS:	Fixed probe aft of engine - closed duct.	Optical or gas sampling access available at engine tailpipe exit plane. Most test cells have room for larger instrumentation installations but particular attention must be directed to its performance and integrity in a severe environment (ie., noise and vibration).	Open access at nozzle exit.
OTHER REMARKS:	NONE	Tests conducted according to rigorous schedules in facilities located in Connecticut, Florida and in government owned facilities. Majority of tests conducted at sea level engine inlet/exhaust conditions.	Very severe environment (heat, noise, vibration, dirt) cells located in Ohio and Massachusetts
CONTACT:	JOEL TOOF - 517/230-3836	BOB LOMMAN - 203/565-7778 DAVE KWIKA - 203/565-4581	WILL DODDS - 513/774 4560

VEHICLE: CURRENT ENGINE (CONTINUED)

ORGANIZATION:	CALSPAN, BUFFALO, NY
TEST CONDITIONS:	
AVAILABILITY:	7/92-1999
TEST FREQUENCY:	SEE NOTE (2)
COST: (\$/DAY)	VERY HIGH - SEE NOTE (3)
SETUP/COORDINATION COST:	VERY HIGH - SEE NOTE (3)
INSTRUMENTATION AVAILABLE:	DOYOD, INC./MOH, INC. OTHER-SEE NOTE (4)
INSTRUMENTATION ACCESS:	SEE FIGURES 1 AND 2
OTHER REMARKS:	SEE NOTES (1) AND (5)
CONTACT:	THOMAS ALBRECHTINSKI 716/631-6766

Calspan Advanced Technology Center

Notes:

- (1) The Large Engine Research Cell (LERC) facility can accommodate engines in the 350 lb/sec class. JT3D, J57 and F100 engines have been run in the test cell at sea level conditions.**
- (2) Testing performed on contract basis for sponsoring agency. Frequency dependent on contract requirements.**
- (3) Basic operating costs include fuel and manpower to operate the facility. (Manpower costs ~\$10K/week). No facility usage fees.**
- (4) Conventional NO/NO_x, CO/CO₂, THC instrumentation available. Other diagnostic support, i.e., non-intrusive laser and optical measurements can be supported/developed on a collaborative basis.**
- (5) Calspan open to discussions regarding teaming arrangements and collaborative engine exhaust measurements programs.**

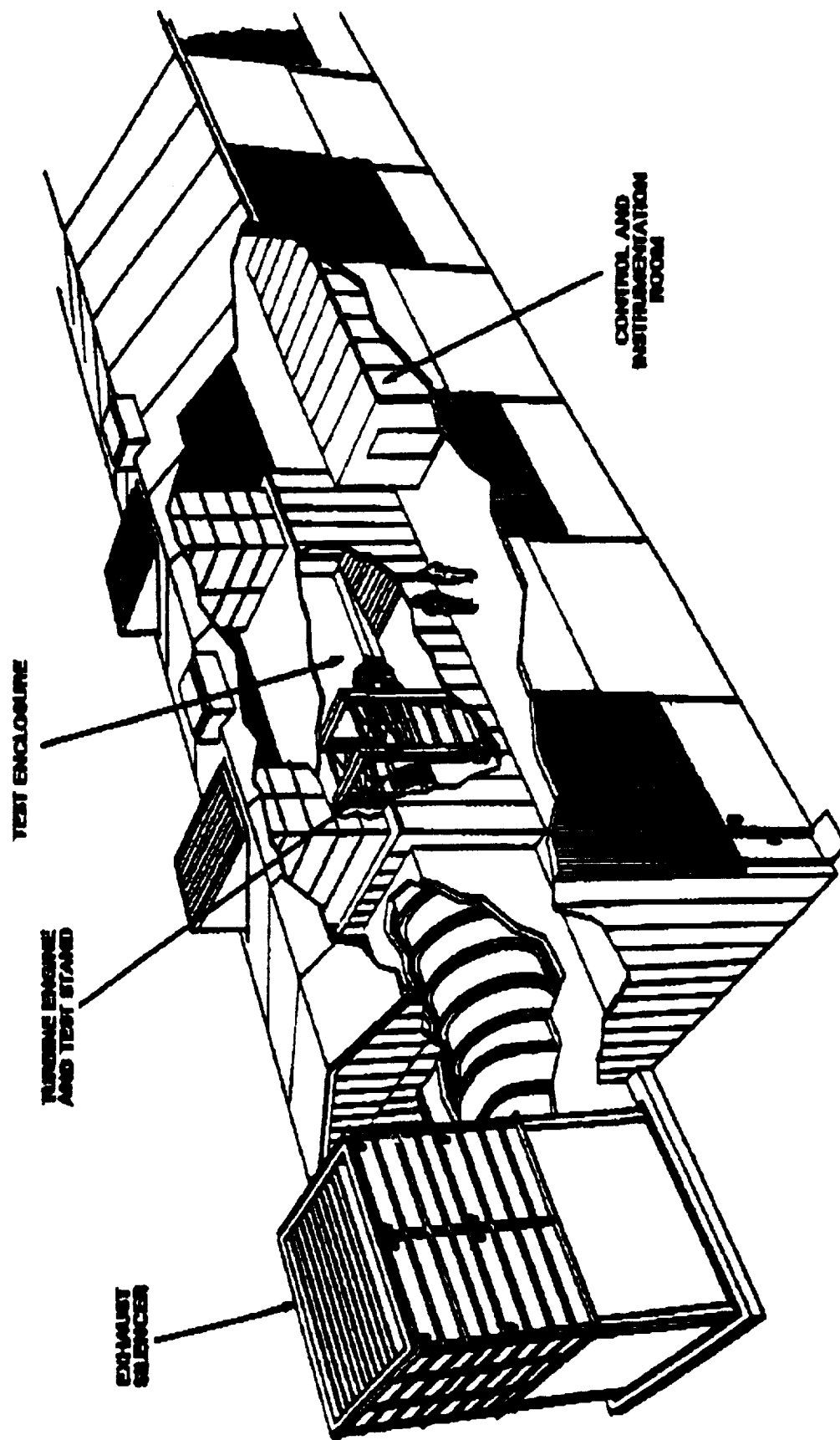


Figure 1 LARGE ENGINE RESEARCH CELL (LERC)

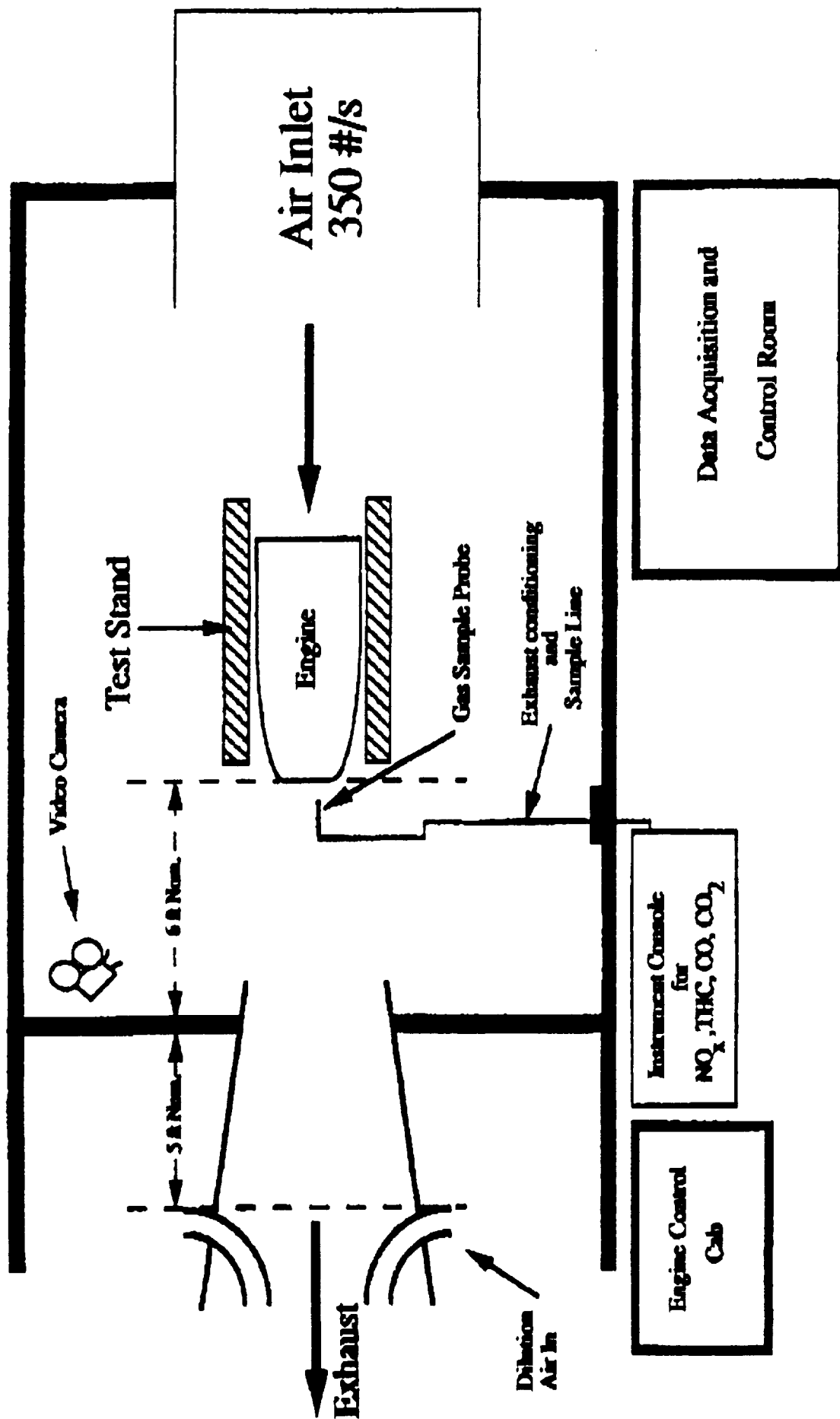


Figure 2 Schematic Diagram of the Engine Research Cell

VENUE: ADVANCED ENGINE

ORGANIZATION:	ALLISON, INDIANAPOLIS, IN	PRATT & WHITNEY, E. HARTFORD, CT
TEST CONDITIONS:	1100°F/400 psia	1200°F/200 psia
AVAILABILITY:	1993	1998
TEST FREQUENCY:	WEEKLY	MONTHLY
COST: (\$/DAY)	LOW	HIGH
SETUP/COORDINATION COST:	LOW	VERY HIGH
INSTRUMENTATION AVAILABLE:	CO/CO ₂ , NO/NO _x , HC, SMOKE	CO/CO ₂ , NO/NO _x , HC, SMOKE
INSTRUMENTATION ACCESS:	Fixed probe aft of engine.	Gas sampling at turbine discharge. Optical access to turbine discharge area difficult. Gas sampling and optical access available at exhaust plane downstream of water cooled turbine exhaust case.
OTHER REMARKS:	NONE	Test vehicle is a core or high spool engine. Tests will be conducted on a rigid schedule. Most likely test site is Arnold Engine Development Center (Tulahoma, TN).
CONTACT:	JOEL TOOF - 317/230-3836	BOB LOHMAN - 203/565-1118 DAVE KUOKA - 203/565-4581

REFERENCES

- Bekki, S., R. Toumi, J. A. Pyle, and A. E. Jones, Future aircraft and global ozone, *Nature* 354, 193-194, 1991.
- CIAP Monograph 2, *Propulsion Effluents in the Stratosphere*, DOT-TST-75-52, U.S. Department of Transportation, Washington, DC, 1975.
- Douglass, A. R., M. A. Carroll, W. B. DeMore, J. R. Holtan, I. S. A. Isaksen, H. S. Johnston, and M. K. W. Ko, *The Atmospheric Effects of Stratospheric Aircraft: A Current Consensus*, NASA Ref. Pub. 1251, Washington, D.C., 1991.
- EPA, Emission standard and test procedures for aircraft, *Federal Register*, 38, No. 136, 19088-19102, July 17, 1973.
- EPA, 1974, Supersonic aircraft pollution, *Federal Register*, 39, No. 141, 26653-266655, July 22, 1974).
- EPA, Control of air pollution from aircraft and aircraft engines, *Federal Register*, 43, No. 58, 12614-12634, March 24, 1978).
- Few, J. D., and H. S. Lowry III, Reevaluation of Nitric Oxide Concentration in Exhaust of Jet Engines and Combustors, Report No. AEDC-TR-80-65, Arnold Engineering Development Center, Arnold AFB, TN. 1981.
- Gradel, T. E., and C. J. Weschler, HO_x chemistry within aqueous atmospheric aerosols and raindrops, *Rev. of Geophys. Space Phys.*, 19, 505-539, 1981.
- Hagen, D. E., M. B. Trueblood and D. R. White, Hydration properties of combustion aerosols, *Aerosol Sci. Technol.*, 10, 63-69, 1989.
- Hallett, J., J. G. Hudson, and C. F. Rogers, Characterization of combustion aerosols for haze and cloud formation, *Aerosol Sci. Tech.*, 10, 70-83, 1989.
- Hansen, A. D. A., H. Rosen, and T. Novakov, Real-time measurement of the absorption coefficient of aerosol particles, *Appl. Optics*, 21, 3060-3062, 1982.
- Hofmann, D. J., Increase in the stratospheric background sulfuric acid aerosol mass in the past ten years, *Nature*, 248, 996, 1990.
- Hofmann, D. J., Aircraft sulphur emissions, *Nature*, 349, 659, 1991.
- Hudson, J. G., J. Hallett, and C. F. Rogers, Field and laboratory measurements of cloud forming properties of combustion aerosols, *J. Geophys. Res.*, 96, 10,847-10,859, 1991.
- Hunten, D. M., R. P. Turco, and O. B. Toon, Smoke and dust particles of meteoric origin in the mesosphere and stratosphere, *J. Atmos. Sci.*, 37, 1342-1357, 1980.
- Johnston, H. S., D. E. Kinnison, and D. J. Wuebbles, Nitrogen oxides from high-altitude aircraft: An update of potential effects on ozone, *J. Geophys. Res.*, 94, 16,351-16,363, 1989.
- Johnston, H. S., M. J. Prather, and R. T. Watson, *The Atmospheric Effects of Stratospheric Aircraft: A Topical Review*, NASA Ref. Pub. 1250, Washington, D.C., 1991.

- Lee, Y-N, and J. A. Lind, Kinetics of aqueous-phase oxidation of nitrogen (III) by hydrogen peroxide, *J. Geophys. Res.*, **91**, 2793-2800, 1986.
- Miake-Lye, R. C., M. Martinez-Sanchez, R. C. Brown, and C. E. Kolb, "Plume and wake dynamics, mixing and chemistry behind an HSCT aircraft," AIAA Paper 91-3158, AIAA Aircraft Design and Systems Meeting, Baltimore, MD, September 1991, in press *J. Aircraft*.
- Park, J. M., and B. Carli, Spectroscopic measurement of HO₂, H₂O₂ and OH in the stratosphere, *J. Geophys. Res.*, **96**, 22,535-22,541, 1991.
- Peter, T., C. Brühl, and P. J. Crutzen, Increase in the PSC-formation probability caused by high flying aircraft, *Geophys. Res. Lett.*, **18**, 1465-1468, 1991.
- Pitchford, M., J. G. Hudson, J. Hallett, Size and critical supersaturation for condensation of jet engine exhaust particles, *J. Geophys. Res.*, **96**, 20,787-20,793, 1991.
- Pueschel, R. F., D. F. Blake, K. G. Suetsinger, A. D. A. Hansen, S. Verma, and K. Kato, Black carbon (soot) aerosol in the lower stratosphere and upper troposphere, *Geophys. Res. Letts.*, **19**, 1659-1662, 1992.
- Prather, M. J., H. L. Wesoky, R. C. Miake-Lye, A. R. Douglass, R. P. Turco, D. J. Wuebbles, M. K. W. Ko, and A.L. Schmeltekopf, *The Atmospheric Effects of Stratospheric Aircraft: A First Program Report*, NASA Ref. Pub. 1272, Washington D.C., 1992.
- McGregor, W. K., B. L. Seiber, and J. D. Few, Second Conference on CIAP, 214-229. U.S. Department of Transportation, Washington, D.C., 1973.
- Meinel, H., and L. Krauss, Monitoring of nitric oxide in flames by UV differential absorption, *Combust. Flame*, **33**, 69-77, 1978.
- Society of Automotive Engineers, "Procedure for the Continuous Sampling and Measurement of Gaseous Emissions from Aircraft Turbine Engines," Aerospace Recommended Practice ARP 1256A. Society of Automotive Engineers, 1980a.
- Society of Automotive Engineers, "Aircraft Gas Turbine Engine Exhaust Smoke Measurement," Aerospace Recommended Practice ARP-1179A. Society of Automotive Engineers, 1980b.
- Spicer, C. W., M. W. Holdren, D. L. Smith, D. P. Hughes, and M. D. Smith, Chemical composition of exhaust from aircraft engines, *J. Eng. Gas Turb and Power*, **114**, 111-117, 1992.
- Stimpfle, R. M., P. O. Weinberg, L. B. Lapson, and J. G. Anderson, Simultaneous in situ measurements of OH and HO₂ in the stratosphere, *Geophys. Res. Letts.*, **17**, 1905-1908, 1990.
- Turco, R. P., R. C. Whitten, and O. B. Toon, Stratospheric aerosols: observation and theory, *Rev. Geophys.Space Phys.*, **20**, 233-279, 1982.
- Weisenstein, D. K., M. K. W. Ko, J. M. Rodriguez, and N. D. Sze, Impact of heterogeneous chemistry on model calculated ozone change due to high speed civil transport aircraft, *Geophys. Res. Lett.*, **18**, 1991-1994, 1991.

Zabielski, M. F., L. G. Doge, M. B. Colhet, III, and D. J. Seery, "The Optical and Probe Measurement of NO: A Comparative Study;" Eighteenth Symp. (Int.) Combust., 1591-1598, The Combustion Institute, Pittsburgh, PA., 1981.

Zolensky, M. E., O. S. McKay, and L. A. Kaczof, A tenfold increase in the abundance of large solid particles in the stratosphere, as measured over the period 1976-1984, *J. Geophys. Res.*, 94, 1047-1056, 1989.

Chapter 6

Exhaust Plume/Aircraft Wake Vortex Interaction Committee Report

Charles E. Kolb
Richard C. Miake-Lye
Aerodyne Research Inc.
Billerica, MA

Todd R. Quackenbush
Continuum Dynamics
Princeton, NJ

Robert C. Oliver
Institute for Defense Analyses
Alexandria, VA

Manuel Martinez-Sanchez
Massachusetts Institute of Technology
Cambridge, MA

William L. Grose
James D. Lawrence, Jr.
Langley Research Center
National Aeronautics and Space Administration
Hampton, VA

INTRODUCTION

Beginning with the Climatic Impact Assessment Program (CIAP) program in the early 1970s, it was recognized that an assessment of the atmospheric effects resulting from a fleet of aircraft operating in the stratosphere must largely depend upon numerical studies conducted with atmospheric simulation models. In turn, the validity of the assessment would ultimately rest upon the fidelity with which the models represent atmospheric processes and the accuracy of the input related to the proposed aircraft fleet (e.g., fleet size, characterization of the engine emissions, deposition altitude, and route structure). Initial simulation studies were based upon calculating a net burden of emission products (based upon assumed fleet size and the emissions at the jet exhaust exit plane of characteristic engines) and then imposing this burden into the models at the design cruise altitude of the aircraft in a narrow latitude corridor (in this instance, the North Atlantic corridor where the principal market existed).

As the CIAP program progressed, some subtle questions emerged related to the assumed emissions burden used for the assessment studies. It was understood that the wake behind an aircraft consisted of several regimes: the jet exhaust plume just aft of the engine, where dispersal of the emissions largely depends upon exhaust velocity, pressure, and temperature; a region farther aft where the plume interacts with the trailing wing-tip vortices; a region even farther aft where the wake is still coherent, but the effects of the wing-tip vortices have decayed, and dispersal is now controlled by local atmospheric processes; and finally a region where the wake begins to break up and disperse at atmospheric scales of motion. The questions concerned themselves with whether the chemical and fluid dynamic processes occurring in the plume and wake change the physical and/or chemical properties of the exhaust species or their deposition altitude in any way which might significantly influence their ultimate effect on the ambient stratosphere.

A number of research efforts were initiated during the CIAP period to address these questions. In the following section a brief review is given of research conducted during CIAP and the intervening years to the present. In subsequent sections, our current understanding of the wake problem is discussed, and a review of ongoing AESA/HSRP-sponsored research is presented. Finally, some perceived strengths and deficiencies of current research related to the wake problem are discussed.

WAKE STUDIES IN THE CLIMATIC IMPACT ASSESSMENT PROGRAM (CIAP)

Wake studies in the CIAP program were concerned with the various physical, chemical and dynamic processes occurring as the exhaust gases from supersonic aircraft mix with and spread into the ambient atmosphere. Major efforts went into the "microscale" regime, which was defined as the region up to 400-1200 km (10-20 minutes) behind a single aircraft (Hoshizaki et al., 1975; Overcamp and Fay, 1973). Attention was also given to the mesoscale regime, defined as the region of the order of 1 hour to 10 days after aircraft passage (Taylor et al., 1975), and the perturbing influences of repeated flights of aircraft were examined. The microscale and mesoscale efforts are reviewed briefly here; effects on the global scale, are not discussed. Aerosols (see Hidy et al., 1975) and contrail and possible cloud formation effects (Welckmann et al., 1975) were treated separately from those phenomena particularly concerned with NO_x and ozone, which were emphasized in the work of Hoshizaki and colleagues (1975). Input data for the wake studies (engine effluent compositions) were provided in CIAP Monograph 2.

The microscale regime studies of Hoshizaki et al. (1975) included both theoretical analyses and flight tests on single aircraft exhausts. The microscale regime was broken down into three subregimes characterized by time after leaving the engines: the jet regime, 1-10 seconds; the vortex regime, 10-100 seconds; and the wake-dispersion regime, 100 to 1000 seconds. The theoretical analyses coupled chemical kinetic modeling and dynamics, following the chemical

composition, temperatures and dimensions of the wake(s) as the exhaust mixed with and was diluted and cooled by the ambient air. The flight tests, which were intended to validate the wake growth models, incorporated both photographic observations of contrails (identifying the wake) from subsonic (B-52) aircraft and wakes from supersonic (YF-12) wake for NO content was also carried out. A particular interest of the wake chemistry studies was in determining the degree of conversion of NO and NO₂ species into the reservoir species HNO₃, which at the time was thought to possibly minimize ozone depletion due to NO_x emissions from the aircraft. Little conversion to HNO₃ was found, and no other sinks for NO_x were discovered.

A separate study of dispersion, subsidence, and chemical processes in an aircraft wake was reported by Overcamp and Fay (1973) prior to completion of the CIAP effort. Both laboratory (towing tank) and theoretical analyses were carried out. The study provided detail on wake dynamics and on effects of stratification of the ambient air, predicting radiative cooling of the stratified plumes (due to enriched moisture and depleted ozone content) and resulting subsidence; the degree of stratospheric turbulence was noted to represent a significant, but poorly established variable. Highly stratified wakes were calculated to be significantly depleted in ozone. Upper limit estimates for wake subsidence suggested that subsidence would not be significant before wake dispersal for aircraft operating at 16-18 km (less than a few hundred meters) but could be significant for aircraft operating at higher altitudes, possibly sinking several kilometers for aircraft operating at 27 km.

The mesoscale (or corridor) regime studies (Taylor et al., 1975) used several simplified models in which sources were assumed, buildup of tracers was followed, and chemistry questions addressed. Eddy transport was parameterized to study effects, it being known that extreme stratification can occur in the stratosphere: Panofsky and Heck (1975) noted layers spreading a kilometer or less vertically in a year; they also noted that the spreading of single wakes is not the dominant process of interest, but rather the superposition of frequent sources moving in different directions, a process which increases the effective dispersion rate. It was observed that wakes computed with low values of eddy diffusivities may lead to high localized losses of ozone, but lead to less total ozone destruction than do wakes that spread the NO_x pollutant more uniformly where the NO_x can be more effective. Aerosol formation from SO₂ and hydrocarbons were studied in this regime by Hidy et al., (1975); it was predicted that particulates from these sources would not be expected to be formed in the microscale regime. Discussion of soot emissions was also included. Theoretical contrail and cloud formation studies were carried out (Welckmann et al., 1975) to determine regions wherein contrails or persistent clouds might be formed.

It was concluded from the CIAP wake studies that any chemistry taking place in the wake would not be significant and that a good first approximation for global models would be to employ directly the aircraft exhaust composition (NO_x water, SO₂) as source terms. However, it should be noted that the wake modeling and computational fluid dynamics capabilities used to represent the wake and vortex interactions were relatively unsophisticated by current standards. Also, the CIAP studies were based on homogeneous chemistry; some possible heterogeneous reactions, both catalytic and consumptive (with soot), were noted, but none were thought to be important (see Corrin, 1975; see also Hidy et al., 1975; and Olszyna et al., 1979). The possibility of nitric acid trihydrate (NAT) formation alone or on other particulates was not recognized at the time, nor were the various complexities of chlorine chemistry as related to ozone destruction. The heterogeneous hydrolysis of N₂O₅, which is now known to be of great importance, was not included. Further studies may thus well provide interesting new insights.

REVIEW OF PROGRESS BETWEEN CIAP AND HSRP/AESA

Plume Mixing and Chemistry

The ability to model aerospace exhaust plume chemical and physical processes increased substantially between the end of CIAP in 1975 and the beginning of the HSRP/AESA program in 1990. Most of this progress was achieved under the sponsorship of the Joint Army, Navy, NASA, and Air Force (JANNAF) Exhaust Plume Technology Committee. Under the guidance of this group a Standardized Plume Flowfield (SPF) program directed the development and testing of a series of SPF models capable of more accurately describing the complex fluid dynamic and chemical kinetic properties of aircraft and rocket exhaust plumes in the troposphere and stratosphere (Dash and Pergament, 1978; Dash et al., 1979). The resulting plume flowfield model most applicable to HSCT exhaust plumes is SPF-2 (Dash et al., 1990); it has served as the baseline model for subsequent HSRP/AESA model upgrade activities. A number of classified Department of Defense ground simulation and flight measurement programs performed between 1975 and 1990 have confirmed the basic validity of the jet mixing and chemical kinetic modules used in SPF-2. Since 1980, extensive aircraft infrared signature modeling and analysis activities at Aerodyne Research, Inc. (ARI) have resulted in full integration of SPF plume models for current supersonic aircraft (Conant et al., 1985; Aerodyne, 1989).

Exhaust plume jet mixing and chemistry models such as SPF-2 require detailed chemical kinetic rate parameter inputs to calculate the evolution of gaseous pollutants within the exhaust plume flowfield. One major advance since 1975 is the establishment of periodic chemical kinetic data evaluation activities and the regular publication of their results. Pertinent data reviews are available for both combustion chemistry (Tsang and Hampson, 1986; Miller and Bowman, 1989; Tsang and Herron, 1991) relevant to exhaust nozzle flow and near nozzle hot plume flows, and from the stratospheric chemistry community, for processes in the colder, well-mixed portions of the exhaust plume and wake (DeMore et al., 1990; 1992).

Finally, any model of HSCT exhaust plume chemistry also requires an accurate representation of the ambient atmospheric pressure, temperature, and chemical composition. The extensive atmospheric measurement and modeling activities of NASA's Upper Atmospheric Research Program (UARP) and its U.S. and international counterparts since the late 1970s have equipped us with more accurate stratospheric composition models (WMO, 1986; 1989).

Aircraft Wake Dynamics

The earlier studies of wake and contrail analyses utilized in CIAP, which covered work from the 1950s through the early 1970s, were significantly extended in a distinct but related body of literature beginning in the 1970s. These analyses of the trailing vortex wake were directed at understanding and assessing the hazard posed by the wakes of large subsonic transport aircraft. The development of analytical and computational tools to study such issues includes the pioneering work of Crow (1970), who identified the major modes of instability of trailing vortex pairs. Further research into the methods for modeling the evolution of the vortex pair was carried out by Moore and Saffman (1971) and Widnall et al. (1971), who refined the understanding of the breakdown of the organized flow in the far wake of the aircraft.

An extended effort to develop and implement more detailed computational models of the roll-up, merging, and decay of aircraft wakes was subsequently conducted by Bilanin and Donaldson (1975), Teske (1976), Bilanin et al. (1978), and Bilanin and Teske (1988). The initial roll-up of the lift circulation distribution and profile drag distribution into distinct trailing vortices was accomplished by a modification of the Betz methodology by Bilanin and Donaldson (1975). The Betz roll-up computation identifies the discrete vortical structure (location, strength, and core size

of swirling and axial velocities) given the computed wing lift circulation distribution. This treatment has proven to be a useful tool for initialization of the wake evolution calculations, particularly in cruise flight, but this model oversimplifies many important features of the wake for aircraft in landing configuration (Bilanin et al., 1977).

Initial efforts to carry out direct numerical simulation of vortex merging and decay behind aircraft included the development of the NASA WAKE code (Teske, 1976; Bilanin et al., 1978). This code solved the parabolized Navier-Stokes equations for the wake downstream of the aircraft carrying out coupled calculations of the velocity, vorticity, turbulence, and temperature fields in the crossflow plane. WAKE featured second-order accurate spatial differencing, which restricted its ability to resolve and preserve the complex, concentrated vorticity fields without creating a very large computational burden. Such limitations were overcome with the completion of the successor UNIWAKE (UNified WAKE analysis) code (Bilanin and Teske, 1988; Teske et al., 1991) by Continuum Dynamics, Inc. (CDI). UNIWAKE combines the four principal elements of the generation, merging, and break-up of the wake: 1) a vortex lattice model to determine the wing loading; 2) a near wake roll-up model of the load distribution based on an extension of the work of Betz by Bilanin and Donaldson (1975); 3) an advanced turbulent transport finite difference model employing a fourth-order accurate solution scheme for the computation of the merging of the trailed wake; and 4) a three-dimensional unsteady analysis replacing the merged vortices by curved vortex elements, leading to vortex linking and pinch-off.

The central feature of the UNIWAKE code is the third element described above, the technique for computing the merging of the individual vortex trailers identified by the Betz initialization. Numerical integration of turbulent merging and decay of these vortices, including the effect of jet engine exhaust, is carried out by a fourth-order accurate solution of the modeled incompressible, stratified Navier-Stokes equations of motion (Hirsh, 1983), which includes second-order closure of the turbulence (Sykes et al., 1986; Mellor and Yamada, 1974). The wake turbulent merging and decay computation evolves from the vortical structure and includes the turbulence and temperature distributions in the aircraft exhaust stream. One of the unique advantages of this formulation is the highly accurate fourth-order spatial differencing in the merging calculation, which produces dramatically reduced numerical diffusion relative to the earlier second-order accurate schemes.

The UNIWAKE model represents the only comprehensive, integrated, validated analysis of aircraft wake development and decay presently available. The code is currently being used by researchers at NASA Langley, the U.S. Air Force, and the Boeing Commercial Airplane Company to evaluate vortex wake hazard and the effect of engine placement on wake evolution. Substantial efforts have also been undertaken to validate the existing code through comparisons of predicted swirl velocity profiles to measured results from experimental tests, including the measurements of velocity fields downstream of subsonic transports (Garodz, 1971; Burnham et al., 1978).

COMPONENTS OF THE HSRP/AESA EXHAUST PLUME/VORTEX WAKE RESEARCH EFFORT

Overview

As developed during the first 3 years of the HSRP/AESA program, the exhaust plume/vortex wake research effort can be divided into four elements, these are:

- Development and exercise of exhaust plume chemistry and mixing models capable of describing the chemical kinetic evolution and condensation physics of exhaust plume species as the plume jet undergoes turbulent mixing with the ambient atmospheric free stream immediately behind the HSCT aircraft. An illustration of the four exhaust plumes behind a schematic HSCT aircraft is shown in Figure 1.

- Analysis of and analytic model development for the fluid dynamic interaction of the exhaust plume structures with the wing wake vortices and the impact of this interaction on the continuing chemical kinetic and condensation processing of the exhaust plume species. A schematic showing the entrainment and roll-up of the exhaust plumes with the wing wake vortices is shown in Figure 2.
- Development and exercise of far wake dispersion models coupled with atmospheric photochemical, heterogeneous chemical and radiative cooling models to assess the chemical, radiative and dynamic properties of the exhaust species rich individual far wake and multi-far wake corridor regions. A schematic of the initial vortex wake breakup and dispersion is shown in Figure 3.
- Assessment of potential stratospheric field measurement techniques which might be utilized to test the coupled fluid dynamic, chemical kinetic, and condensation physics models developed for the three regimes outlined above. These techniques might be utilized to probe the plume/wake vortex and/or far wake regimes behind a suitable surrogate for an HSCT if the evolution of the HSRP/AESA program dictates the need for such an experiment. Possible surrogate aircraft include the Concorde, the TU-144, and the SR-71.

The overall goal of the first three efforts as outlined above, is to develop and utilize a compatible set of modeling tools in order to reliably describe the chemical and physical evolution of relevant HSCT exhaust species from the aircraft engine's nozzle out to dimensional scales capable of being addressed by regional and global atmospheric impact models.

The fourth topic is an initial effort to address whether meaningful field measurements to verify the accuracy of the exhaust plume, vortex wake, and wake dispersion models are technically feasible and affordable.

The exhaust plume/vortex wake research effort is a relatively small component of the overall HSRP/AESA program, and the above topics involve a small number of research organizations. Activity on the first topic, exhaust plume chemical and physical modeling, is centered at Aerodyne Research, Inc. (ARI) with contributing laboratory activity on the reactivity and condensation physics of exhaust soot particles from the University of Missouri at Rolla (UMR) and the modeling of binary water vapor/sulfuric acid nucleation and subsequent contrail condensation physics from the Department of Atmospheric Sciences at the University of California at Los Angeles (UCLA).

Work on the second topic, the interaction of the exhaust plume with the wing wake vortex and the evolution of both the wake vortex structure and the plume exhaust species as chemical and physical properties, is also centered at ARI, with important computational fluid dynamic modeling support from Continuum Dynamics, Inc. (CDI) and overview from NASA Langley Research Center (LaRC) Fluid Mechanics Division.

The modeling of far wake and wake corridor effects, the third topic, is centered at Atmospheric and Environmental Research, Inc. (AER), with collaboration and guidance from the ARI plume/wake modeling team.

Assessment of potential field measurement techniques for the plume, vortex wake, and far wake dispersion regimes, the fourth topic, has been performed by staff from the Atmospheric Sciences Division at LaRC with input from ARI.

Exhaust Plume Chemistry and Condensation Physics Modeling

A model of the relevant exhaust plume mixing, homogeneous gas-phase chemical kinetics and heterogeneous condensation processes necessary to simulate an HSCT exhaust plume has been developed at ARI with HSRP/AESA funding (Miake-Lye et al., 1992; 1993). This model is based on the fluid dynamic and homogeneous chemical modeling framework of the SPF-2 model (Dash et al., 1990). Upgrades made at ARI include the addition of SO₂ and NO/NO₂ (NO_x) oxidation kinetics using evaluated temperature dependent chemical kinetic rate parameters from the combustion chemistry (Tsang and Hampson, 1986; and Tsang and Herron, 1991) and stratospheric chemistry (DeMore et al., 1990; 1992) communities. Modifications to the SPF-2 code include three condensation models: one based on equilibrium condensation (Miake-Lye et al., 1992) and two on kinetic condensation, the first representing heterogeneous condensation on pre-existing exhaust soot and sulfate aerosols (Brown et al., 1992; Miake-Lye et al., 1993) and the second representing binary nucleation of sulfuric acid vapor/water vapor followed by water vapor condensation on the resulting sulfate nuclei (Zhao and Turco, 1992; Miake-Lye et al., 1993).

The reacting plume model is currently initiated with exhaust trace chemistry characteristic of a model Mach 2.4 HSCT engine as specified by a one-dimensional flow/finite rate chemical kinetic model of combustor exhaust gas transported through the turbine, bypass mixing chamber and turbine (Miake-Lye et al., 1992). When nozzle exit plane emission measurements are available from prototype HSCT engines, these measured values will be used for model initiation.

The reacting plume model is designed to cope with coupled chemical kinetic and condensation phenomena. For instance, in the case of condensation on nuclei from homogeneous binary sulfuric acid vapor/water vapor condensation, the kinetically limited oxidation of SO₂ to H₂SO₄ vapor is ongoing at the same time the product H₂SO₄ vapor is triggering nucleation and condensation (Miake-Lye et al., 1993). Initial calculations for a model Mach 2.4 HSCT in cruise at ~18 km indicate that homogeneous plume chemistry driven by nonequilibrium levels of exhaust OH and entrained ambient O₃ can oxidize a significant fraction of exhaust NO_x to HNO₃ (~5%) and exhaust SO₂ to SO₃ (~10%) in the first 600 meters of the plume (Miake-Lye et al., 1992 - see Table 1).

If SO₃ is allowed to react with H₂O vapor at a rate represented by the evaluated upper limit for this reaction's rate constant (DeMore et al., 1992), it is quickly converted to H₂SO₄ vapor and triggers binary nucleation of H₂SO₄ and H₂O vapor as suggested by the UCLA group (Zhao and Turco, 1992) and confirmed by the ARI binary nucleation model embedded into SPF-2 (Miake-Lye et al., 1993). Current calculations indicate that new particle nucleation rates in a Mach 2.4 HSCT exhaust plume can exceed 10¹¹ cm⁻³s⁻¹, indicating that plume-induced new particle creation may cause a significant enhancement of new sulfate aerosol surface available for heterogeneous reactions in the wake and wake dispersion regimes (Miake-Lye et al., 1993). The key to formation of copious H₂SO₄/H₂O particles in the plume/wake is the rate of H₂SO₄ production in the exhaust plume. Production of H₂SO₄ depends primarily on exhaust radical chemistry and is relatively insensitive to atmospheric conditions. However, the degree to which the H₂SO₄/H₂O aerosols, in turn, nucleate water vapor to form contrails, will depend critically on local atmospheric pressure, temperature, and water vapor content.

Furthermore, assessment of whether or not these plume-induced aerosol particles have a significant impact on global aerosol levels will depend on an analysis of their subsequent agglomeration and evaporation kinetics as well as a better model of ambient stratospheric aerosol climatology.

Since model HSCT exhaust plumes for some representative operating parameters cool below the water condensation point from ambient air entrainment before the point where the plumes are entrained into the wing wake vortices, the plume model can be used to study the details of initial

contrail droplet formation. Work to date is focusing on the competition between heterogeneous nucleation on exhaust soot particles activated by oxidizing plume gases (Miake-Lye et al., 1992) and condensation on nuclei created by sulfuric acid vapor/water vapor binary nucleation (Zhao and Turco, 1992).

The rate of soot-induced heterogeneous nucleation depends on the rate of heterogeneous activation of soot which sets the fraction of soot particles at each position of the plume capable of nucleating water vapor at low (~ 1.01) supersaturation ratios (Brown et al., 1992). Ongoing HSRP/AESA-sponsored experimental soot kinetics studies at the University of Missouri at Rolla (UMR) are designed to provide kinetic information on the rates and mechanisms of jet fuel soot activation by combustion exhaust species. When these experiments and the concomitant data analyses are completed, these data will be used in the plume chemistry model to better estimate the level of active soot condensation nuclei. Preliminary results from the UMR effort (Whitefield et al., 1992) indicate that soot activation may be more efficient than indicated by the previous literature (Hallett et al., 1989; Hudson et al., 1991). However, current model calculations with generous estimates of soot activation levels indicate that the high level of condensation nuclei provided by binary homogeneous nucleation of sulfuric acid vapor and water vapor may swamp the soot nucleation mechanism, especially if the homogeneous conversion of $\text{SO}_3(\text{g})$ to $\text{H}_2\text{SO}_4(\text{g})$ is fast (Miake-Lye et al., 1993). This is in accord with the estimates of Zhao and Turco (1992) using estimated plume chemical properties.

The enhanced SPF-2 plume chemistry and condensation model will be used to further evaluate plume chemical kinetic processes and condensation mechanisms during the remainder of the HSRP/AESA program. It will also be used to specify the chemical and physical plume input conditions for the exhaust plume/wake vortex model described in the following subsection. The chemical kinetic and condensation models imbedded in the plume model, as described above, will be carried, as necessary, into this wake vortex regime modeling effort.

Wake Vortex Modeling

The discussion in the Aircraft Wake Dynamics section summarized the post- CIAP work in wake dynamics as well as the technical foundation of the UNIWAKE analysis presently in use as part of the HSRP/AESA computational effort. UNIWAKE is an appropriate computational tool to adapt to the prediction of exhaust plume/wake vortex dynamics, since it provides full flexibility for specifying the type of aircraft, the flight parameters, and the atmospheric conditions. However, substantial modifications have been required to augment the capabilities of the baseline code to assess the importance of wake effects on projected HSCT configurations and to include appropriate chemical models for the reacting flow downstream of the aircraft.

The first step in the HSRP/AESA-funded wake vortex modeling effort involved parametric studies of the interaction of hot exhaust gases with the wake trailing from notional HSCT designs (Teske et al., 1992). The platform and operation conditions were drawn from recent design studies on high-speed stratospheric aircraft (Boeing, 1989). These calculations illustrated the sensitivity of the temperature distribution in the wake far downstream of the wing to the engine placement. The flowfield associated with the wingtip vortices not only produces a temperature drop due to high cross flow velocities (Miake-Lye et al., 1992) but also sets up a recirculating cell that inhibits mixing with the free air and retards the diffusion of warmer than ambient plume hot exhaust gases. Accurate calculation of such competing effects in determining the temperature distribution in the wake is important, both because temperature is a strong driver of the chemical reaction rates and because the extent of condensation and freezing of water vapor is an important determinant of the dynamics of heterogeneous reactions. Calculations of this type are a continuing part of the present effort, using more refined predictions of HSCT spanwise loading in cruise recently obtained from Boeing personnel (R. Kulfan, Boeing Aircraft Co., private communication, 1993).

The primary objective of the present effort, however, is to develop a modified version of UNIWAKE, which can be used to directly compute the heterogeneous chemical reactions occurring between the exhaust products of HSCT engines while acted upon by the aircraft's vortex wake and the atmosphere. The modified code under development uses the mean and fluctuating flowfield predicted by UNIWAKE but is being designed to compute passive convective chemistry, assuming that heat release and subsequent density changes are negligible. These assumptions are consistent with the small concentrations of highly reactive species anticipated in the exhaust of representative aircraft. The code is designed to be a subprogram in the UNIWAKE package and has been designated PCHEM (Passive CHEMistry).

Typically, aircraft engine emissions dilute very rapidly to low concentrations which, when reacting, produce or absorb negligible heat from the air. For this reason these exhaust products, such as water vapor, soot, etc. have a small effect on the fluid dynamic interaction of the jet exhaust and wake vortex in the atmosphere. This uncoupling of the chemistry from the flowfield results in enormous simplifications in the analysis and permits the aircraft wake flowfield to be computed neglecting the exhaust product chemistry. Using this assumption, UNIWAKE predicts the ensemble-averaged velocity field, the ensemble-averaged temperature field, turbulence field (i.e., the rms turbulence level), the turbulence integral scale, and the appropriate turbulent fluctuation terms. The effects of turbulence are included by closing the Reynolds stress equations at the second order with an invariant model (Mellor and Yamada, 1974). Detailed time histories of the cross flow velocities (normal to the free stream) and the vorticity are also computed. These quantities are treated as specified or "frozen" velocity and temperature fields and are used to convect and diffuse the chemical species present in the exhaust as well as to determine chemical reaction rates.

The form of the governing equations for species convection and diffusion is broadly similar to those for the temperature field, and such equations are presently in place in the UNIWAKE/PCHEM code. The production and loss terms associated with the chemical reaction rates have yet to be fully integrated, although stand-alone computations of reacting flows are being carried out using well-known integration methods for stiff mathematical systems (Gear, 1971) as well as chemical reaction rates from standard thermochemical data bases (Miake-Lye et al., 1992). The present code allows for as many as 30 chemical species and 40 reactions, including reverse reactions.

The UNIWAKE/PCHEM code is also being designed with species equations for water vapor, water droplets, and ice crystals. A set of passive Lagrangian tracers have been implemented that can be used to sample the temperature field and water content of the combined wake/plume flowfield to provide input to existing condensation models. Finally, initialization procedures are in place to use the output of the SPF/BOAT plume code (Miake-Lye et al., 1992; Dash and Pergament, 1978) to start the computation.

The primary remaining tasks for the first phase of the development of UNIWAKE/PCHEM will involve competing direct coupling of the flowfield and passive chemistry models and carrying out sample calculations on representative systems, in cooperation with ARI. Extensions of the present modeling work will be carried on by CDI during 1993-1994 and will involve implementing direct computations of the near wake roll-up, bypassing the present Betz/Donaldson model; refinement of compressible flow effects in the crossflow plane; and addition of the full dynamic equations for second-order closure of turbulence. These modifications, which are being supported by HSRP/AESA funding, will result in a follow-on version of UNIWAKE/PCHEM, which will be made available to ARI for its ongoing work in wake/plume analysis.

The outstanding single deficiency identified in the work to date is the lack of a suitable data base for high-speed aircraft in cruise flight to use in validating the present code. While flowfield

information is available for the wakes of subsonic aircraft, most of this is for transports in landing configuration (Gardoz, 1971; Burnham, et al., 1978). Experimental information on the wakes of supersonic transports for validation purposes would be very valuable, even if this information were limited to gross features of wake convection, subsidence, and temperature field. If this proves to be infeasible in the near term, similar data on subsonic transports in the upper troposphere would be useful for carrying out preliminary validation studies that would enhance confidence in the present code.

Wake Dispersion Regime Modeling

Unlike the exhaust plume and wake vortex regimes, the wake break-up and dispersion regime has received very little previous attention in the scientific literature. No serious attempt to understand the dynamics of the mixing and exhaust evolution in this regime occurred in the CIAP program (Taylor et al., 1975), and this situation had not significantly improved by the start of the HSRP/AESA program.

Some semi-quantitative statements can be made about the vortex wake break-up and initial wake dispersion parameters (Miake-Lye et al., 1992; 1993). The descending wake vortex cell is eventually broken up due to the Crow instability (Crow, 1970) when sinusoidal perturbations along the length of the individual vortices are amplified due to mutual Biot-Savart induction. These amplified disturbances result in the trailing vortex pair reconnecting and forming vortex rings elongated in the flight direction (see Figure 3). These descending vortex rings are poorly understood at present, particularly as to how they may continue to confine and transport the exhaust gases to lower altitudes until arrested by the stable stratification of the stratosphere.

A detailed description of the eventual breakup and dissipation of these vortex rings is not currently available. After the rings have broken up, the vorticity is dissipated and/or canceled; the cancellation being due to the baroclinic vorticity generated as the less dense vortex descends into denser surroundings. The exhaust emissions, which have been mixed and confined due to aircraft-generated flow up to this point, are subsequently subject to atmospheric mixing and transport processes including local wind shear and global transport. An analysis (Miake-Lye et al., 1992) of the times scales and distances for mixing beyond the airplane plumes has been performed in order to begin to quantify the chemical environment of the exhaust gases as they mix to global scales. AER and ARI are collaborating on separate analysis of the dissipation and mixing due to atmospheric processes after the wake breakup. This latter effort includes estimates of the effects due to buildup of emissions in flight corridors created by frequent commercial traffic.

As noted above, the effort to study exhaust-driven chemical and condensation processes in the wake dispersion regime cannot draw on previous analyses of mesoscale dispersion of stratospheric pollutants. Phenomenologically, the vortex break-up ring structures illustrated in Figure 3 can be expected to leave, thin flat "pancakes" of exhaust rich air behind and slightly below the HSCT's trajectory. Since horizontal motion in the lower stratosphere is generally believed to be much faster than vertical motion, we can expect this "pancaking" exhaust trail structure to persist for some time as horizontal dispersion thins the exhaust components from the edge of each pancake.

In order to model the chemical/physical and dynamic properties of this far-wake region on time scales of 10^2 to 10^5 seconds, a Lagrangian Box dispersion model has been constructed (Shia et al., 1993). The initial model conditions including far-wake dimensions and exhaust species physical and chemical properties are specified from plume model outputs and estimated wake vortex breakup properties performed at ARI.

Since the actual horizontal and vertical dispersion mechanisms and rates in the lower stratosphere are poorly known, they are parameterized with the Lagrangian Box model

formulation. The model has initially been used to investigate the photochemistry of exhaust species rich single wakes, computing the effects of both heterogeneous and homogeneous chemistry on far wake nitrogen oxide (NO , NO_2 , N_2O_5 , HNO_3) speciation, and ozone depletion (Shia et al., 1993). The possibility of differential radiative cooling in the far-wake, which is enriched in infrared active water vapor and depleted in ultraviolet active ozone, might lead to far-wake subsidence as suggested by Overcamp and Fay (1973) has also been investigated.

Lagrangian Box model calculations of the chemical evolution of the wake corroborate the CIAP results of the mid-1970s (Gelinas and Walton, 1974; Hoshizaki et al., 1975), i.e., that there is very little additional conversion of NO_x to HNO_3 in the far wake if only gas-phase chemistry is assumed to occur. Substantial conversion could occur, however, if heterogeneous chemistry takes place on contrails, which could provide a large enhancement in available surface for heterogeneous reactions. In particular, a speculative heterogeneous conversion of NO_2 to NO_3 could accelerate the NO_x to HNO_3 conversion by heterogeneous reactions. Thus, heterogeneous chemistry provides an additional source of HO_x (produced by photodissociation of HNO_3) and leads to enhanced concentrations of OH in the wake.

The far-wake heterogeneous chemistry calculations performed to date are of an illustrative nature. The duration of heterogeneous chemistry is not well known since confinement of the exhaust products may be for a limited time. There are also varying degrees of uncertainty in the rates of the heterogeneous reactions, depending on the composition of the reacting surface. The heterogeneous conversion of NO_2 to HNO_3 has not been experimentally established. Calculations extended for 2 days indicate that a chemically perturbed environment could persist for the duration of this period after passage of the aircraft (Shia et al., 1993). In particular, concentrations of radiatively important species such as ozone and water could be reduced by about 20% and enhanced by factors of 6 to 12, respectively, during this period of time.

The above results motivated an examination of the radiative balance in aircraft wakes. Enhancements in water and reductions in ozone yield differential cooling rates relative to the background which could be as large as 3 K/day (Shia et al., 1993). Calculated downward vertical velocities range up to 0.3 km/day, depending on the altitude of wake deposition and the assumed water concentration. The net vertical displacement of the wake will be a sensitive function of the rate of dispersion of the wake, but probably will not exceed 0.5 to 1.0 km. The implications of both the photochemical and radiative results depend crucially on the adopted rates of dispersion. Information about this parameter is at present practically non-existent. The required horizontal and vertical dispersion rates for plume species in the lower stratosphere would be an appropriate target for any future field flight measurements carried out in support of the HSRP/AESA studies.

Ongoing modeling studies of the wake dispersal regime are assessing the possible impact of superposed aircraft wakes along flight corridors. Individual plumes from single flights are modeled as they expand and mix with the background atmosphere; their cross sectional areas are time dependent, calculated from the Gaussian plume equations in the model. A flight corridor will contain all the individual flight plumes with their various ages and widths. For most global-scale models, the flight corridors are expected to be smaller than the model grid box.

For simplicity and to provide a worst-case concentration enhancement, the effects of advection are initially neglected. The geographical location of the corridor is then defined solely by the adopted flight path. The chemistry continuity equation can be solved for individual plumes using the methodology developed in the Lagrangian Box model. The background concentration is also assumed to be constant in time for the domain of interest.

A time-independent background concentration implies that this value must include the large-scale perturbations of the adopted flight scenario. These can be estimated from steady-state

solutions of large-scale models. For example, the source of NO_x and other effluents can be diluted through a grid-box, or the calculated concentrations can be averaged over a grid-box, and the process iterated. Particular care will be taken to determine if nitric acid trihydrate (NAT) clouds are formed along a corridor. In this case, heterogeneous chemistry on these clouds could make these regions chemical processors and change the chemical partitioning of trace species over large, possibly global scales.

Analysis of Field Measurement Capabilities for Plume/Wake of Wake Dispersion Regimes

Measurements to directly validate plume/wake or wake dispersion models for a supersonic aircraft at typical operational altitudes are very difficult, if not impossible, to make.

Table 2, compiled primarily by Martinez-Sanchez of ARI and MIT, represents a desired set of measurements in a supersonic wake that would probably serve to evaluate the models being developed.

The basic problem is that the plume/wake/wake dispersion regimes are probably accessible only to remote sensing systems. Operational constraints imposed on a subsonic aircraft carrying in situ sensors would probably require that the aircraft enter the wake at the order of 100 km downstream of the supersonic transport. The CIAP experience established that it was extremely difficult to definitively sample the wake at that distance. In situ sensors operated aboard supersonic aircraft are not presently practical.

An effort has been made to examine remote sensor methods for measurement diagnostics. Most of the effort to date has focused on the potential use of lidar (laser radar). The two lidar research groups at NASA LaRC have examined the problem and reached the following conclusions.

- The only trace gas for which the change in optical depth across the exhaust plume is large enough to allow possible detection by differential absorption lidar is CO_2 in the 2.7 and 4.25 μm wavelength bands. Unfortunately, no practical laser system is currently available at these wavelengths.
- Optically active particles are emitted in sufficient number to be detectable by lidar backscatter during daylight hours, provided there are no intervening clouds. Such measurements are possible even without contrail formation and probably could capture the gross morphology and motion of the plume. A high repetition rate laser (approximately 30 Hz) and fast digitizer could possibly achieve 15-m resolution.

The most critical problems in the use of lidar backscatter for particle measurements are related to actually illuminating a supersonic plume with laser radiation. If the lidar systems were deployed aboard a subsonic aircraft approximately 5000 feet below the altitude of an overtaking supersonic transport, the roll angle of the subsonic aircraft carrying the lidar system could not exceed 0.5 degrees. Experiments conducted aboard a DC-8 attempting to illuminate an engine plume with a laser have established that such precise control is not practical. A lidar system deployed aboard a subsonic aircraft would, therefore, have to have the ability to scan to perform plume measurements. Existing airborne lidar systems could be modified to allow moderate scanning. Both NASA LaRC lidar groups recommended that ground-based lidar measurements (probably at night) be performed to establish the feasibility of airborne measurements.

Various suggestions have been made that measurements of the thermal emission from the plume might be useful in determining the position of the plume or possibly even provide

measurements of specie concentration (e.g., water vapor). A remote sensing group at NASA LaRC experienced in measuring atmospheric thermal emission from satellites is currently assessing the potential of thermal emission techniques for plume measurement. It has also been suggested that the wake vortex dynamics model could perhaps be validated in one of the NASA LaRC wind tunnels. This possibility is also under study.

SUMMARY/EVALUATION OF PROGRAM STRENGTHS AND DEFICIENCIES

In summary, a major theoretical effort has been undertaken to model the physical and chemical processes that occur in the wake aft of a supersonic aircraft. This effort can be considered state of the art in terms of algorithms for studying chemical, radiative, and fluid dynamical processes and their respective interactions within aircraft wakes. At present, there exists no equivalent effort for attacking this problem. British Aerospace is beginning an effort to develop a computer code for modeling aircraft wakes as part of the European AERONOX program. The HSRP/AESA program will maintain cognizance of this developing effort to maximize resources applied to this problem area.

The major concern at this point is the inability in the near-term to validate/assess these algorithms. As indicated earlier in this chapter, locating and sampling the wake of a supersonic aircraft poses extreme difficulties. Some data do exist for the wake fluid dynamics of subsonic jumbo jets in landing configuration. Furthermore, recent measurements from Europe have reported on reactive nitrogen oxide chemical speciation in subsonic plumes (Arnold et al., 1992). These data must be exercised to provide some level of assessment for the existing wake computer codes. However, the general lack of data poses a level of uncertainty for the computer code predictions which cannot be evaluated at this time. The French government is planning a program that includes "chasing" a Concorde aircraft and sampling the trailing wake. This program will be followed carefully to determine the utility of any acquired data for evaluating the existing computer codes.

Table 1. SO_x and Oxidizer Speciation (Mach 2.4; N47; 18.4 km; June 15)

Species	Exit Plane	Mole Fractions		
		152m	305m	610m
OH	1.0×10^{-5}	1.4×10^{-8}	1.4×10^{-8}	1.9×10^{-9}
O ₃	0.0	2.1×10^{-6}	2.4×10^{-6}	2.4×10^{-6}
NO	4.3×10^{-5}	6.2×10^{-6}	2.0×10^{-6}	9.4×10^{-7}
NO ₂	4.8×10^{-6}	6.2×10^{-7}	2.0×10^{-7}	1.0×10^{-7}
NO ₃	0.0	2.1×10^{-11}	4.5×10^{-12}	8.1×10^{-13}
N ₂ O ₅	0.0	2.1×10^{-10}	3.2×10^{-10}	3.4×10^{-10}
HNO ₃	0.0	2.4×10^{-7}	1.1×10^{-7}	5.9×10^{-8}
SO ₂	6.9×10^{-6}	9.5×10^{-7}	3.0×10^{-7}	1.4×10^{-7}
SO ₃	0.0	6.8×10^{-8}	3.2×10^{-8}	1.6×10^{-8}
NO ₂ /NO	0.11	0.10	0.10	0.11
HNO ₃ /NO _x	0.0	0.035	0.05	0.056
SO ₃ /SO ₂	0.0	0.07	0.11	0.11

Table 2. Desired Measurements for Supersonic Wakes

Questions to be Answered	Regime	Data Required & (Accuracy)	Approaches Comments
Degree of Confinement What Morphology? Detrainment?	2-D Plume-Wake Ring Descent Bottom of B.V. Cycle Post-Breakup	Visualization Rough Profiling (Qualitative or Semiquantitative) ($\pm 50\%$?)	ER2 Flights Parallel to Concorde/TU-144 (Extension of CIAP Data)
Descent Speed/Distance	2-D Ring	$\pm 20\%$	
Validation of Vortex/Plume Simulations	2-D Plume-Wake	Tracer Profiling ($\pm 20\%$?) Vortex Pair Separation ($\pm 5\%$ of span)	(a) Laboratory (Buoyant Dye in Tank) (b) Parallel Flights (Difficult)
What Dilution at End of Ring Descent?	Ring Descent Break-Up	Tracer Profiling ($\pm 20\%$?)	Parallel Flights Through Flights
What Distribution After Breakup?	Post-Breakup	Tracer Profiling ($\pm 20\%$?)	Through Flights (10-60 Minutes after Passage)
How Much Vortex Cooling?	2-D Plume-Wake Ring Descent	At ($\pm 0.5^\circ\text{C}$?)	Remote Sensing Parallel Flights (Difficult)
Enhancement of Contrail Formation?	2-D Plume-Wake Ring Descent	Visualization (Qualitative to Semiquantitative)	Can be Done Together with Morphology Studies
How Many Particles? How Big? What Shape?	2-D Plume-Wake Ring Descent Post Breakup?	Scattering ($\pm 50\%$?)	Parallel Flights (Difficult)
What Chemistry at Intermediate Stages?	2-D Plume-Wake Ring Descent	Quantitative Remote Profiling of NO_x , O_3 , HNO_3 ...($\pm 20\%$?)	Parallel Flights (Most Difficult)
What Chemistry by End of Regime?	Post-Breakdown	Quantitative In Situ Profiling of NO_x , O_3 , HNO_3 ...($\pm 20\%$?)	Through Flights

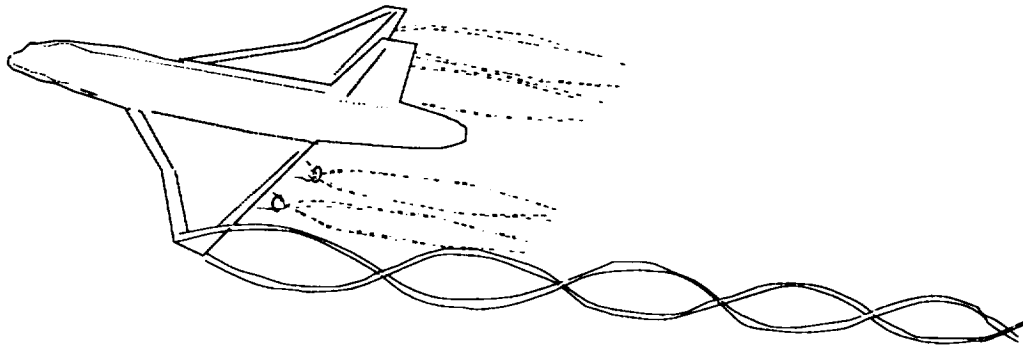


Figure 1. Plume regime with exhaust jet mixing and vortex roll-up.

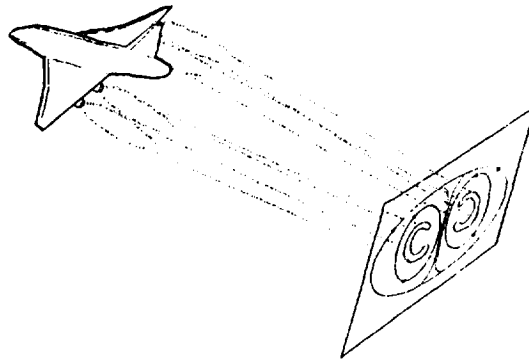


Figure 2. Vortex wake regime with exhaust entrainment, shear, and confinement in the descending vortex cell (not to scale).

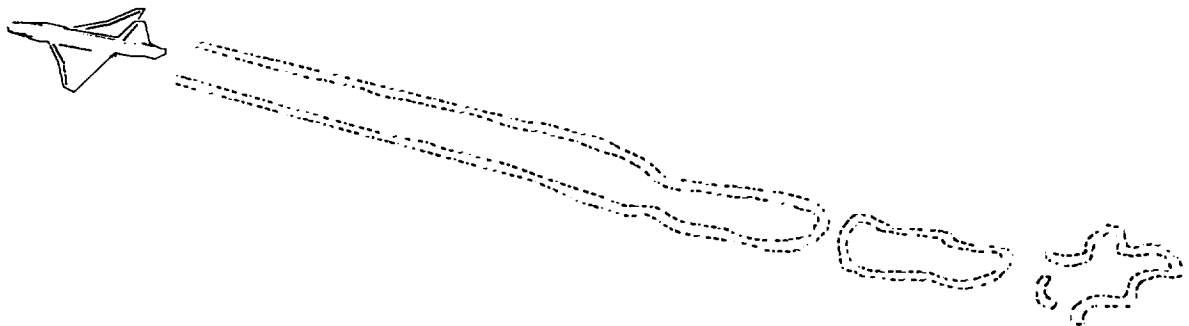


Figure 3. Breakup of vortex wake and formation of reconnected elongated vortex rings (not to scale).

REFERENCES

- Aerodyne Research, Inc., "SPIRITS 4.1 User's Manual," Report No. ARI-RR-754, 1989.
- Arnold, F., J. Scheid, Th. Stulp, H. Schlager, and M. E. Reinhardt, Measurements of jet aircraft emissions at cruise altitude I: The odd-nitrogen gases NO, NO₂, HNO₂, and HNO₃, *Geophys. Res. Lett.*, 12, 1421-1424, 1992.
- Bilanin, A. J., and C. Donaldson, Estimation of velocities and roll-up in aircraft vortex wakes, *J. Aircraft*, 12, 578-585, 1975.
- Bilanin, A. J. and M. E. Teske, Unified Wake Analysis, Continuum Dynamics, Inc., Report No. 88-06, 1988.
- Bilanin, A. J., M. E. Teske, and J. E. Hirsh, Neutral atmosphere effects on the dissipation of aircraft vortex wakes, *AIAA J.*, 16, 9, 1978.
- Bilanin, A. J., M. E. Teske, and G. G. Williamson, Vortex interactions and decay in aircraft wakes, *AIAA J.*, 15, 2, 1977.
- Boeing Commercial Aircraft Company, *High Speed Civil Transport Study*, NASA Contractor Report 4233, NASA, Washington, D.C., 1989.
- Brown, R. C., R. C. Miake-Lye, M. Martinez-Sanchez, and C. E. Kolb, "Heterogeneous Condensation in Stratospheric Aircraft Plumes," Abstracts of the Second Annual HSRP/AESA Meeting, Virginia Beach, VA, *HSRP-AESA Flyer*, NASA, Washington, D.C., 1992.
- Burnham, D. C., J. N. Hallock, I. H. Tombach, M. R. Brashears, and M. R. Barber, "Ground-Based Measurements of the Wake Vortex Characteristics of a B-747 Aircraft in Various Configurations," FAA-RD-78-146, 1978.
- CIAP Monograph 2, Propulsion Effluents in the Stratosphere*, DOT-TST-75-52, September 1975.
- Conant, J., J. Gruninger, T. Spaulding, T. Thompkins, G. Voltin, and B. Sandford, SPIRITS - A model for spectral infrared imaging of targets and scenes, in *Proceedings of the 1985 IRIS Specialty Group Meeting on Targets, Backgrounds, and Discrimination*, Volume I, ERIM IRIA Center, Ann Arbor, MI, pp. 129-147, 1985.
- Corrin, M., Heterogeneous chemistry of the natural stratosphere, Section 5.5, *CIAP Monograph 1, The Natural Stratosphere of 1974*, pp. 5-55 to 5-70, DOT-TST-75-51, September 1975.
- Crow, S. C., Stability theory for a pair of trailing vortices, *AIAA J.*, 8, 2172-2179, 1970.
- Dash, S. M., and H. S. Pergament, *A Computational Model for the Prediction of Jet Entrainment in the Vicinity of Nozzle Boattails (The BOAT Code)*, NASA Contractor Report 32075, NASA, Washington, D.C., 1978.
- Dash, S. M., H. S. Pergament, and R. D. Thorpe, The JANNAF Standard Plume Flowfield Model: Modular approach, computational features and preliminary results, in *Proceedings of the JANNAF 11th Plume Technology Meeting*, CIAP Pub. 306, 345-442, 1979.
- Dash, S. M., H. S. Pergament, D. E. Wolf, N. Sinha, M. W. Taylor, and M. E. Vaughn, Jr.,

- The JANNAF Standardized Plume Flowfield Code Version II (SPF-II)*, Vol. I and II, Technical Report No. CR-RD-55-90-4, U.S. Army Missile Command, Redstone Arsenal, AL, 1990.
- DeMore, W. B., S. D. Sander, D. M. Golden, M. J. Molina, R. F. Hampson, M. J. Kurylo, C. J. Howard, and A. R. Ravishankar, "Chemical Kinetics and Photochemical Data for Using Stratospheric Modeling," JPL Publication 90-1, Jet Propulsion Laboratory, Pasadena, CA, 1990.
- DeMore, W. B., S. P. Sander, D. M. Golden, R. F. Hampson, M. J. Kurylo, C. J. Howard, A. R. Ravishankar, C. E. Kolb, and M. J. Molina, *1992 Chemical Kinetics and Photochemical Data for Use in Stratospheric Modeling*, JPL Publication 92-20, Jet Propulsion Laboratory, Pasadena, CA, 1992.
- Garodz, L. J., Measurements of Boeing 747, Lockheed C5A and other aircraft vortex wake characteristics by the Tower Fly-By Technique, in *Aircraft Wake Turbulence and Its Detection*, J. H. Olsen, A. Goldberg, and M. Rodgers Eds., Plenum Press, 1971.
- Gear, R. J., *Numerical Initial Value Problems in Ordinary Differential Equations*, Prentice Hall, Englewood Cliffs, NJ, 1971.
- Gelinas, R. J., and J. J. Walton, Dynamic-kinetic evolution of a single plume of interacting species, *J. Atmos. Sci.*, *31*, 1807-1813, 1974.
- Hallett, J., J. G. Hudson, and C. F. Rogers, Characterization of Combustion Aerosols for Haze and Cloud Formation, *Aerosol Sci. Tech.*, *10*, 70-83, 1989.
- Hidy, G. M., A. W. Castleman, Jr., J. P. Friend, A. Harker, and J. Huntzicker, Aerosols from engine effluents, *CIAP Monograph 3, The Stratosphere Perturbed by Propulsion Effluents*, pp. 6-1 to 6-63, DOT-TST-75-53, Department of Transportation, Washington, D.C., September 1975.
- Hirsch, R. S., "Higher Order Approximations in Fluid Dynamics - Compact to Spectral," von Karman Institute Lecture Series 1983-04, 1983.
- Hoshizaki, H., L. B. Anderson, R. J. Conti, N. Farlow, J. W. Meyer, T. Overcamp, K.O. Redler, and V. Watson, Aircraft wake microscale phenomena. Chapter 2 in *CIAP Monograph 3, The Stratosphere Perturbed by Propulsion Effluents*, DOT-TST-75-53, Department of Transportation, Washington, D.C., 1975.
- Hudson, J. G., J. Hallett, and C. F. Rogers, Field and laboratory measurements of cloud-forming properties of combustion aerosols, *J. Geophys. Res.*, *96*, 10,847-10,859, 1991.
- Mellor, G. L., and T. Yamada, A hierarchy of turbulent closure models for planetary boundary layers, *J. Atm. Sci.*, *31*, 1791-1806, 1974.
- Miake-Lye, R. C., R. C. Brown, M. Martinez-Sanchez, and C. E. Kolb, High-speed civil transport exhaust mixing and chemistry, *Proceedings of the 1993 JANNAF Exhaust Plume Technology Subcommittee Meeting*, Kirtland AFB, NM, Chemical Propulsion Information Agency, in press, 1993.
- Miake-Lye, R. C., M. Martinez-Sanchez, R. C. Brown, and C. E. Kolb, Plume and wake dynamics, mixing, and chemistry behind an HSCT aircraft, *J. Aircraft*, accepted for publication (1993); also AIAA Paper No. 91-3150.

- Miller, J. A., and C. T. Bowman, Mechanism and modeling of nitrogen chemistry in combustion, *Prog. Energy Combust. Sci.*, **15**, 287-338, 1989.
- Moore, D. W., and P. G. Saffman, Structure of a line vortex in an imposed strain, in *Aircraft Wake Turbulence and Its Detection*, J. H. Olsen, A. Goldberg, and M. Rodgers, Eds., Plenum Press, 1971.
- Olszyna, K., R. D. Cadle, and R. G. de Penna, Stratospheric heterogeneous decomposition of ozone, *J. Geophys. Res.*, **84**, 1771-1775, 1979.
- Overcamp, T. J., and J. A. Fay, Dispersion and subsidence of the exhaust of a supersonic transport in the stratosphere, *J. Aircraft*, **10**, 720-728, 1973.
- Panofsky, H., and W. Heck, "Vertical Dispersion near 20 km," p. 102, Third Conference on CIAP, DOT-TSC-OST-74-15, February 1974; see also Section 6.5.3, p. 6-78 to 6-80, *CIAP Monograph 1, The Natural Stratosphere of 1974*, DOT-TST-75-51, September 1975.
- Shia, R. L., J. Rodriguez, M. K. W. Ko, C. Helsey, R. C. Miake-Lye, and C. E. Kolb, Subsidence of aircraft engine exhaust in the stratosphere and its implication for ozone depletion, Submitted to *Geophys. Res. Lett.*, 1993.
- Sykes, R. I., W. S. Lewellen, and S. F. Parker, On the vorticity dynamics of a turbulent jet in a crossflow, *J. Fluid Mech.*, **168**, 393-413, 1986.
- Taylor, T. D., J. S. Chang, T. V. Crawford, G. R. Hilst, H. Hoshizaki, J. Riley, J. J. Walton, and G. Widhopf, Dispersion and transport at intermediate scales between the microscale and the horizontal mesoscale, *CIAP Monograph 3, The Stratosphere Perturbed by Propulsion Effluents*, pp. 3-1 to 3-32, DOT-TST-75-53, Department of Transportation, Washington, D.C., September 1975.
- Teske, M. E., "Vortex Interactions and Decay in the Aircraft Wakes: User Manual and Program Manual," Aeronautical Research Associates of Princeton, Inc., Report No. 271, 1976.
- Teske, M. E., T. R. Quackenbush, and A. J. Bilanin, Vortex roll-up, merging, and decay with the UNIWAKE computer program, *Proceedings of the FAA International Vortex Wake Symposium*, Washington, D.C., 1991.
- Teske, M. E., A. J. Bilanin, and T. R. Quackenbush, A Parametric Study of Vortex Wake Dynamics Behind and HSCT Aircraft Using the UNIWAKE Code, presentation at the Second Annual HSRP/AESA Annual Meeting, 1992.
- Tsang, W., and R. F. Hampson, Chemical kinetic data base for combustion chemistry. Part I. Methane and related compounds, *J. Phys. Chem. Ref. Data*, **15**, 1087-1279, 1986.
- Tsang, W., and J. T. Herron, Chemical kinetic data base for propellant combustion I. Reactions involving NO, NO₂, HNO, HNO₂, HCN, N₂O, *J. Phys. Chem. Ref. Data*, **20**, 609-663, 1991.
- Welckmann, H., J. Anderson, H. Appleman, E. Barrett, H. Elisaesser, and C. Van Valin, Water vapor and cloud formation from engine effluents, *CIAP Monograph 3, The Stratosphere Perturbed by Propulsion Effluents*, pp. 7-1 to 7-39, DOT-TST-75-53, Department of Transportation, Washington, D.C., September 1975.

- Widnall, S. E., D. B. Bliss, and A. J. Zalay, Theoretical and experimental study of the stability of a vortex pair, in *Aircraft Wake Turbulence and Its Detection*, J. H. Olsen, A. Goldberg, and M. Rodgers, Eds., Plenum Press, 1971
- Whitefield, P. D., D. E. Hagen, R. Holland, K. O'Brien, and M. Trueblood, "Size and Hydration Characteristics of Laboratory Simulated Jet Engine Combustion Aerosols Using a Range of Aviation Fuels in Conventional and Advanced Combustor Configurations," Abstracts of the Second Annual HSRP/AESA Meeting, Virginia Beach, VA, *HSRP/AESA Flyer*, NASA, Washington, D.C., 1992.
- WMO, *Atmospheric Ozone 1985, Assessment of Our Understanding of the Processes Controlling Its Present Distribution and Change*, WMO Global Ozone Research and Monitoring Report NO. 16, World Meteorological Organization, Washington, D.C., 1986.
- WMO, *Atmospheric Ozone 1989*, WMO Global Ozone Research and Monitoring Report No. 20, World Meteorological Organization, Washington, D.C., 1989.
- Zhao, J. and R.P. Turco, Particle nucleation in the wake of a jet aircraft in stratospheric flight, *J. Aerosol Sci.*, submitted for publication (1992).

Chapter 7

HSRP/AESA Research Summaries

This chapter presents individual summaries of research conducted by investigators supported by High Speed Research Program/Atmospheric Effects of Stratospheric Aircraft; see Chapter 1 for an overview of the principal investigators and research areas. The summaries follow this format: (A) title, (B) investigators and institutions, (C) abstract of research objectives, (D) summary of progress and results to date, and (E) journal publications. These summaries have been edited where necessary. The principal investigator (denoted by an asterisk) is the contact person responsible to HSRP/AESA for the proposed research.

HSRP/AESA Principal Investigators

James G. Anderson, Harvard University
Darrel Baumgardner, National Center for Atmospheric Research
David F. Blake, NASA Ames Research Center
Donald R. Blake, University of California, Irvine
Guy P. Brasseur, National Center for Atmospheric Research
William H. Brune, Pennsylvania State University
Karen L. Carleton, Physical Sciences Inc.
K. Roland Chan, NASA Ames Research Center
David R. Crosley, SRI International
Anne R. Douglass, NASA Goddard Space Flight Center
Timothy J. Dunkerton, Northwest Research Associates
James W. Elkins, NOAA Climate Monitoring and Diagnostics Laboratory
David W. Fahey, NOAA Aeronomy Laboratory
Randall R. Friedl, NASA Jet Propulsion Laboratory
Patrick Hamill, San Jose State University
R. Stephen Hipskind, NASA Ames Research Center
Matthew H. Hitchman, University of Wisconsin
Kenneth K. Kelly, NOAA Aeronomy Laboratory
Malcolm K. W. Ko, Atmospheric and Environmental Research, Inc.
Charles E. Kolb, Aerodyne Research, Inc.
John S. Langford, Aurora Flight Sciences Corporation
Ming-Tuan Leu, NASA Jet Propulsion Laboratory
Max Loewenstein, NASA Ames Research Center
Richard C. Miake-Lye, Aerodyne Research, Inc.
Mario J. Molina, Massachusetts Institute of Technology
Daniel M. Murphy, NOAA Aeronomy Laboratory

Paul A. Newman, NASA Goddard Space Flight Center
Samuel J. Oltmans, NOAA Climate Monitoring and Diagnostics Laboratory
Leonhard Pfister, NASA Ames Research Center
G. Pitari, Universita' degli Studi L'Aquila
R. Alan Plumb, Massachusetts Institute of Technology
Michael H. Proffitt, NOAA Aeronomy Laboratory
Rudolph F. Pueschel, NASA Ames Research Center
Richard B. Rood, NASA Goddard Space Flight Center
Philip B. Russell, NASA Ames Research Center
Glen W. Sachse, NASA Langley Research Center
Robert K. Seals, Jr., NASA Langley Research Center
Patrick J. Sheridan, University of Colorado
Run-Lie Shia, Atmospheric and Environmental Research, Inc.
Margaret A. Tolbert, University of Colorado
Owen B. Toon, NASA Ames Research Center
Ka-Kit Tung, University of Washington
Richard P. Turco, University of California, Los Angeles
Christopher R. Webster, NASA Jet Propulsion Laboratory
Andrew J. Weinheimer, National Center for Atmospheric Research
Philip D. Whitefield, University of Missouri-Rolla
James C. Wilson, University of Denver
Steven C. Wofsy, Harvard University
Douglas R. Worsnop, Aerodyne Research, Inc.
Donald J. Wuebbles, Lawrence Livermore National Laboratory
Glenn K. Yue, NASA Langley Research Center

Development of Techniques for the In Situ Observation of OH and HO₂ for Studies of the Impact of High-Altitude Supersonic Aircraft on the Stratosphere

Investigators

*James G. Anderson
Philip Weld
Atmospheric Research Project
Engineering Sciences Laboratory
Harvard University
Cambridge, MA 02138

Research Objectives

The purpose of this study is to add a new capability to the existing ER-2 payload to measure OH and HO₂. The lack of knowledge of the HO_x radical concentrations has been a major impediment in the ability to test fully the photochemical models of the lower stratosphere.

Summary of Progress and Results

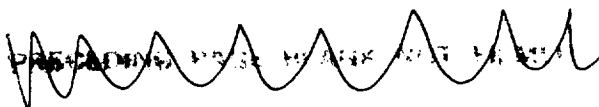
This new instrument had its first test flights in October/November 1992 during the SPADE test flight series. These test flights demonstrated the capability of the experiment to make very high signal-to-noise measurements of OH from the ER-2. Data return rates exceeded 50%. In addition, successful measurements of stratospheric water vapor were made. This in situ hygrometer is located immediately down stream of the OH detection axes and as used as a diagnostic for detection of photochemical interference in the OH measurement.

Following the November deployment, work was done to increase the software and hardware reliability of the instrument, and further work to reduce the overall weight was performed. Additional calibration was performed to determine the absolute sensitivity of the OH system.

Deployment during the SPADE science flights is in progress and to date the instrument performance is excellent. Data return rates are approaching 100%. Measurement of the OH and HO₂ densities from 60°N latitude to 20°N, as well as diurnal measurements, has now been accomplished. These data sets are already yielding surprises which await further analysis.

Journal Publications

None



The Multiangle Spectrometer Probe (MASP)

Investigators

***Darrel Baumgardner**
James E. Dye
Atmospheric Technology Division
National Center for Atmospheric Research
P. O. Box 3000
Boulder, CO 80307-3000

Research Objectives

Our objective is to develop an optical sensor that can fly on a high-speed aircraft and isokinetically measure the size, concentration, and index of refraction of stratospheric aerosol particles.

Summary of Progress and Results

The multiangle aerosol spectrometer probe (MASP) measures the forward and backward components of light scattered from individual aerosol particles and determines the particle size from the magnitude of the combined intensity of these components and, for a select size range, estimates index of refraction from the ratio of the scattered light components.

The prototype optical bench is now assembled and undergoing evaluation. The pulse processing electronics have been designed and breadboarded for evaluation with the prototype optical bench. A major design review was conducted to evaluate the pulse processing design. The design is now being finalized as the various stages are being bench-tested before final incorporation in the airborne version.

Preliminary results from evaluations of the optical design indicate that the scattering geometry and first stage electronics will provide at least a 2:1 signal to noise ratio and will provide adequate signal to detect 0.2 μm diameter particles.

A number of aerodynamic design models of the MASP were evaluated during a one-week period at the Air Force Academy wind tunnel facility. Air speeds near those of the ER-2 were attained but at nonstratospheric pressures (700 mb) and temperatures (25°C). The tests have shown that a shroud around the inlet is a necessity for isokinetic, low turbulence flow but that the inlet length could be shorter than originally anticipated.

The development project is still on schedule for completion of a prototype instrument that can be tested at the Air Force Academy wind tunnel sometime in mid to late summer.

Journal Publications

None

Stratospheric Dust Particles: Composition, Size Distribution, and Surface Chemistry

Investigators:

*David F. Blake
Rudolf F. Pueschel
Sherwood Chang
Theodore Bunch
Ames Research Center
National Aeronautics and Space Administration
Moffett Field, CA 94035-1000

Research Objectives

We are continuing to quantify stratospheric and upper tropospheric carbon soot loading by directly identifying and counting individual soot particles on Ames Wire Impactors (AWI). Large variations in atmospheric soot loading appear to exist between samples from different latitudes in the northern hemisphere and between samples from northern versus southern latitudes. These variations appear to correlate with anthropogenic activities. A paper describing these results is in preparation (see reference below).

Summary of Progress and Results

We have nearly completed the duration of ~20 years of AWI collectors, cataloging them and placing each ring in an individual Fluorware™ clean room container. All new collectors and rings are exposed to laboratory air only in a class-100 clean room (although there is brief exposure to unfiltered air during pumpdown inside the electron microscope). We have performed analyses using collectors that were prepared by not flown, which show that laboratory contamination is not a serious problem.

Our data collection and analyses is now completely electronic. Images of particles are collected digitally from the electron microscope into a workstation-based image analysis system. The images are permanently stored on tape, and measurements are made by computer.

We are preparing collectors for the upcoming SPADE II mission. The collectors hold two wires (500 μm and 75 μm) and a 3-mm EM grid for TEM analysis.

Journal Publications

Blake, D., R. Pueschel, K. Kato, and S. Verma, Analysis and distribution of carbon soot in the lower stratosphere and upper troposphere, in preparation, 1993.

Whole Air Sampling from the DC-8 Aircraft During AASE-2

Investigators

*Donald R. Blake
F. Sherwood Rowland
Department of Chemistry
University of California, Irvine
Irvine, CA 92717

Research Objectives

By collecting whole-air samples from the NASA DC-8 Aircraft and assaying them for selected nonmethane hydrocarbons and halocarbons the perturbation on the lower stratosphere by jet aircraft exhaust will be evaluated. Also, by studying correlations of numerous long and short lived gases the amount of stratospheric photolysis and the age of the sampled airmasses will be estimated.

Summary of Progress and Results

Measurements of the relative concentrations of different halocarbon compounds in sequential samples of stratospheric air demonstrated a very consistent pattern which provides both a rank ordering of susceptibility to stratospheric decomposition and a quantitative estimate for each compound. The halocarbons included in this ranking are five CFCs (CFC-11, -12, -113, -114, -115), two halons (H-1301, -1211), one HCFC (HCFC-22), CH_3CCl_3 , CCl_4 , and several chloro- and bromocarbons (CH_3Cl , CH_2Cl_2 , CHCl_3 , CH_3Br , CH_2Br_2 , CHBr_3).

The concentrations of most nonmethane hydrocarbons (NMHC) were very low, generally less than 10 pptv, for all except C_2H_6 , C_2H_2 , and C_3H_8 in stratospheric air. Vertical spirals made during the northern winter show C_2H_6 concentrations in the 2000-3000 pptv range in the troposphere, decreasing to 35-100 pptv in the stratosphere. The tropospheric concentrations of C_2H_6 , C_2H_2 , and C_3H_8 are very highly correlated with one another, consistent with removal for each by reaction with HO radicals.

Air samples collected in the upper troposphere during the transit flights from San Jose to Tahiti provided latitudinal profiles for more than a dozen each of hydrocarbons and halocarbons. The alkane concentrations all decrease rapidly for latitudes south of 20°N , with very low concentrations (< 10 pptv) for essentially all except C_2H_6 and C_3H_8 . The halocarbon variation with latitude is quite different for $\text{CCl}_2\text{-CCl}_2$ (anthropogenic input from the north temperate zone), CH_3Br and CH_3Cl (small latitudinal variation suggesting major input--presumably much of it natural--from both northern and southern hemispheres) and CH_2Cl_2 (higher concentrations in the tropic latitudes).

Air samples collected at 12 km in the vicinity of a tropical storm with strong upward convection exhibited elevated concentrations of all hydrocarbons and short-lived halocarbons indicative of strong upward transport. These samples can be useful for estimating the natural and anthropogenic inputs of halocarbons into the stratosphere during such convective events.

Journal Publications

"Measured Relative Removal Rates of Halocarbons and N_2O in the Arctic Stratosphere During the Winter 1991-1992," in preparation for submissions to *Science*.

"Arctic Haze Event Encountered at the North Pole, During Winter 1992," in preparation for submission to *J. Geophys. Res.*

Modeling of the Atmospheric Effects of Stratospheric Aircraft

Investigators

*Guy P. Brasseur
Philip J. Rasch
XueXi Tie
Brian Eaton
National Center for Atmospheric Research
P. O. Box 3000
Boulder, CO 80307-3000

Richard P. Turco
Department of Atmospheric Sciences
University of California, Los Angeles
Los Angeles, CA 90024-1565

Research Objectives

In this study we hope to understand and predict the atmospheric effects of a fleet of stratospheric aircraft, using 2-D and 3-D chemical, dynamical, radiative models of the middle atmosphere. In addition, we hope to improve the transport and chemistry formulations in these models and assess the global changes in the atmospheric composition for a variety of scenarios of aircraft emissions.

Summary of Progress and Results

Two-dimensional dynamical and chemical model studies: The NCAR 2-D model has been further developed to include the effects of heterogeneous chemistry on sulfate aerosol and polar stratospheric clouds. A study of the chemical effects of aerosols produced by the eruption of Mt. Pinatubo has been published in *Science*.

A model describing microphysical processes related to aerosol formation and destruction has been completed and coupled to the 2-D model. Heterogeneous nucleation, condensation, evaporation, coagulation, gravitational sedimentation, and washout are treated in detail for aerosols distributed in 25 size bins. The aerosols are also transported. A paper summarizing the results of this model study and simulating the distribution of volcanic aerosols after the eruption of El Chichón is being prepared.

Model calculations based on new NASA scenarios for aircraft emissions have been performed and the effect of atmospheric aerosols on the model predictions has been assessed. The results appear in Chapter 4 of this report.

A detailed model study of ozone response to HSCT operations, including the effect of emission altitude and latitude, the chlorine loading, heterogeneous processes, etc. has been completed and submitted to the *Journal of Atmospheric Chemistry*.

Three-dimensional dynamical and chemical model studies: A new chemical scheme for the stratosphere has been completed, tested, and included in the stratospheric version of the NCAR Community Climate Model. First results obtained by this model have been presented at several international conferences (Japan, France, Canada) and will be discussed at the next HSRP conference, June 1993, Virginia Beach, VA. The 3-D model simulates the behavior of approximately 30 species belonging to the oxygen, hydrogen, nitrogen, and chlorine families.

The development of an off-line version of this model has been completed. A manuscript has been submitted to the *Journal of Geophysical Research* in which 2-D and 3-D simulations of airplane emissions and tracer transport are compared. Simulations of Carbon-14 exchange through the tropopause were also studied.

We have participated in the recent NASA meeting at Satellite Beach, FL, and contributed to the preparation of the HSRP/AESA Interim Assessment Report.

Journal Publications

Granier, C., and G. P. Brasseur, Impact of heterogeneous chemistry on model predictions of ozone change, *J. Geophys. Res.*, 97, 18015-18033, 1992.

Brasseur, G. P., and C. Granier, Pinatubo aerosols, chlorofluorocarbons, and ozone depletion, *Science*, 257, 1239-1242, 1992.

Rasch, P. J., X. X. Tie, B. A. Boville, and D. L. Williamson, A three dimensional transport model for the middle atmosphere, *J. Geophys. Res.*, submitted, 1992.

Rasch, P. J., B. A. Boville, and G. P. Brasseur, "A Three-Dimensional General Circulation Model with Coupled Chemistry for the Middle Atmosphere," manuscript in preparation.

Tie, X., G. Brasseur, P. Friedlingstein, C. Granier, and P. Rasch, The impact of high altitude aircraft on the ozone layer in the stratosphere, *J. Atmos. Chem.*, submitted, 1992.

Tie, X., Lin, X., and G. P. Brasseur, "Two-dimensional Coupled Dynamical/Chemical/Microphysical Simulation of Global Distribution of El Chichón Volcanic Aerosols," manuscript in preparation.

Laboratory Investigations of the Microphysics and Chemistry of Aqueous Particles Typical of the Lower Stratosphere

Investigators

*William H. Brune
Dennis Lamb
Meteorology Department

Bruce R. F. Kendall
Physics Department
Pennsylvania State University
University Park, PA 16802

Research Objectives

This project is designed to investigate the microphysics and chemistry of aqueous particles in a controlled laboratory environment. One important goal of the project is to demonstrate the feasibility of employing the technique of electrodynamic levitation to suspend and isolate micron-sized particles from the unwanted influence of chamber walls and yet let the particles be exposed to air that simulates the pressure, temperature, water, and trace gas environment of the stratosphere. The microphysical investigations focus on the growth rates and phase changes of individual particles as they evolve from small sulfuric acid droplets to hydrated nitric acid crystals under varying humidity and trace gas conditions. Studies of the heterogeneous chemistry involve observing swarms of levitated particles to assess the effects of the microphysical properties on the rates and efficiencies of the heterogeneous transformations.

Summary of Progress and Results

Through various tests conducted over the past year, the electrodynamic cell has been shown to meet our anticipated experimental needs. This cell has interchangeable flat electrodes made of conductive glass, thus simplifying our ability to sense the particle characteristics and position from outside the cell. The cubical shape of the cell also allows us to bathe the levitated particles with a laminar flow of well-characterized air. The optical system used to identify particle composition and phase changes uses an argon laser guided into the center of the cell from below; Raman-scattered radiation is captured by a fast lens near one of the sides of the cell and then focused into a monochromator. System testing with aqueous particles at ambient conditions is about finished, so we will soon begin experiments at reduced temperatures and pressures.

Journal Publications

- Allison, E. E., B. R. F. Kendall, B. V. Bronk, and D. S. Weyandt, Manipulation of microparticles in multiphase levitation traps. Proceedings, 1992 CRDEC Scientific Conference on Observations and Aerosol Research, 1992.
- Lamb, D., Microphysical and chemical aspects of cloud formation at low temperatures. Preprints, 11th International Conference on Clouds and Precipitation, Montreal, Canada, 17-22 August 1992, Am. Meteorol. Soc., Boston, 869-872.

Heterogeneous Nucleation Kinetics of Atmospheric Aerosols by Single Particle Measurements in a Quadrupole Trap

Investigators

*Karen L. Carleton
David M. Sonnenfroh
Barbara Wyslouzil
Steven J. Davis
W. Terry Rawlins
Physical Sciences Inc.
20 New England Business Center
Andover, MA 01810

Research Objectives

Heterogeneous atmospheric chemistry is a critical issue in assessing the potential effects of stratospheric aircraft. The demonstrated impact of polar stratospheric clouds on ozone levels suggests that nucleation and growth of aerosols are important. This work is designed to measure physical and chemical properties of single particles under stratospheric conditions in a quadrupole trap. This electrodynamic trap confines the charged particle in an electric field. The DC voltage necessary to suspend the particle and to offset the gravitational force is proportional to the particle mass. Monitoring this voltage enables studies of particle growth as the gas phase composition and temperature are changed.

Summary of Progress and Results

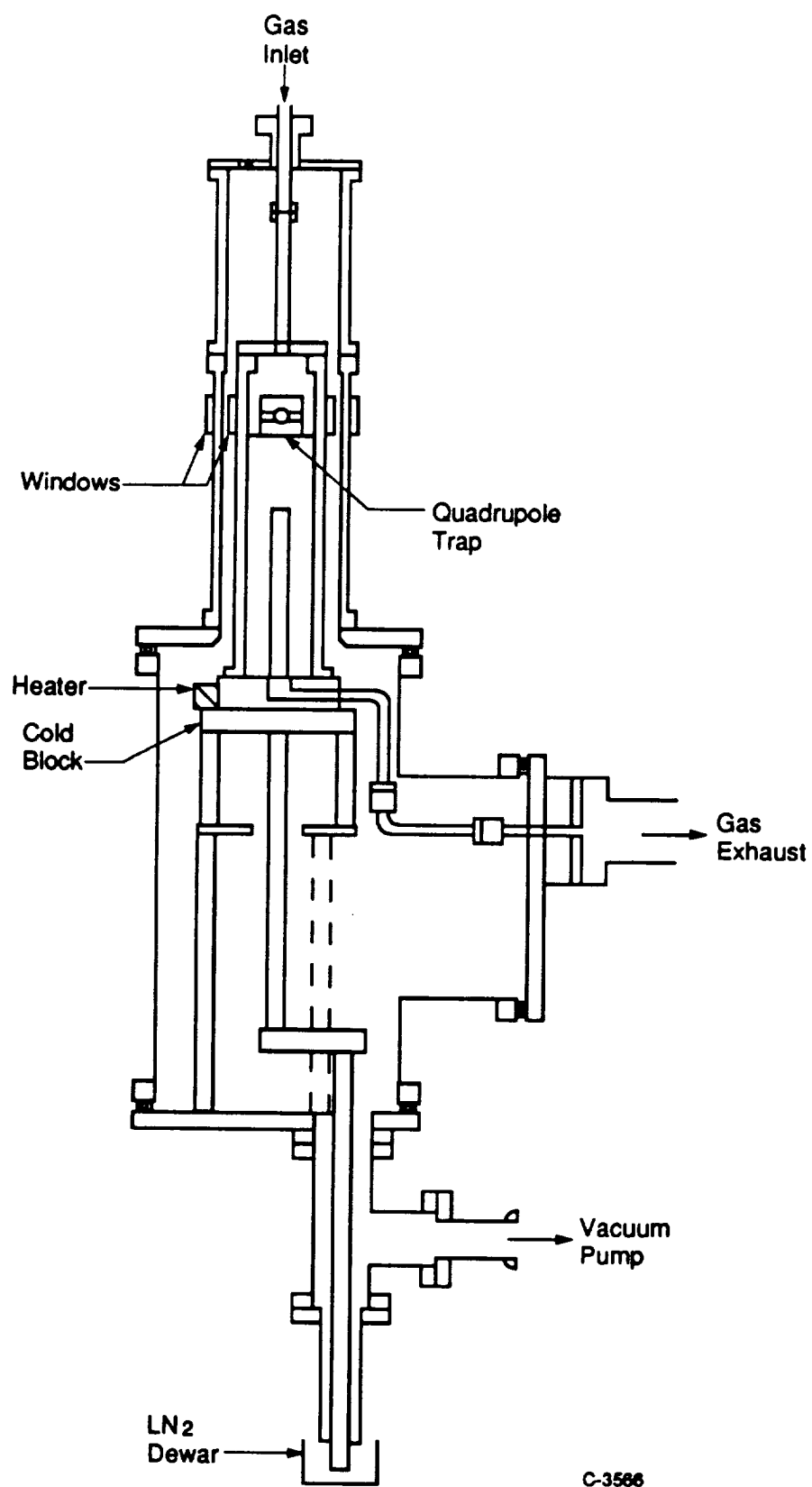
In the first year of this program, built a quadrupole trap apparatus for studying single atmospheric aerosols. This apparatus is used to study aqueous particles including sulfuric acid, ammonium and sodium sulfate, and potassium nitrate as well as solid particles such as carbon and polystyrene latex spheres. Particle sizing is achieved by several techniques including the spring point balance method and angularly resolved Mie scattering. Optical diagnostics including Mie scattering and Raman spectroscopy have been demonstrated on sulfate and nitrate salt particles to supplement the time-dependent mass measurements.

We recently completed construction of a low temperature trap apparatus (Figure 1) which provides a controlled temperature (190 to 300 K) and pressure (10 to 760 Torr) environment to simulate a variety of conditions including those characteristic of the stratosphere. Individual particles can be exposed to variable gas compositions (H_2O , NO_y) for particle growth studies. This trap is automated in that the particle balancing is feedback controlled, enabling us to monitor the balance voltage, and therefore particle mass, as the gas composition and temperature are varied. The trap is designed to optimize optical access.

We have also developed computational capabilities for relating the gas phase and particle compositions. Aqueous particles in the trap quickly equilibrate with the gas phase through exchange of volatile species such as water. This exchange occurs until the species' activities in the particle and in the gas phase are equal. We have implemented a thermodynamic program to calculate particle gas phase equilibria for aqueous sulfuric acid, aqueous nitric acid, and the ternary $\text{H}_2\text{SO}_4/\text{HNO}_3/\text{H}_2\text{O}$ system as a function of gas phase composition and temperature. These data will be useful for interpretation of the particle mass uptake measurements.

Journal Publications

None



C-3566

Figure 1. Cryogenic quadrupole trap apparatus.

Meteorological Measurement System (MMS)

Investigator

K. Roland Chan
Ames Research Center
National Aeronautics and Space Administration
Moffett Field, CA 94035

Summary of Progress and Results

The Meteorological Measurement System (MMS) provides pressure (p), temperature (T), and 3-D wind (u, v, w) measurements at 5 times per second. The MMS participated in the 1987 Stratosphere-Troposphere Exchange Project (STEP), the 1987 Airborne Antarctic Ozone Experiment (AAOE), the 1989 Airborne Arctic Stratospheric Expedition (AASE), and the 1991-92 AASE II.

For the High-Speed Research Program (HSRP), the MMS has to be modified because the position of a new Harvard instrument in the aircraft nose prevents the MMS radome system from measuring airflow angles, and because of the necessity to reduce the total science payload weight.

A new differential pressure (ΔP) system was successfully designed and flight tested. Using an incompressible, inviscid panel code, a new shape for the Harvard instrument inlet was designed to avoid possible boundary layer flow separations and high sonic flow regions. The new ΔP system has two possible configurations: a set of flush-mounted taps or two flow-angle probes (Rosemount 858Y) mounted on the nose behind the radome. Both configurations were tested in the fall of 1992. Test flight results indicate that measurements from flush-mounted taps and flow-angle probes were linear over the whole range, and there was no coupling between the ΔP measurements and flow modulations of the primary duct of the Harvard instrument. Since the flush-mounted taps can be calibrated, the Rosemount flow-angle probes were removed.

The Litton LTN-92 inertial navigation system (INS) with the capability to be updated by Global Positioning System (GPS) satellites was adopted as the primary navigation system for all ER-2 aircraft. By successfully incorporating the LTN-92 INS into the MMS in 1992, we were able to eliminate the Litton LTN-72RH INS (dedicated to the MMS in past missions) and reduce the payload weight by over 100 pounds.

Journal Publications

None

Energy Transfer Effects in Laser Detection of Stratospheric Hydroxyl Radicals

Investigator

David R. Crosley
Molecular Physics Laboratory
SRI International
333 Ravenswood Avenue
Menlo Park, CA 94025

Research Objectives

Measurement of the hydroxyl radical is essential to testing our understanding of atmospheric photochemistry. In the stratosphere, it has been determined using the method of laser-induced fluorescence, instrumentation for which is mounted on balloon platforms or the ER-2. Comparing the OH signals measured during a flight with those obtained from a ground-based calibration cell requires knowledge of the fluorescence quantum yield as a function of pressure, temperature, and composition.

A laboratory determination of the needed collisional energy transfer rate coefficients is the objective of this project. Using temporally and spectrally resolved laser-induced fluorescence measurements of OH in cooled flow cells, we will measure the temperature dependence of vibrational energy transfer in the electronically excited state and the final rotational state distribution following vibrational transfer caused by collisions with nitrogen and oxygen. These data will permit quantitative analysis of OH data over the range of conditions found in the stratosphere.

Summary of Progress and Results

During the first year, measurements have been made at room temperature. Rate coefficients for total decay from $v=1$ and vibrational transfer from $v=1 \rightarrow 0$ have been determined for N_2 and O_2 . The N_2 values agree with those determined previously, but the O_2 results are smaller than previously accepted values. High resolution spectral scans provide the final rotational distribution in $v=0$ following the vibrational transfer event. The distributions are nonthermal and have considerable population in high rotational levels. This means the OH will quench more slowly than previously assumed and explains why the previous value of the O_2 rate coefficient is too large. Distributions for other colliders were also made to understand the vibrational transfer process. CF_4 , N_2O , and CO_2 behave similarly to N_2 ; H_2 , D_2 , and CH_4 produce distributions with less rotation; and argon, surprisingly, is like O_2 .

During the past quarter, through support from a different project (NASA Global Tropospheric Program) studying the temperature dependence of quenching on NO laser-induced fluorescence diagnostics, we have constructed a cooled cell capable of attaining temperatures as low as 203 K. We have just begun to use this cell to investigate the effects of reduced temperature on the OH vibrational transfer. The OH will be produced through laser photolysis of HNO_3 in the cold flow, and a second laser will be used for excitation to $v=1$ of the emitting electronic state.

Journal Publications

Williams, L. R., and D. R. Crosley, Collisional vibration energy transfer of OH ($A^2\Sigma^+$, $v=1$), to be submitted to the *Journal of Chemical Physics*.

Crosley, D. R., Laser detection of atmospheric hydroxyl radicals, to appear in the volume *Current Problems and Progress in Atmospheric Chemistry*, J. R. Barker, Ed.

Two-Dimensional and Three-Dimensional Model Studies of Stratospheric Aircraft Emissions

Investigators

*Anne R. Douglass
Charles H. Jackman
Code 916 Atmospheric Chemistry and Dynamics Branch

Richard B. Rood
Code 910.3 Data Assimilation Office
Goddard Space Flight Center
National Aeronautics and Space Administration
Greenbelt, MD 20771

Research Objectives

This research involves the coordinated use of the NASA/GSFC 2-D model and the 3-D chemistry and transport model (3DCTM). Chemical assessments of the impact of aircraft exhaust on stratospheric ozone employ the 2-D model. In addition to examining required scenarios, the 2-D model is being used for photochemical and transport sensitivity studies. Chemical issues under consideration include the impact of heterogeneous processes, the comparison of calculated values with measurements, and the possibility that increased odd nitrogen and water vapor in flight corridors may lead to an increased probability of nitric acid trihydrate clouds outside the polar vortex. When heterogeneous reactions are included in the model, the response to a perturbation in nitrogen species is complicated by adjustment in the hydrogen and chlorine loss mechanisms of ozone.

Because the size of the perturbation for any exhaust product depends upon its residence time in the lower stratosphere, the model sensitivity to lower stratospheric transport is of particular importance. The 3-D dispersion of tracers is being examined using the 3DCTM. This model uses winds from a data assimilation procedure and provides a realistic simulation of tracer dispersion. The modeled behavior of tracers and species such as ozone is being compared with satellite fields as a means of model validation. Long calculations (greater than 1 year) for inert tracers allow us to determine the altitude, latitude, and seasonal dependence of horizontal and vertical tracer transport, and to provide estimates of the potential build up of pollutants in oceanic flight corridors. Such calculations also allow a direct comparison of 2-D and seasonally averaged 3-D transports. These calculations should serve to reduce the uncertainty in assessments associated with 2-D model transport.

Summary of Progress and Results

All scenarios requested by the program have been completed using the 2-D model. As a result of our participation in the Models and Measurements Comparisons at Satellite Beach, Florida, in February 1992, we have made improvements to the 2-D model transport and photolysis calculations. We have developed a fully diurnal version of the model to enable comparison with measurements of diurnally varying species. Initial studies with a parameterization for Nitric Acid Trihydrate cloud formation as a result of the increased values of HNO_3 and H_2O indicate that the effect on the photochemical assessment is small. There are still questions concerning the 2-D model transport. For example, in 2-D tracer calculations the strat/trop exchange takes place primarily at high latitudes and through horizontal exchange across model tropopause gaps. In the 3-D model, the strat/trop exchange takes place at middle latitudes in association with synoptic scale events. This difference could be significant to assessment calculations, as the HSCT aircraft fly primarily at middle latitudes.

The 3-D model, which uses winds from a stratospheric data assimilation system for transport, has been used for simulations of the transport and dispersion of aircraft exhaust (tracer) and for simulations of ozone. Comparisons with ozone measurements show that although the 3-D simulations capture variations in total ozone caused by synoptic events in the upper troposphere/lower stratosphere, the calculated ozone diverges from measurements as the integration proceeds. The differences, too low ozone in the tropics and excess ozone at middle and high latitudes, result from an excessively strong

residual circulation. The strong residual circulation is produced by the assimilation process, in which data are continually inserted into a general circulation model. The shock of data insertion impacts the thermodynamic balance and results in excessive vertical transport. In addition to diagnosing this problem, a method has been developed to postprocess the assimilation wind fields and provide a set of winds that have a physically realistic thermodynamic balance. The comparison of ozone simulations using these adjusted winds with TOMS and SBUV ozone observations is markedly improved.

Time series of model ozone, tracer, and 500 hPa heights have shown high anticorrelations between tracer and geopotential height. A similar out-of-phase relationship is seen in the model ozone and is suggested by TOMS data. Attention has been placed on mass transfer from the stratosphere into the troposphere associated with cutoff low (COL) and trough/ridge systems. The mechanism for this exchange process is large-scale eddy transport near the polar jet stream region in areas of upper tropospheric cyclonic activity. In the 3-D model, transport of stratospheric ozone into the troposphere is evident within the cutoff low events. Maxima in TOMS data are also observed to occur in conjunction with these systems. Experiments using postprocessed winds provide an improved representation of the influence of synoptic events on the calculated ozone and on the tracer distribution. These studies of strat/trop exchange should lead to an improved representation in the 2-D model.

Journal Publications

- Jackman, C. H., A. R. Douglass, K. F. Brueske, S. A. Klein, The influence of dynamics on two-dimensional model results: simulations of ^{14}C and stratospheric aircraft NO_x injections, *J. Geophys. Res.*, 96, 22,559-22,572, 1991.
- Douglass, A. R. and R. B. Rood, The dynamics of the HSCT Environment, Proceedings of AIAA Aircraft and Design Systems Meeting, Baltimore, MD, 1991.
- Rood, R. B., A. R. Douglass and C. J. Weaver, Tracer exchange between tropics and middle latitudes, *Geophys. Res. Lett.*, 19, 805-808, 1992.
- Weaver, C. J., A. R. Douglass, and R. B. Rood, Thermodynamic balance of three-dimensional stratospheric winds derived from a data assimilation procedure, to appear in *J. Atmos. Sci.*, 1993.
- Douglass, A. R., R. B. Rood, C. J. Weaver, M. C. Cerniglia, and K. F. Brueske, Implications of 3-D tracer studies for 2-D assessments of the impact of supersonic aircraft on stratospheric ozone, to appear in *J. Geophys. Res.*, 1993.
- Considine, D. B., A. R. Douglass, and C. H. Jackman, The effects of a parameterization of Nitric Acid Trihydrate cloud formation on 2D model predictions of stratospheric ozone depletion due to stratospheric aircraft, manuscript in preparation for submission to *J. Geophys. Res.*, 1993.

Inertia-Gravity Waves in the Stratosphere: Excitation, Propagation, and Constituent Transport

Investigators

*Timothy J. Dunkerton
Donal O'Sullivan
Northwest Research Associates
P.O. Box 3027
Bellevue, WA 98009

Research Objectives

This study seeks to understand better the excitation of internal inertia-gravity waves (IGW) in the troposphere, their subsequent propagation and breakdown in the lower stratosphere, generation of secondary instabilities, and resulting vertical transport of trace constituents. Such transport is essential for the removal of exhaust pollutants produced by future high-speed aircraft in order to lessen the severity of ozone depletion. We focus specifically on the role of midlatitude synoptic-scale weather systems (baroclinic instability and frontogenesis) in excitation of IGW, refraction into regions of preferred wavebreaking, and the efficiency of in situ mixing by convective and dynamical instabilities in breaking IGW.

Summary of Progress and Results

High resolution numerical simulations of baroclinic lifecycles have been performed using a 3-D primitive equation, 60 degree sector model, which extends vertically from the ground to 35 km. These simulations reveal episodes of IGWs radiating upwards into the lower stratosphere. The source of these IGWs is related to a tropopause folding event which develops in the model during the baroclinic lifecycle. The IGWs are absorbed in the lower stratosphere, 15-25 km altitude range, apparently by critical level absorption. It appears that model IGWs are efficiently excited in regions of strong parcel accelerations due to the curvature of the jet stream distorted by cyclogenesis. There are several such regions, the most important of which is near the location of vortex "filamentation" where a small amount of potential vorticity is extruded by the breaking synoptic-scale wave in the upper troposphere. (This process is quite similar to its counterpart in stratospheric planetary waves.) Subsequent propagation of IGWs is sensitive to the local wind and the distribution of potential vorticity. Waves radiate into the jet stream but also penetrate the region of anticyclonic potential vorticity to the west.

Journal Publications

"Generation of Inertia-Gravity Waves by Mid-latitude Baroclinic Lifecycles," manuscript in preparation.

Measurement of CFC-11 and CFC-113 During the Stratospheric Photochemistry Aerosols and Dynamics Expedition by the Airborne Chromatograph for Atmospheric Trace Species (ACATS)

Investigators

*James W. Elkins
Climate Monitoring and Diagnostics Laboratory

David W. Fahey
Aeronomy Laboratory
National Oceanic and Atmospheric Administration
325 Broadway
Boulder, CO 80303

Research Objectives

The main research objectives of this work are to measure the mixing ratios of two tracers, chlorofluorocarbon (CFC) -11 and CFC-113 using gas chromatography, on the Stratospheric Photochemistry Aerosols and Dynamics Expedition (SPADE) aboard the NASA ER-2 aircraft. These tracers are extremely useful because of the large dynamic range for mixing ratios in the stratosphere at altitudes covered by the ER-2 aircraft. The goal is to use these tracers as a yard stick to quantify the photochemical loss and production of the reactive species, HO₂, OH, NO, NO_y, NO₂, and O₃ in the lower stratosphere and upper troposphere during the SPADE mission of the HSRP Program.

Summary of Progress and Results

Most of the effort over the past year has been spent on analyzing data from the Airborne Arctic Stratospheric Expedition II during August 1991 through March 1992. This analysis will be important to the SPADE mission because we will establish a climatology for each of these tracer gases against other species. We participated on the first series of test flights for the SPADE mission during November and collected data from three flights. In the laboratory, we have demonstrated that we can measure CFC-12 and nitrous oxide (N₂O) or carbon monoxide (CO) and methane (CH₄) on an additional channel with only minor modifications to the ACATS instrument. Based on highest scientific payoff, we decided to add another channel to our flight instrument to measure CO every two minutes for the upcoming SPADE mission in April and May 1993. The photochemical steady state ratio of HO₂/OH is controlled in the lower stratosphere by reactions involving CO, NO, and O₃. Measurements of CO with the ER-2 gas chromatograph will be combined with simultaneous measurements of OH, HO₂, NO, and O₃ for the first time in the NASA SPADE field program. These measurements will allow for a critical test of our understanding of the processes that control OH.

Journal Publications

Proffitt, M., K. Aikin, J. Margitan, M. Loewenstein, J. Podolske, S. Strahan, A. Weaver, R. Chan, D. Toohey, L. Avallone, J. Elkins, D. Fahey, J. Fast, L. Lait, P. Newman, M. Schoeberl, J. Anderson, Ozone loss inside the northern polar vortex during the 1991-92 winter, submitted to *Science*, 1993.

Salawitch, R. J., S. C. Wofsy, E. W. Gottlieb, D. W. Toohey, L. M. Avallone, L. R. Lait, P. A. Newman, M. R. Schoeberl, M. Loewenstein, J. R. Podolske, S. E. Strahan, M. H. Proffitt, C. R. Webster, R. D. May, D. W. Fahey, D. Baumgardner, J. E. Dye, J. C. Wilson, K. K. Kelly, J. W. Elkins, K. R. Chan, and J. G. Anderson, Chemical loss of ozone in the Arctic polar vortex in the winter of 1991-92, submitted to *Science*, 1993.

Webster, C. R., R. D. May, D. Toohey, L. Avallone, J. G. Anderson, P. Newman, L. Lait, M. Schoeberl, K. R. Chan, J. Elkins, and D. Fahey, Hydrochloric acid loss and chlorine chemistry on polar stratospheric clouds in the arctic winter, submitted to *Science*, 1993.

A Dual Channel Chemiluminescence Detector for Measurements of NO and NO_y Onboard the NASA ER-2 Aircraft

Investigators

*David W. Fahey
S. J. Ciciora
R. S. Gao
S. R. Kawa
E. R. Keim
P. Tin
E. L. Woodbridge

Aeronomy Laboratory
National Oceanic and Atmospheric Administration
325 Broadway
Boulder, CO 80303

Cooperative Institute for Research
in Environmental Sciences
University of Colorado
Boulder, CO 80309

Research Objectives

The research objectives are to design and construct instrumentation for the NASA ER-2 high-altitude aircraft to measure reactive nitrogen species, to participate in field programs that seek measurements of a wide variety of trace species in the lower stratosphere, and to interpret the resulting data in a manner that advances our understanding of the photochemistry and dynamics of the lower stratosphere.

Summary of Progress and Results

The NASA Airborne Arctic Stratospheric Expedition - II (AASE-II) ended in March 1992 with data for NO and NO_y obtained in more than 20 flights in the lower stratosphere. Submission of final data was completed in summer 1993.

Of interest in the interpretation of these data is the role of the heterogeneous reaction $\text{N}_2\text{O}_5 + \text{H}_2\text{O}$ occurring on the surface of sulfate aerosols. The reaction serves to reduce the NO_x/NO_y ratio within an air parcel by producing HNO₃. When the observations of NO and NO_y are used to estimate the ratio and compare it to gas-phase photochemical models, the values observed at midlatitudes are significantly lower than predicted. The inclusion in the model of the N₂O₅ reaction on background aerosol improves the comparison with the observations. As a consequence, the expected importance of nitrogen oxides in ozone destruction at midlatitudes is reduced, while the importance of chlorine and hydrogen chemistry is increased. These results increase model sensitivity of ozone to growth in chlorine abundances in the atmosphere and lessen the predicted impact of NO_x from aircraft exhaust in these models. Observations at elevated aerosol values caused by the eruption of Mt. Pinatubo show further reductions in NO_x/NO_y. The data show a nonlinear response with increasing aerosol surface area, suggesting saturation. The saturation effect agrees well with photochemical models which show that the formation rate of N₂O₅ limits the reduction of NO_x/NO_y at high aerosol values. These results demonstrate that chemical changes resulting from observed increases in sulfate aerosol above background values are limited at midlatitudes, consequently limiting expected changes in ozone loss rates.

Journal Publications

Fahey, D. W., et al., In situ measurements constraining the role of reactive nitrogen and sulfate aerosols in mid-latitude ozone depletion, *Nature*, 363, 509-514, 1993.

Chemical Kinetics Studies of Hydrocarbons From Stratospheric Aircraft

Investigators

*Randall R. Friedl
Stanley P. Sander
Jet Propulsion Laboratory
California Institute of Technology
Pasadena, CA 91109

Research Objectives

We are collecting experimental data on the rates and mechanisms of key elementary gas-phase and gas-surface reactions that relate to the processing of nonmethane hydrocarbon aircraft exhaust in the lower stratosphere. Our focus is on processes that may impact the partitioning of nitrogen oxides. Consequently, we have been investigating chemical production and loss mechanisms of peroxyacetyl nitrate (PAN), an important reservoir of odd nitrogen in the atmosphere and a common intermediate in the atmospheric oxidation of small nonmethane hydrocarbons.

Summary of Progress and Results

We have examined the NO_2 product yield from the photolysis of PAN at 248 nm. NO_2 was detected by laser induced fluorescence (LIF). The probe laser was a pulsed copper vapor laser operating at 511 nm and 20 KHz. NO_2 fluorescence was collected between approximately 550 nm and 900 nm with a combination of high pass optical filters and a red-sensitive photomultiplier. The sensitivity of the technique to NO_2 was quantified by photolyzing HNO_3 .

A complex temporal behavior of the laser induced fluorescence signal following PAN or HNO_3 photolysis was observed. The data indicate that the photolysis of these species produces NO_2 in an electronically or vibrationally excited state. A simple kinetics mechanism consisting of five to seven equally spaced energy levels was found to adequately describe the observed relaxation of the excited species. The collisional quenching rates between excited levels were assumed to be equal.

The derived rate constants for various quenching gases in our experiments were found to be similar to ones measured previously for quenching of excited vibrational states of the NO_2 ground electronic (2A_1) state. We concluded from our analysis that the majority of excess energy following 248 nm photolysis of HNO_3 appears as vibrational excitation of 2A_1 state NO_2 . The photolysis mechanism presumably involves initial excitation of the nascent NO_2 to the 2B_2 state followed by rapid collisional quenching or curve crossing to upper vibrational levels of the 2A_1 state. In support of this conclusion we have observed small amounts of direct fluorescence from the 2B_2 state.

Energy disposal, in the NO_2 photo fragments from HNO_3 and PAN photolysis appears to be similar. This finding suggests that mixing between the 2A_1 and 2B_2 states of NO_2 is relatively constant over a large range of initial energies since the amount of excess energy following 248 nm photolysis is quite different in the HNO_2 (23100 cm^{-1}) and PAN (31400 cm^{-1}) cases. In addition, the findings indicate that collisional quenching of vibrational levels above the 2B_2 state energy threshold must be substantially faster than quenching of levels with pure 2A_1 character.

The determination of the NO_2 quantum yield from PAN photolysis is significantly hindered by the complex internal energy relaxation process. We have been able to derive an accurate quantum yield by employing buffer gases such as O_2 and CO_2 , which are efficient vibrational quenchers, or by comparison of PAN and HNO_3 photolysis data at specific delay times following the photolysis pulse. A NO_2 quantum yield of 0.8 ± 0.2 from PAN photolysis at 248 is obtained from the data.

Journal Publications

None

Modeling of Heterogeneous Processes

Investigator

Patrick Hamill
Physics Department
San Jose State University
San Jose, CA 95192-0106

Research Objectives

The purposes of this study are to assist in modeling efforts for SPADE and to develop a sulfate aerosol model for studying heterogeneous chemical processes in the stratosphere.

Summary of Progress and Results

The project involves formulating an aerosol module to be incorporated into the GUMBO model which is being developed as part of the SPADE program.

At selected points along the ER-2 flight track, parcel trajectory analyses are carried out to predict the time history of the air parcel being monitored. The trajectory analysis predicts the temperature and pressure of the air parcel as a function of time for 9 days prior to its encounter with the ER-2.

The aerosol model predicts the size and composition (weight percentage sulfuric acid) of the aerosol during the 9 days prior to encounter. The calculations are based on the fact that at a given temperature and water vapor content, the composition of a sulfuric acid/water aerosol particle is uniquely determined. The particles adjust to the compositional change by either absorbing or evaporating water. This changes the size of the particles and hence their surface area. The surface area of the aerosols is the primary quantity of interest in studying heterogeneous processes.

The aerosol module has been completed and successfully incorporated into the GUMBO model. The results are realistic, except for the size distribution. For simplicity we assumed a distribution having a single mode, but measurements during SPADE indicate a bi-modal distribution. However, this does not have a detectable effect on the aerosol surface area because the area is dominated by the larger mode.

Journal Publications

None

Project and Data Management Support for HSRP Field Missions

Investigators

*R. Stephen Hipskind
Patricia Hathaway
Steven E. Gaines
Ames Research Center
National Aeronautics and Space Administration
Moffett Field, CA 94035-1000

Research Objectives

The objective of this study is to provide Project Management for HSRP aircraft field campaigns, including data management and computer networking support. Project Management covers a range of activities, including assistance in experiment definition, scheduling, field facility preparation, dissemination of project information, overseeing aircraft payload integration, and projecting and tracking deployment budgets. Data management entails the definition of data exchange standards and implementation of the exchange process in the field. It also includes the dissemination of the field experiment data sets after the mission. Networking support provides the basis for the data exchange in the field; it also provides the communication link for acquiring critical data sets required during the field missions and for communication to home labs.

Summary of Progress and Results

The data from the second Airborne Arctic Stratospheric Expedition (AASE II) were published on CDROM and distributed to the mission participants. This data set includes the measurements taken aboard both the ER-2 and DC-8 aircraft during the AASE II mission and is available by contacting Steve Hipskind at NASA Ames Research Center.

The primary focus of this past year has been on the Stratospheric Photochemical, Aerosols and Dynamics Expedition (SPADE). SPADE is the first field mission devoted to making atmospheric measurements for the HSRP. The mission, originally scheduled to be completed in the fall of 1992, was split into two phases, the first in November of 1992 and the second, in April and May of 1993. The split was necessitated by the time line of the new instruments being developed for SPADE, which could not be ready for a fall mission.

The goal of the November series was redirected to getting all of the instruments integrated onto the ER-2 aircraft, test flown, and flight certified. This goal was successfully met with two 2-hour test flights and two 6-hour flights. The last flight accomplished a terminator crossing, which was crucial for testing the performance of the new instruments. The full payload exceeded the total fuselage weight capacity and center of gravity constraints of the aircraft, so that, except for the first 2-hour flight, partial payloads had to be flown. Weight losses in several instruments were identified and the instrument PIs made commitments to lose instrument weight before the spring 1993 science flight series. At this time it appears that the weight losses were accomplished and it should be possible to fly the full payload during the spring science flights.

Though the SPADE mission is being conducted from NASA Ames, it is the first time that we have conducted a mission of this magnitude from Ames with the full complement of external investigators (70-80 external investigators and support personnel with an equivalent number of Ames personnel). The facility preparation was not unlike a remote field deployment, with much effort spent on negotiating for space and preparing the space for use as lab space by the participating investigators.

The networking and data exchange for the SPADE mission was set up and run essentially the same as was done for the AASE II (which was also partially funded by the HSRP). Because many of the

investigators at Ames were housed in a building with no existing network connections, we utilized a wireless network link to bring the building into the Ames campus network. The networking and data exchange worked smoothly during the November flight series.

We are also preparing for the 1994 combined UARP/HSRP field campaign. This mission is known collectively as the Airborne Southern Hemisphere Ozone Experiment (ASHOE) and Measurements for the Assessing the Effects of Stratospheric Aircraft (MAESA). The mission will be based in Christchurch, New Zealand, with over four deployment periods from March 1994 through October 1994, with MAESA concentrating primarily on the transit flights from Ames to Christchurch. There will also be MAESA flights made locally out of Hawaii on the transit phase. We made a site survey trip to Christchurch in January and are working with both the NSF and the U.S. Navy to construct the required lab space and put in the necessary infrastructure for power and communications.

Journal Publications

AASE II Mission Dataset CDROM, July 1992, S. Gaines, P. Hathaway, S. Hipskind, Eds., UARP-004.

Dynamical and Chemical Studies of Aircraft Emissions Using Satellite Data and a 2-D Model

Investigator

Matthew H. Hitchman
Department of Meteorology
University of Wisconsin Madison
Madison, WI 53706

Research Objectives

The objective is to assess the effects of aircraft emissions on the ozone layer with a fully interactive 2-D model. Specifically, a new stratospheric aerosol climatology is employed, which we created from SAGE and SAM II data, to assess the effects of heterogeneous processes. A second objective is to improve parameterized vertical mixing through the use of aircraft mission data on gravity waves.

Summary of Progress and Results

We have completed our aerosol climatology which exhibits significant seasonal and quasi-biennial variations. We have carried out a variety of scenarios to explore the sensitivity to surface anthropogenic trace gas emissions, conventional aircraft, HSCTs, model mixing coefficients, seasonal aerosol cycle, QBO aerosol variability, and a range of aerosol loadings. These results will be reported at the annual meeting in Virginia Beach.

Journal Publications

McKay, M. A., "A Climatology of Stratospheric Aerosols and Their Impact on Ozone in a 2-D Model," M. S. thesis, University of Wisconsin - Madison.

Hitchman, M. H., M. A. McKay, and C. R. Trepte, Circulation deduced from aerosol data averaged by season and phase of the quasibiennial oscillation, in *Coupling Processes in the Lower and Middle Atmosphere*, Kluwer Academic Publishers, pp. 25-33, 1993.

McKay, M. A., M. H. Hitchman, and C. R. Trepte, A climatology of stratospheric aerosols, manuscript in preparation, to be submitted to *J. Geophys. Res.*

NO/NO_y, O₃, and H₂O Instruments, and Meteorological Analysis

Investigator

Kenneth K. Kelly
Aeronomy Laboratory
National Oceanic and Atmospheric Administration
325 Broadway
Boulder, CO 80303

Research Objectives

The objective is to support of the HSRP-SPADE campaigns.

Summary of Progress and Results

The water instrument did not fly on all flights of the November SPADE I mission because of aircraft weight and balance considerations. Andy Dessler compared the two water instruments for joint flights. The two instruments were within experimental error with the possible exception of ascent and descents. Mike Proffit offered to share a computer to help the weight problem. I have modified my experiment with a weight savings of almost 60 pounds. I am currently trying to hire someone to help with the data analysis. The emphasis will be on relating the aircraft data to satellite data sets and GCMs.

Journal Publications

None

Impact of Engine Emissions of a Proposed High-Speed Stratospheric Aircraft Fleet on the State of the Atmosphere

Investigators

*Malcolm K. W. Ko
Debra K. Weisenstein
Nien-Dak Sze
Jose M. Rodriguez
Atmospheric and Environmental Research, Inc.
840 Memorial Drive
Cambridge, MA 02139

Research Objectives

The AER 2-D chemistry-transport model will be used to investigate the sensitivity of ozone to emissions from HSCT aircraft, including nitrogen oxides, water vapor, carbon monoxide, hydrocarbons, and sulfur dioxide. Because heterogeneous chemistry was found to have a large impact on the predicted change in ozone due to HSCT emissions, a new emphasis is to develop a sulfate model in collaboration with Dr. Glenn Yue of NASA/Langley. AER will develop the gas-phase portion of the model which will be combined with the aerosol microphysics model at Langley. This model will allow us to predict changes in aerosol loading due to aircraft emissions and volcanic eruptions. The impact of changes in aerosol loading on ozone will be explored by varying the rate of the heterogeneous reactions over the expected range of the aerosol surface area.

Summary of Progress and Results

Model improvements in the past year have included updating the chemical rates to the JPL-92 recommendations, implementing a parameterized treatment of the Schumann-Runge bands, and adoption of the NMC 8-year average temperatures. We are now calculating tropopause height based on model temperatures and are also calculating water vapor concentration in the stratosphere. We have created a high-resolution version of our 2-D model with the vertical resolution increased by a factor of three to approximately 1.2 km. This high-resolution model has been used to evaluate the ozone response to HSCT emissions.

Model calculations performed during the past year include the 12 experiments designated for intercomparison at the June 1993 HSRP meeting. These scenarios represent refinements of the basic scenarios used in previous years. Subsonic air traffic is assumed to decrease with the introduction of an HSCT fleet. Mach numbers of 1.6 and 2.4 are assumed for the HSCT cruise speed with NO_x emission indices of 5, 15, 45, and fuel use during ascent and descent are now included. We find results for these scenarios to be quite similar to the less-detailed calculations performed previously. In addition, four scenarios have been evaluated with background Cl_y concentrations at 2.0 ppbv instead of 3.5 ppbv. We find that the lower background chlorine increases the calculated ozone depletion by about 60% at northern midlatitudes with NO_x EI=15, and by 25% at northern midlatitudes with NO_x EI=5 for the Mach 2.4 cases. Also, as a sensitivity test, we have repeated the calculation for the Mach 2.4, NO_x EI=15 case with NO_x emissions only and with NO_x and H_2O emissions only. With only NO_x emissions, the calculated ozone depletion is 25% less than with NO_x , H_2O , CH_4 , and CO emissions. With both NO_x and H_2O emissions included, results are almost identical to when all emissions are included, implying the CH_4 and CO emissions play a very minor role in the impact of HSCT emissions on ozone.

We have continued our gas-phase sulfur model development by including more realistic boundary conditions on SO_2 and CS_2 and have increased the vertical resolution to 1.2 km. The model includes the species CS_2 , DMS , H_2S , MSA , OCS , SO_2 , and SO_4 . Gravitational sedimentation velocities are used for SO_4 below 25 km, based on the size distribution of aerosols measured by SAGE II for January-February 1989. The model calculates a stratospheric sulfate burden of 11.6×10^7 kg of sulfur without aircraft and 11.8×10^7 kg of sulfur with subsonic aircraft. Assuming an EI of 1 for SO_2 , the model predicts maximum local changes in sulfate due to HSCT emissions of 40%, 90%, and 100% for Mach 1.6, 2.4,

and 3.2, respectively. Thus we expect changes of a factor of two or less in the aerosol surface area due to HSCT aircraft emissions with SO_2 EI=1.

Work is under way to include aerosol microphysics in our sulfur model. The aerosol code has been supplied to us by Dr. Glenn Yue of NASA/Langley. There are 25 aerosol size bins in the models, with radii ranging from 0.01 microns to 2.65 microns, each bin containing twice the particle volume of the preceding bin. Aerosol processes included are coagulation, sedimentation, H_2SO_4 condensation, heterogeneous growth, nucleation, advection, and diffusion. When the microphysical model is operational, we plan to (1) perform the Ruiz aerosol experiment from the Models and Measurements Workshop for comparison of the resulting aerosol size distribution with measurements, (2) repeat the HSCT aircraft scenarios, and then use the calculated aerosol surface area to predict ozone changes, and (3) simulate volcanic eruptions by input of SO_2 .

Journal Publications

Weissenstein, D. K., M. K. W. Ko, J. M. Rodriguez, and N. D. Sze, High-speed civil transport and sensitivity to stratospheric aerosol loading, submitted to *Journal of Geophysical Research*, 1993.

Stratospheric Sulfur Oxidation Kinetics

Investigators

*Charles E. Kolb
Douglas R. Worsnop
Mark S. Zahniser
P. Davidovits
Center for Chemical and Environmental Physics
Aerodyne Research, Inc.
45 Manning Road
Billerica, MA 01821-3976

*Mario J. Molina
J. T. Jayne
Department of Earth, Atmospheric and Planetary Sciences
and Department of Chemistry
Massachusetts Institute of Technology
Cambridge, MA 02139

Research Objectives

The purpose of this study is to determine the mechanisms and chemical kinetics rate parameters controlling the homogeneous and heterogeneous oxidation of SO_2 to H_2SO_4 in high-altitude aircraft plume/wakes and in the ambient stratosphere.

Summary of Progress and Results

Since the start of the project in February 1993 we have designed a series of fast-flow tube experiments to measure the temperature dependent rate of the homogeneous reaction of the SO_3 molecule with monomeric and dimeric water vapor to form $\text{H}_2\text{SO}_4(\text{v})$. These reactions will be studied in a novel, high-pressure turbulent fast-flow reactor, previously designed and fabricated at MIT, to minimize the effects of the fast heterogeneous reaction between SO_3 and H_2O on the reactor's wall. This should allow a more definitive rate constant to be determined than the currently evaluated upper limit of $<5.7 \times 10^{-15} \text{ cm}^3/\text{s}$. The reaction with water vapor dimer $(\text{H}_2\text{O})_2$ or bimer e.g. $(\text{H}_2\text{O} \cdot \text{N}_2)$ may proceed much more rapidly than the reaction with the H_2O monomer. The rates of these reactions will be studied by varying the concentrations of H_2O vapor in the flow.

Journal Publications

None

Plume Chemistry and Dispersion Modeling to Evaluate the Atmospheric Effects of Stratospheric Aircraft

Investigators

*Charles E. Kolb
Robert C. Brown
Richard C. Miake-Lye
Manuel Martinez-Sanchez
Aerodyne Research, Inc.
45 Manning Road
Billerica, MA 01821-3976

Jose M. Rodriguez
Malcom K. W. Ko
Run-Lie. Shia
Nien-Dak. Sze
Atmospheric and Environmental Research, Inc.
840 Memorial Drive
Cambridge, MA 02139

Research Objectives

The environmental perturbations caused by the exhaust of a high-speed civil transport (HSCT) depend on the deposition altitude and the amount and composition of the emissions. The chemical evolution and the mixing and vortical motion of the exhaust need to be analyzed to track the exhaust and its speciation as the emissions are mixed to atmospheric scales. A model of the dynamical processes in the plume and wake is being developed to account for plume mixing, the roll-up of the exhaust with trailing vorticity, and the subsequent evolution and motion of the exhaust gases in the descending vortex cell. The eventual dispersion to atmospheric scales after the decay of local emission enhancements along flight corridors, where concomitant chemical and radiative effects may occur, is also being quantified.

Summary of Progress and Results

A model of plume mixing and chemistry has been optimized for HSCT exhaust plumes, and condensation kinetics have been calculated using the mixing and chemistry output of model calculations. Following the chemical kinetics of NO_x and SO_x demonstrates that oxidation to HNO_3 and SO_3 and subsequent formation of H_2SO_4 proceeds in the wake of the aircraft driven by exhaust OH and ambient O_3 . The effects of these acid gases on heterogeneous chemistry and binary homogeneous and heterogeneous condensation are being explored. Analytical modeling of the vortex wake shows that the concentrated vorticity wraps up the buoyant exhaust and suppresses its continued mixing and dilution, while subjecting it to locally perturbed temperatures and pressures. Modeling of the dispersion indicates that radiatively-driven subsidence of the exhaust emissions is likely to be less than 1 km and that conversion of NO_x to HNO_3 can be substantial if heterogeneous chemistry takes place on contrail aerosols. Further modeling of nonlinear chemical effects, particularly on polar stratospheric clouds, in aircraft flight corridors is currently under way.

Journal Publications

Miake-Lye, R. C., M. Martinez-Sanchez, R. C. Brown, and C. E. Kolb, Plume and wake dynamics, mixing, and chemistry behind an HSCT aircraft (AIAA Paper No. 91-3158, September 1991), accepted for publication in *J. Aircraft*.

Miake-Lye, R. C., R. C. Brown, M. Martinez-Sanchez, and C. E. Kolb, "High Speed Civil Transport Exhaust Mixing and Chemistry," presented at the JANNAF Exhaust Plume Technology Subcommittee Meeting, Kirkland AFB, 10 February 1993. To be published in CPIA Publication 595, Chemical Propulsion Information Agency, 1993.

Shia, R-L., J. Rodriguez, M. K. W. Ko, C. Heisey, R. C. Miake-Lye, and C. E. Kolb, "Subsidence of Aircraft Engine Exhaust in the Stratosphere and Its Implication for Ozone Depletion," submitted to *Geophys. Res. Letts.*, 1993.

Design and Development of an Unmanned Research Aircraft in Support of the Small High Altitude Science Aircraft (SHASA) Project

Investigator

John S. Langford
Aurora Flight Sciences Corporation
10601 Observation Road
Manassas, VA 22111

Research Objectives

The purpose of this project is to develop and field two Perseus A science aircraft capable of carrying a 50-kg payload to altitudes in excess of 25 km.

Summary of Progress and Results

During the last quarter the first two Perseus aircraft made the transition from individual component parts to complete airframes. Following a public rollout of December 18, 1992, the aircraft entered an extended period of integrated systems testing. Significant milestones reached during this period included:

- Validation of the closed cycle powerplant output power and fuel specifics better than required to complete the stated mission.
- Accumulation of more than 100 hours of closed cycle operation.
- The first application of power through the drivetrain and the 4.2 meter propeller.
- Demonstration of all command uplink, downlink, and engineering command functions via radio link between ground station and aircraft.
- Completion of the first payload integration and planning meeting with participating P.I.s and payload engineers.

The aircraft development is proceeding on schedule to support initial scientific flights in 1994. The initial flight test has been moved from April to July 1993 to allow the resolution of radio frequency coordination issues and sufficient time for the desert test site to dry out after a very wet winter.

Journal Publications

None

Laboratory Studies of Heterogeneous Processes Important in Stratospheric Aircraft Emissions

Investigators

*Ming-Taun Leu
Leon F. Keyser
Liang T. Chu
Jet Propulsion Laboratory
National Aeronautics and Space Administration
Pasadena, CA 91109

Research Objectives

The objective of this task is the laboratory investigation of heterogeneous processes that are potentially important in assessing the environmental impact of high-altitude aircraft emissions. The work aims to investigate the effects of water ice, nitric acid trihydrate, sulfuric acid aerosol, and soot on atmospheric species important in the ClO_x , NO_x , and HO_x cycles that include: HCl , ClO , ClONO_2 , NO , NO_2 , O_3 , N_2O_5 , HNO_3 , OH , HO_2 , H_2O_2 , and SO_2 . Flow reactor mass spectrometry and discharge flow resonance fluorescence measure sticking or reaction probabilities on these aerosols. Several analytical techniques, which include mass spectrometry, chloride ion electrode, infrared absorption, scanning electron microscopy, x-ray diffraction spectrometry, and BET surface area analysis, monitor gas-phase species and characterize the condensed phase.

Summary of Progress and Results

Heterogeneous reactions of $\text{HOCl} + \text{HCl} \rightarrow \text{Cl}_2 + \text{H}_2\text{O}$ (1) and $\text{ClONO}_2 + \text{HCl} \rightarrow \text{Cl}_2 + \text{HNO}_3$ (2) on ice surfaces at 188 K have been investigated in a flow reactor interfaced with a quadrupole mass spectrometer. Reaction probabilities for these heterogeneous reactions have been determined to be 0.15 and 0.10, respectively.

Journal Publications

- L. T. Chu, M-T. Leu, and L. F. Keyser, Uptake of HCl in water ice and nitric acid trihydrate films, submitted to *J. Phys. Chem.*, 1993.
- L. F. Keyser and M-T. Leu, Surface areas and porosities of ices used to simulate stratospheric clouds, *J. Coll. Interface Sci.*, 155, 137, 1993.
- L. F. Keyser, M-T. Leu, and S. B. Moore, Comment on porosities of ice films used to simulate stratospheric cloud surfaces, submitted to *J. Phys. Chem.*, 1993.
- L. F. Keyser and M-T. Leu, Morphology of nitric acid and water ice films, submitted to *Microscopy Res. Technique*, 1993.

Argus: N₂O and CH₄ Instrument for Perseus

Investigator

Max Loewenstein
Ames Research Center
National Aeronautics and Space Administration
Moffett Field, CA 94035-1000

Summary of Progress and Results

A prototype of one channel of the Argus instrument employing an evacuable Herriott cell has been calibrated over the pressure range 50 to 350 torr and N₂O values ranging from 0 to 320 ppb. The results show that the instrument response is linear and the measurement precision is approximately 0.6 ppb of N₂O. These measurements were made employing a complete simulation of the flight analog and digital electronics. A prototype of the flight analog board consisting of a synchronous amplifier and integrator was used in the detection chain. Instrument precision is now within about a factor of three of achieving the required 1% precision value over the operating range of Perseus.

In the current prototype, the Herriott cell employed is a design close to the flight cell design. It incorporates all the features of the flight cell, but its physical dimensions are somewhat different. 56 cell passes are employed, for a total path of about 12 meters. A pressure and flow measuring system is connected to the Herriott cell to allow monitoring of the cell flow and pressure and the introduction of calibrated N₂O gases, as well as other gases which assist in identification of the N₂O line being employed in the detection process. Candidate flight pressure transducers have been procured and calibrated and soon will be incorporated into the prototype.

Several choices of flight electronics hardware have been made. A commercial 386 processor system, as well as a candidate hard disk having a capacity of 64 megabytes, has been acquired for testing. The entire digital system has been subjected to extended low-pressure tests to determine whether there could be thermal problems associated with operating them in the Perseus experiment bay.

In the coming quarter the prototype will be upgraded to include flight-type optics throughout. Calibrations will be extended to include the entire pressure and N₂O mixing ratio envelope of Perseus operations, and fabrication of flight hardware will begin.

Journal Publications

None

Development of Trace Gas Constituent Measurement Techniques for HSCT Engines and Their Components

Investigators

*Richard C. Miake-Lye
Charles E. Kolb
Joda C. Wormhoudt
Kurt D. Annen
Aerodyne Research, Inc.
45 Manning Road
Billerica, MA 01821-3976

Research Objectives

The objective of this program is the detailed characterization of engine exhaust trace constituents, motivated by the need to quantify levels of species that are active in homogeneous and heterogeneous chemistry and condensation in the plumes and wakes of high-speed civil transport (HSCT) aircraft. Accurate inputs to both plume/wake models and global atmospheric models require complete and accurate accounts of SO_x and NO_y being injected into the atmosphere. Work is divided into three areas: 1) assessment and prioritization of the required exhaust composition measurements for both existing gas turbine engines and prototype HSCT engine components, 2) an optimal Tunable Diode Laser (TDL) absorption technique to measure high-priority species concentrations, and 3) instrument development and characterization based on this design carried out at ARI, followed by a measurement program at HSRP-selected combustor development sites. These measurements will verify the sensitivity and detectability of the trace species and will provide emission estimates of these species for use in the AESA atmospheric assessment program.

Summary of Progress and Results

In conjunction with the Emissions Scenarios Development program (Miake-Lye et al), the AESA Engine Exhaust Trace Chemistry (EETC) Committee met several times in the last year and coordinated a workshop at NASA Lewis Research Center to identify measurement techniques and species to be developed under the AESA Program. These additional species measurements are required to characterize the exhaust emissions more completely than the current suite of standard measurements allows. The criteria for recommending these additional measurements were formulated the EETC Committee by prioritizing engine exhaust gas constituents in the order of their impact on atmospheric processes. These recommendations and their technical basis are described in the referenced report.

Development of a TDL long-path adsorption spectroscopic instrument is under way. Both extractive sampling into a low pressure astigmatic multipass optical cell and line-of-sight in situ absorption measurements will be possible with the same basic optical source/detector combination. Three species, NO, NO₂, and HNO₃, have been chosen for the initial round of development and demonstration measurements. Design of the instrument is complete and fabrication has been initiated. Plans are being made for laboratory calibration measurements, which will be carried out at ARI prior to more HSCT-specific measurements in the final year of this program.

Journal Publications

Miake-Lye, R. C., W. J. Dodds, D. W. Fahey, C. E. Kolb, and S. R. Langhoff, "Engine Trace Constituent Measurements Recommended for the Assessment of the Atmospheric Effects of Stratospheric Aircraft " (Aerodyne Research, Inc., Report ARI-RR-947, August 1992), Chapter 5 of this AESA Third Program Report, 1993.

The Interaction of Engine Exhaust Plumes and Wing Wake Vortices

Investigators

*Richard C. Miake-Lye
Robert C. Brown
Manuel Martinez-Sanchez
Charles E. Kolb
Aerodyne Research, Inc.
45 Manning Road
Billerica, MA 01821-3976

Todd R. Quackenbush
Milton E. Teske
Alan J. Bilanin
Continuum Dynamics, Inc.
P. O. Box 3073
Princeton, NJ 08543

Research Objectives

The environmental perturbations caused by the exhaust of a high-speed civil transport (HSCT) depend on the deposition altitude and the amount and composition of the emissions. The chemical evolution and the mixing and vortical motion of the exhaust need to be analyzed to track the exhaust and its speciation as the emissions are mixed to atmospheric scales. A numerical model of the dynamical and chemical processes in the aircraft vortex wake is being developed based on the existing UNIWAKE wake code. The vortex wake calculation is initialized with plume mixing and chemistry, as calculated using the SPF model developed previously under AESA, and with the rolled-up wing-tip vortices from a representative HSCT configuration. The subsequent chemical evolution and motion of the exhaust gases in the descending vortex cell will be followed in this numerical model. In addition, the resulting flowfield, including both temperature and species concentrations, defines the environment in which aerosol formation and growth may proceed. The species tracked include those that could be heterogeneously reactive on the surfaces of the condensed solid water (ice) particles when condensation occurs and those capable of participating in the formation active contrail and/or cloud condensation nuclei (ccn).

Summary of Progress and Results

A modified version of UNIWAKE has been developed to compute directly the homogeneous and heterogeneous reactions occurring between the exhaust products of HSCT engines while acted upon by the aircraft's vortex wake and the atmosphere. The modified code used the mean and fluctuating flowfield predicted by UNIWAKE and is designed to compute passive convective chemistry, assuming that heat release and subsequent density changes are negligible. The flowfield history will be followed along the trajectories of a number of passive tracers to allow condensation phenomena in the flowfield to be computed in a separate calculation.

Condensation kinetics modeling has been extended beyond the homomolecular heterogeneous condensation previously modeled under AESA sponsorship. In particular, using the results of the SO₂ and NO_x oxidation chemistry, the binary nucleation of sulfuric acid/water (Zhao and Turco, 1992; Miake-Lye et al., 1993) is being modeled to calculate the formation of additional aircraft-generated aerosol, followed by water vapor condensation on the resulting sulfate nuclei. Initial calculations indicate an extremely high rate of new particle creation, much higher than would be predicted if the exhaust were simply spread over atmospheric scales.

Journal Publications

Miake-Lye, R. C., R. C. Brown, M. Martinez-Sanchez, and C. E. Kolb, "High Speed Civil Transport Exhaust Mixing and Chemistry," presented at the JANNAF Exhaust Plume Technology Subcommittee Meeting, Kirtland AFB, 10 February 1993. To be published in CPIA Publication 595, Chemical Propulsion Information Agency, 1993.

Brown, R. C., et al., manuscript(s) in preparation.

Determination of Emission Scenarios for the Program on Atmospheric Effects of Stratospheric Aircraft

Investigators

*Richard C. Miake-Lye
Charles E. Kolb
Aerodyne Research, Inc.
45 Manning Road
Billerica, MA 01821-3976

Research Objectives

Predictive modeling of the dispersal and reaction of stratospheric pollutants must be based on reliable projections of combustion emissions. An independent review and assessment of current efforts at NASA and industry combustor research centers will be directed toward supplying relevant projected emissions data to the plume modeling effort. Current progress and future trends will be assessed for the control of critical species, as required by the concurrent modeling activity. A supplementary analysis stage will facilitate the integration of the emission data into the modeling by identifying pollution chemical mechanisms to which the models may be particularly sensitive. Such integrations will tie the required emissions scenario data to the needs of the plume modeling efforts and global stratospheric models.

Summary of Progress and Results

In conjunction with the Measurement Technique Development program (Miake-Lye et al.), the AESA Engine Exhaust Trace Chemistry Committee met several times in the last year and coordinated a workshop at NASA Lewis Research Center to identify measurement techniques and species to be developed under the AESA program. These additional species measurements are required to characterize the exhaust emissions more completely than the current suite of standard measurements allows. The criteria for recommending these additional measurements were formulated by the EETC Committee by prioritizing engine exhaust gas constituents in the order of their impact on atmospheric processes. These recommendations and their technical basis are described in the referenced report.

Journal Publications

Miake-Lye, R. C., W. J. Dodds, D. W. Fahey, C. E. Kolb, and S. R. Langhoff, Engine trace constituent measurements recommended for the assessment of the atmospheric effects of stratospheric aircraft (Aerodyne Research, Inc, Report ARI-RR-947, August 1992), Chapter 5 of this AESA Third Program Report, 1993.

Laboratory Studies of Stratospheric Aerosol Chemistry

Investigators

Mario J. Molina
Department of Earth, Atmospheric and Planetary Sciences
and Department of Chemistry
Massachusetts Institute of Technology
Cambridge, MA 02139

Research Objectives

The aim of the task is to investigate the physical chemistry of the sulfuric acid-nitric acid-hydrogen chloride-water system, and to generate and characterize in the laboratory aerosol particles similar to those formed in the high-latitude stratosphere. This is being done in order to elucidate the mechanism of the formation of polar stratospheric clouds and their chemical reactivity associated with chlorine activation.

Summary of Progress and Results

Infrared spectra, melting points, and HNO_3 and H_2O vapor pressures have been measured for the $\text{H}_2\text{SO}_4/\text{HNO}_3/\text{H}_2\text{O}$ system under conditions applicable to the polar stratosphere. The results indicate that background aerosols consisting of liquid sulfuric acid solutions will absorb HNO_3 vapor under those conditions to yield solutions containing more than 10% wt HNO_3 . These solutions freeze to form nitric acid trihydrate (NAT) crystals together with H_2SO_4 hydrates, and hence function as precursors to Type I polar stratospheric clouds. Supercooling investigations show that the ternary solutions freeze at temperatures above those corresponding to the frost point in the polar stratosphere but below those corresponding to saturation with respect to NAT formation. Also, HCl vapor pressures have been measured for the liquid $\text{H}_2\text{SO}_4/\text{HNO}_3/\text{H}_2\text{O}$ system. The results indicate that the amount of HCl taken up by liquid H_2SO_4 aerosols in the polar stratosphere is larger than 0.1 % wt, which is sufficient to promote a fast heterogeneous reaction with ClONO_2 to produce Cl_2 .

Journal Publications

- R. Zhang, P. J. Wooldridge, and M. J. Molina, Vapor pressure measurements for the $\text{H}_2\text{SO}_4/\text{HNO}_3/\text{H}_2\text{O}$ and $\text{H}_2\text{SO}_4/\text{HCl}/\text{H}_2\text{O}$ liquid systems: Incorporation of stratospheric acids into background sulfate aerosols, *J. Phys. Chem.*, in press, 1993.
- R. Zhang, P. J. Wooldridge, J. P. D. Abbatt, and M. J. Molina, "Physical chemistry of the $\text{H}_2\text{SO}_4/\text{H}_2\text{O}$ System at Low Temperatures: Stratospheric Implications, " submitted to *J. Phys. Chem.*

Real-Time Measurement of the Composition of Individual Aerosol Particles with a Mass Spectrometer

Investigators

*Daniel M. Murphy
Adrian F. Tuck
Aeronomy Laboratory
National Oceanic and Atmospheric Administration
325 Broadway
Boulder, CO 80303

Research Objectives

Aerosol particles are crucial to both the chemistry and radiative processes in the lower stratosphere. Heterogeneous chemistry is emerging as perhaps the single most crucial issue in the HSRP assessment. Accurate knowledge of the composition of stratospheric aerosols is fundamental to understanding heterogeneous chemistry. The objective of our research is to build an instrument that can measure the size and composition of individual aerosol particles. The proposal was to build a laboratory instrument with technology suitable for an eventual airborne instrument.

Summary of Progress and Results

Progress in 1992 was made in a number of areas:

- We are routinely acquiring high-quality mass spectra of test aerosols. As predicted in our 1990 report, we were able to improve the resolution of the mass spectrometer (m/Dm) from about 50 to about 300. This will resolve all mass peaks of atmospheric interest. It is also the best performance of any time-of-flight mass spectrometer of its size.
- We have obtained mass spectra of particles using a lightweight excimer laser. This laser weighs less than 20 kg complete with power supply and emits 5 mJ/pulse at 248 nm. This laser emits much more peak power and as much average power in the ultraviolet as more exotic diode pumped YAG lasers. Coupled with a mass spectrometer only 67 cm long and less than 10 cm in diameter, we have the core of a highly flyable payload.
- We have pushed the lower size limit of aerosols we can work with from about 1.3 μm down to less than 0.6 μm diameter. We expect to work with particles less than 0.4 μm diameter very soon. This would include most of the mass and about half of the surface area of the pre-Pinatubo background aerosol in the stratosphere, or nearly all of the current stratospheric aerosol. Even our current size limit would include most PSC particles.
- We have measured the pulsed laser energy required for ionization of a number of different test aerosols at 248, 308, and 337 nm. Ionization thresholds are less variable with composition at the shorter wavelength; hence the decision to set up the lightweight laser for 248 nm.
- Work in the near future will focus on obtaining spectra of more particles of atmospheric interest, obtaining spectra of smaller particles, and obtaining negative ion spectra. We also plan to begin to investigate tropospheric aerosols.

Journal Publications

Thomson, D. S. and D. M. Murphy, Laser-induced ion formation thresholds of aerosol particles in vacuum, submitted to *Applied Optics*, 1992.

Meteorological Analysis for SPADE

Investigators

*Paul A. Newman
Mark R. Schoeberl
Leslie R. Lait
Joan E. Rosenfield
Code 916
Goddard Space Flight Center
National Aeronautics and Space Administration
Greenbelt, MD 20771

Julio T. Bacmeister
Code 4141
Naval Research Laboratory
4555 Overlook Avenue, SW
Washington, DC 20375-5000

Ronald M. Nagatani
Climate Analysis Center/NMC
National Oceanic and Atmospheric Administration
Washington, DC 20233

Research Objectives

This project's objective is to provide a variety of meteorological products to SPADE investigators, the science team, and the Project Scientist for flight planning and data analysis purposes. Gridded meteorological observations are captured in near-real time from the National Meteorological Center. From these data, balanced winds and potential vorticity are computed and projected along the flight tracks. Constituent data acquired from various data sources, including PI instruments, are also used to reconstruct along the flight track. Parcel back trajectories are also computed. High-resolution gravity wave computations forecast localized turbulence. A radiative transfer code is also available to estimate cooling rates.

The standard data products to be produced are: global analyses along projected flight tracks of the ER-2, curtain files of global analyses track; back trajectories along the flight track; flight meteorological data derived potential vorticity at various isentropic surfaces; reconstructed ozone, nitrous oxide, and chlorine monoxide distribution gravity wave computations, and cooling rate computations.

Summary of Progress and Results

The GSFC group participated in the SPADE test flight series in November 1992. The meteorological products outlined above were routinely provided to the investigators. Software improvements are currently being implemented for use in the SPADE flight series in April and May 1993.

Journal Publications

- Bacmeister, J. T., M. R. Schoeberl, L. R. Lait, P. A. Newman, Small-scale waves encountered during AASE, *Geophys. Res. Lett.*, 17, 349-352, 1990.
- Lait, L. R. et al. Reconstruction of O_3 and N_2O fields from the ER-2, DC-8, and balloon observations, *Geophys. Res. Lett.*
- Newman, P. A., et al. Meteorological Atlas of the Northern Hemisphere Lower Stratosphere During the Airborne Arctic Stratospheric Expedition, NASA Technical Memorandum 4145, NASA, Washington, DC, 1989.

Rosenfield, J. E., M. R. Schoeberl, P. A. Newman, and L. R. Lait. "Radiative heating rates during the Airborne Arctic Stratospheric Expedition. *Geophys. Res. Lett.* 17, 349-352, 1989.

Schoeberl, M. R., et al. Reconstruction of the constituent distribution and trends in the Antarctic polar vortex from ER-2 data, *Geophys. Res.*, 94, 16, 815-16, 845, 1989.

Ozone and Water Vapor Vertical Profiles to 28 km

Investigator

Samuel J. Oltmans
Climate Monitoring and Diagnostics Laboratory
National Oceanic and Atmospheric Administration
325 Broadway
Boulder, CO 80303-3328

Research Objectives

Our objective is to make simultaneous ozone, water vapor, and temperature profile measurements using balloon platforms. Two profile measurements extending from the surface to 28 km altitude will be made. One profile will be obtained during each of the diurnal mission periods scheduled for approximately May 3 and May 10 from Crow's Landing Naval Facility east of Ames.

Summary of Progress and Results

Simultaneous ozone, water vapor, and temperature profile measurements will be made using balloon platforms. Two profile measurements extending from the surface to 28 km altitude will be made. One profile will be obtained during each of the diurnal mission periods scheduled for approximately May 3 and May 10 from Crow's Landing Naval Facility east of Ames Research Center.

Instrumentation for the balloon packages is under construction and will be completed by April 15, 1993, for deployment to California/

HSRP funding was used to procure needed equipment and to pay a portion of the salary for a research assistant.

Journal Publications

"Long-Term Changes in Lower Stratospheric Water Vapor over Boulder, Colorado", submitted to *Nature*.

Transport Across Regions with Strong Isentropic Meridional Tracer Gradients: An Investigation Using Existing Lower Stratospheric Aircraft Measurements

Investigators

*Leonhard Pfister
Earth Systems Science Division
Ames Research Center
National Aeronautics and Space Administration
Moffett Field, CA 94035-1000

Henry B. Selkirk
Space Physics Research Institute
Sunnyvale, CA 94087

Research Objectives

Our work has two major objectives. The first is to examine the origin and nature of the thin (less than 1 km) layered structures in the tracer fields within the midlatitude lower stratosphere. In particular, we seek to establish the reversibility or irreversibility of these layers, whether they are produced by inertial gravity waves, and the nature and strength of the turbulence that erodes them. The ultimate goal is to show how important or unimportant they are to the overall meridional and vertical transport picture. The second is to extend the description of steep isentropic tracer gradients in the tropics as revealed by recent aircraft and satellite measurements by establishing the relationship to meteorological variables and potential vorticity.

Summary of Progress and Results

The progress so far in FY 1993 is in the second of the two objectives outlined above. We have analyzed data from the 1992 SAGE-2 Pinatubo aerosol validation mission, in which the NASA DC-8 made lidar measurements of stratospheric aerosol along a mostly north-south flight path in the central Pacific extending from 37°N to 52°S. The backscatter from the main stratospheric aerosol cloud was centered at 23 km and was maximized in the tropics, and there were clear poleward boundaries (15-20 degree latitude in the northern hemisphere and ~30 degree in the southern), which corresponded to regions of significant gradients of IPV from the NMC stratospheric analysis. These analyses suggest that the relationship between the regions of horizontal tracer gradients and the subtropical jet is ambiguous at best.

Journal Publications

Selkirk, H., and D. M. Winker, "Pinatubo Aerosol Cloud Edges in the Subtropics: Evidence of Sharp Boundaries Between the Tropics and Midlatitudes?" presented at the 1992 AGU Fall meeting, December 7-11, San Francisco, CA

Modeling the Atmospheric Effects of Stratospheric Aircraft

Investigators

*G. Pitari
R. Ferretti
L. Ricciardulli
V. Rizi
M. Verdecchia
Dipartimento di Fisica
Universita' degli Studi L'Aquila
67010 Coppito, L'Aquila
Italy

Research Objectives

The purpose of this project is to study the effects on stratospheric composition using two- and three-dimensional models, and to model the effluent or plume dispersion using mesoscale models.

Summary of Progress and Results

Recent assessment studies have shown that heterogeneous chemistry could have a significant role on the model predicted ozone changes due to gas injection from high-speed civil transport (HSCT) aircraft. One major limitation of these numerical experiments was the highly simplified scheme adopted for the aerosol particles, and in particular the absence of any explicit feedback between the gas-phase chemistry included in the models with the total aerosol surface density available for heterogeneous reactions. Using a two-dimensional model that includes photochemical reactions for the sulfur cycle and a microphysical code for sulfuric aerosols we were able to predict the size distribution for nitric acid trihydrate (NAT) and ice aerosols, covering globally a particle radius range between 0.01 micron and about 160 micron.

Model results for the aerosol size distribution and for the available surface densities appear reasonable when compared with satellite and balloon measurements and with independent numerical calculations. As shown by previous research work and assessment panels, the ozone sensitivity to HSCT emissions largely decreases when heterogeneous chemistry is included with respect to a pure gas-phase chemistry case. With polar aerosols present, the ozone sensitivity to HSCT emission shows a further decrease, and the time-latitude contours of this modeled ozone column change appear significantly different from the pure sulfate case. In addition we show that the SO₂ injection from supersonic aircraft has a large impact on the sulfate aerosol layer, while the effects on ozone appear to be significant only when polar stratospheric aerosols are included in the numerical simulation.

Journal Publications

Pitari, G., L. Ricciardulli, G. Visconti, and V. Rizi, HSCT impact the role of sulfate, NAT and ICE aerosols studied with a 2D model including aerosol physics, submitted to *J. Geophys. Res.*

Air Parcel Trajectories in the Lower Stratosphere Using Winds from the "SKYHI" General Circulation Model

Investigator

R. Alan Plumb
Department of Earth, Atmospheric
and Planetary Sciences
Massachusetts Institute of Technology
Cambridge, MA 02139

Research Objectives

The objective of this study was to investigate the properties of lower stratospheric transport in the high-resolution (1×1.2 degrees) "SKYHI" general circulation model (GCM), by using model-generated winds to generate trajectories of large numbers of trace particles. Of particular interest is transport across the tropopause, across the edge of the polar vortex, and into and out of the tropics.

Summary of Progress and Results

We have developed a sophisticated contour-following technique, which we refer to as "Contour Advection with Surgery" (CAS), to track the two-dimensional motion of material contours. We have used this technique with the SKYHI winds for the southern hemisphere in June (when the wind data are available more frequently from the model) to model the transport of air from the Antarctic vortex and its edge on isentropic surfaces (an assumption that limits us to time intervals of 10 days or so). Vigorous wave breaking is clearly taking place in the model at this time. It was found that the simulation of material contour evolution in this active flow was remarkably insensitive to the resolution (in space and time) of the winds. The generation of very fine-scale filaments (widths of less than 1 degree) was almost unchanged when the resolution of the advecting winds was degraded from 1 degree to 10 degrees. Experiments with tropical and subtropical contours will be run in the near future.

We are currently developing and testing a three-dimensional trajectory code for long-term simulations with the model.

Journal Publications

Publication partly supported by this project:

Waugh, D. W., and R. A. Plumb, Contour advection with surgery: a technique for investigating fine-scale structure in tracer transport. Submitted to *J. Atmos. Sci.*, 1993.

NO/NO_y, O₃, and H₂O Instruments, and Meteorological Analysis

Investigator

Michael H. Proffitt
Aeronomy Laboratory
National Oceanic and Atmospheric Administration
325 Broadway
Boulder, CO 80303

Research Objectives

Support of the HSRP-SPADE campaigns.

Summary of Progress and Results

The ER-2 ozone photometer was repackaged to reduce weight, reducing from 102 pounds to 54 pounds. It was flown successfully during test flights in August 1992 and during the SPADE field campaign in November 1992. Support was given for the field operation in the form of ozone data reduced in the field and made available to all experimenters within three hours. Minimal reconfiguration of the ozone package was also necessary to accommodate the repackaged water instrument of Ken Kelly. Extensive changes in the computer software have been made to accommodate the shared data computer configuration now in place. All travel expenses for the PI and a support technician were provided. Funds were carried over to cover the upcoming SPADE II field campaign in April-May 1993.

Journal Publications

None

Black Carbon (Soot) Aerosols in the Lower Stratosphere and Upper Troposphere: Abundance and Climatic Effects

Investigators

*Rudolf F. Pueschel
David F. Blake
Kenneth G. Snetsinger
Ames Research Center
National Aeronautics and Space Administration
Moffett Field, CA 24035-1000

Anthony D. A. Hansen
Lawrence Berkeley Laboratory
1 Cyclotron Road
Berkeley, CA 94720

Research Objectives

Our objectives are to (1) characterize existing black carbon (soot) aerosols (BCA) in the stratosphere and upper troposphere in terms of absolute amounts, sources, sinks, and residence times in relation to the total aerosol; (2) determine the single scatter albedo of the stratospheric aerosols and assess its effect on radiative transfer; and (3) assess the impact of BCA emissions from a prospective fleet of supersonic aircraft on BCA abundance and effects in the stratosphere.

Summary of Progress and Results

ER-2 and DC-8 aircraft measurements of stratospheric aerosols show a three fold increase in effective particle radius, and 20- and 60-fold increases in aerosol surface area and volume, respectively, due to the 1991 Pinatubo volcanic eruption. The resulting wavelength-dependent light extinction is increased by up to two orders of magnitude. The particle size distribution has become bimodal near 20 km MSL and trimodal just above the tropopause. Based on post-Pinatubo midvisible aerosol optical depths measured at 3.4 km MSL in Hawaii, radiative transfer calculations for the tropics predict stratospheric warming of +0.3 K/day in the aerosol layer and tropospheric cooling (net flux losses -2.5 W m^{-2} at the tropopause). Model calculations with a global distribution of the bimodal volcanic aerosol with 0.1 midvisible optical depth suggest net flux losses of -1.5 W m^{-2} at the tropopause and -0.75 W m^{-2} at the top of the atmosphere.

Journal Publications

- Pueschel, R. F., D. F. Blake, K. G. Snetsinger, A. D. A. Hansen, S. Verma, and K. Kato, Black carbon (soot) aerosol in the lower stratosphere and upper troposphere, *Geophys. Res. Lett.*, 19, 1659-1662, 1992
- Pueschel, R. F., S. A. Kinne, P. B. Russell, and K. G. Snetsinger, Effects of the 1991 Pinatubo volcanic eruption on the physical and radiative properties of stratospheric aerosols, *Proceedings IRS'92: Current Problems in atmospheric radiation*, S. Keevallik, ed. A. Deepak Publications, Hampton, VA, 1993.

Three-Dimensional Transport Studies with Assimilated Meteorological Data: Annual Cycles

Investigator

Richard B. Rood
Data Assimilation Office
Goddard Space Flight Center
National Aeronautics and Space Administration
Greenbelt, MD 20771

Research Objectives

This research effort is closely coordinated with the project headed by Dr. A. Douglass ("Two-Dimensional and Three-Dimensional Model Studies of Stratospheric Aircraft Emissions"). It is leveraged by the resources of the Data Assimilation Office and the Stratospheric General Circulation with Chemistry Project (SGCCP). The HSRP funding is to improve the long-term fidelity of the winds from the data assimilation models for use in transport studies and to produce data sets of one year duration or longer. During the past year a significant part of the effort has also been directed towards the Stratospheric Photochemistry, Aerosol and Dynamics, Expedition (SPADE).

Summary of Progress and Results

The assimilation data sets have been used to study aircraft emissions along corridors connecting North America with Europe, Asia, and Australia. The 3-D model has been compared with the 2-D models through the Douglass effort. The most important results are:

- Aircraft emissions are likely to build up to very high levels. This will occur in regions of low wind speed or in stable dynamical structures such as the Aleutian Anticyclone or the polar vortex.
- Synoptic-scale events of tropospheric origin have a profound influence on the lower stratosphere. In the model they dominate transport from the stratosphere to the troposphere, and they also are responsible for breaking down the boundaries between different latitude zones (e.g., tropics and middle latitudes; middle latitudes and polar vortex).

Attempts to do annual simulations revealed significant problems with the mean meridional circulation. The mean meridional circulation is difficult to quantify in general, and it is especially difficult to quantify in assimilation data products. Comparisons with ozone observations led to a quantification of the error. Using diabatic information a post-processing procedure was developed that substantially improved the quality of the assimilation. Within the Data Assimilation Office, a new analysis system was developed and implemented based on the information gained from the transport experiments. Baseline transport applications are currently being performed and show substantial improvement in the mean meridional circulation as well as in synoptic variability in the southern hemisphere. Assuming successful completion of the baseline experiments, data production will begin with the period September 1991, and 12-18 months of data should be completed by early summer 1993. Data to allow complete simulation of the dispersion of the Pinatubo cloud will follow as soon as practical (input data acquisition required).

Significant effort has also been directed towards support for the SPADE missions. In the November test flight series analyses and forecasts were provided at both high and low resolutions. These products were determined to be useful in flight planning, and they will be supplied in the April-May SPADE mission. Assimilation data for May 1992 have also been supplied to Dr. H. Selkirk at NASA/Ames to study tropical dispersion of the Pinatubo cloud from observations made from aircraft. As part of the general effort to provide near-real time products for HSRP applications, a data-transfer agreement between NOAA/NMC and NASA/Goddard was formalized and will be upgraded with funds provided by the Earth Observing System (EOS) project.

Current work also utilizes Upper Atmosphere Research Satellite (UARS) data to determine weaknesses in the winds from the assimilation procedures. This work is focused on determining the general characteristics of the vertical motion in the stratosphere. This is particularly important for determining how high aircraft emissions might be transported in the tropics.

Journal Publications

Rood, R. B., A. R. Douglass, and C. J. Weaver, Tracer exchange between tropics and middle latitudes, *Geophys. Res. Lett.*, 19, 805-808, 1992.

Weaver, C. J., A. R. Douglass, and R. B. Rood, Thermodynamic balance of three-dimensional stratospheric winds derived from a data assimilation procedure, *J. Atmos. Sci.*, in press, 1993.

Douglass, A. R., R. B. Rood, C. J. Weaver, M. Cerniglia, and K. F. Brueske, Implications of 3D tracer studies for 2D assessments of the impact of supersonic aircraft on stratospheric ozone, *J. Geophys. Res.*, in press, 1993.

Coy, L., R. B. Rood, and P. A. Newman, A comparison of winds from the STRATAN data assimilation system to geostrophic and balanced wind estimates, submitted to *J. Atmos. Sci.*, 1993

Ames-Moffett Management Support for the Small High-Altitude Science Aircraft (SHASA) Project and the Earth Science Advanced Aircraft (ESAA) Team

Investigators

*Philip B. Russell
Steven S. Wegener
Seth Anderson
George Kidwell
John Arvesen
Lawrence Lemke
Mail Stop 245-5
Ames Research Center
National Aeronautics and Space Administration
Moffett Field, CA 94035-1000

David Hall
David Hall Consulting
1111 West El Camino Real
Suite 109, Box 406
Sunnyvale, CA 94087-3758

Mark Waters
Mail Stop 237-11
Eloret Institute
Palo Alto, CA

Research Objectives

The goal of this task is to increase probability of success in the Small High-Altitude Science Aircraft (SHASA) Project and to investigate other aircraft developments needed by HSRP/AESA. The approach is to provide limited technical oversight of the SHASA contractor (Aurora Flight Sciences, Inc.) and to perform related studies and services. Subsidiary objectives are to:

- Provide reviews of proposals and progress, e.g., by attending design reviews.
- Ensure that aircraft performance and payload accommodations will meet the scientific need.
- Perform independent simulations of the performance of the Perseus aircraft using the latest information on engine performance, propeller and wing specifications, etc.
- Investigate and recommend ways to obtain FAA approval for times and airspaces in which Perseus A missions are to be conducted.

The SHASA Project to develop Perseus A is managed by Ames-Dryden, which supplies the Project Manager, Jennifer Baer-Riedhart. Progress on Perseus-A development is described in a separate Research Summary by John Langford, the PI at Aurora Flight Sciences, Inc. This task supplies the SHASA Deputy Project Manager (S. Wegener) and Project Scientist (P. Russell), plus other functions.

Summary of Progress and Results

Staff from this task attended design reviews at Aurora Flight Sciences, Inc., in June 1992 and February 1993, and the Perseus A rollout in December 1992. Reviews were provided for the Aurora proposal for Perseus A operations in HSRP/MAESA.

David Hall prepared the report, "Perseus A Technical Assessment," (December 1992; available from David Hall Consulting). The report investigated the effects on Perseus A performance of 1) replacing the Norton rotary engine with the Rotax 912 and 2) increasing payload weight above the contractual target of 50 kg. These simulations agreed with those presented by Aurora Flight Sciences at the Critical Design Review in predicting that Perseus A with the Norton rotary would be capable of carrying a 50-kg payload to 25 km altitude for a time-on-station of 1 hour. Substituting the Rotax 912 for the Norton did not degrade this predicted performance. David Hall Consulting predicted that, even with a payload of 100 kg, Perseus A would attain a ceiling of 25 km for a predicted time-on-station of 0.4 hour. Concerns raised in the report included:

- the effects of increased payload on the aircraft center of gravity location and stability margins;
- the possible need for external payload containers to carry payload that greatly exceed the 50 kg design requirement;
- the effect of the Rotax 912 heat rejection requirements on the existing Perseus systems; and
- the vibration environment in the payload bay.

David Hall has recently begun an investigation of FAA approvals and protocols for Perseus flights.

Monthly video conferences with HQ, Ames-Dryden, Lewis, Langley, JPL, and Sandia-Livermore were hosted by Ames-Moffett to report progress on SHASA and to discuss broader issues on Earth Science Advanced Aircraft.

Journal Publications

None in 1993, but the following 1991 publication has not been reported here previously.

Russell, P. B., J. S. Langford, J. Anderson, D. Lux, D. W. Hall, and S. Wegener, Advanced aircraft for atmospheric research, *Unmanned Systems*, Vol. 9, 19-24, 1991.

In Situ Measurements of CO, CH₄, N₂O, and CO₂ for the AASE-II/HSRP Expedition

Investigators

*Glen W. Sachse
Bruce E. Anderson
James E. Collins
Langley Research Center
National Aeronautics and Space Administration
Hampton, VA 23665

Research Objectives

To provide high-precision measurements of combustion and stratospheric tracers on board the NASA Ames DC-8 aircraft for (1) assessing the impact of high-flying aircraft on trace gas budgets in the upper troposphere/lower stratosphere and (2) delineating dynamical from chemical processes occurring within and outside the arctic polar vortex in winter.

Summary of Progress and Results

All CO, CH₄, N₂O, and CO₂ data recorded during the AASE-II/HSRP mission have now been reduced, verified, and submitted to the project data archive. Our recent efforts have focused on addressing the above objectives using the merged, in situ measurement (DADS, hydrocarbons, nitrogen species, O₃, and our measurements) data base.

In pursuit of objective 1 (see Anderson et al., below), time series along with vertical and latitudinal profiles were plotted and examined for enhancements in aircraft-signature emissions over known flight corridors. No clear cases of pollution attributable to aircraft were found. Instead, the analyses showed ubiquitous tropospheric enhancements (when compared to summertime or more southerly observations) for all combustion-derived species over the middle to northern latitudes (> 40°N) during the AASE-II mission. The longer-lived species (e.g., CO, CO₂, and C₂H₆) appeared to accumulate at high northern latitudes over the course of the experiment and reached maximum concentrations during late winter and over arctic latitudes. We attribute this finding to the frequent exchange of air masses between midlatitude and polar regions and the reduced efficiency of atmospheric removal processes during the winter season.

Toward objective 2 (see Collins et al., below), the N₂O and CH₄ (stratospheric tracers) data obtained over polar/arctic regions during each flight series were examined as a function of altitude and potential temperature. Results indicate that air at DC-8 altitudes (< 12 km) in the polar region diabatically cooled and subsided an estimated 10 K and 0.8 km, respectively, between the January and March flight series. In fact, potential temperature/N₂O scatter diagrams for March were similar to ER-2 profiles obtained within the polar vortex, which suggests that processed air had subsided into the lower stratosphere by late winter. DC-8 O₃ mixing ratios on constant N₂O surfaces in this processed air were about 10-20% less in comparison to January and February data. This finding is consistent with the ER-2 observations of early winter O₃ loss in the lower vortex and the modest rate of subsidence (diabatic cooling) occurring in the arctic lower stratosphere. These results imply that vortex-related processes may substantially impact the photochemical state of the lower stratosphere/upper troposphere over polar and midlatitude regions. Thus, since effects from vortex-associated processes are expected to increase in coming years, their cumulative impact on the oxidative capacity of the lower stratosphere/troposphere must be factored into HSRP studies.

Journal Publications

- Whiting, G. J., B. E. Anderson, and G. L. Gregory, Aircraft measurements of CO₂ concentrations across latitude and altitude regions: Instrumentation and preliminary results, *EOS Trans. AGU*, 72, 27, April 23, 1992.
- Anderson, B. E., J. E. Collins, G. W. Sachse, G. W. Whiting, D. Blake, and F. S. Rowland, AASE-II observations of trace carbon species distributions in the mid to upper troposphere, submitted to *Geophys. Res. Lett.* for the AASE-II special issue, March 1993.
- Collins, J. E., G. W. Sachse, B. E. Anderson, A. J. Weinheimer, J. G. Walega, and B. A. Ridley, AASE-II in-situ tracer correlations as observed aboard the DC-8: Evidence for subsidence and O₃ loss, submitted to *Geophys. Res. Lett.* for the AASE-II special issue, March 1993.

Model and Measurements Data Base for Atmospheric Assessment of Aircraft Effects

Investigators

*Robert K. Seals, Jr.
Richard S. Eckman
Mary Ann H. Smith
Langley Research Center
National Aeronautics and Space Administration
Hampton, VA 23665

Linda A. Hunt
Karen H. Sage
Lockheed Engineering and Sciences Co.
Hampton, VA 23665

Research Objectives

The purpose of this task is to support the use of model and measurement data sets to understand the response of the atmosphere to aircraft emissions. The task focuses on compilation, distribution, intercomparison, and archival of such data sets in support of AESA studies and of associated workshops and intercomparison activities. Emphasis is on assembling relevant model prediction results and measurement data sets; making them available in an electronic format; and supporting the intercomparison, manipulation, and display of key parameters. The AESA work is complementary to activity under the Upper Atmosphere Data Program (UADP) funded through the NASA Upper Atmosphere Theory Program.

Summary of Progress and Results

A major effort under this task has been working with the Models and Measurements (M & M) Committee. Revised data from modeling groups participating in the M & M intercomparison activity have been incorporated into the data base. Analyses and plots of the data were prepared for the M & M report entitled "The Atmospheric Effects of Stratospheric Aircraft: Report of the 1992 Models and Measurements Workshop." Investigation into and planning for the publishing of a compact disc containing the report and data has begun.

A second major effort this year has been the development of a series of aircraft emissions scenarios using emissions data compiled for various classes of aircraft by Boeing and McDonnell Douglas. These emission scenario data sets are available on both a three-dimensional (longitude, latitude, altitude) and a two-dimensional (latitude, altitude) grid and include cases for 1990 and 2015 subsonic fleets and for potential Mach 1.6 and Mach 2.4 HSCT fleets. The data were assembled on the UADP system, regridded to the model grids of six AESA modeling groups, and distributed for use in HSCT assessment modeling runs. Resulting model projections were incorporated into the data base, and plots and analyses of the data were provided to the modelers and authors of chapters of the HSRP Program Report. On-site data base support was provided at the 1993 Interim Assessment meeting in Satellite Beach, Florida. Subsequent to the meeting, revised model projections have been submitted to the data base. Analyses and plots of the revised data have been provided for the program report. Support was also provided for the HSRP/AESA annual meeting in June, both prior to the meeting and on-site at Virginia Beach.

Journal Publications

Prather, M. J., and E. E. Remsberg, Eds, *The Atmospheric Effects of Stratospheric Aircraft: Report of the 1992 Models and Measurements Workshop*, NASA Reference Publication, 1292, NASA Washington, DC, 1993.

Electron Microscope Aerosol Analysis for SPADE

Investigator

Patrick J. Sheridan
CIRES, Campus Box 449
University of Colorado
Boulder, CO 80309-0449

Research Objectives

Our first research objective was to determine the collection efficiency of the University of Denver electrostatic aerosol sampler (EAS) for particles of different sizes. The EAS was designed to collect particles directly onto thin films, so that high-resolution analytical electron microscopy (AEM) could be used for aerosol analysis. It now appears that many of the aerosol samples for electron microscope analysis will be collected using a low-pressure impaction technique (the MACS sampler described below). The second goal of this project is to examine the physical and chemical properties of stratospheric particles collected during the SPADE missions. The physicochemical characterizations of these particles and their stratospheric residence times will be of importance in determining the overall impact of HSCT emissions on stratospheric chemistry.

Summary of Progress and Results

During the last Program Report period, electron microscope analyses of laboratory-generated aerosols initially indicated an unacceptable collection efficiency for the EAS over several particle size ranges. The University of Denver Group used this information to make design changes to the sampler which significantly increased the EAS collection efficiency over many of the particle sizes of interest. The approximate collection efficiency of the EAS for particles of various sizes has now been determined.

Aerosol samples collected by the new Multi-sample Aerosol Collection System (MACS) during the Stratospheric Photochemistry, Aerosols and Dynamics Expedition (SPADE) test flights in fall 1992 have been analyzed. Stratospheric aerosol samples were dominated by heavy loadings of ammoniated sulfates. This neutralization of acidic sulfate probably occurred during handling and is the reason for subsequent testing and improvement of the MACS sample isolation mechanism. In some of the samples, the sulfate particles contained large (often supermicrometer) solid inclusions with elemental signatures (e.g., major Si, Fe, Ca, etc., plus O) suggesting crustal or volcanic sources. A few of the samples were heavily contaminated with large, jagged stainless steel (SS) particles, whose source has been attributed to a length of SS tubing in the instrument's inlet. While the SS particles are easily identified by composition and morphology using electron microscopy, heavy particulate contamination from inlets can skew the aerosol size distribution. Disassembly and cleaning of the inlet revealed a gray-black deposit of SS particles on inner inlet surfaces; cleaning of the inlet will be performed between each flight during SPADE. We are currently investigating why only a few of the ~20 MACS aerosol samples collected during the test flights showed as contamination.

Our most recent work has focused on testing the MACS for possible sample contamination by inadequate sealing. Electron microscope analyses on pure sulfuric acid aerosols collected and stored in the MACS sample isolation tubes are under way to determine if these aerosols have changed over time and thus are poorly isolated from air within the instrument and/or laboratory. Recent modifications to this sampling system appear to have significantly improved the sealing mechanism.

Journal Publications

None

Validating the Transport Component of Two-Dimensional Chemical Transport Models Using Excess Carbon 14 Data

Investigators

*Run-Lie Shia
Malcolm K. W. Ko
Rao V. Katamarthi
Min Zou
Atmospheric and Environmental Research, Inc.
840 Memorial Drive
Cambridge, MA 02139

Research Objectives

An important factor in the assessment of the atmospheric effects from the engine emissions of a projected fleet of stratospheric aircraft is the magnitude of the residence time of the emitted materials in the stratosphere. For a species that has a photochemical lifetime longer than a year, the residence time depends on the cross-tropopause exchange rate. Refinements are needed in current two-dimensional chemical transport models to provide better simulation of the exchange processes between the stratosphere and the troposphere. These refinements would include increasing the model resolution in the vertical to about 1 km and improving the model physics through validating the transport component of the model using excess ^{14}C data from nuclear bomb tests.

Summary of Progress and Results

We have completed an analysis in which various combinations of the transport parameters were used in a two-dimensional model to see how well the excess ^{14}C from nuclear tests can be simulated. We found that the set of standard transport parameters used in the AER model produced very favorable results compared with the measurements. Only small adjustment (about 10%) could be justified.

The new version of the model with three times finer vertical resolution ($Dz = 1.2$ km) has been used to investigate the cross-tropopause transport. A detailed sensitivity study of excess ^{14}C simulation to the change of the transport parameters and tropopause height has been performed. The model simulations showed that, in the model, horizontal eddy diffusion along isentropic surfaces is the most important mechanism for transporting excess ^{14}C across the tropopause, but the circulation is the more important contributor to cross-equator transport.

Also from the sensitivity study we found that the model simulation of excess ^{14}C is in better agreement with the measurements if the tropopause position shifts down one level (about 1.2 km) in the model. This shift of the tropopause can cause a 14-22% increase in the accumulation of the aircraft emitted NO_x in the stratosphere, which would result in ozone depletion that is larger by a factor of 1.2 to 1.3.

In accordance with a recent estimate of the air exchange rate through the tropopause folding, the eddy diffusion coefficient K_{yy} there should be much smaller than one currently used in the model. Although the change of K_{yy} only involves several grid boxes, the simulation of excess ^{14}C using new K_{yy} is noticeably improved.

The prescribed parameters (e.g., Rayleigh friction coefficients and eddy diffusion coefficients) in the AER 2-D interactive model have been validated using excess ^{14}C data. The model is then used to investigate the effects of the projected high-speed civil transport emissions on the ozone distribution in the stratosphere. The feedback effects through the change of temperature and circulation is to reduce the ozone depletion by a factor of 0.85 to 0.7 in the middle latitudes of northern hemisphere, in which two-thirds is due to the change of the circulation only.

Journal Publications

Shia, R.-L., M. K. W. Ko, M. Zou, and V. R. Kotamarthi, Cross tropopause transport of excess ^{14}C in a two-dimensional model, submitted to *J. Geophys. Res.*

Heterogeneous Chemistry Related to Stratospheric Aircraft

Investigator

Margaret A. Tolbert
CIRES
Campus Box 216
University of Colorado
Boulder, CO 80309-0216

Research Objectives

We are performing laboratory experiments aimed at characterizing thin films representative of stratospheric aerosols. In particular, we are studying H₂SO₄/H₂O films representative of the global stratospheric sulfate layer and nitric acid/ice films representative of Type I polar stratospheric clouds (PSCs). We have used FTIR spectroscopy to measure the composition, phase, formation, evaporation, freezing, and melting of model stratospheric aerosol films. We hope to understand the microphysical properties of these aerosols so that heterogeneous chemical effects can be properly included in atmospheric models of high-speed civil transport.

Summary of Progress and Results

FTIR spectroscopy was used to examine the competitive growth of nitric acid/ice films representative of Type I PSCs. These experiments show that either crystalline nitric acid trihydrate (β -NAT) or amorphous films with H₂O:HNO₃ ratios close to 3:1 form at temperatures 3-7 K warmer than the ice frost point under stratospheric pressure conditions. In addition, with higher HNO₃ pressures we observe nitric acid dihydrate (NAD) formation at temperatures warmer than ice formation. However, our experiments also show that NAD surfaces convert to β -NAT upon exposure to stratospheric water pressures. These studies suggest that Type I PSCs are probably β -NAT, or possibly NAD with a β -NAT surface.

Other recent studies have used FTIR spectroscopy to examine sulfuric acid films representative of stratospheric sulfate aerosols. Thin films of sulfuric acid were formed in-situ by the condensed phase reaction of SO₃ and H₂O. FTIR spectra show that the sulfuric acid films deliquesce while cooling in the presence of water vapor. With continued cooling, the sulfuric acid films crystallized as sulfuric acid tetrahydrate (SAT). Crystallization occurred either when the composition was about 60 wt% or after ice condensed on the films. Finally, we determined that the melting point for SAT depends on the background water pressure and is ≈ 216 K in the presence of 4×10^{-4} Torr H₂O. Our melting point results suggest that frozen sulfate aerosols in the stratosphere are likely to melt at temperatures 30 K colder than previously thought, thus impacting PSC nucleation and heterogeneous chemistry.

Journal Publications

- Tolbert, M. A., B. G. Koehler, and A. M. Middlebrook, Spectroscopic studies of model polar stratospheric cloud films, *Spectrochimica Acta*, 48A, 1303-1313, 1992.
- Middlebrook, A. M., B. G. Koehler, L. S. McNeill, and M. A. Tolbert, Formation of model polar stratospheric cloud films, *Geophys. Res. Lett.*, 12, 2417-2420, 1992.
- Tolbert, M. A., J. Pfaff, I. Jayaweera, and M. J. Prather, Uptake of formaldehyde by sulfuric acid solutions: impact on stratospheric ozone, *J. Geophys. Res.*, 98, 2957-2962, 1993.
- Koehler, B. G., A. M. Middlebrook, L. S. McNeill, and M. A. Tolbert, FTIR studies of the interaction of HCl with model polar stratospheric cloud films, *J. Geophys. Res.*, in press, 1993.

Middlebrook, A. M., L. T. Iraci, L. S. McNeill, B. G. Koehler, M. A. Tolbert, D. R. Hanson, and O. W. Saastad, FTIR studies of thin sulfuric acid films: formation, water uptake, and phase changes, submitted to *J. Geophys. Res.*, 1993.

Heterogeneous Chemistry and Microphysical Modeling and Analysis in Support of the HSRP

Investigator

Owen B. Toon
Earth Systems Science Division
Ames Research Center
National Aeronautics and Space Administration
Moffett Field, CA 94035-1000

Research Objectives

The first objective of this sub-task of the proposed work is to advise the HSRP project on the use of the DC-8 aircraft for atmospheric measurements. The second objective is to provide a data set on heterogeneous reactions on volcanic aerosols observed from the DC-8 for use in testing UCLA models of heterogeneous chemistry. The third objective is to provide analyzed data sets on polar stratospheric cloud properties to the UCLA group for use in testing their polar stratospheric cloud models.

Summary of Progress and Results

The DC-8 aircraft was successfully flown in the 1992 AASE-II program. As the flight scientist for the DC-8 I considered the interests of the HSRP project in the design of flight plans and in the choice of instruments used on the aircraft. A number of important observations were made from the DC-8 including tracer ratio data near and above the tropopause and other information relevant to the dynamics of the lower stratosphere. These data should be useful to the HSRP and are currently being reduced and described by the relevant PIs. A proposal was prepared for the HSRP on the use of the DC-8 aircraft in the 1994 HSRP field programs. The proposal was forwarded to the appropriate HSRP science management personnel for their consideration. A data set on heterogeneous chemical conversions on volcanic sulfuric acid aerosols was assembled from the DC-8 data in AASE-II. The reaction rate of ClNO_3 on the aerosols and the solubility of HNO_3 in the aerosols was found to be similar to laboratory studies. However, it was inferred that HCl is either much more reactive, or much more soluble in sulfuric acid than laboratory studies have suggested. We also found that in contradiction to some theories, sulfuric acid aerosols do not freeze until temperatures are near the ice frost point. We plan to work on the polar stratospheric cloud data set over the next year.

Journal Publications

O. B. Toon et al., Heterogeneous reaction probabilities, solubilities, and physical state of cold volcanic aerosols, submitted to *Science*, 1992.

Quantifying the Strength of Brewer-Dobson Circulation and Other Strat-Trop Exchange Processes

Investigator

Ka-Kit Tung
Department of Applied Mathematics, FS-20
University of Washington
Seattle, WA 98195

Research Objectives

To quantify the strength of the mass transport across the tropopause and to develop direct and indirect means to validate its strength, in support of HSRP program of assessing the impact of stratospheric aircrafts.

Summary of Progress and Results

In addition to studying the climatological mass transport in the lower stratosphere, we have began a study on its year-to-year change. In particular, we are focusing on the difference in mass transport between the QBO easterly and QBO westerly years. A model has been developed for the variation in tropical and extratropical circulation caused directly and indirectly by the phenomenon of equatorial QBO in zonal wind. We further examine the effect on the transported ozone as an indirect means of validation. We have good success in simulating both the tropical and extratropical QBO components as compared to TOMS data on column ozone.

Journal Publications

In preparation

Investigation of High-Altitude Aircraft Plumes and Contrails: Physical and Chemical Processes and Global Implications

Investigators

*Richard P. Turco
Department of Atmospheric Sciences
University of California
Los Angeles, CA 90024

*Owen B. Toon
Earth System Sciences Division
Ames Research Center
National Aeronautics and Space Administration
Moffett Field, CA 94035

Research Objectives

The objectives of the project are to develop a physical/chemical model describing the evolution and chemical effects of contrails formed behind high-speed stratospheric aircraft; to quantify important environmental effects of high-altitude flight including, chemical transformations in the exhaust contrails and impacts on the formation, distribution, and persistence of stratospheric sulfate aerosols and polar stratospheric clouds (PSCs); and to advise the HSRP program on the use of the DC-8 aircraft in field experiments, and employ aircraft data on heterogeneous chemistry in the models described above.

Summary of Progress and Results

Model Development and Applications: A physical/chemical model describing the formation, evolution and chemical effects of aerosol particles in the exhaust stream of high-speed stratospheric aircraft has been developed. This contrail model predicts the formation and growth of ice and other particles in an expanding jet plume, and the heterogeneous chemical processes that may occur on ice and other aerosols. We have calculated the nucleation rates of sulfuric aerosols and ice crystals in aircraft wake (Zhao and Turco, 1993). Both homogeneous bimolecular ($\text{H}_2\text{SO}_4/\text{H}_2\text{O}$) nucleation and heterogeneous binary nucleation on existing particles were studied. This work established the importance of sulfuric and homogeneous nucleation in high-altitude contrails. The calculations also show that ice nucleation is highly dependent on environmental conditions and is most likely to occur on sulfate aerosols, which deliquesce into droplets that subsequently freeze.

The physical/chemical processes that determine the evolution and chemical effects of stratospheric contrails is being simulated with a detailed microphysics model (e.g., Drdla et al., 1992, 1993). Water vapor condensation and evaporation as liquid droplets and ice crystals, and the ice particles, determines the surface areas available for chemical processing. Such details are important to the HSRP objectives. Simulations of PSC properties were compared to ER-2 aircraft data at the NRC HSRP review in Cleveland in February 1993. The comparison clearly demonstrated the limitations in modeling PSC formation and growth, particularly in regions where PSC occurrence may be marginal. HSCT emissions would have the largest impact on chemical processing leading to ozone depletion in these regions.

Heterogeneous chemistry on ice particles in aircraft contrails is being studied with a model that predicts "sticking coefficients" from basic physical data (Tabazadeh and Turco, 1991, 1992). This surface physics/chemistry model is based on phenomenology taken from surface physics. The model has been applied to interpret and reconcile conflicting laboratory measurements of ice surface properties and chemical reactivities (Tabazadeh and Turco, 1993a,b). The model is flexible enough to show how chlorine can be removed from volcanic eruption clouds before injection into the stratosphere. Heterogeneous chemical processes occurring on ice in aircraft contrails is being investigated with the model. Clusters of trajectories are being calculated for aircraft exhaust parcels subject to mixing and cooling. Coupled microphysical photochemical simulations are being analyzed to understand the basic

mechanisms that influence contrail chemistry, and to define the major sources of uncertainty in modeling such chemistry on hemispheric scales.

Aircraft Data Analysis: The DC-8 aircraft was successfully flown in the 1992 AASE-II program. O. Toon acted as flight scientist for the mission. Flight plans and an instrument package well suited to the goals of the HSRP were given special consideration. A number of observations that are important to the HSRP were carried out, including the concentration ratios of certain tracers near and above the tropopause. These data, which are currently being analyzed, will be useful in studying the dynamics of the lower stratosphere. A proposal was prepared for the HSRP project to use the DC-8 in the 1994 HSRP field campaign. The proposal has been forwarded to the HSRP management team for evaluation. Another relevant data set on sulfuric acid aerosols was obtained during the DC-8 AASE-II flights. The data indicate that the reaction rate of chlorine nitrate on sulfuric acid surfaces, and the solubility of nitric acid in sulfuric acid aqueous solutions, are similar to laboratory measurements of these parameters. However, HCl was found either to be much more reactive or much more soluble in sulfuric acid than laboratory data indicate. Further, it was found that the sulfuric acid aerosols do not freeze until temperatures drop close to the ice frost point, which contradicts some recent theories. These important findings from field data are being applied to improve our models of aerosol microphysics and chemistry. In the next year, a similar analysis of the PSC data from the AASE-II mission will be completed.

Other Activities: R. Turco presented an overview on the background stratosphere and perturbations expected with HSCT traffic to the National Research Council Advisory Committee on the HSRP at the Lewis Center, Cleveland, February 10, 1993. Turco also continues to chair the Stratospheric Aerosol Science Committee (SASC) of the HSRP, and contributed a report recommending priorities for engine-test measurements based on a May 1992 SASC meeting.

Project Personnel (including part-time appointments)

Prof. Richard Turco (UCLA, Principal Investigator)
Dr. O. B. Toon (Ames Research Center, Co-Investigator)
Prof. Patrick Hamill (San Jose University, Consultant on nucleation and microphysics)
Dr. Sajal Kar (UCLA, Postdoctoral Researcher)
Katja Drdla (UCLA, Graduate Student)
Azadeh Tabazadeh (UCLA, Graduate Student)
Jing-Xia Zhao (UCLA, Graduate Student)

Journal Publications

- Drdla, K., "High-Speed Stratospheric Aircraft: Factors Affecting Their Climatic Effect," preprint, 1991.
- Drdla, K., R. P. Turco, Denitrification through PSC formation: A 1-D model incorporating temperature oscillations, *J. Atmos. Chem.*, 12, 319-366, 1991.
- Drdla, K., R. P. Turco, J. Farrara, and C. R. Mechoso, PSC microphysics and heterogeneous chemistry along atmospheric trajectories, *EOS Am. Geophys. Union*, Special Supplement, Fall 1991, AGU Meeting, 1991.
- Drdla, K., R. P. Turco, J. Bacmeister, M. R. Schoeberl, D. Baumgardner, and J. E. Dye, The efficiency of chemical processing in lee-wave polar stratospheric clouds, *Trans Am. Geophys. Union, EOS*, Supplement, 1992 Spring Meeting, Montreal, p. 68, 1992.
- Drdla, K., R. P. Turco, and S. Elliott, Heterogeneous chemistry on Antarctic PSCs: A microphysical estimate of the extent of chemical processing, to appear in *J. Geophys. Res.*, 1993.
- Elliott, S., R. P. Turco, O. B. Toon, and P. Hamill, Incorporation of stratospheric acids into water ice, *Geophys. Res. Lett.*, 17, 425-428, 1990.

- Elliott, S., R. P. Turco, O. B. Toon, and P. Hamill, Application of physical adsorption thermodynamics to heterogeneous chemistry on polar stratospheric clouds, *J. Atmos. Chem.*, 12, 1991.
- Kar, S., R. P. Turco, C. R. Mechoso, and A. Arakawa, A locally one-dimensional semi-implicit scheme for global grid-point shallow-water models, submitted to *Mon. Weather Rev.*, 1993.
- Tabazadeh, A., and R. P. Turco, A surface chemistry model to study heterogeneous processes of atmospheric significance, *EOS*, Supplement, October 29, p. 82, 1991.
- Tabazadeh, A., and R. P. Turco, A model for heterogeneous chemical processes on the surfaces of ice and nitric acid trihydrate particles, to appear in *J. Geophys. Res.*, 1993a.
- Tabazadeh, A., and R. P. Turco, Stratospheric chlorine injection by volcanic eruptions: HCl scavenging and implications for ozone, to appear in *Science*, 1993b.
- Toon, O. B., et al., Heterogeneous reaction probabilities, solubilities and physical state of cold volcanic aerosols, submitted to *Science*, 1992.
- Turco, R., Upper-atmosphere aerosols: Properties and natural cycles, Chapter 3B, *The Atmospheric Effects of Stratospheric Aircraft: A First Program Report*, M. J. Prather and H. L. Wesoky (Eds.), NASA Ref. Publ. 1272, pp. 65-95, NASA, Washington, D.C., 1992.
- Turco, R. P., and P. Hamill, Supercooled sulfuric acid droplets: Perturbed stratospheric chemistry in early winter, *Ber. Bunsenges. Phys. Chem.*, 96, 323-334, 1992.
- Turco, R. P., K. Drdla, A. Tabazadeh, and P. Hamill, "Heterogeneous chemistry of polar stratospheric clouds and volcanic aerosols," to appear in the Proc. NATO Advanced Studies Institute on the Role of the Middle Atmosphere in Global Change, Darquerainne, France, September 14-25, 1992 (1993).
- Zhao, J.-X., and R. P. Turco, Particle nucleation in the wake of a jet aircraft in stratospheric flight, to appear in *J. Aerosol Sci.*, 1993.
- Zhao, J.-X., O. B. Toon, and R. P. Turco, Simulation of condensation nuclei in the spring polar stratosphere, *EOS Am. Geophys. Union*, Special Supplement, 1991 Fall AGU Meeting, 1991.

Aircraft Laser Infrared Absorption Spectrometer (ALIAS-II) for N₂O, CH₄, and H₂O Profiles from Perseus; and HCl, HNO₃, NO₂, N₂O, and CH₄ Measurements from ALIAS-I on the ER-2

Investigators

*Christopher R. Webster
Randy D. May
Jet Propulsion Laboratory
California Institute of Technology
4800 Oak Grove Drive
Pasadena, CA 91109

Kenneth K. Kelly
Adrian F. Tuck
Aeronomy Laboratory
National Oceanic and Atmospheric Administration
325 Broadway
Boulder, CO 80303-3328

Research Objectives

In-situ measurements of HCl, N₂O, CH₄, H₂O, NO₂ and HNO₃ will be used in conjunction with other simultaneous measurements from the ER-2 and Perseus to define the reference state of the atmosphere in the altitude region 10-30 km. These measurements will constrain model simulations, which will assess the impact of a proposed fleet of supersonic aircraft on stratospheric ozone.

Specific objectives over the next year are to complete building the ALIAS-II spectrometer for measurement of H₂O, CH₄, and N₂O during Perseus test flights in late 1993; and to fly ALIAS-I on the ER-2 for measurements of HCl, N₂O, CH₄, NO₂, and HNO₃ during the SPADE campaign out of NASA Ames in April/May 1993.

Summary of Progress and Results

The ALIAS-II construction is well under way, with the basic design completed, purchase orders placed, and electronics fabrication started. With its long optical path over to the Perseus wing, ALIAS-II is expected to have similar measurement sensitivity to ALIAS-I, with HCl included as a candidate gas.

ALIAS-I participated in the SPADE test flight series with mixed success, encountering problems in the N₂O/CH₄ channel, but achieving objectives with regard to NO₂ and HNO₃. Spectral features of HNO₃ were identified for the first time, and upper limits for NO₂ were measured. Improved performance is expected for the spring SPADE campaign.

Journal Publications

None

NO, NO₂, NO_y, and O₃ Measurements Made During the Arctic DC-8 1992 Missions

Investigators

*Andrew J. Weinheimer
James G. Walega
Brian A. Ridley
National Center for Atmospheric Research
P. O. Box. 3000
Boulder, CO 80307-3000

Research Objectives

Our objectives over the past year have been twofold: (1) To measure the distribution of odd nitrogen species (NO, NO₂, and NO_y), in conjunction with O₃, in different regions of the western northern hemisphere to help define a current reference state for assessment studies as well as to look for the effects of NO_x emissions from present-day aircraft. (2) To investigate effects of wintertime polar chemistry on air at DC-8 altitudes.

Summary of Progress and Results

With regard to measurements and data analysis: The four species were successfully measured on all 19 DC-8 flights that were part of AASE II (with the exception of problems with NO_y on the first test flight). The NO_y and O₃ are archived on the 1st edition of the AASE II CDROM. Preliminary analysis of NO and NO₂ has been done. This will soon be finalized for inclusion of all four species on the 2nd edition of the CDROM (NO_y and O₃ at 2 seconds, NO and NO₂ at 1 minute).

Most of our analysis and interpretation to date have been in conjunction with tracers measured by Sachse et al. (NASA Langley). We find: (1) The evolution of the O₃-N₂O correlation over the course of AASE II exhibits a decrease in O₃ that occurred between the February and March flight series. Additional analysis will be pursued to determine the cause of this decrease, whether it reflects chemical loss within the polar vortex, or if transport is responsible. (2) The NO_y-N₂O correlation in AASE II shows an absence of the high-NO_y regions seen by the DC-8 in 1989 in AASE I. In addition, relative to N₂O, there is less NO_y in the month of February, especially on the last flight of the month. (3) There is no marked difference, for DC-8 levels, between air under and not under the Arctic polar vortex.

Journal Publications

To be submitted to the special issue of *Geophysical Research Letters*:

Collins, J. E., G. W. Sachse, B. E. Anderson, Weinheimer, A. J., J. G. Walega, B. A. Ridley, AASE-II in-situ tracer correlations as observed aboard the DC-8: Evidence of subsidence and O₃ loss.

Weinheimer, A. J., J. G. Walega, B. A. Ridley, G. W. Sachse, B. E. Anderson, J. E. Collins, Stratospheric NO_y measurements on the NASA DC-8 during AASE II.

Investigation of Combustion Aerosols as a Potential Sink for NO_x in the Expanding Exhaust Plume of the HSCT

Investigators

*Philip D. Whitefield
Donald E. Hagen
Cloud and Aerosol Science Laboratory (UMR/CASL)
Norwood Hall (G11)
University of Missouri-Rolla
Rolla, MO 65401-0249

Harvey Lilenfeld
Mail Stop 111-1041
McDonnell Douglas Research Laboratories (MDRL)
McDonnell Douglas
Saint Louis, MO 63166-0516

Research Objectives

Experiments are being performed to investigate the role of combustion aerosols as potential sinks for the NO_x in the exhaust plume of supersonic aircraft flying in the stratosphere. Laboratory generated combustion aerosol (both fresh and aged) will be characterized for size distribution and hydration properties. Accommodation coefficients for NO and NO₂ will be measured for the aforementioned, well-defined combustion aerosols as a function of exposure time, relative humidity, pressure and temperature appropriate to conditions expected in the jet/vortex regime.

Summary of Progress and Results

The University of Missouri-Rolla cloud simulation chamber was configured for the initial accommodation coefficient experiments tasked for year two as follows:

- A pre-mixed pre-vaporized laboratory burner aerosol emission was characterized for given samples of JP4 and JP5.
- Monodisperse aerosols in the range 0.01 to 0.10 microns in diameter and with a known critical supersaturation can be routinely delivered to the chamber in concentrations up to and including 500 cm³.
- A quadruple mass spectrometer was connected to the cloud chamber through its critical orifice probe and will sustain a vacuum of 1.0E-6 in the mass analyzer while drawing through the critical orifice from the simulation chamber at a pressure of one atmosphere.
- A trace gas handling and mixing line was installed and calibrated for nitrous oxide (N₂O) and nitrogen dioxide (NO₂). Because of its compatibility with the cloud chamber materials, N₂O was the first oxide of nitrogen studied.
- The N₂O uptake was extremely small and essentially below the limit of detection using the mass spectrometer. Such a limit indicates a gamma of less than 10⁻⁶. This is not anticipated for NO₂. Recent reports in the literature have estimated gamma for NO₂ to be as high as 1.5 x 10⁻³ (J. L. Ponche et al. *J. Atmos. Chem.* 16, 1, 1993).
- Measurements to determine the accommodation coefficient for NO₂ on laboratory-simulated jet engine exhaust carbonaceous aerosols are currently under way in the UMR cloud simulation chamber facility.

Formal requests have been received for the UMR/MDRL team and their Mobile Aerosol Sampling System (MASS) to join lower atmosphere assessment programs initiated in Europe such as the AERONOX and AEROSPEC measurement campaigns at Rolls Royce in the United Kingdom and DLR (Oberpfaffenhofen) in Germany. The UMR/MDRL team and their MASS will join the in flight measurement campaigns at DLR (Oberpfaffenhofen) in Germany during the summer of 1993 and in the North Atlantic Corridor in October. These studies are focused on particulate emissions in the exhaust plumes of conventional commercial transport at cruise in the troposphere. Collaboration with Rolls Royce is still being negotiated.

Recent measurements performed under an independent research project funded by the McDonnell Douglas Corporation have provided us with unique size and hydration property data for the GE 404 engine currently deployed in the F-18E supersonic fighter aircraft.

- These data coupled with engine operating parameters permit us to determine effective emission indices for CN and CCN.
- We are currently discussing with Aerodyne (Dr. Miake Lye) how the aforementioned data on particulate emission indices and accommodation coefficients (reference below) can be coupled with Aerodyne's HSCT plume model to estimate the potential for NO_x scavenging during the plume equilibration.

Journal Publications

Hagen, D. E., M. B. Trueblood, and P. D. Whitefield, A field sampling of jet exhaust aerosols, *Particulate Science and Technology*, 10, 53-63, 1992.

Whitefield, P. D., M. B. Trueblood, and D. E. Hagen, Size and hydration characteristics of laboratory simulated jet engine combustion aerosols, *Particulate Science and Technology*, in press.

Detection and Analysis of Aircraft Produced Particles in the Stratosphere: Participation in the Stratospheric Photochemistry, Aerosols and Dynamics Experiment (SPADE)

Investigators

*James C. Wilson
Charles A. Brock
Department of Engineering
University of Denver
Denver, CO 80208-0177

Research Objectives

The research objective is to operate two instruments in the SPADE experiment. The first instrument, the CNC II, is designed to determine the concentration of nonvolatile particles in the stratosphere and to collect particles for laboratory analysis. The nonvolatile particles are those surviving heating to 180°C. Sulfuric acid particles should vaporize at these temperatures, and the remaining particles are considered to nonvolatile and may include soot from aircraft engines. The measurement of nonvolatile particles is achieved with a two-channel condensation nucleus counter. One channel counts the particles sampled from the stratosphere and the second counts particles in a sample that has been heated to 150°C. Aerosol samples will be collected to determine the differences between volatile and nonvolatile particles. The collector consists of an impactor capable of collecting particles larger than 0.03 micron in diameter. Twenty four samples may be collected in flight and returned to the laboratory for analysis.

The second instrument is the Focused Cavity Aerosol Spectrometer, FCAS. The FCAS permits aerosol size distributions to be measured in the 0.07 to 2 micron diameter range. The FCAS, the CNC II, and the FSSP permit size distributions to be measured in the diameter range from 0.01 to 20 micron. These measurements have been central to determining the role of heterogeneous chemistry in establishing the partitioning of the reactive nitrogen family in the midlatitude stratosphere. The measurements of aerosol size distributions are central to the SPADE objectives of determining the role of heterogeneous chemistry in influencing the chemistry of the stratosphere and in following the evolution of the stratospheric aerosol following the eruption of Mt. Pinatubo.

Summary of Progress and Results

The SPADE mission will start in April 1993. Thus the only work done on this task to date has been to prepare for SPADE.

Journal Publications

None

High Altitude NO and NO_y Measurements Using A New Lightweight Chemiluminescence Instrument

Investigators

*Steven C. Wofsy
Joel D. Burley
Bruce C. Daube, Jr.
Department of Earth and Planetary Sciences
Harvard University
Cambridge, MA 02138

Research Objectives

The objective of the project is to design, construct, and test a lightweight, dual-channel sensor for stratospheric NO and NO_y. This sensor will be incorporated into the first two payloads of the Perseus A aircraft currently being developed by Aurora Flight Sciences Corporation. Test flights of the first Perseus A payload (i.e. the "chemistry" payload) are tentatively scheduled at Dryden A.F.B. for mid-February of 1994. Operational deployment to mid (Dryden) and tropical (Darwin, Australia) latitudes will follow in July and October of 1994.

Summary of Progress and Results

Test flights of a prototype, balloon-borne instrument were conducted over Sondrestrom, Greenland in March of 1992. Analysis of the engineering and science data from these flights is now complete, and a paper outlining the scientific results has been submitted to *Geophysical Research Letters* (see below). A laboratory test-bed system has been assembled, and has been used to complete a series of materials compatibility tests to address questions raised by the test flight. We determined the suitability (or lack thereof) of aluminum, stainless steel, Pyrex, quartz, and PFA Teflon as materials in the inlet and zeroing volume portions of the instrument. Loss of NO sample was observed on the aluminum and stainless surfaces, while no detectable losses were seen for Pyrex, quartz, and PFA Teflon. Current plans envision a Teflon-based system, with minimal sample exposure to stainless steel. Laboratory testing is now concentrating on possible revisions to the chemiluminescence cells and detectors used in the Greenland instrument.

At the same time the laboratory test-bed system was being assembled, the components of the data acquisition system were selected and purchased. The heart of this system -- an Ampro 386SX computer with a small hard disk (Seagate ST9096A) -- is now operational in our laboratory.

Journal Publications

Dessler, A. E. et al., "Balloon-Borne Measurements of ClO, NO, and O₃ in a Volcanic Cloud: An Analysis of Heterogeneous Chemistry Between 20 and 30 km," submitted to *Geophys. Res. Lett.*, 1993.

A High-Precision, Fast-Response Instrument for CO₂

Investigators

*Steven C. Wofsy
Kristie A. Boering
Bruce C. Daube, Jr.
Ralph F. Keeling
Darin W. Toohey
Department of Earth and Planetary Sciences
Harvard University
Cambridge, MA 02138

Research Objectives

The research objective was to construct a CO₂-sensor for deployment on the ER-2, with sensitivity and accuracy sufficient to detect seasonal variations and long-term trends in stratospheric concentrations of the gas. Measurements were intended to determine the mean age of stratospheric air over the height range of interest for operations of future fleets of stratospheric aircraft, and to define exchange rates between the troposphere and the lower stratosphere.

Summary of Progress and Results

A new high-resolution, fast-response instrument for measuring stratospheric CO₂ in situ aboard the NASA ER-2 aircraft was completed in October 1992. Science-quality data are available from the test flights for the Stratospheric Photochemistry, Aerosols, and Dynamics Experiment (SPADE) in November 1992 and from the SPADE test flights and operational missions in April and May, 1993, both conducted from NASA Ames Research Center, Moffett Field, California. Analysis of time series from the instrument, and detailed comparison with other tracers on the ER-2 payload (N₂O, CFC-11, O₃) indicates precision better than ± 0.04 ppm for 2 sec measurement intervals over an 8-hour flight. Analysis of a primary standard carried on all flights indicate long-term accuracy of better than ± 0.05 ppm in routine operation.

Scatter plots of the tracer species from these flights, such as N₂O, O₃, and NO_y versus CO₂, show that CO₂ concentrations vary in a dramatically different way than the other tracers. For example, the correlation coefficient with N₂O changes sign at about 400K on the flight of 16 November, indicating that the stratosphere is influenced by seasonal variations in tropospheric CO₂ up to that level. This reversal was absent in the springtime data. Over the same period, N₂O and CFC-11 retained virtually the same linear correlation.

Changes were observed in tracer relationships throughout the stratosphere, indicating unexpectedly strong mixing in the stratosphere this winter. Preliminary examination of data for H₂O and CO₂ indicate substantial infiltration of tropospheric air during the past 5 months, with dry air entering in the tropics and notably wetter air entering in the subtropics.

The observed seasonal changes are consistent with some views of stratospheric circulation, but seem to contradict other, widely-accepted concepts.

During April, 1993, the SPADE flights intercepted several anomalous layers of air. Concentrations of CO₂ were the lowest observed in all missions, 349 ppm as compared to present tropospheric values near 356 ppm (annual mean). The CO₂ data provide crucial evidence to imply that these layers were derived from remnants of the 1992-93 Arctic polar vortex.

The ER-2 flew through its own wake at least 8 times. Data for CO₂, H₂O, and nitrogen oxides demonstrate a low emission index for the JT-75 engine. This is believed to be the first in situ determination of this key parameter for a jet engine operating normally in the stratosphere. Theoretical studies of this engine will be undertaken to determine the reliability of computed NO_x emission rates.

Journal Publications

None

Laboratory Studies of Stratospheric Heterogeneous Chemistry

Investigators

*Douglas R. Worsnop
Mark S. Zahniser
Charles E. Kolb
Center for Chemical and Environmental Physics
Aerodyne Research, Inc.
Billerica, MA 01821

Steven C. Wofsy
Division of Applied Sciences
Harvard University
Cambridge, MA 02138

P. Davidovits
Department of Chemistry
Boston College
Boston, MA

Research Objectives

The purpose of this study is to determine kinetic and thermodynamic parameters necessary for modeling heterogeneous chemistry of stratospheric aerosol particles.

Summary of Progress and Results

Experiments investigating the uptake of HCl , N_2O_5 , and ClONO_2 on cold sulfuric acid droplets have been completed. Results have largely confirmed those from other laboratories: reaction of $\text{N}_2\text{O}_5 + \text{H}_2\text{O}$ is fast ($\gamma \sim 0.1$) while reaction of $\text{ClONO}_2 + \text{H}_2\text{O}$ is slow, except perhaps in very cold aerosol near the poles. The reaction of ClONO_2 with HCl is constrained by relatively low HCl solubility. The reaction efficiencies of N_2O_5 and ClONO_2 and the solubility and accommodation coefficient of HCl have been systematically studied as a function of sulfuric acid composition (40 to 70 wt%) and temperature (230 to 270 K).

Vapor pressure measurements of condensed $\text{HNO}_3/\text{H}_2\text{O}$ samples have confirmed that nitric acid trihydrate (NAT) is the most stable nitric acid hydrate under stratospheric conditions. Thermodynamic parameters measured for nitric acid dihydrate (NAD) have been determined for the first time. NAD is only slightly less stable than NAT; and metastable NAD may play an important role in Type I PSC nucleation in the stratosphere.

Journal Publications

Worsnop, D. R., L. E. Fox, M. S. Zahniser, and S. C. Wofsy, Vapor pressures of solid hydrates of nitric acid: Implications for stratospheric clouds, *Science* 259, 71, 1993.

2-D MAGI: Two-Dimensional Modeling of Aircraft Global Impacts

Investigators

*Donald J. Wuebbles
Douglas E. Kinnison
Keith E. Grant
Global Climate Research Division, L-262
P.O. Box 808
Lawrence Livermore National Laboratory
Livermore, CA 94550

Research Objectives

This research project emphasizes the application of the LLNL 2-D chemical-radiative-transport model to determine the impact of present and potential future aircraft emissions on the global atmosphere. The intention is to reduce uncertainties and better define the range of possible effects of aircraft emissions on the atmosphere. Realistic scenarios for aircraft emissions are examined to evaluate past as well as future effects on the atmosphere. Further development and improvement of the model will be done to meet the special needs of the HSR Program, with special consideration to understanding the effect of heterogeneous chemistry on changing the chemical species partitioning in the stratosphere.

Summary of Progress and Results

Our research studies during the past year have supported the HSRP/AESA Program by participating in NASAs Model and Measurement Workshop (Prather and Remsberg, 1993) to better understand the strengths and weaknesses of current global chemical-radiative-transport models by stringently comparing model-derived constituents to observed data. This exercise has been useful in guiding our future model development efforts. We contributed to all four chapters and sixteen sections that comprised this report. D. Kinnison was chapter chairman of Section I, Volume III (Kinnison et al., 1993). The goal of this section was to conduct fundamental tests of dynamical transport in the models using carbon-14 and strontium-90 as inert tracers. Results from this section are very important to understanding the uncertainties in model dynamics in the tropopause region and lower stratosphere, and the subsequent effect that transport in this region will have on the atmospheric lifetimes of important trace gases that would be emitted from HSCTs.

The LLNL two-dimensional model has been used to assess the impact of proposed 2015 subsonic and HSCT emissions on ozone and other trace gases. Results from this effort are in the NASA HSRP/AESA 1992 (Ko et al., 1993a) and 1993 (Ko et al., 1993b) assessments of the Atmospheric Effects of Stratospheric Aircraft.

There have been a number of improvements to the LLNL two-dimensional model over the last year. The vertical and latitudinal resolution has been increased by a factor of two. This was done specifically to better represent regions where realistic HSCT emission scenarios would be implemented for the NASA HSRP/AESA 3rd Annual Program Report. In addition, the effect of nitrosyl sulfuric acid was investigated (Kinnison and Wuebbles, 1992). Initial results indicate that this additional heterogeneous process in conjunction with a 2015 HSCT scenario does not add an additional change in ozone to previously derived results. Polar heterogeneous chemistry has been added to the LLNL two-dimensional chemical mechanism to investigate the potential effects of NO_x and H₂O emissions from HSCTs during periods when polar stratospheric clouds are formed.

Results from this study will be presented at the June 1993 Third Annual Meeting. Don Wuebbles has continued to chair the Emission Scenarios Committee (Wuebbles et al. 1993a, Wuebbles et al., 1993b). The outcome of this effort has produced realistic 2015 subsonic and HSCT emission scenarios. These scenarios were used by the participating global models for the 1993 NASA HSRP/AESA assessment.

Journal Publications

- Kinnison, D. E., H. S. Johnston, D. Weisenstein, and G. K. Yue, Radionuclides as exotic tracers, Section I in *The Atmospheric Effects of Stratospheric Aircraft: Report of the 1992 Models and Measurements Workshop*, Vol. III, M. J. Prather and E. E. Remsberg, Eds., NASA Reference Publication 1292, 1993.
- Kinnison, D. E., and D. J. Wuebbles, Impact of current subsonic and proposed supersonic aircraft on ozone: Including heterogeneous chemical reaction mechanisms. International Quadrennial Ozone Symposium, Charlottesville, VA, June 4-13, in press (LLNL Report UCRL-JC-108951), 1992.
- Ko, K. W., and D. Weisenstein, Ozone response to aircraft emissions: Sensitivity to heterogeneous reactions, Chapter 5, in *The Atmospheric Effects of Stratospheric Aircraft: A Second Program Report*, R. S. Stolarski and H. L. Wesoky, Eds., NASA Reference Publication 1293, 1993a.
- Ko, K. W., A. Douglass, W. Gross, and M. McElroy, Update of model simulations for the effects of stratospheric aircraft, Chapter D, in *The Atmospheric Effects of Stratospheric Aircraft: A Third Program Report*, R. S. Stolarski and H. L. Wesoky, Eds., NASA Reference Publication, in review, 1993b.
- Prather, M. J., and E. E. Remsberg, Eds., *The Atmospheric Effects of Stratospheric Aircraft: Report of the 1992 Models and Measurements Workshop*, Vol. I, II, and III, NASA Reference Publication 1292, 1993.
- Wuebbles, D. J., S. L. Baughcum, S. C. Henderson, R. Eckman, D. Maiden, M. Metwally, A. Mortlock, and F. Torres, Report of the emissions scenarios committee: Preparations for the 1993 assessment, Chapter 2, in *The Atmospheric Effects of Stratospheric Aircraft: A Second Program Report*, R. S. Stolarski and H. L. Wesoky, Eds., NASA Reference Publication 1293, 1992.
- Wuebbles, D. J., D. Maiden, R. K. Seals Jr., S. L. Baughcum, M. Metwally, and A. Mortlock, Emissions scenarios committee report, Chapter C, in *The Atmospheric Effects of Stratospheric Aircraft: A Third Program Report*, R. S. Stolarski and H. L. Wesoky, Eds., NASA Reference Publication, in review, 1993.

Modeling of Microphysical Effects on Aerosol Properties Due to Stratospheric Aircraft Emissions

Investigators

*Glenn K. Yue
Lamont R. Poole
Langley Research Center
National Aeronautics and Space Administration
Hampton, VA 23681

Research Objectives

The objectives of this research are: (1) to better understand aerosol formation and growth mechanisms after expected increases in particles and trace gases caused by emissions from stratospheric aircraft and major volcanic eruption and (2) to assess the impact on optical properties of aerosol particles in the lower stratosphere and upper troposphere. The change of aerosol properties due to stratospheric aircraft and volcanic eruptions will be studied by analyzing the temporal and latitudinal variation of aerosol properties derived from the Stratospheric Aerosol and Gas Experiment (SAGE II).

Summary of Progress and Results

- *Aerosol acidity, density and refractive index.* Water vapor concentrations obtained by SAGE II and collocated NMC temperature data were used to deduce seasonally and zonally averaged acidity, density, and refractive index of stratospheric aerosols. The derived acidity was used to estimate the rate coefficient for the heterogeneous reaction $\text{ClONO}_2 + \text{H}_2\text{O}$, and the derived aerosol density was used to estimate stratospheric aerosol loading before and after the Mt. Pinatubo eruption.
- *Sulfate aerosol model.* In collaboration with AER (Atmospheric and Environmental Research, Inc.), a 2-D sulfate model was developed. This model includes diffusion, advection, sedimentation, nucleation, and growth. The change of precursor sulfur-bearing gases such as CS_2 , OCS , SO_2 , and H_2SO_4 is also simulated in this model.
- *Comparison of aerosol and trace gases measured by different experiments.* In order to support the SPADE mission, programs to interpolate results of aerosol and ozone measurements by SAGE II were developed. The derived data will be used for trajectory analyses. In addition, aerosol, ozone, and water vapor properties deduced from SAGE II data have been compared with results obtained by other experiments such as SBUV, ATMOS, AASE II, and SPADE. Most of the intercomparisons are quite favorable. Possible sources for discrepancies of results are being studied.
- *Aerosol properties derived from SAGE II data.* Spatial and temporal variation of aerosol extinction, optical depth, effective size, surface area, and mass loading observed by SAGE II were derived and analyzed. A mysterious volcanic cloud in the stratosphere in the summer of 1990 was discovered and studied.
- *The Ruiz cloud experiment.* As part of the Models and Measurement Intercomparison studies, the 2-D modeling results submitted by seven groups and the dispersion of Ruiz cloud observed by SAGE II were compared. Good agreement of decay rates was observed in the latter months of simulations. A report on this experiment was finished.

Journal Publications

Yue, G. K., L. R. Poole, P. -H. Wang, and E. W. Chiou, Aerosol Acidity, Density, and refractive index deduced from SAGE II and NMC temperature data, submitted to *J. Geophys. Res.*, 1993.

Appendix A

HSRP/AESA Third Program Report Reviewers

Appendix A
HSRP/AESA Third Program Report Reviewers

Dr. James G. Anderson
Atmospheric Research Project
Engineering Sciences Laboratory
Harvard University
40 Oxford Street
Cambridge, MA 02138

Mr. Robert E. Anderson
Code RJH
Headquarters
National Aeronautics and Space Administration
Washington, DC 20546-0001

Dr. Steven L. Baughcum
Boeing Commercial Airplane Group
Mail Stop 6H-FC
P. O. Box 3707
Seattle, WA 98124-2207

Dr. Darrel Baumgardner
Atmospheric Technology Division
National Center for Atmospheric Research
P. O. Box 3000
Boulder, CO 80307-3000

Dr. Guy P. Brasseur
National Center for Atmospheric Research
1850 Table Mesa Drive
P. O. Box 3000
Boulder, CO 80307

Dr. William H. Brune
Department of Meteorology
520 Walker Building
Pennsylvania State University
University Park, PA 16802

Dr. Ralph J. Cicerone
Department of Geosciences
220 Physical Sciences I
University of California, Irvine
Irvine, CA 92717

Ms. Estelle Condon
Mail Stop 239-20
Ames Research Center
National Aeronautics and Space Administration
Moffett Field, CA 94035

Mr. Willard J. Dodds
Mail Drop A-309
GE Aircraft Engines
1 Neumann Way
P. O. Box 156301
Cincinnati, OH 45215-6301

Professor Frederick L. Dryer
Mechanical and Aerospace Engineering
D316 Engineering Quadrangle
Princeton University
Princeton, NJ 08544-5263

Dr. James E. Dye
Mesoscale and Microscale Meteorology Division
National Center for Atmospheric Research
P. O. Box 3000
Boulder, CO 80307-3000

Professor Dieter H. Ehhalt
Institut für Atmosphärische Chemie, ICG-3
Forschungszentrum Jülich
Postfach 1913
W-5170 Jülich
GERMANY

Dr. James W. Elkins
R/E/CG1
Environmental Research Laboratories/CMDL
National Oceanic and Atmospheric Administration
325 Broadway
Boulder, CO 80303-3328

Dr. Randall R. Friedl
Mail Stop 183-901
Jet Propulsion Laboratory
National Aeronautics and Space Administration
4800 Oak Grove Drive
Pasadena, CA 91109

Mr. Edwin J. Graber
Mail Stop 86-1
Lewis Research Center
National Aeronautics and Space Administration
21000 Brookpark Road
Cleveland, OH 44135

Dr. William L. Grose
Mail Stop 401B
Langley Research Center
National Aeronautics and Space Administration
Hampton, VA 23681

Professor Donald E. Hagen
Cloud and Aerosol Science Laboratory
Department of Physics
G-7 Norwood Hall
University of Missouri - Rolla
Rolla, MO 65401-0249

Dr. Neil Harris
Ozone Secretariat
British Antarctic Survey
High Cross
Madingley Road
Cambridge, CB3 0ET
UNITED KINGDOM

Mr. Michael H. Henderson
Mail Stop 6H-FM
Boeing Commercial Airplane Group
P. O. Box 3707
Seattle, WA 98124-2207

Mr. Richard Hines
Mail Stop 165-19
Pratt and Whitney
400 Main Street
East Hartford, CT 06108

Professor James R. Holton
AK-40
Atmospheric Sciences
University of Washington
Seattle, WA 98195

Professor Ivar S. A. Isaksen
Institute of Geophysics
University of Oslo
P. O. Box 1022, Blindern
N-0315 Oslo
NORWAY

Dr. Charles H. Jackman
Code 916
Goddard Space Flight Center
National Aeronautics and Space Administration
Greenbelt, MD 20771

Dr. Thomas A. Jackson
Aero Propulsion and Power Directorate
Wright Laboratory
WL/POSF
Wright-Patterson AFB, OH 45433-6563

Professor Harold S. Johnston
Department of Chemistry
University of California, Berkeley
Berkeley, CA 94720

Dr. Jack A. Kaye
Mail Code Y
Headquarters
National Aeronautics and Space Administration
Washington, DC 20546-0001

Mr. Kenneth Kelly
R/E/AL6
Aeronomy Laboratory
National Oceanic and Atmospheric Administration
325 Broadway
Boulder, CO 80303-3328

Mr. Nicholas P. Krull
AEE-3
Office of Environment and Energy
Federal Aviation Administration
800 Independence Avenue, SW
Washington, DC 20591

Mr. Richard L. Kurkowski
Aircraft Technology Division, Mail Stop 237-11
Ames Research Center
National Aeronautics and Space Administration
Moffett Field, CA 94035

Dr. Michael J. Kurylo
Code Y
Headquarters
National Aeronautics and Space Administration
Washington, DC 20546-0001

Dr. James G. Lawless
Mail Stop 239-20
Ames Research Center
National Aeronautics and Space Administration
Moffett Field, CA 94035-1000

Dr. James D. Lawrence, Jr.
Mail Stop 401
Langley Research Center
National Aeronautics and Space Administration
Hampton, VA 23681

Dr. Ming-Taun Leu
Mail Stop 183-901
Jet Propulsion Laboratory
National Aeronautics and Space Administration
4800 Oak Grove Drive
Pasadena, CA 91109

Dr. Joel M. Levy
Office of Oceanic and Atmospheric Research
Mail Code OGP
National Oceanic and Atmospheric Administration
1335 East-West Highway
Silver Spring, MD 20910

Dr. Max Loewenstein
Mail Stop 245-5
Ames Research Center
National Aeronautics and Space Administration
Moffett Field, CA 94035-1000

Dr. Nicole Louisnard
Physics Department
Office National d'Etudes et Recherches
Aerospatiales
8, rue des Vertugadins
92190 Meudon
FRANCE

Mr. Donald L. Maiden
High-Speed Research Program Office
Mail Stop 403
Langley Research Center
National Aeronautics and Space Administration
Hampton, VA 23681

Dr. James J. Margitan
Mail Stop 183-301
Jet Propulsion Laboratory
National Aeronautics and Space Administration
4800 Oak Grove Drive
Pasadena, CA 91109

Dr. Richard C. Miake-Lye
Aerodyne Research, Inc.
45 Manning Road
Billerica, MA 01821-3976

Professor Mario J. Molina
Atmospheric Chemistry, 54-1312
Department of Earth, Atmospheric, and
Planetary Sciences
Massachusetts Institute of Technology
Cambridge, MA 02139

Mr. Alan K. Mortlock
High Speed Civil Transport, MC 35-29
Douglas Aircraft Company
McDonnell Douglas Corporation
3855 Lakewood Boulevard
Long Beach, CA 90846-0001

Dr. Jarvis Moyers
Division of Atmospheric Sciences, Room 644
National Science Foundation
1800 G Street, NW
Washington, DC 20550

Dr. Paul A. Newman
Code 916
Goddard Space Flight Center
National Aeronautics and Space Administration
Greenbelt, MD 20771

Mr. Richard W. Niedzwiecki
Mail Stop 77-10
Lewis Research Center
National Aeronautics and Space Administration
21000 Brookpark Road
Cleveland, OH 44135

Dr. Robert C. Oliver
Science and Technology Division
Institute for Defense Analyses
1801 North Beauregard Street
Alexandria, VA 22311-1772

Dr. Michael Oppenheimer
Environmental Defense Fund
257 Park Avenue South, 16th Floor
New York, NY 10010

Professor R. Alan Plumb
Room 54-1726
Department of Earth, Atmospheric and
Planetary Sciences
Massachusetts Institute of Technology
Cambridge, MA 02139

Dr. Michael J. Prather
Department of Geosciences
211 Physical Sciences Research Facility
University of California, Irvine
Irvine, CA 92717

Dr. Michael H. Proffitt
R/E/AL5
Aeronomy Laboratory
National Oceanic and Atmospheric Administration
325 Broadway
Boulder, CO 80303

Dr. John A. Pyle
Department of Chemistry
University of Cambridge
Lensfield Road
Cambridge, CB2 1EP
UNITED KINGDOM

Dr. A. R. Ravishankara
R/E/AL2
Environmental Research Laboratories
National Oceanic and Atmospheric Administration
325 Broadway
Boulder, CO 80303

Dr. David H. Rind
Goddard Institute for Space Studies
National Aeronautics and Space Administration
2880 Broadway
New York, NY 10025

Professor F. Sherwood Rowland
Department of Chemistry
University of California, Irvine
Irvine, CA 92717

Dr. Arthur L. Schmeltekopf
410 East Fork Road
Marshall, NC 28753

Mr. Stephen Seidel
Acting Director, Stratospheric Protection Division
Office of Air and Radiation
Mail Code 6205J
Environmental Protection Agency
401 M Street, SW
Washington, DC 20460

Dr. Richard S. Stolarski
Code 916
Goddard Space Flight Center
National Aeronautics and Space Administration
Greenbelt, MD 20771

Dr. Margaret A. Tolbert
Cooperative Institute for Research in
Environmental Sciences - CIRES
Campus Box 216
University of Colorado
Boulder, CO 80309-0216

Dr. Adrian F. Tuck
R/E/AL6
Aeronomy Laboratory
National Oceanic and Atmospheric Administration
325 Broadway
Boulder, CO 80303-3328

Dr. Guido Visconti
Dipartimento di Fisica
Universita' degli Studi L'Aquila
Via Vetoio
67010 Coppito (L' Aquila)
ITALY

Dr. Christopher R. Webster
Mail Code 183-401
Jet Propulsion Laboratory
National Aeronautics and Space Administration
4800 Oak Grove Drive
Pasadena, CA 91109-8099

Professor Philip D. Whitefield
Cloud and Aerosol Sciences Laboratory
Norwood Hall (G-7)
University of Missouri - Rolla
Rolla, MO 65401

Dr. James C. Wilson
Department of Engineering
Knudson Hall
University of Denver
Denver, CO 80208-0177

Dr. Douglas R. Worsnop
Aerodyne Research, Inc.
45 Manning Road
Billerica, MA 01821-3976

Dr. Owen B. Toon
Space Sciences Division, Mail Stop 245-3
Ames Research Center
National Aeronautics and Space Administration
Moffett Field, CA 94035-4000

Dr. Richard P. Turco
Department of Atmospheric Sciences
University of California, Los Angeles
Los Angeles, CA 90024-1565

Dr. Robert T. Watson
Code Y
Headquarters
National Aeronautics and Space Administration
Washington, DC 20546-0001

Mr. Howard L. Wesoky
Code RH
Headquarters
National Aeronautics and Space Administration
Washington, DC 20546-0001

Mr. Allen H. Whitehead, Jr.
Mail Stop 403
Langley Research Center
National Aeronautics and Space Administration
Hampton, VA 23681

Dr. Steven C. Wofsy
Room 100A, Pierce Hall
Department of Earth and Planetary Science
Harvard University
29 Oxford Street
Cambridge, MA 02138

Dr. Donald J. Wuebbles
Atmospheric and Geophysical Sciences
Division, L-262
Lawrence Livermore National Laboratory
7000 East Avenue
P. O. Box 808
Livermore, CA 94550



Report Documentation Page

1. Report No. NASA RP-1313	2. Government Accession No.	3. Recipient's Catalog No.	
4. Title and Subtitle The Atmospheric Effects of Stratospheric Aircraft: A Third Program Report		5. Report Date November 1993	
		6. Performing Organization Code	
7. Author(s) Richard S. Stolarski and Howard L. Wesoky, Editors		8. Performing Organization Report No.	
		10. Work Unit No.	
9. Performing Organization Name and Address NASA Office of Mission to Planet Earth		11. Contract or Grant No.	
		13. Type of Report and Period Covered Reference Publication	
12. Sponsoring Agency Name and Address National Aeronautics and Space Administration Washington, DC 20546		14. Sponsoring Agency Code	
15. Supplementary Notes Stolarski: Goddard Space Flight Center, Greenbelt, MD; Wesoky: NASA Headquarters Office of Aeronautics, Washington, D. C.			
16. Abstract <p>This document presents a third report from the Atmospheric Effects of Stratospheric Aircraft (AESA) component of NASA's High-Speed Research Program (HSRP). Market and technology considerations continue to provide an impetus for high-speed civil transport research. A recent United Nations Environment Program scientific assessment has shown that considerable uncertainty still exists about the possible impact of aircraft on the atmosphere. The AESA has been designed to develop the body of scientific knowledge necessary for the evaluation of the impact of stratospheric aircraft on the atmosphere. The first Program report presented the basic objectives and plans for AESA. This third report marks the midpoint of the program and presents the status of the ongoing research on the impact of stratospheric aircraft on the atmosphere as reported at the third annual AESA Program meeting in June 1993. The focus of the program is on predicted atmospheric changes resulting from projected HSCT emissions. Topics reported on cover how high-speed civil transports (HSCT) might affect stratospheric ozone, emissions scenarios and databases to assess potential atmospheric effects from HSCTs, calculated results from 2-D zonal mean models using emissions data, engine trace constituent measurements, exhaust plume/aircraft wake vortex interactions.</p>			
17. Key Words (Suggested by Author(s)) stratospheric chemistry, ozone, aircraft emissions, upper atmosphere aerosols, stratospheric aircraft, high-speed civil transport		18. Distribution Statement Unclassified - Unlimited Subject Category 45	
19. Security Classif. (of this report) Unclassified	20. Security Classif. (of this page) Unclassified	21. No. of pages 428	22. Price A19

National Aeronautics and
Space Administration
Code JTT
Washington DC 20546
Official Business
Penalty for Private Use, \$300

FOURTH CLASS

SPECIAL FOURTH-CLASS RATE
POSTAGE & FEES PAID
NASA
Permit No. G-27

L1 001 RP-1313 931118S090569A
NASA
CENTER FOR AEROSPACE INFORMATION
ACCESSIONING
800 ELKRIDGE LANDING ROAD
LINTHICUM HEIGHTS MD 210902934

